Total Synthesis of Sorbicillactone A: Inspiration for Methodology and Catalyst Development

A Dissertation
SUBMITTED TO THE FACULTY OF
UNIVERSITY OF MINNESOTA
BY

Kelly A. Volp

IN PARTIAL FULFILLMENT OF THE REQUIREMENTS
FOR THE DEGREE OF
DOCTOR OF PHILOSOPHY

Andrew M. Harned, Advisor

January 2014

Acknowledgements

First, I would like to thank my loving and supporting husband, Adam Denny. You have always kept me grounded and have kept me appreciating the finer things in life. Moving to Minneapolis would not have been as much fun without you; I have enjoyed every minute of our adventure together. I would also like to thank my mom for always believing in me and being there for me – I have always appreciated everything you have done for me; I hope that I have been able to convey that to you over the years.

Second, I want to thank my advisor, Prof. Andrew Harned. Your unwavering enthusiasm for chemistry and dedication to your students is something I did not fully understand the value of until I began research in your group. I appreciate all of the dedication and time you have put into the success of my graduate career over the years. I would also like to thank my group members who have been essential in creating an enjoyable and supportive environment. To Dr. Rodolfo Tello-Aburto, your generous nature and cheery attitude are truly inspirational qualities that I strive for. Kyle Kalstabakken: thank you for your willingness to always help me and answer my questions, no matter how ridiculous they were. And Karen Beckman: thank you for always being there for me – in the lab and as a friend; things would not have been as much fun without you. Nick Moon, Erik Goebel, and to all of the other past members of the Harned Group, it has been a pleasure to have you as my friends and co-workers.

Dedication

to my husband, Adam Denny, and my mother, Rita Volp

Abstract

The unique reactivity and usefulness of cyclohexadienones has been the central focus of my graduate research. Our group has a particular interest in the synthesis and methodology of this structural motif because it can be used as a synthetic building block for the construction of complex molecules, specifically, natural products.

We were inspired to design a synthetic route to sorbicillactone A, a bioactive marine natural product, using a cyclohexadienone as the key building block. Chapter 1 will give a more detailed background on cyclohexadienones: how they are synthesized and how they have been utilized in natural product synthesis. Sorbicillactone A is part of a larger family of natural products called sorbicillinoids, therefore, Chapter 2 is based on a review that we wrote summarizing the various sorbicillinoid compounds that have been isolated, the biosynthetic proposals that have been put forth, and the various synthetic efforts that have already been carried out. Chapter 3 will cover our own synthetic efforts on the total synthesis of sorbicillactone A and a related epimer. Curious diastereoselectivity was encountered during these efforts that were further explored and will be discussed in Chapter 4. Finally, Chapter 5 will highlight our endeavors in designing chiral aryl iodide catalysts for the asymmetric synthesis of cyclohexadienones.

Table of Contents

List of Tables

List of Figures

List of Schemes

List of Abbreviations

Ac	acetyl
aq	aqueous
Bn	benzyl
BP or bp	boiling point, °C
t-Bu	*tertiary*-Butyl
DBU	1,8-diazabicyclo[5.4.0]undec-7-ene
DCC	*N,N*′-dicyclohexylcarbodiimide
DCE	1,2-dichloroethane
DDQ	2,3-dichloro-5,6-dicyano-1,4-benzoquinone
DEAD	diethyl azodicarboxylate
DEPT	Distortionless enhancement by polarization transfer
DFT	density functional theory
DIBAL-H	diisobutylaluminum hydride
DMAP	4-dimethylaminopyridine
DMF	*N,N*-dimethylformamide
DMP	Dess-Martin periodinane
DMSO	dimethylsulfoxide
dr	diastereomeric ratio
EI	electron impact ionization
equiv	equivalent(s)
ESI	electrospray ionization
FCC	flash column chromatography
HMDS	hexamethyldisilazane
HMPA	hexamethylphosphoramide
HPLC	high performance/pressure liquid chromatography
Hz	hertz
IBX	1-hydroxy-1,2-benziodoxol-3(1*H*)-one 1-oxide
IR	infrared spectroscopy

LA	Lewis acid
LAH	lithium aluminum hydride
LDA	lithium diisopropylamine
LiHMDS	lithium bis(trimethylsilyl)amide
Me	Methyl
MP or mp	melting point, °C
MS	mass spectrometry
NaHMDS	sodium bis(trimethylsilyl)amide
NBS	*N*-bromosuccinimide
NMR	nuclear magnetic resonance spectroscopy
NOE	nuclear Overhauser enhancement/effect
[O]	oxidation
ORTEP	Oak Ridge Thermal Ellipsoid Plot
Ph	phenyl
PIDA	phenyliodine diacetate
PIFA	[bis(trifluoroacetoxy)iodo]benzene
ppm	parts per million (NMR spectroscopy)
pyr	pyridine
rt	room temperature
sat'd	saturated
TBAF	tetra-*n*-butylammonium fluoride
TBS	*tertiary*-butyldimethylsilyl
TFA	trifluoroacetic acid
THF	tetrahydrofuran
TIPS	triisopropylsilyl
TLC	thin layer chromatography
TMS	trimethylsilyl
TOF	time of flight
t_R	retention time

Chapter 1

Introduction and Background

The unique reactivity and usefulness of cyclohexadienones, small organic molecules with a specific chemical structure, have been the central focus of my graduate research. Our group has a particular interest in the synthesis and methodology of this structural motif and its application as a synthetic building block for the construction of complex molecules. The overall goal of our research is twofold: the development of new methodologies and their use in the synthesis of bioactive natural products, molecules that have potential to be further developed as pharmaceutical drug therapies.

Synthetic organic chemistry is continuously evolving with reports of cutting edge research; the boundaries for complex molecule synthesis are always being thrust into new territories. New transformations are still being discovered today, with an impressive efficiency and scale that is key to the advancement and significance of the field to society. In a world where we have limited natural resources, and where we are still struggling to discover cures and therapies for diseases, infections, and ailments, it is imperative that we continue to develop new approaches for the improvement of human health. Our role in this overall goal is through synthetic organic chemistry: developing methods for effectively synthesizing small molecules and learning how these can be further elaborated into bioactive molecules. We aim to discover new

reactivity and structural motifs that have an impact in the scientific field and application to the improvement of human health.

This chapter will provide background on the overall topic of cyclohexadienones, followed by an overview of the relevant research being conducted in the Harned group. This will offer insight to the motivation and goals behind our projects.

1.1 CYCLOHEXADIENONES

1.1.1. What are Cyclohexadienones?

Cyclohexadienones are unique small molecules that can be regarded as an oxidized version of a phenol. They come in one of two varieties: 2,4-cyclohexadienone or 2,5-cyclohexadienone (Figure 1.1). Both types undergo an array of different reactions, which make them suitable building blocks for the synthesis of complex molecules.[1] These reactions include Diels-Alder cycloadditions, conjugate additions, epoxidations, and direct additions to the ketone. This reactivity also poses a challenge in harnessing their full potential, as many worthy intentions are often plagued with unwanted side reactions, such as rearomatization or dimerization. Our group is specifically interested in cyclohexadienones of the 2,5-variety as they are underutilized as synthetic building blocks and their use in asymmetric synthesis is relatively unexplored. Therefore, the remainder of this thesis will focus on the 2,5-cyclohexadienone motif.

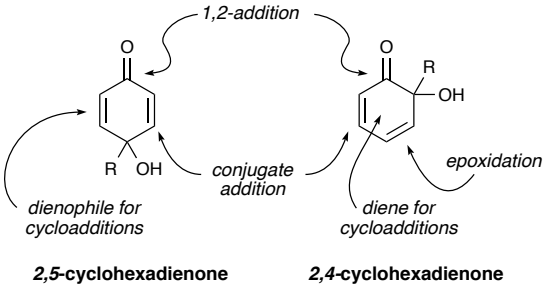

Figure 1.1. Cyclohexadienones can undergo a variety of different reactions.

1.1.2. Synthesis of Cyclohexadienones

The most straightforward and easiest method for accessing cyclohexadienones is through oxidative dearomatization of phenols.[2] This can be accomplished through

several different methods, including electrochemistry, singlet oxygen, hypervalent iodide reagents, and transition metal complexes. Two of these methods, singlet oxygen and hypervalent iodide, will be detailed below, as these are the most relevant methods to our research.

1.1.2.a Singlet Oxygen Methods

Singlet oxygen can be formed by irradiating oxygen with light of the appropriate wavelength in the presence of photosensitizers, which are organic molecules capable of absorbing energy from the light and transferring it to gaseous oxygen, exciting it to the singlet state.[3] The synthesis of *p*-peroxyquinols can be achieved by the reaction of *p*-substituted phenols with singlet oxygen. The *p*-quinol can then obtained upon a reduction.

Matsuura and co-workers reported one of the first examples of oxidative dearomatization with singlet oxygen (Scheme 1.1A).[4] They investigated the photochemical oxidation of hindered phenols using various photosensitizers and analyzed the resulting isolated products. In many of the experiments, the *p*-quinone or diphenoquinone was observed. However, using Eosin Y on phenol **1.1** yielded *p*-quinol **1.2** in 1% yield. Endo and co-workers followed this work by demonstrating that **1.4** could be oxidized to *p*-quinol hydroperoxide **1.5** through photooxygenation by irradiating their reaction mixture with a halogen lamp in the presence of Rose Bengal (Scheme 1.1B). Reduction of the peroxide with dimethylsulfide afforded the *p*-quinol (**1.6**) in 27% yield over the two steps.[5]

Scheme 1.1. Synthesis of *p*-quinols from light and oxygen in the presence of photosensitizers.

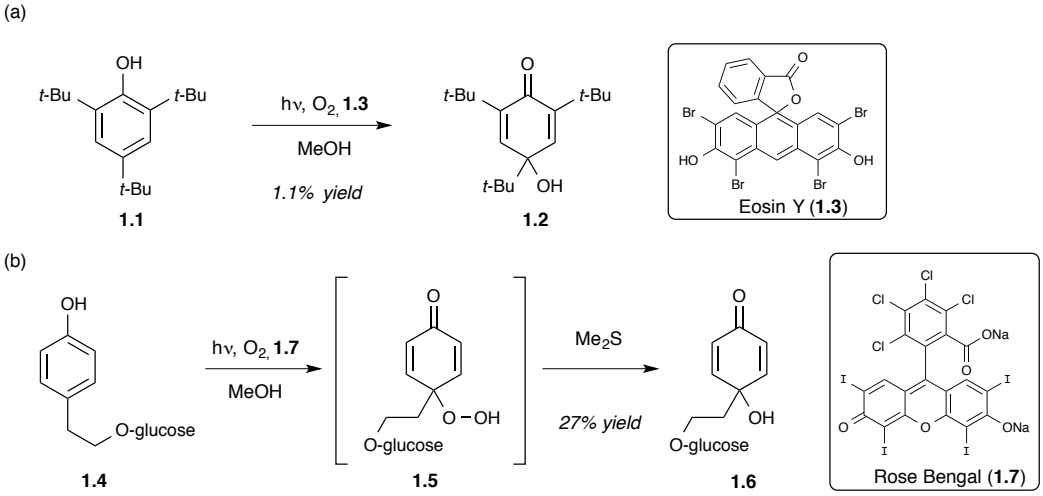

More recently, Carreño and co-workers have reported an Oxone-mediated oxidative dearomatization of substituted phenols.[6] This method is quite general, generating the *p*-peroxyquinol (**1.9**) directly, or the *p*-quinol (**1.10**) upon a reductive workup in excellent yields (Scheme 1.2). This procedure uses Oxone, a mild and safe oxidant, and $NaHCO_3$ to generate singlet oxygen, which undergoes a [4 + 2] cycloaddition with the phenol. Exposure to water results in exclusive formation of the *p*-peroxy product (presumably by facilitating the opening of the peroxide-acetal intermediate); the authors note that water is essential for success of the reaction. Notably, the use of *o*-methoxy substituted phenols can also be used to generate the *p*-quinol in 33% yield, while iodine(III) reagents (see below) exclusively give the *o*-quinone monoacetal.[7]

Scheme 1.2. Synthesis of *p*-peroxyquinol or *p*-quinol with Oxone.

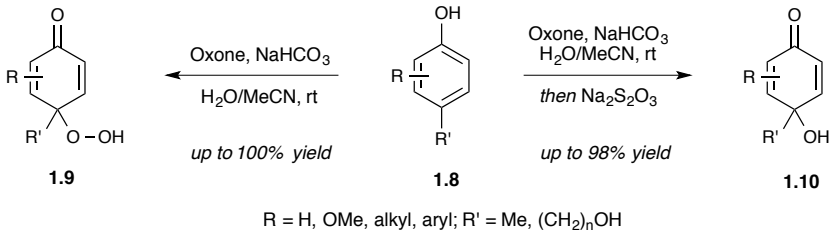

1.1.2.b Hypervalent Iodide Reagents

Hypervalent iodide reagents, such as phenyliodine diacetate (PIDA) and [phenyliodine bis(trifluoroacetate)] (PIFA), have become the reagent of choice for dearomatization of phenols due to their commercial availability, functional group tolerance, and wide versatility as safe and mild oxidants.[8] Highlighted here will be the versatility of these reagents for the synthesis of *p*-quinols and *p*-monoacetals.

Some of the first examples of using PIDA with substituted phenols were provided by Lewis[9] and Pelter.[10] They treated *p*-substituted phenols with PIDA in MeOH and isolated *p*-quinol ethers in good yields (Scheme 1.3A). Wipf and co-workers expanded the substrate scope to include tethered amines during their synthesis of *Stemona* alkaloids (Scheme 1.3B),[11] while Rama Rao and co-workers were among the first to demonstrate intramolecular nucleophilicity with tethered amino acids and PIFA (Scheme 1.3C).[12]

Scheme 1.3. (A) Pelter and Lewis demonstrated the synthesis of *p*-quinol ethers on separate occasions; (B) Wipf expanded the substrate scope; (C) Rama Rao successfully spirolactonized amino acid-tethered phenols.

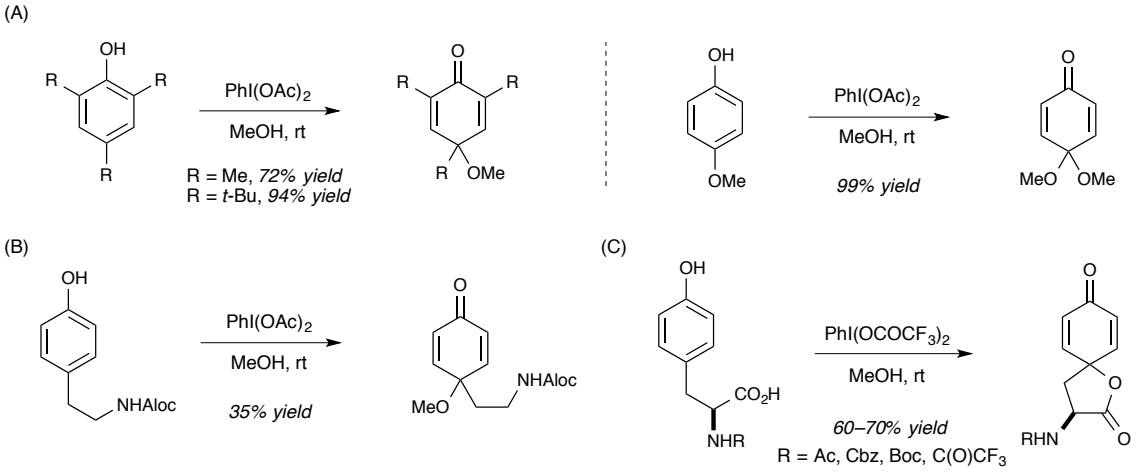

Taylor and co-workers isolated alkyl *p*-quinols in moderate to good yields when substituted phenols were treated with PIFA in a 4:1 mixture of MeCN-H_2O at 0 °C.[13] They noted that simple alkyl phenols, such as *p*-cresol, were prone to over-oxidation, giving only 44% yield of the *p*-quinol (Scheme 1.4).

Scheme 1.4. Oxidation of *p*-cresol with PIFA.

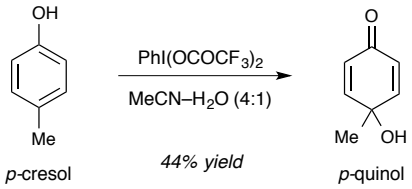

They attempted to optimize conditions by varying the reaction time, temperature, and base additives, such as Triton-B and pyridine. However, they ultimately found that better yields were obtained with silyl ether phenols, rather than the free phenols; this was in accordance to previous findings by Kita and co-workers during their synthesis of discorhabdin C.[14] They further investigated this observation by subjecting various silyl ethers of *p*-cresol to dearomatization with PIFA and found that the tri-*n*-propyl silyl ether gave the best results. They conducted a brief substrate scope

proving that this finding was general, and not exclusive to the *p*-cresol substrate (Table 1.1). They also noted the reactions were generally cleaner than with the free phenols.

Table 1.1. Yields of *p*-quinols with free phenols compared to silyl-ether phenols.

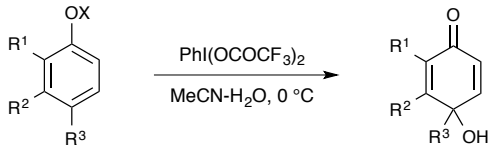

R^1	R^2	R^3	% yield	
			X = H	X = *n*-Pr_3Si
H	H	Me	48	73
Me	H	Me	60	73
Me	Me	Me	67	78
H	H	CH_2CO_2Me	27	59

Kita explored the nucleophilicity preferences of amides and different alcohol solvents to affect product formation from oxidative dearomatization (Scheme 1.5).[15] When phenols containing secondary amides (**1.11**) were treated with PIFA, C–O bond formation occurred via the imidate (**1.12**) in trifluoroethanol (Scheme 1.5A). Alternatively, if solvents such as methanol or ethanol were used, nucleophilic addition of the solvent provided *p*-quinol ethers (**1.13**). Next, Kita employed tertiary amides (**1.14**) and observed initial dearomatization with C–O bond formation (Scheme 1.5B). Upon aqueous workup and hydrolysis, intramolecular conjugate addition of the free amine occurred to give bicyclic amines (**1.15**). Kita's group was the first to exploit the reactivity differences between alcohol solvents and their fluorous congeners for dearomatization reactions, which have now become common for these types of reactions.

Scheme 1.5. (A) Oxidative dearomatizations with trifluoroethanol versus methanol. (B) Synthesis of bicyclic amines.

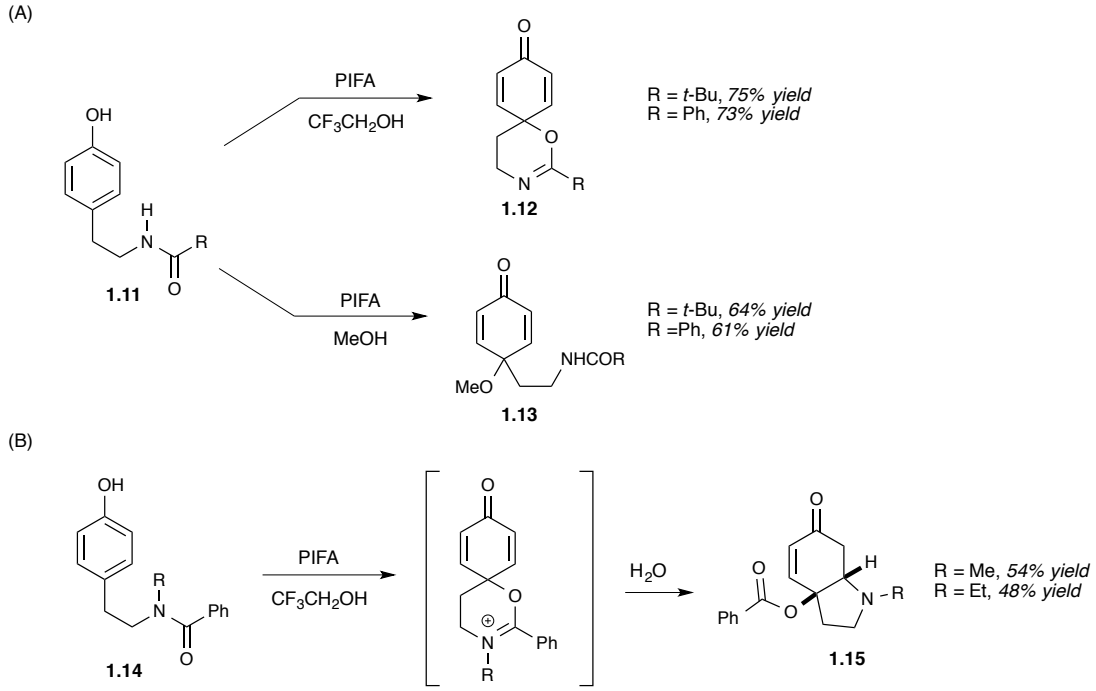

1.1.3. Cyclohexadienones in Natural Product Synthesis

Oxidative dearomatizations of phenols have found great utility in natural product synthesis.[16] Their ease of construction and versatile reactivity make them desirable synthetic building blocks. Additionally, cyclohexadienones are a common motif found in natural products. Notable examples of total syntheses utilizing 2,5-cyclohexadienones are highlighted below.

1.1.3.c Puupehenone

The synthesis of puupehenone, a marine quinonoid with promising antituberculosis activity, by the Quideau group illustrates C–O bond formation through oxidative dearomatization.[17] The authors began their synthesis from commercially available (+)-sclareolide, which afforded their dearomatization precursor **1.16** in 8 steps. Treating phenol **1.16** with PIFA at –25 °C in dichloromethane afforded dienone **1.17** in 67% yield. It is notable that the free *o*-hydroxyl was present during the

dearomatization reaction, but did not interfere with the desired product formation. Subsequent treatment with KH and in situ oxidation afforded their target molecule.

Scheme 1.6. Quideau's synthesis of (+)-puupehenone.

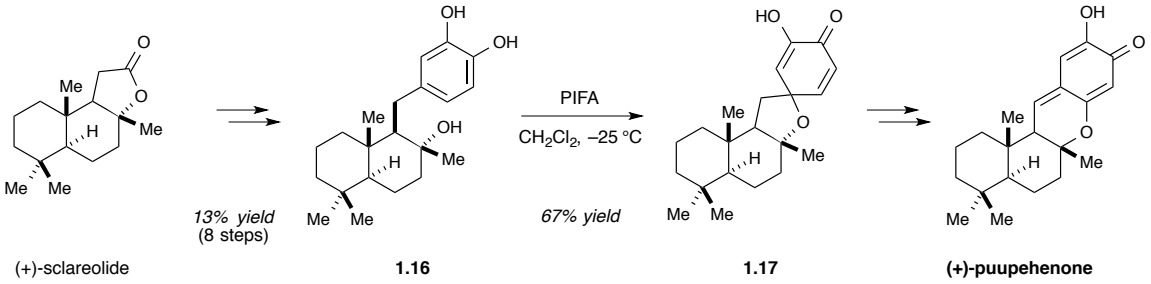

1.1.3.d Discorhabdins

Kita and co-workers were among the first to realize the full potential of oxidative dearomatization with carbon nucleophiles when they utilized this strategy in a total synthesis of the discorhabdins (Scheme 1.7).[14,18] Oxidative dearomatization of **1.18** with PIFA in trifluoroethanol provided discorhabdin C in 42% yield. The benefits of silylphenols in dearomatization reactions had previously been studied (see Section 1.1.2.b).[13,14] More recently, this chemistry was applied to the diastereoselective synthesis of discorhabdin A. The dearomatization precursor (**1.19**) was synthesized in 5 steps from (L)-tyrosine methyl ester·HCl. When the free phenol was subjected to PIFA in the presence of Montmorillonite K-10 (MK-10) with trifluoroethanol as a solvent, dienone **1.20** was afforded in 45% yield with a 1.5:1 dr. If MK-10 was omitted from the reaction, the yield was reduced to 22%, but the diastereoselectivity was unaffected. Interestingly, when the silylated phenol was subjected under these conditions, a more favorable 4.8:1 dr was obtained, with the major diastereomer being the desired one. They postulated this was due to a change of mechanism during the dearomatization, as the reaction proceeded much more slowly, thus enhancing the selectivity. In this manner, Kita was able to obtain discorhabdin A diastereoselectively with the only controlling chiral center coming from the amino acid.

Scheme 1.7. Kita's dearomatization strategy for the synthesis of discorhabdins.

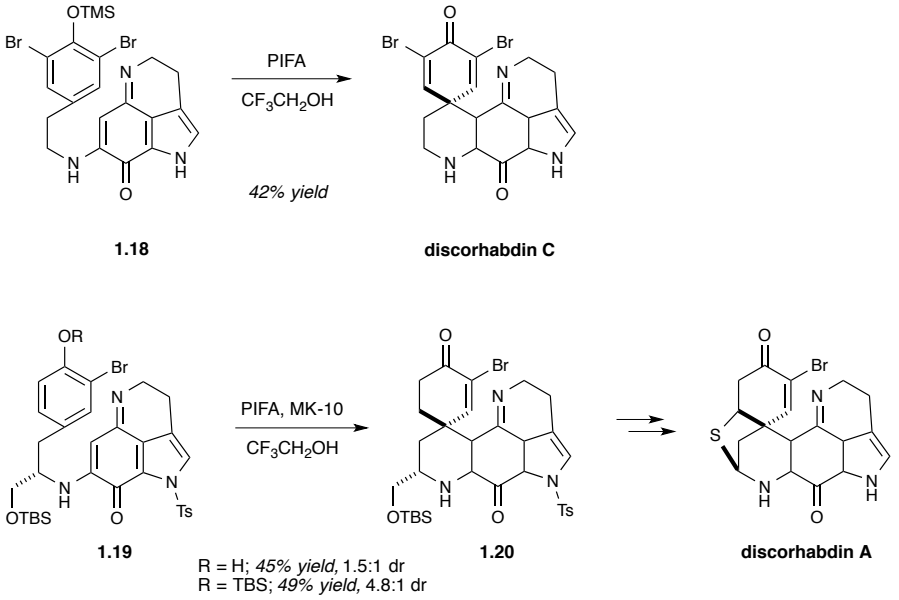

1.1.3.e Rishirilide B

The Pettus group had developed a methodology for enantioselectively dearomatizing resorcinol derivatives and sought to construct a natural product utilizing their new strategy.[19] They envisioned the synthesis of rishirilide B proceeding through cyclohexadienone **1.22**.[20] Their synthesis commenced with the protected resorcinol derivative **1.21**, which was subjected to Mitsunobu conditions with a chiral methoxyamide to generate the inverted product; subsequent deprotection with $ZnBr_2$ afforded (*S*)-**1.22** (Scheme 1.8). With (*S*)-**1.22** in hand, they performed the oxidative dearomatization with a combination of PhIO/TMSOTf in dichloromethane, giving **1.22** exclusively as one enantiomer and in 73% yield. With the core of rishirilide B synthesized, relatively few steps remained. However, they had great difficulty in effectively removing the chiral tether from (–)-**1.22**. In the end, they synthesized rishirilide B in a total of 15 steps with an overall yield of 12.5%. While Pettus and co-workers achieved this total synthesis by means of diastereoselective oxidative dearomatization, they were unable to easily remove the lactone functionality used to influence the configuration. Ideally, a more efficient synthesis would be afforded if

enantioselectivity could be induced using reagent control; this would eliminate several steps and likely result in a higher overall yield.

Scheme 1.8. Synthesis of rishirilide B utilizing a cyclohexadienone as a key intermediate.

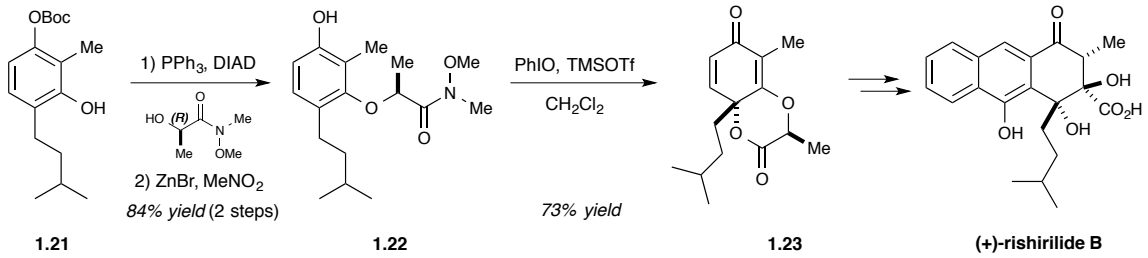

1.21 **1.22** **1.23** **(+)-rishirilide B**

1.2 RESEARCH OVERVIEW

1.2.1. Methodology

Cyclohexadienones offer a unique and challenging platform for reaction discovery and natural product synthesis.[1] Our group aims to utilize cyclohexadienones in two key ways: through their asymmetric synthesis and by their use in desymmetrization reactions. Both methods install stereogenic centers: either upon formation of the cyclohexadienone directly (Figure 1.2A), or through subsequent asymmetric reactions to give chiral derivatives (Figure 1.2B). These chiral molecules can be further elaborated into complex natural products.

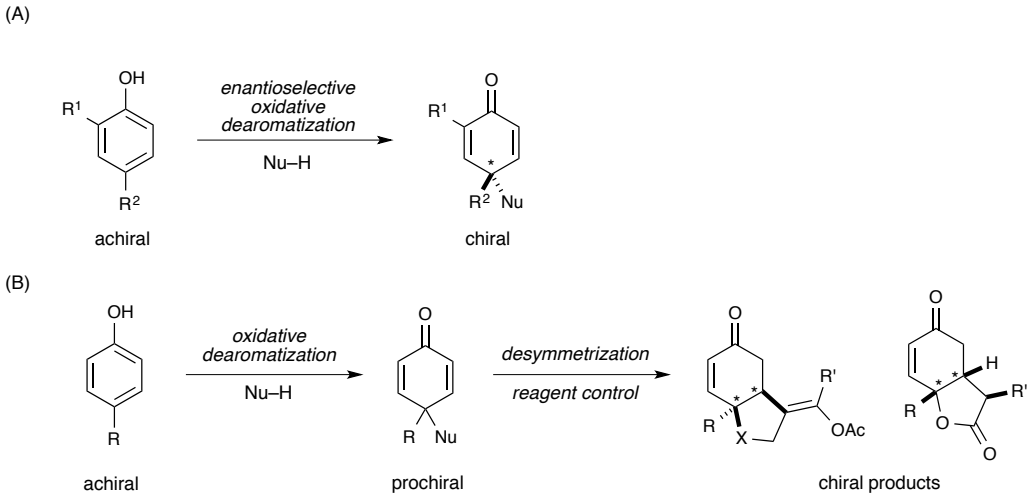

Figure 1.2. (A) Enantioselective reactions of achiral substrates. (B) Desymmetrization of prochiral substrates to give chiral products.

1.2.1.f Enantioselective Oxidative Dearomatization

The principle behind enantioselective synthesis is taking a non-chiral molecule and subjecting it to asymmetric reaction conditions, creating a chiral product. Enantioselective oxidative dearomatization specifically is the transformation of an achiral phenol into a chiral cyclohexadienone. This can be accomplished by either substrate or reagent control (Figure 1.3). Pettus and co-workers have successfully synthesized chiral cyclohexadienones by tethering their nucleophile, containing a chiral center, to the phenol.[19] Subjecting the phenol to an oxidative dearomatization reaction with hypervalent iodide gave enantioenriched cyclohexadienones upon removal of the tether. This is an example of a substrate controlled enantioselective reaction; the asymmetry is being induced from the molecule itself. *Our goal is to induce asymmetry through reagent control.* We aim to accomplish this by synthesizing chiral hypervalent iodide reagents. A benefit of reagent controlled asymmetric reactions is that a wider variety of nucleophiles can be utilized; the reaction is not limited to tethered nucleophiles.

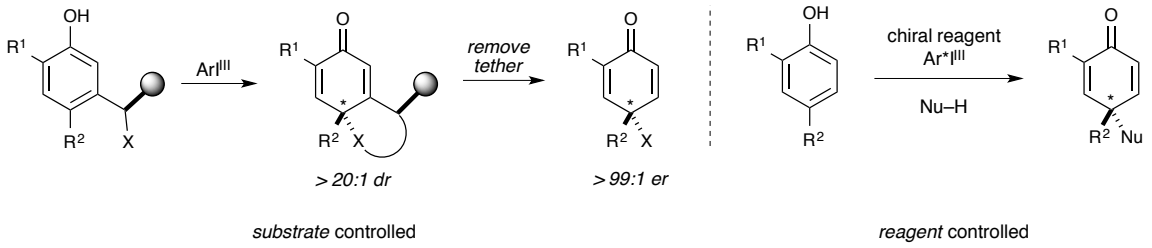

Figure 1.3. Enantioselective dearomatization via substrate or reagent control.

1.2.1.g Desymmetrization of Cyclohexadienones

Another method of synthesizing chiral cyclohexadienone derivatives is through desymmetrization reactions. Enantioselective desymmetrization [21] of prochiral cyclohexadienones has seen limited attention.[22] These reactions are attractive for several reasons. First, the desymmetrization event will not only set the configuration of the fully substituted carbon atom, but under most circumstances will also result in the concomitant installation of a second contiguous stereocenter (and possibly more). Additionally, the symmetry-breaking event will leave behind an enone moiety that can be engaged in further synthetic manipulations.[23]

Our group has investigated the desymmetrization of tethered cyclohexadienones (Figure 1.4A). By tethering the electrophile to the cyclohexadienone, substrate controlled reactivity reduces the number of possible diastereomers and allows for greater selectivity. This is possible due to the fact that, in our systems, the tethered electrophile selectively reacts with the enone on the same face, creating a *cis*-fused ring system. Utilizing cinchonine-derived phase transfer catalysts allowed for the cyclized product to be isolated with up to 91:9 er (Figure 1.4B).

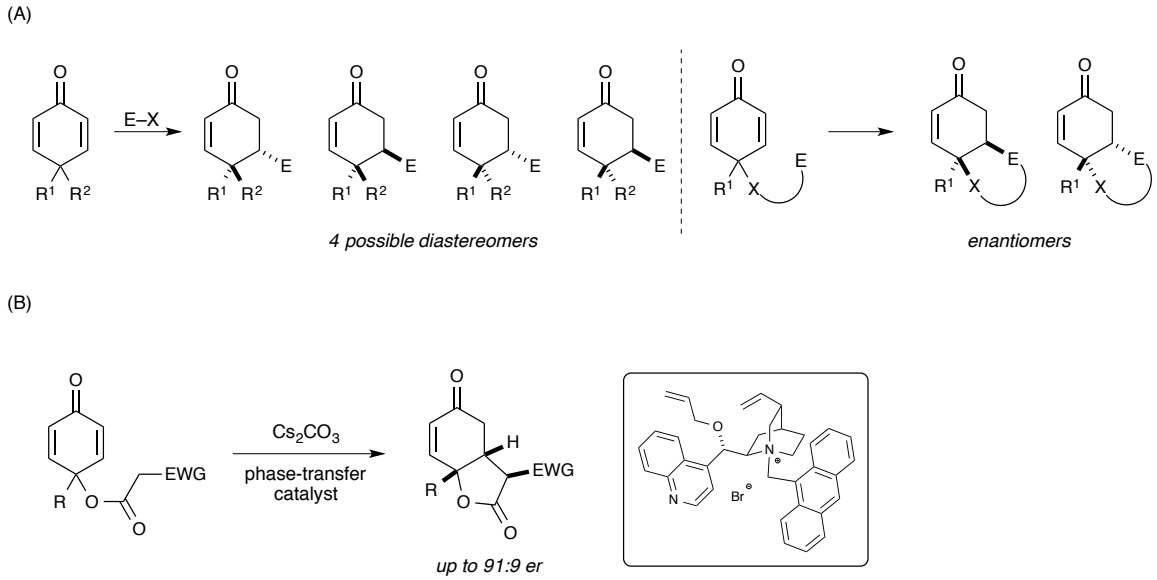

Figure 1.4. (A) Tethering the electrophile eliminates the possibility of diastereomers. (B) Desymmetrization with a phase-transfer catalyst produces enantioenriched bicyclic lactone.

1.2.2. Application to Natural Product Synthesis

In 2005, Bringmann and co-workers reported the isolation and structure determination of sorbicillactone A and B (Figure 1.6).[24] These molecules belong to a larger family of similar structures called the sorbicillinoids. We became interested in sorbicillactone A for a number of reasons: (1) it had a unique molecular structure that we considered to be a worthy target for a total synthesis, (2) we could showcase our methodology, and (3) it had interesting biological activity.

Our goal was not to merely synthesize the natural product: we desired to develop methodology that would be useful for the construction of numerous complex molecules. In addition, the bioactivity was important to us in order for a

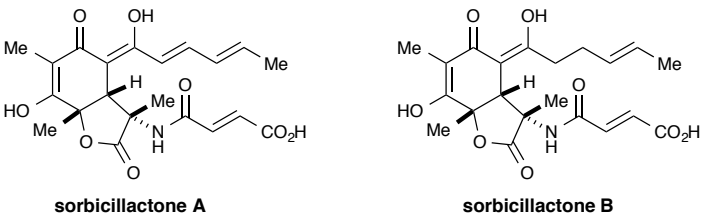

Figure 1.5. Structures of sorbicillactone A and B.

total synthesis to be warranted; an intriguing aspect of the molecular structure of sorbicillactone A was the opportunity to synthesize analogs that could be used for further biological studies. The core skeleton has several useful handles that could be derivatized easily, providing access to structurally diverse analogs. More detail on the sorbicillactones in regards to isolation, biological activity, and proposed biosynthesis can be found in Chapter 2.

We envisioned utilizing enantioselective dearomatization as a strategy for the synthesis of sorbicillactone A (Figure 1.6). Alternatively, asymmetric desymmetrization could also be used to synthesize variations of sorbiciallactone A. These methods also offered unique opportunity for developing scaffolds to synthesize a variety of analogs for use in structure-activity relationship (SAR) studies, bioassays, and target-oriented synthesis. In addition to sorbicillactone A, there are a variety of other natural products our methodology could be applied to.

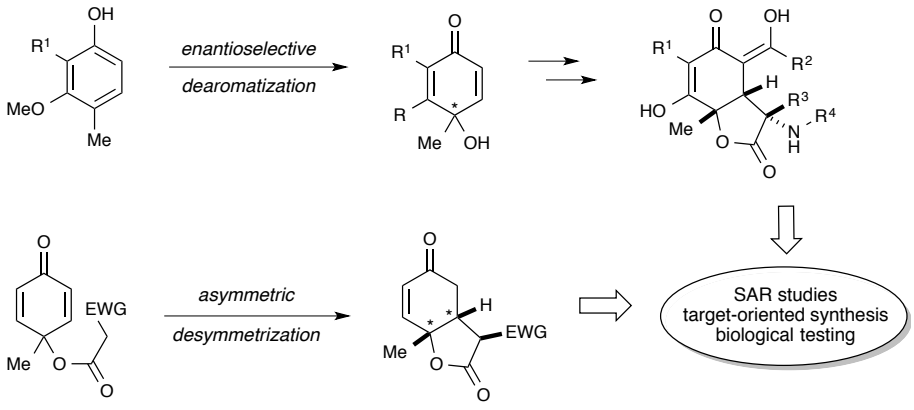

Figure 1.6. Application of our methodology development for the synthesis of natural products and related analogs.

CHAPTER 2

THE SORBICILLINOID FAMILY OF NATURAL PRODUCTS: ISOLATION, BIOSYNTHESIS, AND SYNTHETIC STUDIES§

2.1 INTRODUCTION

In 1948, Cram and Tishler of Merck & Co., Inc. reported the isolation[25] and structure elucidation[26] of several compounds from *Penicillium notatum*. One of these compounds was christened "sorbicillin" and was determined to have the structure represented by **2.1**.[27] The reisolation of sorbicillin would be reported by Japanese workers in 1953.[28] For several decades this remained the only example of a hexaketide in which the cyclization had taken place on the carboxylate terminus.[29] In 1981, Dreiding and co-workers reported the isolation of sorbicillin from *Verticillium intertextum*.[30] In addition, they were able to characterize several other compounds that were structurally related. Over the years, many more members of the family have been isolated from fungal strains collected around the world and from numerous different environments.

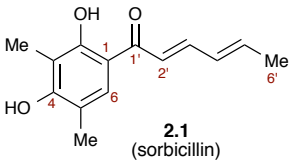

2.1 (sorbicillin)

§ This chapter is part of a more comprehensive review: Harned, A. M.; Volp, K. A. The sorbicillinoid family of natural products: Isolation, biosynthesis, and synthetic studies. *Nat. Prod. Rep.* **2011**, *28*, 1790–1810.

Many of these compounds possess elaborate bicyclic and tricyclic ring systems that, in a very general sense, appear to arise from the oxidative dearomatization and subsequent dimerization of sorbicillin. The presence of the C1′–C6′ sorbyl sidechain is another structural feature that is characteristic of this family. Recognizing this structural similarity and finding that an "official" name had yet to be bestowed on the family, Nicolaou proposed the name "bisorbicillinoids".[31] In practice, a broader term is necessary since many family members are not dimers. Hence, the term "sorbicillinoid" has come to encompass the family as a whole and generally refers to any compound that, at least to a first approximation, contains the carbon skeleton of sorbicillin.

The purpose of this chapter is threefold. First, some of the various sorbicillinoid structures that have been isolated will be introduced and the biological activities briefly discussed. Second, biosynthetic studies that have been put forth will be discussed. And last, the various efforts to synthesize these compounds will be examined.

2.2 ISOLATION AND STRUCTURAL STUDIES

This section will provide a brief survey of the different sorbicillinoids that have been isolated. The structures have been divided into subfamilies corresponding to common structural features. It should be noted that several tautomeric forms of the different structures are possible.[32]

2.2.1. Monomeric sorbicillinoids

Only a handful of monomeric sorbicillinoids have been isolated with an intact sorbicillin skeleton. Crews and co-workers isolated epoxysorbicillinol (**2.2**) from a sponge-derived strain of *Trichoderma longibrachiatum*.[33] A different *Trichoderma* sp. strain was the first source of oxosorbicillinol (**2.3**),[34] which has since been isolated from two other *Penicillium* sp.[35,36] Though Dreiding and co-workers first proposed the intermediacy of quinol **2.4** to explain the formation of the bisorbicillinoids,[30] it would be another 20 years (2000) before the presence of this elusive intermediate would be

detected. In conjunction with their efforts aimed at elucidating the biosynthetic pathways responsible for the formation of the sorbicillinoids, Abe and co-workers were able to isolate small amounts of **2.4** and named it "sorbicillinol."[37] Not surprisingly, this compound was found to be highly reactive, which prevented its isolation in high purity. It is this reactivity that is responsible for the formation of the other members of the sorbicillinoid family.

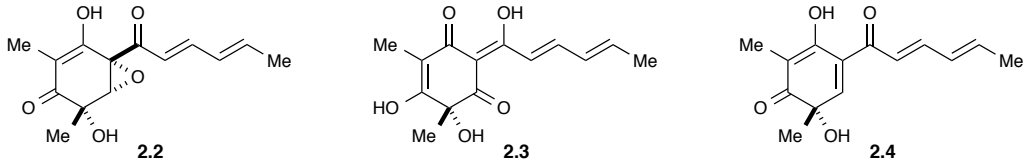

Figure 2.1. Structures of monomeric sorbicillinoids.

2.2.2. Dimeric sorbicillinoids

Only structures that appear to be the product of a reaction between two monomeric sorbicillinoids or a dimerization of a monomeric family member will be described in this section. Briefly, all of these structures can be rationalized by the dual reactivity of sorbicillinol (Figure 2.2). This reactivity leads to three main classes of bisorbicillinoids that can be grouped according to their connectivity. The bisvertinols have a fused [6.5.6] tricyclic core and are likely produced through a conjugate addition mechanism. The trichodimerols have a cage-like core that appears to be unique among secondary metabolites. The formation of these caged structures can be rationalized by invoking the tautomeric form of sorbicillinol (**2.4′**). There is also a group of compounds with a bicyclo[2.2.2]octanedione core that appears to be formed by a formal [4+2] cycloaddition.

As will be seen, many of the bisorbicillinoids have derivatives in which only one of the sorbicillin C2′-C3′ double bonds has been reduced. This particular modification is quite common and, as first discussed by Dreiding,[38] has important

implications about when and how the dimerization occurs with respect to sidechain modification.

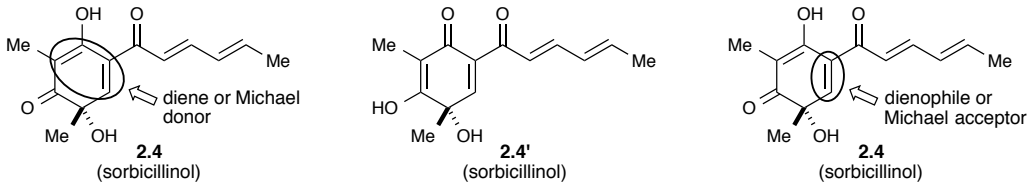

Figure 2.2 Structural features of sorbicillinol that account for the formation of the bisorbicillinoids.

2.2.2.a Bisvertinols

The first bisvertinols were reported by Dreiding and co-workers in 1986.[39] These compounds were isolated from *Verticillium intertextum* and were named bisvertinol (**2.5**), dihydrobisvertinol (11,12-dihydro), isodihydrobisvertinol (20,21-dihydro), and bisvertinolone (Figure 2.3).

The relative configuration of the bisvertinol stereocenters shown in **2.5** are those originally proposed by Dreiding.[39] It was assumed, correctly, that the stereocenters at C4 and C5a were conserved during biosynthesis. The configuration at C9a was suggested based on a biosynthetic proposal put forth at the time. Dreiding and co-workers did not attempt to assign the configuration of both C4a and C9b.

Several years later (1992), Ayer and co-workers isolated bisvertinol and bisvertinolone from *Trichoderma longibrachiatum*.[40] By performing NOE experiments on these compounds, they were able to propose revised structures for bisvertinol (**2.6**) and bisvertinolone (**2.9**), and by extension dihydrobisvertinol (**2.7**) and isodihydrobisvertinol (**2.8**).

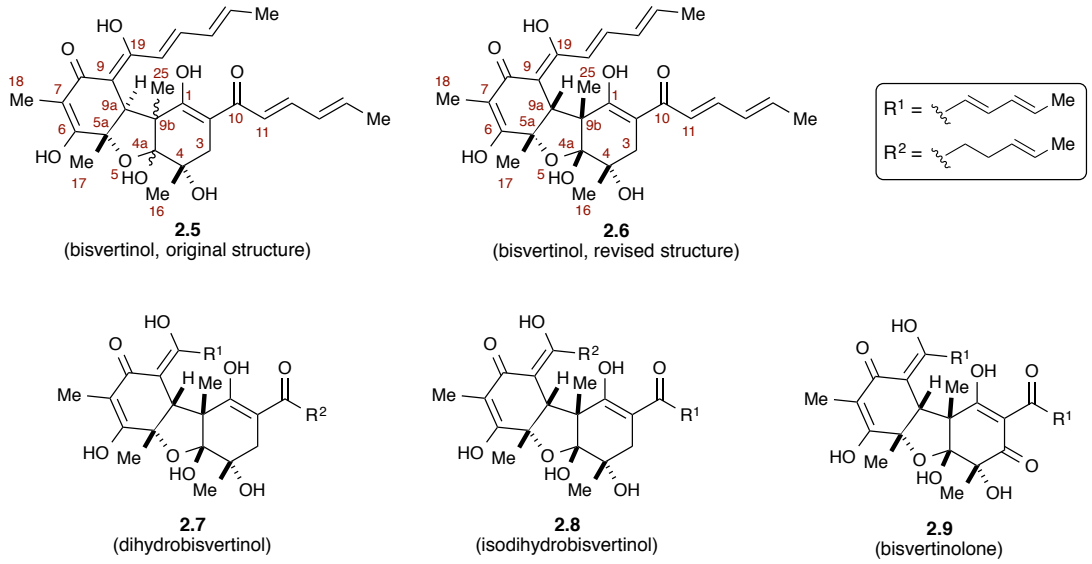

Figure 2.3. Structures of the bisvertinols.

2.2.2.b Trichodimerols

Though highly unusual, the cage-like core that is characteristic of the trichodimerols can be rationalized if one redraws bisvertinol as the structure represented by **2.6′** (Figure 2.4). The first report of trichodimerol (**2.10**) came from Ayer and co-workers (1992), who isolated it from *Trichoderma longibrachiatum*.[40] This compound was subsequently isolated from *Penicillium chrysogenum* by workers at Bristol-Myers Squibb,[41] who initially named it BMS-182123. X-ray crystallography confirmed that these two compounds were indeed the same.[42]

In the late 1990s, reports on the first derivatives of trichodimerol came from Abe and co-workers, who isolated demethyltrichodimerol (**2.11**)[43] and bisorbibetanone (**2.12**)[44] from a *Trichoderma* sp. strain that was cultured from a soil sample collected in Japan. In 2005, the isolation of trichodimerol and dihydrotrichodimerol (**2.13**) were reported independently by Lee and co-workers, from an "unidentified fungal strain" collected from a soil sample in Korea,[45] and by Gu and co-workers, from a marine-derived sample of *Penicillium terrestre*.[46] The latter group also reported the isolation of

tetrahydrotrichodimerol (**2.14**). In 2009 came a report by Evidente and co-workers on the isolation of trichodimerol and dihydrotrichodimerol from *Trichoderma citrinoviride*, collected from a soil sample in Austria.[47] Trichodimerol has also been isolated from a sponge-derived strain of *Trichoderma* sp.[48]

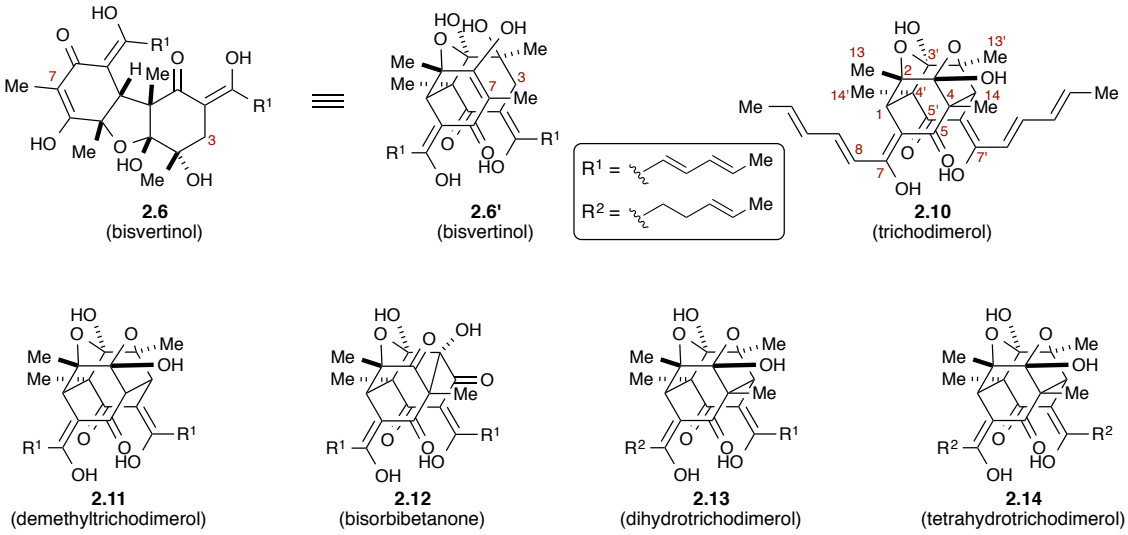

Figure 2.4 Structures of the trichodimerols and their relationship to the bisvertinols.

2.2.2.c Bridged bicyclic bisorbicillinoids

The formation of the bisvertinols and trichodimerols can be rationalized by the ability of sorbicillinol to serve as both a Michael acceptor and a Michael donor. However, sorbicillinol can also dimerize through a formal [4+2] cycloaddition. Such a reaction would produce compounds with a bicyclo[2.2.2]octanedione ring system. Indeed, this structural motif has been found in a number of bisorbicillinoid structures (Figure 2.5).

Dreiding and co-workers first reported the isolation of bisvertinoquinol (**2.15**) from *Verticillium intertextum* in 1981.[30] X-ray analysis[38] confirmed the unusual structure. In 1998, Abe and co-workers reported the isolation of bisorbicillinol (**2.16**)

from a *Trichoderma* sp.[43] in which both sorbyl chains are intact. Identifying the two sorbicillinol units in structures **2.15** and **2.16** is trivial.

However, there are also several compounds for which it is more difficult to account for one molecule of sorbicillinol. The butenolide-containing compound **22** was independently isolated from a *Trichoderma* sp. by three separate groups at approximately the same time. Consequently, it has been given three different names. Ayer and co-workers named **2.17** bislongiquinolide,[49] while Abe and co-workers deemed it bisorbibutenolide.[50] Finally, Satake and co-workers called it trichotetronine.[51]

Other groups have also isolated **2.17** from considerably different environments following these initial reports. Crews[33] and König[48] have isolated **2.17** from a sponge-derived *Trichoderma* species, while Evidente and co-workers isolated **2.17** from an Austrian source of *T. citrinoviride*.[47]

Abe and co-workers also isolated another related compound from *Trichoderma* sp: bisorbicillinolide (**2.18**)[50] in which the bicyclo[2.2.2]octanedione ring system appears to have undergone several bond reorganizations.

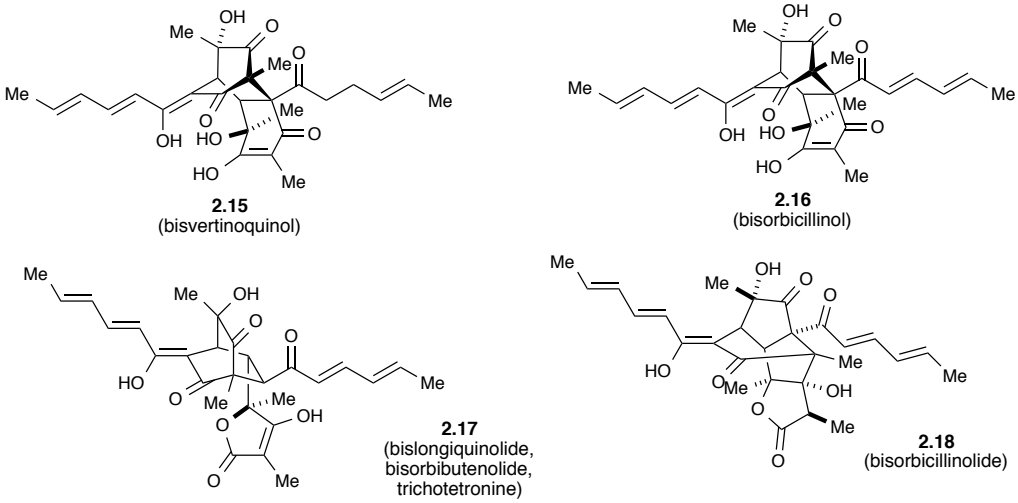

Figure 2.5. Bridged bisorbicillinoid structures.

2.2.3. Other Sorbicillinoids

2.2.3.d Nitrogen-containing sorbicillinoids

The incorporation of nitrogen into the sorbicillinoids is rare. The first examples came in 2005 with the isolation of sorbicillactone A (**2.19**) and B (**2.20**) by Bringmann and co-workers (Figure 2.6).[36] These compounds are produced by a *Penicillium chrysogenum* strain that was cultured from the Mediterranean sponge *Ircinia fasciculata*. In later work, the authors were able to develop a fermentation protocol for the large-scale production of sorbicillactone A.[52] While this protocol requires the use of HPLC to separate sorbicillactone A and B, it was sufficient to deliver 100 g of pure sorbicillactone A. As will be seen in Section 2.4.3, the amino acid alanine serves as the source for the nitrogen atom and C9–C11 of the sorbicillactones. Though such structures have yet to be reported, one might expect sorbicillactones derived from other amino acids to also exist.

To date, the only other nitrogen-containing sorbicillinoid that has been isolated is the unnamed urea **2.21**. This compound was isolated by Cabrera and co-workers from a cultured strain of *Paecilomyces marquandii* that was obtained from marine sediment collected at Miramar, Argentina.[53] A biosynthetic proposal to account for the formation of **2.21** was not provided by the authors.

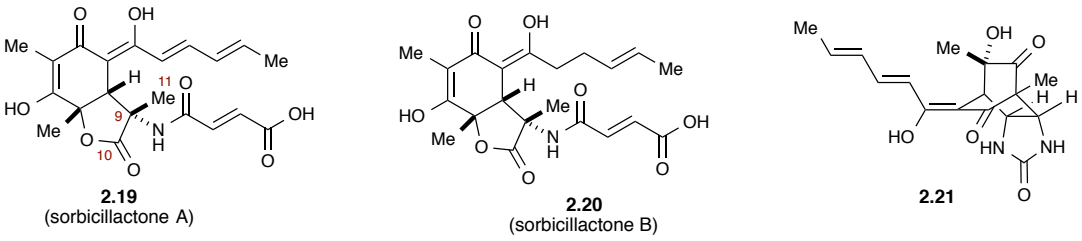

Figure 2.6. Structures of nitrogen-containing sorbicillinoids.

2.2.3.e Vertinolides

Though not immediately recognizable as such, the vertinolides can be considered to be a subfamily of the sorbicillinoids and have been isolated along with many of the compounds that have already been discussed. In addition to the discrete molecules discussed here, the tetronic acid moiety found in the vertinolides is also present in several of the bisorbicillinoid structures already presented.

Vertinolide (**2.22**) itself was first reported by Trifonov and co-workers in 1981, who isolated it from *Verticillium intertextum*.[30] It was later isolated from *Trichoderma* sp. by König[48] and Wright.[54] Dreiding was able to confirm the constitution of vertinolide through X-ray analysis,[55] but its absolute configuration remained unknown. Takaiwa and Yamashita were able to determine the natural configuration by synthesizing the tetrahydro derivative **2.23** from vertinolide and comparing the optical rotation to a sample of known configuration prepared independently.[56]

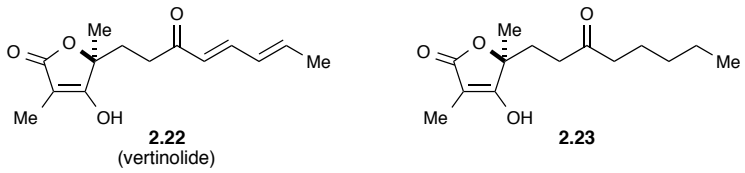

Figure 2.7. Vertinolide structures.

2.3 BIOLOGICAL ACTIVITY

The unique structural features of the sorbicillinoid family make them attractive candidates for developing new pharmaceutical agents. With this in mind, the aforementioned isolates have been screened in a number of different biological assays. This section will focus on the biological activity of the sorbicillactones and give a brief overview of the notable bioactivity of a few select sorbicillinoids.

2.3.1. Sorbicillactones

The sorbicillactones are two notable examples of sorbicillinoids with cell growth inhibitory activity. Bringmann and co-workers found that sorbicillactone A (**2.19**) has significant activity against the L5178y (murine leukemic lymphoblasts) cell line (IC_{50} = 2.2 μg/mL), but had much lower activity against the PC12 (rat adrenal pheochromocytoma), HeLa S3 (human cervix carcinoma), and H9 (human T lymphocytes) cell lines (all >10 μg/mL). However, sorbicillactone B (**2.20**) had IC_{50} values >10 μg/mL for all cell lines tested,[36] which highlights the importance of the intact sorbyl sidechain on anticancer activity.

Additionally, preincubation of neurons with 10 μg/mL sorbicillactone A blocked the effects of both serotonin and L-glutamic acid on calcium concentrations. This suggests that sorbicillactone A could serve as a possible neuroprotective agent for in vivo models.[36]

Finally, most interestingly, it inhibited expression of HIV-1 proteins in infected human stem cells in the concentration range of 0.3 and 3.0 μg/mL, which resulted in a decrease of reverse transcriptase activity. While the exact molecular target still needs to be established, it is known that the expression of viral proteins is inhibited in the presence of sorbicillactone A.[57] This is significant because to date, most prescription drugs on the market that inhibit reverse transcriptase are flat, aromatic structures, and overtime HIV-infected patients can become resistant to their therapeutic effects due to viral mutations.[58] Sorbicillactone A would offer an alternative to what is already on the market for these patients since it most likely has a different mode of binding to the HIV-1 proteins due to its unusual structure.

2.3.2. Radical-scavenging activity

Free radicals have been implicated as causative agents in several different disease states including atherosclerosis, arthritis, and cancer.[59] Identifying novel antioxidants to serve as free radical scavengers is important for developing new treatments for these conditions. Over a series of papers, Abe and co-workers have found that the unique structural features of the bisorbicillinoids make them effective scavengers of the 2,2-diphenyl-1-picrylhydrazyl (DPPH) radical. To date, the most active sorbicillinoid in this assay has been bisorbicillinol (**2.16**, ED_{50} = 31.4 μM).[43] By way of comparison, the known radical scavengers 2,6-di-*tert*-butyl-4-methylphenol (BHT) and α-tocopherol (vitamin E) have ED_{50} values of 27.0 and 22.0 μM, respectively, in this same assay.

2.3.3. Antimicrobial activity

In 1994 Kontani and co-workers reported evidence that suggested bisvertinolone (**2.9**) can function as a β-1,6-glucan biosynthesis inhibitor.[60] While a direct *in vitro* assay was not available at the time, they found that **2.9** induced morphological changes in the growing hyphae of *Phytophthora capsici*, a microbial organism that is pathogenic to plants. It also produced morphological changes in

Saccharomyces cerevisiae (a bacterium with a cell wall comprised of both β-1,6-glucans and β-1,3-glucans). However, it was inactive against *Acetobacter xylinum* (a Gram negative bacterium). Further investigations into this promising activity have yet to emerge.

2.3.4. Other biological activities

The sorbicillinoids have also been tested for biological activity in other areas. One of the more promising results was reported by workers at Bristol-Myers Squibb, who found trichodimerol (**2.10**) to be a potent inhibitor of tumor necrosis factor-α (TNF-α) production from macrophages (IC_{50} = 200 ng/mL) and blood monocytes (IC_{50} = 600 ng/mL).[41] Subsequent work at BMS revealed that the basis for this TNF-α inhibition was due to a diminution of prostaglandin synthesis. Specifically, trichodimerol targets prostaglandin H synthase-2.[61] TNF-α is a cytokine that serves a key role in the immune response and inflammation. Abnormal regulation of TNF-α has been implicated in several diseases: depression, Alzheimer's disease, arthritis, and cancer.[62]

2.4 BIOSYNTHETIC STUDIES

One source of controversy surrounding the sorbicillinoids is related to their biosynthesis. In particular, there has been a significant debate regarding which compound is the biosynthetic precursor to the rest of the family: sorbicillin or sorbicillinol. As will be described in this section, much of this debate has initially been settled with the elegant feeding experiments conducted by Abe and co-workers. However, recent studies have shown this may no longer be the case. In this section we will describe ^{13}C feeding studies that were conducted in order to elucidate the various pathways and will introduce proposed biosynthetic routes that have not been examined experimentally. Finally, a brief synopsis of the new experimental findings will be given.

2.4.1. Original proposals and identification of sorbicillinol

The first hypotheses were put forth by Dreiding and co-workers,[30,38,39] who were the first to suggest the intermediacy of sorbicillinol (**2.4**). Their proposal, outlined in Scheme 2.1,[63] was based on the previous suggestion[29] that sorbicillin (**2.1**) is constructed from the methylated hexaketide **2.25** by cyclization on the carboxyl terminus. Dreiding was the first to suggest that sorbicillin was the key biosynthetic precursor to all of the compounds isolated up to that point. Dreiding and co-workers were also the first to propose that the bisorbicillinoids could arise by various transformations involving intermediates **2.26**, **2.27**, and **2.4**.[30,39] They envisioned this occurring by oxidation of **2.1** to give epoxide **2.26**. While direct evidence for this transformation was lacking, a similar oxidation had been proposed for the biosynthesis of penicillic acid from orsellinic acid.[64,65,66] A reductive opening of epoxide **2.26** would form alcohol **2.27**, which was postulated to be an early intermediate on the way to vertinolide (**2.22**). Alternatively, sorbicillinol (**2.4**) could be formed from epoxide **2.26** through a simple elimination process. Though not shown in Scheme 2.1, Dreiding and co-workers were also the first to propose that the bisorbicillinoids could arise by various transformations involving intermediates **2.26**, **2.27**, and **2.4**.[30,39] It should be noted that the authors recognized the possibility that sorbicillinol (**2.4**) could be formed from **2.25** without going through sorbicillin first, but preferred the route shown due to the lack of specific precedence to support another pathway.[30]

Scheme 2.1. Dreiding's biosynthetic hypothesis.

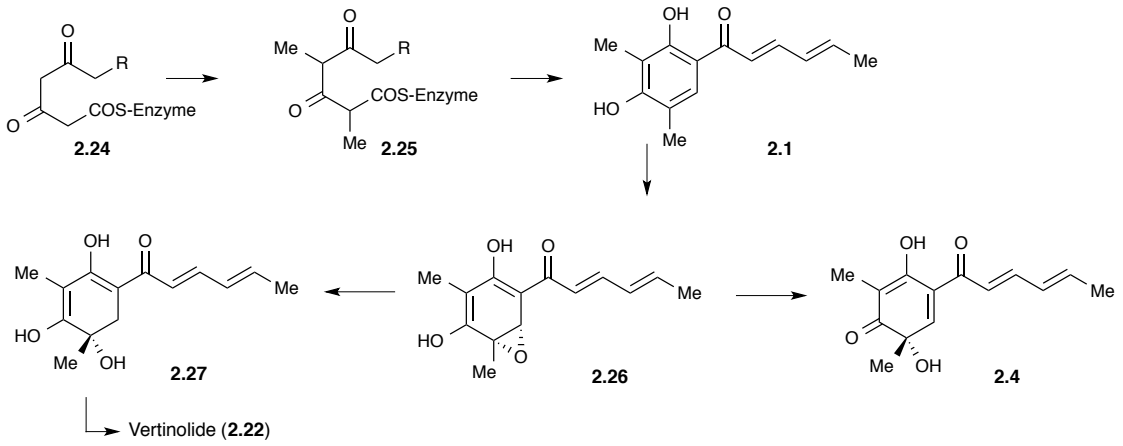

The intermediacy of sorbicillinol (**2.4**) would also serve as a launching point for several biomimetic syntheses, which will be described in the following section. A breakthrough came in 2000 with Abe's identification of sorbicillinol during HPLC analysis of the early stages of fermentation studies carried out with *Trichoderma* sp. USF-2690.[37,67] Not surprisingly, this metabolite was found to be quite reactive and could only be isolated as an aqueous solution in ~75% purity, which rapidly formed trichodimerol (**15**) upon extraction and solvent evaporation.

2.4.2. Biosynthesis of sorbicillinol

Having confirmed the existence of sorbicillinol (**2.4**), Abe and co-workers then embarked on a series of elegant studies to further elucidate the biosynthesis of this compound and other members of the family.[68,69,70,71] While all of their work was carried out with *Trichoderma* sp. USF-2690, one would expect the pathways to be similar in other organisms. By feeding fungal cultures [1,2-$^{13}C_2$] and [1-^{13}C] labeled sodium acetate, Abe was able to confirm the polyketide origin of sorbicillinol and establish the positions where ring closure, methylation, and oxidation had occurred. These same studies also established that sorbicillin is formed from sorbicillinol.

When [1-^{13}C] sodium acetate was fed to the culture, the $^{13}C\{H\}$-NMR spectrum of isolated labelled sorbicillinol[72] indicated that ^{13}C incorporation had occurred at C1,

C3, C5, C1′, C3′, and C5′ (Scheme 2.2). This observation firmly established the polyketide origin of this family of compound, presumably through hexaketide **2.28**. We have chosen to include the intact dienoyl sidechain in structure **2.28**. This was done under the assumption that the typical polyketide synthase machinery is operating in this case and that the ketoreductase and dehydratase enzymes are active while the two-carbon subunits are being added (the formation of the 2′-3′ dihydro sidechain would also require the action of enoylreductase). It is also safe to assume that *S*-adenosylmethionine serves as the methyl donor for the alkylation of C2 and C4. As will be described later, Bringmann and co-workers would confirm this hypothesis during their work on the biosynthesis of the sorbicillactones.

However, the intermediacy of **2.28** raises the question as to whether the oxidation of C2 was occurring after cyclization (as proposed by Drieding) or before cyclization. If the C2 oxidation occurs before cyclization (via path I, Scheme 2.2), one would expect the formation of intermediate **2.29**. Cyclization of **2.29** to form the C1–C6 bond would then give isotopomer **2.4*** directly.[73] On the other hand, if cyclization occurs first (via path II, Scheme 2.2), then compound **2.30** would be formed as the direct product of the cyclization. The symmetrical nature of intermediate **2.30** means that C2 and C4 are equivalent and, consequently, that the oxidation at these two positions are equally likely. As such one should expect that the oxidation of **2.30** would lead to the formation of *both* isotopomeric products **2.4*** and **2.4****.

Scheme 2.2 Abe's labeling studies to deduce the biosynthetic origins of sorbicillinol.[73]

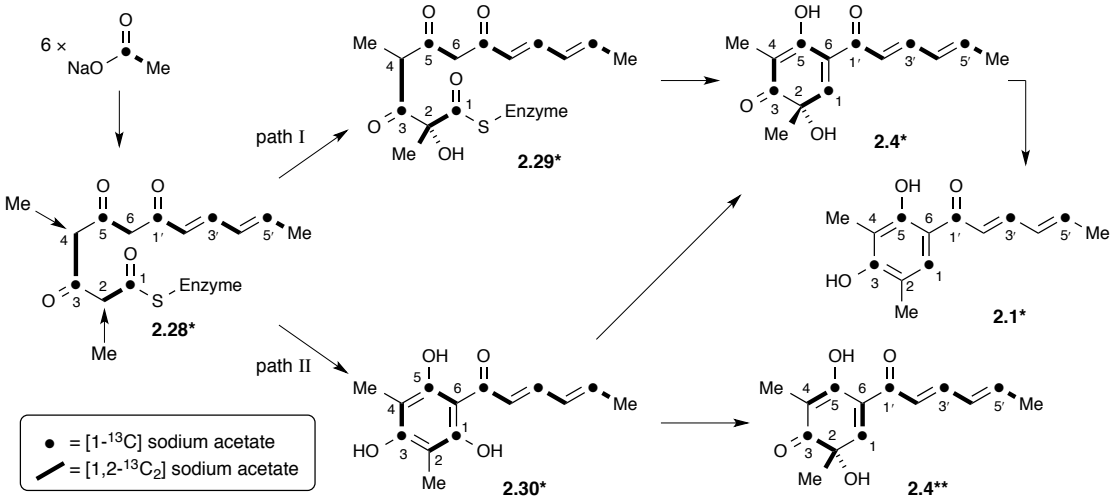

Abe and co-workers were able to answer this question by analysis of the one-bond ^{13}C-^{13}C coupling constants ($^{1}J_{C-C}$) observed in the $^{13}C\{H\}$-NMR spectrum and ^{13}C-^{13}C correlations observed in the INADEQUATE spectrum following feeding of [1,2-$^{13}C_2$] sodium acetate. This analysis revealed acetate incorporation into **4** at C1/C2, C3/C4, C5/C6, C1′/C2′, C3′/C4′, and C5′/C6′. Importantly, *only a single set of ^{13}C enhanced peaks were observed in isolated **2.4**.*[69] This isotope pattern indicates that the sorbicillinol formed was labelled as illustrated by **2.4*** and not **2.4****. Abe concluded that the only explanation consistent with these observations is if *the key oxidation of C2 occurs before cyclization (e.g., in **2.28**) and that sorbicillinol is formed through path I, and not through the intermediacy of **2.30** or, by extension, sorbicillin.*[69]

These results raise the question that sorbicillinol (**2.4**) is not only the direct precursor to the bisorbicillinoids, but could also give rise to sorbicillin (**2.1**). In an attempt to answer this question, isolated **2.4***, produced from [1-^{13}C] sodium acetate, was added to a separate fermentation medium. Abe found that when sorbicillin (**2.1**) was isolated from this batch, significant ^{13}C enrichment had occurred at C1, C3, C5, C1′, C3′, and C5′, as shown by **2.1***. This indicates that sorbicillinol (**2.4**) can indeed function as a precursor to sorbicillin.[69] However, this experiment does not rule out the possibility that **2.30** is being formed through path II and then continues on to sorbicillin

(**2.1**). It also does not completely eliminate the possibility of forming sorbicillinol (**2.4**) from sorbicillin (**2.1**) as proposed by Dreiding. A seemingly simple test for this would be to feed labeled sorbicillin to the fungal culture and look for downstream incorporation of the label. To the best of our knowledge, this experiment has not been reported.

2.4.3. Biosynthesis of the sorbicillactones

As previously mentioned, all of Abe's label studies were carried out using a single organism: *Trichoderma* sp. USF-2690. Fortunately, Bringmann and co-workers have confirmed much of Abe's work through studies aimed at determining the biosynthetic origins of the sorbicillactones, which were isolated from a sponge-derived *Penicillium chrysogenum* strain. As shown in Scheme 2.3, feeding experiments with sodium acetate revealed the same ^{13}C incorporation pattern into **2.19*** as was observed for **2.4***. No ^{13}C incorporation was observed at C9, C10, or C11. Bringmann was also able to confirm that methionine was the biogenetic source of the methyl groups attached to C3 and C5 by feeding [methyl-^{13}C]-L-methionine. While they were unable to specifically detect sorbicillinol itself, they were able to trap it by a cycloaddition with ethyl vinyl ether.[36]

As expected, when $^{13}C_3$-L-alanine was used, significant ^{13}C incorporation was observed at C9, C10, and C11. However, minor amounts were also observed in the sorbicillinoid portion of the molecule. This is likely due to partial metabolism of the alanine by the fungus to give acetyl CoA. When compared to the rest of the molecule, the fumarate sidechain in **2.19** showed weaker ^{13}C incorporation when ^{13}C-acetate or ^{13}C-alanine were used. The labeling also appeared to be non-symmetric, indicating that fumaric acid itself was likely not the biogenetic source of the amide sidechain. This was confirmed with the observation that no isotopic label occurred when [$^{13}C_4$]-fumaric acid was fed to the culture.[36] The identity of the C_4 unit used to form the fumarate chain remains unknown.

Scheme 2.3. Biosynthetic pathway toward the sorbicillactones. Sorbicillactone numbering used for **2.19**.

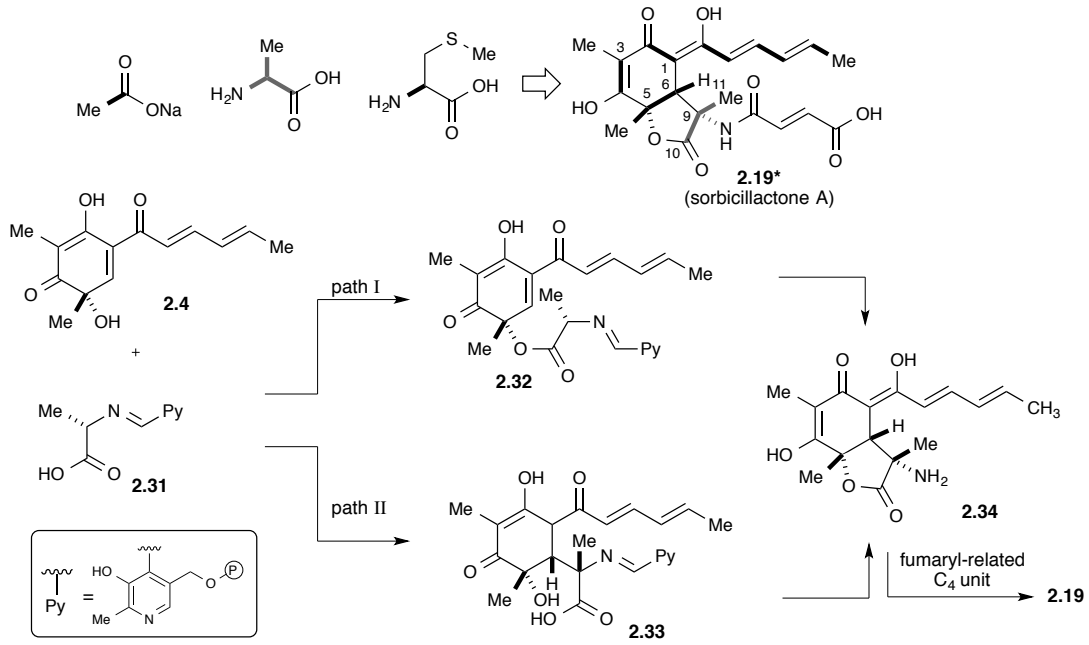

While the above labeling studies shed light on the identity of the building blocks needed for the sorbicillactones, exactly how the alanine is incorporated is still an open question. Two conceivable pathways were put forth by Bringmann and co-workers (Scheme 2.3).[36] The first (path I) involves esterification of sorbicillinol by alanine, which may be present as the pyridoxal phosphate-derived Schiff base **2.31**. This would give intermediate **2.32**, which would then undergo intramolecular Michael addition to give **2.34**. Alternatively, path II requires an initial intermolecular Michael reaction between Schiff base **2.31** and **2.4** in order to form **2.33**. A final lactonization would then be required to give amine **2.34**. Bringmann clearly favored path I, because cyclization of **2.32** would be expected to give **2.34** with the required configuration at C5 and C6.[36] However, path II cannot be discounted due to the so-called "*syn* oxygen phenomenon" in which nucleophiles will add to oxygenated cyclohexadienones from the same face as the oxygen atom.[74]

2.4.4. Biosynthesis of the bisorbicillinoids

There are also several biosynthetic proposals that have yet to be tested by feeding studies. These proposals are instructive when attempting to understand the reactivity of these interesting molecules and will help to guide further developments in this field.

Nicolaou31 and Corey[75] simultaneously recognized that the unusual caged structure characteristic of the trichodimerols contains two molecular equivalents of sorbicillinol. This led to the biosynthetic proposal outlined in Scheme 2.4. This proposal requires the two tautomeric forms of sorbicillinol (**2.4** and **2.4′**) to join together though a Michael reaction/ketalization sequence as depicted by **2.10A**. This results in the construction of the two red bonds highlighted in **2.10B**. A second, and presumably rapid, Michael reaction/ketalization reaction would then forge the remaining bonds needed for trichodimerol (**2.10**). Both Nicolaou and Corey would go on to confirm this hypothesis by carrying out a biomimetic synthesis of trichodimerol (Section 2.5.3).

Scheme 2.4. Proposed biosynthesis of trichodimerol.

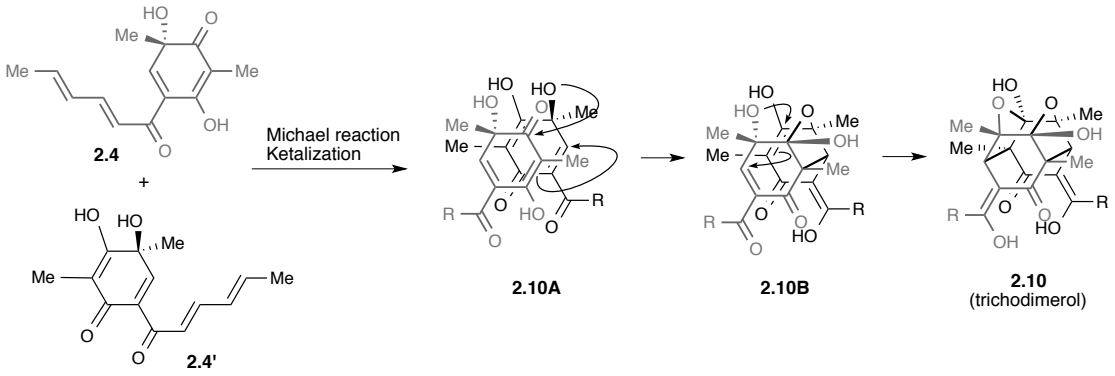

2.4.5. A Recent Report

Recently, new evidence has emerged that supports sorbicillinol arising from an oxidative dearomatization of sorbicillin.[76] The authors had successfully isolated and identified the gene responsible for the enzyme (*sorbC*) from *Penicillium chrysogenum*

E01-10/3, the strain that produces the sorbicillactones. Expressing the protein and incubating it with sorbicillin in the presence of NADPH and a phosphate buffer provided sorbicillinol, which was trapped as the bis-acetate upon treatment with acetic anhydride. A revised biosynthetic proposal was put forth based on their new findings. The authors agree that polyketide **2.28** is formed by acetate followed by methylation, but instead of an oxidative hydroxylation and subsequent ring closure proposed previously (see Section 2.4.2), that a reductive release occurs, giving aldehyde **2.35**. This aldehyde is then poised to undergo Knoevenagel cyclization to afford sorbicillin (**2.1**), which is then oxidatively dearomatized by *sorbC* to give sorbicillinol (**2.4**). They note that these findings are consistent with the data provided by previous studies, that their proposal is simpler, as well as comparable to the biosynthesis of a number of other fungal secondary metabolites.[77]

Scheme 2.5. New biosynthetic proposal for the formation of sorbicillinol.

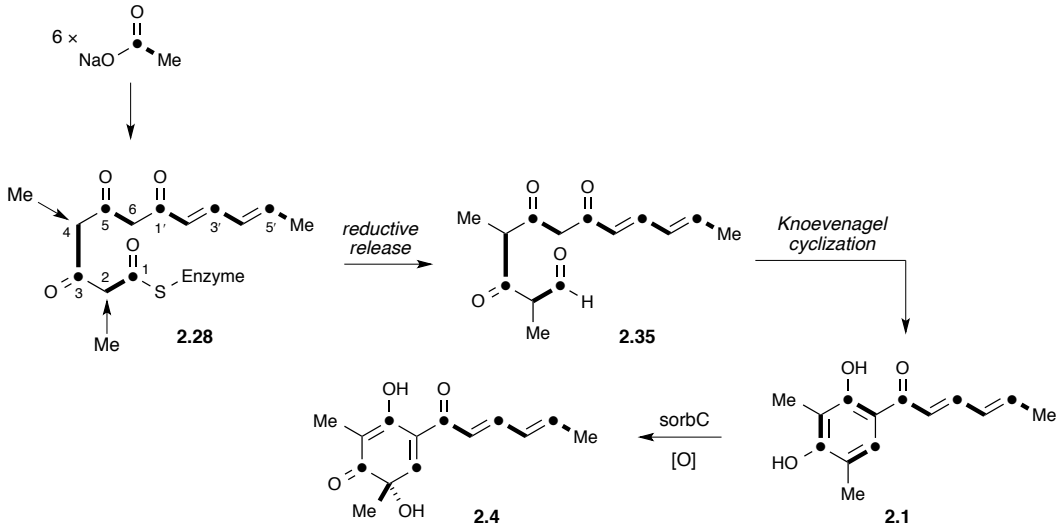

2.5 SYNTHETIC STUDIES

The synthetic community has shown a healthy interest in the sorbicillinoids. Much of this interest stems from the unusual structures present throughout the family, as well as a drive to further the study of their biological activity. In this section, we aim

to give an overview of the synthetic work that has been completed with the hope that this discussion will continue to spur synthetic work with these molecules.

2.5.1. Sorbicillin

Kuhn and Staab reported the first synthesis of sorbicillin in 1954 (Scheme 2.6A). Conversion of 2,4-dimethylresorcinol (**2.36**) to chloroacetophenone **2.37** allowed them to perform a Reformatsky reaction with crotonaldehyde, which resulted in the isolation of clavatol (2,4-dihydroxy-3,5-dimethylacetophenone) as the major product and trace amounts (0.26%) of sorbicillin (**2.1**).[78] McOmie and Tute were able to improve on these results by performing a BF_3-mediated Friedel-Crafts reaction between **2.36** and sorbic acid. This afforded the boron complex **2.38**, which liberated sorbicillin in 33% yield when heated in aqueous methanol (Scheme 2.6B).[79] Nicolaou and co-workers further improved this method by employing THF as a solvent instead of methanol. This prevented the formation of the Michael addition products that were originally observed.[80] In this manner, they were able to isolate the desired product in yields up to 80%. This method was also more convenient on multigram scale then that of Sartori and co-workers, who utilized anionic conditions to install the sorbyl sidechain (**2.40a**, Scheme 15C).[81] However, the latter method proved to be a convenient route for the synthesis of sorbicillin analogs (**2.40b-c**).

Scheme 2.6. (A) Kuhn and Staab's synthesis of sorbicillin. *Reagents and conditions:* (a) Zn, crotonaldehyde, 0.26%; (B) McOmie and M. S. Tute's synthesis. *Reagents and conditions:* (a) sorbic acid, 45% BF_3•OEt_2, then heating in MeOH/H_2O, 33%; (C) Sartori's synthesis. *Reagents and conditions:* (a) EtMgBr, ether, rt (b) RCOCl, toluene, 25 °C, 75%.

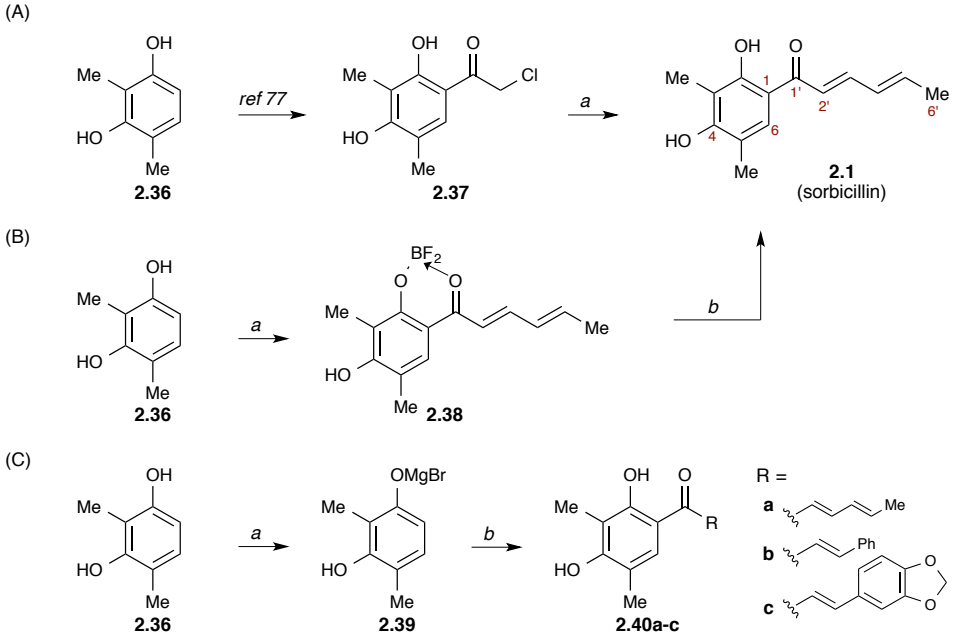

2.5.2. Epoxysorbicillinol

To date, there have only been two racemic syntheses of epoxysorbicillinol reported. These were simultaneously published in 2001 by the Pettus (Scheme 2.7)[82] and Wood (Scheme 2.8)[83] groups.

Pettus and co-workers began their route with an oxidative dearomatization of sorbicillin derivative **2.41**, which contained a tethered amide**.** By using two equivalents of PIFA they not only accomplished the oxidative dearomatization of phenol **2.41**, but the epoxidation of the resulting cyclohexadienone also occurred. In this manner, epoxide **2.42** was obtained in 40% yield as a single diastereomer. All that remained was to hydrolyze and dealkylate the vinylogous ester to free the quinol; however this proved to be much more difficult than anticipated. Eventually, it was discovered that conversion of the lactone to amide **2.43** could be achieved using a protocol developed

by Weinreb.[84] This was then followed by a $SnCl_4$-mediated dealkylation of the vinylogous ester to give (±)-epoxysorbicillinol (**2.2**) in 72% yield over the two steps.

Scheme 2.7 Pettus' synthesis of (±)-epoxysorbicillinol. *Reagents and conditions:* (a) 2.2 equiv $PhI(O_2CCF3)_2$, CH_2Cl_2/CH_3NO_2 (3:1), 40%; (b) dimethylaluminum amide, CH_2Cl_2, 90%; (c) $SnCl_4$, CH_2Cl_2, 80%.

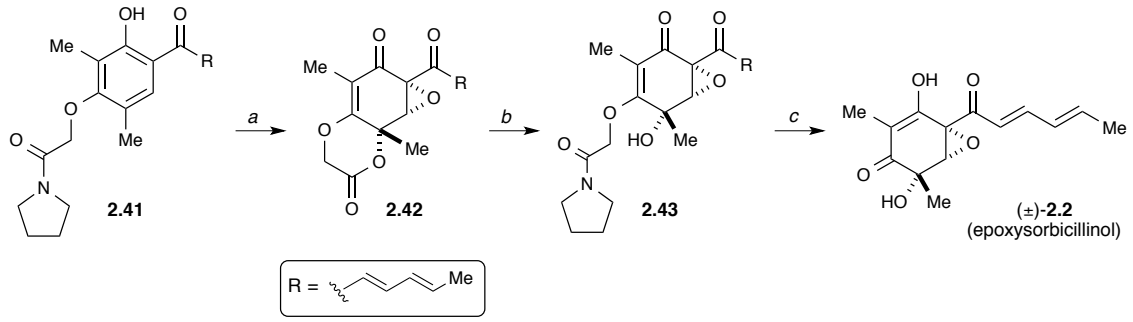

Wood and co-workers took a much different approach with their synthesis of epoxysorbicillinol. Their strategy was to utilize a rhodium-catalyzed 1,3-dipolar cyclization as the key reaction (Scheme 2.8). They also decided to delay the installation of the sorbyl chain in order to prevent polymerization issues. They were also concerned about facile rearomatization of the quinol intermediate. Ultimately, adjustments had to be made to their synthetic plan in order to address these issues. Beginning with diethyl malonate **2.44**, the construction of diazoketone **2.45** could be achieved in five steps. A rhodium-catalyzed 1,3-dipolar cycloaddition between **2.45** and allyl propiolate (**2.46**) afforded oxabicycle **2.47** in 73% yield. In three straightforward steps, **2.47** was converted to ketone **2.48** with an overall yield of 41%. Key intermediate **2.49** was generated as a single diastereomer through a TFA induced ring opening, followed by nucleophilic epoxidation. The endgame involved decarboalkoxylation using an excess of TFA to give **2.50** and oxidation of the side chain with DDQ to give epoxysorbicillinol. The presence of the epoxide was enough to prevent rearomatization of the quinol during the acid-promoted ring opening.

Scheme 2.8 Wood's synthesis of (±)-epoxysorbicillinol. *Reagents and conditions:* (a) $Rh_2(OAc)_4$, **2.46**, toluene, 60 °C, 73%; (b) 1.5 equiv TFA; (c) *t*-BuOOH, DBU, 62%; (d) TFA, 81%; (e) DDQ, toluene, reflux, 40%.

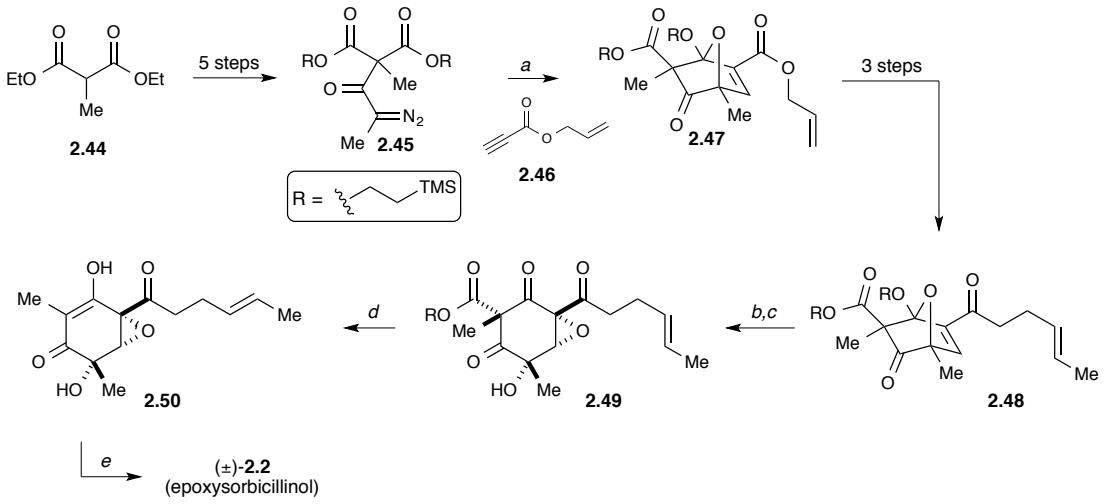

2.5.3. Bisorbicillinoids and related compounds

Trichodimerol has arguably been one of the most desired bisorbicillinoid targets because of its unique biological activity and interesting cage-like structure. Barnes-Seeman and Corey[75] were the first to complete a total synthesis of trichodimerol, with Nicolaou and his group reporting their syntheses of trichodimerol and related compounds shortly thereafter.[80]

Both groups synthesized trichodimerol in just two steps from sorbicillin (Scheme 2.9A). Treating sorbicillin with $Pb(OAc)_4$ gave the isomeric products **2.51** and **2.52** in a 1:5 ratio, favoring the desired product **2.52**. Acetate **2.52** was resolved by chiral HPLC to obtain the natural enantiomer (*S*)-**2.52**. When Corey subjected acetate (*S*)-**2.52** to 10 equiv of NaOMe in MeOH, followed by neutralization with $NaH_2PO_4 \bullet H_2O$, trichodimerol (**2.10**) was produced in a 10% yield after purification (Scheme 2.9B). Nicolaou and his group arrived at trichodimerol with nearly the same sequence, except with slightly different reagent choices and procedures. Through much trial and error, they learned that the workup procedure greatly affected the outcome of the reaction and isolated products. By treating (*S*)-**2.52** with $CsOH \bullet H_2O$ in MeOH for 7

hours, followed by an extremely careful neutralization with $NaH_2PO_4 \bullet H_2O$ and stirring at 25 °C for 12 hours, trichodimerol (**2.10**) was produced in a 16% yield along with bisorbicillinol (**2.16**, 22% yield) and sorbicillin (**2.1**, 12% yield). The presence of only a stoichiometric amount of H_2O was key to the success of this reaction, as it allowed for the formation of the needed quinolate under limited protic conditions.

However, if (*S*)-**2.52** was instead treated with 10 equiv of KOH in a 9:1 ratio of THF/H_2O at 0 °C, followed by 1 N HCl, bisorbicillinol (**2.16**) could be isolated as the only product in a 40% yield (or 12.1 N HCl in THF/H_2O (9:1) at 25 °C, 43% yield) (Scheme 2.9C). In order to confirm the biosynthetic relationship between bisorbicillinol (**2.16**) and bisorbibutenolide (**2.17**), compound **2.16** was treated with 1.1 equiv of KHMDS. This induced a biomimetic anionic rearrangement and afforded **2.17** in 80% yield after acidic workup.

Scheme 2.9. (A) Corey's and Nicolaou's dearomatization of sorbicillin. *Reagents and conditions:* (a) Corey: 0.4 M $Pb(OAc)_4$ (1.2 equiv), $AcOH/CH_2Cl_2$ (5:1), 23 °C, 30 min, 35% **2.51**, 38% **2.52**; (b) Nicolaou: $Pb(OAc)_4$ (1.05 equiv), $AcOH/CH_2Cl_2$ (1:1), 0 °C, 30 min, ~5:1 **2.52**:**2.51**, 40%. (B) Synthesis of trichodimerol. *Reagents and conditions:* (a) Corey: NaOMe (10 equiv), MeOH; then $NaH_2PO_4 \bullet H_2O$, HCl/MeOH, 10%; (b) Nicolaou: $CsOH \bullet H_2O$ (10 equiv), MeOH, 25 °C, 7 h; then $NaH_2PO_4 \bullet H_2O$, 25 °C, 12 h, 16% **2.10**, 22% **2.16**, 12% **2.1**. (C) Nicolaou's synthesis of bisorbicillinol and bisorbibutenolide. *Reagents and conditions:* (c) KOH (10 equiv), THF/H_2O (9:1), 0 °C, 2 h; then 1 N HCl, 40%; (d) KHMDS (1.1 equiv), THF, 25 °C, 24 h; then aq 1 N HCl, 80%.

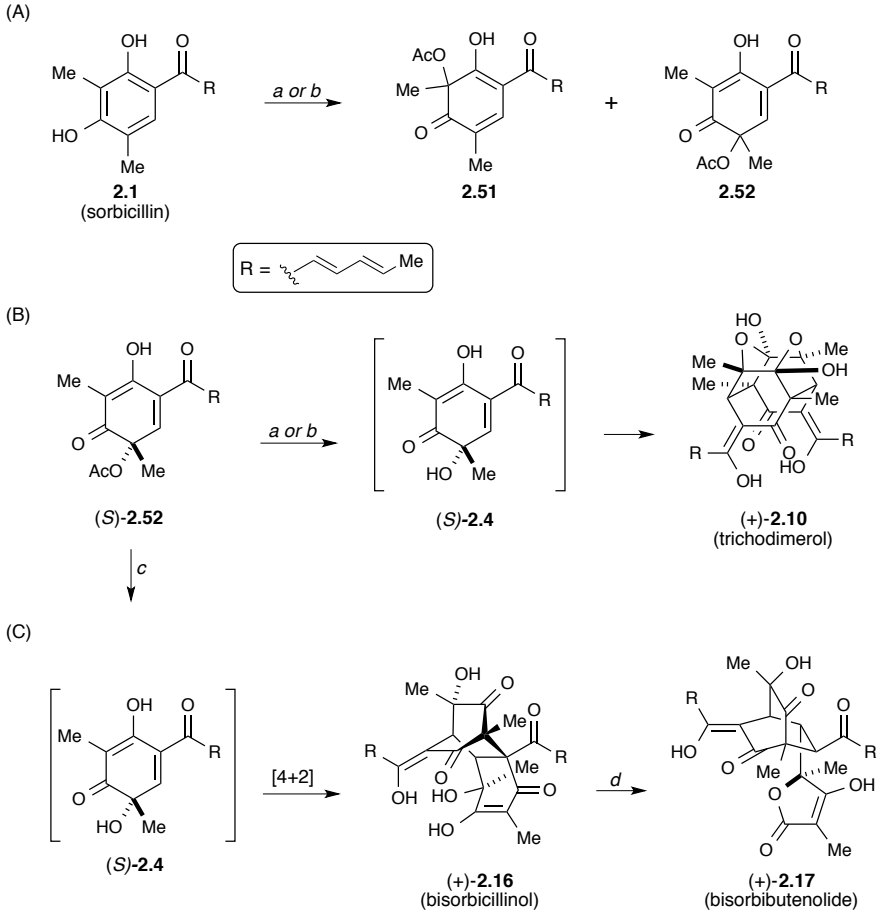

The Pettus group was also able to access bisorbicillinol during their studies on the synthesis of epoxysorbicillinol (Scheme 2.10A).[82] When they treated phenol **2.41** with just 1 equiv of $PhI(O_2CCF_3)_2$, they obtained dienone **2.53** in 45% yield. Subjecting **2.53** to concentrated HCl in THF produced what they hypothesized to be the mixed ketal intermediate **2.54**, which upon quenching with aqueous KOH, gave bisorbicillinol (**2.16**) in 83% yield.

In order to achieve an enantioselective synthesis of bisorbicillinol, asymmetry was introduced during the oxidative dearomatization and cyclization step (Scheme 2.10B). This was accomplished by installing a stereocenter on the amide tether (**2.55**). As a result, the cyclized product **2.56** was generated as a mixture of diastereomers. Carrying this mixture forward without separation gave (+)-**2.16** in a 30% overall yield and 51% ee after purification.

Scheme 2.10 Pettus' synthesis of bisorbicillinol. *Reagents and conditions:* (a) $PhI(O_2CCF_3)_2$ (1 equiv), CH_2Cl_2/CH_3CN (3:1), 45%; (b) HCl (8 equiv), THF (not isolated); (c) KOH (15 equiv), H_2O, 83%. B Pettus' asymmetric synthesis of bisorbicillinol. *Reagents and conditions:* (a) $PhI(O_2CCF_3)_2$ (1 equiv), CH_2Cl_2/CH_3CN (b) HCl (8 equiv), THF (not isolated); (c) KOH (15 equiv), H_2O, 30% overall, 51% *ee*.

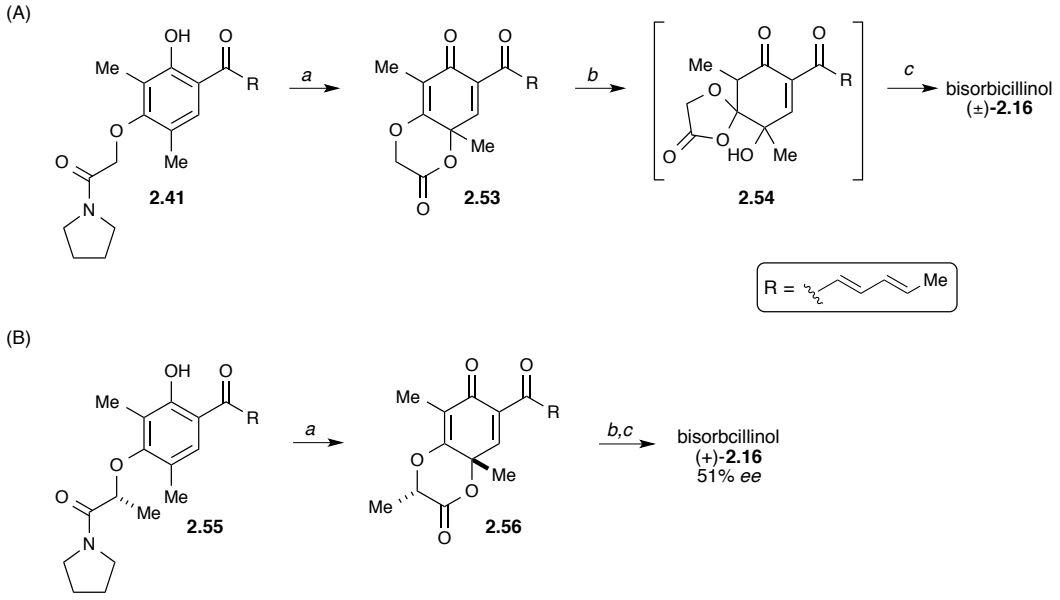

The Deng group was the first to succeed at synthesizing bisorbicillinolide (**2.18**), doing so in an enantioselective fashion (Scheme 2.11).[85] They employed a modified cinchona alkaloid catalyst to generate the enantioenriched starting material, which through a novel route was advanced to the chiral quinol. This intermediate allowed them to access both bisorbicillinol and bisorbibutenolide enantioselectively. Enantioselective cyanosilylation of ketone **2.57** produced multigram quantities of cyanohydrin (*R*)-**2.58** in quantitative yield and 92% ee. Four steps (Grignard reaction, alcohol protection, Wittig reaction, acetal hydrolysis) advanced **2.58** to aldehyde **2.59**. This intermediate readily underwent Knoevenagel condensation with ketoester **2.60**.

Regioselective ozonolysis of the condensation product then afforded ynone **2.61** in 68% yield over the two steps. Isomerization of the ynone to the requisite sorbyl chain was accomplished using a modified Trost-Lu procedure.[86,87] The PMB-protected quinol was formed in 67% yield by a Dieckmann-type condensation in the presence of aqueous NaOH. Deprotection of the quinol with TFA produced sorbicillinol ((*S*)-**2.4**), which rapidly underwent [4+2] dimerization to give bisorbicillinol ((+)-**2.16**) in 54% yield. Simply allowing (+)-**2.16** to stand in MeOH for 48 hours furnished the rearranged product, bisorbicillinolide ((+)-**2.18**), in 64% yield along with 10% of recovered (+)-**2.16**. This completed the first total synthesis of (+)-**2.18** in 11 steps and an impressive 19% overall yield. Borrowing conditions from Nicolaou and co-workers, the Deng group converted bisorbicillinol ((+)-**2.16**) to bisorbibutenolide ((+)-**2.17**), completing an enantioselective synthesis of of this compound in 11 steps and 15% overall yield.

Scheme 2.11 Deng's synthesis of bisorbicillinol and bisorbicillinolide. *Reagents and conditions:* (a) TMSCN, $(DHQ)_2AQN$ (2 mol%), $CHCl_3$, 100%, 92% ee; (b) **2.60**, $TiCl_4$, NMM, THF, 93%; (c) O_3, pyridine, CH_2Cl_2, 99%; (d) $Pd(OAc)_2$ (cat.), *p*-tol_3P, benzene, 92%; (e) Ph_3COH, KH, THF, 90%; (f) TFA, CH_2Cl_2, 54%; (g) MeOH, rt, 48 h, 64% (+)-**2.18**, 10% (+)-**2.16**.

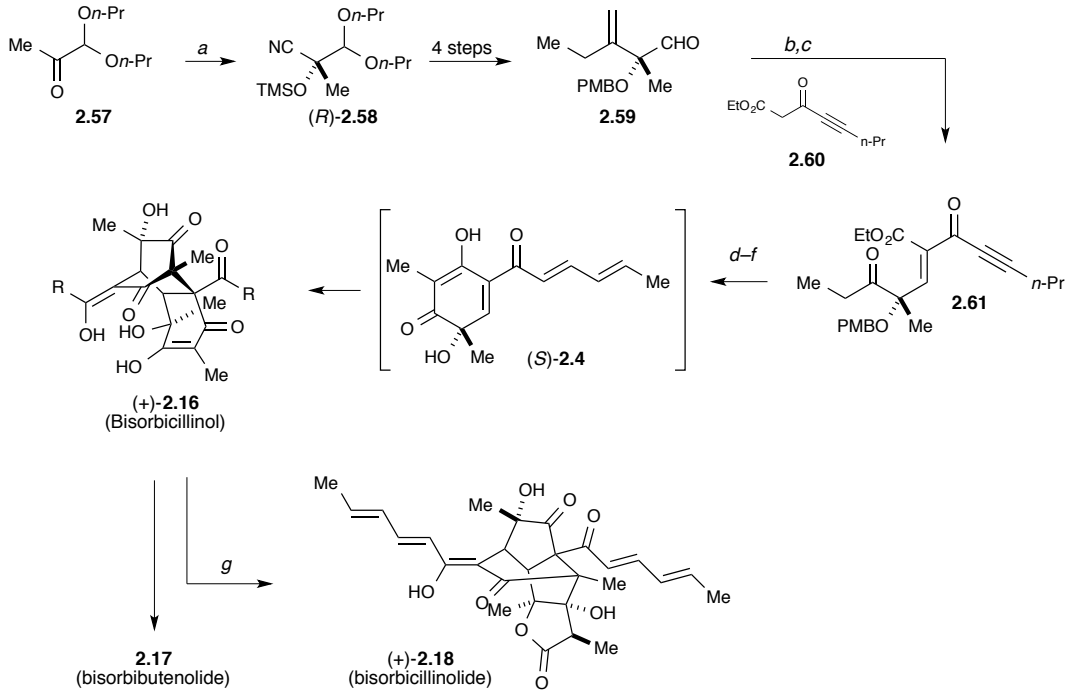

CHAPTER 3

TOTAL SYNTHESIS OF SORBICILLACTONE A AND 9-*EPI*-SORBICILLACTONE A

3.1 SYNTHETIC PROPOSAL

3.1.1. Retrosynthesis

The synthetic strategy that we devised for sorbicillactone A was motivated by several factors. We wanted to (1) showcase methodology that our group was developing by utilizing a cyclohexadienone as a key building block and (2) devise a synthesis in which a library of analogs could easily be obtained. Most previous sorbicillinoid syntheses have started with oxidation of sorbicillin; however, this approach does not allow variation of the C1′ side chain, which we were very interested in investigating due to the profound difference in biological activity between sorbicillactone A and sorbicillactone B.[88] The most convergent synthesis would be one where the side chains are installed in the final steps; therefore, **3.2** would be our key building block (Scheme 3.1). This bicyclic intermediate would arise from an intramolecular conjugate addition (Michael addition) of tethered cyclohexadienone **3.3** equipped with an activating group (Z). A coupling of quinol **3.4** and the tether provides **3.3**. Lastly, the quinol would be afforded through an oxidative dearomatization of the corresponding phenol **3.5**.

Scheme 3.1. Retrosynthetic analysis of sorbicillactone A.

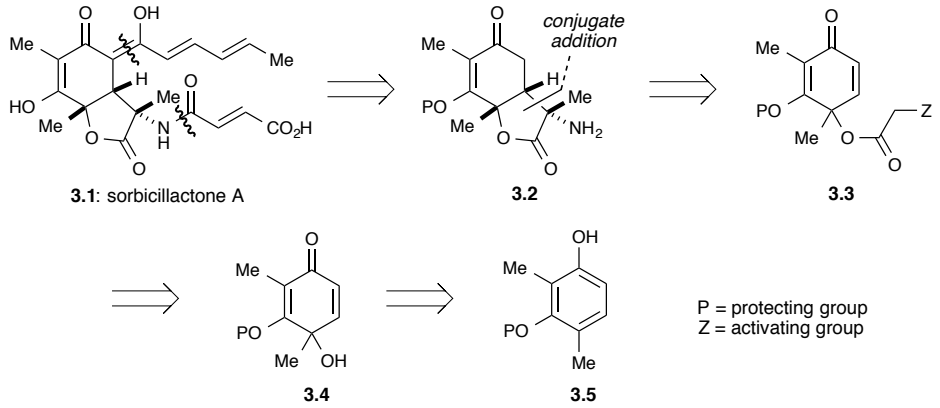

3.1.2. Library Development

Our synthetic plans for the total synthesis of sorbicillactone A allows for facile derivatization to generate useful analogs for further biological testing and SAR studies. This would give insight to the mechanism of action that sorbicillactone has as an anti-retroviral drug therapy. Sorbicillactone A has several key points of diversification. Due to the lack of bioactivity of sorbicillactone B, it is clear that the sorbyl chain has a profound effect; therefore we want to probe this further by synthesizing analogs at the C1′ sidechain. Another point of diversification is at the C1″ sidechain. By varying the acylating reagents used, substrates differing at C1′ and C1″ can be obtained (Figure 3.1). We are specifically interested in changing the size and electronics of these sidechains, in addition to changing the number of unsaturations.

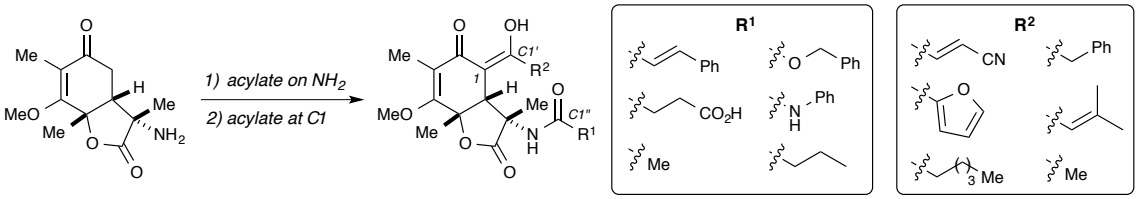

Figure 3.1. Library analogs derivatized at C1′ and C1″.

Additionally, sulfonamide derivatives can be generated by *N*-sulfonylation (Figure 3.2). Sulfonamides are an important class of pharmacophores that are found in nearly 200 drugs currently on the market. The presence of a sulfonamide can increase pharmacologic potency as well as alter the absorption, distribution, metabolism, and excretion of the molecule.[89]

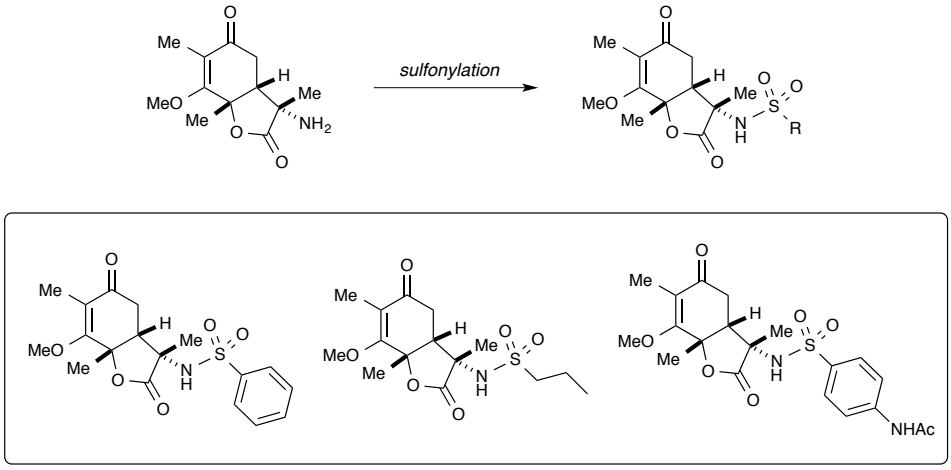

Figure 3.2. Library synthesis of sulfonamide derivatives.

Finally, because we plan to install the C11 methyl group via electrophilic substitution, one can imagine a variety of different electrophiles being added to vary the substituent at C9, which is representative of employing various amino acids in a biomimetic synthesis (Figure 3.3).

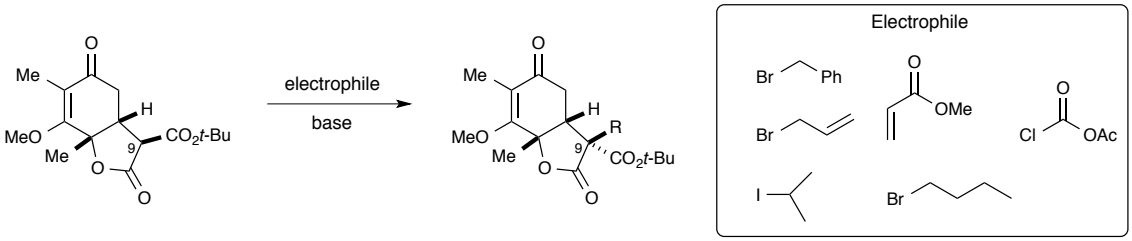

Figure 3.3. Employing various electrophiles will generate analogs at C9.

3.2 INITIAL STUDIES WITH A MODEL SUBSTRATE

Our initial studies to elaborate the cyclohexadienone were conducted with a model substrate that was accessible in one step from commercially available *p*-cresol. Using *p*-cresol as the model substrate would save several synthetic steps and allow the details for the remaining steps to be optimized, which could then be applied to the sorbicillactone substrate.

3.2.1. Synthesis of the Bicyclic Lactone

Cyclohexadienone **3.6** was synthesized by treating *p*-cresol with Oxone and $NaHCO_3$ to give the *p*-quinol after a mild reductive workup of the resulting peroxide with $Na_2S_2O_3$ (Scheme 3.2).[90] This reaction was easy to conduct and its use of mild reagents made it an attractive method to synthesize *p*-quinols. The product was usually sufficiently pure, avoiding the need for further purification by column chromatography. However, the reaction also had several drawbacks. First, the scale at which the reaction could be executed was severely limited; a closed vessel was required for complete conversion due to the production of singlet oxygen from the reaction of Oxone and $NaHCO_3$. This meant only a few hundred milligrams could be synthesized at a time. Second, the yields varied drastically (30–75%) each time the reaction was performed, with an average obtained yield of ~45%.

Scheme 3.2. Synthesis of *p*-quinol **3.6** using an Oxone-mediated singlet-oxygen oxidation.

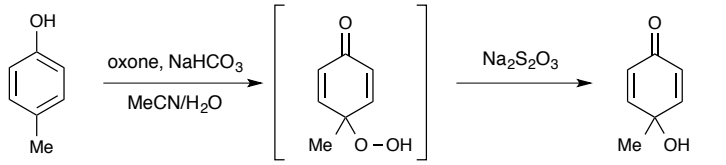

With the *p*-quinol in hand, the next step was the synthesis of the lactone ring. We were initially interested in conditions reported by Nicolaou and co-workers in their syntheses of bisorbicillinoid compounds.[91] When they treated acetate **3.7** with 3 equiv

of KHMDS at –78 °C, an intramolecular Michael-addition occurred to give the bicyclic lactone **3.8** (Scheme 3.3A). They noted that the use of LiHMDS only gave the enolate, which did not undergo intramolecular cyclization. They also found that the addition of various Lewis acids to the reaction, such as TBSOTf, only led to rearomatization. We decided to test these conditions with dienone **3.9**, which was synthesized easily from *p*-cresol with phenyliodine diacetate (PIDA) and acetic acid (Scheme 3.3B). We did observe consumption of the starting material, but there was unfortunately no evidence of the cyclized product.

Scheme 3.3. (A) Nicolaou's synthesis of the bicyclic lactone using an intramolecular Michael addition of an acetoxy dienone. (B) Failed cyclization of our substrate.

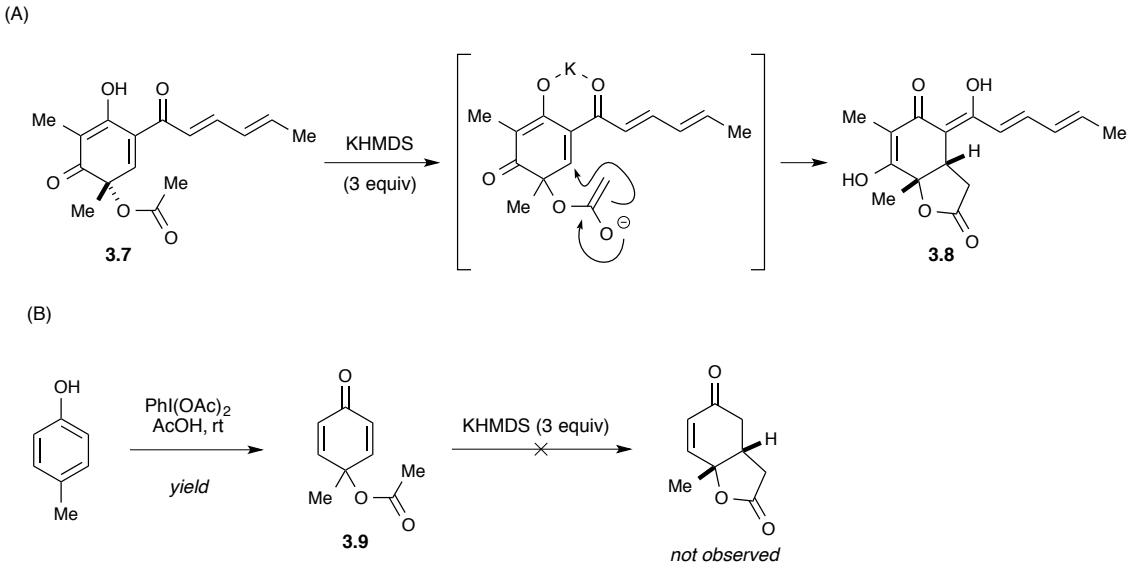

Previous studies have indicated that cyclohexadienones are sensitive to strong bases due to their propensity to rearomatize.[92] In Nicolaou's case, the highly electron deficient Michael acceptor may have mitigated this problem. We recognized that our system would be restricted to a mild base; therefore, an activating group tethered to the quinol was essential (Scheme 3.4). The activating group would also need to serve as a handle for the amide installation after formation of the lactone ring. We sought to unearth a functional group that would meet both of these criteria.

Scheme 3.4. Synthetic plan for an activating group to induce cyclization and function as a handle for amide bond formation.

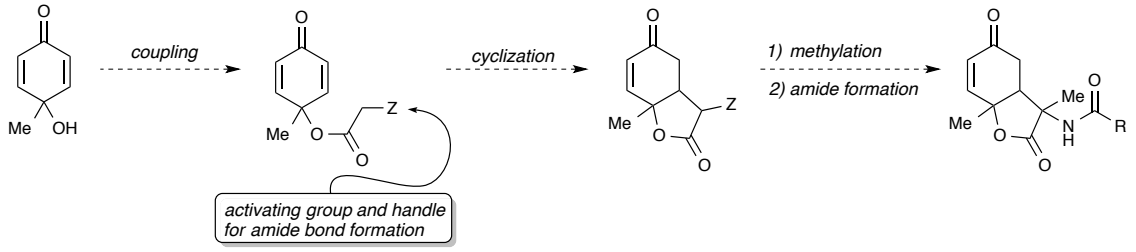

We first explored the use of an azide as our activating group, which could then be converted to the amine via a Staudinger reduction. Unfortunately, not only was the synthesis of the α-azido acetic acid difficult (as well as dangerous),[93] neither DCC coupling nor acylation with the acid chloride produced the tethered dienone (Scheme 3.5).

Scheme 3.5. Attempts at tethering an α-azido acetate to the *p*-quinol.

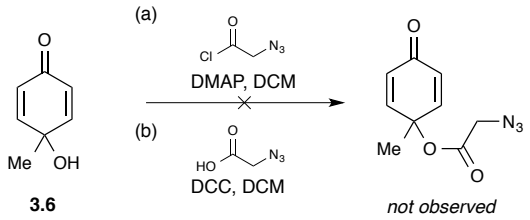

The use of chlorine as an activating group proved to be slightly more fruitful and significantly less dangerous (Scheme 3.6). Chloroacetate-tethered cyclohexadienone **3.10** in 54% yield was obtained through a DCC coupling with **3.6** and chloroacetic acid. We first attempted the Michael addition with mild bases such as K_2CO_3 and Cs_2CO_3; unfortunately, these failed at promoting the cyclization. Consequently, we decided to try Nicolaou's conditions once again, but with only one equivalent of base. Treating **3.10** with 1 equiv of KHMDS yielded only the *p*-quinol and recovery of the chloroacetic acid. When 3 equiv of KHMDS was used, the rearomatized product was observed. It appeared that not only was chlorine an insufficient activating group, but also that even with an activating group, our system was not stable to strong bases, which is not too surprising. A more activating functional

group was needed in order to employ a mild enough base that would promote the Michael addition instead of rearomatization.

Scheme 3.6. Synthesis of the tethered dienone and attempts at cyclization.

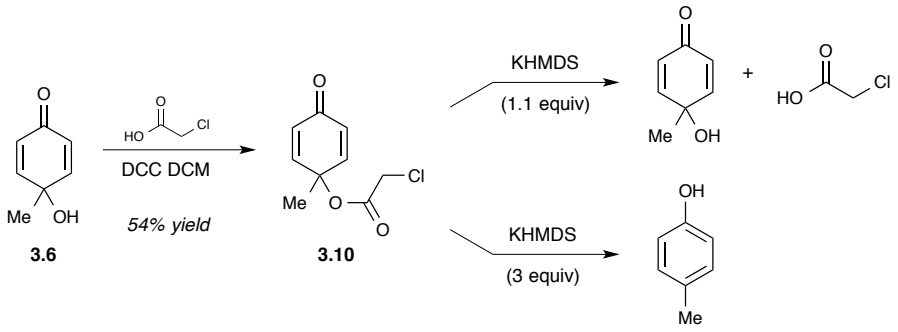

We decided to explore the use of a dithiocarbamate as a duel activating and protecting group, which could be unmasked to reveal the amine. Dithiocarbamate amino acid derivatives have previously been utilized in peptide synthesis due to the fact the nitrogen atom is unlikely to be nucleophilic enough for unwanted addition reactions.[94] The synthesis of the dithiocarbamate acetic acid was straightforward (Scheme 3.7A).[95] With **3.11** in hand, we attempted to couple the acid to the *p*-quinol with various coupling reagents (e.g. DCC, CDI), to no avail (Scheme 3.7B). Next, the acid was converted to the methyl ester in hopes that Otera's catalyst would be a sufficient coupling reagent, as it is often used for hindered alcohols.[96] Even with an excess amount of the *p*-quinol, no product (**3.12**) was observed.

Scheme 3.7. (A) Synthesis of dithiocarbamate glycine; (B) Coupling attempts.

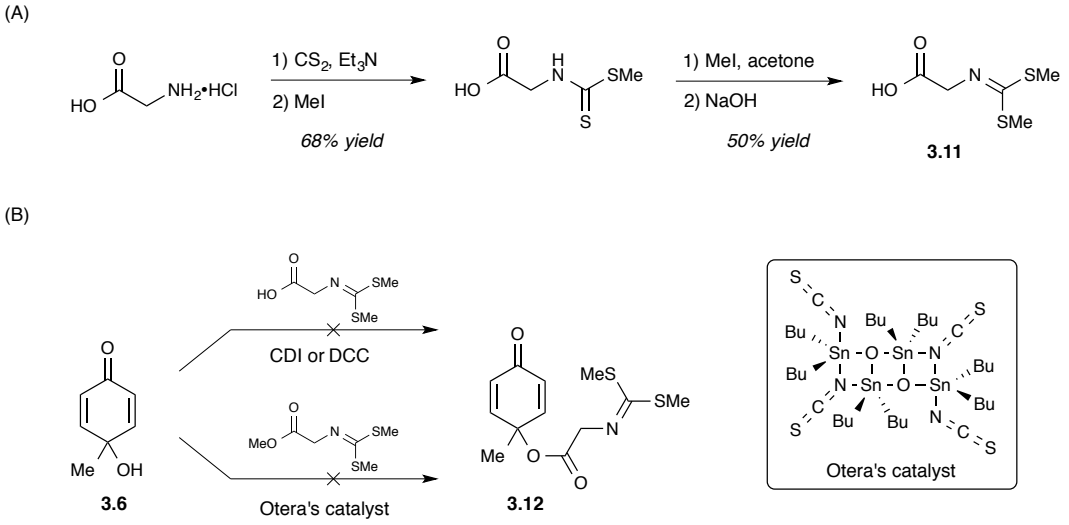

At this time, we decided to revisit the idea of utilizing an azide as an activating group. Our previous attempts were thwarted at the coupling stage, so if we could first couple a halo-acetic acid to the quinol, and then perform a displacement of the halogen with NaN_3, our azide-tethered dienone could be obtained. Coupling iodoacetic acid to the *p*-quinol under the same conditions previously employed gave **3.13** in 67% yield (Scheme 3.8). Curiously, when this was subsequently treated with NaN_3 in DMF, instead of displacing the iodine with the azide to afford **3.14**, an addition-elimination occurred providing phenol **3.15.** This was determined by the observation of an IR stretch at 2118 cm^{-1}, indicating the presence of an azide, as well as the lack of a carbonyl stretch. The ^1H NMR spectrum was also consistent with an aromatic compound.

Scheme 3.8. Attempts at halogen displacement with NaN_3 led to rearomatization of the dienone.

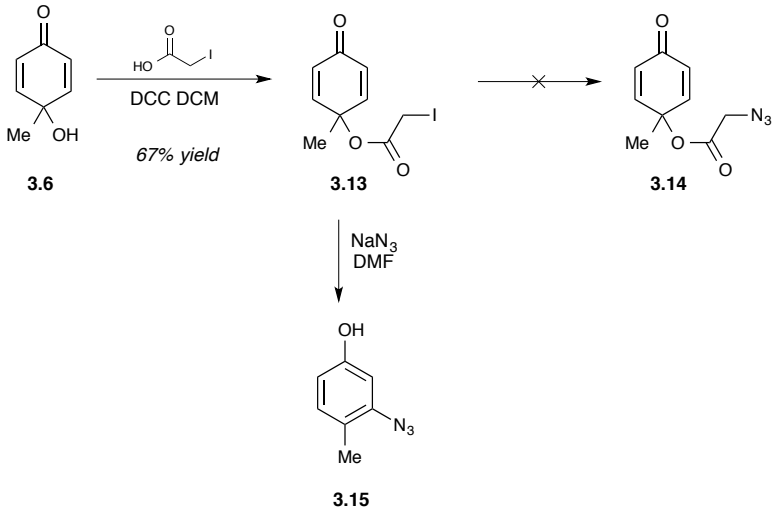

At this point, we decided to try a simpler activating group. Malonates are relatively potent carbon acids, allowing for deprotonation of the α-carbon by mild bases, such as Cs_2CO_3 or K_2CO_3. We hypothesized that coupling a malonic half ester to the *p*-quinol would allow for facile cyclization using a carbonate base (Scheme 3.9). The resulting ester could then be used to install the amine through a Curtius or Lossen rearrangement.[97]

Scheme 3.9. New synthetic route utilizing an ester as an activating group and handle for nitrogen installation.

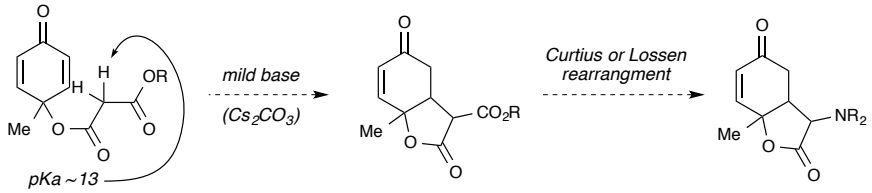

A *t*-butyl ester was chosen due to its ease of removal at a later stage. Thus, mono-*t*-butyl malonate was coupled to the *p*-quinol (**3.6**) through the mixed anhydride **3.16**,[98] giving the malonate-tethered cyclohexadienone **3.17** in 43% yield after purification (Scheme 3.10).[A]

[A] This work was in conjunction with Rodolfo Tello-Aburto.

With the malonate now appended to the quinol, we sought to induce the cyclization. We decided to use Cs_2CO_3 as our carbonate base of choice due to its better solubility in organic solvents.[99] To our delight, treatment of **3.17** with Cs_2CO_3 in acetonitrile cleanly afforded the bicyclic lactone (**3.18**) in 80% yield. Subsequent methylation provided **3.19** in 67% yield, which now resembled the core structure of sorbicillactone A. At this time, two diastereomers were observed in an approximately 5:1 ratio.[B] The cyclization and methylation could also be conducted in a one-pot procedure by treating **3.17** with 2 equiv of Cs_2CO_3, followed by iodomethane, to give **3.19** in 43% yield from the *p*-quinol.

Scheme 3.10. Synthesis of the bicyclic lactone.

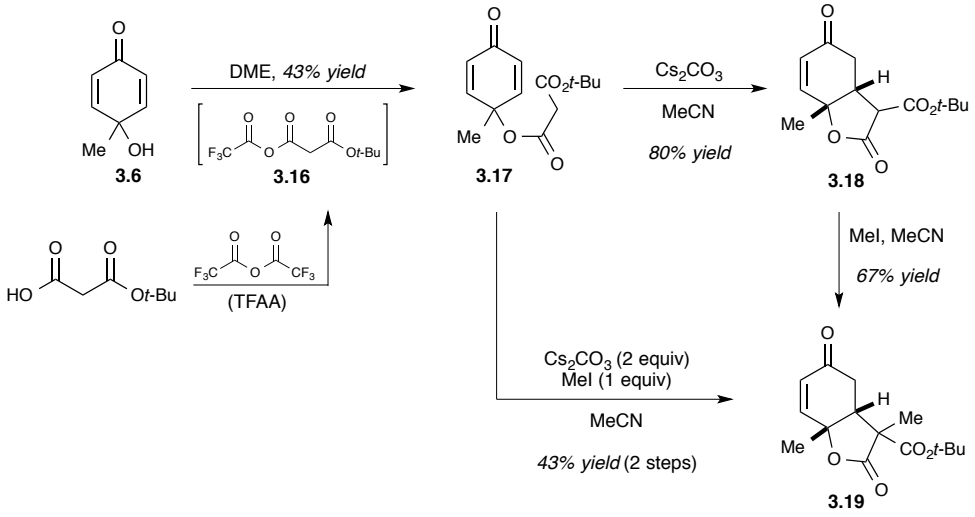

We tentatively assigned the major diastereomer as the exo product, as we had predicted that the electrophile should approach from the less-hindered convex face of the bicyclic ring system (Figure 1.4A).[100] An NOE experiment on the major diastereomer confirmed the cis-fused ring system, however an NOE was not observed for the C9 methyl group (Figure 1.4B). NOE experiments for the minor diastereomer were inconclusive as both methyl groups had the same chemical shift. Because we

[B] [KAV-I-186]

could not definitively assign the C9 stereocenter at this point, the proceeding structures in this section will indicate ambiguous stereochemistry.

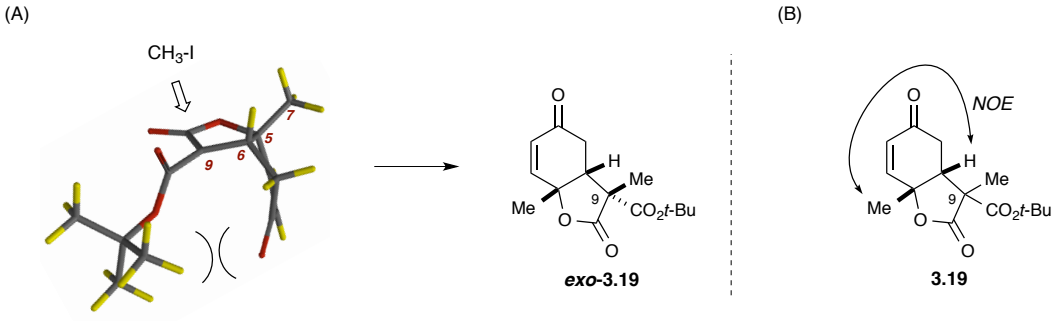

Figure 3.4. (A) Iodomethane should approach from the exo face of the bicyclic ring system. (B) Observed NOE for the major diastereomer.

3.2.2. Installation of the Amide Sidechain

With the bicyclic lactone in hand, the next step was to convert the *t*-butyl ester to an amide containing a fumarate residue. We envisioned utilizing a Curtius rearrangement to afford this transformation. Initially, this was achieved by first converting the ester (**3.19**) to acyl azide **3.20** in a three step procedure without purification of any of the intermediates (Scheme 3.11). The crude acyl azide was then refluxed in toluene to yield isocyanate **3.21**, which was quenched by heating with *t*-BuOH to afford Boc-protected amine **3.22** in 48% yield over the four steps and after purification. The rearrangement could easily be followed by IR as the azide and the isocyanate had distinct stretches ~100 cm^{-1} apart. Alternatively, the acyl azide could be heated directly in *t*-BuOH in a microwave reactor, affording **3.22** in quantitative yield and a much shorter reaction time. The Boc-protected amine will be a suitable core molecule to base a library scaffold off of; it is stable and can be stored for long periods of time. Deprotection followed by acylation would give rise to derivatives. However, for the natural product synthesis, a direct conversion to the fumarate amide would be more efficient.

Eventually, reaction conditions were found that converted the acid directly to the acyl azide by treatment with trichloroacetonitrile, NaN_3, and triphenylphosphine.[101] The purified acyl azide was then heated in THF using a microwave reactor. When the acyl azide was no longer present by IR, the isocyanate was quenched with aqueous K_2CO_3 and subsequently treated with fumarate **3.23** to afford amide **3.24** in 52% yield from the azide.

Scheme 3.11. Curtius rearrangement.

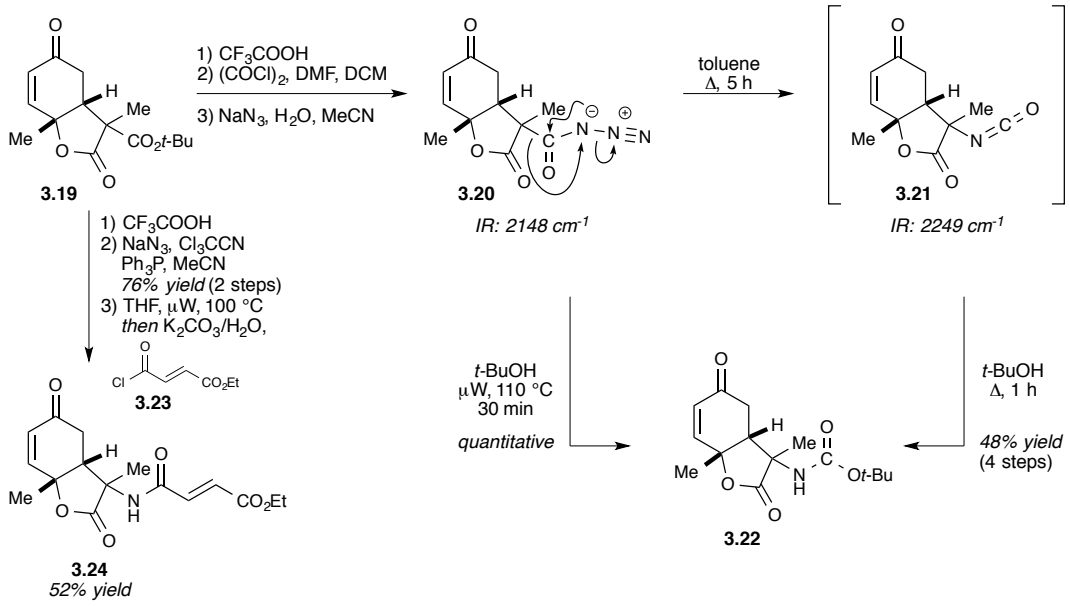

With a viable route the core of the molecule, we turned our attention to the synthesis of the natural product substrate. The model substrate served an important purpose of allowing us to work through the chemistry efficiently with accessible material. The model substrate will be revisited during the sorbyl chain investigation (Section 3.3.3), where we explored a variety of conditions in attempts to install the second side chain.

3.3 SYNTHESIS OF SORBICILLACTONE A AND 9-*EPI*-SORBICILLACTONE A[§]

3.3.1. Synthesis of the phenol

The C3 position was a point of diversification for analog synthesis in our original route to sorbicillactone A (Scheme 3.12). Ideally, the same phenolic precursor could be used for the library synthesis as well as the natural product synthesis, eliminating the need for developing multiple synthetic routes. A bromine atom in the C3 position would allow for cross-coupling reactions with a variety of different boronic acids, including methyl boronic acid, generating the methyl group necessary for the natural product.

Scheme 3.12. Proposed synthetic plan for the synthesis of sorbicillactone A and library development.

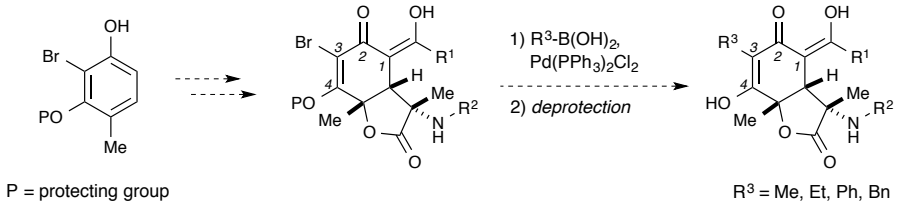

3.3.1.a Synthesis of the bromo-phenol

Phenol **3.25** was the key phenolic precursor needed for the oxidative dearomatization reaction (Scheme 3.13). It was necessary to have a protecting group on the C4 hydroxyl group to prevent regioisomers and unwanted reactions from occurring during the oxidation event. In addition, it would be present for the remainder of the synthesis, so it needed to be robust, yet also be able to be removed selectively in the presence of other functional groups; therefore, the silyl group TIPS was chosen. A TIPS group is relatively stable to mild acidic conditions compared with other silyl groups; it can also be selectively removed with fluorinating reagents such as TBAF.[102] In order to accomplish a regioselective protection of the C4 hydroxyl group, we would need to

[§] Part of this section has previously been published: Volp, K. A.; Johnson, D. M.; Harned, A. M. A Concise Synthetic Approach to the Sorbicillactones: Total Synthesis of Sobicillactone A and 9-*epi*-Sorbicillactone A. *Org. Lett.* **2011**, *13*, 4486–4489.

temporarily protect the C1 hydroxyl group with an orthogonal protecting group that could be removed in the presence of the TIPS group.

We envisioned phenol **3.25** being obtained from the protection and subsequent hydrogenation of dihydroxybenzaldehyde **3.27**. Our strategy was to install the protecting groups sequentially by first regioselectively acylating the C1 hydroxyl group in the presence of a Lewis acid, which should interact with both the formyl group and the ortho hydroxyl group, preventing acylation at the unwanted hydroxyl group.[103] We chose an acyl protecting group because of its ease of installation and removal. With the first hydroxyl group acylated, the second could then be silylated to give bis-protected benzaldehyde **3.26**. Bromo-benzaldehyde **3.27** could be obtained through a bromination of 2,4-dihydroxybenzaldehyde (**3.28**).

Scheme 3.13. Retrosynthetic analysis for the target phenol.

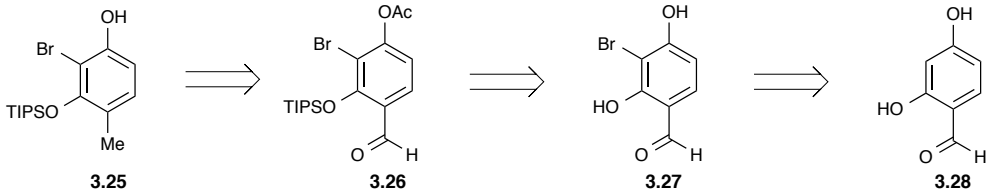

Initially, a direct bromination of 2,4-dihydroxybenzaldehyde was attempted,[104] however, this method proved to be low yielding and messy. Alternatively, bromination of resorcinol, followed by formylation would achieve the same goal. Therefore, resorcinol was tribrominated and subsequently reduced with NaOH and Na_2SO_3 to remove the unwanted bromine atoms, resulting in monobrominated **3.29** in 98% overall yield (Scheme 3.14).[105,106]

Formylation under Vilsmeier-Haack conditions produced **3.27** in poor yield. After encountering difficulty in the following acylation step (**3.31**), we decided to forego the synthesis of the library substrate and instead focus solely on the synthesis of the phenol needed for the natural product.

Scheme 3.14. Synthesis of phenol **3.31**.

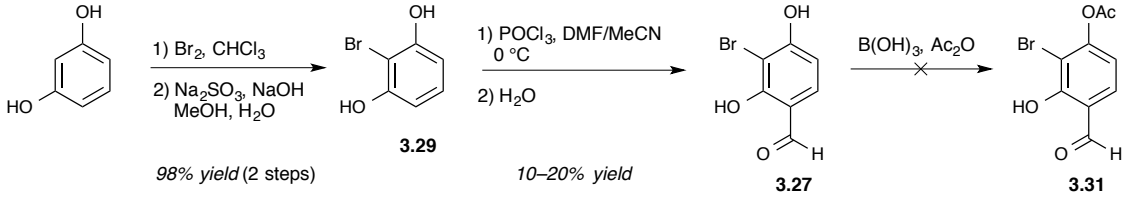

3.3.1.b Synthesis of the sorbicillactone phenol

Now focusing on the phenol for the synthesis of the natural product, a methyl group (instead of a bromine atom) on the aryl ring was required. We envisioned the same protecting group strategy as with the bromo-phenol. Our synthesis commenced with 2-methylresorcinol, which was formylated under the same Vilsmeier-Haack conditions to provide **3.32** with an improved yield of 52% (Scheme 3.15). Unfortunately, the acylation conditions once again did not work well. A maximum conversion of 83% and inability to separate the product (**3.33**) from the starting material forced us to rearrange the order of steps. Therefore, 2-methylresorcinol was first mono-benzylated,[107] and then treated under Vilsmeier-Haack conditions, which unfortunately led to regioisomers. Alternative formylation conditions were found that used paraformaldehyde and $MgCl_2$; this reaction relies upon a free hydroxyl group to coordinate to the $MgCl_2$, therefore regioselectively directing the formaldehyde to the correct position.[108] Following this new procedure provided the desired benzaldehyde **3.34** in 62% yield. These conditions proved to be far superior to the Vilsmeier-Haack conditions, resulting in easier handling and higher yields of product. Finally, protection of the second hydroxyl group with TIPSCl gave **3.35** in 98% yield.

Scheme 3.15. Synthesis of phenol precursor.

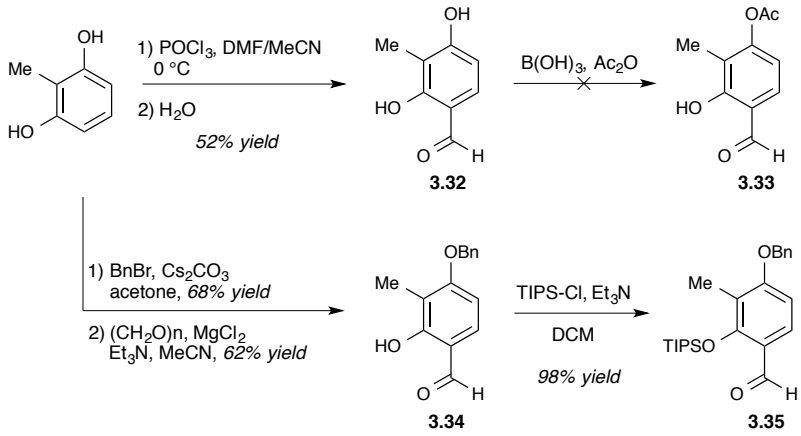

The final step in the phenol synthesis was a hydrogenation that would simultaneously reduce the aldehyde and orthogonally remove the benzyl group. However, this proved to be more challenging than anticipated. Achieving full conversion of the aldehyde to the methyl group was difficult: the reaction often stalled out at the benzyl alcohol (**3.36**, Scheme 3.16). Addition of excess HCl led to poisoning of the palladium catalyst and removal of the TIPS group. Therefore, two submissions to reaction conditions were necessary for full conversion. Alternatively, treatment of benzyl alcohol **3.36** with $BF_3{\cdot}OEt_2$ and Et_3SiH afforded phenol **3.37** in 29% yield. When benzaldehyde **3.35** was treated directly with $BF_3{\cdot}OEt_2$ and Et_3SiH, no product was observed. Despite the poor yields for the reduction of benzaldehyde **3.35**, it was carried forward to the dearomatization step. Initially, we sought to synthesize the acetate, with the intention of treating it with K_2CO_3 to reveal the *p*-quinol. Unfortunately, subjecting **3.37** to PIFA in the presence of acetic acid did not provide **3.38**, despite many attempts under different reaction conditions. This could be due to incompatibility of the TIPS group with strong acidic conditions. At the time, we also considered steric crowding around the newly forming stereocenter due to the TIPS group could be a reason, but subsequent dearomatization studies have shown this was probably not the case (see Chapter 5, Section 5.2.3.a).

Scheme 3.16. Synthesis of **3.37** and attempted dearomatization.

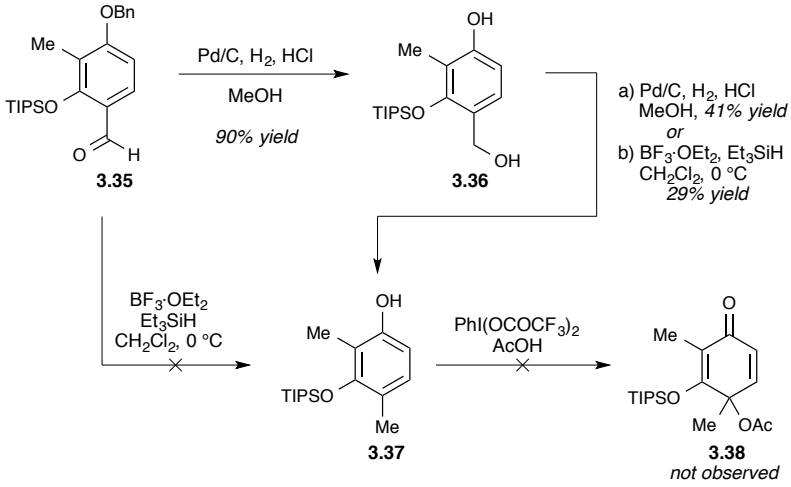

We decided to employ a methyl ether as our next choice of protecting group due its robustness, ease of installation, and small size. Phenol **3.34** was methylated with iodomethane to achieve a nearly quantitative yield of **3.39** (Scheme 3.17). Subsequent hydrogenation gave phenol **3.40** in 48% yield. With the phenol in hand, the stage was set to attempt the dearomatization reaction. To our delight, treatment of **3.40** with PIFA and acetic acid gave dienone **3.41** in 48% yield.

Scheme 3.17. Synthesis of cyclohexadienone **3.41**.

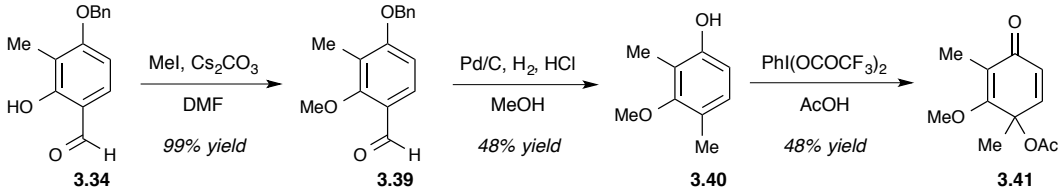

With the success of the dearomatization, we sought to optimize the synthesis of phenol **3.40**. By testing various formylation conditions, we found yields up to 75% could be achieved under modified Vilsmeier-Haack conditions (Scheme 3.18). Recrystallization gave pure product that could be carried forward to the benzylation step, giving the mono-protected phenol. After a chromatographic purification, methylation with iodomethane and Cs_2CO_3 cleanly afforded the bis-protected benzaldehyde (**3.39**).

Scheme 3.18. Optimized synthesis of benzaldehyde **3.39**.

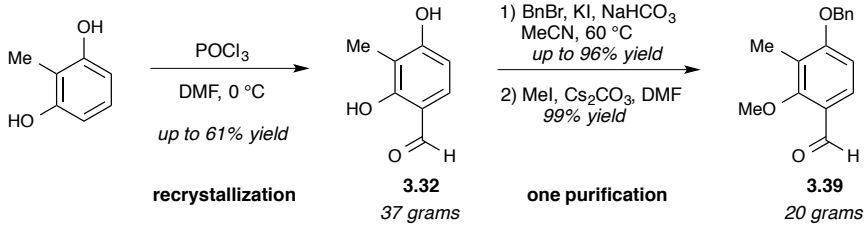

The hydrogenation conditions were also optimized using various Pd/C reagents that were obtained from Johnson Matthey (Table 3.1). Previously, 10 wt % of Pd/C (dry) from Sigma-Aldrich was employed; however, the reaction needed to be performed twice for full conversion of the aldehyde to the methyl group (entry 1). Simply adding more catalyst did not seem to improve yields; the reaction needed to be fully worked up and resubjected to reaction conditions. Ultimately, we found a catalyst that gave superior yields of phenol **3.40** (entry 2). Scale-up of these reactions provided the phenol in up to 20 g at a time.

Table 3.1. Hydrogenation conditions.

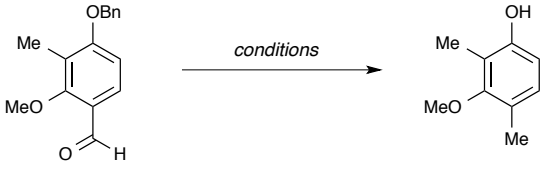

Entry	Pd/C reagent	Solvent	Conditions	Time	Yield
1[a]	Sigma-Aldrich, dry	MeOH	cat. HCl, rt	16 h	77%[D]
2	Johnson Matthey Type 10R39 (56% H_2O)	MeOH	30 min, then add cat. HCl	16 h	86%[E]
3	Johnson Matthey Type A501023-10 (53% H_2O)	MeOH	30 min, then add cat. HCl	16 h	81%[F]

[a] Crude product was resubjected to reaction conditions.

[D] [KAV-I-224]
[E] [KAV-II-118A]
[F] [KAV-II-118B]

3.3.2. Synthesis of the Bicyclic Lactone

Adhering to the steps we had optimized for the model substrate synthesis, we attempted to oxidize phenol **3.40** under the Oxone conditions. However, these conditions failed to yield any product, most likely due to the presence of the methyl ether.[109] Fortunately, by employing PIDA as the oxidation reagent in acetonitrile-water, *p*-quinol **3.42** was initially obtained in 51% yield (Scheme 3.19A). This was then treated with the mixed anhydride of TFAA and mono-*t*-butyl malonate to give the tethered cyclohexadienone **3.43** in nearly quantitative crude yield. However, the yields of these two reactions were quite variable and capricious, especially when performing the reactions on larger scales (greater than 200 mg). To circumvent this problem, we sought to find more reliable conditions that would also be more amenable to scale-up. For the dearomatization of the phenol, reports were found in the literature where TMS phenols led to better yields of the cyclohexadienone under hypervalent iodine conditions than unsilylated phenols.[110] Thus, phenol **3.40** was first transformed to the trimethylsilyl ether by heating in the microwave with an excess of hexamethyldisilazane (Scheme 3.19B). Removal of the excess HMDS in vacuo, followed by subsequent treatment with PIDA and H_2O/MeCN, provided the quinol (**3.42**) on larger scale (up to ~1 g) and with improved yields (77–95%). Next, instead of the using the mixed anhydride to append the malonate, DCC was used to couple the acid to the quinol, affording **3.43** in yields up to 98%. These conditions proved to be much more reliable and scalable than the conditions that were employed with the model substrate. We would eventually perform these reactions on a 12 g scale.

Scheme 3.19. Synthesis of the malonate-tethered dienone.

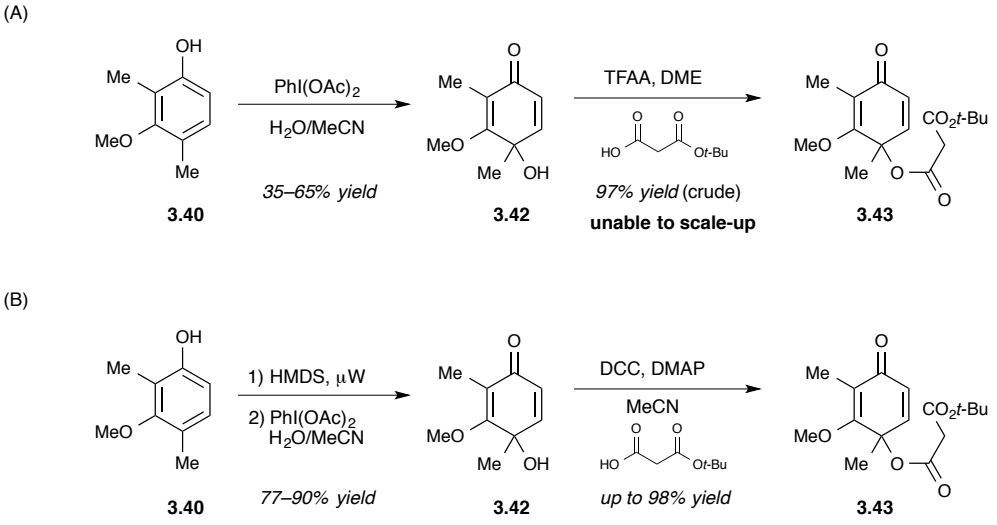

With the tethered dienone (**3.43**) in hand, the cyclization-methylation sequence was carried out, providing the bicyclic lactone **3.44** in 43% yield (Scheme 3.20). A single diastereomer was isolated and NOE experiments once again confirmed the cis-fused ring system. However, an NOE was not observed between the C6-H and the methyl group. Again, we were not overly concerned with the absence of an NOE; unobserved through-space interactions by NMR do not definitively confirm molecular structure. Next, the bicyclic lactone was converted to the acyl azide in the same fashion as the model substrate, affording **3.45** in 76% yield. Heating the acyl azide in a solution of *t*-BuOH under microwave conditions, gave the rearranged product as Boc-protected amine **3.46** in 43% yield. Alternatively, acyl azide **3.45** could be heated in THF under microwave conditions to induce the rearrangement to the isocyanate, which was subsequently treated with aqueous K_2CO_3 and the fumoryl chloride to give **3.47** in 56% yield.

Scheme 3.20. Synthesis of fumarate **3.47**.

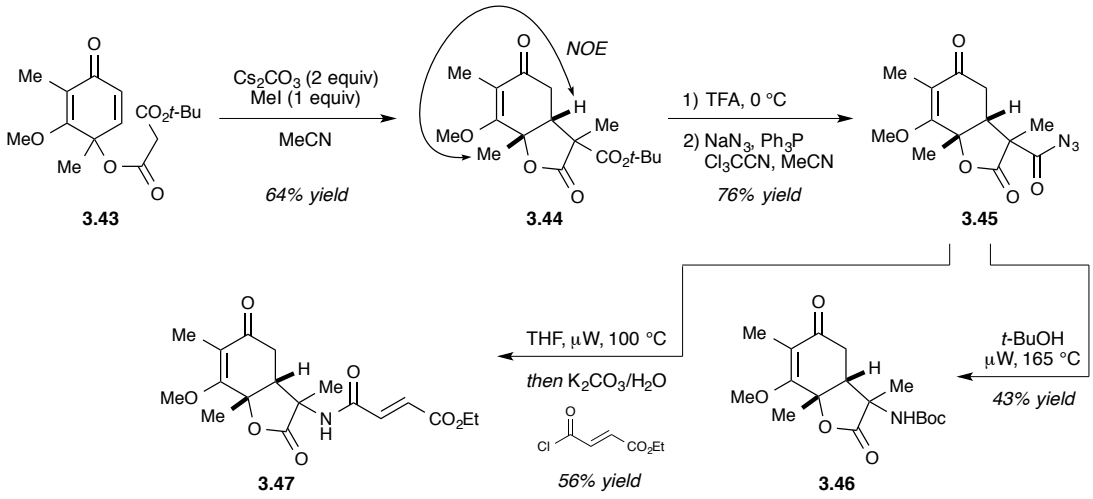

3.3.3. Installation of the Sorbyl Chain

With the success of the Curtius rearrangement, we turned our attention to appending the sorbyl sidechain (Table 3.2). Conditions were initially employed on the model substrate, but were also tested on the sorbicillactone substrate. Using sorboyl chloride at –78 °C with LiHMDS to our delight gave a trace amount of product (entry 1) from the model substrate, detected by a singlet in the ^{1}H NMR spectrum at ~16 ppm indicating the presence of a 1,3-diketone in the enol tautomer. Switching the base to LDA also resulted in a trace amount of product (entry 2). Next, we tried appending the side chain before the Curtius rearrangement; unfortunately, this only led to a 12% yield with the model substrate (entry 3) and decomposition with the sorbicillactone substrate (entry 4). Smaller lithium amine bases were also used to attempt to overcome possible steric interactions that may be hindering the formation of the enolate, but this also led to decomposition (entries 5 and 6). Instead of trying to achieve a direct acylation, we also tried aldol reactions with LDA and the sorbaldehyde with either the ester sidechain (entry 7) or the fumarate side chain (entry 8); however, these also did not yield any desired product.

Table 3.2. Attempted acylation and aldol reactions of the bicyclic lactone.

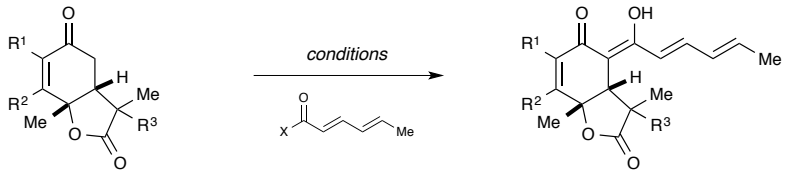

Entry	R^1, R^2	R^3	X	Base	Temp (°C)	Yield
1	H, H	NHBoc	Cl	LiHMDS	–78	trace
2	H, H	NHBoc	Cl	LDA	–78	trace
3	H, H	CO_2t-Bu	Cl	LiHMDS	–78	12%
4	Me, OMe	CO_2t-Bu	Cl	LiHMDS	–78	decomp
5	Me, OMe	CO_2t-Bu	CN	LDA	–78	decomp
6	Me, OMe	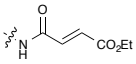	Cl	$LiEt_2N$	–78	decomp
7	Me, OMe	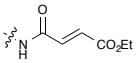	CN	$LiEt_2N$	–78	decomp
8	Me, OMe	CO_2t-Bu	H	LDA	–78	decomp
9	Me, OMe	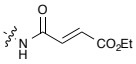	H	LDA	–78	sm + decomp

3.3.3.c Boron aldol attempts

We began to investigate the side-chain problem with an even simpler system in order to grasp the feasibility of the transformation we were attempting. Utilizing a truncated version of our substrate (**3.48**), a variety of aldol and acylation conditions were examined. Claisen condensation conditions failed to give the desired product, as did Mukaiyama aldol conditions. Fortunately, treating **3.48** under standard boron aldol conditions gave **3.49** in 57% yield, which could then be subsequently oxidized with Dess-Martin periodinane to give **3.50**.[111]

Scheme 3.21. Boron aldol conditions.

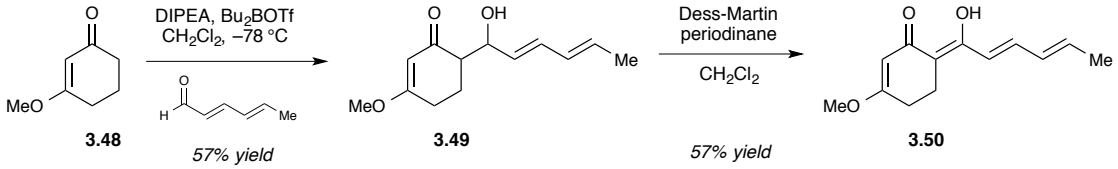

Encouraged by these results, we employed the same conditions to the model and natural product substrates (Table 3.3). Unfortunately, the boron-aldol conditions failed to give the desired product (entries 1–4). We also tried Lewis acid promoted aldol conditions (entry 5), but no reaction was observed.

Table 3.3. Boron aldol attempts.

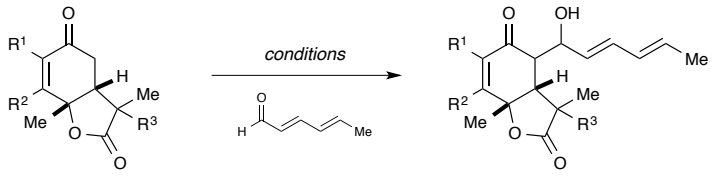

Entry	R^1, R^2	R^3	Base	Reagent	Temp (°C)	Yield
1	H, H	NHBoc	DIPEA	Bu_2BOTf	–78 → rt	decomp
2	Me, OMe	CO_2t-Bu	DIPEA	Bu_2BOTf	–78 → rt	decomp
3	Me, OMe	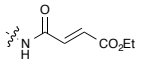	DIPEA	Bu_2BOTf	–78 → rt	decomp
4	Me, OMe	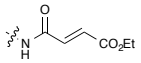	TEA	Cy_2BOTf	–78	decomp
5[112]	Me, OMe	CO_2t-Bu	Et_3N	$Yb(OTf)_3$, TMSCl	rt	no reaction

3.3.3.d One-Pot Trapping Experiments

Due to the many unsuccessful acylation and aldol attempts, we began to look at different ways the sorbyl chain could be installed. We reasoned that because an enolate is generated during the Michael addition step, it could perhaps be trapped out either as the silyl enol ether, which could then be used in a Mukaiyama aldol addition (Scheme 3.22A), or with sorbaldehyde itself (Scheme 3.22B). Unfortunately, neither of these approaches afforded any product. The enolate is likely trapped with a proton much

faster than the lifetime it would need to undergo an intermolecular reaction with another reagent.

Scheme 3.22. Enolate-trapping attempts.

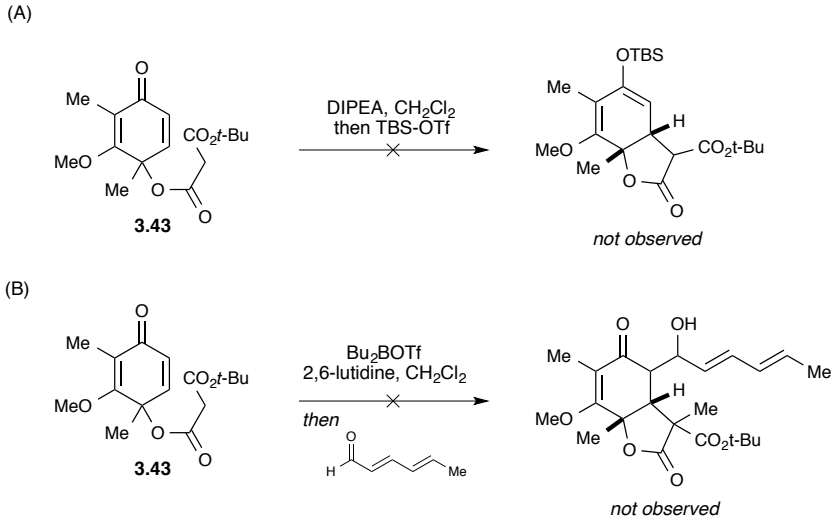

3.3.3.e Reformatsky Reaction and Unexpected Outcome

We also attempted to utilize a Reformatsky reaction to install the sorbyl sidechain. This would be accomplished by treating bromine bicyclic lactone **3.52** with sorbaldehyde and activated zinc, followed by an oxidation to afford **3.51** (Scheme 3.23). The bicyclic lactone would come from the malonate-tethered dienone (**3.53**), which would ultimately be synthesized from bromophenol **3.54**.

Scheme 3.23. Reformatsky reaction retrosynthesis.

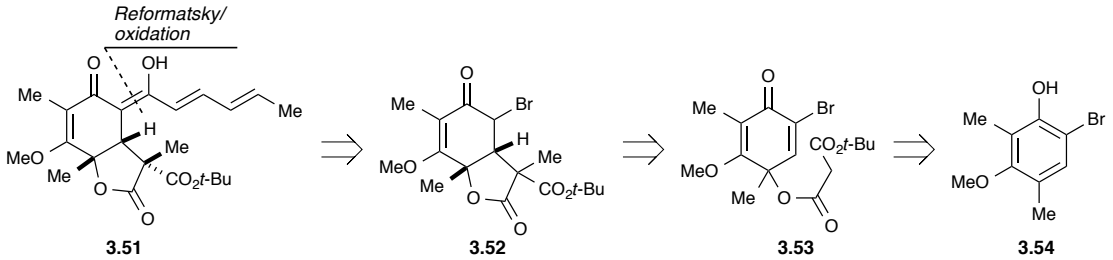

Installing the bromine on phenol **3.40** was easily accomplished with dibromantin, affording **3.54** in 97% yield (Scheme 3.24). However, the bromophenol appeared to be light sensitive, as the color would change from ivory color to dark

brown upon standing after purification by column chromatography; the NMR spectrum confirmed degradation. Therefore, the bromophenol was dearomatized with PIDA immediately after purification to give **3.55** in 51% yield, which was subsequently treated with the mixed anhydride of TFAA and mono-*t*-butyl malonate to give **3.53** in 55% yield (and 19% of recovered starting material). Initially, treating **3.53** with Cs_2CO_3 gave two compounds, which, after analysis, were determined to be **3.57** (6% yield) and the unexpected cyclopropane **3.56** (21% yield). Interestingly, both products were present as a single diastereomer. We hypothesized that only one diastereomer of the anionic intermediate could proceed to form the cyclopropane, as the configuration of the bromine-bearing stereocenter in **3.57** does not allow for nucleophilic attack by the malonate. Resubjecting **3.57** to the reaction conditions provided complete conversion to cyclopropane **3.56**, indicating that the reaction likely proceeds through epimerization of the relevant stereocenter.

Finally, treating **3.53** with 1.1 equiv Cs_2CO_3 overnight gave the cyclopropane directly in 65% yield. Cyclopropane **3.56** was treated with SmI_2 in hopes the cyclopropane would open and undergo an aldol with sorbaldehyde, but unfortunately no product was observed.[G]

[G] This transformation has since been further investigated by Nicholas Moon.

Scheme 3.24. Attempted synthesis of the Reformatsky reaction substrate.

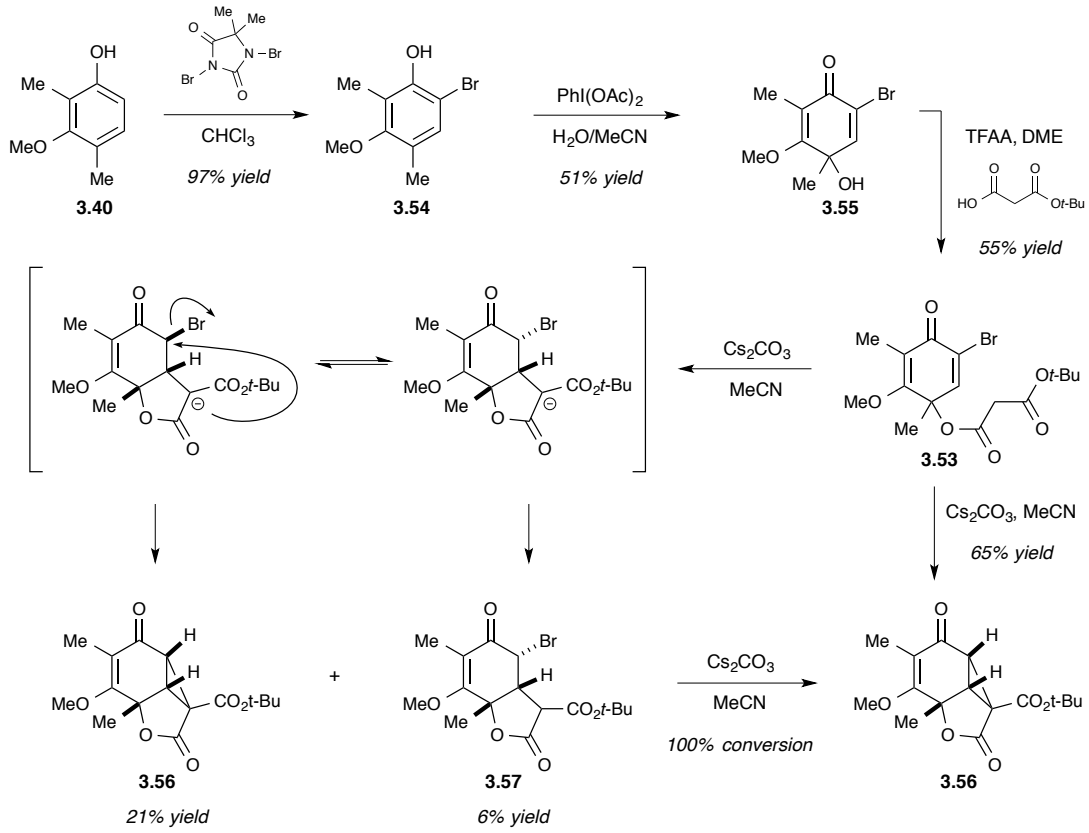

3.3.3.f Direct acylation

It was to our serendipitous advantage that Helmchen and co-workers reported the acylation of a similar bicyclic structure with an unsaturated acyl reagent.[113] The authors had successfully performed a boron aldol on substrate **3.58** with *trans*-cinnamaldehyde using *n*-Bu_2BOTf and DIPEA to generate the enolate (Scheme 3.25A). A Dess-Martin oxidation of the resulting product gave them **3.59** in 64% yield, which is the overall transformation that we desired. They noted that enolate formation with lithium amine bases gave poor and inconsistent results. Unfortunately, applying the successful conditions found for **3.58** to the bicyclic structure (**3.60**) did not lead to their desired product (Scheme 3.25B).

Scheme 3.25. (A) Helmchen's boron aldol of an intermediate in his synthesis of (+)-infectocaryone; (B) Failed boron-aldol with bicyclic **3.60**.

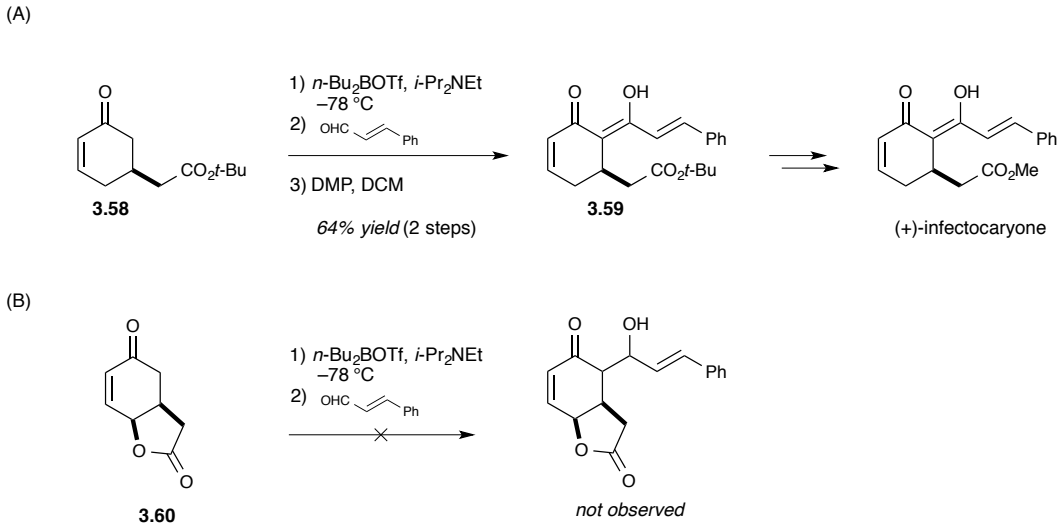

They decided to attempt direct acylation and tested a variety of conditions (Table 3.4). Using LiHMDS as the base, they first varied the acyl substituent. Employing the standard acid chloride gave 26% yield of product (entry 1). Moving to softer electrophiles, the acyl imidazole led to no product (entry 2), while the benzotriazole only gave product with LiHMDS as a base (compare entries 3 and 4). When an acyl nitrile was used, an improved yield of 39% was obtained. This yield was further increased when they shortened the time allowed for enolate formation (entry 6).

Table 3.4. Helmchen's acylation conditions.

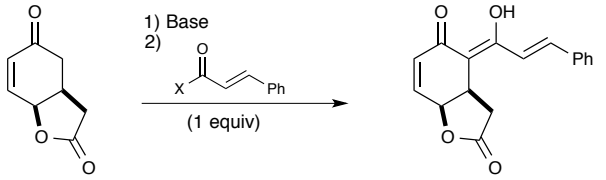

3.60 **3.61**

Entry	X	Deprotonation conditions	Acylation conditions	Yield
1	Cl	LiHMDS (1.1 equiv) THF, 10 min, –78 °C	15 min at –78 °C	26
2	Imd	LiHMDS, (1.05 equiv) THF, 45 min, –78 °C	3 h at –78 °C	–
3	Bt	LDA, (1.0 equiv) THF, 30 min, –78 °C	20 h at –78 °C	–
4	Bt	LiHMDS, (1.05 equiv) THF, 55 min, –78 °C	3 h at –78 °C	18
5	CN	LiHMDS, (1.1 equiv) THF, 55 min –78 °C	30 min at –78 °C	39
6	CN	LiHMDS, (1.1 equiv) THF, 10 min, –78 °C	5 min at –78 °C	47
7	CN	LiHMDS (1.1 equiv) THF, 20 min, –100 °C	30 min at –100 °C	74

[1] Bt: benzotriazole

However, the most pronounced change in yield occurred when the temperature was lowered further to –100 °C as opposed to the standard –78 °C. These results clearly indicate the required enolate is very sensitive; a soft lithium base, shortened enolate formation time, and lowered temperature all contribute to success of the reaction. These results correlated closely with our acylation experience (Table 3.3 and Table 3.5). As Helmchen had discovered, the colder temperature for enolate formation was key for the success of the reaction; however, in our case the mixture needed to be warmed to –78 °C after addition of the acyl nitrile due it solidifying at the colder temperature. Gratifyingly, a yield of 66% (entry 2) was obtained for the model substrate under rigorous drying conditions. This was achieved by evaporating the starting material several times from benzene. These conditions transferred well to the sorbicillactone substrate (entry 3). Surveying other lithium bases (entries 4 and 5) revealed LiHMDS

was best suited for the task. However, we were unable to convince the reaction to go to completion: prolonged reaction time led to decomposition rather than full conversion. Therefore, the reaction was terminated early and the starting material recovered. Eventually, we found that these conditions were also successful with the bicyclic lactone with the ester (entry 6), whereas previously, the reaction only led to decomposition at –78 °C (see Table 3.2, entries 4 and 5) .

Table 3.5. Acylation conditions.

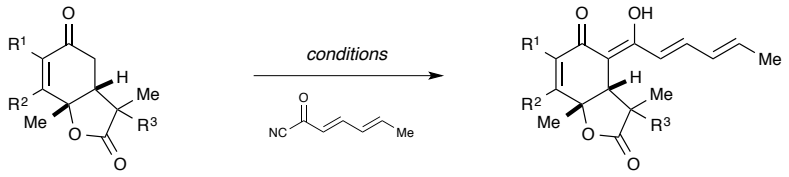

Entry	R^1, R^2	R^3	Product	Base	Temp (°C)	Yield
1	H, H	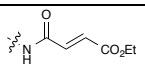	**3.62**	LiHMDS	–98 → –78	39% (62% brsm)
2[a]	H, H	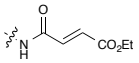	**3.62**	LiHMDS	–98 → –78	66%
3	Me, OMe	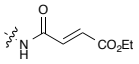	**3.63**	LiHMDS	–98 → –78	45% (82% brsm)
4	Me, OMe	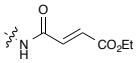	**3.63**	LDA	–98 → –78	11% (19% brsm)
5	Me, OMe	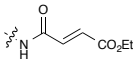	**3.63**	$LiEt_2N$	–98 → –78	decomp
6	Me, OMe	CO_2t-Bu	**3.64**	LiHMDS	–98 → –78	56%

[a] Starting material was rigorously dried by evaporation from benzene.

3.3.4. Reexamining the Stereoconfiguration

After the installation of the sorbyl sidechain, we began to have serious doubts regarding the C9 configuration. The ^{1}H NMR spectrum of the fully protected compound (**3.63**) matched nearly every peak in that of the natural material, except for the C11 methyl group and the C6 proton; there was an approximately 0.3 ppm

difference between the signals for the protected synthetic material and those for the natural material (Figure 3.5).[H]

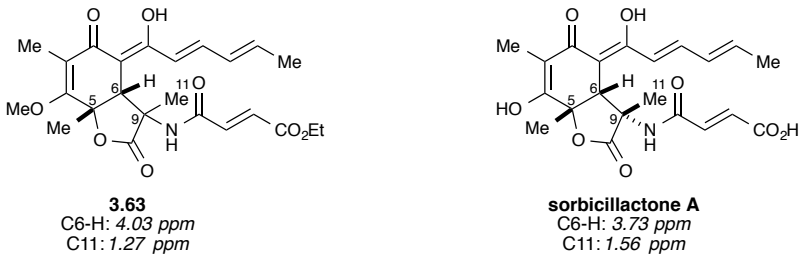

Figure 3.5. Comparison of chemical shifts between the natural substrate and our protected substrate.

It seemed unlikely this would change significantly after deprotection of the methyl ether and the ethyl ester. We had previously sought to determine the configuration unambiguously through X-ray analysis; unfortunately, we struggled to obtain crystals of sufficient quality despite attempts with numerous intermediates. We decided to employ the Curtius rearrangement sequence with *p*-bromobenzoyl chloride in place of the fumaroyl chloride in order to obtain a compound more suitable for crystal growth (Scheme 3.26). The moderate yield (42%) of amide **3.65** was likely due to the insoluble nature of the compound.

Scheme 3.26. Synthesis of **3.65** for X-ray analysis.

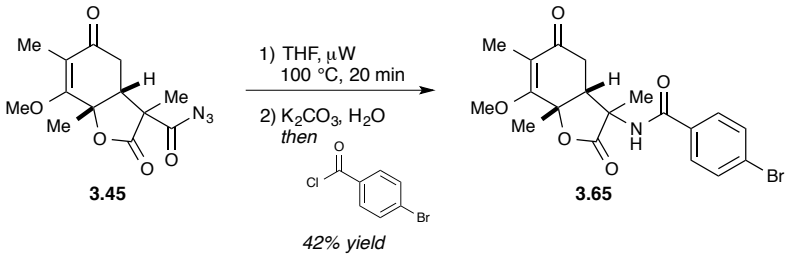

After many attempts at growing X-ray quality crystals (and enduring a twinned crystal that was not suitable for X-ray analysis), a mixed solvent system[114] yielded suitable crystals, the analysis of which revealed the true configuration of the C9

[H] Both NMR samples were prepared in acetone-d_6.

stereocenter. Unfortunately, our worst fears were true: the diastereomer was epimeric to the natural product (Figure 3.6). The ORTEP diagram clearly shows a trans relationship between the C11 methyl group and the bridgehead methyl group (C7).

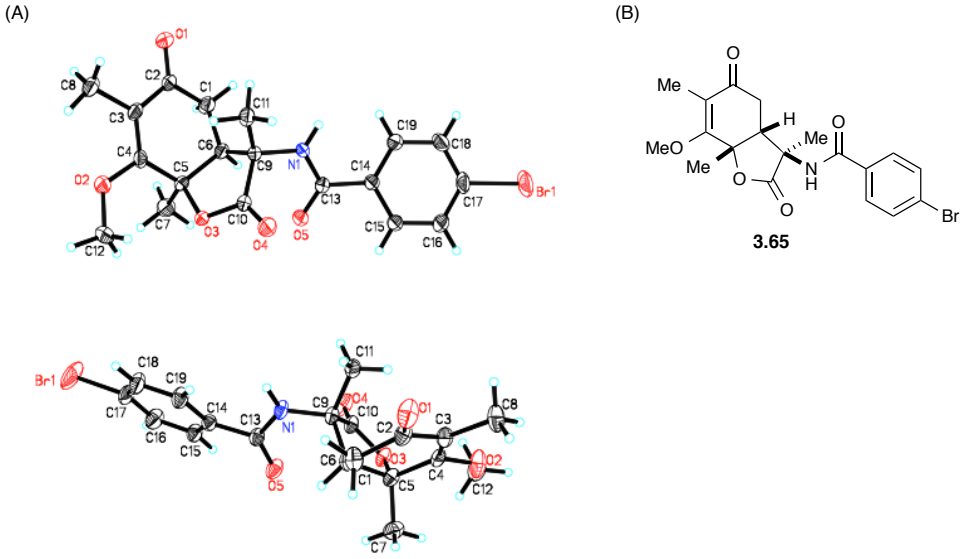

Figure 3.6. (A) ORTEP diagram of **3.65** in two different orientations. (B) Correct configuration of **3.65**.

At approximately the same time the X-ray was obtained, a scale-up of the cyclization-methylation sequence revealed a second diastereomer (Scheme 3.27), recovery of which improved the overall average yield (84% versus 60%). ^{1}H NMR and subsequent NOE studies determined that the minor diastereomer was, in fact, the one with the correct configuration of the natural product. The scaled up reaction gave a diastereomeric ratio of 6:1 (endo:exo) bicyclic products. Scaling up the reaction even further allowed us to isolate over 1 g of the correct diastereomer.

Scheme 3.27. Scale-up of the cyclization-methylation sequence revealed a minor diastereomer.

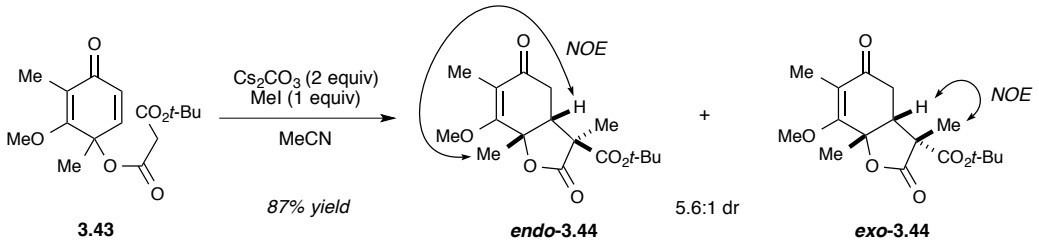

Fortunately, an R_f difference of approximately 0.2 between the two diastereomers allowed them to be easily visualized by TLC and separated by column chromatography. Additionally, there were defining peaks in each of the ^{1}H NMR spectra that allowed for identification of each diastereomer (Figure 3.20). The most prominently different peaks correspond to the C6 proton and the C11 methyl group. Each has significantly different chemical shifts and unique splitting patterns. The bridgehead proton in ***endo*-3.44** is a dd and has a chemical shift of 3.31 ppm; the same proton in ***exo*-3.44** has chemical shift of 2.99 and is doublet. The methyl group attached to the C9 stereocenter is shifted much further upfield (1.33 ppm) in the ***endo*-3.44** spectrum than in the ***exo*-3.44** spectrum (1.47 ppm). These differences greatly aided in determining the diastereomeric ratio of the reaction mixture.

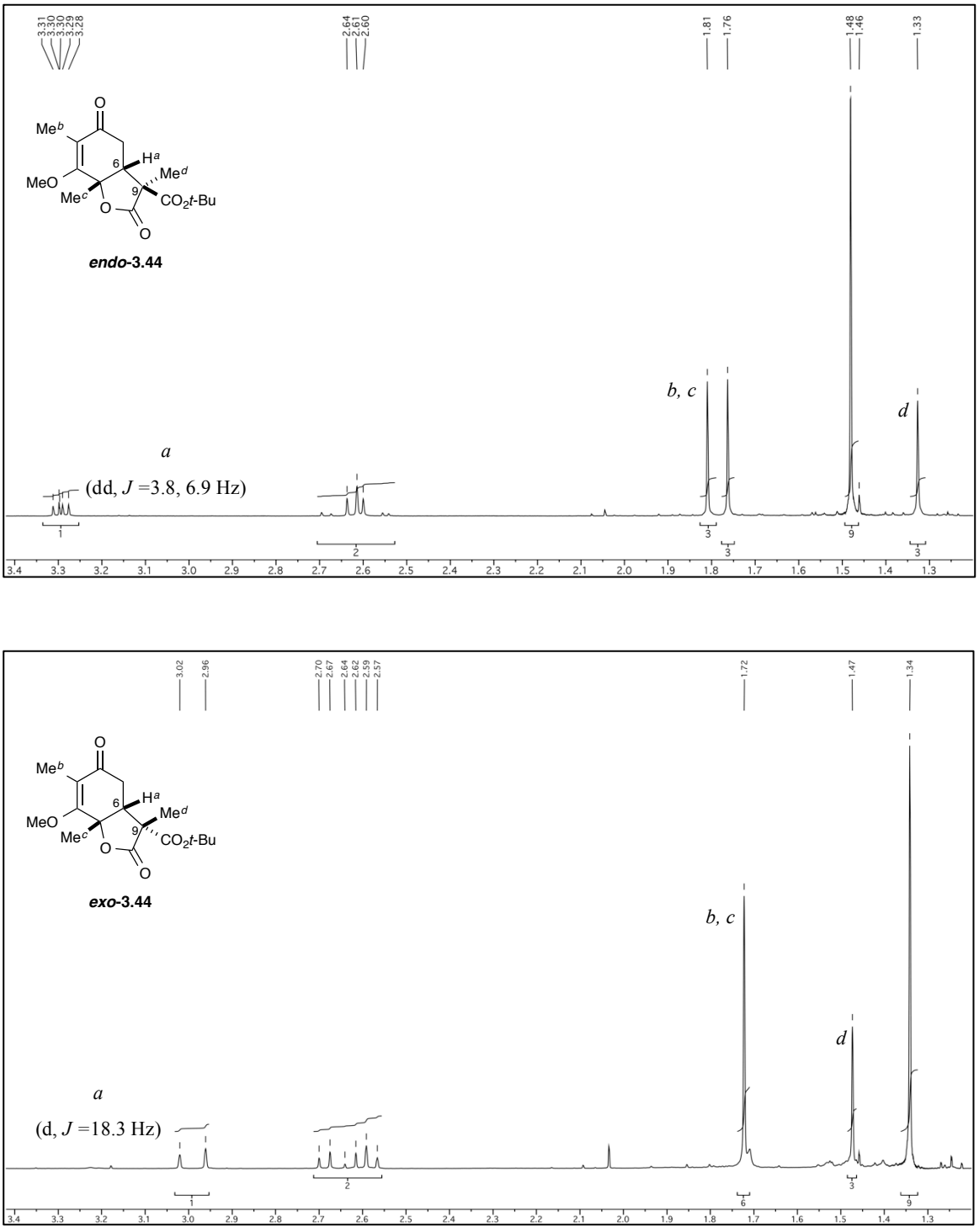

Figure 3.20. ^{1}H NMR comparison of ***endo*-3.44** and ***exo*-3.44**.

Now that the stereoconfiguration at C9 was no longer ambiguous, it is important to note that all reactions involving the bicyclic lactone up until this point were conducted with the epimer (which was the major diastereomer), not the correct diastereomer. We were uncertain which diastereomer we possessed, therefore the stereochemistry had been labeled ambiguous; all proceeding reactions will now be labeled with the correct configuration, as we now have full knowledge of which diastereomer was being obtained and used.

3.3.5. Epimerization and Other Attempts at Altering the Diastereomeric Ratio

Many attempts were made at altering the diastereomeric ratio to favor the desired diastereomer. During our pursuit of the total synthesis, we were unsuccessful; however, in our later studies involving the alkylation of the bicyclic lactone (Chapter 4), we uncovered more useful results. Several of the attempts that were made during the total synthesis studies are listed below.

3.3.5.g Equilibration Conditions

We hypothesized that we could affect the diastereomeric ratio through equilibration of the anionic intermediates. To test this, the reaction was performed at 80 °C overnight (Scheme 3.28). We initially thought we had successfully increased amount exo product, as we observed a 3.9:1 dr.[I] However, we subsequently identified an additional product with the same R_f as ***exo*-3.44**: the decarboxylated product **3.66**. It appears that ***endo*-3.44** decarboxylates at a faster rate than ***exo*-3.44**, which was accounting for the change in diastereomeric ratio. Performing the reaction with catalytic amounts of Cs_2CO_3 (5 mol%) did not improve the diastereoselectivity and trace amounts of decarboxylated product were still observed.

[I] [KAV-II-160]

Scheme 3.28. Equilibration attempt.

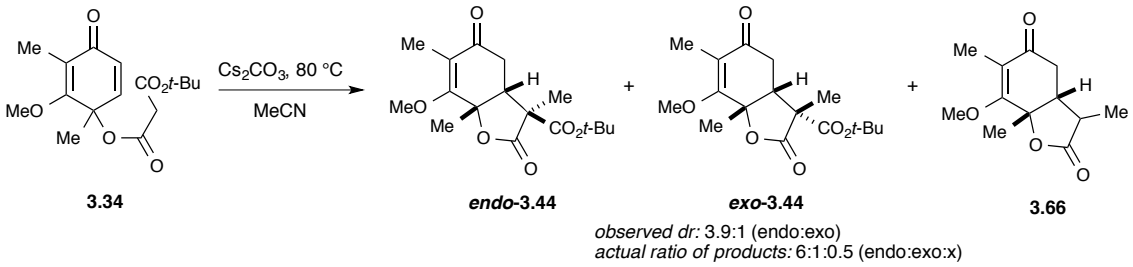

3.3.5.h Epimerization Experiments

Because the bicyclic lactone is formed through a potential reversible conjugate addition, we decided to attempt epimerization through a retro-Michael process (Scheme 3.29). We subjected the mixture of diastereomers to a variety of experimental conditions varying: the amount and kind of base, the reaction temperature, and the heating method (microwave and oil bath). Unfortunately, we only observed the starting material or the decarboxylated product.

Scheme 3.29. Proposed retro-Michael addition.

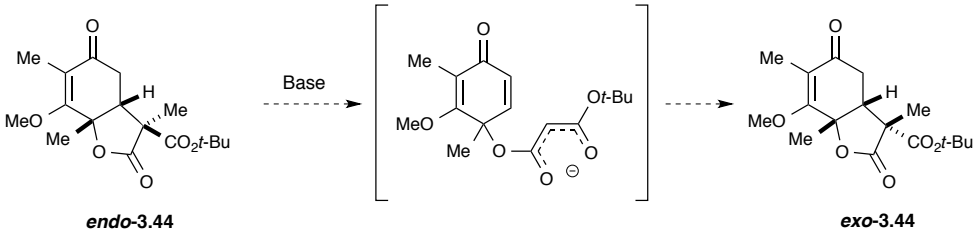

Table 3.6. Epimerization attempts of ***endo*-3.44**.

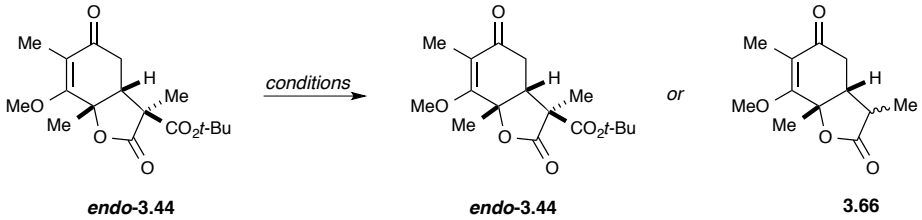

***endo*-3.44** ***endo*-3.44** **3.66**

Entry	Base	Solvent	Temp	Time	Results (*endo*-3.44:3.66)
1[J]	Cs_2CO_3 (1 equiv)	MeCN	80 °C	23 h	3.4:1
2[K]	Cs_2CO_3 (1 equiv)	MeOH	80 °C	24 h	2:1
3[L]	Cs_2CO_3 (5 mol %)	MeCN	80 °C	24 h	1:0
4[M]	DBU (5 mol %)	MeCN	145 °C (μW)	45 min	1:0
5[N]	DBU (1 equiv)	MeCN	80 °C	16 h	1.0

3.3.5.i Phase-Transfer Catalysts

We also attempted to utilize *Cinchona* alkaloid-derived phase-transfer catalysts for the alkylation of the bicyclic lactone. Trifluorotoluene was used as the solvent based on previous studies.[115] Employing Catalyst A (Figure 3.8) with Cs_2CO_3 afforded the same selectivity, indicating the catalyst had no effect on the diastereomeric ratio. However, changing the base to K_2CO_3 gave only the undesired endo diastereomer. This also occurred when Catalyst B (the pseudo-enantiomer of Catalyst A) was used. The reasons for these results are unclear, and we did not pursue this method any further as only increased amounts of undesired diastereomer were observed.

[J] [KAV-II-163]
[K] [KAV-II-139B]
[L] [KAV-III-11A]
[M] [KAV-III-11B]
[N] [KAV-II-139A]; analyzed by TLC

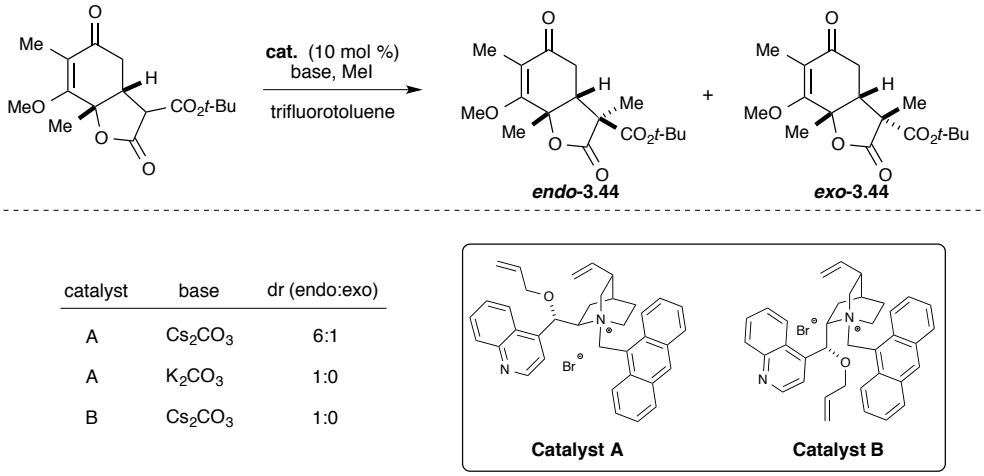

catalyst	base	dr (endo:exo)
A	Cs_2CO_3	6:1
A	K_2CO_3	1:0
B	Cs_2CO_3	1:0

Figure 3.8. Utilizing phase-transfer catalysts to induce selectivity.

3.3.5.j Biomimetic substrate

Finally, one of the more promising methods we tried was a biomimetic approach. As previously mentioned in Chapter 2, Section 2.4.3, Bringmann and co-workers deduced that the lactone and α-amide were derived from alanine, indicating the methyl group is already in place when the conjugate addition takes place. Consequently, we considered that if the methyl group were already in place on our substrate, the conjugate addition would perhaps favor the exo product. The methyl-malonic half ester was synthesized[116] and subsequently coupled to the quinol with DCC to give **3.67** in quantitative yield (Scheme 3.30). Subjecting **3.67** to basic conditions afforded bicyclic lactone **3.44**; unfortunately, very little exo product was observed.

When it became evident that we were unlikely to improve the diastereomeric ratio, we decided to continue on with the synthesis with the separate diastereomers.

Scheme 3.30. Coupling and cyclization with methyl-malonate.

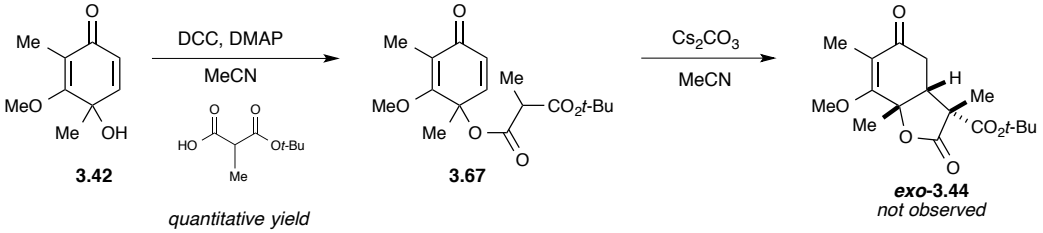

3.3.6. Synthesis of 9-*epi*-sorbicillactone A.

Because we had an abundance of the epimer, we first sought to optimize the remainder of the synthesis with this diastereomer. With **3.63** (see Table 3.5, entry 3) in hand, all that remained was removal of the methyl ether and hydrolysis of the ethyl ester. We first tried typical hydrolysis conditions to remove the ethyl ester; however, basic and acidic conditions failed (Scheme 3.31). The methyl ether can also be considered as a vinylogous ester, so we had hoped it might react differently than typical methyl ethers. Unfortunately this was not the case. We subjected **3.63** to a number of different deprotection conditions (BBr_3,[117] TMSI,[118,119,120] TMSOK[121]), but all failed to hydrolyze the ester or remove the methyl ether in any appreciable yield, and in most cases, led to decomposition or a complex mixture.

Scheme 3.31. Hydrolysis of the ethyl ester failed.

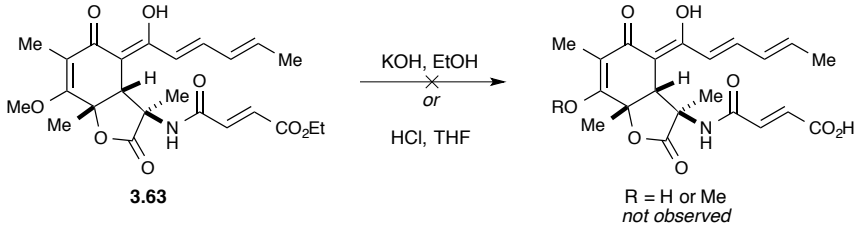

3.3.6.k Deprotection Difficulties

We began to consider a different protecting group for the fumaric acid. Switching to a *t*-butyl ester would allow for a wider variety of deprotection methods than those available for the ethyl ester. Surprisingly, the synthesis of the acid chloride was more difficult than expected. Variable and low yields were obtained each time the

reaction was performed. Eventually, we learned that the reaction conditions greatly altered the outcome; specifically, the HCl that was generated during the reaction had a detrimental effect on the product yield. This was overcome by bubbling N_2 through the reaction mixture along with adequate ventilation. Once these conditions were discovered, improved yields were obtained. However, the purity of the mono-*t*-butyl fumarate also had a significant impact. Fortunately, the acid could easily be purified by flash column chromatography.

Finally, with *t*-butyl fumaroyl chloride in hand, the new fumarate ester was appended to afford **3.68** in 56% yield (Scheme 3.32). To our delight, when **3.68** was treated with TMSI (formed in situ),[118,122] both the methyl ether and *t*-butyl ester were cleanly removed to give **3.69** in 56% yield.[O]

Scheme 3.32. Synthesis of *t*-butyl fumarate **3.68** and deprotection.

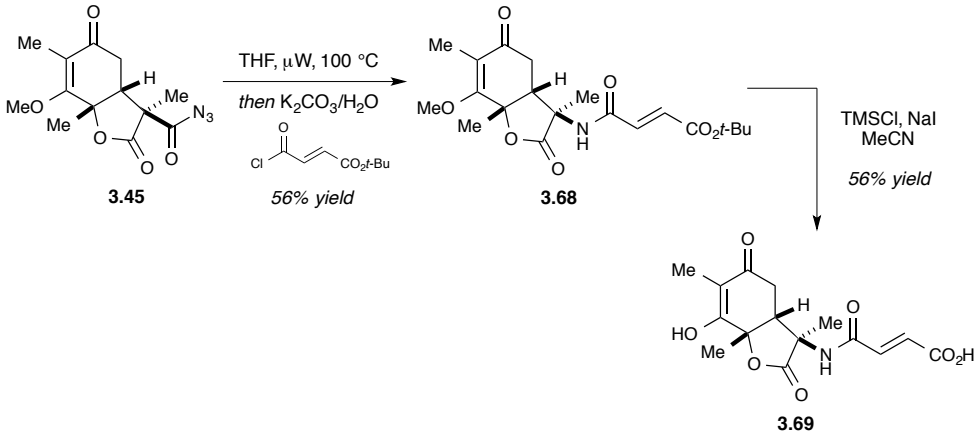

Having successfully established conditions to remove both protecting groups, the sorbyl chain was appended to **3.68** in 45% yield (Scheme 3.33). However, when **3.70** was subjected to the deprotection conditions, the TMSI failed to cleave the methyl ether, but cleanly and quantitatively afforded the acid **3.71**. It was now evident that the sorbyl chain must be playing a crucial role in the inability to remove the methyl ether. Subjecting **3.71** to BBr_3 led to decomposition. Finally, treating **3.70** with LiI in

[O] [KAV-II-137]

acetonitrile under microwave conditions gave demethylated **3.72** in 23% yield after purification.[123] This could then be subjected to the TMSI conditions to give the fully deprotected 9-*epi*-sorbicillactone A (***epi*-2.1**) in 64% yield. Fortunately, these two deprotections could be carried out in one pot, first treating **3.70** with LiI in the microwave, and then adding the NaI and TMSCl into the reaction mixture. This allowed for deprotection of the both the *t*-butyl ester and the methyl ether in one pot with an improved yield of 64%.

Scheme 3.33. Synthesis with *t*-butyl fumarate and deprotection.

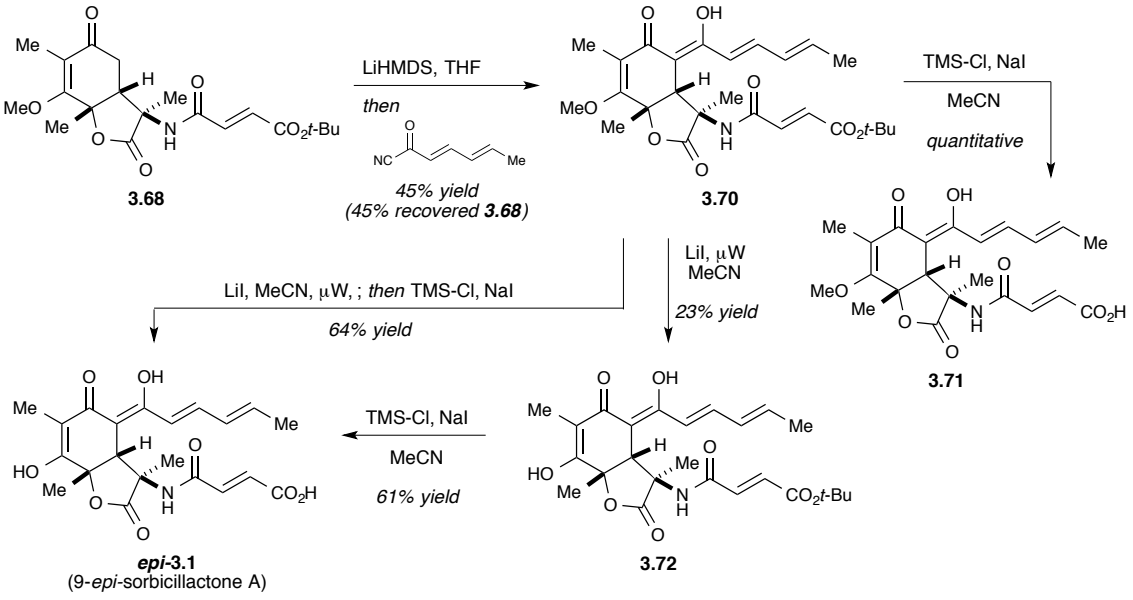

3.3.7. Synthesis of Sorbicillactone A

With the successful synthesis of 9-*epi*-sorbicillactone A, we returned to the pursuit of completing a total synthesis of sorbicillactone A. Because we were unable to persuade the cyclization-methylation sequence to favor the correct configuration, we performed the reaction on a nearly 10 g scale, which provided us with over 1 g of material with which to complete the synthesis.[P]

[P] [KAV-III-43]; [KAV-III-202]

3.3.7.l Curtius Rearrangement Troubles

Bicyclic lactone ***exo*-3.44** was converted to the acyl azide in the same fashion as the epimer, affording **3.73** in 55% yield (Scheme 3.34). Heating **3.73** in THF under microwave conditions induced the Curtius rearrangement, which was followed by addition of aqueous K_2CO_3 to quench the isocyanate to the amine. However, the amine did not react with the fumaroyl chloride under these conditions. Instead, it was necessary to isolate the amine (**3.2**) and then treat with the acid chloride and Cs_2CO_3; this produced amide **3.74** in 80% yield. The acylation of amine **3.2** proved to be much more sluggish than with the epimeric substrate. We were able to overcome this reactivity difference by extending the reaction times and using multiple additions of the fumarate. Interestingly, when the Curtius rearrangement reaction was scaled up to 500 mg, the reaction failed, producing a complex mixture of extremely polar products. Fortunately, we were able to circumvent this problem by heating the acyl azide in the presence of water to immediately quench the isocyanate, before it could undergo unwanted side reactions. Treating the amine with the fumaroyl chloride and Cs_2CO_3 as previously established afforded **3.74** in 45% yield over the two steps.

Scheme 3.34. Synthesis of amide **3.74**.

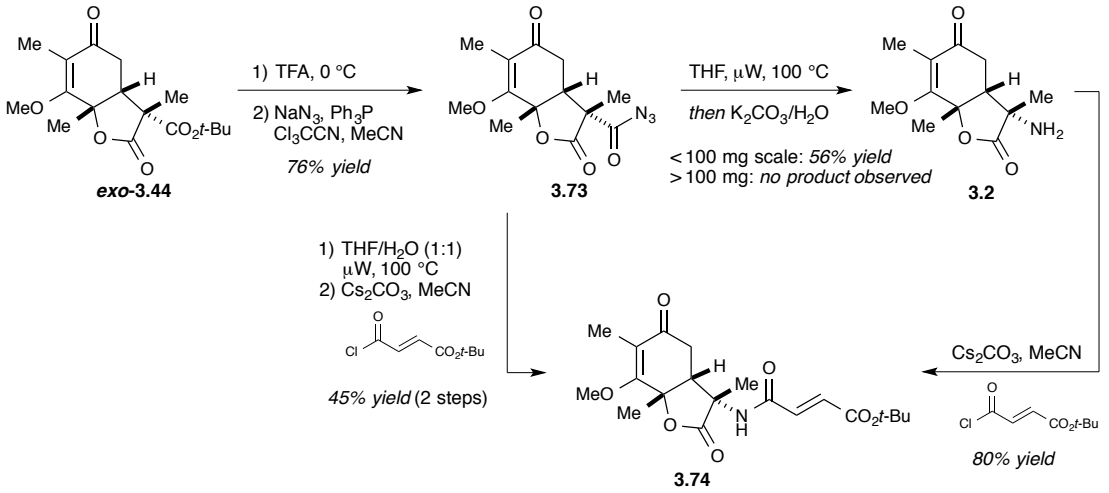

3.3.7.m Completing the Synthesis

The sorbyl chain was attached without any difficulties, producing protected sorbicillactone A (**3.75**) in a satisfying yield of 64% along with isolation of 12% starting material (Scheme 3.35). The chemical shifts of the C11 methyl group and the C6 proton in the ^{1}H NMR spectrum now closely matched the chemical shifts of the natural product, indicating that this was the correct diastereomer.

Scheme 3.35. Synthesis of **3.75** and ^{1}H NMR comparison with the natural material (in d_6-acetone).

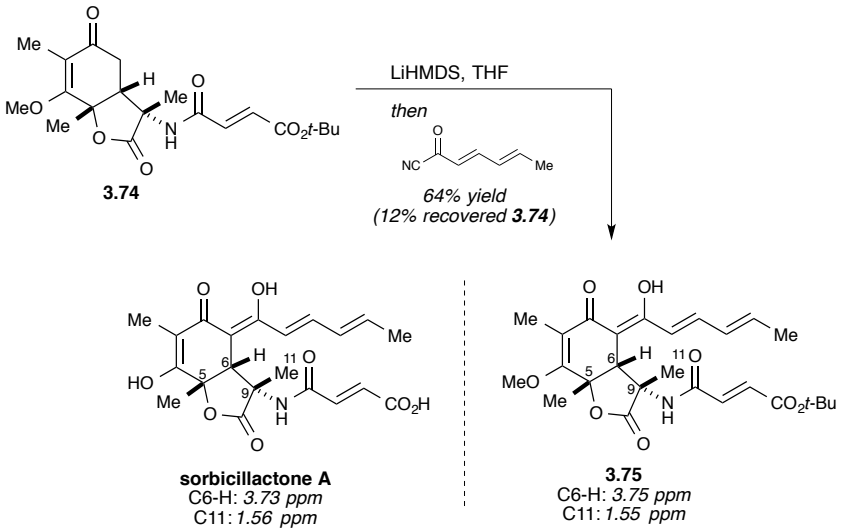

The first time the deprotection sequence was applied to **3.75**, sorbicillactone A was produced in a quantitative crude yield; however, after purification attempts the product quickly decomposed and only a 14% yield was obtained (Scheme 3.36). Unfortunately, the deprotection conditions were also unreliable; we were unable to successfully repeat the reaction. Therefore, the deprotection sequence needed to be altered. This was accomplished by reversing the order of deprotection. First treating **3.75** with TFA (neat) at room temperature afforded acid **3.76**. We were able to obtain quality spectral data for **3.76**, which, except for the presence of the vinylogous methyl ester, closely resembled the data for sorbicillactone A. Treating **3.76** with LiI under the microwave conditions caused the substrate to completely decompose. We found that adding 2,6-lutidine helped keep the mixture from becoming too acidic. Lowering the temperature to 80 °C and using conventional heating also proved to be beneficial. Once again, we were able to obtain a decent crude ^{1}H NMR spectra, but purification attempts left us with decomposed yellow material. Several different methods were attempted, including size-exclusion gel filtration (Sephadex) and reverse-phase prep HPLC. In all cases, we found that in our hands sorbicillactone A rapidly decomposed after deprotection. This could be due to a number of reasons, including the close proximity of the amide to the vinylogous acid as well as the harsh deprotection conditions.

Although these were very disappointing results, we learned that the C9 stereocenter must be the reason for the instability of sorbicillactone A, as the epimer has proven to be very stable. Perhaps the epimer would make a better candidate for drug discovery efforts – it would be very interesting to obtain biological data to compare to the natural product.

Scheme 3.36. Synthesis of sorbicillactone A.

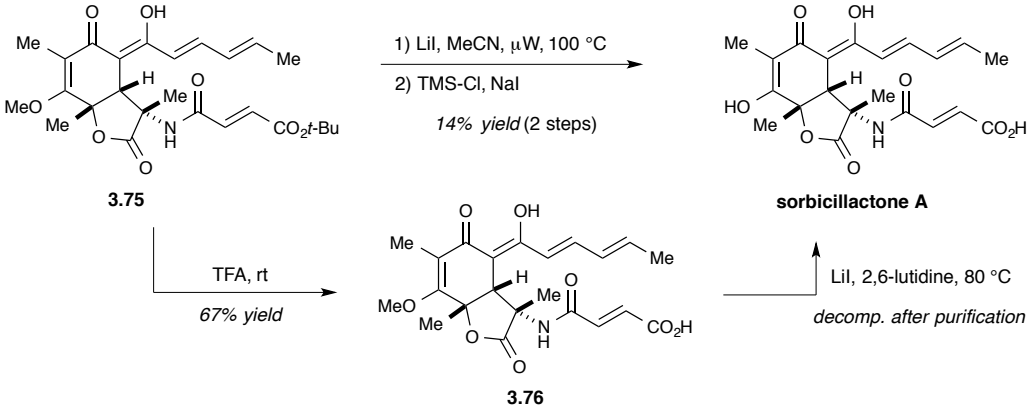

3.3.8. Completion of Synthesis of the Model Substrate

With the synthesis of the natural product complete and the stereochemistry determined, the model substrate was revisited utilizing the new methods that were discovered. The endo bicyclic structure (***endo*-3.19**) was converted to the acyl azide in 62% yield followed by the Curtius rearrangement with *t*-butyl fumaroyl chloride to give **3.77** in 56% yield. Next, the sorbyl chain was appended under similar conditions as previously, however, the temperature was kept at –98 °C. This could have contributed to the lower yield of **3.78** and a large recovery of the starting material (**3.77**). Finally, the *t*-butyl ester was removed with TFA to give the deprotected model substrate (**3.79**) in 39% yield after purification by column chromatography. Interestingly, when these steps were attempted with ***exo*-3.19**, the Curtius rearrangement was unsuccessful. These results indicate that the lack of the vinylogous ester with the exo configuration may be leading to additional unwanted reactions due to the more exposed and less hindered enone.

Scheme 3.37. Synthesis of the endo model substrate.

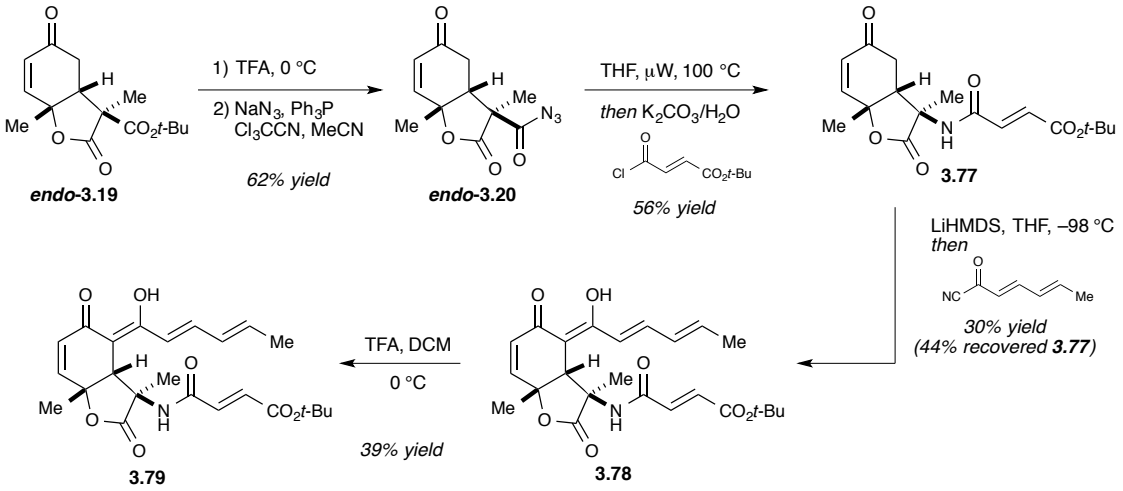

CHAPTER 4

ORIGIN OF STEREOSELECTIVITY OF THE ALKYLATION OF CYCLOHEXADIENONE-DERIVED BICYCLIC MALONATES[§]

4.1 INTRODUCTION

Recently, we have further investigated the intriguing selectivity that was observed during the cyclization/alkylation reaction of bicycle **4.1** that resulted with ***endo*-4.3**[†] being the major product (Scheme 4.1). The stereoselectivity displayed in this reaction sequence was quite surprising considering that formation of the major diastereomer (***endo*-4.3**) requires the electrophile to approach bicyclic malonate anion **4.2** from the seemingly more crowded endo (concave) face. This is counter to what is commonly perceived as a reliable strategy for stereoinduction.[124] Indeed, a search of the literature revealed that alkylations of similar bicyclic lactones typically do proceed from the exo (convex) face.[125,126,127] At the time, we had tried several experiments attempting to alter the diastereoselectivity, but to no avail. In the end, we reluctantly accepted the unfavorable dr and concentrated on carrying each diastereomer forward with the total synthesis. With the completion of the natural product, we returned to the

[§] This chapter is based on previously published work: Volp, K. A.; Harned, A. M. Origin of Stereoselectivity of the Alkylation of Cyclohexadienone-Derived Bicyclic Malonates. *J. Org. Chem*. **2013**, *78*, 7554–7564.

[†] Throughout this chapter, the terms endo and exo are being used to describe the orientation of the C7 alkyl group relative to the cis-fused bicyclic ring.

question of why were we seeing this unexpected diastereoselectivity? The discovery of examples that run counter to established models provides an opportunity to further refine these models and deepen our understanding of stereoselective processes in general.

This chapter highlights our efforts toward understanding the reason behind the selectivity by systematically analyzing how base, solvent, and structure affect the stereochemical outcome. We conducted our investigation experimentally as well as computationally.

Scheme 4.1. Diastereoselectivity of the cyclization/alkylation of sorbicillactone substrate **4.1**.

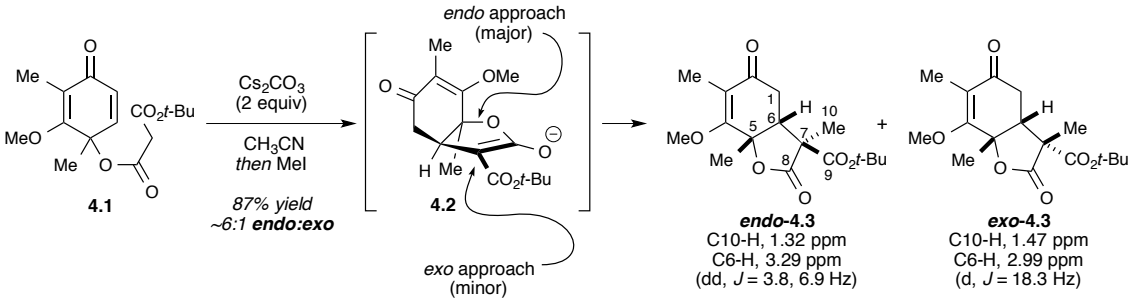

4.2 RESULTS AND DISCUSSION

For this project, we were concentrating on the stereochemical outcome of the alkylation reaction. Therefore, we needed a substrate that would focus on the reaction in question, as well as be easily accessible. The model substrate we used for the sorbicillactone studies was a suitable candidate, as it did not have extraneous substituents that would interfere with or alter results. Although we had performed the cyclization-alkylation sequence, we had not fully recognized the diastereoselectivity that was occurring; we also did not establish the stereoconfiguration of each diastereomer at that time. Consequently, we repeated the reaction with the model substrate that was derived from *p*-cresol to confirm that the same dr was observed as the sorbicillactone substrate (Scheme 4.2). Indeed this was the case. The reaction proceeded with the same level of diastereoselectivity as the original system (i.e., **4.1** → **4.3**). The identity of ***endo*-4.5** and ***exo*-4.5** was established by comparing the chemical

shifts of the methyl groups and C6 methyne protons in **4.5** with those of the analogous protons in **4.3** (refer to Scheme 4.1), the structure of which was established through X-ray analysis of a derivative (see Chapter 3, Figure 3.6).

Scheme 4.2. Cyclization/alkylation sequence with the model substrate.

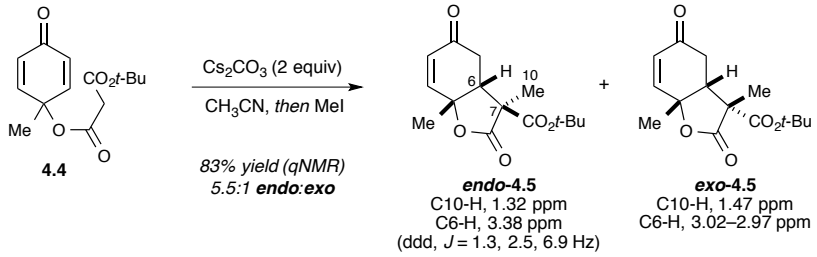

Confirming that the cyclization/alkylation of **4.4** is indeed a valid model reaction, it was subsequently cyclized to give bicyclic malonate **4.6** (Scheme 4.3) in order to evaluate the influence of reaction conditions during the alkylation event. Bicycle **4.6** had previously been synthesized during a related methodology study.[128] With **4.6** in hand, we proceeded with our analysis.

Scheme 4.3. Cyclization of dienone **4.4** afforded the substrate needed for experimental analysis.

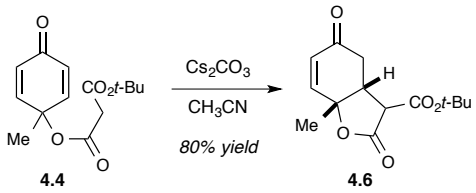

4.2.1. Experimental Results

4.2.1.a Model system: Influence of reaction conditions.

First, we sought to evaluate the influence of solvent on the stereochemical outcome of the alkylation reaction. However, we had presumed that the cyclization/alkylation process proceeded with the conjugate addition occurring first, resulting in a bicyclic anion being alkylated, rather than the alkylation initially occurring followed by the cyclization. To ensure the validity of this hypothesis, we employed the same reaction conditions as the cyclization/alkylation sequence. This

indeed seemed to be the case, as the alkylation of **4.6** in acetonitrile proceeded to give **4.5** with the same diastereoselectivity as the one-pot process (Table 4.1, entries 1 and 2). We proceeded forward with our solvent screen beginning with changing the solvent from acetonitrile to DMF, had a negligible influence on the endo:exo ratio (entry 3). In contrast, using a solvent of either moderate (acetone) or low polarity (CH_2Cl_2) proceeded with lower endo selectivity (entries 4 and 5). Curiously, all ethereal solvents (entries 6–11) had diminished endo selectivity, irrespective of their polarity (entries 6, 9–11) or conversion (entries 7–9). Modified reaction conditions were required when methyl *t*-butyl ether (MTBE) was used as solvent (entry 11).

Table 4.1. Influence of solvent on diastereoselectivity.

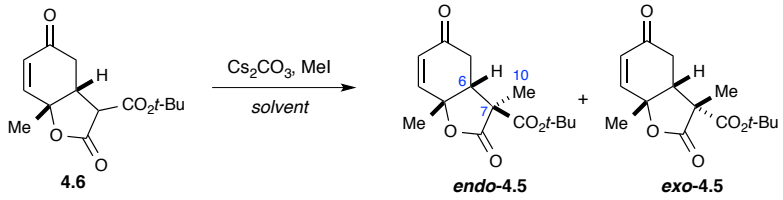

entry[a]	solvent	dielectric constant[b]	time (h)	% conversion[c]	dr (endo:exo)[c]	% yield[d]
1	CH_3CN	36.64	2	79	5.3:1	65
2	CH_3CN	36.64	6	100	5.5:1	93
3	DMF	38.25	18	100	5.8:1	95
4	acetone	21.01	5.5	100	3.7:1	89
5	CH_2Cl_2	8.93	24	71	3.6:1	60
6	DME	7.30	12	100	1.6:1	93
7	THF	7.52	2	58	1.5:1	51
8	THF	7.52	6	84	1.5:1	76
9	THF	7.52	14	100	1.5:1	91
10	dioxane	2.22	18	84	1.3:1	66
11[e]	MTBE	~ 4[f]	48	96	1.7:1	71

[a] All reactions performed at rt using 0.131 mmol **4.6**, 1.2 equiv Cs_2CO_3, and 1.2 equiv MeI in the listed solvent (0.08 M). [b] Values obtained from ref 129. [c] Measured by HPLC. [d] Combined yield calculated by quantitative NMR (qNMR), Ph_3CH as an internal standard. [e] After 24 h at rt, the temperature was raised to 60 °C and stirred for another 24 h. [f] The dielectric constant of MTBE has not been reported. The estimated value is based on the dielectric constant of diethyl ether (4.27) and diisopropyl ether (3.81).

The choice of base had a complex influence on both reaction efficiency and diastereoselectivity (Table 4.2). Switching from Cs_2CO_3 to K_2CO_3 lowered

diastereoselectivity of the alkylation (entries 1 and 2). In contrast, the strong amine base DBU resulted in somewhat higher diastereoselectivity, albeit with diminished reactivity (entry 6). No reaction was observed with Na_2CO_3, Li_2CO_3, or MgO (entries 3–5), likely due to a lack of solubility.

The use of DBU presumably results in a coordination environment that is much different from that formed when inorganic bases are used. To further explore this, the reaction was performed with K_2CO_3 in the presence of 18-crown-6, in order to make the counterion less coordinating. This increased the diastereoselectivity to levels consistent to those obtained with the amidine base (compare entries 2, 6, 7). Based on this success, we then returned to the use of ethereal solvents. Using K_2CO_3 with 18-crown-6 in THF increased the amount of ***endo*-4.5** produced, relative to Cs_2CO_3 in THF (compare Table 4.2, entry 8 with Table 4.1, entry 9). To study the influence of additives with Cs_2CO_3, increasing amounts of HMPA was added. Lower concentrations of HMPA had little impact on the diastereoselectivity (compare Table 4.1, entry 9 and Table 4.2, entry 9), but higher concentrations resulted in an increase in the amount of ***endo*-4.5** produced (entry 10).

The final base examined was NaH in THF. This reaction was sluggish and resulted in no diastereoselectivity (Table 4.2, entry 11). Another notable observation was that the selectivity at partial and full conversion was the same (Table 4.1, entries 1, 2, 7–9). This suggests that epimerization through a retro-Michael process is not important.[130]

Table 4.2. Influence of base.

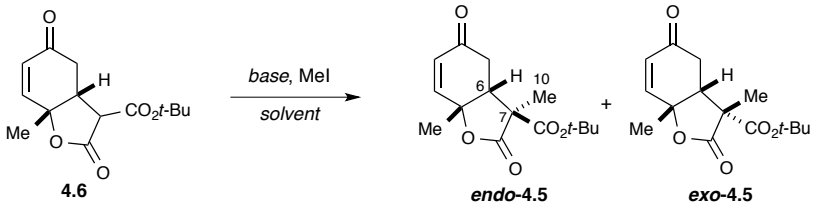

entry[a]	base	solvent	time (h)	% conversion[b]	dr (endo:exo)[b]	% yield[c]
1	Cs_2CO_3	CH_3CN	6	100	5.5:1	93
2	K_2CO_3	CH_3CN	16	88	4.6:1	85
3	Na_2CO_3	CH_3CN	16	0	–	–
4	Li_2CO_3	CH_3CN	16	0	–	–
5	MgO	CH_3CN	16	0	–	–
6	DBU	CH_3CN	16	45	6.2:1	43
7[d]	K_2CO_3/ 18-crown-6	CH_3CN	24	100	6.4:1	88
8[d]	K_2CO_3/ 18-crown-6	THF	24	94	3.3:1	74
9	Cs_2CO_3	THF/HMPA (10:1)	30	100	1.6:1	82
10	Cs_2CO_3	THF/HMPA (1:1)	30	92	3.1:1	67
11[e]	NaH	THF	48	100	0.9:1	79

[a] All reactions performed at rt using 0.131 mmol **4.6**, 1.2 equiv of the listed base, and 1.2 equiv MeI in the listed solvent (0.08 M). [b] Measured by HPLC. [c] Combined yield calculated by qNMR, Ph_3CH as an internal standard. [d] 1.2 equiv 18-crown-6 was used. [e] After 24 h at rt, the temperature was raised to 60 °C and stirred for another 24 h.

4.2.1.b Influence of electrophile.

Having examined the influence of both solvent and base, we turned our attention to the electrophile (Table 4.3). Given the high degree of endo selectivity observed with MeI, we were surprised to find that all other carbon-based electrophiles were quite selective toward formation of the exo diastereomer.[131] Only allyl bromide gave any appreciable amount of the endo isomer (entry 4). Although these results were quite disparate from that obtained with MeI, it was gratifying to see that our original hypothesis of alkylation from the convex (exo) face was not without merit. Rather, it

became clear that the use of MeI with these particular nucleophiles was an unusual case that warranted closer attention.

Table 4.3. Influence of electrophile on diastereoselectivity.

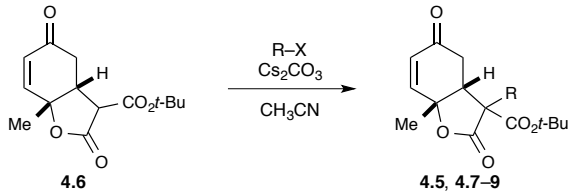

entry[a]	electrophile (R–X)	product	dr (endo:exo)[b]	% yield[c]
1	MeI	**4.5**	5.5:1	93
2	BnBr	**4.7**	<1:20	92 (89)[d]
3[e]	2-iodopropane	**4.8**	<1:20	19[d]
4	allyl bromide	**4.9**	1:6.3	89 (81)[d]

[a] All reactions performed at room temperature using 0.131 mmol **4.6**, 1.2 equiv Cs_2CO_3, and 1.2 equiv electrophile in acetonitrile (0.08 M) for 16 h. [b] Calculated by ^{1}H NMR of the crude material and confirmed by HPLC. [c] Combined yield calculated from qNMR, Ph_3CH used as an internal standard. [d] Isolated yield after purification by flash column chromatography (SiO_2). [e] Reaction performed at 80 °C for 6 days.

4.2.1.c Influence of nucleophile.

Finally, we decided to test other bicyclic malonates as nucleophiles. The results of this study are reported in Table 4.4. Switching the *t*-butyl ester for a benzyl ester (**4.10**, entry 3) resulted in a slight increase in the endo:exo ratio. Adding a methyl group to the β-position of the enone (**4.12**, entry 4) had little influence on the diastereoselectivity. Alkylation of the same substrate in THF resulted in diminished selectivity (entry 5), matching the results observed with the model substrate (entry 2). We were also interested in whether these same solvent effects would result in an increase in the formation of the desired exo isomer using our sorbicillactone substrate. Gratifyingly, the alkylation of **4.14** proceeded with diminished endo selectivity when Cs_2CO_3 or NaH were used in THF (compare entries 6, 7 with Scheme 4.1).

Table 4.4. Influence of nucleophile on diastereoselectivity.

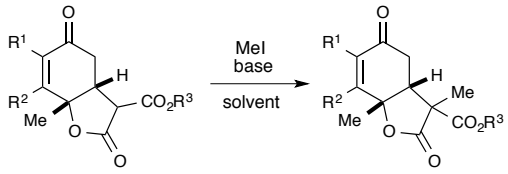

entry[a]	substrate	product	R^1	R^2	R^3	base	solvent	dr (endo:exo)[b]	% yield[c]
1	**4.6**	**4.5**	H	H	*t*-Bu	Cs_2CO_3	CH_3CN	5.5:1	93
2	**4.6**	**4.5**	H	H	*t*-Bu	Cs_2CO_3	THF	1.5:1	91
3[d]	**4.10**	**4.11**	H	H	Bn	Cs_2CO_3	CH_3CN	7.9:1	85
4	**4.12**	**4.13**	H	Me	*t*-Bu	Cs_2CO_3	CH_3CN	6.5:1	88
5	**4.12**	**4.13**	H	Me	*t*-Bu	Cs_2CO_3	THF	1.5:1	80
6	**4.14**	**4.3**	Me	OMe	*t*-Bu	Cs_2CO_3	THF	2.5:1	82
7[e]	**4.14**	**4.3**	Me	OMe	*t*-Bu	NaH	THF	1.8:1	40 (60)[f]

[a] All reactions performed at rt using 0.13 mmol of the substrate, 1.2 equiv base, and 1.2 equiv MeI in the listed solvent (0.08M) for 16 h. [b] Calculated by achiral HPLC. [c] Combined yield calculated by qNMR, Ph_3CH as an internal standard. [d] Performed using 0.07 mmol of the substrate. [e] After 24 h at rt, the temperature was raised to 60 °C and stirred for another 24 h. [f] Calculated yield based on presence of 38% starting material.

4.2.2. Computational Results

In order to better understand the origin of the stereoselectivity observed with MeI, we performed molecular modeling of several key structures. Specifically, the structures of the deprotonated malonate, diastereomeric products, and alkylation transition states for the model transformation shown in Scheme 4.5 were considered. Calculations were performed at both the M06-2X[132] and B3LYP[133] level using the 6–31G(d)[134] basis set (see Experimental Section for more details). In order to simplify the calculations, MeI was replaced with MeCl during the transition state analysis.[135] In general, the computational results using M06-2X and B3LYP led to somewhat different energy differences. This is likely due to the ability of the former to better handle both noncovalent interactions (to include dispersion binding forces and solvation)[136,137,138,139,140,141] and transition state analysis.[142,143] Importantly, both methods led to the same conclusions. Wherever relative energy differences are reported, results from B3LYP are given in parentheses.

Scheme 4.4. Alkylation with methyl chloride.

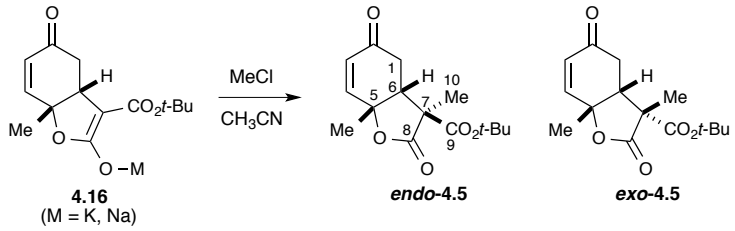

4.2.2.d Structure of the deprotonated bicyclic malonate.

As stated above, the diastereoselectivity of the alkylation was surprising given that the major diastereomer seemingly arises from the more sterically crowded face of the intermediate bicyclic anion. This supposition was evaluated by modeling malonate anion **4.16** in the presence of either a Na or K cation.[144] Three potential cation coordination modes were examined (Figure 4.1a): one syn conformation (**4.16S**) and two anti conformations (**4.16A$_1$** and **4.16A$_2$**).[145] With both Na and K, coordination of the metal via syn conformation **4.16S** was clearly preferred over coordination through either anti conformation. Qualitatively, the concave face (endo approach) of **4.16S** appeared to be more sterically crowded than the convex face (exo approach) due to the cyclohexenone ring being roughly perpendicular to the plane formed by the metal-coordinated malonate anion (Figure 4.1b and 4.1c). This analysis confirmed that our initial hypothesis, with respect to which face is more sterically accessible, was not flawed. It also confirms that the observed stereoselectivity is likely due to a confluence of factors, rather than a pure steric influence.

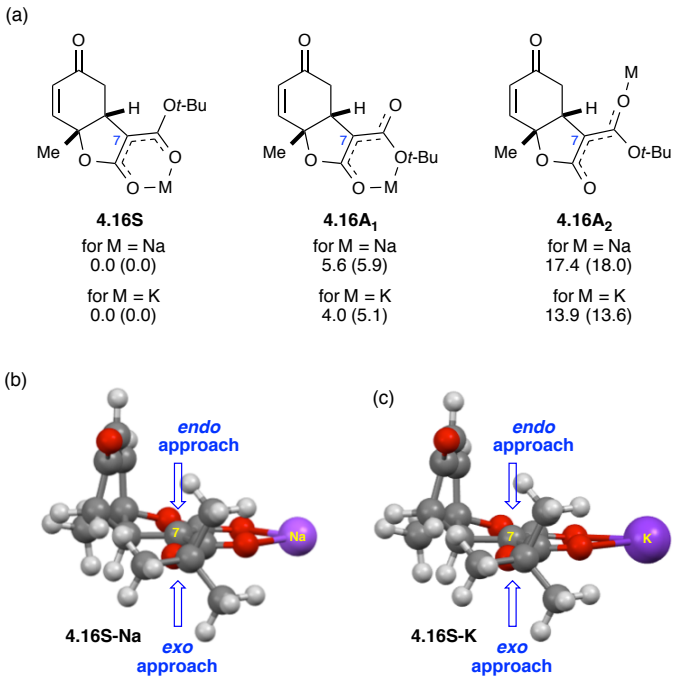

Figure 4.1. (a) Structure of the sodium and potassium malonates. Values below each structure are relative energies (kcal/mol) calculated by M06-2X (B3LYP). (b) Side view of the calculated (M06-2X) structure of 16S, M = Na. (c) Side view of the calculated (M06-2X) structure of 16S, M = K. Front views and structures calculated using B3LYP can be found in the supporting information.

4.2.2.e Relative energy of alkylated products.

We also considered the possibility that an unidentified equilibration process was responsible for the observed product distribution. This was evaluated by considering the relative energies of the alkylation products ***endo*-4.5** and ***exo*-4.5** (Figure 4.2). In order to account for conformational flexibility with the exocyclic ester, a relaxed scan around the C7–C9 σ-bond was performed (see Experimental Section for details). Neither method (M06-2X or B3LYP) produced results that were entirely consistent with our experimental findings. Using M06-2X, diastereomer ***exo*-4.5** was found to be lower in energy than ***endo*-4.5** (the major diastereomer produced during the experiment). Conversely, when B3LYP was used, diastereomer ***endo*-4.5** was lower in energy but the magnitude was not entirely consistent with the observed selectivity. These results indicated that the observed selectivity was likely not due to product equilibration,[130]

instead they pointed toward a difference in transition state structure as the source of the observed selectivity.

Figure 4.2. Relative energy (kcal/mol) of the lowest energy conformers of ***endo*-4.5** and ***exo*-4.5**. Energies below each structure are calculated by M06-2X (B3LYP).

4.2.2.f Transition state structures.

Because syn malonate salt **4.16S** was found to be lower in energy than either anti malonate isomer (Section 2.2.1), only transition states arising from **4.16S** were fully considered.[146] Transition state calculations (using both M06-2X and B3LYP) for the endo and exo approach were performed with both Na and K counterions. These are shown (for M = K) in Figure 4.3, along with the final structures optimized using M06-2X.

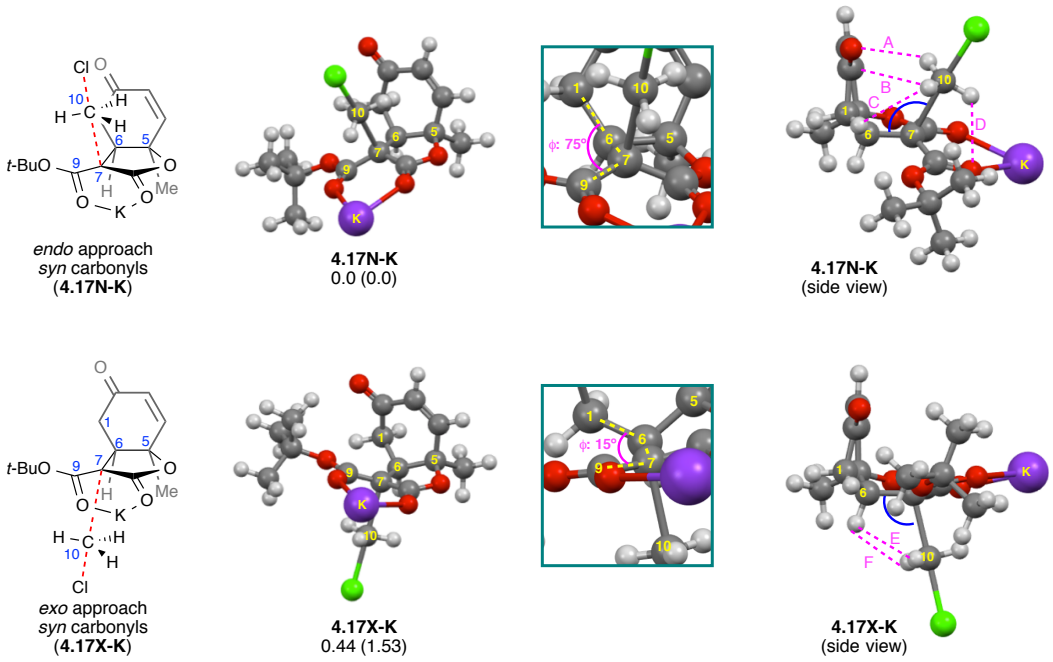

Figure 4.3. Structure of the calculated transition states incorporating a K counterion. Only structures optimized with M06-2X are shown. Values below the middle structures are relative energies (kcal/mol) calculated by M06-2X (B3LYP). Carbon numbering is the same as that shown in Scheme 4.5. The blue lines represent the C6–C7–C10 angle. The pink dashed lines represent through space distances.

Both M06-2X and B3LYP returned endo transitions states (**4.17N-K**) that were lower in energy than the corresponding exo transition states (**4.17X-K**). The $\Delta G^{\ddagger}$ obtained with M06-2X (0.44 kcal/mol) was slightly smaller than that obtained with B3LYP (1.53 kcal/mol) and is more consistent with the level of diastereoselectivity observed during the reaction. Closer inspection of the two transition states revealed the basis for their energy difference. As shown in Figure 4.3 (insets), the C7 carbon atom (the nucleophile) of transition state **4.17N** is in a staggered orientation. In contrast, the C7 carbon atom in transition state **4.17X** is in an eclipsed orientation; this is evident by measuring the C9–C7–C6–C1 dihedral angle (Table 4.5 and Table S2). In **4.17N-K** this angle is ~75º but is only ~15º in **4.17X-K**. Similar angles can be found in the transition state of the sodium salt. The compression of this dihedral angle introduces torsional strain into the system, which in turn raises the energy of the exo transition states. These

observations are quite similar to the "torsional steering" model advanced by Houk and co-workers.[147,148] This model has proven effective for rationalizing the stereoselectivity of several different reaction types, including: epoxidation,[149,150,151] dihydroxylation,[152] Mannich-type reactions,[153] Diels-Alder reactions,[154] iodocyclizations,[155] and Michael additions of β-iminoesters[156] and iodocyclizations. Torsional effects have also been used to explain[157] the unexpected diastereoselectivity observed by Meyers and co-workers during α-alkylations of chiral lactams.[158,159,160]

Table 4.5. Selected measurements of the transition states incorporating a K or Na counterion that were calculated using M06-2X.

C7–C10/C10–Cl bond length (Å)				
4.17N-K	2.243/2.230		**4.17X-K**	2.207/2.237
4.17N-Na	2.233/2.246		**4.17X-Na**	2.194/2.249
C9–C7–C6–C1 dihedral angle (º)				
4.17N-K	75.2		**4.17X-K**	14.6
4.17N-Na	75.1		**4.17X-Na**	12.1
C6–C7–C10 angle (º)				
4.17N-K	115.0		**4.17X-K**	103.9
4.17N-Na	114.7		**4.17X-Na**	103.5
Distance A (C10H–C3, Å)				
4.17N-K	2.715		**4.17N-Na**	2.706
Distance B (C10H–C2, Å)				
4.17N-K	2.775		**4.17N-Na**	2.770
Distance C (C10H–C1H, Å)				
4.17N-K	2.666		**4.17N-Na**	2.678
Distance D (C10H–O, Å)				
4.17N-K	2.500		**4.17N-Na**	2.558
Distance E (C10H–C6H, Å)				
4.17X-K	2.548		**4.17X-Na**	2.502
Distance F (C10H–C6H, Å)				
4.17X-K	2.302		**4.17X-Na**	2.310

Even with less torsional strain being present in **4.17N**, there is still the question of potential steric hindrance during endo approach of the electrophile. One explanation for this is shown at the bottom of Figure 4.3. Here the structures of **4.17N-K** and **4.17X-K** are rotated 90º. Upon inspection, the C6–C7–C10 bond angle appears to be

larger in the endo transition state than in the exo transition state. This is confirmed by the measurements (Table 4.5 and S2). In **4.17X-K** this angle is ~104º, while in **4.17N-K** this angle is ~115º. It is plausible that by approaching at a larger angle, the electrophile can not only engage in a staggered transition state but also avoid potential steric clashes with the cyclohexenone ring. Further evidence for this can be found by measuring the closest neighbors to the three hydrogen atoms of C10 (pink dashed lines in Figure 4.3). In **4.17N-K** the closest contact (distance D, 2.50 Å) is between the C10 hydrogen atom and one of the malonate oxygen atoms (Table 4.5 and S2). There are also contacts between the C10 hydrogen atoms and C3 and C2 (distances A and B) that are closer than the sum of the Van der Waal radii (2.9 Å).[161] Distance C, between one C10-H and C1-H, is outside the sum of the Van der Waal radii for two hydrogen atoms (2.4 Å),[161] and is likely unimportant. All other measurements from the C10 hydrogen atoms are >2.8 Å. In contrast, with **4.17X-K** there are close contacts between two C10 hydrogen atoms and the C6 hydrogen atom (2.30–2.55 Å). In both cases, these distances are shorter than those found in endo transition states. The distance between the C10-H and the malonate oxygen atoms in **4.17X-K** (2.725 and 2.729 Å, not shown) is slightly larger than the sum of the Van der Waal radii (~2.7 Å)[161] and are likely unimportant. Overall, this analysis implies that with a small electrophile like MeI, the endo transition state is favored on both torsional and steric (through-space) grounds.

These same measurements also explain why electrophiles larger than MeI prefer an exo approach (Table 4.3). Clearly, any extended carbon chain on C10 will orient itself away from the cyclohexenone ring during endo approach. However, the C6–C7–C10 bond angle preferred by transition states **4.17N** means that any extended carbon chain will be oriented toward the exocyclic ester of the malonate nucleophile. Alternatively, approach from the exo direction will allow the carbon chain to be oriented away from the exocyclic ester. Thus, larger electrophiles will experience decreased through-space steric interactions when engaging the malonate anion from an exo approach, compensating for the energetic cost associated with the torsional strain of the exo transition state.

What is not adequately addressed by our calculations is the observed influence on the diastereoselectivity by solvent (Table 4.1). As stated before, the observed selectivity does not correlate well with solvent polarity. More specifically, reactions performed in ethereal solvents demonstrated greatly diminished endo selectivity, regardless of their polarity. This is likely related to the Lewis basic nature of the oxygen atoms that are necessarily present. One possible explanation is that coordination of the solvent to the metal cation in **4.16S** creates a solvent shell that blocks access to the endo face of the malonate. While a coordinated solvent shell is certainly possible with acetonitrile, the shape of the shell formed will be quite different. This difference is related to the hybridization of the Lewis basic atoms involved. Coordination of a linear acetonitrile through an sp-hybridized nitrogen would result in a solvent shell that is shaped much differently from that formed by coordination of an ether molecule through an sp^3-hybridized oxygen atom.

Another possibility is that relative differences in Lewis basicity between the various solvents[162] are able to influence the coordination of the malonate anion to the metal cation, and any solvent shell that accompanies it. Some evidence for this can be found with our experiments in the presence of known metal chelators. For instance, when 18-crown-6 was used with K_2CO_3, the endo selectivity increased (Table 4.2, entries 7 and 8). Similarly, adding increasing amounts of HMPA also results in increased endo selectivity in THF (Table 4.2, compare entries 9 and 10). Given the small energy differences involved and the inherent errors associated with solvation models,[163] using computational methods to rationalize our observations does not seem to be reasonable at this time.[164] Moreover, testing the hypotheses proposed above would likely require the use of explicit (atomistic) solvent molecules, which would significantly increase the computational cost.

4.2.3. Further Experimental Results

4.2.3.g Comparison With Literature Examples.

The computational results described above have uncovered several factors that influence the stereochemical outcome of alkylation reactions involving cyclohexadienone-derived bicyclic malonates. However, they do not fully explain why our results with MeI differ so much from the literature reports on similar alkylations, selected examples[125–127] of which are shown in eq 1–4. While details regarding the diastereoselectivity cannot be found with all of these literature examples, they are all overwhelmingly exo-selective.

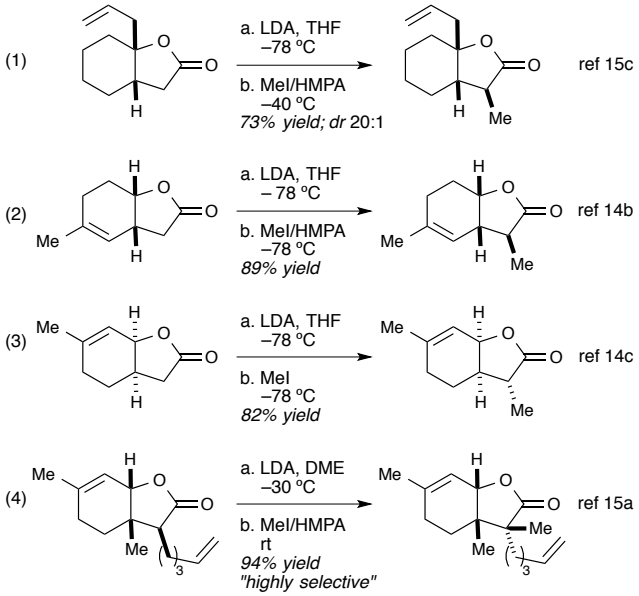

There are two aspects of these reactions that might contribute to their exo preference. First, all of the literature examples were performed with LDA in ethereal solvents. Unfortunately, lithium bases were not successful in promoting our alkylation reaction (Table 4.2), so at this time we can only speculate on the influence of the lithium cation. However, we have found that ethereal solvents have a profound influence on the diastereoselectivity (Table 4.1). More specifically, they lead to more exo selective reactions.

The second potentially important difference between our alkylation and the literature examples is a structural one. Comparing **4.6** and the conjugate acid of **4.2** to the literature examples revealed that ours is the only system with three sp^2 carbons in the six-membered ring. This imparts a great deal of planarity to the ring. In contrast, the extra sp^3 carbons present in the literature reports (eq 1–4) would be expected to increase steric interactions between a methyl group approaching the enolate from the concave face and the six-membered ring (i.e., shorten distance A and/or B in Figure 4.3). It stands to reason that adding even one more sp^3-hybridized carbon atom to the six-membered ring would increase steric interactions with the incoming electrophile to such an extent that they can override the torsional strain associated with the exo approach. Houk and co-workers have found that steric control can outweigh torsional steering during the alkylation of certain substrates.[165]

4.2.4. Manipulating the steric environment.

The level of diastereoselectivity observed during the studied alkylation reactions suggest that the difference between the energetic gains afforded by a staggered transition state and the unfavorable sterics of an endo approach are quite small. This is supported by the free energy differences obtained from our calculations. These results, coupled with the ability to manipulate the steric environment of an α,β-unsaturated ketone, suggest that the structure of our substrates can be manipulated to override the inherent stereoselectivity observed with MeI.

This hypothesis was tested as shown in Scheme 4.6. Enone **4.6** was hydrogenated with Pd/C to provide cyclohexanone **4.18**. The malonate in **4.18** was then alkylated to afford an inseparable mixture of ***endo*-4.19** and ***exo*-4.19**. The structural assignment of the alkylated products was accomplished by comparing the chemical shifts of the methyl groups in ***endo*-4.19** and ***exo*-4.19** with those of the methyl groups in ***endo*-4.5** and ***exo*-4.5**. This assignment was confirmed by hydrogenating purified samples of ***endo*-4.5** and ***exo*-4.5**. Gratifyingly, when the alkylation of **4.18** was performed in acetonitrile, a diastereomeric ratio of 4.9:1 favoring ***exo*-4.19** was

observed. Interestingly, when the solvent was changed to THF, the diastereoselectivity increased to 12.3:1, again favoring ***exo*-4.19**. The finding that the alkylation of saturated ketone **4.18** with MeI is selective for the exo diastereomer confirms that the enone in **4.6** (and by extension **4.2**) plays an important role in making the endo approach accessible to small electrophiles.

Scheme 4.5. (a, b) Hydrogenation of each diastereomer separately. (c) Hydrogenation of **4.6** and subsequent alkylation in different solvents.

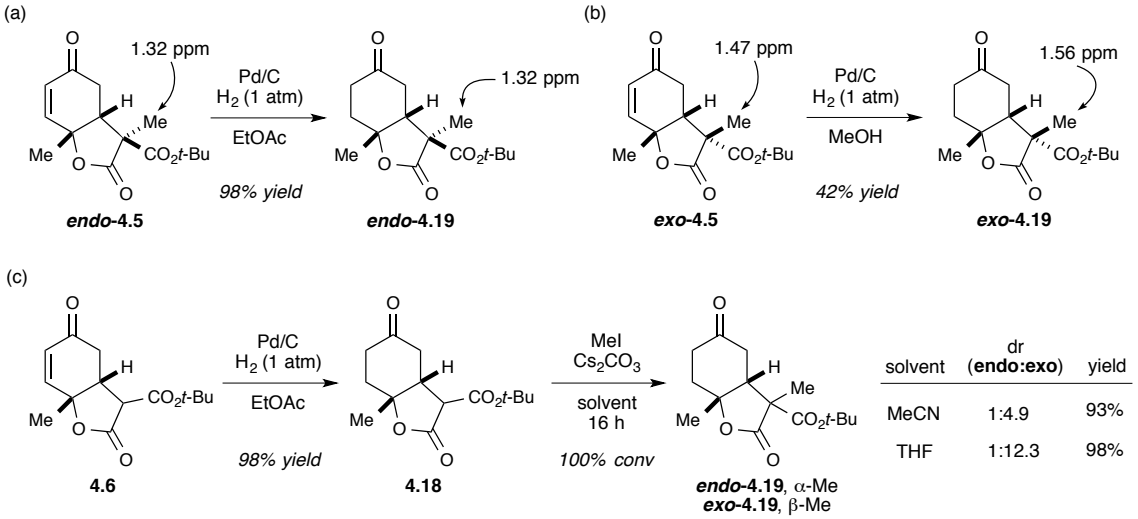

4.2.5. Conclusions

Our studies have revealed the origin for the endo selectivity observed during alkylation reactions of cyclohexadienone-derived bicyclic malonates with MeI. This result can be traced to an energetically favorable endo transition state that experiences less torsional strain. This is in line with the torsional steering model advanced by Houk and co-workers. However, the line between the favorable energetics offered by a staggered transition state and unfavorable steric interactions is razor thin. With even a modest increase in electrophile size, the steric penalties accrued during an endo trajectory are such that they force the electrophile to take an exo approach. Similar steric arguments can be used to explain why our observed diastereomeric ratios with MeI differ significantly from literature examples with otherwise very similar substrates. These arguments are related to the planarity and rigidity that arise from replacing one

sp^3 carbon (in the literature cases) with an sp^2 carbon (in the present case) in a fused 5,6 ring system. This slight decrease in steric crowding is seemingly sufficient to provide access to the energetically favorable endo transition state.

Finally, we have shown that the steric environment of these substrates can be modified by harnessing the reactivity of the enone moiety. In this case, hydrogenation of the C–C double bond can be used to overcome the endo selectivity observed with enone **4.6**. While this specific approach will not provide direct access to the originally targeted vinylogous ester ***exo*-4.3**, it sets the stage for developing a strategy in which the steric environment of the substrate is temporarily modified to allow for an exo selective alkylation event. The development of such a strategy is underway[166] and will be reported in due course.

CHAPTER 5

DEVELOPMENT OF CHIRAL ARYL IODIDE CATALYSTS FOR DEAROMATIZATION REACTIONS

Hypervalent iodine compounds have broad applications in organic synthesis due to their oxidative and electrophilic properties, which can effect a variety of transformations including oxidation of alcohols, radical cyclizations, dearomatizations, and oxidative coupling.[167] In addition, their low toxicity make them reagents of choice over toxic metals (such as lead, mercury and thallium) that once were commonly used for the same reactions.

This chapter will provide an introduction to hypervalent iodide catalysis in dearomatization reactions (Section 5.1), followed by an account of our recent endeavors in designing chiral aryl iodide catalysts capable of generating enantioenriched *p*-quinols (Section 5.2).

5.1 INTRODUCTION AND BACKGROUND

5.1.1. Hypervalent Iodine Complexes

Iodine is most commonly found in the +1 oxidation state. "Hypervalent iodide" is used to describe iodine found in higher oxidation states, specifically iodine(III) and iodine(V). Complexes that include iodine in these states are known as λ^3- and λ^5-iodanes, respectively. The iodine oxidation state dictates the geometry of the complex: trigonal bipyramidal for λ^3-iodanes and octahedral for λ^5-iodanes (Figure 5.1).[168]

Iodine(III) has a total of 10 valence electrons and prefers the two heteroatom ligands to occupy the apical positions with the less electronegative carbon ligand and both electron pairs in the equatorial positions. This geometry is often referred to and depicted as "T-shaped".[169] Iodine(V) prefers the organic carbon ligand and electron pair to occupy the apical groups while the heteroatom ligands occupy all four basal positions. The heteroatom bonds are referred to as the hypervalent bonds because they are three-center, four-electron bonds (X–I–X), making them longer and weaker compared to a regular covalent bond. It is the presence of the hypervalent bonds that make λ^3- and λ^5-iodanes highly electrophilic and thus good oxidizing reagents. In general, aryl iodides are the only stable hypervalent complexes that can be isolated; however, there are a few examples of alkyl-substituted iodine(III) complexes that are stabilized by strong electron-withdrawing groups.

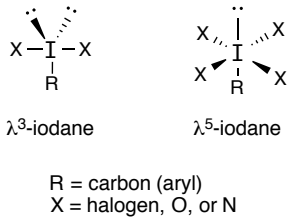

Figure 5.1. Hypervalent iodine geometries.

5.1.1.a Common Reagents

Many hypervalent iodine reagents have achieved wide use in organic synthesis, becoming commonplace for certain transformations. Iodine(III) reagents (such as PIDA and PIFA) are often used for phenolic oxidations, while iodine(V) reagents, such as DMP and IBX are more commonly used for the oxidation of alcohols (Figure 5.2).

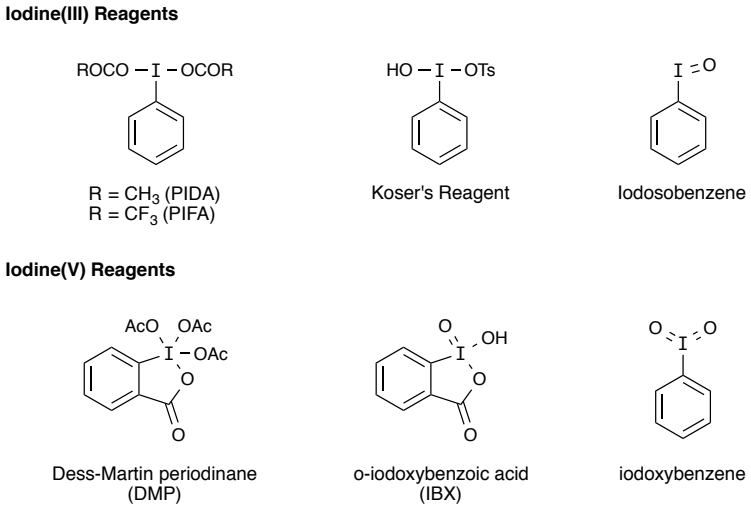

Figure 5.2. Commercially available hypervalent iodine reagents.

Although reagents such as PIDA and PIFA are employed stoichiometrically, aryl iodine reagents can also be used catalytically with a stoichiometric oxidant (Scheme 5.1).[170] A monovalent iodine reagent (sometimes referred to as a pre-catalyst) is oxidized in situ by the terminal oxidant, generating iodine(III) or iodine(V), which then undergoes the oxidative reaction of interest to regenerate the reduced iodine reagent. Kita and co-workers reported the use of *m*-CPBA as an effective oxidizing reagent for iodine(III),[171] while Vinod's group found Oxone to be a suitable oxidant to generate iodine(V) in situ.[172]

Scheme 5.1. Catalytic cycle with hypervalent iodine compounds; X = ligand (OH, OAc, OTs, $OCOCF_3$).

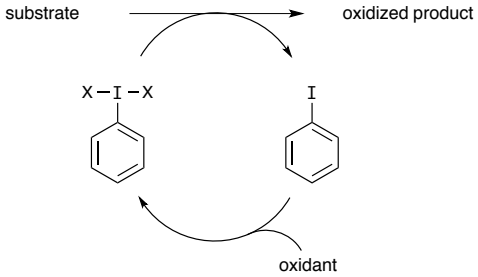

5.1.2. Oxidative Dearomatization with Hypervalent Iodine

Recent years have seen great progress in the development of asymmetric hypervalent iodine reagents and catalysts for use in enantioselective oxidation reactions.[173] Although high levels of enantiocontrol (>90:10 er) can be achieved for oxidative lactonization,[174] dioxygenation[175] and amination,[176] of olefins, analogous results for oxidative dearomatization reactions have been slow to develop.[177] Additionally, the number of studies on the asymmetric synthesis of 2,4-cyclohexadienones far exceeds those focusing on the synthesis of 2,5-cyclohexadienones. Prior to our work, to best of our knowledge, there had been no reports of using asymmetric hypervalent iodine reagents for the enantioselective construction of 2,5-cyclohexadienones (e.g., **5.1** → **5.3**, Scheme 5.2), and a general solution to this problem remains elusive.

Scheme 5.2 Iodine(III)-mediated oxidative dearomatization of phenols to access 2,5-cylohexadienones.

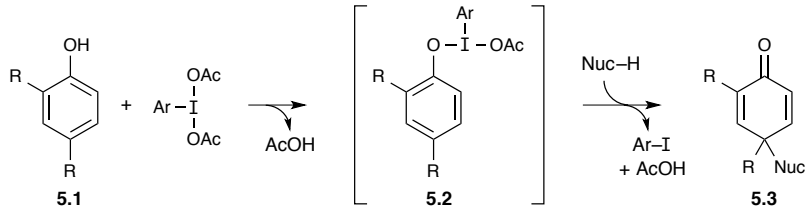

5.1.2.b Mechanism

The overall behavior of the reaction outlined in Scheme 5.3 is generally well understood. However, the mechanism of the conversion of **5.1** into **5.3** is still unclear due to the highly reactive nature of the intermediates in question. The mechanism likely

lies somewhere between direct nucleophilic attack on the aromatic ring of the phenoxide (S_N2'-like, Scheme 5.3A), and ionization to a highly reactive and short-lived[178] phenoxenium ion (S_N1-like, Scheme 5.3B).[179]

Scheme 5.3. Oxidative dearomatization mechanisms: (A) associative (B) dissociative.

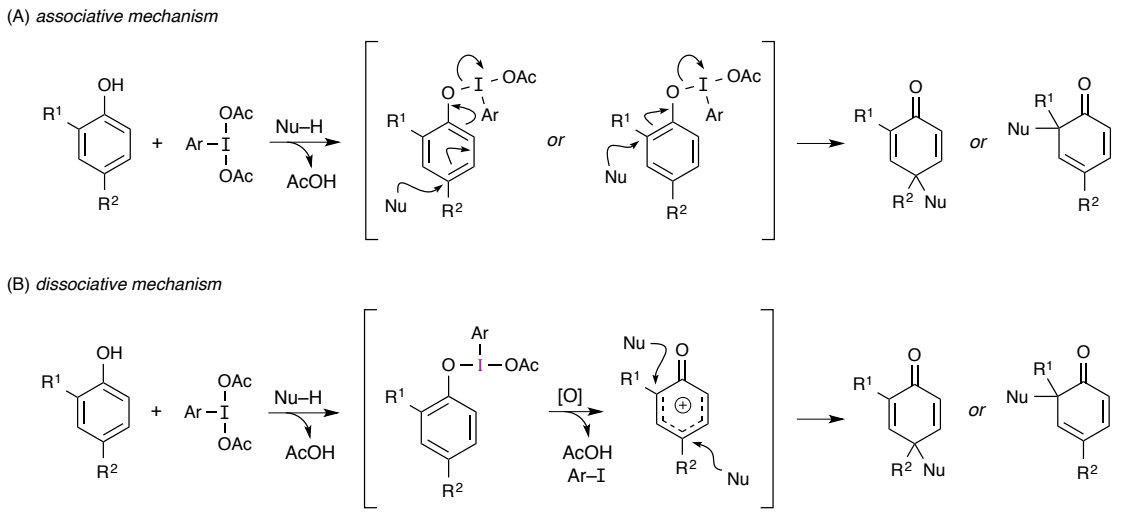

As will be seen, our initial results, and those of Kita and Ishihara, indicate that the approach of the nucleophile can be influenced by a hypervalent iodine catalyst no matter where on the S_N1/S_N2' continuum the dearomatization reaction of interest lies. In these systems, the incoming nucleophile either attacks an iodine(III) phenolate intermediate (S_N2') or traps the phenoxenium ion so rapidly that the dissociating iodine complex is still present (S_N1'). In either case, the iodine reagent selectively shields one face of the substrate.

5.1.3. Previous Dearomatization Reactions with Chiral Iodide Catalysts

5.1.3.c Chiral Spirocyclic Diiodides – Kita

The first successful enantioselective dearomatization using a chiral hypervalent iodine reagent was performed by Kita in 2008.[180] The authors hypothesized that a tethered nucleophile would favor an associative mechanism, with the intramolecular reaction occurring faster than dissociation of the iodine reagent. They performed

extensive experimentation on intramolecular oxidative spirolactonizations of **5.4** with a variety of previously reported iodine(III) carboxylates (**5.6**–**5.8**); obtaining **5.5** with low enantioselectivity (Scheme 5.4). This inspired them to design new chiral aryl iodide reagents, postulating that a rigid backbone on the iodide catalyst would more effectively maintain the chiral environment around the iodine(III). They successfully synthesized **5.9** and tested it in the dearomatization reactions, achieving an encouraging 80:20 er.

Scheme 5.4. Enantiomeric ratios obtained from spirolactonization of **5.4** with iodide reagents.

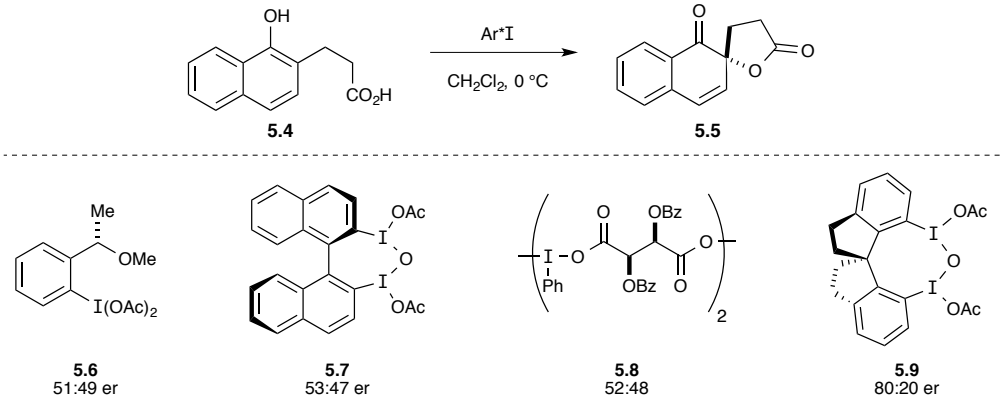

Pleased with this result, they performed a solvent screen and found that enantioselectivity was highly dependent on the solvent polarity. Mechanistic insight was procured by using more polarizable solvents, such as CH_3CN, AcOH and $(CF_3)_2CHOH$ (Table 5.1, entries 1–3). These solvents reduced the enantioenrichment, consistent with a dissociative mechanism being favored due to greater stabilization of the cationic intermediate. Further experimentation concluded that noncoordinating solvent systems (Table 1, entries 4–7) provided higher enantioselectivity.

Table 5.1. Effect of solvent polarity on enantioselectivity of the reaction in **Scheme 5.4**[a]

entry	solvent	er	% yield
1[b]	$(CF_3)_2CHOH$	50:50	87
2	CH_3CN/AcOH (10:1)	58:42	77
3	CH_3CN	60:40	50
4	$ClCH_2CH_2Cl$	80:20	69
5	CH_2Cl_2	80:20	65
6	CCl_4	85:15	47
7	$CHCl_3$	86:14	64

[a] Reactions were performed with 0.55 equiv (110 mol% of iodine) for 2 h. [b] Reaction time was 0.5 h.

Kita was also able to use iodide **5.9** catalytically by employing *m*-CPBA as a co-oxidant, albeit with slightly diminished yields and selectivity (Scheme 5.5). Afterwards, they were able to recover their catalyst by silica gel column chromatography. At the time, these results had demonstrated the highest levels of asymmetric induction by iodine(III)-mediated dearomatizations.

Scheme 5.5. Catalytic utilization of chiral aryl iodide **5.9**.

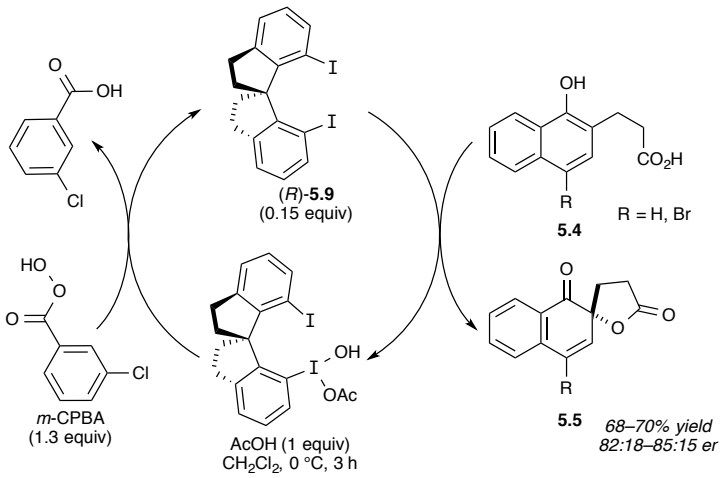

Recently, Kita has improved the selectivity even further with a modified version of spirobiindane **5.9** that has an ethyl substituent ortho to the iodine atoms (**5.10**, Scheme 5.6).[181] Under catalytic conditions, a 94:6 er was obtained for the spirolactonization product (**5.5**). He rationalizes the better selectivity is due to effective extension of the equatorial substituents surrounding the iodine center, thus affecting the chiral environment to a greater degree.

Scheme 5.6. New catalyst provides enhanced selectivity.

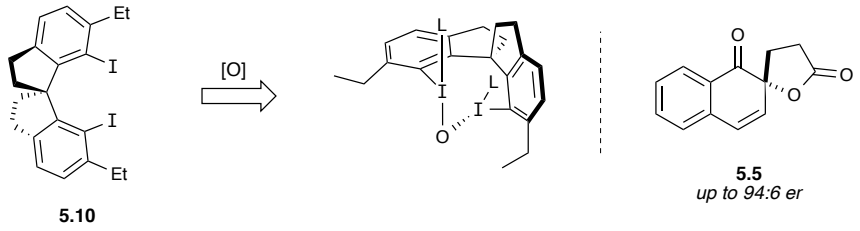

5.1.3.d C$_2$-symmetric Lactate-Derived Aryl Iodides – Ishihara

Ishihara and his group improved upon Kita's enantioselective spirolactonization of naphthols by synthesizing various conformationally flexible C_2-symmetric iodoarene catalysts (Scheme 5.7). Iodides **5.11** were synthesized in just 3 steps from (–)-ethyl lactate and iodoresorcinol. Varying the aniline used for the amide-bond formation allowed a range of iodoarenes to be synthesized easily. They hypothesized that upon oxidation of **5.11**, hydrogen bonding between the acidic proton of the C(O)X–H moiety and an acetoxy ligand on the iodine(III) atom would contribute to creating a chiral environment surrounding the iodine(III) center (**5.11‡**).

Scheme 5.7. Synthesis of C_2-symmetric iodoarene reagents.

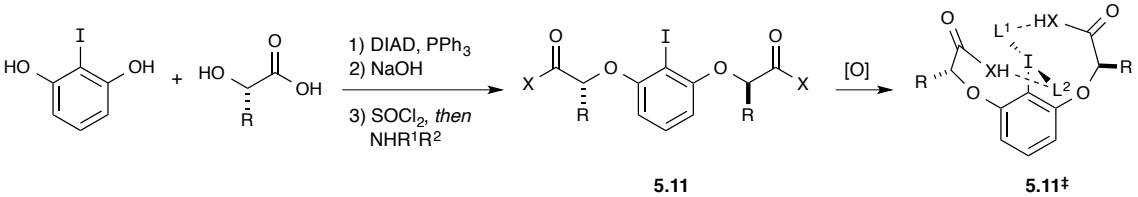

A library of catalysts were synthesized and tested under the same catalytic reaction conditions employed by Kita (Table 5.2, entries 1–9). The diester and diacid gave poor selectivity (62:38 and 72:28 er respectively, entries 1 and 2), while the bis(primary amide) gave a better er of 85:15 (entry 3). They progressed to the bis(*N*-aryl amides), which further increased the selectivity (entries 4–7). The use of a bis(tertiary amide) lowered the er to 76:24 (entry 8), which indicates the hydrogen bond donor of the previous catalysts may be contributing to better enantioselectivity. Using the mesityl amide, the R group was changed from a methyl to an isopropyl group, which also gave

high selectivity (entry 9). The authors felt that the catalyst with the bis(mesityl amide) and methyl R group gave the best combination of yield and enantioselectivity, so they decided to use this to optimize their reaction conditions (entries 10–13). Lowering the temperature and increasing the reaction time increased the yield and selectivity (entry 10). In contrast to Kita's report, significant changes in enantioselectivity was not observed with solvents of varying polarity (entries 11 and 12).

Table 5.2. Reaction optimization for the spirolactonization of **5.4**.

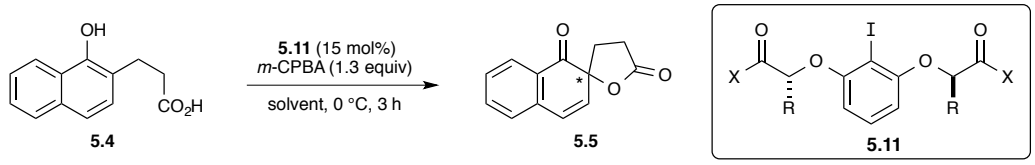

Entry	cat. 5.11		solvent	temp	time	% yield	er
	R	X					
1	Me	OEt	CH_2Cl_2	0 °C	3 h	27	62:38
2	Me	OH	CH_2Cl_2	0 °C	3 h	26	72:28
3	Me	NH_2	CH_2Cl_2	0 °C	3 h	40	85:15
4	Me	NHPh	CH_2Cl_2	0 °C	3 h	25	89:11
5	Me	NH[3,5-$(CF_3)_2C_6H_3$]	CH_2Cl_2	0 °C	3 h	53	88:12
6	Me	NH(3,5-*t*-$Bu_2C_6H_3$)	CH_2Cl_2	0 °C	3 h	36	92:8
7	Me	NHMes	CH_2Cl_2	0 °C	3 h	64	91:9
8	Me	NPh_2	CH_2Cl_2	0 °C	3 h	39	76:24
9	*i*-Pr	NHMes	CH_2Cl_2	0 °C	3 h	70	92:9
10	Me	NHMes	CH_2Cl_2	–20 °C	48 h	75	95:5
11	Me	NHMes	CH_3NO_2	0 °C	5 h	82	93:7
12	Me	NHMes	$CHCl_3$	–20 °C	48 h	55	96:4

Notably, the use of monosubstituted iodoarenes **5.12** gave low enantioselectivity, indicating that the C_2-symmetry was essential (Scheme 5.8).

Scheme 5.8. Enantioselective spirolactonization with mono-substituted iodoarene **5.4**.

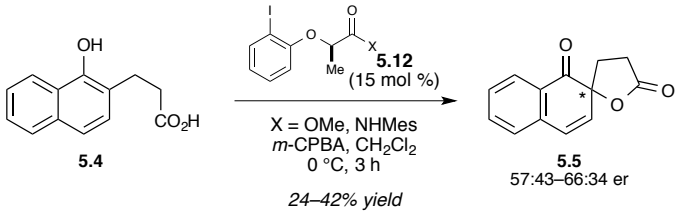

Finally, a substrate scope was performed (Table 5.3). They conducted the reactions under two sets of conditions, one with catalytic amounts of iodoarene **5.11a** (Method A), and the other with stoichiometric iodosyl arene **5.11‡** (Method B). Both conditions gave the unsubstituted and alkyl substituted products with consistent selectivity and yields (entries 1 and 2). However, greater enantioselectivity and significantly better yields were obtained under the stoichiomentric conditions for the methoxy-substituted substrates (entries 3 and 4). By conducting the reactions with the iodine(III) reagent, they were also able to confirm that *m*-CPBA was not acting as the oxidizing reagent in the spirolactonization reaction.

Table 5.3. Catalytic versus stoichiometric chiral iodine reagents for enantioselective intramolecular spirolactonization.

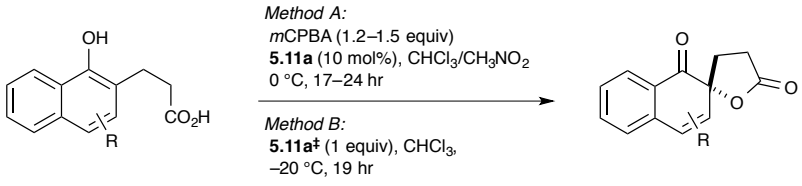

		Method A		Method B	
Entry	R	% yield	er	% yield	er
1[a]	H	75	95:5	70	95:5
2	4-Me	59	92:8	85	95:5
3	6-OMe	40	94:6	89	95:5
4	3-OMe	3	94:6	87	98:2

Ishihara's results demonstrated that the flexible, C_2-symmetric catalysts were more selective than Kita's rigid spirobiindane **5.9**. However, a better understanding of the transition state is clearly needed considering that significantly different catalysts provide comparable yields and selectivity. Recently, Ishihara has provided additional insight regarding the influence of hydrogen bond interactions in transition state conformations with C_2-symmetric catalysts.[182]

5.1.3.e Chiral Iodine(V) Reagents and Catalysts – Quideau and Birman

Quideau and co-workers have also made a profound impact in the field of chiral hypervalent iodine reagents with their display of enantioselective *ortho*-hydroxylative phenol dearomatization (Scheme 5.9).[183] Many examples of using *o*-iodoxybenzoic acid (IBX) to dearomatize phenols existed in the literature,[184] so naturally a chiral IBX derivative would be a logical choice in performing an enantioselective dearomatization. Surprisingly, after screening a variety of chiral iodine reagents, it was found that iodoarenes featuring axial chirality (**5.13** and **5.14**) were much more effective at inducing asymmetry than those with a chiral benzylic center (**5.15**).

Scheme 5.9. Enantioselective hydroxylative dearomatization with chiral iodoarene and *m*-CPBA.

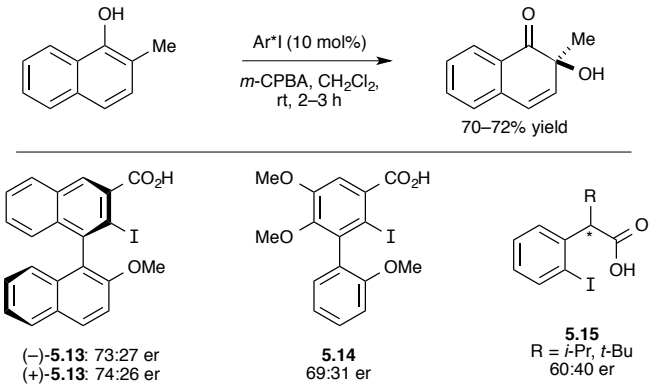

Interestingly, varying the equivalents of iodoarene **5.13** and *m*-CPBA in the dearomatization of naphthol **5.16** led to exclusive formation of either quinol **5.17** or epoxide **5.18** (Table 5.4). Using only a catalytic amount of (–)-**5.13** and 2.5 equiv of *m*-CPBA gave epoxide **5.18** in 90% yield and 65:35 er. However, when equimolar

amounts of (–)-**5.13** and *m*-CPBA were used, *o*-quinol **5.17** was the only isolated product in 67% yield and 73:27 er. Despite the moderate selectivity that was obtained, this was the first example of an enantioselective dearomatization being accomplished with hypervalent iodine and a non-substrate-tethered oxygenating source. Presumably, iodine(V) is the active reagent and an intramolecular delivery of the hydroxyl group is occurring. This is in direct contrast of the Kita and Ishihara catalysts, where iodine(III) is thought to be the active reagent.

Table 5.4. Effect of reagent stoichiometry on isolated product.

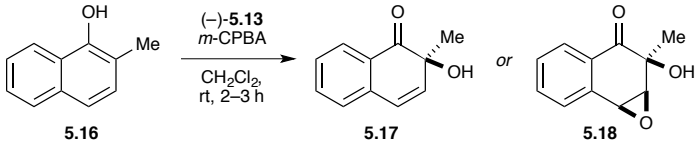

Entry	(–)-5.13 (equiv)	*m*-CPBA (equiv)	5.17 (yield)	5.18 (yield)	er
1	0.1	2.5	–	90%	65:35
2	1.0	1.0	67%	–	73:27

Finally, Birman has reported the enantioselective dearomatization of *o*-alkylphenols with oxazoline-derived iodoxy arene reagents.[185] The reactive *o*-quinols that were generated dimerized spontaneously by a Diels-Alder cycloaddition, affording an enantioenriched bicyclic system with 82:18 er (Scheme 5.10).

Scheme 5.10. Enantioselective dearomatization with 2-(*o*-iodoxyphenyl)-oxazoline

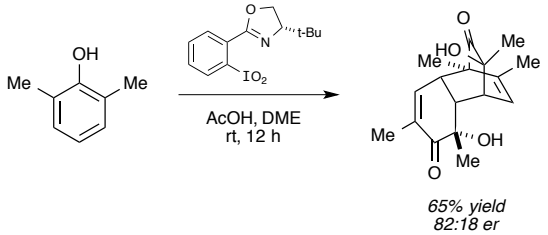

5.2 DEVELOPMENT OF NEW CHIRAL ARYL IODIDE CATALYSTS

5.2.1. Synthetic Goal

The goal of this project was to design new chiral aryl iodide catalysts for dearomatizing phenols asymmetrically to afford 2,5-cyclohexadienones. To the best of our knowledge, no previous research has been conducted in this topic. Kita and Ishihara had successfully developed chiral aryl iodide reagents to dearomatize naphthol derivatives, however there are still limitations with these catalysts. We sought to develop an aryl iodide catalyst capable of asymmetrically dearomatizing phenols in a direct and general manner to generate 2,5-cyclohexadienones. Initially, we wanted to employ simple oxygen-based nucleophiles, such as water, which would allow us to gain access to chiral *p*-quinols that could be utilized in an asymmetric synthesis of sorbicillactone A. Eventually, we aim to expand the scope to encompass carbon- and nitrogen-based nucleophiles. Finally, the catalytic oxidations by Kita inspired us to employ our own novel aryl iodide reagents catalytically. This would greatly reduce the amount of reagent needed and also contribute to the overall efficiency of the reaction.

5.2.1.f Challenges

Controlling bond rotation presents a significant challenge when designing any chiral catalyst. In the context of oxidative dearomatization, there are several modes in which this can occur. One is rotation about the C–O bond of the phenol; this rotation exposes both faces of the phenol to nucleophilic attack, thus degrading any stereochemical bias. Second, rotation of the I-O bond when the phenol is attached to the iodine can cause the aryl rings to splay out, preventing the catalyst from blocking either face of the phenol. This would also cause both faces of the phenol to be exposed to nucleophilic attack. In addition, rotation around this bond would significantly increase the distance between the stereogenic elements on the iodide catalyst and the newly forming stereocenter.

Scheme 5.11. Bond rotation exposes both faces of the phenol to nucleophilic attack and increases the distance between the chiral catalyst and newly forming stereocenter.

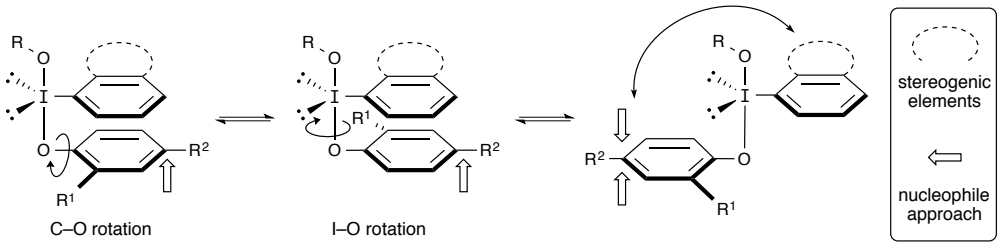

5.2.2. Ishihara Catalysts

5.2.2.g Initial Results[A]

We first decided to explore the possibility of using the iodide catalysts developed by Ishihara. These catalysts worked well with his dearomatization of substituted naphthols; however, the fact that his work utilized a tethered nucleophile represented a significant difference from our desired system. Furthermore, because the nucleophile was adding into the phenol at the ortho position, it was in closer proximity to the chiral information present in the catalyst. However, these catalysts remained attractive because of their ease of preparation. Due to our previous interest and success in accessing racemic *p*-quinols, we chose water as the nucleophile. Gratifyingly, we found that the reaction was indeed successful, affording *p*-quinol **5.20a** with fair selectivity (Scheme 5.12). Minor modifications, including changes to the amide and alkyl substituents of the catalyst, did not significantly affect the selectivity.

[A] Most of this work was conducted by Alison Thorsness and Andrew Harned.

Scheme 5.12. Synthesis of quinol **5.20a** with Ishihara's catalysts.

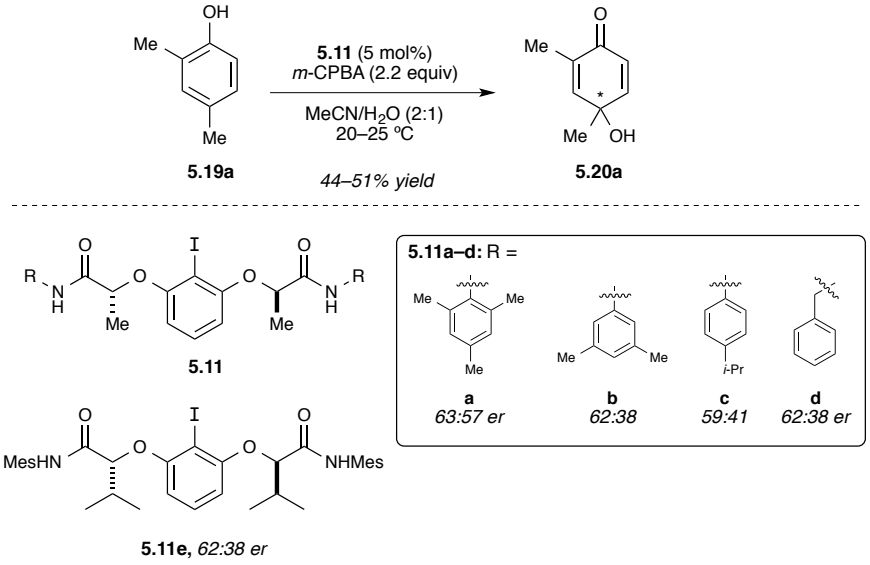

5.2.2.h Modified Ishihara Catalysts

We decided to modify the tether by lengthening the chain in order to place the chiral information further from the iodine, potentially positioning it closer to the para position of the phenol in the transition state and thus providing greater influence on the approach of the nucleophile. The amide was also inverted so that hydrogen bonding with the acetoxy ligand on the iodine would remain relatively unchanged. The synthesis of these new catalysts was accomplished using chiral sulfonamides (synthesized easily from amino alcohols),[186] which underwent electrophilic substitution with iodoresorcinol to achieve bis(Boc-protected amine) **5.21** (Scheme 5.13).[187] Treatment of **5.21** with TFA removed the Boc group and subsequent addition of an acid chloride and K_2CO_3 in dichloromethane gave the bis(amino acid)-derived catalysts (**5.22a-c**) in 30–40% overall yield. These catalysts were used in the same dearomatization conditions as above (see Scheme 5.12) and were found to have lower selectivity than the Ishihara catalysts.

Scheme 5.13. Synthesis and selectivity results of Ishihara-inspired iodoarenes **5.22**.

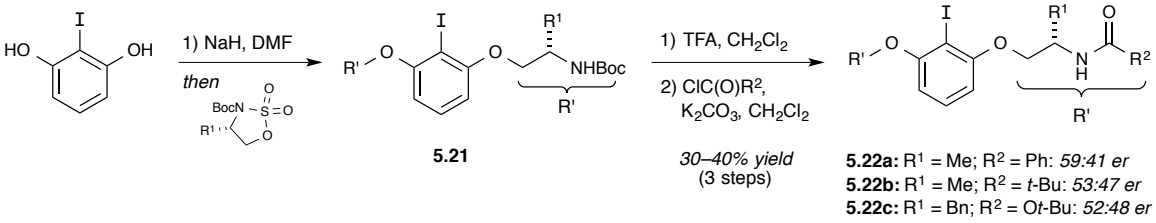

5.2.3. Tartrate-Derived Catalysts[§]

The poor selectivities observed with the Ishihara and novel Ishihara-inspired catalysts led us to develop new chiral iodoarene catalysts based on computational studies. In order to gather additional information about the structure of iodine(III) phenolates, DFT calculations were performed on intermediate **5.23**, which arises from a ligand exchange of diacetoxy iodine(III) with the phenol (Figure 5.3A). The calculations were carried out using Truhlar's M06-2X functionals[188] and a mixed basis set (6–31+G(d) for C,H,O and SDD[189] for iodine). The calculations revealed a dramatic conformational change upon switching from a gas phase to a solvated system. In the gas phase, both faces of the phenolic substrate are accessible. However, in both MeCN and CH_2Cl_2 the aryl ring of the iodide reagent partially blocks one face of the substrate (Figure 5.3B). This suggests that enantiofacial descrimination may be possible. We saw this as an opportunity to use this structural feature as a basis for the rational design of new chiral aryl iodides. Specifically, it was envisioned that asymmetry could be introduced using a tether bearing stereogenic centers to link one *ortho* position of the aryl iodide to the α-carbon of an iodine-bound carboxylate.

[§] This work has previously been published: Volp, K. A.; Harned, A. M. Chiral Aryl Iodide Catalysts for the Enantioselective Synthesis of *para*-Quinols. *Chem. Commun.* **2013**, *49*, 3001–3003.

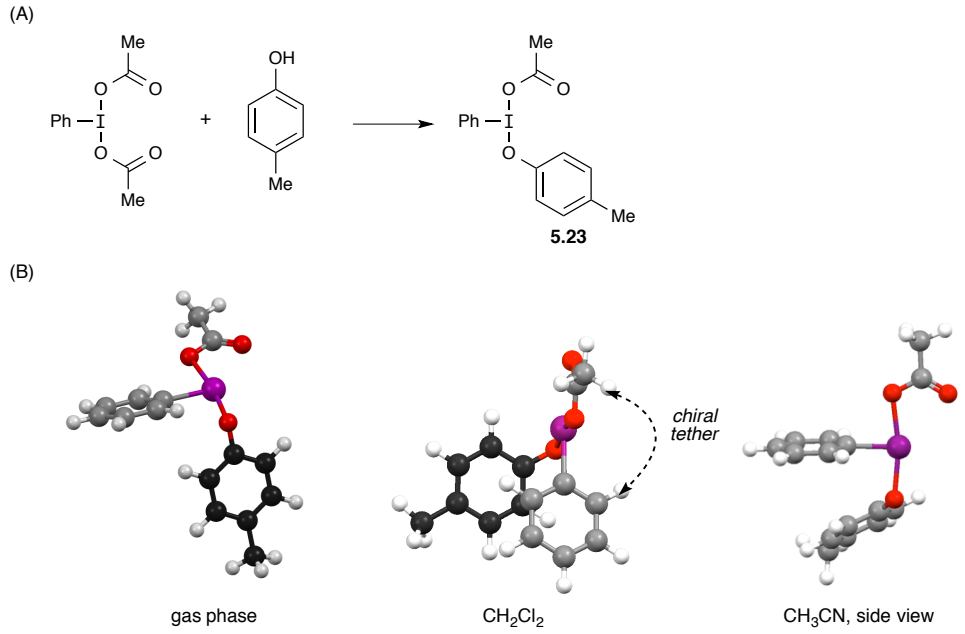

Figure 5.3. (A) Molecular modeling of intermediate **5.23** (B) in gas phase, CH_3CN, and CH_2Cl_2.

We needed a chiral linker that would be readily available and easy to install on the aryl iodide. Dimethyl tartrate was a decent candidate for use with aryliodoketones as the chiral moiety could easily be installed by ketalization (Scheme 5.14). It was our hopes that upon oxidation, the chiral tether would interact with the iodine(III) ligand through hydrogen bonding, similar to that seen in Ishihara's concept. Alternatively, an acid moiety could directly serve as a ligand for the iodine(III) center.

Scheme 5.14. Ketalization of an iodoketone with tartrate would provide the chiral linker upon oxidation.

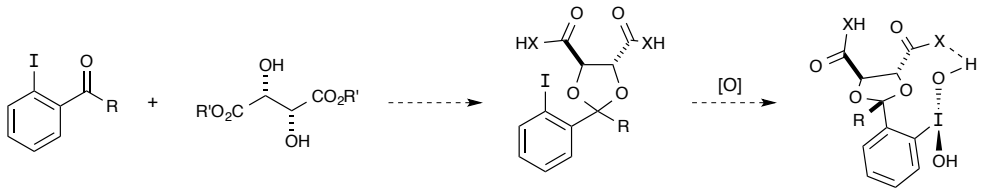

The synthesis of our first catalyst with a chiral tether is outlined in Scheme 5.15, starting from commercially available 2-iodoacetophenone. Initial attempts to directly convert the ketone to the tartrate ketal failed to yield any product. Therefore, the

ketalization of commercially available 2-iodoacetophenone (**5.24**) was accomplished by first converting the ketone to the dimethyl ketal with trimethylorthoformate, which immediately after isolation, was treated with the tartrate under Lewis acidic conditions to afford **5.25**. Next, the esters were hydrolyzed to give bis(acid)iodoarene (**5.26**) in 70% yield. This was subsequently converted to the bis(acid chloride), which was treated with mesityl aniline to afford bis(mesityl-amide)iodoarene **5.27** in 81% yield over the two steps.

Scheme 5.15. Synthesis of tartrate-derived iodoarene **5.27**.

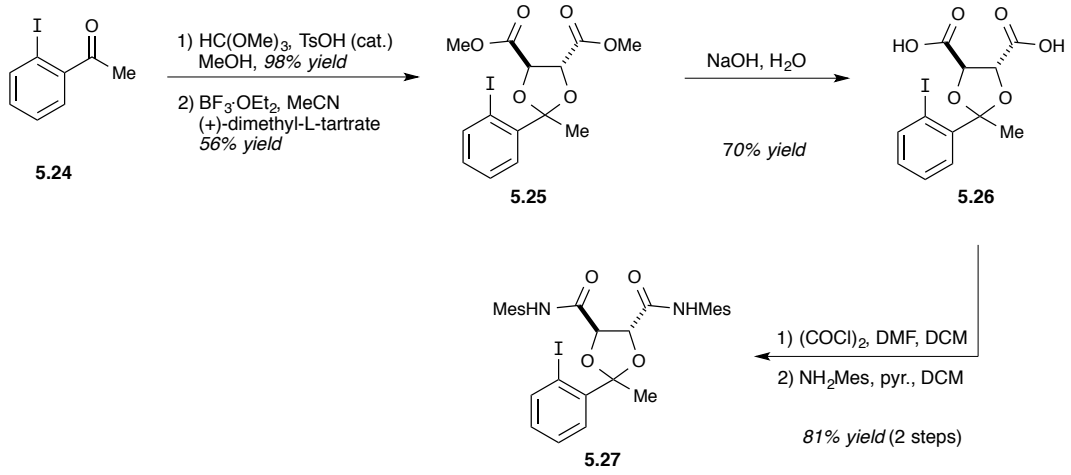

A number of other related structures were constructed in a similar manner, affording a small library of iodide catalysts to be tested under the conditions previously used for the Ishihara catalysts (Table 5.5). All of the catalysts gave similar low enantioselectivity and yields (entries 1–5). It was encouraging that even a low level of enantioselectivity was being achieved: it provided proof-of-concept as well as inspiration to investigate this novel class of chiral aryl iodide catalysts further.

Table 5.5. Screening of tartrate-derived catalysts.

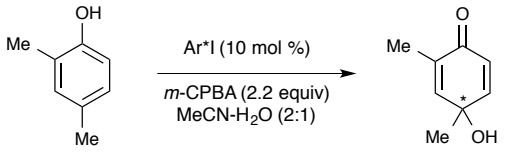

5.19a **5.20a**

entry	Ar*I		time	% yield	er
1	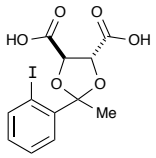	(**5.26**)	1 h	27	44:56
2	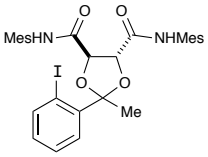	(**5.27**)	1.5 h	29	46:54
3	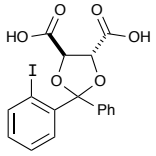	(**5.28**)	1 h	28	47:53
4	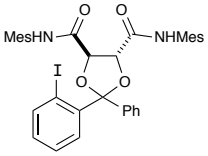	(**5.29**)	1 h	35	46:54
5	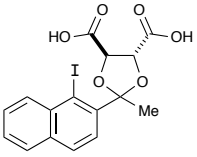	(**5.30**)	1 h	39	45:55

Analyzing our new catalysts more closely, we realized that undesired bond rotation was likely occurring (Figure 5.4). All of the catalysts we had synthesized contained freely rotating bonds, potentially contributing to the low levels of selectivity. Indeed, computational studies confirmed this with two low energy conformers of the same structure, each with opposite orientation of the tartrate. This results in minimal bias of the orientation of the phenol, which exposes each face of the phenol (shaded darker) and allows the nucleophile to approach from either direction.

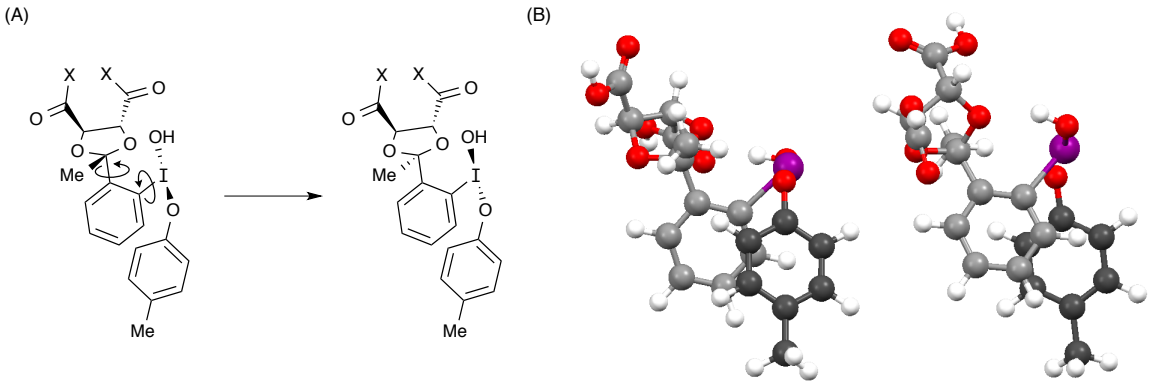

Figure 5.4. (A) Rotation around the indicated bonds exposes both faces of the phenol; (B) two lowest energy conformers, one with the phenol (shaded darker) in front of the iodoarene, and the other behind the iodoarene.

5.2.3.i Iodo-tetrahydronaphthalene Catalysts

In an effort to avoid this problem, we sought to restrict bond rotation by creating a more rigid structure; tethering the R group back to the aryl iodide would eliminate rotation around the aryl ring. This was accomplished by synthesizing iodotetralone **5.31** from α-naphthalamine using a known procedure,[190] followed by ketalization to give **5.32** and finally hydrolysis to afford bis(acid)iodo-tetrahydronaphthalene **5.33** in 63% yield over the three steps (Scheme 5.16).

Scheme 5.16. (A) Synthesis of iodo-tetrahydronaphthalene **5.33**.

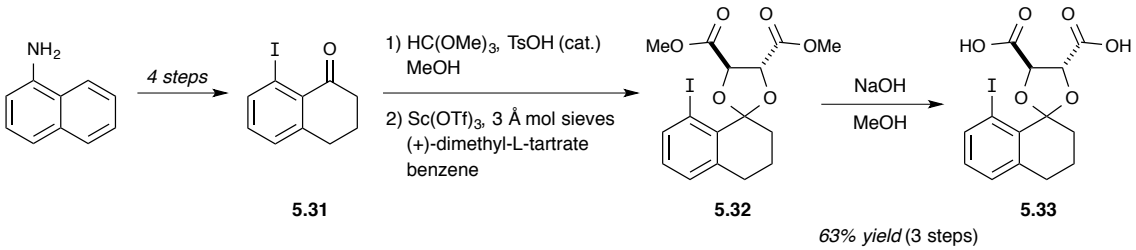

Encouraged by the computational results, we synthesized a small set of the new tetrahydronaphthalene catalysts (Scheme 5.17). Treating the acid with oxalyl chloride afforded the acid chloride, which was subsequently converted to various amides using either morpholine (**5.34a**) or aniline derivatives (**5.34b-h**).

Scheme 5.17. Synthesis of tartrate-derived catalysts **5.34**.

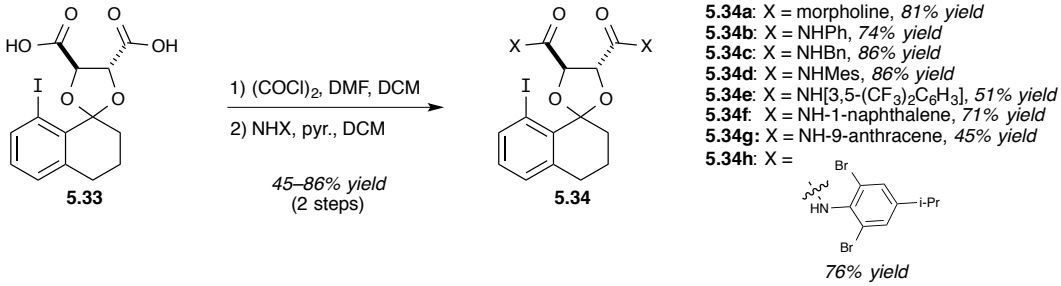

Gratifyingly, the newly designed chiral aryl iodides were successful in providing enantioenriched *p*-quinols **5.20** (Table 5.6). Among the various amides that were tested, catalysts **5.34a-d** gave approximately the same level of selectivity. We were surprised to find that comparable selectivity was observed when a tertiary amide was incorporated into the catalyst (entry 2). This indicates that factors beyond simple hydrogen bonding are important when biasing the conformation of the presumed iodine(III) phenoxide (vide infra). Catalysts **5.34f**, **5.34g**, and **5.34h** resulted in a higher yield of the quinol product (entries 10–13), but the enantioselectivity was not appreciably improved. One of the more intriguing results obtained was with catalyst **5.34e** (entry 9), where a reversal of selectivity was observed in comparison to the other catalysts. Taken as a whole, these results show that the identity of the amide has some influence on the enantioselectivity, but this is a rather minor fine tuning of the selectivity inherent to the structure of catalyst **5.34**. In the end, we decided that the mesityl amide **5.34d** (entry 5) offered the most favorable combination of yield and selectivity; therefore, this catalyst was chosen for further studies.[191]

Table 5.6. Catalyst screening.

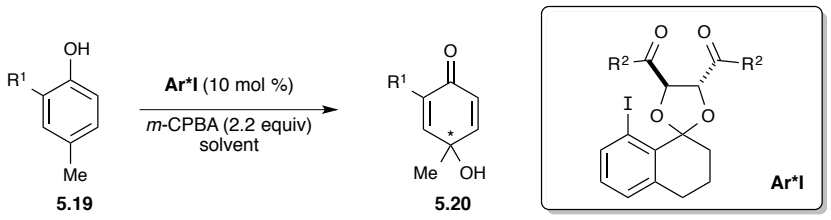

entry	R^1	R^2		temp	MeCN:H_2O	time (h)	yield (%)	er
1	Me	OH	(**5.33**)	rt	2:1	1.5	36	60:40
2	Me	morpholine	(**5.34a**)	rt	3:1	1.5	33	59:41
3	Me	NHPh	(**5.34b**)	rt	3:1	1.5	19	60:40
4	Me	NHBn	(**5.34c**)	rt	3:1	1.5	34	61:39
5	Me	NHMes	(**5.34d**)	rt	2:1	1.5	47	63:37
6	Br	NHPh	(**5.34b**)	rt	9:1	16	48	60:40
7	Br	NHBn	(**5.34c**)	rt	2:1	1.5	20	60:40
8	Br	NHMes	(**5.34d**)	rt	2:1	0.3	45	65:35
9	Br	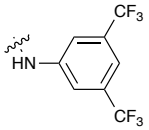	(**5.34e**)	rt	9:1	16	75	43:57
10	Br	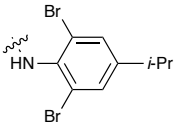	(**5.34h**)	rt	9:1	16	80	63:37
11	TMS			rt	9:1	16	94	72:28
12	Br	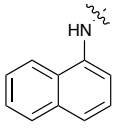	(**5.34f**)	rt	9:1	16	52	60:40
13	Br	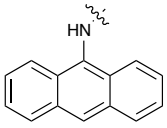	(**5.34g**)	rt	9:1	16	70	63:37

[a] All reactions were performed on a 0.17 mmol scale. [b] 2:1 MeCN/H_2O was used. [c] All yields are following purification using silica gel chromatography. [d] Determined by chiral HPLC (see ESI for details).

Following the catalyst screening, we did a brief solvent screen using catalyst **5.34d** (Table 5.7). In general, the yields were increased slightly when the ratio of acetonitrile-water was changed from 2:1 to 9:1 (entries 1 and 2). Following this observation, various other organic solvents were tested using the same ratio with water.

The yields decreased when THF or trifluoroethanol was used (entries 4 and 5), while nitromethane provided similar yields but diminished selectivity (entry 6). Acetone provided yields and selectivity to comparable to acetonitrile; however, the reaction was not as clean (entry 7).

Table 5.7. Solvent screen.

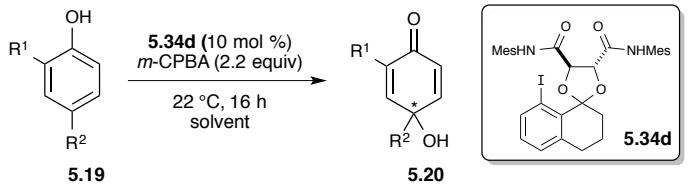

entry	R^1	R^2	solvent	yield (%)	er
1	Me	Me	MeCN-H_2O (2:1)	47	62:38
2	Me	Me	MeCN-H_2O (9:1)	52	62:38
3	TMS	*i*-Pr	MeCN-H_2O (9:1)	53	67:33
4	TMS	*i*-Pr	THF-H_2O (9:1)	33	62:38
5	TMS	*i*-Pr	CF_3CH_2OH-H_2O (9:1)	<10	nd
6	TMS	*i*-Pr	$MeNO_2$-H_2O (9:1)	62	53:47
7	TMS	*i*-Pr	acetone-H_2O (9:1)	66	68:32

Next, the substrate scope was investigated using catalyst **5.34d** and various substituted phenols (Table 5.8). Overall, the enantioselectivity was moderate and ranged from 63:37 to 80:20 er. In general, an approximately 10% (relative) increase in selectivity was observed when the temperature was lowered to 0 °C; however, this often came at the expense of yield. Increasing the size of the ortho substituent had a generally positive effect on selectivity (**5.19a–c**, **4g**), but negative effects were seen when larger para substituents were present (**5.19i** and **5.19j**). Substrate **5.19e** shows that an ortho substituent is required to achieve effective enantiofacial discrimination. However, substrate **5.19f** demonstrates that a meta substituent is tolerated as long as an ortho substituent is also present. Our recent synthesis of sorbicillatone A demonstrates the utility of quinol **5.19f** along with the synthetic potential of an asymmetric synthesis of *p*-quinols. The highest enantioselectivity (80:20 er) was observed with substrate **5.19c**.

Table 5.8. Influence of substrate structure.[a]

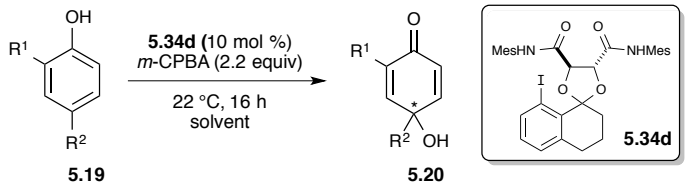

compound	R^1	R^2	R^3	temp (°C)	time (h)	yield (%) [b]	er [c]
a	Me	H	Me	25	16	52	64:36
b	Br	H	Me	0	3	21 [d]	69:31
b	Br	H	Me	25	16	52	65:35
c	TMS	H	Me	0	7	58	80:20
c	TMS	H	Me	25	16	79	75:25
d	Cl	H	Me	25	16	65	65:35
e	H	Me	Me	0	0.5	23 [d]	53:47
e	H	Me	Me	25	16	43	50:50
f	Me	OMe	Me	0	1	20 [d]	69:31
g	TBS	H	Me	0	16	64	77:23
g	TBS	H	Me	25	16	48	71:29
h	TIPS	H	Me	0	16	56	64:36
i	TMS	H	*i*-Pr	25	16	53	67:33
j	TBS	H	*i*-Pr	25	16	41	63:37

[a] All reactions were performed on a 0.17 mmol scale. [b] All yields are following purification using silica gel chromatography. [c] Determined by chiral HPLC (see ESI for details). [d] 2:1 MeCN/H_2O was used.

In order to form the enantioenriched *p*-quinols, the chiral catalyst must control the approach of a relatively small, external nucleophile (i.e., H_2O). The stereoselective delivery of such a nucleophile is further complicated by the aforementioned mechanistic uncertainties associated with this reaction. With this in mind, we wanted to evaluate the ability of catalyst **5.34d** to control the approach of other nucleophiles. To this end, several other nucleophiles were tested (Scheme 5.18). Gratifyingly, spirocyclization of phenol **5.35** afforded spirocycle **5.36** in 70:30 er, and performing the reaction in methanol gave methyl ether **5.37** in 60% yield and 65:35 er. These levels of yields and stereoselectivity were consistent with those reported in Table 5.8. Other substrates were dearomatized with methanol as a nucleophile (**5.19c** and **5.19g**), however, we were unable to separate the enantiomers using chiral HPLC.

Scheme 5.18. Other nucleophiles (A) tethered alcohol, and (B) methanol.

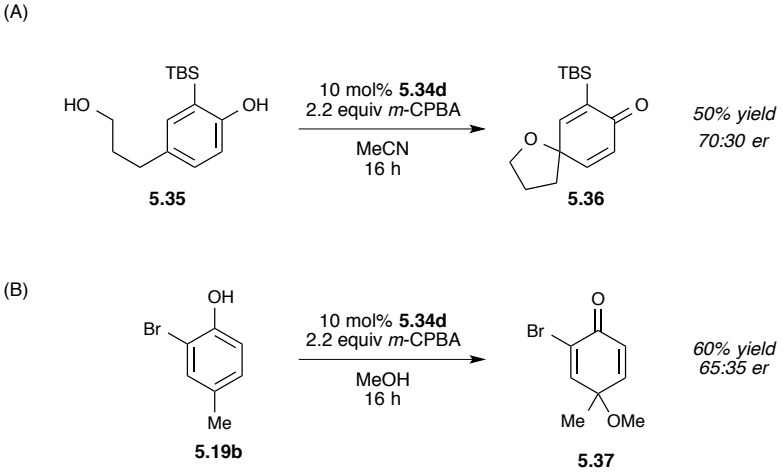

In summary, we have shown that computational methods can be used to gain some insight into the structure of short-lived hypervalent iodine intermediates and that the results of this modeling can serve as a basis for the design of chiral aryl iodine catalysts. More importantly, we have demonstrated for the first time, that chiral aryl iodide catalysts can be used for the enantioselective synthesis of 2,5-cyclohexadienones. Our results indicate that this is a tractable problem, but new catalyst architectures are needed in order to achieve high selectivity.

(1) Magdziak, D.; Meek, S. J.; Pettus, T. R. R. Cyclohexadienone Ketals and Quinols: Four Building Blocks Potentially Useful for Enantioselective Synthesis. *Chem. Rev.* **2004**, *104*, 1383–1430.

(2) Quideau, S.; Pouységu, L.; Deffieux, D. Oxidative dearomatization of phenols: Why, how and what for? *Synlett* **2008**, 467–495.

(3) DeRosa, M. C.; Crutchley, R. J. Photosensitized Singlet Oxygen and its Applications. *Coord. Chem. Rev.* **2002**, 351–371.

(4) Matsuura, T.; Omura, K.; Nakashima, R. Photo-Induced Reaction. II. the Photo-Sensitized Oxidation of Hindered Phenols. *Bull. Chem. Soc. Jpn.* **1965**, *38*, 1358–1362.

(5) Endo, K.; Seya, K.; Hikino, H. Biogenesis-Like Transformation of Salidroside to Rengyol and its Related Cyclohexyletanoids of Forsythia Suspensa. *Tetrahedron* **1989**, *45*, 3673-3682.

(6) Carreño, M. C.; González-López, M., Urbano, A. Oxidative De-aromatization of *para*-Alkyl Phenols into *para*-Peroxyquinols and *para*-Quinols Mediated by Oxone as a Source of Singlet Oxygen. *Angew. Chem. Int. Ed*. **2006**, *45*, 2737–2741.

(7) Gao, S.; Ko, S.; Lin, Y.; Peddinti, R. K.; Liao, C. Inverse-Electron-Demand Diels–Alder Reactions of Masked *o*-Benzoquinones with Enol Ethers and Styrene. *Tetrahedron* **2001**, *57*, 297–308.

(8) (a) Moriarty, R. M.; Prakash, O. Oxidation of Phenolic Compounds with Organohypervalent Iodine Reagents. *Org. React. (New York)* **2001**, *57*, 327–415. (b) Zhdankin, V. V.; Stang, P. J. Chemistry of Polyvalent Iodine. *Chem. Rev.* **2008**, *108*, 5299–5358.

(9) Lewis, N.; Wallbank, P. Formation of Quinol Ethers using (Diacetoxyiodo)benzene. *Synthesis*, **1987**, 1103–1106.

(10) (a) Pelter, A.; Elgendy, S. Phenolic Oxidation with (Diacetoxyiodo)Benzene. *Tetrahedron Lett.* **1988**, *29*, 677–680. (b) Pelter, A.; Elgendy, S. M. A. Phenolic Oxidations with Phenyliodonium Diacetate. *J. Chem. Soc., Perkin Trans. 1* **1993**, 1891–1896.

(11) Goldstein, D. M.; Wipf, P. Studies Toward the Synthesis of *Stemona* Alkaloids; a Short Synthesis of the Tricyclic Core of Tuberostemonines. *Tetrahedron Lett.* **1996**, *37*, 739–742.

(12) Rama Rao, A. V.; Gurjar, M. K.; Sharma, P. A. Studies Directed Towards the Total Synthesis of Aranorosin. *Tetrahedron Lett.* **1991**, *32*, 6613–6616.

(13) McKillop, A.; McLaren, L.; Taylor, R. J. K. A Simple and Efficient Procedure for the Preparation of p-Quinols by Hypervalent Iodine Oxidation of Phenols and Phenol Tripropylsilyl Ethers. *J. Chem. Soc., Perkin Trans. 1* **1994**, 2047–2048.

(14) Kita, Y.; Tohma, H.; Inagaki, M.; Hatanaka, K.; Yakura, T. Total Synthesis of Discorhabdin C: A General Aza Spiro Dienone Formation from O-Silylated Phenol Derivatives using a Hypervalent Iodine Reagent. *J. Am. Chem. Soc.* **1992**, *114*, 2175–2180.

(15) Kita, Y.; Tohma, H.; Kikuchi, K.; Inagaki, M.; Yakura, T. Hypervalent Iodine Oxidation of N-Acyltyramines: Synthesis of Quinol Ethers, Spirohexadienones, and Hexahydroindol-6-Ones. *J. Org. Chem.* **1991**, *56*, 435–438.

(16) Reviews: (a) Roche, S. P.; Porco, J. A. Dearomatization Strategies in the Synthesis of Complex Natural Products. *Angew. Chem. Int. Ed.* **2011**, *50*, 4068–4093. (b) Pouységu, L.; Deffieux, D.; Quideau, S. Hypervalent iodine-mediated phenol dearomatization in natural product synthesis. *Tetrahedron* **2010**, *66*, 2235–2261.

(17) Quideau, S.; Lebon, M.; Lamidey, A.-M. Enantiospecific Synthesis of the Antituberculosis Marine Sponge Metabolite (+)-Puupehenone. the Arenol Oxidative Activation Route. *Org. Lett.* **2002**, *4*, 3975–3978.

(18) (a) Tohma, H.; Harayama, Y.; Hashizume, M.; Iwata, M.; Egi, M.; Kita, Y. Synthetic Studies on the Sulfur-Cross-Linked Core of Antitumor Marine Alkaloid, Discorhabdins: Total Synthesis of Discorhabdin A. *Angew. Chem. Int. Ed.* **2002**, *41*, 348–350. (b) Tohma, H.; Harayama, Y.; Hashizume, M.; Iwata, M.; Kiyono, Y.; Egi, M.; Kita, Y. The First Total Synthesis of Discorhabdin A. *J. Am. Chem. Soc.* **2003**, *125*, 11235–11240.

(19) (a) Hoarau, C.; Pettus, T. R. R. General Synthesis for Chiral 4-Alkyl-4-Hydroxycyclohexenones. *Org. Lett.* **2006**, *8*, 2843–2846. (b) Mejorado, L. H.; Hoarau, C.; Pettus, T. R. R. Diastereoselective Dearomatization of Resorcinols Directed by a Lactic Acid Tether: Unprecedented Enantioselective Access to p-Quinols. *Org. Lett.* **2004**, *6*, 1535–1538.

(20) (a) Wang, J.; Pettus, L. H.; Pettus, T. R. R. Cycloadditions of *o*-Quinone Dimethides with p-Quinol Derivatives: Regiocontrolled Formation of Anthracyclic Ring Systems. *Tetrahedron Lett.* **2004**, *45*, 1793–1796. (b) Wang, J.; Pettus, T. R. R. A Short Diastereoselective Synthesis of the (±)-Rishirilide B Core Structure. *Tetrahedron Lett.* **2004**, *45*, 5895–5899. (c) Mejorado, L. H.; Pettus, T. R. R. Total Synthesis of (+)-Rishirilide B: Development and Application of General Processes for Enantioselective Oxidative Dearomatization of Resorcinol Derivatives. *J. Am. Chem. Soc.* **2006**, *128*, 15625–15631.

(21) (a) T. Rovis, in *New Frontiers in Asymmetric Catalysis*, ed. K. Mikami, M. Lautens, Wiley, Hoboken, NJ, 2007, pp 275-311. (b) Studer, A.; Schleth, F. Desymmetrization and Diastereotopic Group Selection in 1,4-Cyclohexadienes. *Synlett*, **2005**, 3033–3041. (c) García-Urdiales, E.; Alfonso, I.; Gotor, V. Enantioselective Enzymatic Desymmetrizations in Organic Synthesis. *Chem. Rev.*, **2005**, *105*, 313–354. (d) Anstiss, M.; Holland, J. M.; Nelson, A.; Titchmarsh, J. R. Beyond Breaking the Mirror Plane: The Desymmetrisation of Centro-symmetric Molecules as an Efficient Strategy for Asymmetric Synthesis. *Synlett*, **2003**, 1213–1220. (e) Willis, M. C. New strategies for new organic molecules with large second order hyperpolarizabilities. *J. Chem. Soc., Perkin Trans. 1*, 1999, 1765–1770.

(22) (a) Takemoto, Y.; Kuraoka, S.; Hamaue, N.; Aoe, K.; Hiramatsu, H.; Iwata, C. Enantioselective Cu-catalyzed 1,4-addition of Me3Al to a 4,4-disubstituted cyclohexa-2,5-dienone. *Tetrahedron*, **1996**, *52*, 14177–14188. (b) Imbos, R.; Brilman, M. H. G.; Pineschi, M.; Feringa, B. L. Highly Enantioselective Catalytic Conjugate Additions to Cyclohexadienones. *Org. Lett.* **1999**, *1*, 623–626. (c) Imbos, R.; Minnaard, A. J.; Feringa, B. L. A Highly Enantioselective Intramolecular Heck Reaction with a Monodentate Ligand. *J. Am. Chem. Soc.*, **2002**, *124*, 184–185. (d) Hayashi, Y.; Gotoh, H.; Tamura, T.; Yamaguchi, H.; Masui, R.; Shoji, M. Cysteine-Derived Organocatalyst in a Highly Enantioselective Intramolecular Michael Reaction. *J. Am. Chem. Soc.* **2005**, *127*, 16028–16029. (e) Elliott, M. C.; El Sayed, N. N. E.; Ooi, L. Sulfoxide-Directed Desymmetrisation of Cyclohexa-1,4-Dienes. *Tetrahedron Lett.* **2007**, *48*, 4561–4564. (f) Vo, N. T.; Pace, R. D. M.; O'Har, F.; Gaunt, M. J. An Enantioselective Organocatalytic Oxidative Dearomatization Strategy. *J. Am. Chem. Soc.* **2008**, *130*, 404–405. (g) Liu, Q.; Rovis, T. Asymmetric Synthesis of Hydrobenzofuranones Via Desymmetrization of Cyclohexadienones using the Intramolecular Stetter Reaction. *J. Am. Chem. Soc.* **2006**, *128*, 2552–2553. (h) Gu, Q.; Rong, Z.; Zheng, C.; You, S. Desymmetrization of Cyclohexadienones Via Brönsted Acid-Catalyzed Enantioselective Oxo-Michael Reaction. *J. Am. Chem. Soc.* **2010**, *132*, 4056–4057. (i) Leon, R.; Jawalekar, A.; Redert, T.; Gaunt, M. J. Catalytic Enantioselective Assembly of Complex Molecules Containing Embedded Quaternary Stereogenic Centres from Simple Anisidine Derivatives. *Chem. Sci.* **2011**, *2*, 1487–1490. (j) Gu, Q.; You, S. Desymmetrization of Cyclohexadienones Via Cinchonine Derived Thiourea-Catalyzed Enantioselective Aza-Michael Reaction and Total Synthesis of (–)-Mesembrine. *Chem. Sci.* **2011**, *2*, 1519–1522.

(23) Wenderski, T. A.; Hoarau, C.; Mejorado, L.; Pettus, T. R. R. Dearomatization Applications of I(III) Reagents and some Unusual Reactivity Amongst Resorcinol Derived Cyclohexadienones. *Tetrahedron* **2010**, *66*, 5873–5883.

(24) Bringmann, G.; Lang, G.; Gulder, T. A. M.; Tsuruta, H.; Mühlbacher, J.; Maksimenka, K.; Steffens, S.; Schaumann, K.; Stöhr, R.; Wiese, J.; Imhoff, J. F.; Perović-Ottstadt, S.; Boreiko, O.; Müller, W. E. G. The First Sorbicillinoid Alkaloids, the Antileukemic Sorbicillactones A and B, from a Sponge-Derived Penicillium Chrysogenum Strain. *Tetrahedron* **2005**, *61*, 7252–7265.

(25) Cram, D. J.; Tishler, M. Mold Metabolites. I. Isolation of several Compounds from Clinical Penicillin. *J. Am. Chem. Soc.* **1948**, *70*, 4238–4239.

(26) Cram, D. J. Mold Metabolites. II. the Structure of Sorbicillin, a Pigment Produced by the Mold Penicillium Notatum. *J. Am. Chem. Soc.* **1948**, *70*, 4240–4243.

(27) The numbering used for sorbicillin was proposed by Dreiding in ref. 38. All other numbering used in this review was taken from that proposed by the original isolators.

(28) Arima, K.; Nakamura, H.; Komagata, K. Studies on variation of penicillin producing mold. Part 11. Biochemical genetical studies on the yellow pigments losing mutation of Penicillium chrysogenum Q 176 to pigmentless sultant Penicillium chrysogenum Q 176 Arima et Ogasawara. *J. Agric. Chem. Soc. Jpn.* **1953**, *27*, 345–348.

(29) W. B. Turner, in *Fungal Metabolites*, Academic Press, New York, 1971, ch. 5, pp.136.

(30) Trifonov, L. S.; Dreiding, A. S.; Hoesch, L.; Rast, D. M. Isolation of Four Hexaketides from *Verticillium Intertextum*. Preliminary Communication. *Helv. Chim. Acta* **1981**, *64*, 1843–1846.

(31) Nicolaou, K. C.; Jautelat, R.; Vassilikogiannakis, G.; Baran, P. S.; Simonsen, K. B. Studies Towards Trichodimerol: Novel Cascade Reactions and Polycyclic Frameworks. *Chem. Eur. J.* **1999**, *5*, 3651–3665.

(32) When these tautomeric structures become important (e.g., when discussing a biosynthetic mechanism) the same number will be given followed by a “prime” symbol. For example: **2.4′**.

(33) Sperry, S.; Samuels, G. J.; Crews, P. Vertinoid Polyketides from the Saltwater Culture of the Fungus *Trichoderma Longibrachiatum* Separated from a *Haliclona* Marine Sponge. *J. Org. Chem.* **1998**, *63*, 10011–10014.

(34) Abe, N.; Yamamoto, K.; Hirota A. Novel fungal metabolites, demethylsorbicillin and oxosorbicillinol, isolated from *Trichoderma* sp. USF-2690. *Biosci. Biotechnol. Biochem.* **2000**, *64*, 620–622.

(35) Maskey, R. P.; Grün-Wollny, I.; Laatsch, H. Sorbicillin Analogues and Related Dimeric Compounds from *Penicillium Notatum*. *J. Nat. Prod.* **2005**, *68*, 865–870.

(36) Bringmann, G.; Lang, G.; Gulder, T. A. M.; Tsuruta, H.; Mühlbacher, J.; Maksimenka, K.; Steffens, S.; Schaumann, K.; Stöhr, R.; Wiese, J.; Imhoff, J. F.; Perović-Ottstadt, S.; Boreiko, O.; Müller, W. E. G. The First Sorbicillinoid Alkaloids, the Antileukemic Sorbicillactones A and B, from a Sponge-Derived *Penicillium Chrysogenum* Strain. *Tetrahedron* **2005**, *61*, 7252–7265.

(37) Abe, N.; Sugimoto, O.; Tanji, K.; Hirota, A. Identification of the Quinol Metabolite "Sorbicillinol", a Key Intermediate Postulated in Bisorbicillinoid Biosynthesis. *J. Am. Chem. Soc.* **2000**, *122*, 12606–12607.

(38) Trifonov, L. S.; Bieri, J. H.; Prewo, R.; Dreiding, A. S.; Hoesch, L.; Rast, D. M. Isolation and Structure Elucidation of Three Metabolites from Verticillium Intertextum: Sorbicillin, Dihydrosorbicillin and Bisvertinoquinol. *Tetrahedron* **1983**, *39*, 4243–4256.

(39) Trifonov, L. S.; Hilpert, H.; Floersheim, P.; Dreiding, A. S.; Rast, D. M.; Skrivanova, R.; Hoesch, L. Bisvertinols: A New Group of Dimeric Vertinoids from Verticillium Intertextum. *Tetrahedron* **1986**, *42*, 3157–3179.

(40) Andrade, R.; Ayer, W. A.; Mebe, P. P. The Metabolites of *Trichodermalongibrachiatum*. Part 1. Isolation of the Metabolites and the Structure of Trichodimerol. *Can. J. Chem.* **1992**, *70*, 2526–2535.

(41) Warr, G. A.; Veitch, J. A.; Walsh, A. W.; Hesler, G. A.; Pirnik, D. M.; Leet, J. E.; Lin, P.-F. M.; Medina, I. A.; McBrien, K. D. et al. BMS-182123, a Fungal Metabolite that Inhibits the Production of TNF-α by Macrophages and Monocytes. *J. Antibiot.* **1996**, *49*, 234–240.

(42) Gao, Q.; Leet, J. E.; Thomas, S. T.; Matson, J. A.; Bancroft, D. P. Crystal Structure of Trichodimerol. *J. Nat. Prod.* **1995**, *58*, 1817–1821.

(43) Abe, N.; Murata, T.; Hirota, A. Novel DPPH Radical Scavengers, Bisorbicillinol and Demethyltrichodimerol, from a Fungus. *Biosci. Biotechnol. Biochem.* **1998**, *62*, 661–666.

(44) Abe, N.; Murata, T.; Yamamoto, K.; Hirota, A. Bisorbibetanone, a Novel Oxidized Sorbicillin Dimer, with 1,1-Diphenyl-2-Picrylhydrazyl Radical Scavenging Activity from a Fungus. *Tetrahedron Lett.* **1999**, *40*, 5203–5206.

(45) Lee, D.; Lee, J. H.; Cai, X. F.; Shin, J. C.; Lee, K.; Hong, Y.-S.; Lee, J. J. Fungal Metabolites, Sorbicillinoid Polyketides and Their Effects on the Activation of Peroxisome Proliferator-activated Receptor γ. *J. Antibiot.* **2005**, *58*, 615–621.

(46) Liu, W.; Gu, Q.; Zhu, W.; Cui, C.; Fan, G. Dihydrotrichodimerol and Tetrahydrotrichodimerol, Two New Bisorbicillinoids, from a Marine-derived *Penicillium terrestre*. *J. Antibiot.* **2005**, *58*, 621–624.

(47) Evidente, A.; Andolfi, A.; Cimmino, A.; Ganassi, S.; Altomare, C.; Favilla, M.; Cristofaro, A.; Vitagliano, S.; Agnese Sabatini, M. Bisorbicillinoids Produced by the Fungus *Trichoderma citrinoviride* Affect Feeding Preference of the Aphid *Schizaphis graminum*. *J. Chem. Ecol.* **2009**, *35*, 533–541.

(48) (a) Neumann, K.; Abdel-Lateff, A.; Wright, A. D.; Kehraus, S.; Krick, A.; König, G. M. Novel Sorbicillin Derivatives with an Unprecedented Carbon Skeleton from the Sponge-Derived Fungus Trichoderma Species. *Eur. J. Org. Chem.* **2007**, 2268–2275. (b) Correction: *Eur. J. Org. Chem.* **2007**, 4125.

(49) Andrade, R.; Ayer, W. A.; Trifonov, L. S. The Metabolites of *Trichoderma Longibrachiatum*. III. Two New Tetronic Acids: 5-Hydroxyvertinolide and Bislongiquinolide. *Aust. J. Chem.* **1997**, *50*, 255–258.

(50) Abe, N.; Murata, T.; Hirota, A. Novel Oxidized Sorbicillin Dimers with 1,1-Diphenyl-2-Picrylhydrazyl-Radical Scavenging Activity from a Fungus. *Biosci. Biotechnol. Biochem.* **1998**, *62*, 2120–2126.

(51) Shirota, O.; Pathak, V.; Faiz Hossain, C.; Sekita, S.; Takatori, K.; Satake, M. Structural Elucidation of Trichotetronines: Polyketides Possessing a bicyclo2.2.2]Octane Skeleton with a Tetronic Acid Moiety Isolated from *Trichoderma* Sp. *J. Chem. Soc., Perkin Trans. 1* **1997**, 2961–2964.

(52) Bringmann, G.; Gulder, T. A. M.; Lang, G.; Schmitt, S.; Stöhr, R.; Wiese, J.; Nagel, K.; Imhoff, J. F. Large-Scale Biotechnological Production of the Antileukemic Marine Natural Product Sorbicillactone A. *Marine Drugs* **2007**, *5*, 23–30.

(53) Cabrera, G. M.; Butler, M.; Rodriguez, M. A.; Godeas, A.; Haddad, R.; Eberlin, M. N. A Sorbicillinoid Urea from an Intertidal *Paecilomyces Marquandii*. *J. Nat. Prod.* **2006**, *69*, 1806–1808.

(54) Abdel-Lateff, A.; Fisch, K.; and Wright, A. D. Trichopyrone and Other Constituents from the Marine Sponge-Derived Fungus *Trichoderma* sp. *Z. Naturforsch.* **2009**, *64c*, 186–192.

(55) Trifonov, L.; Bieri, J. H.; Prewo, R.; Dreiding, A. S.; Rast, D. M.; Hoesch, L. The Constitution of Vertinolide, a New Derivative of Tetronic Acid, Produced by *Verticillium Intertextum*. *Tetrahedron* **1982**, *38*, 397–403.

(56) Takaiwa, A.; Yamashita, K. Stereochemistry of (–)-Vertinolide. *Agric. Biol. Chem.* **1983**, *47*, 429–430.

(57) G. Bringmann, G. Lang, J. Mühlbacher, K. Schaumann, S. Steffens, P. G. Rytik, U. Hentschel. J. Morschhäuser and W. E. G. Müller, in *Sponges (Porifera)*, ed. W. E. G. Müller, Springer, New York, 2003, pp. 231–253.

(58) Mehellou, Y.; De Clereq, E. Twenty-Six Years of Anti-HIV Drug Discovery: Where Do We Stand and Where Do We Go? *J. Med. Chem.* **2010**, *53,* 521–538.

(59) (a) Pham-Huy, L. A.; He, H.; Pham-Huy, C. Free Radicals, Antioxidants in Disease and Health. *Int. J. Biomed. Sci. (Monterey Park, CA, U.S.)*, **2008**, *4*, 89–96. (b) Federico, A.; Morgillo, F.; Tuccillo, C.; Ciardiello, F.; Loguercio, C. Chronic Inflammation and Oxidative Stress in Human Carcinogenesis. *Int. J. Cancer*, **2007**, *121*, 2381–2386. (c) Fearon, I. M.; Faux, S. P. Oxidative Stress and Cardiovascular Disease: Novel Tools Give (Free) Radical Insight. *J. Mol. Cell. Cardiol.* **2009**, *47*, 372–381.

(60) Kontani, M.; Sakagami, Y.; Marumo, S. First β-1,6-Glucan Biosynthesis Inhibitor, Bisvertinolone Isolated from Fungus, *Acremonium Strictum* and its Absolute Stereochemistry. *Tetrahedron Lett.* **1994**, *35*, 2577–2580.

(61) Mazzucco, C. E.; Warr, G. Trichodimerol (BMS-182123) inhibits lipopolysaccharide-induced eicosanoid secretion in THP-1 human monocytic cells. *J. Leukoc. Biol.* **1996**, *60*, 271–277.

(62) (a) (1)Clark, I. A.; Alleva, L. M.; Vissel, B. The Roles of TNF in Brain Dysfunction and Disease. *Pharmacol. Ther.* **2010**, *128*, 519–548. (b) Mewar, D.; Wilson, A. G. Treatment of Rheumatoid Arthritis with Tumour Necrosis Factor Inhibitors. *Br. J. Pharmacol.* **2011**, *162*, 785–791. (c) Bertazza. L.; Mocellin, S. The Dual Role of Tumor Necrosis Factor (TNF) in Cancer Biology. *Curr. Med. Chem.* **2010**, *17*, 3337–3352.

(63) At the time that Trifonov and co-workers made their proposal, the absolute configuration of the sorbicillinoids had not been established. As a result, they did not indicate a configuration for the stereogenic carbon atom in these structures. We have drawn the now established stereoisomers in Scheme 2.1 to avoid confusion.

(64) Bentley, R.; Keil, J. G. Tetronic Acid Biosynthesis in Molds: II. FORMATION OF PENICILLIC ACID IN PENICILLIUM CYCLOPIUM *J. Biol. Chem.* **1962**, *237*, 867–873.

(65) Al-Rawi, J.; Elvidge, J. A.; Jaiswal, D. K.; Jones, J. R.; Thomas, R. Use of Tritium Nuclear Magnetic Resonance for the Direct Location of 3H in Biosynthetically-Labelled Penicillic Acid. *J. Chem. Soc., Chem. Commun.* **1974**, 220–221.

(66) Elvidge, J. A.; Jaiswal, D. K.; Jones, J. R.; Thomas, R. Tritium Nuclear Magnetic Resonance Spectroscopy. Part 7. New Information from the Tritium Distribution

in Biosynthetically Labelled Penicillic Acid. *J. Chem. Soc., Perkin Trans. 1* **1977**, 1080–1083.

(67) Abe, N.; Sugimoto, O.; Arakawa, T.; Tanji, K.-i.; Hirota, A. Sorbicillinol, a Key Intermediate of Bisorbicillinoid Biosynthesis in Trichoderma sp. USF-2690. *Biosci. Biotechnol. Biochem.* **2001**, *65*, 2271–2279.

(68) Abe, N.; Yamamoto, K.; Arakawa, T.; Hirota, A. The Biosynthesis of Bisorbicillinoids: Evidence for a Biosynthetic Route from Bisorbicillinol to Bisorbibutenolide and Bisorbicillinolide. *Chem. Commun.* **2001**, 23–24.

(69) Abe, N.; Arakawa, T.; Yamamoto, K.; Hirota, A. Biosynthesis of bisorbicillinoid in Trichoderma sp. USF-2690; evidence for the biosynthetic pathway, via sorbicillinol, of sorbicillin, bisorbicillinol, bisorbibutenolide, and bisorbicillinolide. *Biosci. Biotechnol. Biochem.* **2002**, *66*, 2090–2099.

(70) Abe, N.; Arakawa, T.; Hirota, A. The Biosynthesis of Bisvertinolone: Evidence for Oxosorbicillinol as a Direct Precursor. *Chem. Commun.* **2002**, 204–205.

(71) Sugaya, K.; Koshino, H.; Hongo, Y.; Yasunaga, K.; Onose, J.; Yoshikawa, K.; Abe, N. The Biosynthesis of Sorbicillinoids in *Trichoderma* Sp. USF-2690: Prospect for the Existence of a Common Precursor to Sorbicillinol and 5-Epihydroxyvertinolide, a New Sorbicillinoid Member. *Tetrahedron Lett.* **2008**, *49*, 654–657.

(72) Because of the instability of sorbicillinol, Abe found it necessary to convert it into the stable 6-*O*-acetyl derivative prior to carrying out the 13C measurements. For clarity, sorbicillinol is shown in Scheme 2.2, rather than the acetate.

(73) When discussing these feeding studies, the isotopolog has been given the same number as the naturally occurring structure, but a "*" will be used to indicate that it is isotopically enriched. If two structures are isotopomeric to each other (i.e., both labeled, but the label has a different pattern), then one will be designated with a "*" and the other with a "**". For example: **2.4*** and **2.4****.

(74) Ohkata, K.; Tamura, Y.; Shetuni, B. B.; Takagi, R.; Miyanaga, W.; Kojima, S.; Paquette, L. A. Stereoselectivity Control by Oxaspiro Rings during Diels-Alder Cycloadditions to Cross-Conjugated Cyclohexadienones: the *Syn* Oxygen Phenomenon. *J. Am. Chem. Soc.* **2004**, *126*, 16783–16792.

(75) Barnes-Seeman, D.; Corey, E. J. A Two-Step Total Synthesis of the Natural Pentacycle Trichodimerol, a Novel Inhibitor of TNF-α Production. *Org. Lett.* **1999**, *1*, 1503–1504.

(76) Fahad, A. a.; Abood, A.; Fisch, K. M.; Osipow, A.; Davison, J.; Avramovic, M.; Butts, C. P.; Piel, J.; Simpson, T. J.; Cox, R. J. Oxidative Dearomatisation: The

Key Step of Sorbicillinoid Biosynthesis. *Chem. Sci.* DOI: 10.1039/C3SC52911H, **2014**.

(77) (a) Davison, J.; al Fahad, A.; Cai, M.; Song, Z.; Yehia, S. Y.; Lazarus, C. M.; Bailey, A. M.; Simpson, T. J.; Cox, R. J. Genetic, molecular, and biochemical basis of fungal tropolone biosynthesis. *Proc. Natl. Acad. Sci. U. S. A.* **2012**, *109*, 7642–7647. (b) Chiang, Y.-M.; Szewczyk, E.; Davidson, A. D.; Keller, N.; Oakley, B. R.; Wang, C. C. C. A Gene Cluster Containing Two Fungal Polyketide Synthases Encodes the Biosynthetic Pathway for a Polyketide, Asperfuranone, in Aspergillus Nidulans. *J. Am. Chem. Soc.* **2009**, *131*, 2965–2970.

(78) Kuhn, R.; Staab, H. A. Synthese Kernsubstituierter Sorbophenone. *Chem. Ber.* **1954**, *87*, 266–272.

(79) McOmie, J. F. W.; Tute, M. S. A new synthesis of clavatol and of sorbicillin. *J. Chem. Soc.* **1958**, 3226–3227.

(80) Nicolaou, K. C.; Vassilikogiannakis, G.; Simonsen, K. B.; Baran, P. S.; Zhong, Y.; Vidali, V. P.; Pitsinos, E. N.; Couladouros, E. A. Biomimetic Total Synthesis of Bisorbicillinol, Bisorbibutenolide, Trichodimerol, and Designed Analogues of the Bisorbicillinoids. *J. Am. Chem. Soc.* **2000**, *122*, 3071–3079.

(81)Bigi, F.; Casiraghi, G.; Casnati, G.; Marchesi, S.; Sartori, G.; Vignali, G. The first addition of silyl enol ethers to internal unactivated alkynes. *Tetrahedron*, **1984**, *40*, 4081–4084.

(82) Pettus, L. H.; Van de Water, R. W.; Pettus, T. R. R. Synthesis of (±)-Epoxysorbicillinol using a Novel Cyclohexa-2,5-Dienone with Synthetic Applications to Other Sorbicillin Derivatives. *Org. Lett.* **2001**, *3*, 905–908.

(83) Wood, J. L.; Thompson, B. D.; Yusuff, N.; Pflum, D. A.; Matthäus, M. S. P. Total Synthesis of (±)-Epoxysorbicillinol. *J. Am. Chem. Soc.* **2001**, *123*, 2097–2098

(84) Basha, A.; Lipton, M.; Weinreb, S. M. A Mild, General Method for Conversion of Esters to Amides. *Tetrahedron Lett.* **1977**, *18*, 4171–4172.

(85) Hong, R.; Chen, Y.; Deng, L. Catalytic Enantioselective Total Syntheses of Bisorbicillinolide, Bisorbicillinol, and Bisorbibutenolide. *Angew. Chem. Int. Ed.* **2005**, *44*, 3478–3481.

(86) Trost, B. M.; Schmidt, T. A Simple Synthesis of Dienones Via Isomerization of Alkynones Effected by Palladium Catalysts. *J. Am. Chem. Soc.* **1988**, *110*, 2301–2303.

(87) Ma, D.; Lin, Y.; Lu, X.; Yu, Y. A Novel Stereoselective Synthesis of Conjugated Dienones. *Tetrahedron Lett.* **1988**, *29*, 1045–1048.

(88) Bringmann, G.; Lang, G.; Gulder, T. A. M.; Tsuruta, H.; Mühlbacher, J.; Maksimenka, K.; Steffens, S.; Schaumann, K.; Stöhr, R.; Wiese, J.; Imhoff, J. F.; Perović-Ottstadt, S.; Boreiko, O.; Müller, W. E. G. The First Sorbicillinoid Alkaloids, the Antileukemic Sorbicillactones A and B, from a Sponge-Derived *Penicillium Chrysogenum* Strain. *Tetrahedron* **2005**, *61*, 7252–7265.

(89) (a) Kalgutkar, A.; Jones, R.; Sawant, A. In *Metabolism Pharmacokinetics and Toxicity of Functional Groups*; Smith, D. A., Ed.; RSC: Cambridge, UK, 2010; RSC Drug Discovery Series No. 1, Chapter 5. (b) Hansch, C.; Sammes, P. G.; Taylor, J. B. *Comprehensive Medicinal Chemistry*; Pergamon Press: Oxford, UK, 1990; Vol. 2, Chapter 7.1.

(90) Carreño, M. C.; González-López, M., Urbano, A. Oxidative De-aromatization of *para*-Alkyl Phenols into *para*-Peroxyquinols and *para*-Quinols Mediated by Oxone as a Source of Singlet Oxygen. *Angew. Chem. Int. Ed*. 2006, 45, 2737–2741.

(91) Nicolaou, K. C.; Vassilikogiannakis, G.; Simonsen, K. B.; Baran, P. S.; Zhong, Y-L., Vidali, V. P.; Pitsinos, E. N.; Couladouros, E. A., Biomimetic Total Synthesis of Bisorbicillinol, Bisorbibutenolide, Trichodimerol, and Designed Analogues of the Bisorbicillinoids. *J. Am. Chem. Soc.* **2000**, *122*, 3071–3079.

(92) Magdziak, D.; Meek, S. J.; Pettus, T. R. R. Cyclohexadienone Ketals and Quinols: Four Building Blocks Potentially Useful for Enantioselective Synthesis. *Chem. Rev.* **2004**, *104*, 1383–1430.

(93) (a) Lundquist, IV, J. T.; Pelletier, J. C. Improved Solid-Phase Petptide Synthesis Method Utilizing α-Azide-Protected Amino Acids. *Org. Lett.* **2001**, *3*, 781–783. (b) Dyke, J. M.; Groves, A. P.; Ogden, J. S.; Dias, A. A.; Oliveira, A. M. S.; Costa, M. L.; Barros, M. T.; Cabral, M. H.; Moutinho, A. M. C. Study of the Thermal Decomposition of 2-Azidoacetic Acid by Photoelectron and Matrix Isolation Infrared Spectroscopy. *J. Am. Chem. Soc.* **1997**, *119*, 6883–6887.

(94) Greene, T. W.; Wuts, P. G. M. Protecting Groups in Organic Synthesis, 3rd ed.; Wiley Interscience: New York, 1999, p 484.

(95) (a) Berges, D. A.; Chan, G. W.; Polansky, T. J.; Taggart, J. J.; Dunn, G. L. [4,5-Dihydro-5-thioxo-]H-tetrazoie-l-alkanoic and alkanesulfonic acids and their amide derivatives. *J. Hetero. Chem.* **1978**, *15*, 981–985. (b) Vaillancourt, V. A.; Larsen, S. D.; Tanis, S. P.; Burr, J. E.; Connell, M. A.; Cudahy, M. M.; Evans, B. R.; Fisher, P. V.; May, P. D.; Meglasson, M. D.; Robinson, D. D.; Stevens, F. C.; Tucker, J. A.; Vidmar, T. J.; Yu, J. H. Synthesis and Biological Activity of Aminoguanidine and Diaminoguanidine Analogues of the Antidiabetic/Antiobesity Agent 3-Guanidinopropionic Acid. *J. Med. Chem.* **2001**, *44*, 1231–1248.

(96) Otera, J.; Danoh, N.; Nozaki, H. Novel Template Effects of Distannoxane Catalysts in Highly Efficient Transesterification and Esterification. *J. Org. Chem*. **1991**, *56*, 5307–5311.

(97) (a) Saunders, J. H.; Slocombe, R. J. The Chemistry of the Organic Isocyanates. *Chem. Rev.* **1948**, *43*, 203–218. (b) Bräse, S.; Gil, C.; Knepper, K.; Zimmermann, V. Organic Azides: An Exploding Diversity of a Unique Class of Compounds. *Angew. Chem. Int. Ed.* **2005**, *44*, 5188–5240.

(98) La Clair, J. J.; Spargo, P.; Nargund, R. P.; Totah, N., Stereocontrolled Synthesis of (±)-12a-Deoxytetracycline. *J. Am. Chem. Soc.* **1996**, *118*, 5304–5305.

(99) Cella, J. A.; Bacon, S. W. Preparation of Dialkyl Carbonates Via the Phase-Transfer-Catalyzed Alkylation of Alkali Metal Carbonate and Bicarbonate Salts. *J. Org. Chem.* **1984**, *49*, 1122–1125.

(100) (a) Davis, K. M.; Carpenter, B. K. Unusual Facial Selectivity in the Cycloaddition of Singlet Oxygen to a Simple Cyclic Diene. *J. Org. Chem.* **1996**, *61*, 4617–4622. (b) Liu, C.; Bao, G.; Burnell, D. J. Synthetic studies toward the kempane diterpenes. Diels–Alder additions to bicyclic dienes. *J. Chem. Soc., Perkin Trans. 1* **2001**, 2644–2656. (c) Jung, M. E.; Im, G.-Y. J. Total Synthesis of Racemic Laurenditerpenol, an HIF-1 Inhibitor. *J. Org. Chem.* **2009**, *74*, 8739–8753. (d) Welch, S. C.; Prakasa Rao, A. S. C.; Gibbs, C. G.; Wong, R. Y. Stereoselective total synthesis of (±)-trichodiene: biogenetic precursor of the trichothecane sesquiterpenoids. *J. Org. Chem.* **1980**, *45*, 4077–4085. (e) Ishihara, J.; Nonaka, R.; Terasawa, Y.; Tadano, K.-i.; Ogawa, S. Synthetic studies on the trichothecene family from D-glucose. *Tetrahedron: Asymmetry* **1994**, *5*, 2217–2232. (f) Molander, G. A.; Harris, C. R. Sequenced Reactions with Samarium(II) Iodide. Tandem Intramolecular Nucleophilic Acyl Substitution/Intramolecular Barbier Cyclizations. *J. Am. Chem. Soc.* **1995**, *117*, 3705–3716.

(101) Kim, J.-G.; Jang, D. O. Direct Synthesis of Acyl Azides from Carboxylic Acids by the Combination of Trichloroacetonitrile, Triphenylphosphine and Sodium Azide. *Synlett* **2008**, 2072–2074.

(102) Ref. 7, p 410.

(103) Gentry, E. J.; Telikepalli, H.; Srinivas, P.; Mitscher, L. A. Tetraacyldiborates: Selective and efficient acylation reagents suitable for multiple parallel synthetic applications. *Comb. Chem. High Throughput Screening* **2003**, *6*, 139–145.

(104) Bui, E.; Bayle, J. P.; Perez, F.; Liebert, L.; Courtieu, J. Syntheses of Nematogen Copper Complexes using Halogen Substituted Ligands. *Liq. Cryst.* **1990**, *8*, 513–526.

(105) Luning, U.; Abbass, M.; Fahrenkrug, F. Concave Reagents, 37. A Facile Route to Aryl-Substituted 1,10-Phenanthrolines by Means of Suzuki Coupling

Reactions between Substituted Areneboronic Acids and Halogeno-1,10-Phenanthrolines. *Eur. J. Org. Chem.* **2002**, 3294–3303.

(106) Davis, T. L.; Hill, J. W. Oxidation of Tribromoresorcinol. *J. Am. Chem. Soc.* **1929**, *51*, 493–504.

(107) Frlan, R.; Gobec, S.; Kikelj, D. Synthesis of Ethyl 3-(Hydroxyphenoxy)Benzyl Butylphosphonates as Potential Antigen 85C Inhibitors. *Tetrahedron* **2007**, *63*, 10698–10708.

(108) Hofslokken, N. U.; Skattebol, L. Convenient Method for the Ortho-Formylation of Phenols. *Acta Chem. Scand.* **1999**, *53*, 258–262.

(109) Gao, S.-Y.; Ko, S.; Lin, Y.-L.; Peddinti, R. K.; Liao, C.-C. Inverse-electron-demand Diels–Alder reactions of masked o-benzoquinones with enol ethers and styrene. *Tetrahedron* **2001**, *57*, 297–308.

(110) (a) McKillop, A.; McLaren, L.; Taylor, R. J. K. A Simple and Efficient Procedure for the Preparation of p-Quinols by Hypervalent Iodine Oxidation of Phenols and Phenol Tripropylsilyl Ethers. *J. Chem. Soc., Perkin Trans. 1* **1994**, 2047–2048. (b) Kita, Y.; Tohma, H.; Inagaki, M.; Hatanaka, K.; Yakura, T. Total Synthesis of Discorhabdin C: A General Aza Spiro Dienone Formation from O-Silylated Phenol Derivatives using a Hypervalent Iodine Reagent. *J. Am. Chem. Soc.* **1992**, *114*, 2175–2180. (c) Felpin, F.-X. Oxidation of 4-arylphenol trimethylsilyl ethers to *p*-arylquinols using hypervalent iodine(III) reagents. *Tetrahedron Lett.* **2007**, *48*, 409–412.

(111) (a) Gage, J. R.; Evans, D. A. Diastereoselective aldol condensation using a chiral oxazolidinone auxiliary. *Org. Synth.* **1990**, *68*, 83–91. (b) Abiko, A.; Liu, J.; Masamune, S. Concerning the Boron-Mediated Aldol Reaction of Carboxylic Esters. *J. Org. Chem.* **1996**, *61*, 2590–2591.

(112) Kagawa , N.; Toyota , M.; Ihara, M. Yb(OTf)3–TMSCl, a Novel Catalytic System in Cross-Aldol Reactions. *Aust. J. Chem.* **2004**, *57*, 655–657.

(113) Franck, G.; Brödner, K.; Helmchen, G. Enantioselective Modular Synthesis of Cyclohexenones: Total Syntheses of (+)-Crypto- and (+)-Infectocaryone. *Org. Lett.* **2010**, *12*, 3886–3889.

(114) The compound (**3.62**) was dissolved in dichloromethane in a 1 dram vial, which was placed inside a scintillation vial containing methanol and capped tightly for one week.

(115) Tello-Aburto, R.; Kalstabakken, K. A.; Volp, K. A.; Harned, A. M. Regioselective and Stereoselective Cyclization of Cyclohexadienones Tethered to Active Methylene Groups. *Org. Biomol. Chem.* **2011**, *9*, 7849–7859.

(116) (a) Niwayama, S.; Cho, H.; Lin, C. Highly Efficient Selective Monohydrolysis of Dialkyl Malonates and their Derivatives. *Tetrahedron Lett.* **2008**, *49*, 4434–4436. (b) Shelkov, R.; Nahmany, M.; Melman, A. Acylation through Ketene Intermediates. *J. Org. Chem.* **2002**, *67*, 8975–8982.

(117) Felix, A. M. Cleavage of protecting groups with boron tribromide. *J. Org. Chem.* **1974**, *39,* 1427–1429.

(118) Jung, M. E.; Lyster, M. A. Quantitative dealkylation of alkyl esters via treatment with trimethylsilyl iodide. A new method for ester hydrolysis. *J. Am. Chem. Soc.* **1977**, *99*, 968–969.

(119) Morita, T.; Okamoto, Y.; Sakurai, H. Novel Method for Dealkylation of Esters, Ethers, and Acetals by Chlorotrimethylsilane-Sodium Iodide. *J. Chem. Soc., Chem. Commun.* **1978**, 874–875.

(120) Olah, G. A.; Narang, S. C.; Gupta, B. G. B.; Malhotra, R. Synthetic Methods and Reactions. 62. Transformations with chlorotrimethylsilane/sodium Iodide, a Convenient in Situ Iodotrimethylsilane Reagent. *J. Org. Chem.* **1979**, *44*, 1247–1251.

(121) (a) Denmark, S. E.; Regens, C. S.; Kobayashi, T. Total Synthesis of Papulacandin D. *J. Am. Chem. Soc.* **2007**, *129*, 2774–2776. (b) Laganis, E. D.; Chenard, B. L. Metal Silanolates: Organic Soluble Equivalents for O-2. *Tetrahedron Lett.* **1984**, *25*, 5831–5834.

(122) Nudelman, A.; Braun, F.; Karoly, E. Novel 7-Pyrrolocephalosporins. *J. Org. Chem.* **1978**, *43*, 3788–3788.

(123) (a) Tsukano, C.; Siegel, D. R.; Danishefsky, S. J. Differentiation of Nonconventional "Carbanions"—The Total Synthesis of Nemorosone and Clusianone. *Angew. Chem., Int. Ed.* **2007**, *46*, 8840–8844. (b) Waizumi, N.; Stankovic, A. R.; Rawal,V. H. A General Strategy to Elisabethane Diterpenes: Stereocontrolled Synthesis of Elisapterosin B via Oxidative Cyclization of an Elisabethin Precursor. *J. Am. Chem. Soc*. **2003**, *125*, 13022–13023.

(124) Ho, T.-L. *Stereoselectivity in Synthesis*; Wiley: New York, 1999, pp 191–211.

(125) For examples of γ-butyrolactones fused to a saturated six-membered ring, see: (a) Smith, A. B., III; Richmond, R. E. Total synthesis of the paniculides. *J. Am. Chem. Soc.* **1983**, *105*, 575–585. (b) Taschner, M. J.; Shahripour, A. Total synthesis of (–)-upial. *J. Am. Chem. Soc.* **1985**, *107*, 5570–5572. (c) Carda, M.; Marco, J. A. Total synthesis of the monoterpenes (−)-mintlactone and (+)-isomintlactone. *Tetrahedron* **1992**, *48*, 9789–9800. (d) Bermejo, F. A.; Rico-Ferreira, R.; Bamidele-Sanni, S.; García-Granda, S. Total Synthesis of (+)-Ampullicin and (+)-Isoampullicin: Two Fungal Metabolites with Growth Regulatory Activity Isolated from *Ampulliferina* Sp. 27. *J. Org. Chem.* **2001**, *66*,

8287–8292. (e) Maulide, N.; Markó, I. E. Stereoselective synthesis of bicyclic lactones by annelation with functionalised orthoesters. *Chem. Commun.* **2006**, 1200–1202.

(126) For examples of γ-butyrolactones fused to an unsaturated six-membered ring, see: (a) Davis, K. M.; Carpenter, B. K. Unusual Facial Selectivity in the Cycloaddition of Singlet Oxygen to a Simple Cyclic Diene. *J. Org. Chem.* **1996**, *61*, 4617–4622. (b) Liu, C.; Bao, G.; Burnell, D. J. Synthetic studies toward the kempane diterpenes. Diels–Alder additions to bicyclic dienes. *J. Chem. Soc., Perkin Trans. 1* **2001**, 2644–2656. (c) Jung, M. E.; Im, G.-Y. J. Total Synthesis of Racemic Laurenditerpenol, an HIF-1 Inhibitor. *J. Org. Chem.* **2009**, *74*, 8739–8753.

(127) For examples in which a second alkyl group is added to a bicyclic γ-butyrolactone, see: (a) Welch, S. C.; Prakasa Rao, A. S. C.; Gibbs, C. G.; Wong, R. Y. Stereoselective total synthesis of (±)-trichodiene: biogenetic precursor of the trichothecane sesquiterpenoids. *J. Org. Chem.* **1980**, *45*, 4077–4085. (b) Ishihara, J.; Nonaka, R.; Terasawa, Y.; Tadano, K.-i.; Ogawa, S. Synthetic studies on the trichothecene family from D-glucose. *Tetrahedron:Asymmetry* **1994**, *5*, 2217–2232. (c) Molander, G. A.; Harris, C. R. Sequenced Reactions with Samarium(II) Iodide. Tandem Intramolecular Nucleophilic Acyl Substitution/Intramolecular Barbier Cyclizations. *J. Am. Chem. Soc.* **1995**, *117*, 3705–3716.

(128) Tello-Aburto, R.; Kalstabakken, K. A.; Volp, K. A.; Harned, A. M. Regioselective and stereoselective cyclizations of cyclohexadienones tethered to active methylene groups. *Org. Biomol. Chem.*, **2011**, *9*, 7849–7859.

(129) *CRC Handbook of Chemistry and Physics*, 93rd ed., Boca Raton, FL, 2012, pp. 15-13–15-22.

(130) We have made several attempts at utilizing a retro-Michael process to epimerize the C7 stereocenter. Unfortunately, all efforts have resulted in either no change of d.r., or decarboxylation of the *t*-butyl ester after elevated temperatures and prolonged reaction times (see Chapter 3, section 3.3.5.h).

(131) Diastereomers were identified as endo or exo based on the chemical shifts and splitting patterns of the C6 methyne proton compared to the known diastereomers of **3.3** and **3.5** as well as observed NOE enhancements (see Appendix for details).

(132) Zhao, Y.; Truhlar, D. G. The M06 suite of density functionals for main group thermochemistry, thermochemical kinetics, noncovalent interactions, excited states, and transition elements: two new functionals and systematic testing of four M06-class functionals and 12 other functionals. *Theor. Chem. Acc.* **2008**, *120*, 215–241.

(133) (a) Becke, A. D. Density-functional thermochemistry. III. The role of exact exchange. *J. Chem. Phys.* **1993**, *98*, 5648–5652. (b) Lee, C.; Yang, W.; Parr, R. G. Development of the Colle-Salvetti correlation-energy formula into a functional of the electron density. *Phys. Rev. B* **1988**, *37*, 785–789.

(134) Hehre, W. J.; Radom, L.; Schleyer, P. v. R.; Pople, J. A. *Ab Initio Molecular Orbital Theory*, Wiley, New York, 1986.

(135) When MeCl was used to alkylate malonate **4.6** (Cs2CO3, MeCN, rt, 24 h) the alkylation product **4.5** was formed (61% yield, 64% conversion) with a 5.4:1 d.r. (*endo*:*exo*) as measured by HPLC. See Appendix for details.

(136) Zhao, Y.; Truhlar, D. G. Density Functionals with Broad Applicability in Chemistry. *Acc. Chem. Res.* **2008**, *41*, 157–167.

(137) Johnson, E. R.; Mackie, I. D.; DiLabio, G. A. Dispersion interactions in density-functional theory. *J. Phys. Org. Chem.* **2009**, *22*, 1127–1135.

(138) Steinmann, S. N.; Wodrich, M. D.; Corminboeuf, C. Overcoming systematic DFT errors for hydrocarbon reaction energies. *Theor. Chem. Acc.* **2010**, *127*, 429–442.

(139) Zhao, Y.; Truhlar, D. G. Applications and validations of the Minnesota density functionals. *Chem. Phys. Lett.* **2011**, *502*, 1–13.

(140) Wheeler, S. E.; Houk, K. N. Substituent Effects in the Benzene Dimer are Due to Direct Interactions of the Substituents with the Unsubstituted Benzene. *J. Am. Chem. Soc.* **2008**, *130*, 10854–10855.

(141) Wheeler, S. E.; McNeil, A. J.; Müller, P.; Swager, T. M.; Houk, K. N. Probing Substituent Effects in Aryl−Aryl Interactions Using Stereoselective Diels−Alder Cycloadditions. *J. Am. Chem. Soc.* **2010**, *132*, 3304–3311.

(142) Zheng, J.; Zhao, Y.; Truhlar, D. G. The DBH24/08 Database and Its Use to Assess Electronic Structure Model Chemistries for Chemical Reaction Barrier Heights. *J. Chem. Theory Comput.* **2009**, *5*, 808–821.

(143) Tang, S.-Y.; Shi, J.; Guo, Q.-X. Accurate prediction of rate constants of Diels–Alder reactions and application to design of Diels–Alder ligation. *Org. Biomol. Chem.* **2012**, *10*, 2673–2682.

(144) Including Cs in these calculations would require expanded basis sets, which would make the calculations more involved. However, the experimental results using K_2CO_3 and Cs_2CO_3 are quite similar (Table 4.2), indicating that models including K should be a reasonable approximation for experiments with Cs.

(145) We are using the syn and anti descriptors to define the relative orientation of the carbonyl oxygen atoms.

(146) The endo and exo transition states leading from **4.16A1** and **4.16A2** (M = Na and K) were calculated using B3LYP. In all cases, these transition states were higher in energy than those leading from **4.16S** (for M = Na: $\Delta G^{\ddagger}$*syn*–$\Delta G^{\ddagger}$*anti* = –5.0 to –15.0 kcal; for M = K: $\Delta G^{\ddagger}$*syn*–$\Delta G^{\ddagger}$*anti* = –4.4 to –11.1 kcal). Other than the orientation of the exocyclic ester and counterion, there were no major structural deviations in these transition states.

(147) (a) Caramella, P.; Rondan, N. G.; Padden-Row, M. N.; Houk, K. N. Origin of π-facial stereoselectivity in additions to π-bonds: generality of the anti-periplanar effect. *J. Am. Chem. Soc.* **1981**, *103*, 2438–2440. (b) Rondan, N. G.; Paddon-Row, M. N.; Caramella, P.; Mareda, J.; Mueller, P. H.; Houk, K. N. Origin of Huisgen's factor x: staggering of allylic bonds promotes anomalously rapid exo attack on norbornenes. *J. Am. Chem. Soc.* **1982**, *104*, 4974–4976. (c) Paddon-Row, M. N.; Rondan, N. G.; Houk, K. N. Staggered models for asymmetric induction: attack trajectories and conformations of allylic bonds from ab initio transition structures of addition reactions. *J. Am. Chem. Soc.* **1982**, *104*, 7162–7166. (d) Houk, K. N.; Paddon-Row, M. N.; Rondan, N. G.; Wu, Y.-D.; Brown, F. K.; Spellmeyer, D. C.; Metz, J. T.; Li, Y.; Loncharich, R. J. Theory and modeling of stereoselective organic reactions. *Science* **1986**, *231*, 1108–1117.

(148) The Houk model is based on previous observations made by Felkin, Seebach, Fukui, and Anh. See: (a) Cherest, M.; Felkin, H.; Prudent, N. Torsional strain involving partial bonds. The stereochemistry of the lithium aluminium hydride reduction of some simple open-chain ketones. *Tetrahedron Lett.* **1968**, 2199–2204. (b) Cherest, M.; Felkin, H. Torsional strain involving partial bonds. The steric course of the reaction between allyl magnesium bromide and 4-t-butyl-cyclohexanone. *Tetrahedron Lett.* **1968**, 2205–2208. (c) Seebach, D.; Maetzke, T.; Petter, W.; Klötzer, B.; Plattner, D. A. Pyramidalization and reactivity of trigonal centers. X-ray crystal structure analysis of two silyl enol ethers from 1-benzoyl- and 1-(methoxycarbonyl)-2-tert-butyl-3,5-dimethyl-4-imidazolidinone (reagents for amino acid synthesis) *J. Am. Chem. Soc.* **1991**, *113*, 1781–1786. (d) Inagaki, S.; Fukui, K. Origin and Direction of Nonequivalent Orbital Extension and Stereochemical Behaviors of Plane-Asymmetric Olefins. Exo-Electrophilic Addition to Nornornene. *Chem. Lett.* **1974**, 509–514. (e) Anh, N. T.; Eisenstein, O.; Lefour, J.-M.; Dau, M.-E. T. H. Orbital factors and asymmetric induction. *J. Am. Chem. Soc.* **1973**, *95*, 6146–6147.

(149) Martinelli, M. J.; Peterson, B. C.; Khau, V. V.; Hutschison, D. R.; Leanna, M. R.; Audia, J. E.; Droste, J. J.; Wu, Y.-D.; Houk, K. N. Stereoselective Epoxidations and Electrophilic Additions to Partial Ergot Alkaloids and Conformationally-Fixed Styrenes. Experimental and Theoretical Modeling Evidence for the Importance of Torsional Steering as a Stereocontrol Element. *J. Org. Chem.* **1994**, *59*, 2204–2210.

(150) Lucero, M. J.; Houk, K. N. Torsional Control of Epoxidation Stereoselectivity in 1,2-Dihydronaphthalenes. Transition State Modeling with Semiempirical Quantum Mechanics. *J. Org. Chem.* **1998**, *63*, 6973–6977.

(151) Cheong, P. H.-Y.; Yun, H.; Danishefsky, S. J.; Houk, K. N. Torsional Steering Controls the Stereoselectivity of Epoxidation in the Guanacastepene A Synthesis. *Org. Lett.* **2006**, *8*, 1513–1516.

(152) Wang, H.; Kohler, P.; Overman, L. E.; Houk, K. N. Origins of Stereoselectivities of Dihydroxylations of cis-Bicyclo[3.3.0]octenes. *J. Am. Chem. Soc.* **2012**, *134*, 16054–16058.

(153) Bur, S. K.; Martin, S. F. Vinylogous Mannich Reactions: Some Theoretical Studies on the Origins of Diastereoselectivity. *Org. Lett.* **2000**, *2*, 3445–3447.

(154) Carreño, M. C.; García-Cerrada, S.; Urbano, A.; Di Vitta, C. Studies of Diastereoselectivity in Diels−Alder Reactions of Enantiopure (SS)-2-(p-Tolylsulfinyl)-1,4-naphthoquinone and Chiral Racemic Acyclic Dienes. *J. Org. Chem.* **2000**, *65*, 4355–4363.

(155) Tredwell, M.; Luft, J. A. R.; Schuler, M.; Tenza, K.; Houk, K. N.; Gouverneur, V. Fluorine-Directed Diastereoselective Iodocyclizations. *Angew. Chem. Int. Ed.* **2008**, *47*, 357–360.

(156) Lucero, M. J.; Houk, K. N. Conformational Transmission of Chirality: The Origin of 1,4-Asymmetric Induction in Michael Reactions of Chiral Imines. *J. Am. Chem. Soc.* **1997**, *119*, 826–827.

(157) Ando, K.; Green, N. S.; Li, Y.; Houk, K. N. Torsional and Steric Effects Control the Stereoselectivities of Alkylations of Pyrrolidinone Enolates. *J. Am. Chem. Soc.* **1999**, *121*, 5334–5335.

(158) Meyers, A. I.; Seefeld, M. A.; Lefker, B. A. Chiral Bicyclic Lactams. A New Study on Facial Alkylation. *J. Org. Chem.* **1996**, *61*, 5712–5713, and references therein.

(159) Calculations reported by Meyers and co-workers postulated that electronic factors were responsible for the diastereoselectivity. See: (a) Meyers, A. I.; Seefeld, M. A.; Lefker, B. A.; Blake, J. F. Origin of Stereochemistry in Simple Pyrrolidinone Enolate Alkylations. *J. Am. Chem. Soc.* **1997**, *119*, 4565–4566. (b) Meyers, A. I.; Seefeld, M. A.; Lefker, B. A.; Blake, J. F.; Williard, P. G. Stereoselective Alkylations in Rigid Systems. Effect of Remote Substituents on π-Facial Additions to Lactam Enolates. Stereoelectronic and Steric Effects. *J. Am. Chem. Soc.* **1998**, *120*, 7429–7438. This was refuted by the work reported in ref 157.

(160) Meyers was able to rule out a Cieplak-type effect (Cieplak, A. S. Stereochemistry of nucleophilic addition to cyclohexanone. The importance of

two-electron stabilizing interactions. *J. Am. Chem. Soc.* **1981**, *103*, 4540–4552.) as the controlling influence. See: Meyers, A. I.; Wallace, R. H. Some observations on the validity and generality of the "Cieplak stereoelectronic effect". *J. Org. Chem.* **1989**, *54*, 2509–2510.

(161) van der Waals radii: (H: 1.20 Å, C: 1.70 Å, O: 1.52 Å). See: Bondi, A. van der Waals Volumes and Radii. *J. Phys. Chem.* **1964**, *68*, 441–451.

(162) (a) Maria, P.-C.; Gal, J.-F. A Lewis basicity scale for nonprotogenic solvents: enthalpies of complex formation with boron trifluoride in dichloromethane. *J. Phys. Chem.* **1985**, *89*, 1296–1304. (b) Gal, J.-F.; Maria, P.-C.; Massi, L.; Mayeux, C.; Burk, P.; Tammiku-Taul, J. Cesium cation affinities and basicities. *Int. J. Mass Spectrom.* **2007**, *267*, 7–23. (c) Laurence, C.; Gal, J.-F. *Lewis Basicity and Affintiy Scale. Data and Measurement*; Wiley: West Sussex, U.K., 2010; pp 323–399.

(163) Marenich, A. V.; Cramer, C. J.; Truhlar, D. G. Universal Solvation Model Based on Solute Electron Density and on a Continuum Model of the Solvent Defined by the Bulk Dielectric Constant and Atomic Surface Tensions. *J. Phys. Chem. B* **2009**, *113*, 6378–6396.

(164) For a discussion on strengths and limitations associated with solvent models, see: Cramer, C. J. *Essentials of Computational Chemistry: Theories and Models*, 2nd ed.; Wiley: West Sussex, U.K., 2004; pp 385–427.

(165) Wang, H.; Michalak, K.; Michalak, M.; Jinénez-Osés, G.; Wicha, J.; Houk, K. N. Steric Control of α- and β-Alkylation of Azulenone Intermediates in a Guanacastepene A Synthesis. *J. Org. Chem.* **2010**, *75*, 762–766.

(166) The alkylation of a thioether-containing malonate derived from enone **6** was also attempted. Unfortunately, this reaction was complicated by the production of a significant amount of ***endo*-4.5**, ***exo*-4.5**, and **4.6**.

(167) Reviews: (a) Zhdankin, V. V.; Stang, P. J. Recent Developments in the Chemistry of Polyvalent Iodine Compounds. *Chem. Rev.* **2002**, *102*, 2523–2584. (b) Zhdankin, V. V.; Stang, P. J. Chemistry of Polyvalent Iodine. *Chem. Rev.* **2008**, *108*, 5299–5358. (c) Wirth, T. Hypervalent Iodine Chemistry in Synthesis: Scope and New Directions. *Angew. Chem. Int. Ed.* **2005**, *44*, 3656–3665. (d) Moriarty, R. M. Organohypervalent Iodine: Development, Applications, and Future Directions. *J. Org. Chem.* **2005**, *70*, 2893–2903.

(168) (a) Stang, P. J.; Zhadankin, V. V. Chemistry of Polyvalent Iodine. *Chem. Rev.* **2008**, *108*, 5299–5358. (b) Akiba, K. y. In *Chemistry of Hypervalent Compounds*; Akiba, K. y. Ed.; VCH Publishers: New York, 1999.

(169) Koser,G.F. Hypervalent Halogen Compounds. In *The Chemistry of Functional Groups. Supplement D;* Patai, S.,Rappoport, Z., Eds.; Wiley: Chichester, 1983; Chapter 18.

(170) (a) Richardson, R. D.; Wirth, T. Hypervalent Iodine Goes Catalytic. *Angew. Chem. Int. Ed.* **2006**, *45*, 4402–4404. (b) Dohi, T.; Kita, Y. Hypervalent iodine reagents as a new entrance to organocatalysts. *Chem. Commun.* **2009**, 2073–2085.

(171) (a) Tohma, H.; Maruyama, A.; Maeda, A.; Maegawa, T.; Dohi, T.; Shiro, M.; Morita, T.; Kita, Y. Preparation and reactivity of 1,3,5,7-tetrakis[4-(diacetoxyiodo)phenyl]adamantane, a recyclable hypervalent iodine(III) reagent. *Angew. Chem. Int. Ed.* **2004**, *43*, 3595–3598. (b) Dohi, T.; Maruyama, A.; Yoshimura, M.; Morimoto, K.; Tohma, H.; Kita, Y. Versatile hypervalent-iodine(III)-catalyzed oxidations with *m*-chloroperbenzoic acid as a cooxidant. *Angew. Chem. Int. Ed.* **2005**, *44*, 6193–6196. (c) Dohi, T.; Maruyama, A.; Minamitsuji, Y.; Takenaga, N.; Kita, Y. First hypervalent iodine(III)-catalyzed C–N bond forming reaction: catalytic spirocyclization of amides to *N*-fused spirolactams. *Chem. Commun.* **2007**, 1224–1226.

(172) Thottumkara, A. P.; Bowsher, M. S.; Vinod, T. K. In Situ Generation of *o*-Iodoxybenzoic Acid (IBX) and the Catalytic Use of It in Oxidation Reactions in the Presence of Oxone as a Co-oxidant. *Org. Lett*. **2005**, *7*, 2933–2936.

(173) Reviews: (a) M. Ngatimin and D. W. Lupton, The Discovery of Catalytic Enantioselective Polyvalent Iodine Mediated Reactions. *Aust. J. Chem.* 2010, **63**, 653–658. (b) Liang, H.; Ciufolini, M. A Chiral Hypervalent Iodine Reagents in Asymmetric Reactions. *Angew. Chem. Int. Ed.* **2011**, *50*, 11849–11851.

(174) (a) Fujita, M.; Yoshida, Y.; Miyata, K.; Wakisaka, A.; Sugimura, T. Enantiodifferentiating endo-Selective Oxylactonization of ortho-Alk-1-enylbenzoate with a Lactate-Derived Aryl-λ3-Iodane. *Angew. Chem. Int. Ed.* **2010**, *49*, 7068–7071. (b) Fujita, M.; Mori, K.; Shimogaki, M.; Sugimura, T. Asymmetric Synthesis of 4,8-Dihydroxyisochroman-1-one Polyketide Metabolites Using Chiral Hypervalent Iodine(III). *Org. Lett.* **2012**, *14*, 1294–1297.

(175) Fujita, M.; Wakita, M.; Sugimura, T. Enantioselective Prévost and Woodward reactions using chiral hypervalent iodine(III): switchover of stereochemical course of an optically active 1,3-dioxolan-2-yl cation. *Chem. Commun.* **2011**, *47*, 3983–3985.

(176) (a) Röben, C.; Souto, J. A.; González, Y.; Lishchynskyi, A.; Muñiz, K. Enantioselective Metal-Free Diamination of Styrenes. *Angew. Chem. Int. Ed.* **2011**, *50*, 9478–9482. (b) Farid, U.; Wirth, T. Highly Stereoselective Metal-Free

Oxyaminations Using Chiral Hypervalent Iodine Reagents. *Angew. Chem. Int. Ed.* **2012**, *51*, 3462–3465.

(177) Kürti, L.; Herczegh, P.; Visy, J.; Simonyi, M.; Antus, S.; Pelter, A. New insights into the mechanism of phenolic oxidation with phenyliodonium(III) reagents. *J. Chem. Soc., Perkin Trans. 1* **1999**, 379–380.

(178) Lifetimes of phenoxenium ions generated via laser-flash photolysis have been measured and do not exceed ~170 ns. See: (a) Wang, Y.-T.; Wang, J.; Platz, M. S.; Novak, M. Direct Detection of a Transient Oxenium Ion in Water Generated by Laser Flash Photolysis. *J. Am. Chem. Soc.* **2007**, *129*, 14566–14567. (b) Wang, Y.-T.; Jin, K. J.; Leopold, S. H.; Wang, J.; Peng, H.-L.; Platz, M. S.; Xue, J.; Phillips, D. L.; Glover, S. A.; Novak, M. Characterization of Reactive Intermediates Generated During Photolysis of 4-Acetoxy-4-aryl-2,5-cyclohexadienones: Oxenium Ions and Aryloxy Radicals. *J. Am. Chem. Soc.* **2008**, *130*, 16021–16030, and references therein. (c) Hanway, P. J.; Xue, J.; Bhattacharjee, U.; Milot, M. J.; Z. Ruixue, Z.; Phillips, D. L.; Winter, A. H. Direct Detection and Reactivity of the Short-Lived Phenyloxenium Ion. *J. Am. Chem. Soc.* **2013**, *135*, 9078–9082.

(179) L. Kürti; Herczegh, P.; Visy, J.; Simonyi, M.; Antus, S.; Pelter, A. New insights into the mechanism of phenolic oxidation with phenyliodonium(III) reagents. *J. Chem. Soc., Perkin Trans. 1* **1999**, 379–380.

(180) Dohi, T.; Maruyama, A.; Takenaga, N.; Senami, K.; Minamitsuji, Y.; Fujioka, H.; Caemmerer, S. B.; Kita, Y. A chiral hypervalent iodine(III) reagent for enantioselective dearomatization of phenols. *Angew. Chem. Int. Ed.* **2008**, *47*, 3787–3790.

(181) Dohi, T.; Takenaga, N.; Nakae, T.; Toyoda, Y.; Yamasaki, M.; Shiro, M.; Fujioka, H.; Maruyama, A.; Kita, Y. Asymmetric Dearomatizing Spirolactonization of Naphthols Catalyzed by Spirobiindane-Based Chiral Hypervalent Iodine Species. *J. Am. Chem. Soc.* **2013**, *135*, 4558–4566.

(182) Uyanik, M.; Yasui, T.; Ishihara, K. Hydrogen Bonding and Alcohol Effects in Asymmetric Hypervalent Iodine Catalysis: Enantioselective Oxidative Dearomatization of Phenols. *Angew. Chem. Int. Ed.* **2013**, *52*, 9215–9218.

(183) Quideau, S.; Lyvinec, G.; Marguerit, M.; Bathany, K.; Ozanne-Beaudenon, A.; Buffeteau, T.; Cavagnat, D.; Chénedé, A. Asymmetric Hydroxylative Phenol Dearomatization through In Situ Generation of Iodanes from Chiral Iodoarenes and *m*-CPBA. *Angew. Chem. Int. Ed.* **2009**, *48*, 4605–4609.

(184) (a) Magdziak, D.; Rodriguez, A. A.; Van De Water, R. W.; Pettus, T. R. R. Regioselective Oxidation of Phenols to o-Quinones with o-Iodoxybenzoic Acid (IBX). *Org Lett*. **2002**, *4*, 285–288. (b) Gagnepain, J.; Castet, F.; Quideau, S.;

Total Synthesis of (+)-Aquaticol by Biomimetic Phenol Dearomatization: Double Diastereofacial Differentiation in the Diels–Alder Dimerization of Orthoquinols with a C_2-Symmetric Transition State. *Angew. Chem. Int. Ed.* **2007**, *46*, 1533–1535. (c) Lebrasseur, N.; Gagnepain, J.; Ozanne-Beaudenon, A.; Leger, J. M.: Efficient Access to Orthoquinols and Their [4 + 2] Cyclodimers via SIBX-Mediated Hydroxylative Phenol Dearomatization. *J. Org. Chem.* **2007**, *72*, 6280–6283.

(185) Boppisetti, J. K.; Birman, V. B. Asymmetric Oxidation of *o*-Alkylphenols with Chiral 2-(*o*-Iodoxyphenyl)-oxazolines. *Org. Lett.* **2009**, *11*, 1221–1223.

(186) (a) Posakony, J. J.; Grierson, J. R.; Tewson, T. J. New Routes to N-Alkylated Cyclic Sulfamidates. *J. Org. Chem.* **2002**, *67*, 5164–5169. (b) Moss, T.; Alonso, B.; Fenwick, D.; Dixon, D. Catalytic Enantio- and Diastereoselective Alkylations with Cyclic Sulfamidates. *Angew. Chem. Int.l Ed.* **2010**, *49*, 568–571.

(187) Bower, J. F.; Szeto, P.; Gallagher, T. Enantiopure 1,4-Benzoxazines Via 1,2-Cyclic Sulfamidates. Synthesis of Levofloxacin. *Org. Lett.* **2007**, *9*, 3283–3286.

(188) Zhao, Y.; Truhlar, D. G. The M06 suite of density functionals for main group thermochemistry, thermochemical kinetics, noncovalent interactions, excited states, and transition elements: two new functionals and systematic testing of four M06-class functionals and 12 other functionals. *Theor. Chem. Acc.* **2008**, *120*, 215–241.

(189) Bergner, A.; Dolg, M.; Küchle, W.; Stoll, H.; Preuß, H. Ab initio energy-adjusted pseudopotentials for elements of groups 13–17. *Mol. Phys.* **1993**, *80*, 1431–1441.

(190) Nguyen, P.; Corpuz, E.; Heidelbaugh, T. M.; Chow, K.; Garst. M. E. A Convenient Synthesis of 7-Halo-1-indanones and 8-Halo-1-tetralones. *J. Org. Chem.* **2003**, *68*, 10195–10198.

(191) The oxidation of **5.19b** was attempted using a stoichiometric amount of an iodine(III) reagent derived from aryl iodide **5.33**. This produced quinol **5.20b** with 62:38 er. See supporting information for details.

Appendix

Materials and Methods

Unless otherwise stated, reactions were performed in flame- or oven-dried glassware under an argon or nitrogen atmosphere using anhydrous solvents. Tetrahydrofuran (THF) was distilled from sodium/benzophenone. Methanol was dried over 3Å molecular sieves. 3-Chloroperoxybenzoic acid (≤ 77%) was purchased from Aldrich. Labeled ^{18}O water was obtained from Isoflex USA (98.03% enrichment). Unless otherwise stated, reactions were monitored using thin-layer chromatography (TLC) using plates precoated with silica gel XHL w/ UV254 (250 mm) and visualized by UV light or $KMnO_4$, phosphomolybdic acid, or anisaldehyde stains, followed by heating. Silica gel (particle size 32–63 mm) was used for flash column chromatography. ^1H and ^{13}C NMR spectra are reported relative to the residual solvent peak (δ 7.26 and δ 77.2 for ^1H and ^{13}C in $CDCl_3$, δ 3.31 and δ 49.0 for ^1H and ^{13}C in CD_3OD, δ 2.05 and δ 29.8 for ^1H and ^{13}C in $(CD_3)_2CO$, δ 2.50 and 128.1 for ^1H and ^{13}C in $(CD_3)_2SO$ respectively), or tetramethylsilane (δ 0.00 for ^1H) when the residual solvent peak is obscured. Data for ^1H NMR spectra are reported as follows: chemical shift (ppm) (multiplicity, coupling constant (Hz), integration). Multiplicity is described using the following abbreviations: s = singlet, d = doublet, t = triplet, q = quartet, m = multiplet, bs = broad singlet, app = apparent. IR samples were prepared on NaCl plates either neat or by evaporation from $CHCl_3$ or CH_2Cl_2.

CHAPTER 3
EXPERIMENTAL

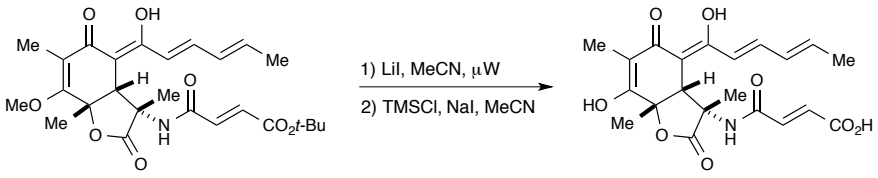

3.75 **3.1**
sorbicillactone A

Sorbicillactone A (3.1).

Compound **3.75** (12 mg, 0.025 mmol) was dissolved in MeCN (1 mL) in a microwave vial and lithium iodide (20 mg, 0.15 mmol) was added. The mixture was heated in a microwave reactor at 140 °C for 35 minutes. The product was extracted with EtOAc until the aqueous layer was no longer yellow, washed with 10% aq. $Na_2S_2O_3$ (1 mL) and brine (2 mL), dried ($MgSO_4$), filtered and concentrated. The yellow residue was dissolved in acetonitrile (1 mL) and treated with NaI (22 mg, 0.15 mmol) followed by TMSCl (20 μL, 0.15 mmol) and stirred 2 hrs. The mixture was concentrated, acidified to pH 2 with 10% aq. HCl and extracted with EtOAc until the aqueous layer was no longer yellow. The combined organic layers were washed with 10% aq. $Na_2S_2O_3$ (1 mL) and brine (2 mL), dried (Na_2SO_4), filtered and concentrated to give a quantitative yield of crude product (confirmed by ^{1}H NMR). The residue was purified by flash column chromatography (C_{18}, 80% to 50% MeCN/H_2O) affording an amorphous yellow solid (1.4 mg, 14%).

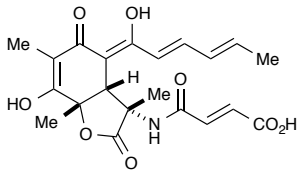

Sorbicillactone A (3.1).

Acid **3.76** was stirred in 2,6-lutidine (0.2 mL) with LiI (10 mg, 0.0738 mmol) for 1.5 h at 80 °C protected from light. After such time, the mixture was cooled to rt, diluted with EtOAc, and stirred with 10% aq. HCl for 2 min. The organic layer was separated and the aqueous layer extracted with EtOAc (2x). The combined organic layers were washed with 0.5 M HCl and brine, dried (Na_2SO_4), filtered, and concentrated to obtain 9.1 mg of amorphous yellow-orange solid. Purification by preparatory HPLC (C18, 15% to 80% acetonitrile:water) gave a yellow solid (1.2 mg, 12%).

^{1}H NMR (500 MHz, $(CD_3)_2CO$) δ 7.73 (s, NH), 7.17 (dd, *J* = 10.9, 14.7 Hz, 1H), 6.86 (d, *J* = 15.5 Hz, 1H), 6.55 (d, *J* = 14.4 Hz, 1H), 6.53 (d, *J* = 15.5 Hz, 1H), 6.34–6.29 (m, 1H), 6.19–6.12 (m, 1H), 3.73 (s, 1H), 1.84 (dd, *J* = 1.0, 6.9 Hz, 3H), 1.63 (s, 3H), 1.59 (s, 3H), 1.55 (s, 3H)

HRMS (ESI–) *m/z* 416.1340 calc for $C_{21}H_{22}NO_8$ found 416.1351

R_f 0.15 (1% AcOH/EtOAc)

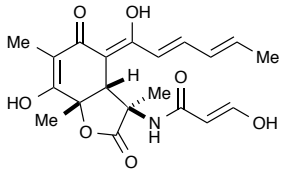

9-*epi*-sorbicillactone A (*epi*-3.1):

Compound **3.70** (39 mg, 0.079 mmol) was dissolved in MeCN (2.5 mL) in a microwave vial and lithium iodide (64 mg, 0.48 mmol) was added. The mixture was heated in a microwave reactor at 140 °C for 35 minutes.[1] At this time, NaI (71 mg, 0.48 mmol) was added followed by TMSCl (0.070 mL, 0.55 mmol) and the reaction was stirred overnight.[2] The mixture was concentrated, acidified to pH 2 with 10% aq. HCl and extracted with EtOAc until the aqueous layer was no longer yellow. The combined organic layers were washed with 10% aq. $Na_2S_2O_3$ (1 mL) and brine (2 mL), dried (Na_2SO_4), filtered and concentrated. Residue was purified by flash column

(1) Tsukano, C.; Siegel, D. R.; Danishefsky, S. J. Differentiation of Nonconventional "Carbanions"—The Total Synthesis of Nemorosone and Clusianone. *Angew. Chem., Int. Ed.* **2007**, *46*, 8840–8844.

(2) Olah, G. A.; Narang, S. C.; Gupta, B. G. B.; Malhotra, R. Synthetic methods and reactions. 62. Transformations with chlorotrimethylsilane/sodium iodide, a convenient in situ iodotrimethylsilane reagent. *J. Org. Chem.* **1979**, *44*, 1247–1251.

chromatography (C_{18}, 70:30 H_2O:MeCN) affording an amorphous yellow solid (21 mg, 64%).

^{1}H NMR (500 MHz, $(CD_3)_2CO$) δ 8.18 (s, 1H), 7.12 (dd, *J* = 10.8, 14.9 Hz, 1H), 7.05 (d, *J* = 15.6 Hz, 1H), 6.83 (d, *J* = 15.6 Hz, 1H), 6.16–6.09 (m, 1H), 6.02 (dd, *J* = 10.8, 14.5 Hz, 1H), 5.92 (d, *J* = 14.9 Hz, 1H), 4.36 (s, 1H), 1.78–1.75 (m, 9H), 1.25 (s, 3H)

^{13}C NMR (75 MHz, $(CD_3)_2CO$, DEPT) δ 191.7 (C), 174.1 (C), 171.7 (C), 166.2 (C), 165.0 (C), 164.0 (C), 139.8 (CH), 138.2 (CH), 136.5 (CH), 132.0 (CH), 131.0 (CH), 121.6 (CH), 111.0 (C), 99.4 (C), 80.5 (C), 62.0 (C), 45.3 (CH), 25.9 (CH_3), 18.8 (CH_3), 18.7 (CH_3), 7.5 (CH_3)

IR (thin film) 3303, 3075, 2983, 2926, 1771, 1713, 1660, 1614, 1546, 1413, 1382, 1349, 1261, 1214, 1067, 946 cm^{-1}

HRMS (ESI–) *m/z* 416.1340 calc for $C_{21}H_{22}NO_8$ found 416.1356

R_f 0.3 (1% AcOH/EtOAc)

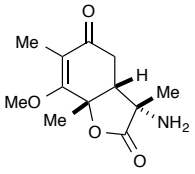

(3*S*,3a*R*,7a*S*)-3-Amino-7-methoxy-3,6,7a-trimethyl-3a,7a-dihydrobenzofuran-2,5(3*H*,4*H*)-dione (3.2).

Azide **3.73** (20.0 mg, 0.068 mmol) was dissolved in a THF-H_2O mixture (1 mL, 1:1) in a microwave vial and heated to 100 °C for 35 min. The mixture was partially concentrated, extracted with EtOAc (3 × 0.5 mL), washed with brine (0.5 mL), dried ($MgSO_4$), filtered and concentrated affording a yellow solid (12.5 mg, 77% yield). No further purification was performed.

^{1}H NMR (300 MHz, $CDCl_3$) δ 3.97 (s, 3H), 2.75 (dd, *J* = 17.5, 1.5 Hz, 1H), 2.60 (t, *J* = 12.2 Hz, 1H), 2.49 (dd, *J* = 6.9, 1.5 Hz, 1H), 1.80 (s, 3H), 1.74 (s, 3H), 1.33 (s, 3H)

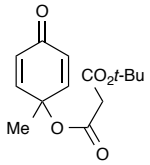

***tert*-Butyl (1-methyl-4-oxocyclohexa-2,5-dien-1-yl) malonate (3.17).**[3]

^{1}H NMR (300 MHz, C_6D_6) δ 6.35 (d, *J* = 10.2 Hz, 2 H), 6.07 (d, *J* = 10.2 Hz, 2 H), 2.97 (s, 2 H), 1.30 (s, 9 H), 1.04 (s, 3 H)

^{13}C NMR (75 MHz, C_6D_6, DEPT) δ 189.6 (C), 165.4 (C), 165.1 (C), 147.8 (CH × 2), 128.6 (CH × 2), 81.7 (C), 75.0 (C), 43.0 (CH_2), 27.9 (CH_3 × 3), 25.9 (CH_3)

IR (thin film) 2983, 2937, 1755, 1728, 1671, 1629, 1144, 1055, 854 cm^{-1}

HRMS (ESI+) 289.1046 calcd for $C_{14}H_{18}O_5Na$, found 289.1059

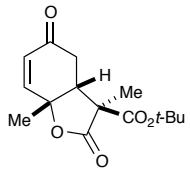

(3*R,3a*S**,7a*S**)-*tert*-Butyl 3,7a-dimethyl-2,5-dioxo-2,3,3a,4,5,7a-hexahydrobenzofuran-3-carboxylate (*endo*-3.19).**[4]

^{1}H NMR (500 MHz, $CDCl_3$) *δ* 6.72 (dd, *J* = 10.4, 1.2 Hz, 1H), 6.06 (d, *J* = 10.4 Hz, 1H), 3.38 (ddd, *J* = 6.9, 2.5, 1.3 Hz, 1H), 2.70 (dd, *J* = 18.2, 6.9 Hz, 1H), 2.59 (dd, *J* = 18.2, 2.5 Hz, 1H), 1.70 (s, 3H), 1.46 (s, 9H), 1.32 (s, 3H)

^{13}C NMR (125 MHz, $CDCl_3$, DEPT) *δ* 194.9 (C), 173.9 (C), 169.2 (C), 147.7 (CH), 129.4 (CH), 83.4 (C), 79.5 (C), 55.8 (C), 47.6 (CH), 34.5 (CH_2), 27.9 (CH_3 × 3), 26.5 (CH_3), 16.0 (CH_3)

HRMS (ESI+) *m/z* calcd for $C_{15}H_{20}O_5Na$ $[M + Na]^+$ 303.1203, found 303.1198

(3) This compound has previously been published: Tello-Aburto, R.; Kalstabakken, K. A.; Volp, K. A.; Harned, A. M. Regioselective and Stereoselective Cyclization of Cyclohexadienones Tethered to Active Methylene Groups. *Org. Biomol. Chem.* **2011**, *9*, 7849–7859.

(4) For experimental procedure and characterization of the exo compound, please see Appendix: Chapter 4 Experimental.

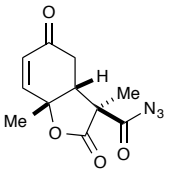

(3*S*,3a*R*,7a*R*)-3,7a-Dimethyl-2,5-dioxo-2,3,3a,4,5,7a-hexahydrobenzofuran-3-carbonyl azide (*endo*-3.20).

Ester **3.19** (268.8 mg, 1.009 mmol) was cooled to 0 °C in a rb flask and to this, TFA (3 mL) was added dropwise and the resulting mixture stirred for 4 h, slowly warming to rt. After such time, the excess TFA was removed in vacuo and placed under high vacuum until a white solid formed. Triphenylphosphine (531.0 mg, 2.018 mmol) and NaN_3 (78.7 mg, 1.121 mmol) was added and the flask flushed with N_2. Acetonitrile (10 mL) was added and after the solids were completely dissolved, the mixture was cooled to 0 °C and trichloroacetonitrile (0.2 mL) added dropwise. The mixture stirred for 5 h, slowly warming to rt and was then partially concentrated, diluted with DCM (10 mL), washed with H_2O (2 × 15 mL) and brine (15 mL), dried (Na_2SO_4), filtered and concentrated. Residue was purified by flash column chromatography (SiO_2, 2:1 hexane:EtOAc) to give a white solid (156.3 mg, 62% yield).

IR (thin film) 2982, 2148, 1775, 1686 cm^{-1}

^{1}H NMR (500 MHz, $CDCl_3$) δ 6.75 (dd, *J* = 10.4, 1.4 Hz, 1H), 6.09 (d, *J* = 10.4 Hz, 1H), 3.47-3.46 (m, 1H), 2.73 (dd, *J* = 18.3, 7.2 Hz, 1H), 2.63 (d, *J* = 18.1 Hz, 1H), 1.74 (s, 3H), 1.40 (s, 3H)

^{13}C NMR (125 MHz, $CDCl_3$, DEPT) δ 194.2 (C), 177.5 (C), 172.7 (C), 147.4 (CH), 129.6 (CH), 80.0 (C), 56.6 (C), 47.5 (CH), 34.2 (CH_2), 26.5 (CH_3), 15.9 (CH_3)

IR (thin film) 2982, 2148, 1775, 1686 cm^{-1}

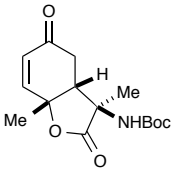

***tert*-Butyl ((3*R*,3a*R*,7a*R*)-3,7a-dimethyl-2,5-dioxo-2,3,3a,4,5,7a-hexahydrobenzofuran-3-yl)carbamate (3.22).**

Azide **3.20** was placed in a microwave vial equipped with a stir bar and *t*-BuOH (2 mL) was added. The vial was heated in a microwave reactor at 165 °C for 35 min. After such time, the excess *t*-BuOH was removed by vacuum to give a beige solid that was analytically pure (49.5 mg, quantitative yield).

^{1}H NMR (500 MHz, $CDCl_3$) δ 6.72 (d, *J* = 10.4 Hz, 1H), 6.04 (d, *J* = 10.4 Hz, 1H), 4.89 (s, 1H), 3.53 (d, *J* = 0.4 Hz, 1H), 2.73-2.64 (m, 2H), 1.74 (s, 3H), 1.42 (s, 9H), 1.23 (s, 3H)

^{13}C NMR (125 MHz, $CDCl_3$, DEPT) δ 195.7 (C), 175.3 (C), 154.3 (C), 148.2 (CH), 129.2 (CH), 81.1 (C), 78.4 (C), 60.3 (C), 46.1 (C), 33.8 (CH_2), 28.4 (CH_3 × 3), 26.5 (CH_3), 19.2 (CH_3)

IR (thin film) 3345, 2977, 1782, 1688, 1516 cm^{-1}

HRMS (ESI+) *m/z* 318.1312 calc for $C_{15}H_{21}NNaO_5$ found 318.1308

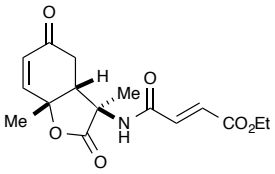

Ethyl (*E*)-4-(((3a*R*,7a*R*)-3,7a-dimethyl-2,5-dioxo-2,3,3a,4,5,7a-hexahydrobenzofuran-3-yl)amino)-4-oxobut-2-enoate (*endo*-3.24).

Azide **3.20** (88.0 mg, 0.353 mmol) was dissolved in THF (3 mL) in a microwave vial and heated to 100 °C in a microwave reactor for 20 min. Aqueous K_2CO_3 (97.0 mg, 3 mL H_2O) was added and the mixture stirred for 15 min. Ethyl fumaroyl chloride (75 μL, 0.388 mmol) was added and the mixture was stirred for another 30 min. The product was then extracted with DCM (3 × 3 mL) and the combined organic layers were washed with brine (3 mL), dried with $MgSO_4$, filtered, and concentrated. The crude material was purified by FCC to give a white solid (59 mg, 52% yield).

^{1}H NMR (300 MHz, CDCl3): δ 7.42 (s, 1H), 6.96 (d, *J* = 15.5 Hz, 1H), 6.83-6.76 (m, 2H), 6.07 (d, *J* = 10.4 Hz, 1H), 4.21 (q, *J* = 7.1 Hz, 2H), 3.56 (dd, *J* = 4.1, 1.6 Hz, 1H), 2.69-2.67 (m, 2H), 1.77 (s, 3H), 1.29 (dd, *J* = 14.3, 7.2 Hz, 6H)

^{13}C NMR (75 MHz, $CDCl_3$): δ 195.8, 174.6, 165.8, 163.3, 148.3, 135.2, 131.7, 129.2, 79.0, 61.6, 60.5, 45.8, 33.8, 26.3, 18.5, 14.2

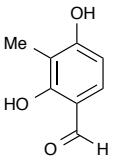

2,4-Dihydroxy-3-methylbenzaldehyde (3.32).

Phosphorous oxychloride (83 mL, 0.89 mol) was added dropwise to DMF (250 mL) stirring at 0 °C in a round-bottom flask under N_2. The mixture was then transferred via cannula to a solution of 2-methylresorcinol (50.0 g, 0.403 mol) in DMF (250 mL) stirring at 0 °C in a round-bottom flask under N_2. The mixture was stirred for 1.5 hr, slowly warming to rt. The mixture was then cooled to 0 °C and quenched with 2 M NaOH until pH 6. The product was extracted with ethyl acetate (3 x 150 mL) and concentrated. The resulting residue was dissolved in hot 10% IPA/H_2O in an Erlenmeyer flask and allowed to slowly cool overnight. The beige crystalline needles

were filtered and dried to obtain 30.3 g. A second crop of crystals gave another 6.99 g for a total of 37.29 g (61%).

^{1}H NMR (500 MHz, DMSO-d_6): δ 11.61 (s, 1H), 10.77 (s, 1H), 9.68 (s, 1H), 7.41 (d, J = 8.6 Hz, 1H), 6.55 (d, J = 8.5 Hz, 1H), 1.97 (s, 3H).

^{13}C NMR (125 MHz, DMSO-d_6) δ 195.1, 163.5, 161.3, 133.1, 114.1, 110.2, 108.1, 7.4

IR (thin film, NaCl)**:** 3276, 2780, 1622,1596, 1493, 1435, 1306, 1251, 1217, 1095 cm^{-1}

MP (uncorrected): 153.0 – 154.4 ºC

R_f 0.35 (3:1 hexane:EtOAc)

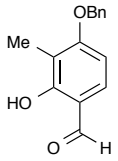

4-(Benzyloxy)-2-hydroxy-3-methylbenzaldehyde (3.34).

A literature procedure was adapted.[5] Into a round-bottom flask equipped with a stir bar was placed 2,4-dihydroxy-3-methylbenzaldehyde (**3.32**) (30.0 g, 0.197 mol), sodium bicarbonate (18.88 g, 0.2247 mol), KI (6.54 g, 0.0394 mol) and MeCN (500 mL). The flask was fitted with a reflux condenser and slowly warmed to 60 ^{o}C. At this time, benzyl bromide (28.3 mL, 0.238 mol) was added and the mixture warmed to 80 ^{o}C. After refluxing overnight, $KHCO_3$ (9.86 g, 0.0985 mol) was added and the mixture was stirred for an additional 5 hours. The mixture was then cooled to room temperature and concentrated by rotary evaporation. The residue was quenched with 10% aq. HCl (100 mL) and extracted with EtOAc (3 x 100 mL). The combined organic extracts were washed with brine (100 mL), dried with Na_2SO_4, filtered, and concentrated. The resulting oil was purified by flash chromatography (SiO_2, 100% hexane until removal of benzyl bromide, then 6:1 hexane:EtOAc) to afford an amorphous yellow solid (46.89 g, 98%).

^{1}H NMR (300 MHz, $CDCl_3$) δ 11.47 (s, 1H), 9.71 (s, 1H), 7.42–7.34 (m, 6H), 6.61 (d, J = 8.7, 1H), 5.19 (s, 2H), 2.17 (s, 3H)

^{13}C NMR (75 MHz, $CDCl_3$) δ 194.9, 163.5, 161.3, 136.4, 133.3, 128.8, 128.3, 127.2, 115.6, 104.4, 104.2, 70.4, 7.7

IR (thin film) 3030, 2923, 2839, 1641, 1626, 1498, 1289, 1250, 1111 cm^{-1}

HRMS (CI, CH_4) *m/z* 243.1016 calc for $[C_{15}H_{14}O_3 + H]^+$ found 243.1030

R_f 0.65 (3:1 hexane:EtOAc)

(5) Mendelson, W. L.; Holmes, M.; Dougherty, J. The Regioselective 4-Benzylation of 2,4-Dihydroxybenzaldehyde. *Synth. Commun.* **1996**, *26*, 593–601.

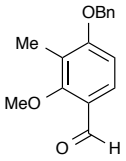

4-(Benzyloxy)-2-methoxy-3-methylbenzaldehyde (3.39).

Benzaldehyde **3.34** (18.5 g, 0.0764 mol) was placed into a round-bottom flask equipped with stir bar and DMF (300 mL) was added. To the resulting solution was added K_2CO_3 (31.7 g, 0.229 mol), followed by MeI (5.14 mL, 0.826 mol). A reflux condenser was added and the mixture heated to 80 ^oC for 3 hours. The reaction was then cooled to r.t., poured onto water (100 mL) and extracted with ether (3 x 100 mL). The organic layers were combined and washed with water (100 mL), 10% aq. NaOH (75 mL) and brine (100 mL), dried with $MgSO_4$, filtered and concentrated to obtain an amorphous yellow solid (19.1 g, 97%).

^{1}H NMR (300 MHz, $CDCl_3$) δ 10.24 (s, 1H), 7.73 (d, *J* = 8.7 Hz, 1H), 7.43–7.35 (m, 5H), 6.81 (d, *J* = 8.7 Hz, 1H), 5.16 (s, 2H), 3.87 (s, 3H), 2.23 (s, 3H)

^{13}C NMR (75 MHz, $CDCl_3$) δ 189.3, 163.2, 162.8, 136.4, 128.8, 128.3, 128.0, 127.3, 123.1, 120.7, 107.9, 70.5, 63.4, 8.9

IR (thin film) 2934, 2861, 1678, 1591, 1277, 1256, 1100 cm^{-1}

HRMS (ESI+) *m/z* 279.0992 calc for $C_{16}H_{16}NaO_3$ found 279.0986

R_f 0.7 (6:1 hexane:EtOAc)

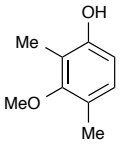

3-Methoxy-2,4-dimethylphenol (3.40).

A round bottom flask was charged with benzaldehyde **3.34** (15.0 g, 58.5 mmol) and 10% Pd/Carbon[6] (3 mol %, 3.2 g) under N_2. To this mixture was added MeOH (250 mL) and the N_2 was replaced by a H_2 balloon. The reaction mixture was stirred at ambient temperature for 3 hours. At this time, 1 drop of conc. HCl was added and the reaction continued to stir under H_2 overnight. The mixture was then filtered through a pad of celite, concentrated, and the crude residue was purified by flash column chromatography (SiO_2, 4:1 hexane:EtOAc) giving **3.40** as a pale yellow amorphous solid (8.6 g, 96%).

^{1}H NMR (500 MHz, $CDCl_3$) δ 6.87 (d, *J* = 8.0 Hz, 1H), 6.50 (d, *J* = 8.0, 1H), 4.58 (s, OH), 3.71 (s, 3H), 2.21 (s, 3H), 2.18 (s, 3H)

^{13}C NMR (75 MHz, $CDCl_3$) δ 157.5, 153.0, 128.2, 122.9, 117.4, 110.8, 60.1, 15.8, 9.0

(6) Pd/Carbon catalyst obtained from Johnson Matthey (56% H_2O, Type 10R39).

IR (thin film) 3388, 2940, 2861, 1603, 1496, 1469, 1411, 1285, 1079, 999 cm^{-1}

HRMS (CI, CH_4) *m/z* 153.0910 calc $[C_9H_{12}O_2 + H]^+$ found 153.0930

R_f 0.6 (6:1 hexane:EtOAc)

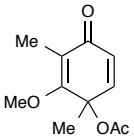

2-Methoxy-1,3-dimethyl-4-oxocyclohexa-2,5-dien-1-yl acetate (3.41).

Phenol **3.40** (328.4 mg, 2.158 mmol) was dissolved in AcOH (4 mL) and to this, PIDA (729.8 mg, 2.266 mmol) was added and the mixture stirred for 3 h. After such time, the mixture was diluted with H_2O (5 mL) and sat'd aq $NaHCO_3$ until bubbling stopped. The product was extracted with EtOAc (3 × 10 mL), washed with sat'd aq $NaHCO_3$ (2 × 10 mL) and brine (10 mL), dried (Na_2SO_4), filtered and concentrated. An orange oil that solidified overnight was isolated (183.8 mg, 41% yield).

^{1}H NMR (500 MHz, $CDCl_3$) δ 6.59 (dd, *J* = 9.9, 0.4 Hz, 1H), 6.21 (d, *J* = 9.9 Hz, 1H), 3.90 (d, *J* = 0.5 Hz, 3H), 2.07 (d, *J* = 0.5 Hz, 3H), 1.92 (s, 3H), 1.54 (s, 3H).

^{13}C NMR (125 MHz, $CDCl_3$, DEPT) δ 187.9 (C), 170.5 (C), 169.5 (C), 145.2 (CH), 127.6 (CH), 118.1 (C), 75.6 (C), 61.3 (CH_3), 25.6 (CH_3), 21.2 (CH_3), 9.7 (CH_3)

HRMS (ESI+) *m/z* 233.0784 calc for $C_{11}H_{14}NaO_4$ found 233.0788

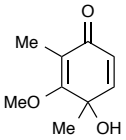

4-Hydroxy-3-methoxy-2,4-dimethylcyclohexa-2,5-dienone (3.42).

A heterogeneous mixture of phenol **3.40** (8.0 g, 53 mmol) and hexamethyldisilazane (17 mL) was heated at 125 °C for 10 minutes in a microwave reactor.[7] The resulting homogeneous solution was transferred to a round-bottom flask and concentrated. The silylated phenol was dissolved in a mixture of MeCN/H_2O (2.5:1, 178 mL) mixture and then treated with $PhI(OAc)_2$ (17.8 g, 55.2 mmol) and allowed to stir for 4 hours. The reaction mixture was then partially concentrated, diluted with saturated aq. $NaHCO_3$ (60 mL) and extracted with EtOAc (3 x 60 mL). The combined organic layers were washed with sat'd $NaHCO_3$ (30 mL) and brine (30 mL), and then dried ($MgSO_4$), filtered, and concentrated. The resulting viscous orange oil was purified by flash

(7) Mojtahedi, M. M.; Saidi, M. R.; Bolourtchian, M.; Heravi, M. M. Silylation of Hydroxy Groups with HMDS Under Microwave Irradiation and Solvent-Free Conditions. *Phosphorus, Sulfur Silicon Relat. Elem.* **2002**, *177*, 289–292.

column chromatography (SiO_2, 100% hexane to 50:50 hexane:EtOAc) to obtain an amorphous orange solid (7.07 1 g, 80%).

^{1}H NMR (300 MHz, $CDCl_3$) δ 6.66 (d, *J* = 9.9 Hz, 1H), 6.09 (d, *J* = 9.9 Hz, 1H), 4.02 (s, 3H), 2.61 (s, OH), 1.87 (s, 3H), 1.51 (s, 3H)

^{13}C NMR (75 MHz, $CDCl_3$, DEPT) δ 188.5 (C), 171.5 (C), 147.8 (CH), 126.5 (CH), 117.6 (C), 69.8 (C), 61.7 (CH_3), 26.5 (CH_3), 9.2 (CH_3)

IR (thin film, NaCl) 3391, 2981, 2932, 2851, 1662, 1608, 1456, 1214, 1094 cm^{-1}

HRMS (ESI+) *m/z* 191.0679 calc for $C_9H_{12}NaO_3$ found 191.0674

R_f 0.2 (3:1 hexane:EtOAc)

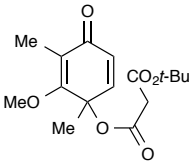

***tert*-Butyl (2-methoxy-1,3-dimethyl-4-oxocyclohexa-2,5-dien-1-yl) malonate (3.43).** While stirring at ambient temperature, a solution of dienone **3.42** (6.39 g, 38.0 mmol) in MeCN (50 mL) was treated with DMAP (0.46 g, 3.8 mmol) and mono-*t*-butyl malonic acid[8] (11.2 mL, 72.7 mmol). A solution of DCC (23.5 g, 114 mmol) in MeCN (45 mL) was added and the reaction mixture was stirred at room temperature overnight. The mixture was filtered, concentrated and purified by flash column chromatography (SiO_2, 1:4 hexane:EtOAc) giving **3.43** as a viscous orange oil (11.53 g, 98%).

^{1}H NMR (300 MHz, $CDCl_3$) δ 6.61 (d, *J* = 10.0 Hz, 1H), 6.23 (d, *J* = 10.0 Hz, 1H), 3.91 (s, 3H), 3.29 (s, 2H), 1.92 (s, 3H), 1.56 (s, 3H), 1.48 (s, 9H)

^{13}C NMR (75 MHz, $CDCl_3$) δ 187.7, 170.1, 165.40, 165.36, 144.4, 128.1, 118.2, 82.4, 76.6, 61.5, 43.1, 28.1, 25.4, 9.7

IR (neat) 2987, 2922, 1753, 1730, 1665, 1614, 1321, 1143, 1056 cm^{-1}

HRMS (ESI+) *m/z* 333.1309 calc for $C_{16}H_{22}NaO_6$ found 333.1307

R_f 0.45 (3:1 hexane:EtOAc)

([8]) Shelkov, R.; Nahmany, M.; Melman, A. Acylation through Ketene Intermediates. *J. Org. Chem.* **2002**, *67*, 8975–8982.

3.1.1. Scale-up Procedure of Cyclization/Alkylation of 3.43.

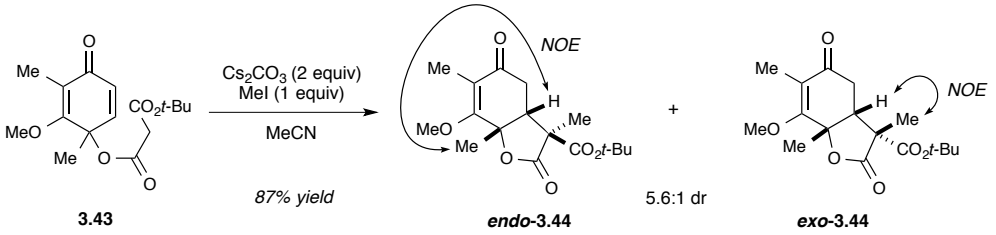

Malonate **3.42** (8.4 g, 27 mmol) was dissolved in MeCN (270 mL) and to this solution was added Cs_2CO_3 (18.52 g, 56.84 mmol) at room temperature. The mixture was stirred for 40 min at which time MeI (1.77 mL, 28.4 mmol) was added slowly. Upon complete addition of MeI, the mixture was stirred for 3 hours at room temperature before being diluted with EtOAc (50 mL), filtered, and concentrated. The crude mixture was purified and the diastereomers separated by flash column chromatography (SiO_2, 4:1 hexane:EtOAc) to give the major diastereomer ***endo*-3.44** as an amorphous beige solid (6.60 g) and the minor diastereomer ***exo*-3.44** as an amorphous yellow solid (1.08 g) for a combined yield of 87%.

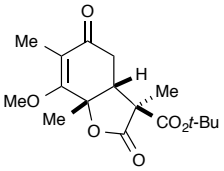

***tert*-Butyl (3*S*,3a*R*,7a*S*)-7-methoxy-3,6,7a-trimethyl-2,5-dioxo-2,3,3a,4,5,7a-hexahydrobenzofuran-3-carboxylate (*endo*-3.44).**

^{1}H NMR (500 MHz, $CDCl_3$) δ 3.95 (s, 3H), 3.29 (dd, *J* = 3.8, 6.9 Hz, 1H), 2.64 (dd, *J* = 6.9, 17.6 Hz, 1H), 2.58 (dd, *J* = 3.8, 17.6 Hz, 1H), 1.80 (s, 3H), 1.76 (s, 3H), 1.47 (s, 9H), 1.32 (s, 3H)

^{13}C NMR (75 MHz, $CDCl_3$, DEPT) δ 195.8 (C), 173.9 (C), 169.4 (C), 166.8 (C), 121.7 (C), 83.5 (C), 82.0 (C), 61.3 (CH_3), 55.5 (C), 46.8 (CH), 34.4 (CH_2), 27.9 (CH_3), 25.1 (CH_3), 16.3 (CH_3), 9.2 (CH_3)

IR (thin film) 2980, 2944, 1781, 1734, 1673, 1457, 1370, 1278, 1257, 1155, 1076 cm^{-1}

HRMS (ESI+) *m/z* 347.1465 calc for $C_{17}H_{24}NaO_6$ found 347.1466

R_f 0.45 (3:1 hexane:EtOAc)

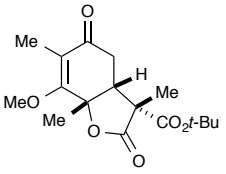

***tert*-Butyl (3R,3aR,7aS)-7-methoxy-3,6,7a-trimethyl-2,5-dioxo-2,3,3a,4,5,7a-hexahydrobenzofuran-3-carboxylate (*exo*-3.44).**

^{1}H NMR (500 MHz, $CDCl_3$) δ 3.98 (s, 3H), 2.99 (d, *J* = 18.3 Hz, 1H), 2.65 (dd, *J* = 7.6, 18.3 Hz, 1H), 2.58 (d, *J* = 7.5 Hz, 1H), 1.72 (s, 6H), 1.47 (s, 3H), 1.34 (s, 9H)

^{13}C NMR (75 MHz, $CDCl_3$, DEPT) δ 194.1 (C), 173.8 (C), 168.6 (C), 167.1 (C), 121.3 (C), 84.4 (C), 81.4 (C), 61.1 (CH_3), 55.0 (C), 51.4 (CH), 33.1 (CH_2), 27.7 (CH_3), 25.2 (CH_3), 21.5 (CH_3), 9.1 (CH_3)

IR (thin film, NaCl) 2980, 2935, 2857, 1791, 1719, 1669, 1370, 1313, 1260, 1150 cm^{-1}

HRMS (ESI+) *m/z* 347.1465 calc for $C_{17}H_{24}NaO_6$ found 347.1458

R_f 0.25 (3:1 hexane:EtOAc)

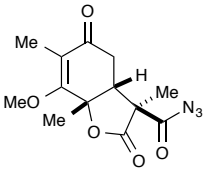

(3*S*,3a*R*,7a*S*)-7-Methoxy-3,6,7a-trimethyl-2,5-dioxo-2,3,3a,4,5,7a-hexahydrobenzofuran-3-carbonyl azide (3.45).

Compound ***endo*-3.44** (0.277 g, 0.85 mmol) was cooled to 0 °C in a round-bottom flask and trifluoroacetic acid (0.9 mL) was added dropwise. The mixture was stirred and allowed to slowly warm to room temperature. After stirring for 5 hrs the volatiles were removed in vacuo. Sodium azide (0.067 g, 1.0 mmol) and triphenylphospine (0.45 g, 1.7 mmol) were added and the reaction was cooled to 0 °C under N_2. MeCN (10 mL) was added and the mixture was stirred until homogenous. Trichloroacetonitrile (0.17 mL, 1.7 mmol) was added dropwise and reaction mixture allowed to slowly warm to room temperature and continued to stir for another 5 hours. The mixture was partially concentrated, diluted with dichloromethane (20 mL), washed with H_2O (2 x 10 mL) and brine (10 mL), dried (Na_2SO_4), filtered and concentrated. The residue was purified by flash column chromatography (SiO_2, 3:1 hexane:EtOAc) to give azide **3.45** as an amorphous white solid (180 mg, 72%).

^{1}H NMR (300 MHz, $CDCl_3$) δ 3.97 (s, 3H), 3.38 (dd, *J* = 3.21, 6.39 Hz, 1H), 2.67 (dd, *J* = 3.39, 6.36 Hz, 2H), 1.82–1.81 (m, 6H), 1.38 (s, 3H)

IR (thin film, NaCl) 2992, 2946, 2147, 1775, 1713, cm^{-1}

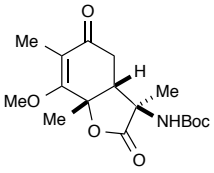

***tert*-Butyl ((3*R*,3a*R*,7a*S*)-7-methoxy-3,6,7a-trimethyl-2,5-dioxo-2,3,3a,4,5,7a-hexahydrobenzofuran-3-yl)carbamate (3.46).**

Carbamate **3.46** was synthesized from **3.45** (53 mg, 0.182 mmol) in the same fashion as **3.22.** A yellow solid (26.8 mg, 43% yield) was isolated after purification by column chromatography.

^{1}H NMR (300 MHz, $CDCl_3$) δ 4.77 (s, 1H), 3.98 (s, 3H), 3.47 (d, *J* = 5.5 Hz, 1H), 2.77-2.59 (m, 3H), 1.84 (s, 3H), 1.79 (s, 3H), 1.44 (s, 9H), 1.22 (s, 3H)

IR (thin film, NaCl) 3344, 2979, 2933, 1784, 1707, 1668, 1205 cm^{-1}

HRMS (ESI+) *m/z* 362.1574 calc for $C_{17}H_{25}NNaO_6$ found 362.1572

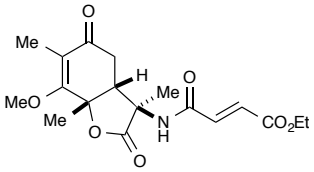

Ethyl (*E*)-4-(((3*R*,3a*R*,7a*S*)-7-methoxy-3,6,7a-trimethyl-2,5-dioxo-2,3,3a,4,5,7a-hexahydrobenzofuran-3-yl)amino)-4-oxobut-2-enoate (3.47).

Fumarate **3.47** was synthesized from **3.45** (200 mg, 0.682 mmol) in the same fashion as **3.24**. A white solid (139 mg, 56% yield) was obtained after purification by column chromatography.

^{1}H NMR (300 MHz, $CDCl_3$): δ 6.89 (d, *J* = 15.5 Hz, 1H), 6.84 (d, *J* = 15.2 Hz, 1H), 6.30 (s, 1H), 4.25 (q, *J* = 7.2 Hz, 2H), 4.00 (s, 3H), 3.52 (dd, *J* = 7.0, 2.0 Hz, 1H), 2.74 (dd, *J* = 18.0, 1.9 Hz, 1H), 2.69-2.60 (m, 1H), 1.87 (s, 3H), 1.81 (s, 3H), 1.34-1.29 (m, 5H)

HRMS (ESI+) *m/z* 388.1367 calc for $C_{18}H_{23}NNaO_7$ found 388.1376

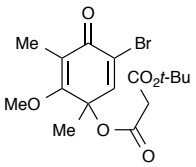

5-Bromo-2-methoxy-1,3-dimethyl-4-oxocyclohexa-2,5-dien-1-yl-*tert*-butyl malonate (3.53).

A mixture of **3.55** (130 mg, 0.53 mmol), mono-*tert*-butyl malonate (169 mg, 1.06 mmol) and DMAP (7 mg, 0.05 mmol) was dissolved in dry MeCN (1.3 mL) and treated with DCC (327 mg, 1.58 mmol). The reaction mixture was stirred at rt overnight, before diluting with 20 mL of EtOAc, and filtering through a plug of celite. The solvent was removed in vacuo and the title compound was purified by FCC using 9:1 hexanes-EtOAc to give 79 mg of a yellow oil (**3.53**) in 55% yield and 19% of recovered **3.55**.

^{1}H NMR (300 MHz, $CDCl_3$) δ 7.04 (s, 1 H), 3.90 (s, 3 H), 3.27 (s, 2 H), 1.95 (s, 3 H), 1.56 (s, 3 H), 1.45 (s, 9 H)

^{13}C NMR (75 MHz, $CDCl_3$, DEPT) δ 180.5 (C), 170.2 (C). 165.3 (C), 165.1 (C), 144.1 (CH), 124.7 (C), 117.0 (C), 82.5 (C), 77.6 (C), 61.7 (CH_3), 42.9 (CH_2), 28.0 (CH_3 × 3), 25.1 (CH_3), 10.6 (CH_3)

IR (neat) 2979, 2933, 2853, 1754, 1730, 1657, 1651, 1613, 1309, 1214, 1143, 1054 cm^{-1}

HRMS (ESI+) 441.0414 calc for $C_{16}H_{21}BrO_6Na$ found 411.0432

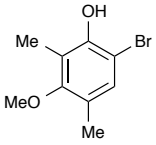

6-Bromo-3-methoxy-2,4-dimethylphenol (3.54).

Phenol **3.40** (500 mg, 3.29 mmol) was dissolved in chloroform (30 mL). To this, 1,3-dibromo-5,5-dimethylhydantoin (70 mg, 2.46 mmol) was added portionwise at rt under dark conditions. The mixture was stirred overnight before being quenched with 10% aq $Na_2S_2O_3$ (10 mL) and then extracted with CH_2Cl_2 (3 × 10 mL). The combined organic layers were washed with brine (15 mL), dried ($MgSO_4$), filtered and concentrated. The resulting brown solid was purified by FCC using 9:1 hexane-EtOAc to afford **3.54** as a yellow solid (39 mg, 51%), which quickly turned brown (product is suspected to be light sensitive).

^{1}H NMR (300 MHz, $CDCl_3$) δ 7.12 (s, 1 H), 5.42 (s, 1 H), 3.69 (s, 3 H), 2.23 (s, 3 H), 2.20 (s, 3 H)

^{13}C NMR (75 MHz, $CDCl_3$, DEPT) δ 157.3 (C), 149.3 (C), 129.8 (CH), 124.3 (C), 119.2 (C), 104.7 (C), 60.1 (CH_3), 15.6 (CH_3), 10.1 (CH_3)

IR (neat) 3511, 2939, 1596, 1470, 1405, 1308, 1235, 1209, 1085, 1003, 778 cm^{-1}

HRMS (ESI+) 229.9937 calc for $C_9H_{11}BrO_2$ found 229.01

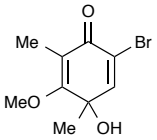

6-Bromo-4-hydroxy-3-methoxy-2,4-dimethylcyclohexa-2,5-dienone (3.55).

Bromo-phenol **3.54** was dissolved in a mixture of MeCN/H_2O (2.5:1, 9.4 mL) and then treated with phenyliodine diacetate (572 mg, 1.78 mmol) and allowed to stir rt for 5 h. The reaction mixture was quenched with sat'd $NaHCO_3$ (10 mL), partially concentrated, then diluted with and extracted with EtOAc (3 × 10 mL). The combined organic layers were washed with sat'd $NaHCO_3$ (15 mL) and brine (10 mL), and then dried (Na_2SO_4), filtered, and concentrated. The resulting viscous brown oil was purified by FCC using 100% hexane to 50:50 hexane-EtOAc to obtain a yellow solid (215 mg, 51%).

^{1}H NMR (300 MHz, $CDCl_3$) δ 7.08 (s, 1 H), 4.05 (s, 3 H), 1.85 (s, 3 H), 1.51 (s, 3 H)

^{13}C NMR (75 MHz, $CDCl_3$, DEPT) δ 181.6 (C), 171.7 (C), 148.7 (CH), 122.7 (C), 116.8 (C), 71.6 (C), 61.6 (CH_3), 25.8 (CH_3), 9.9 (CH_3)

IR (neat) 3397, 2928, 2853, 1640, 1601, 1370, 1299, 1208, 1150, 1062, 868, 762 cm^{-1}

HRMS (ESI+) 268.9784 calc for $C_9H_{11}BrO_3Na$ found 268.9784

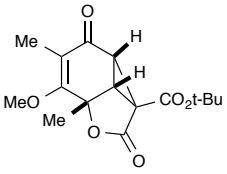

***tert*-Butyl (2a^1*R*,2b*S*,5a*S*)-5-methoxy-4,5a-dimethyl-2,3-dioxo-2a^1,2b,3,5a-tetrahydrocyclopropa[*cd*]benzofuran-2a(2*H*)-carboxylate (3.56).**

Malonate **3.53** (74 mg, 0.19 mmol) was dissolved in MeCN (3.0 mL) and to this was added Cs_2CO_3 (68 mg, 0.21 mmol) at 0 °C and stirred overnight at rt before being diluted with EtOAc (3 mL), filtered, and concentrated. The crude mixture was purified by FCC using 3:1 hexane-EtOAc to give **3.56** as a white solid (38 mg, 65%).

^{1}H NMR (300 MHz, $CDCl_3$) δ 3.90 (s, 3 H), 3.08 (d, J = 7.7 Hz, 1 H), 3.02 (d, J = 7.7 Hz, 1 H), 1.86 (s, 3 H), 1.71 (s, 3 H), 1.49 (s, 9 H)

^{13}C NMR (75 MHz, $CDCl_3$, DEPT) δ 189.3 (C), 170.4 (C), 166.0 (C), 163.5 (C), 84.2 (C), 78.3 (C), 61.6 (CH_3), 43.8 (C), 41.6 (CH), 35.4 (CH), 28.0 (CH_3 × 3), 22.1 (CH_3), 9.8 (CH_3)

IR (thin film) 2980, 2936, 1784, 1723, 1661, 1607, 1370, 1316, 1164, 1034 cm^{-1}

HRMS (ESI+) 331.1152 calc for $C_{16}H_{20}O_6Na$ found 331.1158

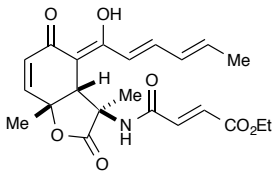

Ethyl ester model substrate (3.62).

A solution of ***endo*-3.24** (24.0 mg, 0.075 mmol) in THF (0.6 mL) was cooled to –98 °C (liq. N_2/MeOH) in a vial under N_2. To this was added 1 M LiHMDS (freshly prepared from HMDS and *n*-butyl lithium in THF) (0.16 mL, 0.163 mmol) dropwise and reaction stirred for 30 minutes. After such time, sorbyl cyanide[9] (11 mg, 0.093 mmol) in THF (0.1 mL) was added by syringe. The reaction was warmed to –78 °C after 15 minutes and stirred an additional 1 hr at –78 °C. The reaction was quenched with saturated aq. NH_4Cl (1 mL) and warmed to room temperature. The mixture was partially concentrated and extracted with EtOAc (3 x 1 mL). Combined organic layers were washed with brine, dried (Na_2SO_4), filtered and concentrated. The resulting residue was purified by flash column chromatography (SiO_2, 9:1 hexane:EtOAc) affording **3.62** (12.1 mg, 39%) as an amorphous yellow solid and 9 mg of recovered ***endo*-3.24**.

^{1}H NMR (300 MHz, $CDCl_3$): δ 16.32 (d, *J* = 0.8 Hz, 1H), 7.31-7.22 (m, 1H), 6.99-6.88 (m, 2H), 6.54 (d, *J* = 10.1, 1H), 6.46 (s, 1H), 6.22-6.08 (m, 1H), 6.09 (d, *J* = 10.1, 1H), 5.98-5.89 (m, 2H), 4.35 (s, 1H), 4.24 (q, *J* = 7.1 Hz, 2H), 1.79 (d, *J* = 6.8 Hz, 3H), 1.69 (s, 3H), 1.33-1.29 (m, 6H)

^{13}C NMR (75 MHz, $CDCl_3$): δ 186.7, 176.7, 174.2, 165.2, 163.3, 144.9, 142.7, 140.7, 134.6, 132.4, 130.8, 128.4, 119.6, 100.0, 80.8, 61.72, 61.69, 44.3, 27.3, 19.1, 19.05, 14.3

IR (thin film) 2985, 1740, 1374, 1244 cm^{-1}

(9) Santelli, M.; El Abed, D.; Jellal, A. α,β-Unsaturated acyl cyanides. 6. Self-condensation and conjugate addition of allyl-, allenyl-, propargyl-, and alkynyltrimethylsilanes. *J. Org. Chem.* **1986**, *51*, 1199–1206.

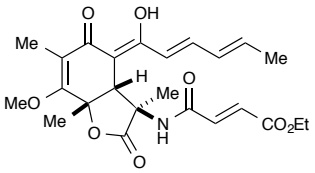

Ethyl (*E*)-4-(((3*R*,3a*R*,7a*S*,*Z*)-4-((2*E*,4*E*)-1-hydroxyhexa-2,4-dien-1-ylidene)-7-methoxy-3,6,7a-trimethyl-2,5-dioxo-2,3,3a,4,5,7a-hexahydrobenzofuran-3-yl)amino)-4-oxobut-2-enoate (3.63).

Compound **3.63** was synthesized from **3.47** (44.0 mg, 0.121 mmol) in the same fashion as **3.62**. A yellow solid (24.6 mg, 45%) was isolated after purification and 44% of **3.47** (20.0 mg) was recovered.

^{1}H NMR (500 MHz, acetone-d_6): δ 8.17 (s, 1H), 7.17 (dd, *J* = 14.6, 11.0 Hz, 1H), 7.05 (d, *J* = 15.5 Hz, 1H), 6.83 (d, *J* = 15.5 Hz, 1H), 6.17 (dd, *J* = 14.9, 7.0 Hz, 1H), 6.00 (ddd, *J* = 15.0, 11.1, 1.5 Hz, 1H), 5.92 (d, *J* = 14.9 Hz, 1H), 4.37 (s, 1H), 4.24 (q, *J* = 7.1 Hz, 2H), 4.03 (s, 3H), 1.83 (s, 3H), 1.77 (dd, *J* = 6.8, 1.0 Hz, 3H), 1.75 (s, 3H), 1.29 (t, *J* = 7.1 Hz, 3H), 1.27 (s, 3H).

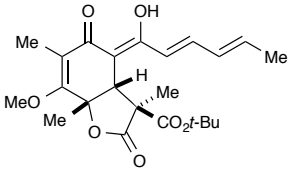

***tert*-Butyl (3*S*,3a*R*,7a*S*,*Z*)-4-((2*E*,4*E*)-1-hydroxyhexa-2,4-dien-1-ylidene)-7-methoxy-3,6,7a-trimethyl-2,5-dioxo-2,3,3a,4,5,7a-hexahydrobenzofuran-3-carboxylate (3.64).**

t-Butyl ester **3.64** was synthesized from ***endo*-3.44** (200 mg, 0.617 mmol) in the same fashion as **3.62**. A yellow solid was obtained (140 mg, 56% yield) after purification.

^{1}H NMR (300 MHz, $CDCl_3$) δ 16.48-16.47 (m, 1H), 7.30-7.21 (m, 1H), 6.19-6.09 (m, 2H), 6.01 (d, *J* = 14.8 Hz, 1H), 4.12 (s, 1H), 3.94 (d, *J* = 0.6 Hz, 3H), 1.83-1.81 (m, 6H), 1.70 (s, 3H), 1.47 (3, 9 H), 1.22 (s, 3H)

^{13}C NMR (75 MHz, $CDCl_3$, DEPT) δ 190.3 (C), 174.9 (C), 172.8 (C), 169.6 (C), 164.6 (C), 141.9 (CH), 139.5 (CH), 130.7 (C), 119.4 (C), 119.1 (CH), 98.8 (C), 83.6 (C), 83.1 (C), 61.0 (CH_3), 57.1 (C), 49.3 (CH), 27.8 (CH_3 × 3), 25.9 (CH_3), 18.9 (CH_3), 15.4 (CH_3), 8.9 (CH_3)

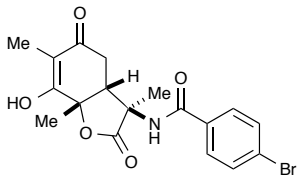

4-Bromo-*N*-(-7-methoxy-3,6,7a-trimethyl-2,5-dioxo-2,3,3a,4,5,7a-hexahydrobenzofuran-3-yl)benzamide (3.65).

Azide **3.45** (0.10 g, 0.34 mmol) was dissolved in THF (1.7 mL) and heated to 100 °C for 30 min in a microwave reactor. The observance of the isocyanate peak (2246 cm^{-1}) by IR spectroscopy confirmed the rearrangement had occurred. A mixture of K_2CO_3 (0.094 g, 0.68 mmol) in H_2O (1.7 mL) was added to the reaction mixture and stirring was continued for another 20 minutes at r.t. At this time, p-bromobenzoyl chloride (0.082 g, 0.38 mmol) was added and the mixture was stirred for another 1 hr. The mixture was acidified to pH 6 with 5% aq. HCl and extracted with EtOAc (3 x 15 mL). The combined organic layers were washed with brine, dried (Na_2SO_4), filtered and concentrated. The residue was purified by flash column chromatography (SiO_2, 3:1 hexane:EtOAc), giving **3.65** as an amorphous white solid (60 mg, 42% yield).

^{1}H NMR (500 MHz, CD_3CN) δ 7.73 (d, *J* = 8.7 Hz, 2H), 7.65 (d, *J* = 8.7 Hz, 2H), 7.29 (s, 1H), 3.93 (s, 3H), 3.47 (dd, *J* = 1.6, 7.5 Hz, 1H), 2.70 (dd, *J* = 7.5, 18.1 Hz, 1H), 2.61 (dd, *J* = 1.6, 18.1 Hz, 1H), 1.78 (s, 3H), 1.76 (s, 3H), 1.29 (s, 3H)

^{13}C NMR (75 MHz, $CDCl_3$, DEPT) δ 196.4 (C), 167.1 (C), 166.0 (C), 132.1 (CH), 131.7 (C), 128.9 (CH), 127.3 (C), 121.4 (C) 81.3 (C), 61.4 (C), 60.3 (CH_3), 45.5 (CH), 33.8 (CH_2), 25.0 (CH_3), 19.3 (CH_3), 9.1 (CH_3)

IR (thin film) 3348, 2995, 2949, 1771, 1667, 1481, 1315, 1260, 1202, 1047 cm^{-1}

HRMS (ESI+) *m/z* 446.0399 calc for $C_{19}H_{20}{}^{81}BrNNaO_5$ found 446.04

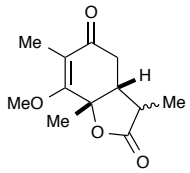

(3a*R*,7a*S*)-7-Methoxy-3,6,7a-trimethyl-3a,7a-dihydrobenzofuran-2,5(3*H*,4*H*)-dione (3.66).

Bicycle ***endo*-3.44** (500 mg, 1.54 mmol) was stirred in TFA (1.2 mL) overnight. The excess TFA was removed in vacuo until a white solid remained. The residue was dissolved in THF (10 mL) and treated with triethylamine (1.1 mL, 7.705 mmol). The mixture was heated at 65 °C for 1.5 h. After such time, the mixture was concentrated in vacuo and purified by flash column chromatography (SiO_2, 3:1 hexane:EtOAc) to give a mixture of diastereomers as a beige solid (315 mg, 91% yield).

^{1}H NMR (300 MHz, CDCl3): δ 3.95 (s, 3H, major), 3.90 (s, 3H, minor), 3.11 (quintet, *J* = 7.4 Hz, 1H, minor), 2.73-2.59 (m, 4H, mixed), 2.50-2.33 (m, 2H, mixed), 2.21 (dd, *J* = 15.5, 11.8 Hz, 1H, minor), 1.82 (s, 3H, minor), 1.76 (s, 3H, major), 1.73 (s, 3H, major), 1.63 (s, 3H, minor), 1.22 (d, *J* = 6.5 Hz, 3H, major), 1.18 (d, *J* = 7.3 Hz, 3H, minor).

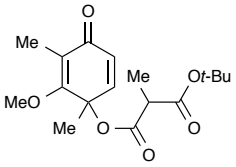

1-(*tert*-Butyl) 3-(2-methoxy-1,3-dimethyl-4-oxocyclohexa-2,5-dien-1-yl) 2-methylmalonate (3.67).

While stirring at ambient temperature, a solution of dienone **3.42** (105 mg, 0.624 mmol) in MeCN (2 mL) was treated with DMAP (8 mg, 0.062 mmol) and mono-*t*-butyl methyl malonic acid (210 mg, 1.25 mmol). A solution of DCC (386 mg, 1.87 mmol) in MeCN (2 mL) was added and the reaction mixture was stirred for 15 min. The mixture was filtered, concentrated and purified by flash column chromatography (SiO_2, 3:1 hexane:EtOAc) giving **3.67** as a beige semi-solid (200 mg, quantitative yield).

^{1}H NMR (500 MHz, CDCl3): δ 6.59 (dd, *J* = 12.2, 10.0 Hz, 1H), 6.23 (d, *J* = 9.9 Hz, 1H), 3.89 (d, *J* = 3.5 Hz, 3H), 3.39-3.31 (m, 1H), 1.92 (s, 3H), 1.56 (d, *J* = 2.6 Hz, 3H), 1.47 (s, 9H), 1.36 (dd, *J* = 7.2, 0.8 Hz, 3H).

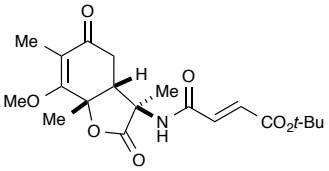

***tert*-Butyl (*E*)-4-(((3*R*,3a*R*,7a*S*)-7-methoxy-3,6,7a-trimethyl-2,5-dioxo-2,3,3a,4,5,7a-hexahydrobenzofuran-3-yl)amino)-4-oxobut-2-enoate (3.68).**

Azide **3.45** (0.20 g, 0.68 mmol) was dissolved in THF (3 mL) and heated to 100 °C for 20 min in a microwave reactor. The observance of the isocyanate peak (2246 cm^{-1}) by IR spectroscopy confirmed the rearrangement had occurred. A mixture of K_2CO_3 (0.19 g, 1.4 mmol) in H_2O (3 mL) was added to the reaction mixture and stirring continued for another 20 minutes at room temperature. At this time, mono-*t*-butyl fumaroyl chloride[10] (0.12 g, 0.75 mmol) was added and the mixture was stirred for another 1 hr.

(10) (a) Neises, B.; Steglich, W. ESTERIFICATION OF CARBOXYLIC ACIDS WITH DICYCLOHEXYLCARBODIIMIDE/4-DIMETHYLAMINOPYRIDINE: tert-BUTYL ETHYL FUMARATE. *Org. Synth.* **1985**, *63*, 183–187. (b) Denmark, S. E.; Thorarensen, A.; Middleton, D. S. Tandem [4 + 2]/[3 + 2] Cycloadditions of Nitroalkenes. 9. Synthesis of (−)-Rosmarinecine. *J. Am. Chem. Soc.* **1996**, *118*, 8266–8277.

The mixture was acidified to pH 6 with 5% aq. HCl and extracted with EtOAc (3 x 15 mL). The combined organic layers were washed with brine, dried (Na_2SO_4), filtered and concentrated. The residue was purified by flash column chromatography (SiO_2, 3:1 hexane:EtOAc) giving **3.68** as an amorphous white solid (0.139 g, 56%).

^{1}H NMR (300 MHz, $CDCl_3$) δ 7.27 (s, NH), 6.83 (d, *J* = 15.4 Hz, 1H), 6.72 (d, *J* = 15.5 Hz, 1H), 3.98 (s, 3H), 3.5 (dd, *J* = 1.7, 7.0 Hz, 1H), 2.71 (dd, *J* = 1.9, 18.2 Hz, 1H), 2.61 (dd, *J* = 7.1, 18.2 Hz, 1H), 1.84 (s, 3H), 1.78 (s, 3H), 1.46 (s, 9H), 1.29 (s, 3H)

^{13}C NMR (75 MHz, $CDCl_3$, DEPT) δ 196.5 (C), 174.4 (C), 167.2 (C), 164.6 (C), 163.5 (C), 134.0 (CH), 133.9 (CH), 121.3 (C), 82.2 (C), 81.3 (C), 61.3 (CH_3), 60.2 (C), 45.4 (CH), 33.6 (CH_2), 28.1 (CH_3), 25.0 (CH_3), 18.9 (CH_3), 9.1 (CH_3)

IR (thin film) 3323, 2978, 2936, 1782, 1715, 1669, 1531, 1370, 1310, 1151 cm^{-1}

HRMS (ESI+) *m/z* 416.1680 calc for $C_{20}H_{27}NNaO_7$ found 416.1684

R_f 0.3 (3:1 hexane:EtOAc)

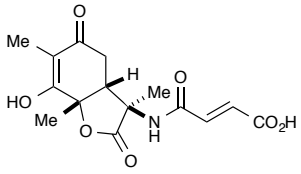

(*E*)-4-(((3*R*,3a*R*,7a*S*)-7-Hydroxy-3,6,7a-trimethyl-2,5-dioxo-2,3,3a,4,5,7a-hexahydrobenzofuran-3-yl)amino)-4-oxobut-2-enoic acid (3.69).

Fumarate **3.68** (14 mg, 0.036 mmol) was stirred in acetonitrile (0.2 mL) with sodium iodide (21 mg, 0.142 mmol) at rt under N_2. To this, freshly distilled TMSCl (18 μL, 0.142 mmol) was added and the mixture stirred 40 min. After such time, the reaction was acidified to pH 2 with 10% aq. HCl and extracted with EtOAc. The combined organic layers were washed with 10% aq. $Na_2S_2O_3$ (1 mL) and brine (2 mL), dried (Na_2SO_4), filtered and concentrated to afford a white solid (6.5 mg, 56% yield).

^{1}H NMR (500 MHz, acetone-d_6): δ 8.11 (s, 1H), 7.02 (d, *J* = 15.5 Hz, 1H), 6.69 (d, *J* = 15.5 Hz, 1H), 3.57 (d, *J* = 7.8 Hz, 1H), 2.88 (dd, *J* = 18.6, 7.9 Hz, 1H), 2.63 (d, *J* = 18.6 Hz, 1H), 1.76 (s, 3H), 1.70 (s, 3H), 1.26 (s, 3H).

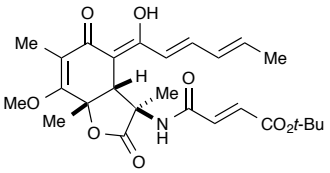

Protected 9-*epi*-sorbicillactone A (3.70):

A solution of **3.68** (44 mg, 0.12 mmol) in THF (1.2 mL) was cooled to –98 °C (liq. N_2/MeOH) in a vial under N_2. To this was added 1 M LiHMDS (freshly prepared from HMDS and *n*-butyllithium in THF) (0.26 mL, 0.253 mmol) dropwise and reaction stirred for 30 minutes. After such time, sorbyl cyanide[11] (**15**, 18 mg, 0.15 mmol) in THF (0.2 mL) was added by cannula. The reaction was warmed to –78 °C after 15 minutes and stirred an additional 1 hr at –78 °C. The reaction was quenched with saturated aq. NH_4Cl (1 mL) and warmed to room temperature. The mixture was partially concentrated and extracted with EtOAc (3 x 1 mL). Combined organic layers were washed with brine, dried (Na_2SO_4), filtered and concentrated. The resulting residue was purified by flash column chromatography (SiO_2, 9:1 hexane:EtOAc) affording **16** (40 mg, 45%) as an amorphous yellow solid and 20 mg (45%) of recovered **13**.

^{1}H NMR (500 MHz, $(CD_3)_2CO$) δ 16.47 (s, 1H), 8.15 (s, NH), 7.18 (dd, *J* = 10.9, 14.9 Hz, 1H), 6.97 (d, *J* = 15.5 Hz, 1H), 6.75 (d, *J* = 15.5, 1H), 6.22–6.15 (m, 1H), 6.02 (ddd, J = 1.1, 10.9, 14.4 Hz, 1H), 5.93 (d, *J* = 14.9 Hz, 1H), 4.37 (s, 1H), 4.03 (s, 3H), 1.83 (s, 3H), 1.80 (dd, *J* = 1.1, 6.8 Hz, 3H), 1.75 (s, 3H), 1.50 (s, 9H), 1.26 (s, 3H)

^{13}C NMR (75 MHz, $CDCl_3$, DEPT) δ 190.4 (C), 174.1 (C), 172.5 (C), 164.9 (C), 164.3 (C), 163.6 (C), 141.0 (CH), 139.1 (CH), 134.2 (CH), 133.7 (CH) 130.9 (CH), 120.0 (CH), 119.1 (C), 98.6 (C), 82.2 (C), 81.7 (C), 61.4 (CH_3), 61.0 (C), 45.4 (CH), 28.1 (CH_3), 26.2 (CH_3), 19.0 (CH_3), 18.9 (CH_3), 8.9 (CH_3)

IR (thin film) 3327, 2983, 2928, 1791, 1717, 1674, 1616, 1542, 1310, 1150, 944 cm^{-1}

HRMS (ESI+) *m/z* 510.2098 calc for $C_{26}H_{33}NNaO_8$ found 510.2120

R_f 0.75 (3:1 hexane:EtOAc)

(11) Santelli, M.; El Abed, D.; Jellal, A. α,β-Unsaturated acyl cyanides. 6. Self-condensation and conjugate addition of allyl-, allenyl-, propargyl-, and alkynyltrimethylsilanes. *J. Org. Chem.* **1986**, *51*, 1199–1206.

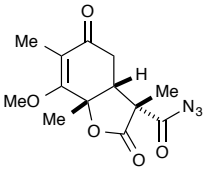

(*E*)-*tert*-Butyl-4-((7-methoxy-3,6,7a-trimethyl-2,5-dioxo-2,3,3a,4,5,7a-hexahydrobenzofuran-3-yl)amino)-4-oxobut-2-enoate (3.73).

Compound ***endo*-3.44** (0.50 g, 1.54 mmol) was cooled to 0 °C in a round-bottom flask and trifluoroacetic acid (6 mL) was added dropwise. The mixture was stirred and allowed to slowly warm to room temperature. After stirring overnight the volatiles were removed in vacuo. Sodium azide (0.12 g, 1.85 mmol) and triphenylphospine (0.81 g, 3.08 mmol) were added and the reaction was cooled to 0 °C under N_2. MeCN (15 mL) was added and the mixture was stirred until homogenous. Trichloroacetonitrile (0.31 mL, 3.08 mmol) was added dropwise and the reaction mixture was allowed to slowly warm to room temperature and continued to stir for another 3 hours. The mixture was diluted with EtOAc (7 mL), filtered over a pad of celite, and concentrated. The residue was purified by flash column chromatography (SiO_2, 2:1 hexane:EtOAc) to give **3.73** as an amorphous yellow solid (0.288 g, 64%).

^{1}H NMR (300 MHz, $CDCl_3$) δ 4.02 (s, 3H), 3.00 (d, J = 16.2 Hz, 1H), 2.75-2.65 (m, 2H), 1.75 (s, 6H), 1.52 (s, 3H)

IR (thin film, NaCl) 2987, 2948, 2143, 1790, 1700, 1668, 1624, 1311, 1195, 1179 cm^{-1}

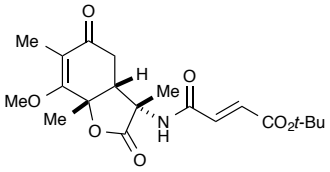

***tert*-Butyl (*E*)-4-(((3*S*,3a*R*,7a*S*)-7-methoxy-3,6,7a-trimethyl-2,5-dioxo-2,3,3a,4,5,7a-hexahydrobenzofuran-3-yl)amino)-4-oxobut-2-enoate (3.74).**

Azide **3.73** (0.172 g, 0.58 mmol) was dissolved in a mixture of THF/H_2O (2.4:1, 3.4 mL) in a microwave vial and heated to 100 °C for 20 min in a microwave reactor. The mixture was concentrated and evaporated from acetonitrile (2 x 5 mL). The resulting white residue was dissolved in acetonitrile and treated with Cs_2CO_3 (0.382 g, 1.17 mmol), DMAP (0.020 g, 0.164 mmol), and mono-*t*-butyl fumaroyl chloride[10] (0.020 g, 0.11 mmol) and stirred overnight. The mixture was acidified to pH 6 with 5% aq. HCl and extracted with EtOAc (3 x 10 mL). The combined organic layers were washed with brine, dried (Na_2SO_4), filtered and concentrated. The residue was purified by flash column chromatography (SiO_2, 2:1 hexane:EtOAc) giving **3.74** as an amorphous white solid (0.112 g, 49%) and recovering 11% (0.019 g) of the amine intermediate.

^{1}H NMR (500 MHz, $CDCl_3$) δ 7.46 (s, 1H), 6.66 (d, *J* = 15.0 Hz, 1H), 6.59 (d, *J* = 15.5 Hz, 1H), 4.17 (s, 3H), 2.76 (dd, *J* = 7.5, 18.0 Hz, 1H), 2.64–2.60 (m, 2H), 1.77 (s, 3H), 1.63 (s, 3H), 1.60 (s, 3H), 1.46 (s, 9H)

^{13}C NMR (75 MHz, $CDCl_3$, DEPT) δ 196.3 (C), 173.6 (C), 167.6 (C), 164.7 (C), 162.8 (C), 134.0 (CH), 133.2 (CH), 119.5 (C), 82.0 (C), 81.5 (C), 60.9 (CH_3), 58.3 (C), 52.2 (CH), 33.5 (CH_2), 28.1 (CH_3), 25.8 (CH_3), 25.3 (CH_3), 9.0 (CH_3)

IR (thin film) 3300, 3056, 2980, 1783, 1719, 1682, 1540, 1456, 1370, 1310, 1226, 1152, 1047, 276 cm^{-1}

HRMS (ESI+) *m/z* 416.1680 calc for $C_{20}H_{27}NNaO_7$ found 416.1680

R_f 0.25 (1:1 hexane:EtOAc)

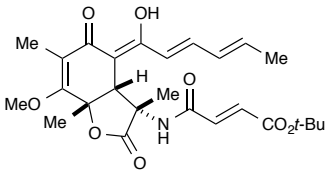

Protected sorbicillactone A (3.75).

A solution of **3.74** (0.033 g, 0.084 mmol) in THF (0.8 mL) was cooled to –98 °C (liq. N_2/MeOH) in a vial under N_2. To this was added 1 M LiHMDS (freshly prepared from HMDS and *n*-butyllithium in THF) (0.18 mL, 0.18 mmol) dropwise and reaction stirred for 30 minutes. After such time, sorbyl cyanide (12 mg, 0.10 mmol) in THF (0.2 mL) was added by cannula. The reaction was warmed to –78 °C after 10 min and stirred an additional 20 min at –78 °C. The reaction was quenched with saturated aq. NH_4Cl (1 mL) and warmed to room temperature. The mixture was partially concentrated and extracted using EtOAc (3 x 1 mL). The combined organic layers were washed with brine, dried (Na_2SO_4), filtered and concentrated. The residue was purified by flash column chromatography (SiO_2, 9:1 hexane:EtOAc) affording **3.75** (26 mg, 64%) as an amorphous yellow solid and 4 mg (12%) of **3.74**.

^{1}H NMR (300 MHz, $CDCl_3$) δ 16.33 (s, 1H) 7.30 (dd, *J* = 10.2, 14.7 Hz, 1H), 6.56 (s, 2 H), 6.24–6.10 (m, 3H), 5.68 (s, 1H), 4.17 (s, 3H), 3.27 (s, 1H), 1.88 (d, *J* = 5.7, 3H), 1.67 (m, 6H), 1.55 (s, 3H), 1.46 (s, 9H)

^{13}C NMR (75 MHz, $CDCl_3$, DEPT) δ 190.8 (C), 173.1 (C), 170.5 (C), 165.2 (C), 164.3 (C), 162.6 (C), 141.0 (CH), 139.2 (CH), 133.8 (CH), 133.3 (CH), 130.8 (CH), 119.3 (CH), 116.8 (C), 98.1 (C), 82.6 (C), 82.1 (C), 60.6 (CH_3), 59.7 (C), 54.0 (CH), 28.1 (CH_3), 26.5 (CH_3), 26.1 (CH_3), 19.0 (CH_3), 8.6 (CH_3)

IR (thin film) 3320, 2978, 2935, 2858, 1783, 1683, 1616, 1558, 1541, 1332, 1309, 1150, 1064, 940 cm^{-1}

HRMS (ESI+) *m/z* 510.2098 calc for $C_{26}H_{33}NNaO_8$ found 510.2114

R_f 0.75 (1:1 hexane:EtOAc)

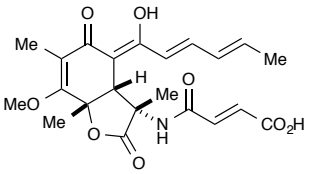

(*E*)-4-(((3*S*,3a*R*,7a*S*,*Z*)-4-((2*E*,4*E*)-1-Hydroxyhexa-2,4-dien-1-ylidene)-7-methoxy-3,6,7a-trimethyl-2,5-dioxo-2,3,3a,4,5,7a-hexahydrobenzofuran-3-yl)amino)-4-oxobut-2-enoic acid (3.76).

Compound **3.75** (12 mg, 0.0246 mmol) was stirred for 1.5 h in TFA (0.3 mL) at rt and protected from light. After such time, the mixture was concentrated in vacuo, filtered through a plug of silica (1:1 hexane:EtOAc), and concentrated to afford an amorphous yellow solid.

^{1}H NMR (500 MHz, $(CD_3)_2CO$) δ 16.39 (d, *J* = 1.3, 1H), 7.81 (s, 1H), 7.21 (dd, *J* = 14.7, 10.9, 1H), 6.87 (d, *J* = 15.4, 1H), 6.58–6.55 (m, 2H), 6.36–6.30 (m, 1H), 6.19 (dq, *J* = 14.7, 7.2, 1H), 4.17 (s, 3H), 3.75 (s, 1H), 1.84 (d, *J* = 6.7, 3H), 1.65 (s, 3H), 1.61 (s, 3H), 1.56 (s, 3H)

IR (thin film) 3297, 2930, 2855, 1777, 1678, 1610, 1554, 1419, 1231, 1151, 938 cm^{-1}

HRMS (ESI–) *m/z* 430.1496 calc for $C_{22}H_{24}NO_8$ found 430.1490

R_f 0.25 (100% EtOAc)

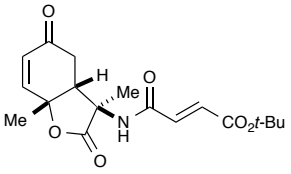

***tert*-Butyl (*E*)-4-(((3*R*,3a*R*,7a*R*)-3,7a-dimethyl-2,5-dioxo-2,3,3a,4,5,7a-hexahydrobenzofuran-3-yl)amino)-4-oxobut-2-enoate (3.77).**

Fumarate **3.77** was synthesized in the same fashion from ***endo*-3.20** (35.9 mg, 0.144 mmol) as ***endo*-3.24** except that *t*-butyl fumaroyl chloride was used. The crude material was purified by FCC (SiO_2, 1:1 hexane:EtOAc) to give a white solid (28.1 mg, 56% yield).

^{1}H NMR (500 MHz, $CDCl_3$): δ 6.96 (s, 1H), 6.82 (d, *J* = 15.4 Hz, 1H), 6.77 (dd, *J* = 10.4, 1.2 Hz, 1H), 6.73 (d, *J* = 15.4 Hz, 1H), 6.07 (d, *J* = 10.4 Hz, 1H), 3.57 (d, *J* = 6.9 Hz, 1H), 2.74-2.64 (m, 2H), 1.77 (s, 3H), 1.47 (s, 9H), 1.33 (s, 3H).

^{13}C NMR (125 MHz, $CDCl_3$, DEPT) 195.6 (C), 174.5 (C), 164.7 (C), 163.6 (C), 148.2 (CH), 134.0 (CH), 133.9 (CH), 129.2 (CH), 82.1 (C), 78.9 (C), 60.6 (C), 45.8 (CH), 33.9 (CH_2), 28.1 (CH_3 × 3), 26.4 (CH_3), 18.7 (CH_3)

IR 3329, 2979, 2932, 1785, 1718, 1677, 1534 cm^{-1}

HRMS (ESI+) *m/z* 372.141 calc for $C_{18}H_{23}NNaO_6$ found 372.1423

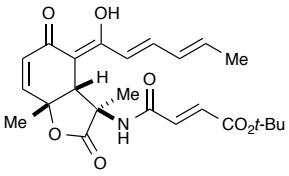

***tert*-Butyl (*E*)-4-(((3*R*,3a*R*,7a*R*,*Z*)-4-((2*E*,4*E*)-1-hydroxyhexa-2,4-dien-1-ylidene)-3,7a-dimethyl-2,5-dioxo-2,3,3a,4,5,7a-hexahydrobenzofuran-3-yl)amino)-4-oxobut-2-enoate (3.78).**

A solution of **3.77** (28.0 mg, 0.0814 mmol) in THF (0.2 mL) was cooled to –98 °C (liq. N_2/MeOH) in a vial under N_2. To this was added 1 M LiHMDS (freshly prepared from HMDS and *n*-butyllithium in THF) (0.17 mL, 0.168 mmol) dropwise and reaction stirred for 30 minutes. After such time, sorbyl cyanide[9] (12 mg, 0.098 mmol) in THF (0.1 mL) was added by syringe and the reaction stirred 30 min. After such time, the reaction was quenched with saturated aq. NH_4Cl (1 mL) and warmed to room temperature. The mixture was partially concentrated and extracted with EtOAc (3 x 1 mL). Combined organic layers were washed with brine, dried (Na_2SO_4), filtered and concentrated. The resulting residue was purified by flash column chromatography (SiO_2, 9:1 hexane:EtOAc) affording **3.78** (10.9 mg, 30%) as an amorphous yellow solid and 12.4 mg of recovered **3.77**.

^{1}H NMR (500 MHz, $CDCl_3$) δ 16.31 (d, *J* = 1.2 Hz, 1H), 7.29 (dd, *J* = 14.8, 7.4 Hz, 1H), 6.83 (d, *J* = 15.4 Hz, 1H), 6.81 (d, *J* = 15.4 Hz, 1H), 6.53 (dd, *J* = 10.1, 1.0 Hz, 1H), 6.17 (dq, *J* = 14.6, 7.2 Hz, 1H), 6.10-6.08 (m, 2H), 6.00-5.97 (m, 1H), 5.94 (d, *J* = 14.8 Hz, 1H), 4.37 (d, *J* = 0.6 Hz, 1H), 1.81 (d, *J* = 6.8 Hz, 3H), 1.69 (s, 3H), 1.50 (s, 9H), 1.32 (s, 3H)

^{13}C NMR (125 MHz, $CDCl_3$, DEPT) δ 186.6 (C), 176.9 (C), 174.1 (C), 164.2 (C), 163.6 (C), 144.9 (CH), 142.7 (CH), 140.6 (CH), 134.4 (CH), 133.5 (CH), 130.8 (CH), 128.4 (CH), 119.6 (CH), 100.1 (C), 82.2 (C), 80.8 (C), 61.7 (C), 44.3 (CH), 28.1 (CH_3 × 3), 27.3 (CH_3), 19.2 (CH_3), 19.1 (CH_3)

IR 3316, 2977, 2927, 2854, 1790, 1772, 17718, 1675 cm^{-1}

HRMS (ESI+) *m/z* 466.1836 calc for $C_{24}H_{29}NNaO_7$ found 466.1860

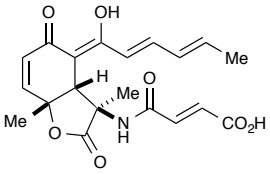

Deprotected model substrate (3.79).

t-Butyl ester **3.78** (10.0 mg) was dissolved in DCM (0.2 mL) and cooled to 0 °C and then TFA (0.2 mL) was added slowly. The mixture was stirred 5 h, slowly warming to

rt. After such time, the mixture was concentrated in vacuo. The crude NMR revealed two similar products. The residue was purified by column chromatography (SiO_2, 9:1 D_2O/MeOH) and one fraction contained pure product isolated as a yellow solid (3.4 mg, 39% yield).

^{1}H NMR (500 MHz, acetone-d_6): δ 7.24 (dd, J = 14.8, 11.0 Hz, 1H), 7.03 (d, J = 15.5 Hz, 1H), 6.86 (d, J = 15.3 Hz, 1H), 6.70 (dd, J = 10.2, 0.9 Hz, 1H), 6.23 (dq, J = 14.6, 7.1 Hz, 1H), 6.12 (d, J = 10.1 Hz, 1H), 6.10-6.04 (m, 1H), 6.01 (d, J = 14.9 Hz, 1H), 4.40 (s, 1H), 1.79 (d, J = 6.7 Hz, 3H), 1.66 (s, 3H), 1.29 (s, 3H).

CHAPTER 4
EXPERIMENTAL

4.1 COMPUTATIONAL METHODS

All calculations were performed using the *Gaussian* 09 Rev C.01 suite[12] of electronic structure programs. All geometries were fully optimized at both the M06-2X[13] and B3LYP[14] level using the 6–31G(d)[15] basis set. An ultrafine grid density was used for numerical integration.[16] Optimizations were performed with no frozen

(12) M. J. Frisch, G. W. Trucks, H. B. Schlegel, G. E. Scuseria, M. A. Robb, J. R. Cheeseman, G. Scalmani, V. Barone, B. Mennucci, G. A. Petersson, H. Nakatsuji, M. Caricato, X. Li, H. P. Hratchian, A. F. Izmaylov, J. Bloino, G. Zheng, J. L. Sonnenberg, M. Hada, M. Ehara, K. Toyota, R. Fukuda, J. Hasegawa, M. Ishida, T. Nakajima, Y. Honda, O. Kitao, H. Nakai, T. Vreven, J. A. Montgomery, Jr., J. E. Peralta, F. Ogliaro, M. Bearpark, J. J. Heyd, E. Brothers, K. N. Kudin, V. N. Staroverov, T. Keith, R. Kobayashi, J. Normand, K. Raghavachari, A. Rendell, J. C. Burant, S. S. Iyengar, J. Tomasi, M. Cossi, N. Rega, J. M. Millam, M. Klene, J. E. Knox, J. B. Cross, V. Bakken, C. Adamo, J. Jaramillo, R. Gomperts, R. E. Stratmann, O. Yazyev, A. J. Austin, R. Cammi, C. Pomelli, J. W. Ochterski, R. L. Martin, K. Morokuma, V. G. Zakrzewski, G. A. Voth, P. Salvador, J. J. Dannenberg, S. Dapprich, A. D. Daniels, O. Farkas, J. B. Foresman, J. V. Ortiz, J. Cioslowski, and D. J. Fox, *Gaussian 09*, Rev A.02; Gaussian, Inc.: Wallingford, CT, 2010.

(13) Zhao, Y.; Truhlar, D. G. The M06 suite of density functionals for main group thermochemistry, thermochemical kinetics, noncovalent interactions, excited states, and transition elements: two new functionals and systematic testing of four M06-class functionals and 12 other functionals. *Theor. Chem. Acc.* **2008**, *120*, 215–241.

(14) (a) Becke, A. D. Density-functional thermochemistry. III. The role of exact exchange. *J. Chem. Phys.* **1993**, *98*, 5648–5652. (b) Lee, C.; Yang, W.; Parr, R. G. Development of the Colle-Salvetti correlation-energy formula into a functional of the electron density. *Phys. Rev. B* **1988**, *37*, 785–789.

(15) Hehre, W. J.; Radom, L.; Schleyer, P. v. R.; Pople, J. A. *Ab Initio Molecular Orbital Theory*, Wiley, New York, 1986.

(16) Wheeler, S. E.; Houk, K. N. Integration Grid Errors for Meta-GGA-Predicted Reaction Energies: Origin of Grid Errors for the M06 Suite of Functionals. *J. Chem. Theory Comput.* **2010**, *6*, 395–404.

coordinates. In order to account for solvation effects, the SMD solvation model[17] for acetonitrile was employed during geometry optimizations. Energy minima and transition states were identified through frequency analysis.

In order to account for conformational flexibility with the exocyclic ester of ***endo*-4.5** and ***exo*-4.5** a relaxed scan of the C6–C7–C9–O dihedral was performed. A full 360º scan was performed in 11 steps (30º intervals) and the geometry of the molecule was optimized at each interval. With ***exo*-4.5** there were two conformers within 1 kcal of each other. Both were used to calculate the free energy differences given in Figure 4.2, which is why an energy range is reported. The Gibbs energy and coordinates for all relevant minima (one for ***endo*-4.5**, two for ***exo*-4.5**) are reported in the supporting information.

Houk and co-workers have found that the conformation of cyclopentene rings can be crucial for the torsional effects we are observing.[18] Conformational analysis of the two envelope conformations of the lactone enolate for **4.16S**, **4.17N**, and **4.17X** (M = Na and K) were performed. The two conformations of **4.16S** were within 1 kcal/mol of each other, but the transition states leading from these alternate conformations were both higher in energy than those shown in Figure 4.3.

For the full computational experimental of the calculated structures, please see the Supporting Information.[19]

(17) Marenich, A. V.; Cramer, C. J.; Truhlar, D. G. Universal Solvation Model Based on Solute Electron Density and on a Continuum Model of the Solvent Defined by the Bulk Dielectric Constant and Atomic Surface Tensions. *J. Phys. Chem. B* **2009**, *113*, 6378–6396.

(18) Wang, H.; Kohler, P.; Overman, L. E.; Houk, K. N. Origins of Stereoselectivities of Dihydroxylations of cis-Bicyclo[3.3.0]octenes. *J. Am. Chem. Soc.* **2012**, *134*, 16054–16058.

(19) Volp, K. A.; Harned, A. M. Origin of Stereoselectivity of the Alkylation of Cyclohexadienone-Derived Bicyclic Malonates. *J. Org. Chem.* **2013**, *78*, 7554–7564

4.2 Experimental Procedures

4.2.1. Sample Preparation.

Samples requiring quantitative NMR (qNMR) yields and diastereomeric ratios were prepared by diluting the reaction mixture with EtOAc, filtering the mixture over a plug of silica, adding Ph_3CH as an internal standard and concentrating. Reaction mixtures containing THF, DME, acetone, or MTBE were first concentrated before being diluted with EtOAc. Reaction mixtures containing dioxane, DMF, or HMPA were subjected to an aqueous workup and extracted with EtOAc (3×). The combined organic layers were washed with H_2O and brine, dried (Na_2SO_4), filtered, and then treated with the internal standard (Ph_3CH) before being concentrated. In all cases, the entire crude mixture was taken up in $CDCl_3$ and the yield determined by qNMR. The sample was then concentrated and diluted with isopropanol/hexanes for HPLC analysis. Diastereomers were separated by FCC (20% EtOAc in hexanes) and characterized individually.

4.2.2. General Procedure for Alkylation.

The substrate (0.131 mmol) was weighed into a 1 dram vial and dissolved in solvent (0.08 M). Base (1.2 equiv, 0.157 mmol) was then added to this mixture, followed by the electrophile (1.2 equiv, 0.157 mmol). The reaction mixture was stirred at rt for 8–16 h. For reactions using compound **4.6** as the starting material, the reaction progress was monitored by HPLC. After such time, the mixture was diluted with EtOAc, filtered over a plug of silica, and concentrated.

4.2.3. Procedure for the one-pot cylization/alkylation of 4.4.

Malonate-tethered cyclohexadienone **4.4** (35.2 mg, 0.131 mmol) was stirred in acetonitrile (1.6 mL). Cs_2CO_3 (90.0 mg, 0.276 mmol) was added, followed by iodomethane (9 μL). The reaction progress was followed using TLC to monitor the disappearance of the UV active starting material as the product is not UV active, but

stains with $KMnO_4$ (both starting material and product have the same R_f). The mixture was stirred for 16 h at rt, then diluted with EtOAc (2 mL) and filtered over a plug of silica, eluting with EtOAc. The internal standard (Ph_3CH) was added and the mixture concentrated under reduced pressure. Compound **4.5** was obtained in 83% yield (30.6 mg) for both diastereomers. The diastereomers were separated by FCC (20% EtOAc in hexanes).

4.2.4. Procedure for Alkylation of 4.6 with Chloromethane.

Chloromethane (450 mg) was condensed into a pressure tube that was cooled to –78 °C. Acetonitrile (1.6 mL), substrate **4.6** (35.6 mg, 0.134 mmol), and Cs_2CO_3 (51.3 mg, 0.158 mmol) were added quickly and the tube was capped, allowed to warm to rt, and stirred overnight. After 24 h, the cap was removed and the mixture was concentrated under a stream of nitrogen. The residue was diluted with EtOAc and filtered over a plug of silica. The internal standard was added and the mixture was concentrated under reduced pressure.

4.3 CHARACTERIZATION

Compounds **4.1**, **4.3**, **4.6** are reported in Chapter 3. Compounds **4.4** and **4.10** have previously been synthesized and reported.[20] HPLC retention times (t_R) are reported for **4.3** and **4.6.**

(20) Tello-Aburto, R.; Kalstabakken, K. A.; Volp, K. A.; Harned, A. M. Regioselective and Stereoselective Cyclization of Cyclohexadienones Tethered to Active Methylene Groups. *Org. Biomol. Chem.* **2011**, *9*, 7849–7859

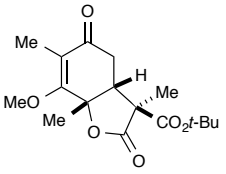

(3*R,3a*S**,7a*R**)-*tert*-butyl 7-methoxy-3,6,7a-trimethyl-2,5-dioxo-2,3,3a,4,5,7a-hexahydrobenzofuran-3-carboxylate (*endo*-4.3).**[21]

HPLC t_R = 6.6 min (λ = 254 nm).

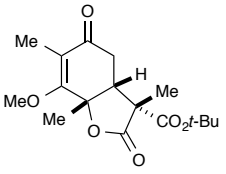

(3*R,3a*R**,7a*S**)-*tert*-butyl 7-methoxy-3,6,7a-trimethyl-2,5-dioxo-2,3,3a,4,5,7a-hexahydrobenzofuran-3-carboxylate (*exo*-4.3).**[21]

HPLC t_R = 8.9 min (λ = 254 nm).

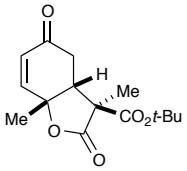

(3*R,3a*S**,7a*S**)-*tert*-butyl 3,7a-dimethyl-2,5-dioxo-2,3,3a,4,5,7a-hexahydrobenzofuran-3-carboxylate (*endo*-4.5).**

Beige amorphous solid (24.0 mg, 65%).

^{1}H NMR (500 MHz, $CDCl_3$) δ 6.72 (dd, J = 10.4, 1.2 Hz, 1H), 6.06 (d, J = 10.4 Hz, 1H), 3.38 (ddd, J = 6.9, 2.5, 1.3 Hz, 1H), 2.70 (dd, J = 18.2, 6.9 Hz, 1H), 2.59 (dd, J = 18.2, 2.5 Hz, 1H), 1.70 (s, 3H), 1.46 (s, 9H), 1.32 (s, 3H)

^{13}C NMR (125 MHz, $CDCl_3$, DEPT) δ 194.9 (C), 173.9 (C), 169.2 (C), 147.7 (CH), 129.4 (CH), 83.4 (C), 79.5 (C), 55.8 (C), 47.6 (CH), 34.5 (CH_2), 27.9 (CH_3 × 3), 26.5 (CH_3), 16.0 (CH_3)

HRMS (ESI-TOF) *m/z* calcd for $C_{15}H_{20}O_5Na$ $[M + Na]^+$ 303.1203, found 303.1198;

HPLC t_R = 9.7 min; R_f 0.4 (3:1 hexanes/EtOAc).

(21) See Chapter 3 Experimental for full characterization.

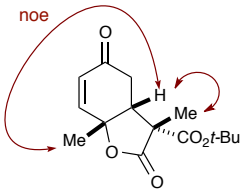

(3*R,3a*R**,7a*R**)-*tert*-butyl 3,7a-dimethyl-2,5-dioxo-2,3,3a,4,5,7a-hexahydrobenzofuran-3-carboxylate (*exo*-4.5).**

White amorphous solid (4.4 mg, 12%).

^{1}H NMR (500 MHz, $CDCl_3$) δ 6.72 (dd, J = 10.4, 1.6 Hz, 1H), 5.93 (d, J = 10.4 Hz, 1H), 3.00-2.95 (m, 1H), 2.69-2.63 (m, 2H), 1.64 (s, 3H), 1.47 (s, 3H), 1.34 (s, 9H)

^{13}C NMR (125 MHz, $CDCl_3$, DEPT) δ 193.3 (C), 173.6 (C), 168.6 (C), 147.4 (CH), 129.6 (CH), 84.6 (C), 79.2 (C), 55.0 (C), 51.8 (CH), 33.3 (CH_2), 27.7 (CH_3 × 3), 26.1 (CH_3), 21.6 (CH_3)

HRMS (ESI-TOF) *m/z* calcd for $C_{15}H_{20}O_5Na$ $[M + Na]^+$ 303.1203, found 303.1204

IR (thin film) 2979, 2937, 1787, 1728, 1679, 1258, 1146, 1077 cm^{-1}

HPLC t_R = 13.9 min; R_f 0.2 (3:1 hexanes/EtOAc).

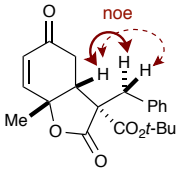

(3*R,3a*R**,7a*R**)-*tert*-butyl 3-benzyl-7a-methyl-2,5-dioxo-2,3,3a,4,5,7a-hexahydrobenzofuran-3-carboxylate (4.7).**

Isolated a white amorphous solid after purification by FCC (41.7 mg, 89% yield).

^{1}H NMR (500 MHz, $CDCl_3$) δ 7.33-7.27 (m, 3H), 7.22 (d, J = 6.8 Hz, 2H), 6.69 (dd, J = 10.4, 1.6 Hz, 1H), 5.95 (d, J = 10.4 Hz, 1H), 3.44 (d, J = 14.1 Hz, 1H), 3.09 (d, J = 14.1 Hz, 1H), 2.97 (d, J = 18.5 Hz, 1H), 2.69 (d, J = 7.7 Hz, 1H), 2.57 (dd, J = 18.5, 7.7 Hz, 1H), 1.37 (s, 9H), 1.36 (s, 3H)

^{13}C NMR (125 MHz, $CDCl_3$, DEPT) δ 193.4 (C), 172.6 (C), 168.3 (C), 147.5 (CH), 134.7 (C), 130.9 (CH × 2), 129.6 (CH), 128.9 (CH × 2), 127.7 (CH), 85.0 (C), 79.1 (C), 60.5 (C), 45.7 (CH), 38.8 (CH_2), 33.0 (CH_2), 27.7 (CH_3 × 3), 26.0 (CH_3)

IR (thin film) 2979, 2930, 1783, 1726, 1685 cm^{-1}

HRMS (ESI-TOF) *m/z* calcd for $C_{21}H_{24}O_5Na$ $[M + Na]^+$ 379.1516, found 379.1524

HPLC t_R = 9.3 min

TLC R_f 0.5 (3:1 hexanes/EtOAc)

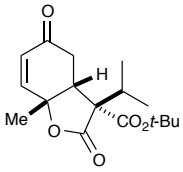

(3*R,3a*R**,7a*R**)-*tert*-butyl 3-isopropyl-7a-methyl-2,5-dioxo-2,3,3a,4,5,7a-hexahydrobenzofuran-3-carboxylate (4.8).**

Isolated a beige amorphous solid after purification by FCC (7.7 mg, 19% yield).

^{1}H NMR (500 MHz, $CDCl_3$) δ 6.70 (dd, J = 10.4, 1.7 Hz, 1H), 5.95 (d, J = 10.4 Hz, 1H), 3.04 (d, J = 18.6 Hz, 1H), 2.91 (d, J = 7.6 Hz, 1H), 2.63 (dd, J = 18.6, 7.5 Hz, 1H), 2.22 (qq, J = 6.8, 6.8 Hz, 1H), 1.65 (s, 3H), 1.39 (s, 9H), 1.16 (d, J = 6.8 Hz, 3H), 1.10 (d, J = 6.8 Hz, 3H)

^{13}C NMR (125 MHz, $CDCl_3$, DEPT) δ 193.6 (C), 171.9 (C), 167.9 (C), 147.6 (CH), 129.7 (CH), 84.7 (C), 78.4 (C), 61.4 (C), 46.7 (CH), 33.9 (CH_2), 33.0 (CH), 27.8 ($CH_3 \times 3$), 26.1 (CH_3), 18.0 (CH_3), 17.7 (CH_3)

IR (thin film) 2977, 2934, 1782, 1724, 1685 cm^{-1}

HRMS (ESI-TOF) *m/z* calcd for $C_{17}H_{24}O_5Na$ $[M + Na]^+$ 331.1516, found 331.1514

TLC R_f 0.3 (3:1 hexanes/EtOAc)

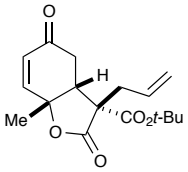

(3*R,3a*R**,7a*R**)-*tert*-butyl 3-allyl-7a-methyl-2,5-dioxo-2,3,3a,4,5,7a-hexahydrobenzofuran-3-carboxylate (4.9).**

Two fractions were isolated after purification by FCC. The first contained two diastereomers (beige solid, 14.4 mg) and the second contained one diastereomer (white solid, 18.7 mg) for a combined isolated yield of 81% (32.7 mg). Only the major diastereomer was characterized.

^{1}H NMR (500 MHz, $CDCl_3$) δ 6.72 (dd, J = 10.4, 1.9 Hz, 1H), 5.95 (dd, J = 10.4, 0.8 Hz, 1H), 5.82 (dddd, J = 16.9, 10.2, 8.1, 6.7 Hz, 1H), 5.24-5.16 (m, 2H), 2.94 (dt, J = 18.6, 1.1 Hz, 1H), 2.84 (dt, J = 7.5, 1.6 Hz, 1H), 2.72-2.67 (m, 1H), 2.61 (dd, J = 18.6, 7.5 Hz, 1H), 2.51 (dd, J = 14.1, 8.1 Hz, 1H), 1.63 (s, 3H), 1.36 (s, 9H)

^{13}C NMR (125 MHz, $CDCl_3$, DEPT) δ 193.4 (C), 172.4 (C), 167.9 (C), 147.5 (CH), 131.5 (CH), 129.6 (CH), 121.4 (CH_2), 84.9 (C), 79.3 (C), 58.3 (C), 47.3 (CH), 38.5 (CH_2), 33.2 (CH_2), 27.7 ($CH_3 \times 3$), 26.0 (CH_3)

HRMS (ESI-TOF) *m/z* calcd for $C_{17}H_{22}O_5Na$ $[M + Na]^+$ 329.1350, found 329.1361

IR (thin film) 2979, 2932, 1784, 1724, 1685, 1251, 1152, 1091 cm^{-1}

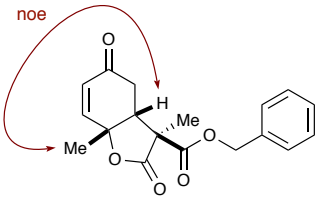

(3*R,3a*S**,7a*S**)-benzyl 3,7a-dimethyl-2,5-dioxo-2,3,3a,4,5,7a-hexahydrobenzofuran-3-carboxylate (*endo*-4.11).**

Pale yellow amorphous solid (14.6 mg, 71% yield).

^{1}H NMR (500 MHz, $CDCl_3$) δ 7.39-7.33 (m, 5H), 6.75 (dd, J = 10.4, 1.5 Hz, 1H), 6.08 (d, J = 10.4 Hz, 1H), 5.22 (s, 2H), 3.42 (dt, J = 6.9, 1.8 Hz, 1H), 2.68 (dd, J = 18.3, 7.0 Hz, 1H), 2.61 (dd, J = 18.2, 1.6 Hz, 1H), 1.69 (s, 3H), 1.43 (s, 3H)

^{13}C NMR (125 MHz, $CDCl_3$, DEPT) δ 194.6 (C), 173.3 (C), 170.1 (C), 147.6 (CH), 135.1 (C), 129.5 (CH), 128.8 (CH × 2), 128.7 (CH), 128.1 (CH × 2), 79.8 (C), 68.2 (CH_2), 55.3 (C), 47.5 (CH), 34.4 (CH_2), 26.5 (CH_3), 16.1 (CH_3)

IR (thin film) 3035, 2949, 1778, 1738, 1686 cm^{-1}

HRMS (ESI-TOF) *m/z* calcd for $C_{18}H_{18}O_5Na$ $[M + Na]^+$ 337.1046, found 337.1052

HPLC t_R = 17.2 min

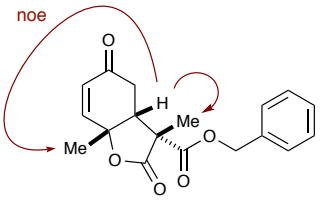

(3*R,3a*R**,7a*R**)-benzyl 3,7a-dimethyl-2,5-dioxo-2,3,3a,4,5,7a-hexahydrobenzofuran-3-carboxylate (*exo*-4.11).**

White amorphous solid (1.8 mg, 9% yield).

^{1}H NMR (500 MHz, $CDCl_3$) δ 7.36-7.30 (m, 5H), 6.55 (dd, J = 10.4, 1.9 Hz, 1H), 5.60 (d, J = 10.4 Hz, 1H), 5.07 (d, J = 12.2 Hz, 1H), 4.91 (d, J = 12.2 Hz, 1H), 2.99 (d, J = 18.1 Hz, 1H), 2.73-2.72 (m, 1H), 2.67 (dd, J = 18.1, 7.3 Hz, 1H), 1.65 (s, 3H), 1.55 (s, 3H)

^{13}C NMR (125 MHz, $CDCl_3$, DEPT) δ 192.9 (C), 173.3 (C), 169.5 (C), 147.2 (CH), 128.9 (CH), 128.80 (CH × 4), 128.79 (CH), 79.5 (C), 67.9 (CH_2), 54.1 (C), 52.4 (CH), 33.4 (CH_2), 25.9 (CH_3), 21.3 (CH_3)

HRMS (ESI-TOF) *m/z* calcd for $C_{18}H_{18}O_5Na$ $[M + Na]^+$ 337.1046, found 337.1044

HPLC t_R = 24.1 min

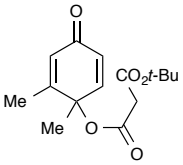

***tert*-butyl (1,2-dimethyl-4-oxocyclohexa-2,5-dien-1-yl) malonate (4.12).**

A mixture of (500 mg, 3.63 mmol), mono-*tert*-butyl malonate (1.07 mL, 7.25 mmol) and DMAP (44 mg, 0.36 mmol) was dissolved in dry MeCN (9 mL) and treated with DCC (2.24 g, 10.88 mmol). The reaction mixture was stirred at rt overnight before diluting with 20 mL of EtOAc and filtering through a plug of celite. The solvent was removed in vacuo and the title compound was purified by FCC using 9:1 hexanes-EtOAc to give 560 mg of a yellow solid in 73% yield.

^{1}H NMR (300 MHz, $CDCl_3$) δ 6.83 (d, J = 10.1, 1 H), 6.21 (dd, J =1.8, 10.0, 1 H), 6.10–6.08 (m, 1 H), 3.29 (s, 2 H), 1.97 (d, J = 1.4 Hz, 3 H), 1.51 (s, 3 H), 1.47 (s, 9 H)

^{13}C NMR (75 MHz, $CDCl_3$, DEPT) δ 185.4 (C), 165.4 (C), 165.1 (C), 158.7 (C), 149.3 (CH), 128.2 (CH), 127.0 (CH), 82.6 (C), 77.3 (C), 43.0 (CH_2), 28.1 (CH_3 × 3), 26.3 (CH_3), 17.9 (CH_3)

IR (thin film) 2979, 2932, 1753, 1729, 1670, 1635, 1142, 1958 cm^{-1}

HRMS (ESI-TOF) *m/z* calc for $C_{15}H_{20}O_5Na$ $[M + Na]^+$ 303.1203, found 303.1206

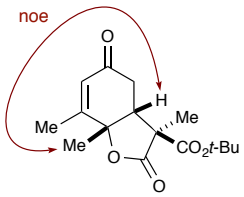

(3*R,3a*S**,7a*R**)-*tert*-Butyl 3,7,7a-trimethyl-2,5-dioxo-2,3,3a,4,5,7a-hexahydrobenzofuran-3-carboxylate (*endo*-4.13).**

White amorphous solid (40.1 mg, 50% yield).

^{1}H NMR (500 MHz, $CDCl_3$) δ 5.92 (s, 1H), 3.38 (dd, J = 7.3, 1.8 Hz, 1H), 2.68 (dd, J = 18.4, 7.3 Hz, 1H), 2.60-2.56 (m, 1H), 2.04 (d, J = 1.4 Hz, 3H), 1.72 (s, 3H), 1.45 (s, 9H), 1.30 (s, 3H)

^{13}C NMR (125 MHz, $CDCl_3$, DEPT) δ 194.5 (C), 173.9 (C), 161.2 (C), 158.6 (C), 128.0 (CH), 83.3 (C), 81.7 (C), 55.5 (C), 48.5 (CH), 34.1 (CH_2), 27.9 (CH_3 × 3), 25.5 (CH_3), 18.7 (CH_3), 16.0 (CH_3)

IR (thin film) 2981, 2935, 1780, 1734, 1676 cm^{-1}

HRMS (ESI-TOF) *m/z* calcd for $C_{16}H_{22}O_5Na$ $[M + Na]^+$ 317.1359, found 317.1353

HPLC t_R = 8.2 min.

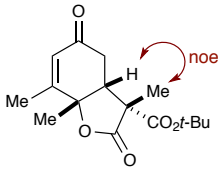

(3*R,3a*R**,7a*S**)-*tert*-Butyl 3,7,7a-trimethyl-2,5-dioxo-2,3,3a,4,5,7a-hexahydrobenzofuran-3-carboxylate (*exo*-4.13).**

Pale yellow amorphous solid (14.0 mg, 17% yield).

^{1}H NMR (500 MHz, $CDCl_3$) δ 5.80 (s, 1H), 3.00-2.95 (m, 1H), 2.68-2.63 (m, 2H), 2.05 (d, J = 1.3 Hz, 3H), 1.67 (s, 3H), 1.47 (s, 3H), 1.36 (s, 9H)

^{13}C NMR (125 MHz, $CDCl_3$, DEPT) δ 193.1 (C), 173.7 (C), 168.7 (C), 158.8 (C), 128.2 (CH), 84.5 (C), 81.5 (C), 54.6 (C), 52.6 (CH), 33.1 (CH_2), 27.6 (CH_3 × 3), 25.2 (CH_3), 21.1 (CH_3), 18.5 (CH_3)

HRMS (ESI-TOF) *m/z* calcd for $C_{16}H_{22}O_5Na$ $[M + Na]^+$ 317.1359, found 317.1359

HPLC t_R = 12.0 min

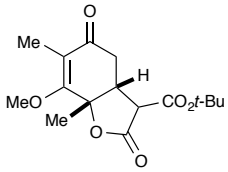

(3*R,3a*S**,7a*R**)-*tert*-Butyl 7-methoxy-6,7a-dimethyl-2,5-dioxo-2,3,3a,4,5,7a-hexahydrobenzofuran-3-carboxylate (4.14).**

Substrate **4.14** was synthesized from malonate-tethered cyclohexadienone **4.1** in the same manner as compound **4.6**. Crude residue was purified by FCC and isolated as an amorphous white solid (320 mg, 87% yield).

^{1}H NMR (500 MHz, $CDCl_3$) δ 3.95 (s, 3H), 3.33 (d, J = 12.3 Hz, 1H), 3.20 (ddd, J = 12.3, 5.3, 2.5 Hz, 1H), 2.68 (dd, J = 17.5, 5.4 Hz, 1H), 2.62 (dd, J = 17.5, 2.5 Hz, 1H), 1.78 (s, 3H), 1.77 (s, 3H), 1.48 (s, 9H)

^{13}C NMR (125 MHz, $CDCl_3$, DEPT) δ 195.1 (C), 169.4 (C), 166.4 (C), 165.4 (C), 121.2 (C), 83.8 (C), 82.6 (C), 61.3 (CH), 52.0 (CH), 44.1 (CH), 35.7 (CH_2), 28.0 (CH_3 × 3), 22.9 (CH_3), 9.1 (CH_3)

IR (thin film) 2989, 2933, 1784, 1734, 1650, 1610 cm^{-1}

HRMS (ESI-TOF) *m/z* calcd for $C_{16}H_{22}O_6Na$ $[M + Na]^+$ 333.1309, found 333.1321

HPLC t_R = 6.5 min (λ = 254 nm)

TLC R_f 0.4 (3:1 hexanes/EtOAc)

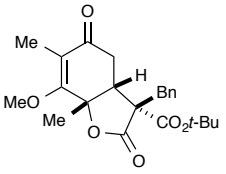

(3*R,3a*R**,7a*S**)-*tert*-Butyl 3-benzyl-7-methoxy-6,7a-dimethyl-2,5-dioxo-2,3,3a,4,5,7a-hexahydrobenzofuran-3-carboxylate (*exo*-4.15).**

White amorphous solid after purification by FCC (41.2 mg, 92% yield).

^{1}H NMR (500 MHz, $CDCl_3$) δ 7.32-7.21 (m, 5H), 3.96 (s, 3H), 3.41 (d, J = 14.1 Hz, 1H), 3.09 (d, J = 14.1 Hz, 1H), 3.00 (d, J = 16.6 Hz, 1H), 2.60-2.53 (m, 2H), 1.72 (s, 3H), 1.43 (s, 3H), 1.34 (s, 9H)

^{13}C NMR (75 MHz, $CDCl_3$, DEPT) δ 194.2 (C), 172.7 (C), 168.2 (C), 167.1 (C), 134.6 (C), 130.9 (CH × 2), 128.9 (CH × 2), 127.7 (CH), 121.2 (C), 84.8 (C), 81.2 (C), 61.0 (CH3), 60.4 (C), 45.3 (CH), 38.6 (CH_2), 32.8 (CH_2), 27.7 (CH_3 × 3), 25.2 (CH_3), 9.1 (CH_3);

IR (thin film) 2980, 2929, 1790, 1729, 1668 cm^{-1}

HRMS (ESI-TOF) *m/z* calcd for $C_{23}H_{28}O_6Na$ $[M + Na]^+$ 423.1778, found 423.1785

TLC R_f 0.4 (3:1 hexanes/EtOAc).

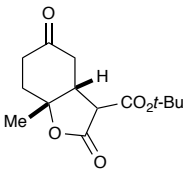

(3*R,3a*S**,7a*S**)-*tert*-Butyl 7a-methyl-2,5-dioxooctahydrobenzofuran-3-carboxylate (4.18).**

Prepared by hydrogenation of **4.6** (127 mg, 0.477 mmol) using Degussa Pd/C (Type E101 Ne/W, obtained from Sigma-Aldrich, 98 mg) in EtOAc (5 mL) with a balloon of H_2 (1 atm) at rt for 1 h. The reaction mixture was filtered over a pad of celite and concentrated under reduced pressure. An amorphous white solid was isolated (126 mg, 98% yield). No further purification was necessary.

^{1}H NMR (500 MHz, $CDCl_3$) δ 3.22 (d, J = 7.7 Hz, 1H), 3.08 (td, J = 7.0, 4.3 Hz, 1H), 2.63 (dd, J = 16.2, 6.4 Hz, 1H), 2.41 (dd, J = 16.3, 4.1 Hz, 1H), 2.32 (tdd, J = 18.5, 10.1, 5.2 Hz, 2H), 2.19-2.07 (m, 2H), 1.63 (s, 3H), 1.46 (s, 10H)

^{13}C NMR (125 MHz, $CDCl_3$, DEPT) δ 208.5 (C), 170.0 (C), 166.1 (C), 83.6 (C), 83.4 (C), 54.7 (CH), 43.1 (CH), 41.1 (CH_2), 35.1 (CH_2), 33.0 (CH_2), 27.9 (CH_3 × 3), 27.3 (CH_3);

IR (thin film) 2978, 2935, 1771, 1727 cm^{-1};

HRMS (ESI-TOF) *m/z* calcd for $C_{14}H_{20}O_5Na$ $[M + Na]^+$ 291.1203, found 291.1200

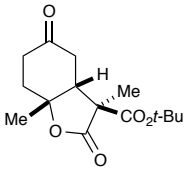

(3*R,3a*S**,7a*S**)-*tert*-Butyl 3,7a-dimethyl-2,5-dioxooctahydrobenzofuran-3-carboxylate (*endo*-4.19).**

Prepared by hydrogenation of ***endo*-4.5** (42.1 mg, 0.1502 mmol) in the same fashion as **4.18**. An amorphous beige solid (41.5 mg, 98% yield) was isolated. No further purification was necessary.

^{1}H NMR (500 MHz, $CDCl_3$) δ 3.00 (t, J = 6.8 Hz, 1H), 2.48-2.41 (m, 2H), 2.32 (ddd, J = 16.1, 8.0, 5.1 Hz, 2H), 2.20 (ddd, J = 14.4, 7.3, 5.2 Hz, 1H), 2.11 (ddd, J = 14.3, 9.0, 5.1 Hz, 1H), 1.58 (s, 3H), 1.46 (s, 9H), 1.32 (s, 3H)

^{13}C NMR (125 MHz, $CDCl_3$, DEPT) δ 209.5 (C), 174.5 (C), 170.4 (C), 83.6 (C), 82.6 (C), 55.7 (C), 45.8 (CH), 38.6 (CH_2), 34.7 (CH_2), 33.1 (CH_2), 27.8 (CH_3 × 3), 27.5 (CH_3), 17.3 (CH_3)

IR (thin film) 2978, 2936, 1771, 1719 cm^{-1}

HRMS (ESI-TOF) *m/z* calcd for $C_{15}H_{22}O_5Na$ $[M + Na]^+$ 305.1359, found 305.1392

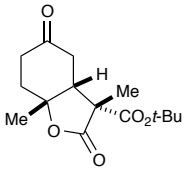

(3*R,3a*R**,7a*R**)-*tert*-Butyl 3,7a-dimethyl-2,5-dioxooctahydrobenzofuran-3-carboxylate (*exo*-4.19).**

Prepared by hydrogenation of ***exo*-4.5** (35.5 mg, 0.127 mmol) in the same fashion as **4.18** except MeOH was used instead of EtOAc. Product was purified via FCC and an amorphous beige solid (15.0 mg, 42% yield) was isolated.

^{1}H NMR (500 MHz, $CDCl_3$) δ 2.57-2.46 (m, 4H), 2.39-2.27 (m, 2H), 2.02 (ddd, J = 13.3, 9.4, 3.8 Hz, 1H), 1.61 (s, 3H), 1.56 (s, 3H), 1.44 (s, 9H)

^{13}C NMR (125 MHz, $CDCl_3$, DEPT) δ 207.8 (C), 175.3 (C), 168.4 (C), 84.9 (C), 82.0 (C), 56.8 (C), 38.8 (CH_2), 35.0 (CH_2), 32.7 (CH_2), 29.1 (CH_3), 27.7 (CH_3 × 3), 24.4 (CH_3)

HRMS (ESI-TOF) *m/z* calcd for $C_{15}H_{22}O_5Na$ $[M + Na]^+$ 305.1359, found 305.1366

Chapter 5
Experimental

5.1 Computational Methods

All geometries were fully optimized at the M06-2X level[13] of density functional theory. A mixed basis set comprised of 6–31G(d)[22] for C, H and O and the Stuttgart/Dresden basis set and pseudopotential (SDD)[23] for iodine. An ultrafine grid density was used for numerical integration.[16] Optimizations were performed with no frozen coordinates. The effects of CH_2Cl_2 (a lower polarity solvent that is commonly used in oxidative dearomatization reactions) and CH_3CN (a polar, non-nucleophilic solvent) solvation were included in the geometry optimizations using the SMD solvation model.[17] Energy minima and transition states were identified though frequency analysis. All calculations made use of the *Gaussian* 09 Rev A.02 suite[12] of electronic structure programs. The Gibbs energies are included below with the atomic coordinates.

5.2 Synthesis of Phenol Substrates

Substrates **5.19a–f** were synthesized as previously described.[20]

(22) W. J. Hehre, L. Radom, P. v. R. Schleyer, and J. A. Pople, *Ab Initio Molecular Orbital Theory*, Wiley, New York, 1986.

(23) Bergner, A.; Dolg, M.; Küchle, W.; Stoll, H.; Preuß, H. Ab initio energy-adjusted pseudopotentials for elements of groups 13–17. *Mol. Phys.* **1993**, *80*, 1431–1441.

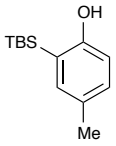

2-(*tert*-Butyldimethylsilyl)-4-methylphenol (5.19g).[24]

Into a round bottom flask was placed commercially available 2-bromo-4-methyl phenol (1.96 g, 10.5 mmol), imidazole (0.93 g, 13.6 mmol) and DCM (12 mL) and cooled to 0 °C. The TBS-Cl (1.9 g, 12.6 mmol) was then added and the reaction stirred overnight, allowing to slowly warm to r.t. The DCM was removed in vacuo, giving a colorless oil. Into the same flask was added THF (30 mL) and the solution was cooled to –78 °C under N_2. To this, *n*-BuLi (2.5 M, 4.2 mL) was slowly added. The reaction was allowed to slowly warm to rt and after 2 h was quenched with saturated aq. NH_4Cl. The mixture was extracted with EtOAc and the combined organic layers were washed with brine, dried over Na_2SO_4, filtered, and concentrated under reduced pressure. The crude oil was purified by flash column chromatography (1:0 hexanes → 9:1 hexanes/EtOAc) to give a pale yellow oil (1.99 g, 86% yield).

^{1}H NMR (300 MHz, $CDCl_3$) δ 7.15 (d, *J* = 2.2 Hz, 1H), 7.05 (dd, *J* = 8.1, 2.3 Hz, 1H), 6.62 (d, *J* = 8.1 Hz, 1H), 4.68 (s, 1H), 2.30 (s, 3H), 0.94 (s, 9H), 0.34 (s, 6H)

^{13}C NMR (75 MHz, $CDCl_3$, DEPT) δ 158.5 (C), 137.2 (CH), 131.3 (CH), 129.1 (C), 122.5 (C), 114.9 (CH), 27.0 (CH_3 × 3), 20.7 (CH_3), 17.7 (C), -4.6 (CH_3 × 2)

IR (thin film) 3537, 2953, 2927, 2855, 1493, 1388, 1254, 822 cm^{-1}

LRMS (ESI+) 221.14 calculated for $C_{13}H_{21}NaOSi$ found 221.19

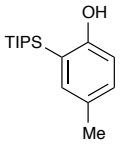

4-Methyl-2-(triisopropylsilyl)phenol (5.19h).

Phenol **5.19h** was synthesized from 2-bromo-4-methyl phenol in the same fashion as **5.19g**, except that TIPSCl was used instead of TBSCl. A white solid (30% yield) was obtained after purification by flash column chromatography (50:1 hexanes/EtOAc).

^{1}H NMR (300 MHz, $CDCl_3$) δ 7.17 (d, *J* = 2.1 Hz, 1H), 7.03 (dd, *J* = 8.1, 2.2 Hz, 1H), 6.59 (d, *J* = 8.1 Hz, 1H), 4.53 (s, 1H), 2.28 (s, 3H), 1.48 (sept, *J* = 7.5 Hz, 3H), 1.10 (d, *J* = 7.4 Hz, 18H)

^{13}C NMR (75 MHz, $CDCl_3$, DEPT) δ 158.6 (C), 137.7 (CH), 130.9 (CH), 129.1 (C), 120.3 (C), 114.8 (CH), 19.03 (CH_3 × 7), 11.8 (CH × 3)

IR (thin film) 3522, 2942, 2861, 1492, 1386, 1175 cm^{-1}

(24) Adapted from A. N. Thadani, Y. Huang, and V. H. Rawal. *Org. Lett.* **2007***, 9*, 3873.

HRMS (ESI+) 263.1837 calculated for $C_{16}H_{27}NaOSi$ found 263.1211

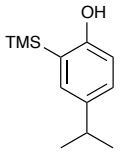

4-Isopropyl-2-(trimethylsilyl)phenol (5.19i).[20]

Phenol **5.19i** was synthesized from commercially available 2-bromo-4-isopropyl phenol in the same fashion as **5.19g**. A colorless oil (61% yield) was obtained after purification by flash column chromatography (95:5 hexanes/EtOAc).

^{1}H NMR (300 MHz, $CDCl_3$) 7.29 (d, J = 2.0 Hz, 1H), 7.17 (dd, J = 8.2, 2.3 Hz, 1H), 6.66 (d, J = 8.2 Hz, 1H), 4.84 (d, J = 3.3 Hz, 1H), 2.93 (hept, J = 6.9 Hz, 1H), 1.31 (d, J = 6.9 Hz, 6H), 0.41 (s, 9H)

^{13}C NMR (75 MHz, $CDCl_3$, DEPT) δ 158.5 (C), 140.7 (C), 133.5 (CH), 128.4 (CH), 125.2 (C), 114.5 (CH), 33.5 (CH), 24.5 (CH_3 × 2), -0.72 (CH_3 × 3)

IR (thin film) 3535, 2958, 2898, 2870, 11596, 1403, 1314, 1245, 1074, 862, 838 cm^{-1}

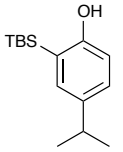

2-(*tert*-Butyldimethylsilyl)-4-isopropylphenol (5.19j).[24]

Into a round bottom flask was placed commercially available 2-bromo-4-isopropyl phenol (763 mg, 3.55 mmol), imidazole (314 mg, 4.61 mmol) and DCM (3.5 mL) and cooled to 0 °C. The TBS-Cl (64 mg, 4.3 mmol) was then added and the reaction stirred overnight, allowing to slowly warm to r.t. The DCM was removed in vacuo, giving a colorless oil. Into the same flask was added THF (20 mL) and the solution was cooled to –78 °C under N_2. To this, *n*-BuLi (2.5 M, 1.4 mL) was slowly added. The reaction was allowed to slowly warm to r.t. and after 2 h was quenched with saturated aq. NH_4Cl. The mixture was extracted with EtOAc and the combined organic layers were washed with brine, dried over Na_2SO_4, filtered, and concentrated under reduced pressure. The crude oil was purified by flash column chromatography (1:0 hexanes → 9:1 hexanes/EtOAc) to give a pale yellow oil (696 mg, 78% yield).

^{1}H NMR (300 MHz, $CDCl_3$) δ 7.20 (d, J = 2.3 Hz, 1H), 7.11 (dd, J = 8.2, 2.3 Hz, 1H), 6.64 (d, J = 8.2 Hz, 1H), 4.67 (s, 1H), 2.87 (hept, J = 6.9 Hz, 1H), 1.24 (d, J = 6.9 Hz, 6H), 0.93 (s, 9H), 0.35 (s, 6H)

^{13}C NMR (75 MHz, $CDCl_3$, DEPT) δ 158.7 (C), 140.3 (C), 134.8 (CH), 128.4 (CH), 122.3 (C), 114.8 (CH), 33.5 (CH), 26.9 (CH_3 × 3), 24.4 (CH_3 × 2), 17.8 (C), -4.6 (CH_3 × 2)

IR (thin film) 3610, 3011, 2957, 2927, 2856, 1595, 1487, 1402, 1314, 1176, 1073 cm^{-1}

LRMS (CI) 251 calculated for $C_{15}H_{27}OSi^+$ found 251

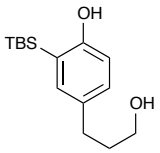

2-(*tert*-Butyldimethylsilyl)-4-(3-hydroxypropyl)phenol (5.35).

Into a vial was placed 3-(3-bromo-4-hydroxyphenyl)propanoic acid (206 mg, 0.841 mmol) and dissolved in THF (4 mL). At 0 °C, $BH_3{\cdot}S(CH_3)_2$ (110 μL) was added dropwise. The mixture was stirred for 2 h and MeOH was then added slowly until bubbling ceased. The mixture was diluted with EtOAc and washed with brine (3 × 2 mL), dried with Na_2SO_4, filtered and concentrated. The crude oil was dissolved in DCM (1 mL), cooled to 0 °C and treated with imidazole (143 mg, 2.10 mmol) followed by TBS-Cl (317 mg, 2.10 mmol). The mixture stirred overnight, slowly warming to rt. After such time, the mixture was diluted with EtOAc and filtered over a plug of celite. The solvent was removed and the crude oil was stirred in THF (5 mL) and cooled to –98 °C under N_2. *n*-BuLi (400 μL) was added slowly dropwise. The mixture was allowed to warm to rt slowly and stir for 1 h. After such time, a saturated solution of NH_4Cl was added and the product extracted with EtOAc (3 × 3 mL). The combined organic layers were washed with brine, dried with Na_2SO_4, filtered and concentrated. The crude product was dissolved in ethanol (8 mL) and pyridinium *p*-toluenesulfonate (21 mg, 0.084 mmol) was added and the mixture stirred rt overnight. After such time, the ethanol was removed in vacuo and the product was purified by flash column chromatography (4:1 hexanes/EtOAc). A white solid was obtained (66.0 mg) in 29% yield over four steps.

^{1}H NMR (500 MHz, $CDCl_3$) δ 7.14 (s, 1H), 7.05 (d, J = 8.1 Hz, 1H), 6.62 (dd, J = 8.1, 1.9 Hz, 1H), 4.82 (s, 1H), 3.69-3.68 (m, 2H), 2.63 (t, J = 6.8 Hz, 2H), 1.86 (quintet, J = 6.6 Hz, 2H), 0.90 (s, 9H), 0.32 (s, 6H)

^{13}C NMR (125 MHz, $CDCl_3$, DEPT) δ 159.0 (C), 136.6 (CH), 133.1 (C), 130.6 (CH), 122.7 (C), 115.0 (CH), 62.6 (CH_2), 34.8 (CH_2), 31.5 (CH_2), 27.0 (CH_3 × 3), 17.8 (C), -4.6 (CH_3 × 2)

IR (thin film) 3335, 2951, 2928, 2855, 1509, 1471, 1401, 1254, 836 cm^{-1}

HRMS (ESI+) 289.1594 calculated for $C_{15}H_{26}NaO_2Si$ found 289.1595

5.3 Synthesis of Racemic Quinols

Quinols **5.20a, 5.20b, 5.20c, 5.20e,** and **5.20f** were prepared as previously described.[25]

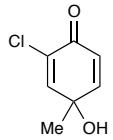

2-Chloro-4-hydroxy-4-methylcyclohexa-2,5-dienone (5.20d).

Commercially available 2-chloro-4-methyl phenol (20 μL, 0.16 mmol) was dissolved in a mixture of MeCN/H_2O (0.17 M, 2:1). (Diacetoxyiodo)benzene (56 mg, 0.17 mmol) was added and the mixture was stirred r.t. overnight. The mixture was then quenched with saturated aq. $NaHCO_3$ and extracted with EtOAc. The combined organic layers were washed with brine, dried (Na_2SO_4), filtered, and concentrated under reduced pressure. The resulting residue was purified by flash column chromatography (4:1 hexanes/EtOAc) and a yellow crystalline solid (18 mg, 67% yield) was isolated.

^{1}H NMR (300 MHz, $CDCl_3$) δ 7.05 (d, *J* = 2.9 Hz, 1H), 6.90 (dd, *J* = 10.0, 2.9 Hz, 1H), 6.21 (d, *J* = 10.0 Hz, 1H), 2.44 (s, 1H), 1.53 (s, 4H)

^{13}C NMR (75 MHz, $CDCl_3$, DEPT) δ 178.5 (C), 152.4 (CH), 148.0 (CH), 131.7 (C), 126.2 (CH), 69.4 (C), 26.8 (CH_3)

IR (thin film) 3406, 3047, 2981, 2930, 1673, 1644, 1603, 1130, 1057 cm^{-1}

HRMS (ESI+) 181.0027 calculated for $C_7H_7ClNaO_2^+$ found 181.0021

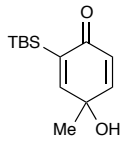

2-(*tert*-Butyldimethylsilyl)-4-hydroxy-4-methylcyclohexa-2,5-dienone (5.20g).

Into a 1 dram vial was placed **5.19g** (48.1 mg, 0.22 mmol) and 4-iodotoluene (10 mol %, 7 mg) in a mixture of acetonitrile/H_2O (1.3 mL, 9:1). Last was added *m*-CPBA (107 mg, 0.41 mmol) and the mixture was capped and stirred overnight at r.t. After such time, the reaction was quenched with 10% aq $Na_2S_2O_3$ (1 mL) and stirred 5 min before saturated aq. $NaHCO_3$ (1 mL) was added. The mixture was extracted with EtOAc (3 × 1 mL) and

(25) Tello-Aburto, R.; Kalstabakken, K. A.; Volp, K. A.; Harned, A. M. Regioselective and Stereoselective Cyclization of Cyclohexadienones Tethered to Active Methylene Groups. *Org. Biomol. Chem.* **2011**, *9*, 7849–7859

the combined organic layers were washed with brine, dried (Na_2SO_4), filtered and concentrated under reduced pressure. The residue was purified by flash column chromatography (5:1 hexanes/EtOAc). A white solid was obtained (23.5 mg, 46% yield).

^{1}H NMR (500 MHz, $CDCl_3$) δ 7.04 (d, *J* = 2.9 Hz, 1H), 6.82 (dd, *J* = 10.0, 2.9 Hz, 1H), 6.08 (d, *J* = 10.0 Hz, 1H), 2.11 (s, 1H), 1.45 (s, 3H), 0.87 (s, 9H), 0.17 (app d, 6H)

^{13}C NMR (125 MHz, $CDCl_3$, DEPT) δ 188.0 (C), 161.6 (CH), 150.6 (CH), 137.6 (C), 128.4 (CH), 67.1 (C), 27.3 (CH_3). 27.2 (CH_3 × 3), 17.0 (C), -5.2 (CH_3), -5.3 (CH_3)

IR (thin film) 3384, 2954, 2928, 2856, 1655, 1618, 1363, 1249, 1058, 838 cm^{-1}

HRMS (ESI+) 261.1281 calculated for $C_{13}H_{22}NaO_2Si$ found 261.1297

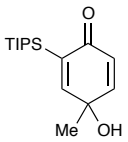

4-Hydroxy-4-methyl-2-(triisopropylsilyl)cyclohexa-2,5-dienone (5.20h).

Dienone **5.20h** was synthesized from **5.19h** in the same fashion as **5.20g**. A white solid (59% yield) was obtained after purification by flash column chromatography (5:1 hexanes/EtOAc).

^{1}H NMR (500 MHz, $CDCl_3$) δ 7.08 (d, *J* = 2.2 Hz, 1H), 6.83 (dd, *J* = 10.0, 2.2 Hz, 1H), 6.09 (d, *J* = 10.0 Hz, 1H), 2.24 (bs, 1H), 1.45 (s, 3H), 1.36 (dt, *J* = 7.5 Hz, 3H), 1.03 (dd, *J* = 7.3, 2.5 Hz, 18H)

^{13}C NMR (75 MHz, $CDCl_3$, DEPT) δ 188.6 (C), 162.6 (CH), 150.6 (CH), 135.0 (C), 128.4 (CH), 67.2 (C), 27.5 (CH_3), 18.9 (CH_3 × 6), 11.2 (CH × 3)

IR (thin film) 3383, 2944, 2889, 2866, 1654, 1617, 1464, 1228, 883 cm^{-1}

HRMS (ESI+) 303.1751 calculated for $C_{16}H_{28}NaO_2Si$ found 303.1749

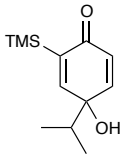

4-Hydroxy-4-isopropyl-2-(trimethylsilyl)cyclohexa-2,5-dienone (5.20i).

Dienone **5.20i** was synthesized from **5.19i** in the same fashion as **5.20d**, except that a mixture of 3:1 acetonitrile-H_2O was used. A white crystalline solid (55% yield) was obtained after purification by flash column chromatography (9:1 hexanes/EtOAc).

^{1}H NMR (300 MHz, $CDCl_3$) δ 6.93 (d, *J* = 3.2 Hz, 1H), 6.76 (dd, *J* = 10.1, 3.2 Hz, 1H), 6.19 (d, *J* = 10.1 Hz, 1H), 2.13 (bs, 1H), 1.97 (hept, 6.9 Hz, 1H), 0.95 (d, *J* = 6.9 Hz, 3H), 0.90 (d, *J* = 6.9 Hz, 3H), 0.18 (s, 9H)

^{13}C NMR (75 MHz, $CDCl_3$, DEPT) δ 188.7 (C), 158.0 (CH), 149.0 (CH), 141.7 (C), 130.1 (CH), 72.1 (C), 36.9 (CH), 17.2 (CH_3 × 3), 17.3 (CH_3), 17.1 (CH_3), -1.38 (CH_3 × 3)

IR (thin film) 3373, 2961, 2549, 1694, 1650, 1304, 1263, 844 cm^{-1}

HRMS (ESI+) 247.1125 calculated for $C_{12}H_{20}NaO_2Si^+$ found 247.1141

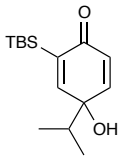

2-(*tert*-Butyldimethylsilyl)-4-hydroxy-4-isopropylcyclohexa-2,5-dienone (5j).

Dienone **5.20j** was synthesized from **5.19j** in the same fashion as **5.20g**. A white crystalline solid (61% yield) was obtained after purification by flash column chromatography (1:0 → 9:1 hexanes/EtOAc).

^{1}H NMR (300 MHz, $CDCl_3$) δ 6.97 (d, *J* = 3.2 Hz, 1H), 6.74 (dd, *J* = 10.1, 3.2 Hz, 1H), 6.18 (d, *J* = 10.1 Hz, 1H), 2.05 (bs, 1H), 1.97 (hept, *J* = 6.9 Hz, 1H), 0.94 (app t, *J* = 6.9 Hz, 3H), 0.89 (s, 9H), 0.17 (s, 3H), 0.15 (s, 3H)

^{13}C NMR (75 MHz, $CDCl_3$, DEPT) δ 188.4 (C), 159.9 (CH), 148.4 (CH), 139.9 (C), 130.3 (CH), 72.3 (C), 36.9 (CH), 27.3 (CH_3 × 3), 17.3 (CH_3), 17.1 (CH_3), 17.0 (C), -5.1 (CH_3), -5.2 (CH_3)

IR (thin film) 3385, 2958, 2928, 2881, 2856, 1653, 1617, 1470, 1363, 1249, 1004, 838 cm^{-1}

HRMS (ESI+) 289.1594 calculated for $C_{15}H_{26}NaO_2Si^+$ found 289.1593

5.4 Synthesis of Aryl Iodide Catalysts

5.4.1. General Procedures:

5.4.1.a General Procedure A: Ketalization with (+)-Dimethyl l-tartrate

The aryl iodoketone (1 equiv) was dissolved in methanol (0.65 M) and treated with trimethyl orthoformate (5 equiv) followed by *p*-toluenesulfonic acid monohydrate (10 mol %). The mixture was refluxed overnight and then concentrated in vacuo. In the same flask, the residue was dissolved in toluene (0.2 M) and (+)-dimethyl L-tartrate (2.1

equiv) was added, followed by $BF_3 \cdot OEt_2$ (5 mol %). The mixture was heated and the methanol removed by azeotrope. After 3 h, the reaction was cooled to r.t., quenched with saturated aq. $NaHCO_3$, and extracted with EtOAc (3×). The combined organic layers were washed with brine and then concentrated under reduced pressure to give a viscous oil. The oil was treated with a 1:1 mixture of MeOH and 2 N NaOH for 1 hr, and then transferred to a separatory funnel. The aqueous layer was washed with ether, acidified with 10% aq. HCl, and then extracted with EtOAc. The combined organic layers were washed with brine, dried over Na_2SO_4, and concentrated under reduced pressure.

5.4.1.b General Procedure B: Amide Synthesis

The aryl iodotartrate was dissolved in DCM (0.1 M) and treated with oxalyl chloride (3.5 equiv) and DMF (10 μL) at room temperature for 3 h. The resulting dark solution was concentrated in vacuo and re-dissolved in DCM (0.2 M). Into the same flask was added the respective aniline or amine (4 equiv) and pyridine (4 equiv). The mixture was stirred at r.t. overnight, then quenched with 10% aq. HCl and extracted with DCM. The organic layer was washed with brine, dried (Na_2SO_4), filtered, and concentrated under reduced pressure. The resulting residue was purified by flash column chromatography (hexanes/EtOAc).

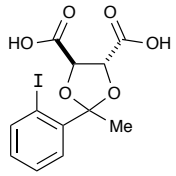

(4*R*,5*R*)-2-(2-Iodophenyl)-2-methyl-1,3-dioxolane-4,5-dicarboxylic acid (5.26).

Using general procedure A, **5.26** was synthesized from commercially available 2-iodoacetephenone. A yellow solid was obtained (38% yield).

^{1}H NMR (300 MHz, CD_3OD): δ 7.92 (dd, *J* = 7.8, 1.2 Hz, 1H), 7.87 (dd, *J* = 7.9, 1.7 Hz, 1H), 7.33 (td, *J* = 7.6, 1.1 Hz, 1H), 6.96 (td, *J* = 7.6, 1.7 Hz, 1H), 5.04 (bs, exchangeable OHs), 4.61 (d, *J* = 8.0 Hz, 1H), 4.39 (d, *J* = 8.0 Hz, 1H), 1.84 (s, 3H)

^{13}C NMR (75 MHz, $CDCl_3$, DEPT) δ 173.4 (C), 173.1 (C), 144.8 (CH), 143.2 (C), 130.8 (CH), 129.4 (CH), 128.8 (CH), 112.5 (C), 93.5 (C), 78.4 (CH), 77.5 (CH), 26.6 (CH_3)

IR (thin film) 3405, 3059, 2991, 2933, 1727, 1605, 1426, 1191, 1085 cm^{-1}

HRMS (ESI–) 376.9528 calculated for $C_{12}H_{10}IO_6$ found 376.9483

$[\alpha]_D^{26}$ + 28.6 (*c* 0.03, MeOH)

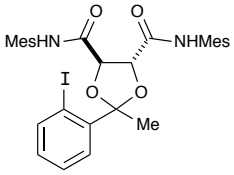

(4*R*,5*R*)-2-(2-Iodophenyl)-*N*^{4},*N*^{5}-dimesityl-2-methyl-1,3-dioxolane-4,5-dicarboxamide (5.27).

Compound **5.27** was synthesized from **5.26** using general procedure B and purified by flash column chromatography (1:0 hexanes → 4:1 hexanes/EtOAc) to obtain a brown solid (81% yield).

^{1}H NMR (300 MHz, $CDCl_3$) δ 8.96 (s, 1H), 8.48 (s, 1H), 7.94 (dd, *J* = 7.9, 1.2 Hz, 1H), 7.89 (dd, *J* = 7.9, 1.7 Hz, 1H), 7.43 (td, *J* = 7.6, 1.2 Hz, 1H), 7.02 (td, *J* = 7.6, 1.8 Hz, 1H), 6.88 (s, 2H), 6.84 (s, 2H), 4.94 (d, *J* = 8.3 Hz, 1H), 4.77 (d, *J* = 8.3 Hz, 1H), 2.26 (s, 3H), 2.24 (s, 3H), 2.22 (s, 6H), 2.07 (s, 3H), 1.87 (bs, 6H)

^{13}C NMR (75 MHz, $CDCl_3$, DEPT) δ 169.1 (C), 165.5 (C), 142.9 (C), 142.6 (CH), 137.6 (C), 136.9 (C), 135.0 (C), 134.8 (C), 130.5 (CH), 129.5 (C), 129.1 (CH), 129.0 (CH), 127.4 (CH), 112.5 (C), 93.7 (C), 78.4 (CH), 77.3 (CH), 26.6 (CH_3), 21.1 (CH_3), 18.6 (CH_3), 18.0 (CH_3)

IR (thin film) 3358, 3269, 2919, 1695, 1506, 1189 cm^{-1}

HRMS (ESI+) 635.1277 calculated for $C_{30}H_{33}IN_2NaO_4$ found 635.1418

$[\alpha]_D^{25}$ + 12.3 (*c* 0.01, EtOAc)

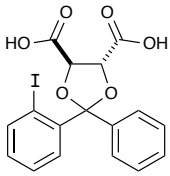

(4*R*,5*R*)-2-(2-Iodophenyl)-2-phenyl-1,3-dioxolane-4,5-dicarboxylic acid (5.28).

Using general procedure A, **5.28** was synthesized from known compound 2-iodoacetephenone.[26] A beige solid was obtained (37% yield).

^{1}H NMR (300 MHz, CD_3OD) δ 7.93 (dd, *J* = 7.8, 1.2 Hz, 1H), 7.86 (dd, *J* = 7.8, 1.7 Hz, 1H), 7.45–7.37 (m, 3H), 7.32–7.30 (m, 3H), 7.03 (td, *J* = 7.6, 1.7 Hz, 1H), 5.06 (bs, exchangeable OHs), 4.88 (d, *J* = 6.9 Hz, 1H), 4.82 (d, *J* = 6.9 Hz, 1H)

^{13}C NMR (75 MHz, $CDCl_3$, DEPT) δ 171.8 (C), 171.6 (C), 143.3 (CH), 143.0 (C), 140.5 (C), 131.28 (CH), 130.3 (CH), 129.9 (CH), 129.8 (CH), 128.8 (CH), 128.4 (CH), 114.1 (C), 96.2 (C), 78.8 (CH), 78.1 (CH)

(26) Krasnokutskaya, E. A.; Semenischeva, N. I.; Filimonov, V. D.; Knochel, P. A New, One-Step, Effective Protocol for the Iodination of Aromatic and Heterocyclic Compounds via Aprotic Diazotization of Amines. *Synthesis*, **2007**, 81–84.

IR (thin film) 3061, 2627, 1733, 1450, 1248, 1202, 1105 cm^{-1}

HRMS (ESI–) 438.9684 calculated for $C_{17}H_{12}IO_6$ found 438.9621

$[\alpha]_D^{25}$ + 22.0 (*c* 0.01, EtOH)

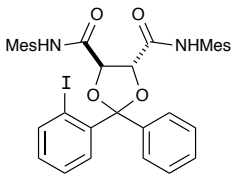

(4*R*,5*R*)-2-(2-Iodophenyl)-*N*^{4},*N*^{5}-dimesityl-2-phenyl-1,3-dioxolane-4,5-dicarboxamide (5.29).

Using general procedure B, **5.29** was synthesized from **5.28** and purified by flash column chromatography (1:0 → 4:1 hexanes/EtOAc) to afford a beige solid (55% yield).

^{1}H NMR (300 MHz, $CDCl_3$) δ 8.53 (s, 1H), 8.39 (s, 1H), 8.03 (dd, *J* = 7.8, 1.7 Hz, 1H), 7.94 (dd, *J* = 7.8, 1.2 Hz, 1H), 7.53–7.45 (m, 3H), 7.39–7.34 (m, 3H), 7.08 (td, *J* = 7.6, 1.7 Hz, 1H), 6.87 (s, 2H), 6.84 (s, 2H), 5.18 (d, *J* = 7.6 Hz, 1H), 5.07 (d, *J* = 7.6 Hz, 1H), 2.25 (d, *J* = 3.9 Hz, 6H), 2.16 (s, 6H), 1.92 (s, 6H)

^{13}C NMR (75 MHz, $CDCl_3$, DEPT) δ 168.0 (C), 166.1 (C), 142.6 (CH), 141.4 (C), 138.4 (C), 137.4 (C), 137.1 (C), 135.0 (C), 134.9 (C), 130.9 (CH), 130.3 (C), 129.8 (C), 129.5 (CH), 129.1 (CH), 128.6 (CH), 128.3 (CH), 127.8 (CH), 113.5 (C), 95.8 (C), 79.1 (CH), 78.3 (CH), 21.0 (CH_3), 18.6 (CH_3), 18.2 (CH_3).

IR (thin film) 3370, 3267, 3059, 2919, 2857, 1699, 1506, 1201, 1100 cm^{-1}

HRMS (ESI+) 697.1534 calculated for $C_{35}H_{35}IN_2NaO_4$ found 697.1580

$[\alpha]_D^{25}$ + 44.0 (*c* 0.004, EtOAc)

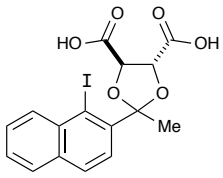

(4*R*,5*R*)-2-(1-iodonaphthalen-2-yl)-2-methyl-1,3-dioxolane-4,5-dicarboxylic acid (5.30).

Compound **5.30** was synthesized from known compound 1-(1-iodonaphthalen-2-yl)ethanone[27] using general procedure A, affording a brown solid (34% yield).

(27) Hirt, U. H.; Schuster, M. F. H.; French, A. N.; Wiest, O. G.; Wirth, T. Chiral Hypervalent Organo-Iodine(III) Compounds**.** *Eur. J. Org. Chem*., **2001**, 1569–1579.

^{1}H NMR (300 MHz, CD_3OD): δ 8.45 (dd, *J* = 8.4, 1.1 Hz, 1H), 7.90 (d, *J* = 8.6 Hz, 1H), 7.83–7.76 (m, 2H), 7.58–7.47 (m, 2H), 4.97 (bs, exchangeable OHs), 4.77 (d, *J* = 6.1 Hz, 1H), 4.72 (d, *J* = 6.1 Hz, 1H), 2.00 (s, 3H)

^{13}C NMR (75 MHz, CD_3OD, DEPT) δ 172.4 (C), 171.8 (C), 144.4 (C), 136.9 (C), 135.1 (CH), 134.8 (C), 129.8 (CH), 129.3 (CH), 128.7 (CH), 128.0 (CH), 126.0 (CH), 114.3 (C), 100.7 (C), 78.9 (CH), 77.3 (CH), 26.9 (CH_3)

IR (thin film) 3057, 2934, 1734, 1224, 1092 cm^{-1}

HRMS (ESI–) 426.9684 calculated for $C_{16}H_{12}IO_6$ found 426.9688

$[\alpha]_D^{26}$ + 45.4 (*c* 0.01, MeOH)

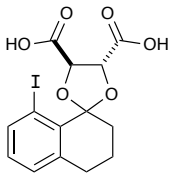

(4*R*,5*R*)-8'-Iodo-3',4'-dihydro-2'*H*-spiro[[1,3]dioxolane-2,1'-naphthalene]-4,5-dicarboxylic acid (5.33).

The iodo tetralone[28] (902 mg, 3.31 mmol) was dissolved in dry methanol (5 mL, 0.65 M) and to this was added trimethyl orthoformate (2.5 mL, 23 mmol), which was followed by *p*-toluenesulfonic acid monohydrate (2 mg). The reaction was refluxed overnight, concentrated in vacuo, and carried on immediately without isolation. Into the same flask was added dry benzene (4 mL), 3 Å molecular sieves, (+)-dimethyl L-tartrate (890 mg, 4.97 mmol), and scandium triflate (2 mg). The resulting mixture was stirred, heated to 90 °C, and left open to the atmosphere for 3 h. After such time, the reaction mixture was concentrated in vacuo and the resulting residue was dissolved in EtOAc, transferred to a separatory funnel and washed with saturated aq. $NaHCO_3$, H_2O, and brine. It was then dried (Na_2SO_4), filtered, and concentrated under reduced pressure, affording a viscous, colorless oil. This was treated with MeOH (2 mL) and 2 N NaOH (2 mL) for 1.5 h. After such time, the mixture was washed with EtOAc and the aqueous layer acidified with 10% aq. HCl. The product was extracted with EtOAc, dried (Na_2SO_4), filtered, and concentrated under reduced pressure to give a reddish orange solid (844 mg, 63% yield). No further purification was performed.

^{1}H NMR (300 MHz, CD_3OD): δ 7.85 (dd, *J* = 7.7, 1.1 Hz, 1H), 7.16 (dd, *J* = 7.6, 1.1 Hz, 1H), 6.92 (t, *J* = 7.7 Hz, 1H), 5.19 (d, *J* = 7.0 Hz, 1H), 5.08 (d, *J* = 7.0 Hz, 1H), 5.00 (bs, exchangeable OHs), 2.85 (t, *J* = 6.1 Hz, 2H), 2.24–2.16 (m, 1H), 2.07 (dd, *J* = 7.9, 5.9 Hz, 1H), 1.85 (dt, *J* = 11.2, 5.6 Hz, 2H)

(28) Nguyen, P.; Corpuz, E.; Heidelbaugh, T. M.; Chow, K.; Garst, M. E. A Convenient Synthesis of 7-Halo-1-indanones and 8-Halo-1-tetralones. *J. Org. Chem.* **2003**, *68*, 10195–10198.

^{13}C NMR (75 MHz, $CDCl_3$, DEPT) δ 174.1 (C), 171.5 (C), 143.7, (C) 141.9 (CH), 134.8 (C), 131.4 (CH), 130.6 (CH), 111.9 (C), 94.7 (C), 78.0 (CH), 35.7 (CH_2), 32.1 (CH_2), 20.8 (CH_2)

IR (thin film) 3052, 2942, 2624, 1728, 1437, 1165, 1096 cm^{-1}

HRMS (ESI–) 402.9684 calculated for $C_{14}H_{12}IO_6$ found 402.9672

$[\alpha]_D^{24}$ – 10.2 (*c* 0.02, MeOH)

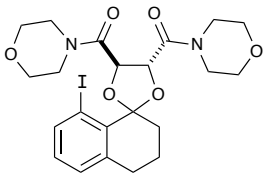

(4*R*,5*R*)-8'-Iodo-3',4'-dihydro-2'*H*-spiro[[1,3]dioxolane-2,1'-naphthalene]-4,5-dicarboxylic acid (5.34a).

Using general procedure B, **5.34a** was synthesized from **5.33** in 81% yield after flash column chromatography (4:1 hexanes/EtOAc).

^{1}H NMR (300 MHz, CDCl3): δ 7.87 (dd, *J* = 7.7, 1.3 Hz, 1H), 7.12 (dd, *J* = 7.6, 1.2 Hz, 1H), 6.90 (t, *J* = 7.7 Hz, 1H), 5.77 (d, *J* = 6.8 Hz, 1H), 5.66 (d, *J* = 6.8 Hz, 1H), 3.92–3.49 (m, 16H), 2.84 (t, *J* = 6.2 Hz, 2H), 2.11–2.07 (m, 2H), 1.85–1.77 (m, 2H)

IR (thin film) 2958, 2924, 2857, 1644, 1441, 1274, 1114, 978 cm^{-1}

HRMS (ESI+) 565.0806 calculated for $C_{22}H_{27}IN_2NaO_6$ found 565.0799

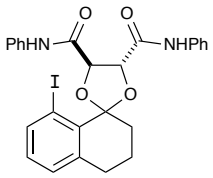

(4*R*,5*R*)-8'-Iodo-N^4,N^5-diphenyl-3',4'-dihydro-2'*H*-spiro[[1,3]dioxolane-2,1'-naphthalene]-4,5-dicarboxamide (5.34b).

Using general procedure B, **5.34b** was obtained from **5.33** and isolated as an orange solid in 74% yield after purification by flash column chromatography (4:1 hexanes/EtOAc).

^{1}H NMR (300 MHz, $CDCl_3$) δ 9.03 (s, 1H), 8.63 (s, 1H), 7.92 (dd, *J* = 7.8, 0.7 Hz, 1H), 7.67–7.63 (m, 4H), 7.41–7.33 (m, 4H), 7.21–7.12 (m, 3H), 6.97 (t, *J* = 7.7 Hz, 1H), 5.25 (d, *J* = 7.6 Hz, 1H), 5.05 (d, *J* = 7.6 Hz, 1H), 2.91 (dq, *J* = 9.7, 5.1 Hz, 2H), 2.30–2.14 (m, 2H), 1.92 (qd, *J* = 9.1, 4.3 Hz, 2H)

^{13}C NMR (75 MHz, $CDCl_3$, DEPT) δ 168.3 (C), 167.1 (C), 142.8 (C), 141.2 (CH), 137.6 (C), 136.6 (C), 133.0 (C), 130.8 (CH), 129.9 (CH), 129.3 (CH × 2), 129.2

(CH × 2), 125.3 (CH), 124.7 (CH), 120.5 (CH × 2), 119.8 (CH × 2), 111.5 (C), 94.0 (C), 78.4 (CH), 77.3 (CH), 34.9 (CH_2), 31.3 (CH_2), 19.9 (CH_2)

IR (thin film) 3383, 3288, 3055, 2933, 1699, 1599, 1538, 1445, 1095 cm^{-1}

HRMS (ESI+) 577.0595 calculated for $C_{26}H_{23}IN_2NaO_4$ found 577.0641

$[\alpha]_D^{25}$ – 37.2 (*c* 0.01, EtOAc)

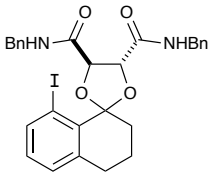

(4*R*,5*R*)-*N*^{4},*N*^{5}-Dibenzyl-8'-iodo-3',4'-dihydro-2'*H*-spiro[[1,3]dioxolane-2,1'-naphthalene]-4,5-dicarboxamide (5.34c).

Using general procedure B, **5.34c** was obtained from **5.33** and isolated as a brown solid in 86% yield after purification by flash column chromatography (3:1 hexanes/EtOAc).

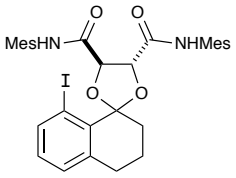

(4*R*,5*R*)-8'-Iodo-*N*^{4},*N*^{5}-dimesityl-3',4'-dihydro-2'*H*-spiro[[1,3]dioxolane-2,1'-naphthalene]-4,5-dicarboxamide (5.34d).

Using general procedure B, **5.34d** was obtained from **5.33** and isolated as a brown solid in 86% yield after purification by flash column chromatography (3:1 hexanes/EtOAc).

^{1}H NMR (500 MHz, $CDCl_3$) δ 8.44 (s, 2H), 7.91 (d, *J* = 7.5 1H), 7.15 (d, *J* = 7.6 Hz, 1H), 6.95–6.90 (m, 5H), 5.44 (d, *J* = 8.2 Hz, 1H), 5.13 (d, *J* = 8.2 Hz, 1H), 2.93–2.87 (m, 2H), 2.40–2.35 (m, 1H), 2.27 (s, 12H), 2.25 (s, 6H), 2.00–1.93 (m, 2H)

^{13}C NMR (75 MHz, $CDCl_3$, DEPT) δ 169.3 (C), 166.4 (C), 142.6 (C), 141.2 (CH), 137.3 (C), 135.0 (C × 2), 134.9 (C × 2), 133.2 (C), 130.7 (CH), 130.3 (C), 130.2 (C), 129.8 (CH), 129.2 (CH × 4), 111.1 (C), 94.1 (C), 78.0 (CH), 77.7 (CH), 34.8 (CH_2), 31.4 (CH_2), 21.0 (CH_3 × 2), 20.0 (CH_2), 19.1 (CH_3 × 2), 18.7 (CH_3 × 2)

IR (thin film) 3368, 3267, 3006, 2947, 2920, 2863, 1704, 1510, 1093 cm^{-1}

HRMS (ESI+) 661.1534 calculated for $C_{32}H_{35}IN_2NaO_4$ found 661.1531

$[\alpha]_D^{24}$ + 4.4 (*c* 0.01, MeOH)

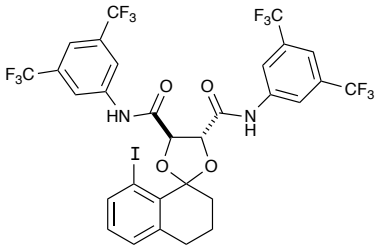

(4*R*,5*R*)-*N*^{4},*N*^{5}-Bis(3,5-bis(trifluoromethyl)phenyl)-8'-iodo-3',4'-dihydro-2'*H*-spiro[[1,3]dioxolane-2,1'-naphthalene]-4,5-dicarboxamide (5.34e).

Using general procedure B, **5.34e** was obtained from **5.33** and isolated as a yellow solid in 51% yield after purification by flash column chromatography (5:1 hexanes/EtOAc).

^{1}H NMR (300 MHz, $CDCl_3$): δ 9.11 (s, 1H), 8.77 (s, 1H), 8.15 (s, 4H), 7.92 (d, *J* = 7.8 Hz, 1H), 7.70 (s, 1H), 7.66 (s, 1H), 7.16 (d, *J* = 7.7 Hz, 1H), 6.98 (t, *J* = 7.7 Hz, 1H), 5.30 (d, *J* = 7.3 Hz, 1H), 5.11 (d, *J* = 7.3 Hz, 1H), 2.88 (t, *J* = 6.0 Hz, 2H), 2.27–2.06 (m, 2H), 1.93 (t, *J* = 4.6 Hz, 2H).

^{13}C NMR (75 MHz, $CDCl_3$, DEPT) δ 168.8 (C), 167.7 (C), 142.8 (C), 141.2 (CH), 138.8 (C), 137.9 (C), 132.9 d, *J* = 18.8 Hz, C–CF_3), 132.6 (d, *J* = 18.8 Hz, C–CF_3), 131.2 (CH), 130.1 (CH), 123.15 (d, *J* = 271.3 Hz, CF_3), 123.08 (d, *J* = 272.5 Hz, CF_3), 120.0 (CH), 119.6 (CH), 118.8 (m, CH),[29] 118.2 (m, CH),[29] 112.19 (C), 78.3 (CH), 77.0 (CH), 34.9 (CH_2), 31.2 (CH_2), 19.8 (CH_2).

IR (thin film) 3267, 2924, 1708, 1381, 1278, 1137 cm^{-1}

HRMS (ESI+) 849.0090 calculated for $C_{30}H_{19}F_{12}IN_2NaO_4$ found 849.0080

$[\alpha]_D^{25}$ – 4.0 (*c* 0.01, EtOAc)

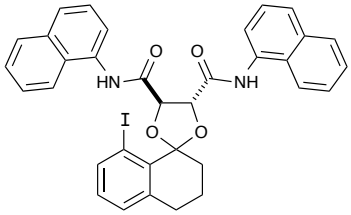

(4*R*,5*R*)-8'-Iodo-*N*^{4},*N*^{5}-di(naphthalen-1-yl)-3',4'-dihydro-2'*H*-spiro[[1,3]dioxolane-2,1'-naphthalene]-4,5-dicarboxamide (5.34f).

Using general procedure B, **5.34f** was obtained from **5.33** and isolated as a brown solid in 71% yield after purification by flash column chromatography (8:1 hexanes/EtOAc).

^{1}H NMR (500 MHz, $CDCl_3$) δ 9.52 (s, 1H), 9.17 (s, 1H), 8.26 (d, *J* = 7.5 Hz, 1H), 8.19 (d, *J* = 7.5 Hz, 1H), 8.13 (d, *J* = 8.4 Hz, 1H), 8.05–8.03 (m, 1H), 7.94 (d, *J* = 7.7 Hz, 1H), 7.90–7.88 (m, 2H), 7.77 (d, *J* = 8.2 Hz, 1H), 7.71 (d, *J* = 8.2 Hz, 1H), 7.56–7.50 (m, 6H), 7.20 (d, *J* = 7.6 Hz, 1H), 6.97 (t, *J* = 7.7 Hz, 1H), 5.59 (d, *J* =

(29) Complex splitting due to multiple C–F coupling interactions.

7.7 Hz, 1H), 5.31 (d, *J* = 7.7 Hz, 1H), 3.00–2.90 (m, 2H), 2.35 (qt, *J* = 13.1, 6.3 Hz, 2H), 2.00 (dt, *J* = 11.3, 5.9 Hz, 2H)

^{13}C NMR (125 MHz, $CDCl_3$, DEPT) δ 169.1 (C), 167.8 (C), 142.8 (C), 141.2 (CH), 134.3 (C), 134.2 (C), 133.2 (C), 132.2 (C), 131.4 (C), 130.8 (CH), 129.9 (CH), 128.9 (CH), 126.9 (C), 126.7 (CH), 126.6 (CH), 126.49 (C), 126.46 (CH), 126.3 (CH), 126.2 (CH), 125.9 (CH), 125.8 (CH), 125.6 (CH), 121.3 (CH), 120.8 (CH), 120.4 (CH), 119.5 (CH), 111.8 (C), 94.1 (C), 78.8 (CH), 78.0 (CH), 35.1 (CH_2), 31.4 (CH_2), 20.01 (CH_2)

IR (thin film) 3296, 3054, 2925, 2854, 1711, 1670, 1598, 1503, 1260, 1095 cm^{-1}

HRMS (ESI+) 677.0908 calculated for $C_{34}H_{27}IN_2NaO_4^+$ found 677.0914

$[\alpha]_D^{26}$ – 51.6 (*c* 0.01, EtOAc)

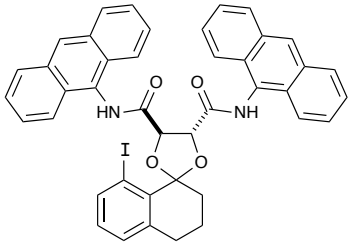

(4*R*,5*R*)-*N*^{4},*N*^{5}-Di(anthracen-9-yl)-8'-iodo-3',4'-dihydro-2'*H*-spiro[[1,3]dioxolane-2,1'-naphthalene]-4,5-dicarboxamide (5.34g).

Using general procedure B, **5.34g** was obtained from **5.33** and isolated as a yellow solid in 45% yield after purification by flash column chromatography (9:1 hexanes/EtOAc).

^{1}H NMR (500 MHz, $CDCl_3$) δ 9.23 (s, 1H), 9.05 (s, 1H), 8.49 (s, 1H), 8.43 (s, 1H), 8.30 (d, *J* = 8.7 Hz, 2H), 8.13 (d, *J* = 8.7 Hz, 2H), 8.04 (d, *J* = 8.4 Hz, 1H), 8.00 (app d, *J* = 8.1 Hz, 2H, 1H), 7.58 (app t, *J* = 7.3 Hz, 2H), 7.52–7.44 (m, 6H), 7.22 (d, *J* = 7.6 Hz, 1H), 6.99 (t, *J* = 7.7 Hz, 1H), 5.98 (d, *J* = 8.0 Hz, 1H), 5.68 (d, *J* = 8.0 Hz, 1H), 3.02–2.92 (m, 2H), 2.60 (dt, *J* = 9.3, 4.4 Hz, 1H), 2.45 (td, *J* = 12.4, 3.3 Hz, 1H), 2.11–2.01 (m, 2H)

^{13}C NMR (75 MHz, $CDCl_3$, DEPT) δ 169.9 (C), 168.5 (C), 142.9 (C), 141.2 (CH), 133.2 (C), 131.71 (C), 131.66 (C), 130.8 (CH), 130.0 (CH), 128.9 (CH × 2), 128.8 (CH × 2), 128.2 (C), 128.0 (C), 127.7 (CH), 127.2 (CH), 126.8 (C), 126.7 (CH × 2), 126.6 (CH × 2), 126.1 (C), 125.5 (CH × 2), 125.4 (CH × 2), 123.4 (CH × 2), 123.2 (CH × 2), 111.9 (C), 94.2 (C), 78.6 (CH), 78.4 (CH), 35.0 (CH_2), 31.4 (CH_2), 20.1 (CH_2)

IR (thin film) 3358, 3053, 2924, 2853, 1670, 1496, 1354 cm^{-1}

HRMS (ESI+) 777.1221 calculated for $C_{42}H_{31}IN_2NaO_4^+$ found 777.1296

$[\alpha]_D^{24}$ + 30.6 (*c* 0.004, EtOAc)

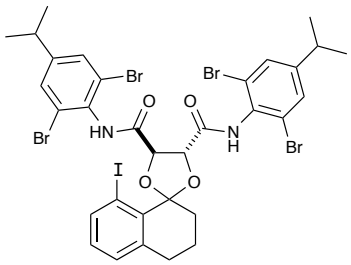

(4*R*,5*R*)-*N*^{4},*N*^{5}-Bis(2,6-dibromo-4-isopropylphenyl)-8'-iodo-3',4'-dihydro-2'*H*-spiro[[1,3]dioxolane-2,1'-naphthalene]-4,5-dicarboxamide (5.34h).

Using general procedure B, **5.34h** was obtained from **5.33** and isolated as a brown solid in 76% yield after purification by flash column chromatography (9:1 hexanes/EtOAc).

^{1}H NMR (500 MHz, $CDCl_3$) δ 8.73 (s, 1H), 8.63 (s, 1H), 7.91 (d, *J* = 8.0, 1H), 7.46 (s, 2H), 7.44 (s, 2H), 7.14 (d, *J* = 7.6 Hz, 1H), 6.92 (t, *J* = 7.7 Hz, 1H), 5.56 (d, *J* = 8.1 Hz, 1H), 5.28 (d, *J* = 8.1 Hz, 1H), 2.95–2.83 (m, 4H), 2.40–2.27 (m, 2H), 1.98–1.95 (m, 2H), 1.232 (d, *J* = 6.9, 6H), 1.227 (d, *J* = 6.9)

^{13}C NMR (125 MHz, $CDCl_3$, DEPT) δ 169.3 (C), 166.1 (C), 151.7 (C), 151.6 (C), 142.6 (C), 141.1 (CH), 133.1 (C), 131.11 (C), 131.05 (C), 130.74 (CH), 130.69 (CH), 129.6 (CH), 123.7 (C), 123.6 (C), 111.5 (C), 94.6 (C), 77.6 (CH), 77.2 (CH), 35.0 (CH_2), 33.75 (CH), 33.73 (CH), 31.4 (CH_2), 23.7 ($CH_3 \times 4$), 20.1 (CH_2)

IR (thin film) 3379, 3258, 2961, 2869, 1724, 1681, 1501, 1096 cm^{-1}

HRMS (ESI+) 976.7917 calculated for $C_{32}H_{31}Br_4IN_2NaO_4$ found 976.7964

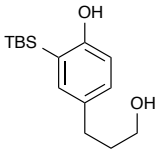

2-(*tert*-butyldimethylsilyl)-4-(3-hydroxypropyl)phenol (5.35).

Into a vial was placed 3-(3-bromo-4-hydroxyphenyl)propanoic acid (206 mg, 0.841 mmol) and dissolved in THF (4 mL). At 0 °C, BH_3•$S(CH_3)_2$ (110 μL) was added dropwise. The mixture was stirred for 2 h and MeOH was then added slowly until bubbling ceased. The mixture was diluted with EtOAc and washed with brine (3 × 2 mL), dried with Na_2SO_4, filtered and concentrated. The crude oil was dissolved in DCM (1 mL), cooled to 0 °C and treated with imidazole (143 mg, 2.10 mmol) followed by TBS-Cl (317 mg, 2.10 mmol). The mixture stirred overnight, slowly warming to rt. After such time, the mixture was diluted with EtOAc and filtered over a plug of celite. The solvent was removed and the crude oil was stirred in THF (5 mL) and cooled to –98 °C under N_2. *n*-BuLi (400 μL) was added slowly dropwise. The mixture was allowed to warm to rt slowly and stir for 1 h. After such time, a saturated solution of NH_4Cl was added and the product extracted with EtOAc (3 × 3 mL). The combined

organic layers were washed with brine, dried with Na_2SO_4, filtered and concentrated. The crude product was dissolved in ethanol (8 mL) and pyridinium *p*-toluenesulfonate (21 mg, 0.084 mmol) was added and the mixture stirred rt overnight. After such time, the ethanol was removed in vacuo and the product was purified by flash column chromatography (4:1 hexanes/EtOAc). A white solid was obtained (66.0 mg) in 29% yield over four steps.

^{1}H NMR (500 MHz, $CDCl_3$) δ 7.14 (s, 1H), 7.05 (d, *J* = 8.1 Hz, 1H), 6.62 (dd, *J* = 8.1, 1.9 Hz, 1H), 4.82 (s, 1H), 3.69-3.68 (m, 2H), 2.63 (t, *J* = 6.8 Hz, 2H), 1.86 (quintet, *J* = 6.6 Hz, 2H), 0.90 (s, 9H), 0.32 (s, 6H).

^{13}C NMR (125 MHz, $CDCl_3$, DEPT) δ 159.0 (C), 136.6 (CH), 133.1 (C), 130.6 (CH), 122.7 (C), 115.0 (CH), 62.6 (CH_2), 34.8 (CH_2), 31.5 (CH_2), 27.0 (CH_3 × 3), 17.8 (C), -4.6 (CH_3 × 2).

IR (thin film) 3335, 2951, 2928, 2855, 1509, 1471, 1401, 1254, 836 cm^{-1}

HRMS (ESI+) 289.1594 calculated for $C_{15}H_{26}NaO_2Si$ found 289.1595

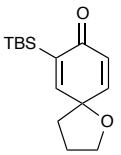

7-(*tert*-Butyldimethylsilyl)-1-oxaspiro[4.5]deca-6,9-dien-8-one (5.36).

Spirocycle **5.36** was obtained from **5.35** in the same fashion as **5.20g** except that MeCN was used as the solvent. A white solid was obtained in 34% yield after purification by flash column chromatography (6:1 hexanes/EtOAc).

^{1}H NMR (500 MHz, $CDCl_3$) δ 6.95 (d, *J* = 3.1 Hz, 1H), 6.76 (dd, *J* = 10.0, 3.1 Hz, 1H), 6.08 (dd, *J* = 10.0, 0.6 Hz, 1H), 4.08 (t, *J* = 6.9 Hz, 2H), 2.15 (quintet, *J* = 6.9 Hz, 2H), 2.02 (t, *J* = 7.2 Hz, 2H), 0.87 (s, 9H), 0.16 (s, 6H)

^{13}C NMR (125 MHz, $CDCl_3$, DEPT) δ 188.4 (C), 159.5 (CH), 148.4 (CH), 137.6 (C), 128.2 (CH), 77.35 (C), 69.4 (CH_2), 37.6 (CH_2), 27.3 (CH_3 × 3), 27.1 (CH_2), 17.0 (C), -5.3 (CH_3 × 2)

IR (thin film) 2953, 2927, 2856, 1656, 1628, 1248, 1229, 1035, 835 cm^{-1}

HRMS (ESI+) 287.1438 calculated for $C_{15}H_2NaO_2Si$ found 287.1429

5.5 Other Experiments

5.5.1. General Procedure for the Synthesis of Enantioenriched Quinols 5.20a–h

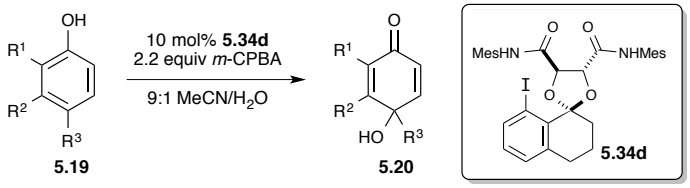

Into a 1 dram vial was placed phenol **5.19** (0.165 mmol) and iodine catalyst **5.34d** (10 mol %) in a mixture of acetonitrile/H_2O (0.16 M, 9:1). Last was added *m*-CPBA (2.2 equiv) and the mixture was stirred overnight at r.t. After such time, the reaction was quenched with 10% aq $Na_2S_2O_3$ (1 mL) and stirred 5 min before saturated aq. $NaHCO_3$ (1 mL) was added. The mixture was extracted with EtOAc (3 × 1 mL) and the combined organic layers were washed with brine, dried (Na_2SO_4), filtered and concentrated under reduced pressure. The residue was purified by flash column chromatography (1:0 → 9:1 hexanes/EtOAc) to afford quinol **5.20**.

5.5.2. Procedure for the synthesis of O^{18} labeled quinol 5.20a

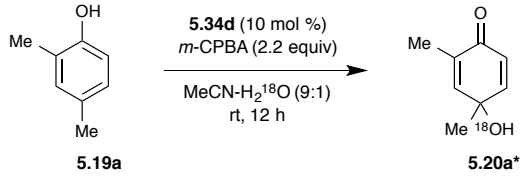

Into a 1 dram vial was placed phenol **5.19a** (0.165 mmol, 19 μL) and iodine catalyst **5.34d** (10 mol %, 11.0 mg) in a mixture of acetonitrile (0.9 mL) and ^{18}O labeled water (0.1 mL). Last was added *m*-CPBA (0.364 mmol, 81.6 mg) and the mixture was stirred overnight at r.t. After such time, the reaction was quenched with 10% aq $Na_2S_2O_3$ (1 mL) and stirred 5 min before saturated aq. $NaHCO_3$ (1 mL) was added. The mixture was extracted with EtOAc (3 × 1 mL) and the combined organic layers were washed with brine, dried (Na_2SO_4), filtered and concentrated under reduced pressure. The residue was purified by flash column chromatography (1:0 → 6:1 hexanes/EtOAc) to afford quinol **5.20a*** (9.5 mg, 41% yield) as a beige solid.

5.5.3. Stoichiometric Iodine Experiment

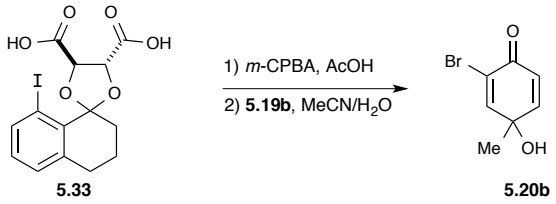

5.33 **5.20b**

A literature procedure was adapted.[30] Aryl iodide **5.33** (103 mg, 0.255 mmol) was stirred in acetic acid (0.25 mL) at rt. To this was added *m*-CPBA (63 mg, 0.280 mmol) and the homogenous mixture stirred for 2 h. After such time, the mixture became heterogeneous and was filtered. The filtrate was dried under vacuum to obtain a yellow solid, which was subsequently dissolved in a mixture of acetonitrile (440 μL) and water (50 μL). The mixture was treated with an excess of 2-bromo-4-methylphenol (**5.19b**) and stirred rt for 4 h. After such time, the reaction was quenched with 10% aq $Na_2S_2O_3$ (1 mL) and stirred 5 min before saturated aq. $NaHCO_3$ (1 mL) was added. The mixture was extracted with EtOAc (3 × 1 mL) and the combined organic layers were washed with brine, dried (Na_2SO_4), filtered and concentrated under reduced pressure. The residue was purified by flash column chromatography (1:0 → 9:1 hexanes/EtOAc) to afford quinol **5.20b**.

5.6 HPLC Data

Entry	Compound	Sample Solution	HPLC Column	HPLC conditions	Retention Time Major Isomer (min)	Retention Time Minor Isomer (min)
1	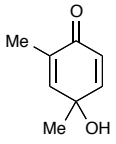 (**5.19a**)	*i*-PrOH	Chiralcel OD-H	8% *i*-PrOH in hexane isocratic, 1 mL/min	8.03	4.43
2	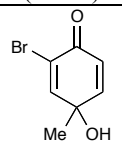 (**5.19b**)	*i*-PrOH	Chiralcel OD-H	10% *i*-PrOH in hexane isocratic, 1 mL/min	8.59	7.65

(30) Iinuma, M.; Moriyama, K.; Togo, H. Simple and Practical Method for Preparation of [(Diacetoxy)iodo]arenes with Iodoarenes and *m*-Chloroperoxybenzoic Acid. *Synlett* **2012**, *23*, 2663.

3	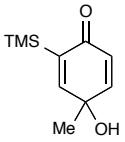 (**5.19c**)	100:1 hexane:*i*-PrOH	Chiralcel OD	2% EtOH in hexane isocratic, 0.3 mL/min	9.27	7.92
4	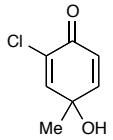 (**5.19d**)	*i*-PrOH	Chiralcel OD-H	10% *i*-PrOH in hexane isocratic, 1 mL/min	31.01	28.92
5	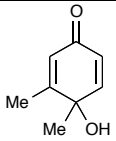 (**5.19e**)	100:1 hexane:*i*-PrOH	Chiralcel OJ	5% EtOH in hexane isocratic, 1 mL/min	11.0	11.9
6	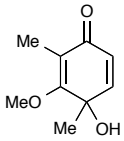 (**5.19f**)	*i*-PrOH	Chiralpak AS	10% *i*-PrOH in hexane isocratic, 1 mL/min	9.85	11.29
7	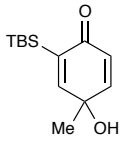 (**5.19g**)	100:1 hexane: *i*-PrOH	Chiralcel OD-H	3% EtOH in hexane isocratic, 0.5 mL/min	13.34	12.04
8	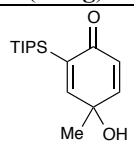 (**5.19h**)	100:1 hexane:*i*-PrOH	Chiralcel OD	2% EtOH in hexane isocratic, 0.3 mL/min	22.94	21.63
9	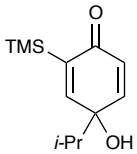 (**5.19i**)	100:1 hexane:*i*-PrOH	Chiralcel OD	3% EtOH in hexane isocratic, 0.5 mL/min	11.53	12.22
10	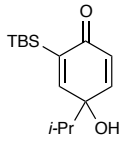 (**5.19j**)	100:1 hexane:*i*-PrOH	Chiralcel OJ	1% EtOH in hexane isocratic, 0.5 mL/min	12.01	11.27
11	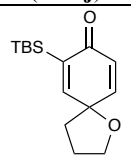 (**5.36**)	100:1 hexane:*i*-PrOH	Chiralcel OD-H	2% EtOH in hexane isocratic, 0.5 mL/min	8.91	9.82

Chapter 3

Spectra

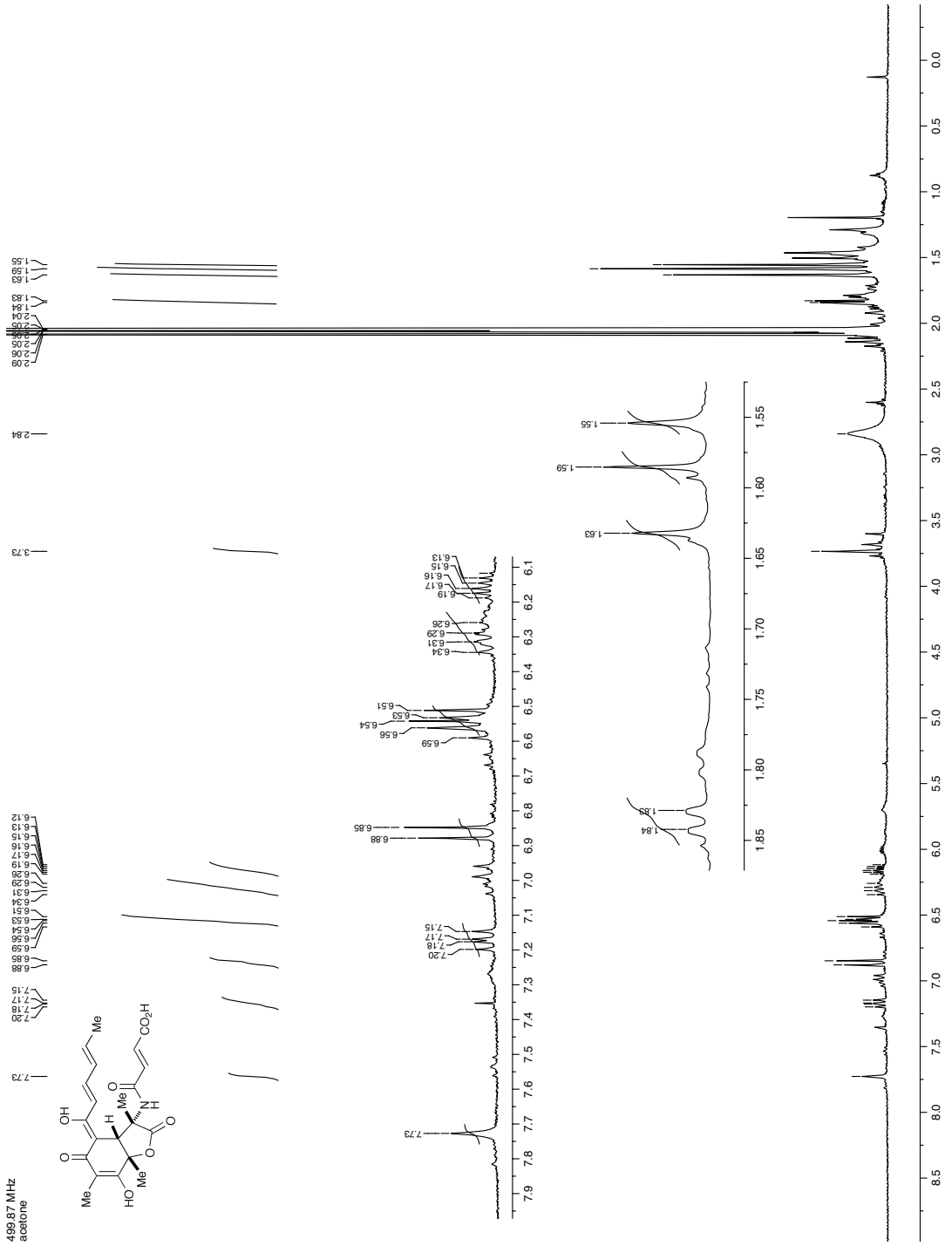
499.87 MHz
acetone
Me
OH
O
H
Me
N
H
O
O
Me
Me
HO
O
CO2H
7.73
7.20
7.18
7.17
7.15
6.88
6.85
6.59
6.56
6.54
6.53
6.51
6.34
6.31
6.29
6.26
6.19
6.17
6.16
6.15
6.13
6.12
3.73
2.84
2.09
2.08
2.06
2.04
1.84
1.83
1.63
1.59
1.55
1.85
1.84
1.83
1.63
1.59
1.55

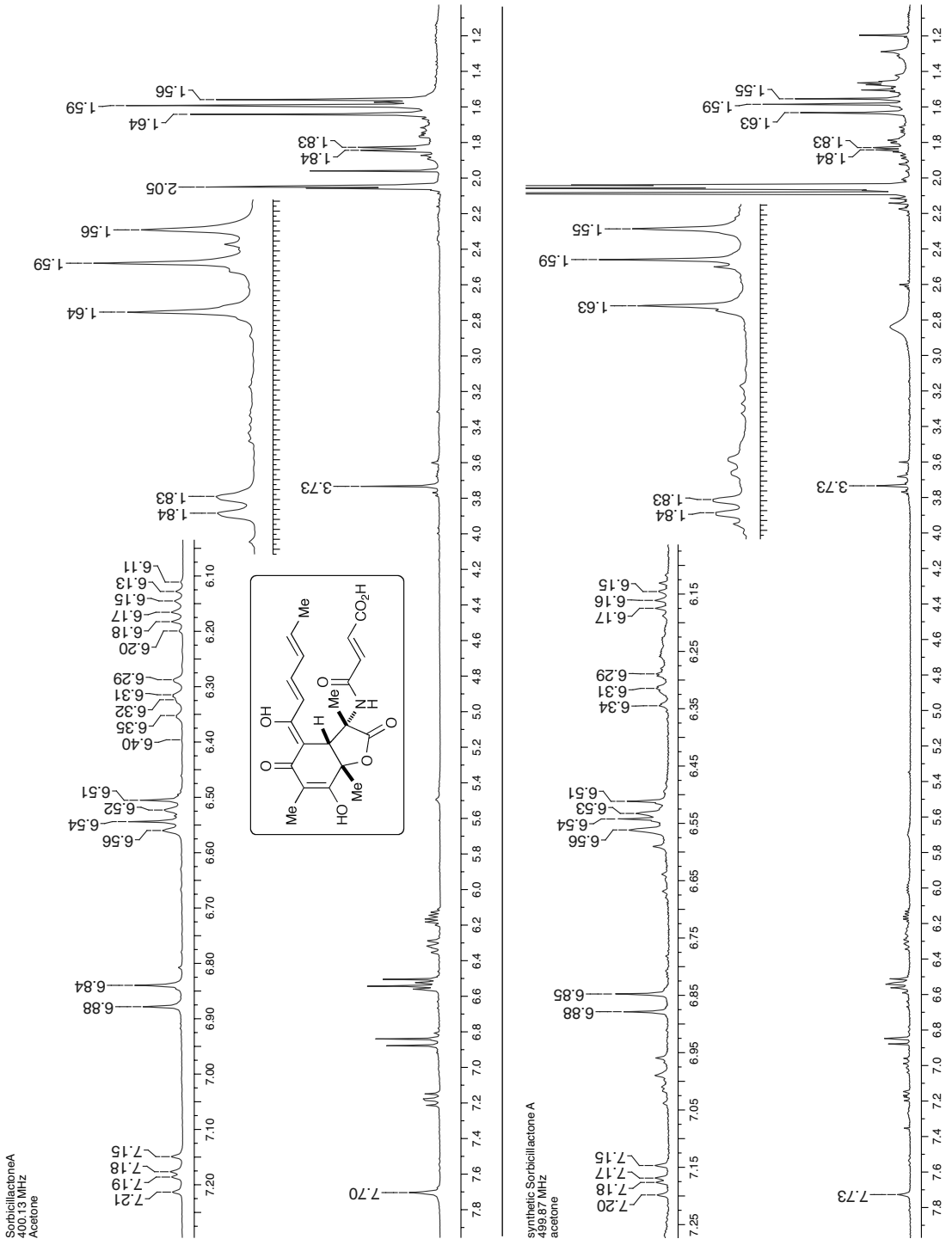
SorbicillactoneA
400.13 MHz
Acetone
synthetic Sorbicillactone A
499.87 MHz
acetone
Me
CO2H
OH
H
Me
O
N
H
O
O
Me
HO
Me
O

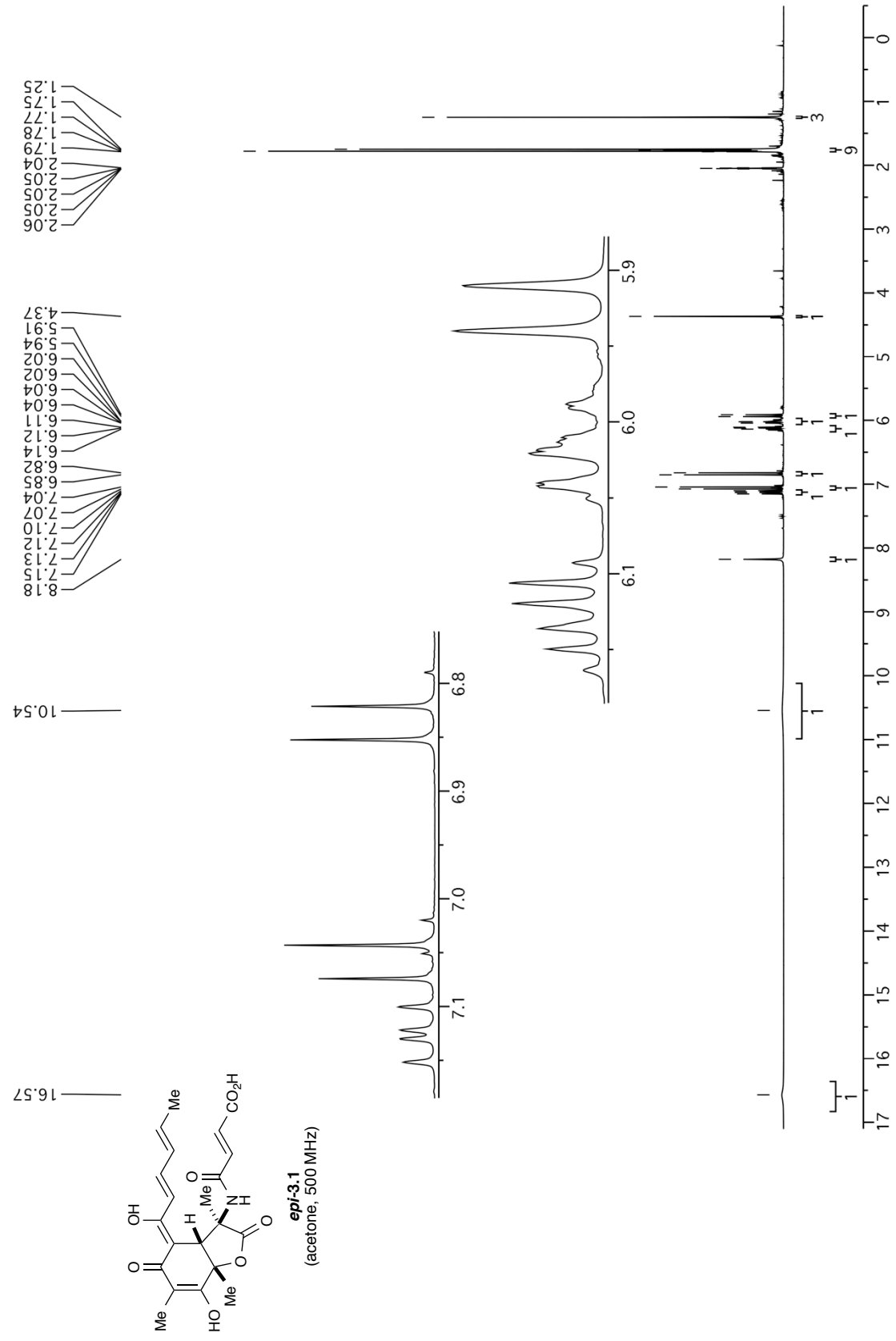
16.57
10.54
8.18
7.15
7.13
7.12
7.10
7.07
7.04
6.85
6.82
6.14
6.12
6.11
6.04
6.04
6.02
6.02
5.94
5.91
4.37
2.06
2.05
2.05
2.05
2.04
1.79
1.78
1.77
1.75
1.25
epi-3.1
(acetone, 500 MHz)

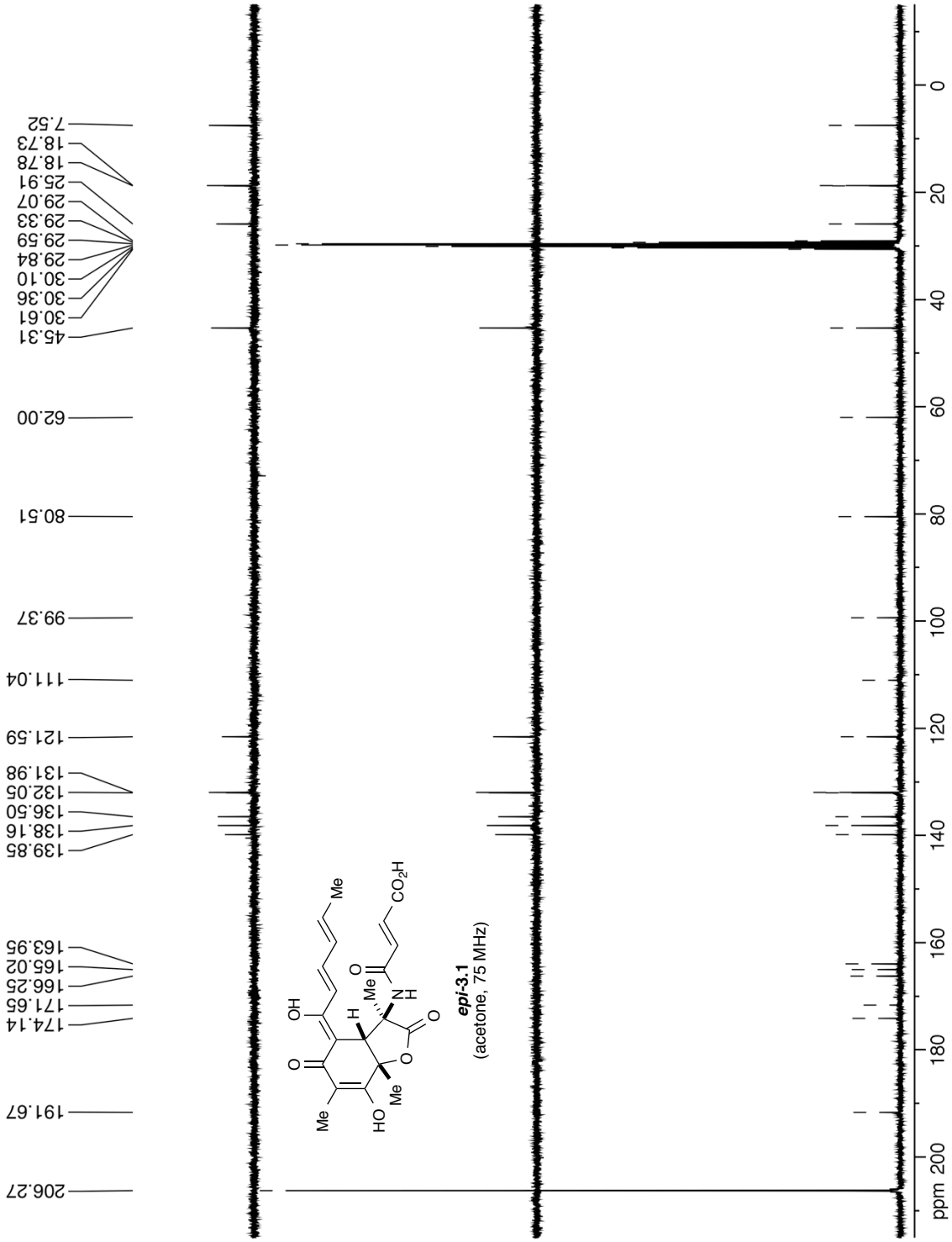
7.52
18.73
18.78
25.91
29.07
29.33
29.59
29.84
30.10
30.36
30.61
45.31
62.00
80.51
99.37
111.04
121.59
131.98
132.05
136.50
138.16
139.85
163.95
165.02
166.25
171.65
174.14
191.67
206.27
ppm 200 180 160 140 120 100 80 60 40 20 0
Me
CO2H
OH
O
Me
H
N
H
O
O
O
Me
Me
HO
epi-3.1
(acetone, 75 MHz)

Natural Sorbicillactone A (acetone-d6, 400 MHz)
Synthetic Sorbicillactone A (acetone-d6, 500 MHz)
9-epi-sorbicillactone A (acetone-d6, 500 MHz)
1.85
1.80
1.75
1.70
1.65
1.60
1.55
1.50
1.45
1.40
1.35
1.30
1.25
1.20
1.15

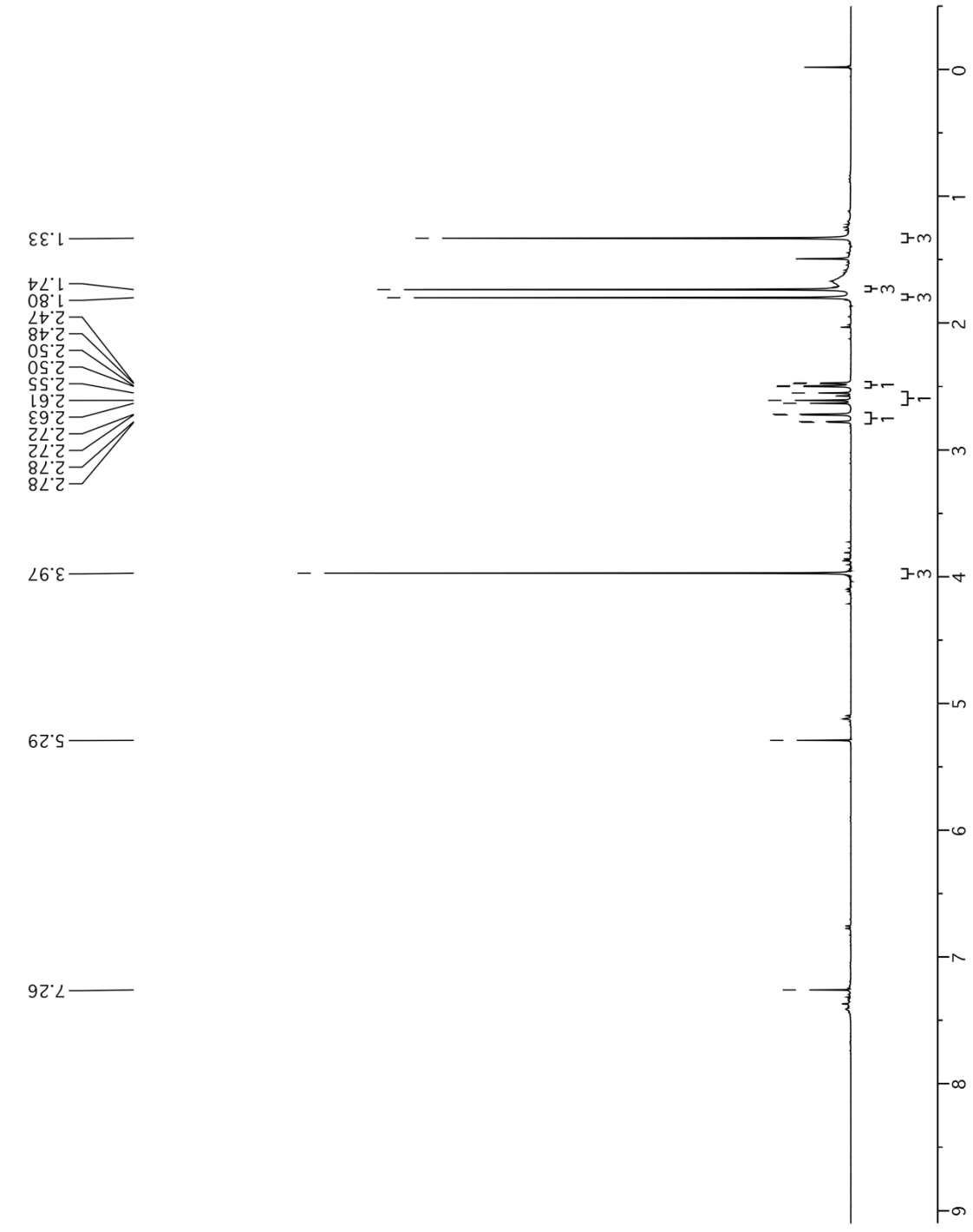

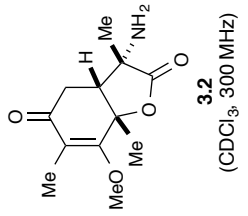

3.2
($CDCl_3$, 300 MHz)

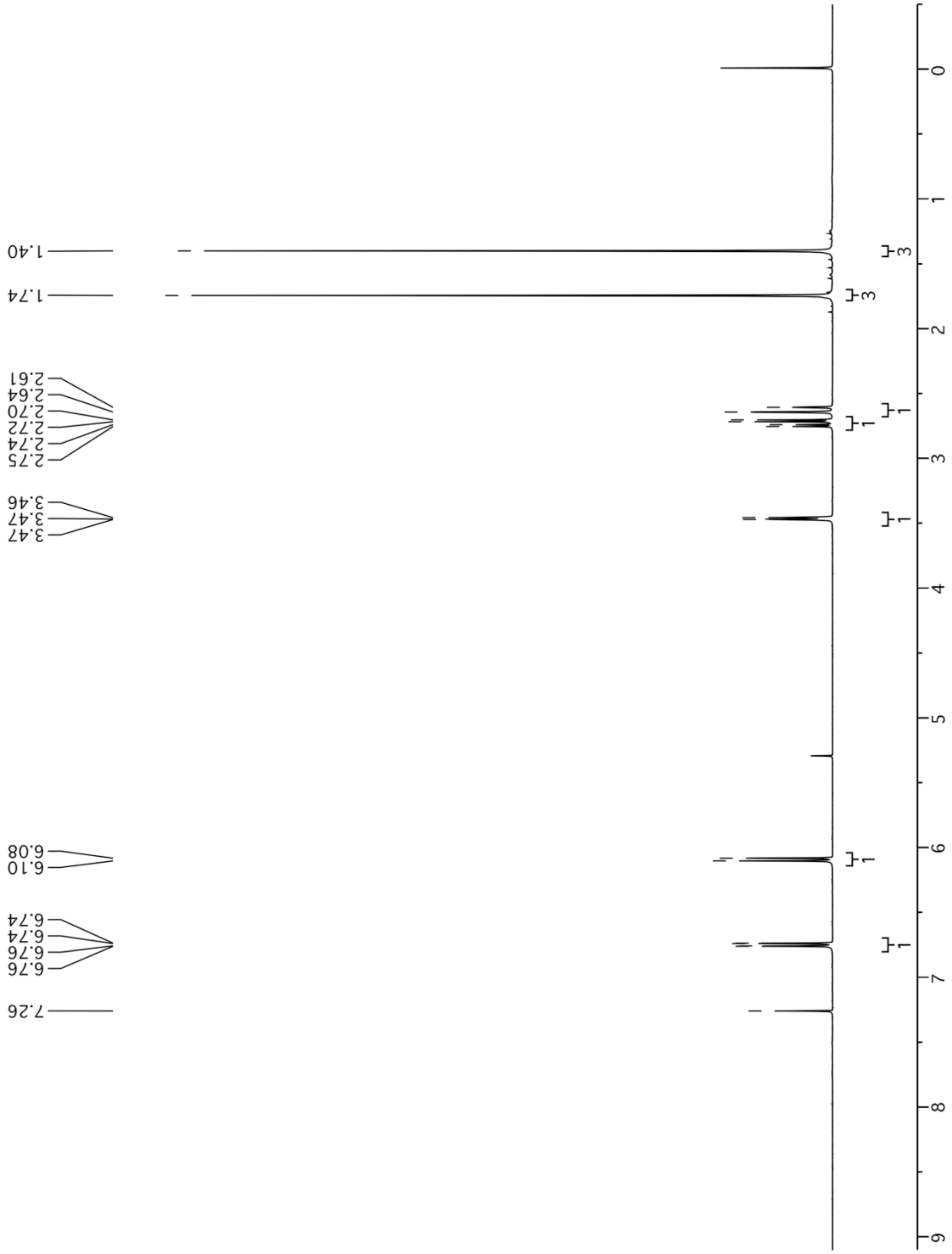

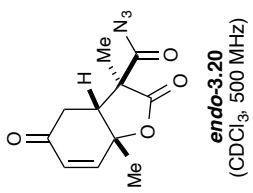

***endo*-3.20**
($CDCl_3$, 500 MHz)

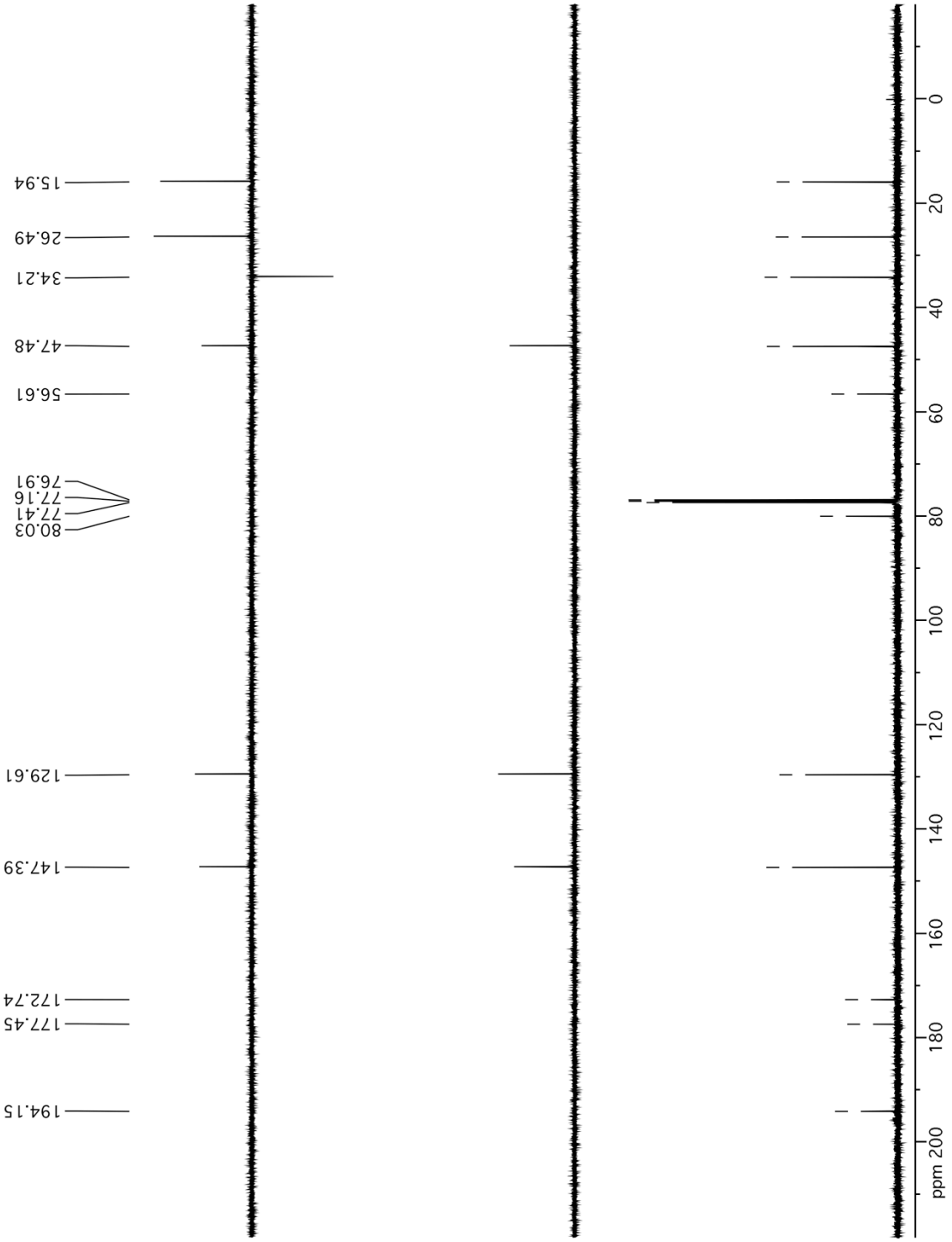

***endo*-3.20**
($CDCl_3$, 125 MHz)

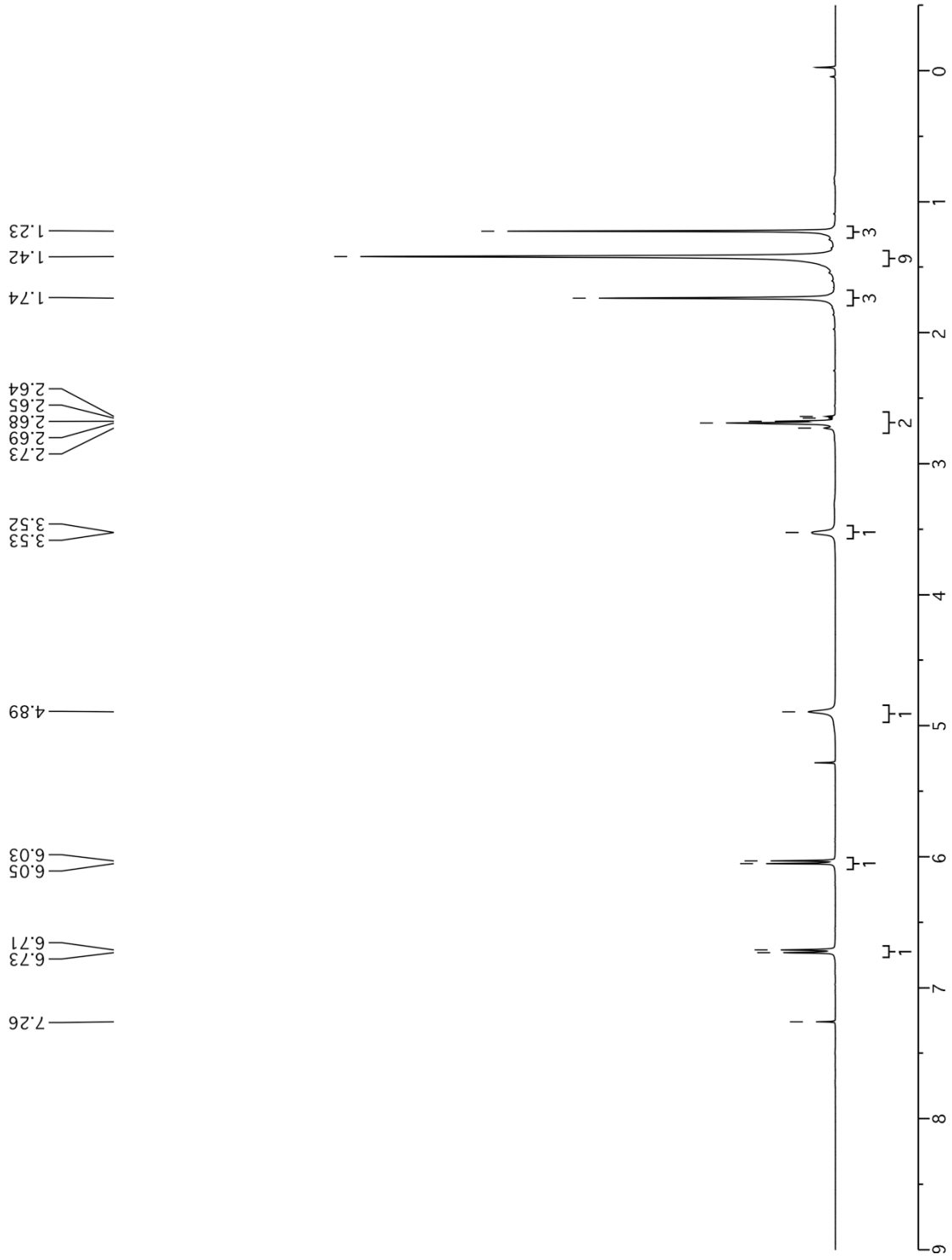

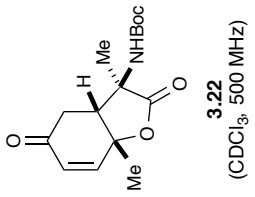

3.22
($CDCl_3$, 500 MHz)

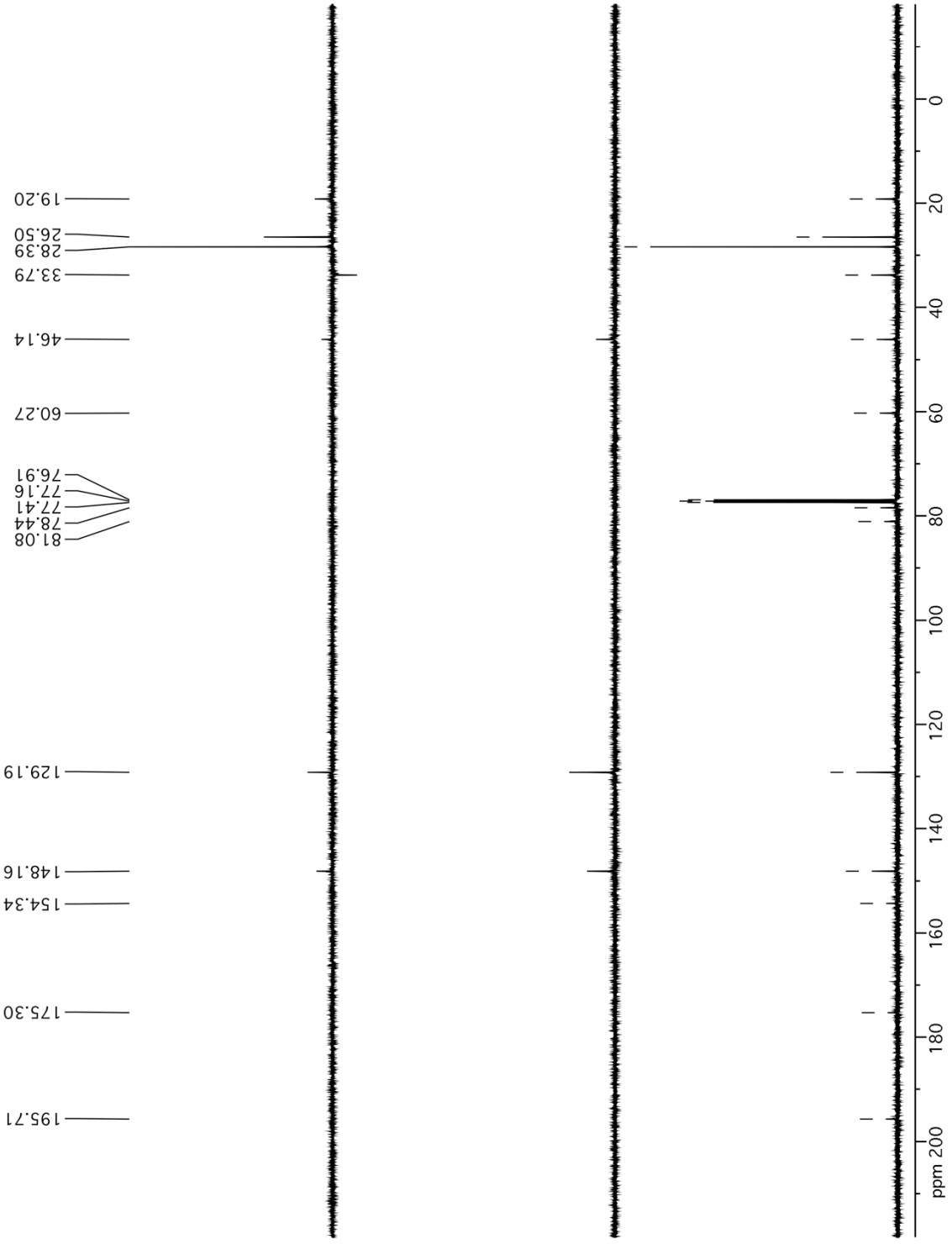

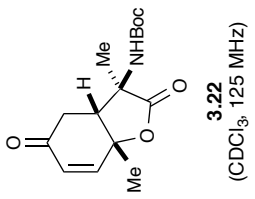

3.22
($CDCl_3$, 125 MHz)

3.24
($CDCl_3$, 300 MHz)

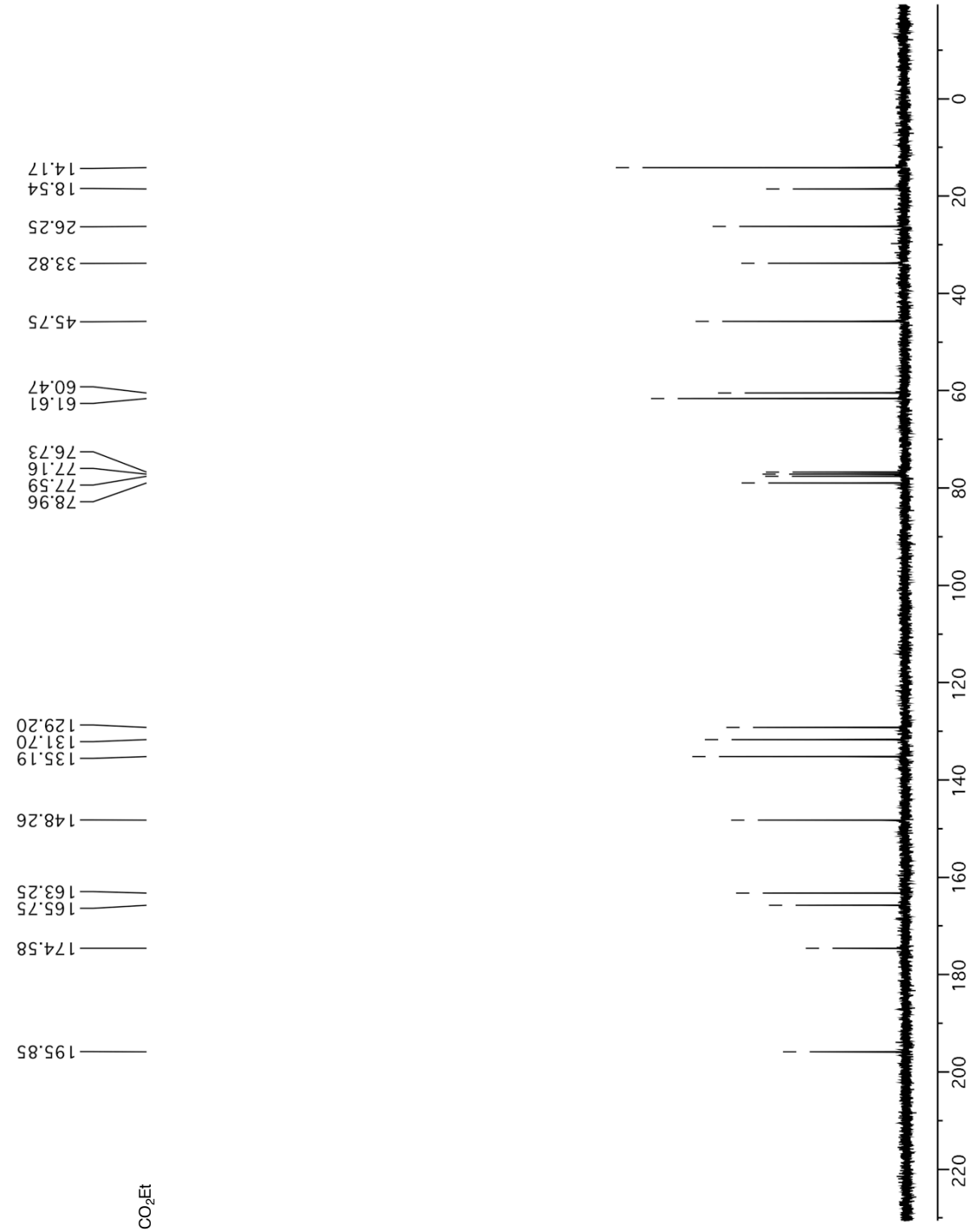

3.24
($CDCl_3$, 75 MHz)

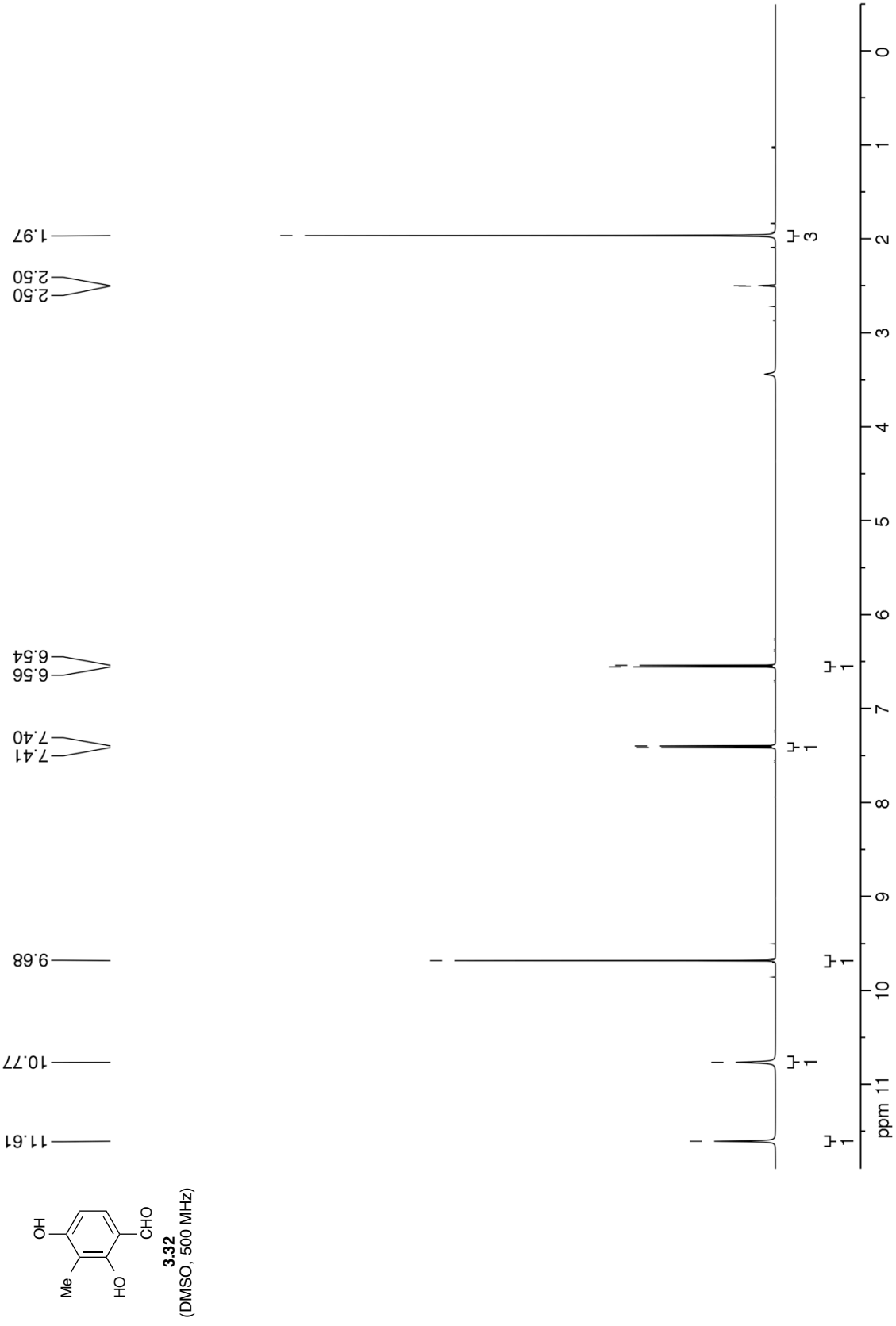

3.32
(DMSO, 500 MHz)

3.32
(DMSO, 125 MHz)

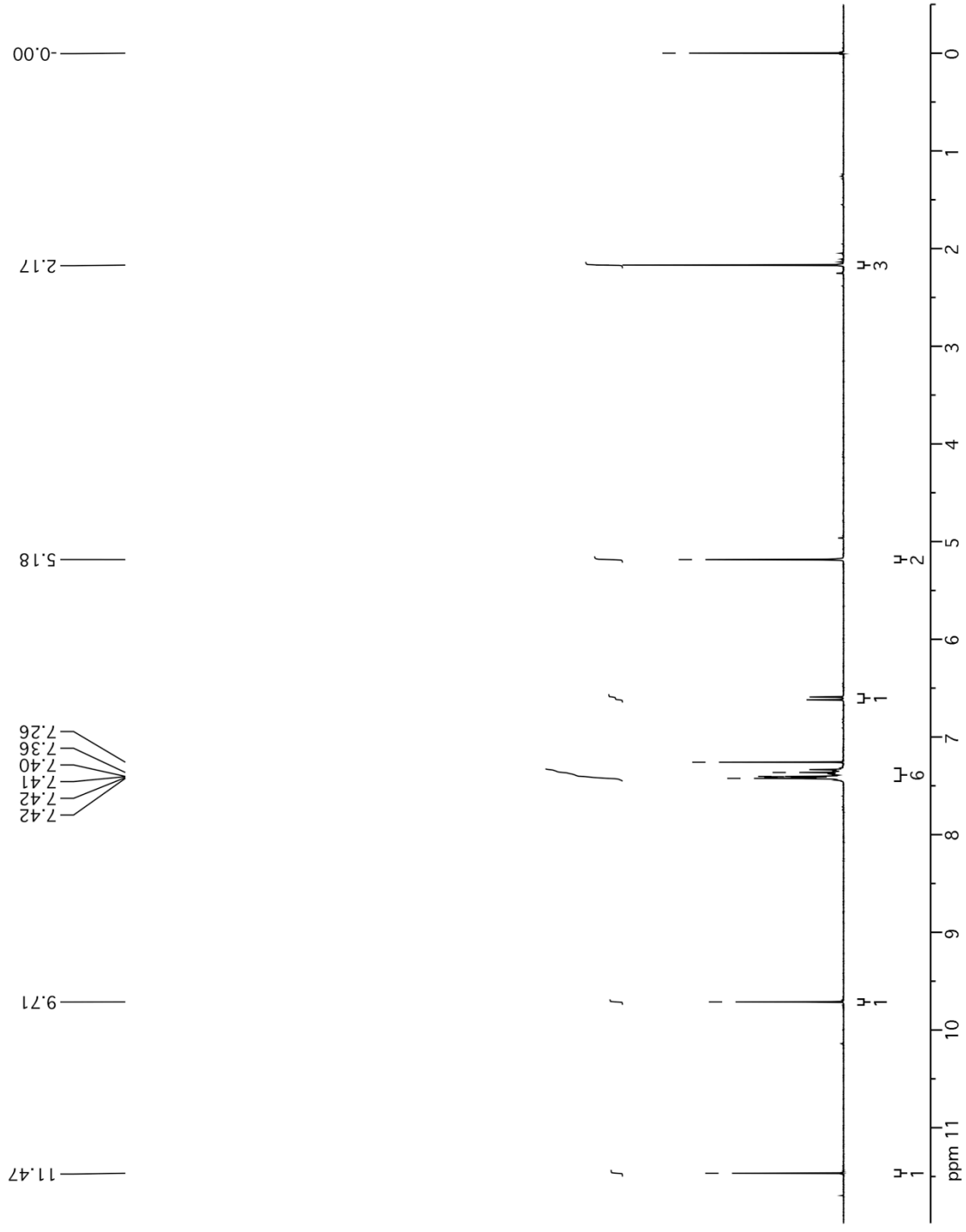

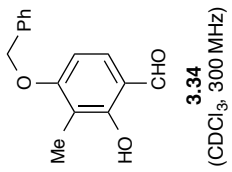

3.34
($CDCl_3$, 300 MHz)

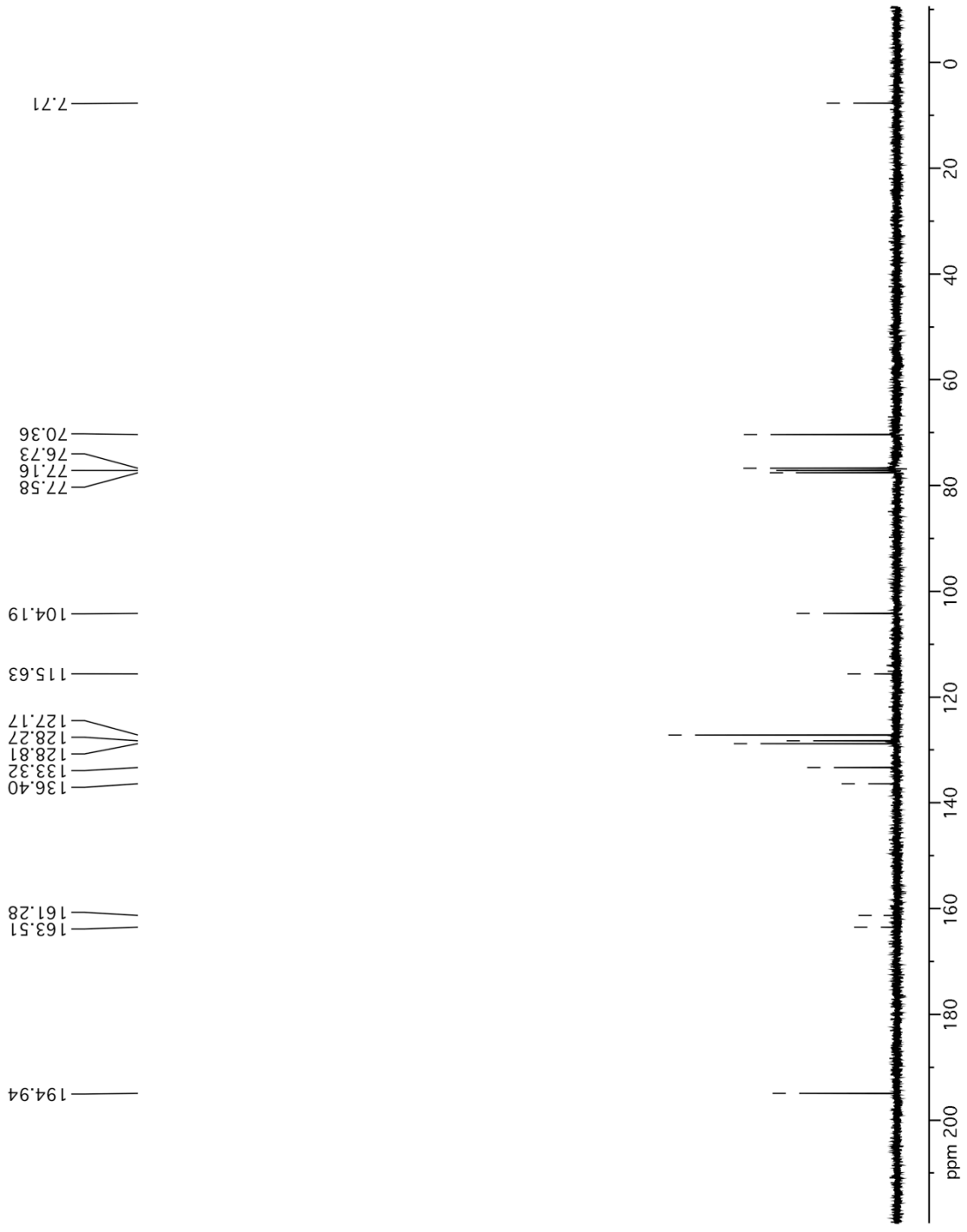

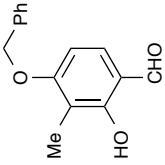

3.34
($CDCl_3$, 75 MHz)

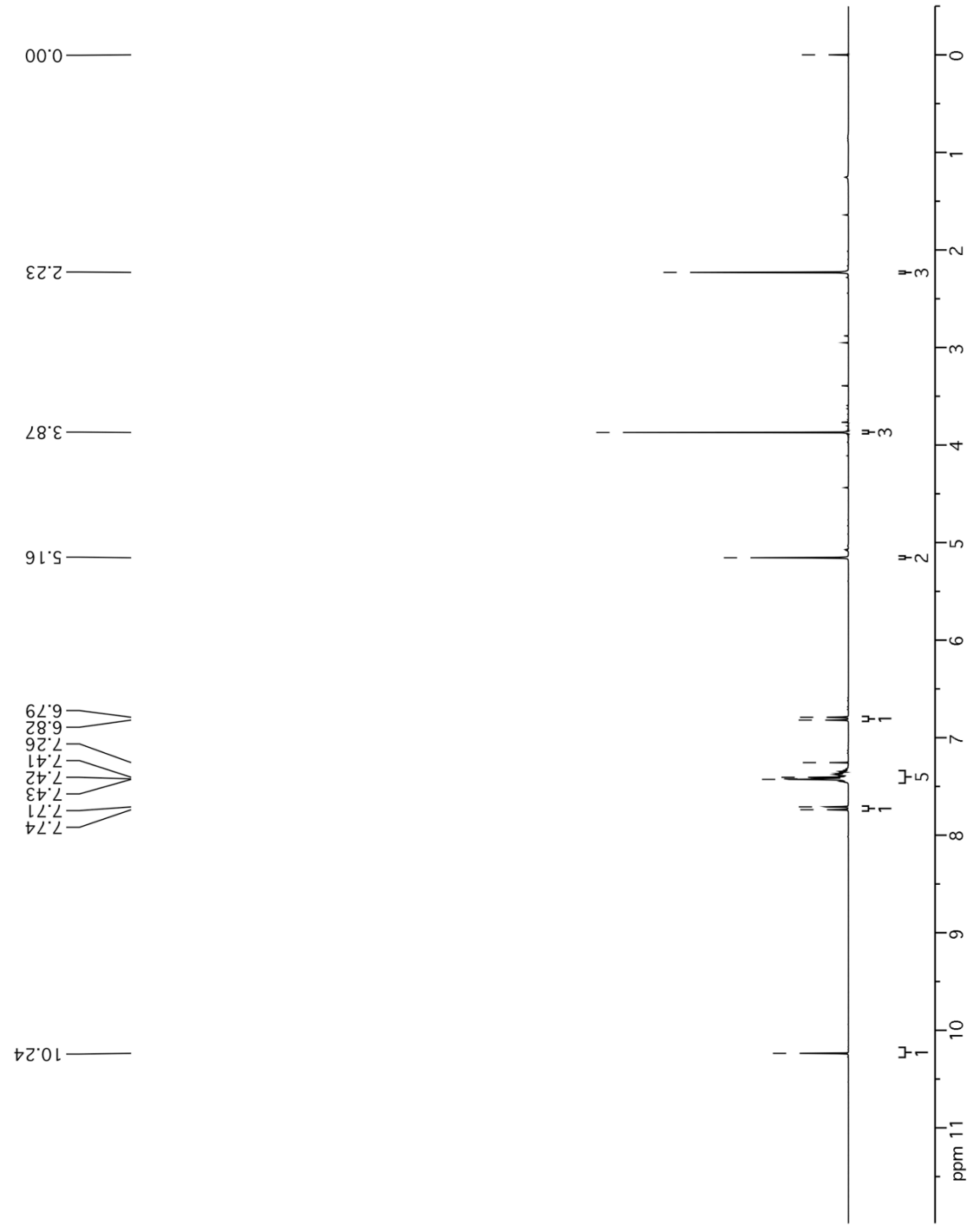

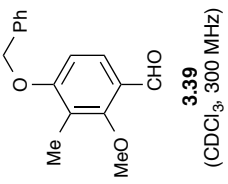

3.39
($CDCl_3$, 300 MHz)

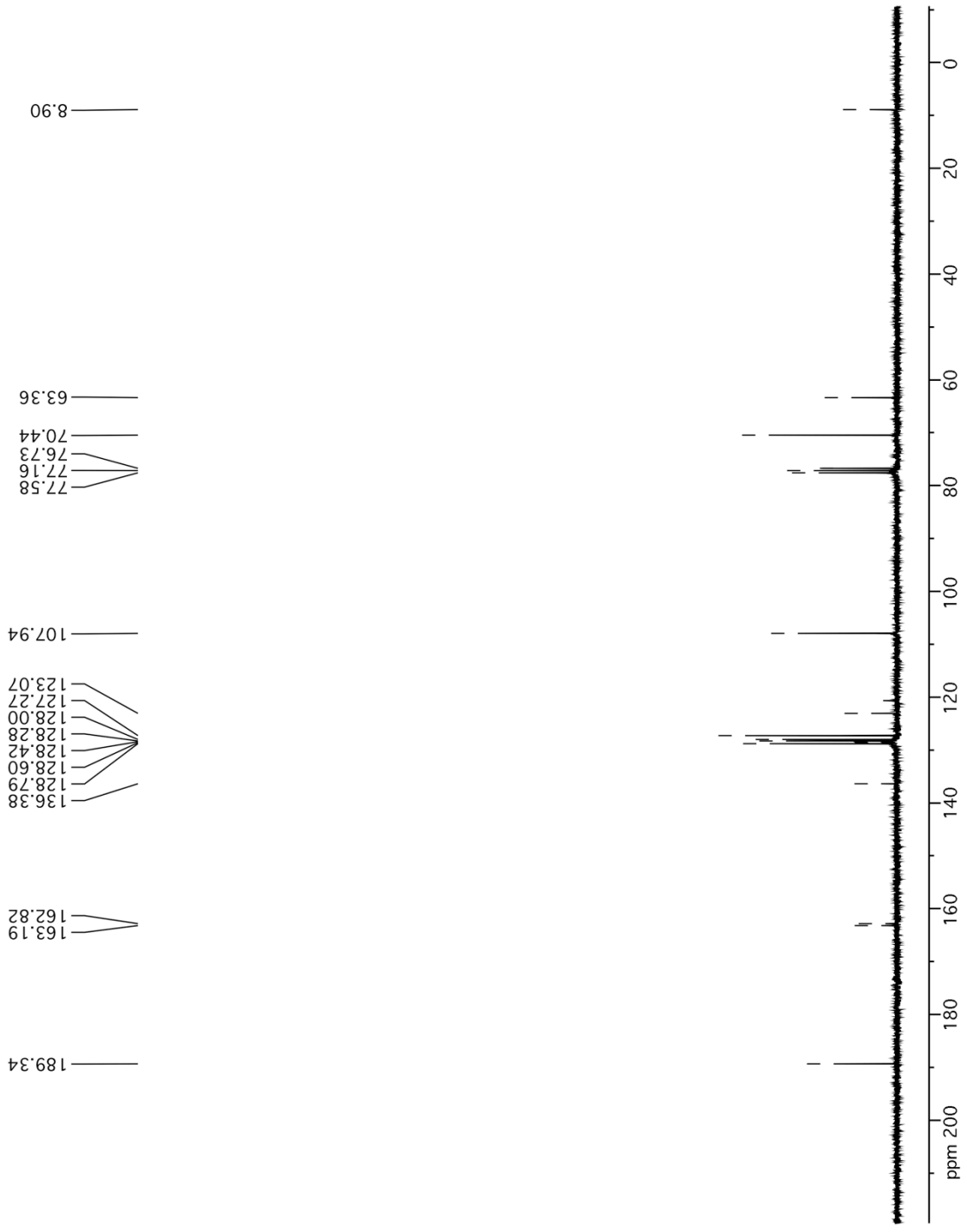

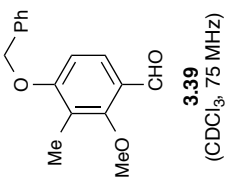

3.39
($CDCl_3$, 75 MHz)

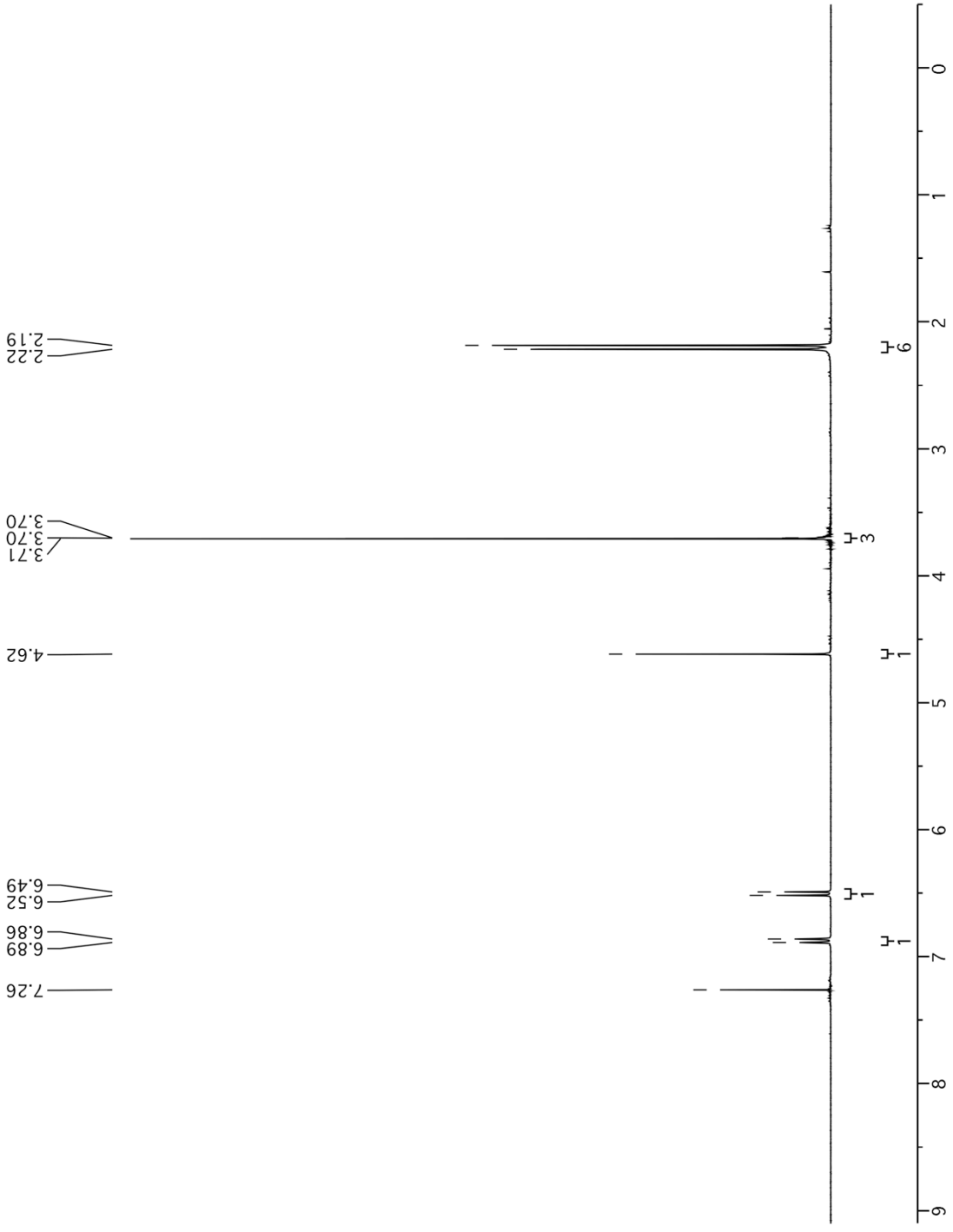

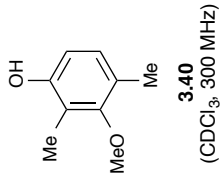

3.40
($CDCl_3$, 300 MHz)

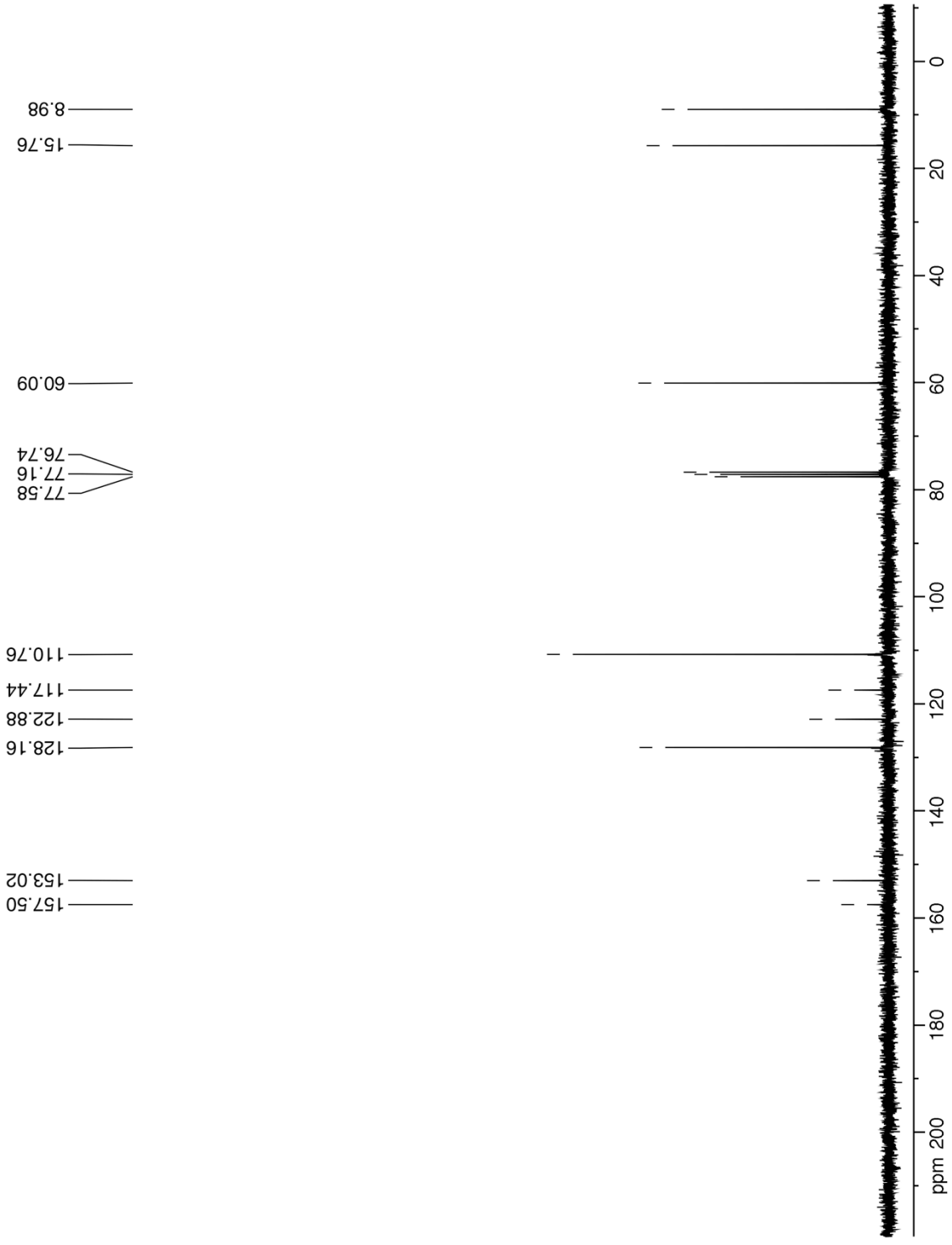

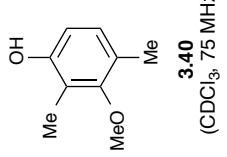

3.40
($CDCl_3$, 75 MHz)

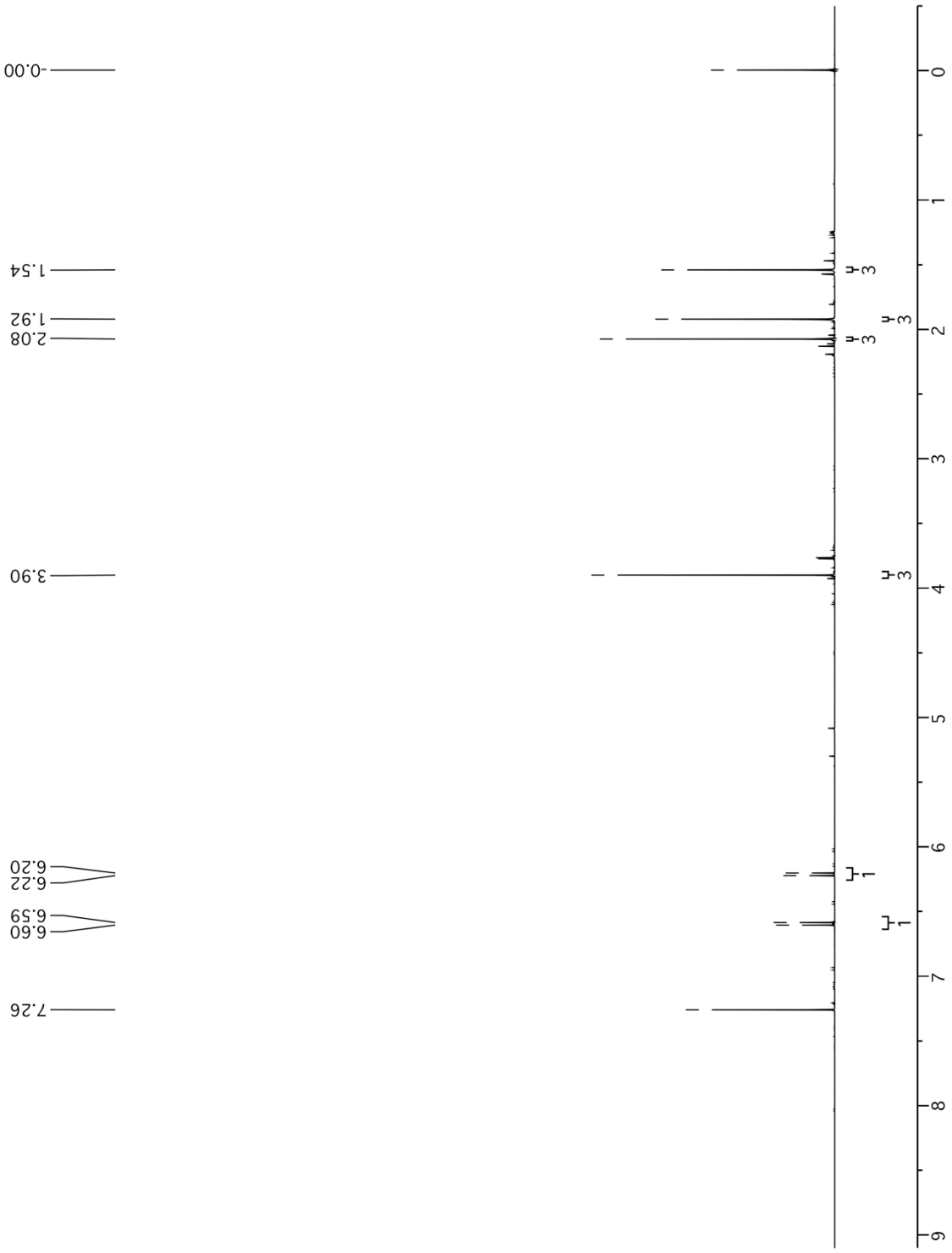

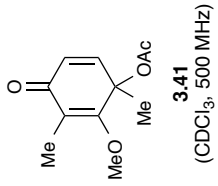

3.41
($CDCl_3$, 500 MHz)

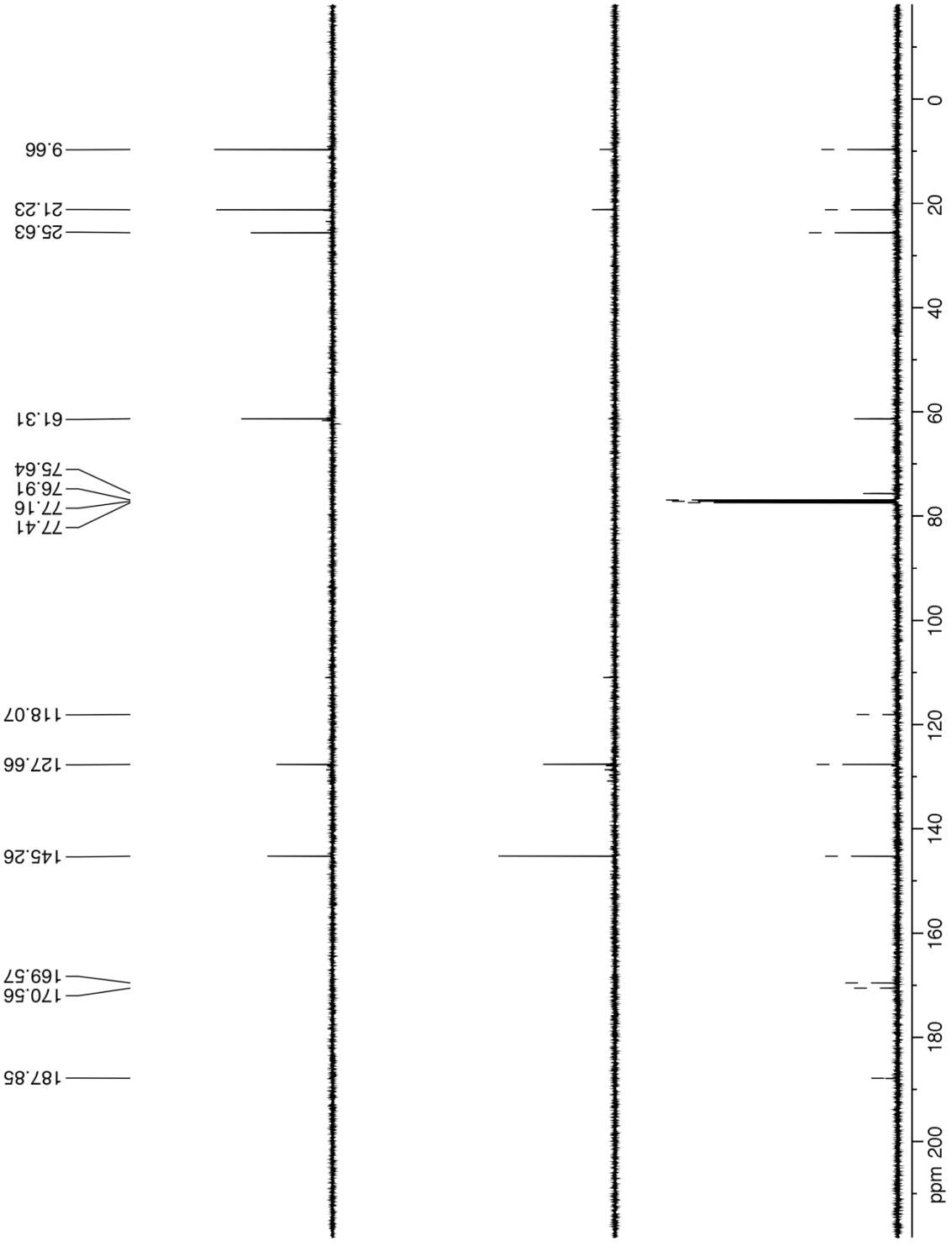

3.41
($CDCl_3$, 125 MHz)

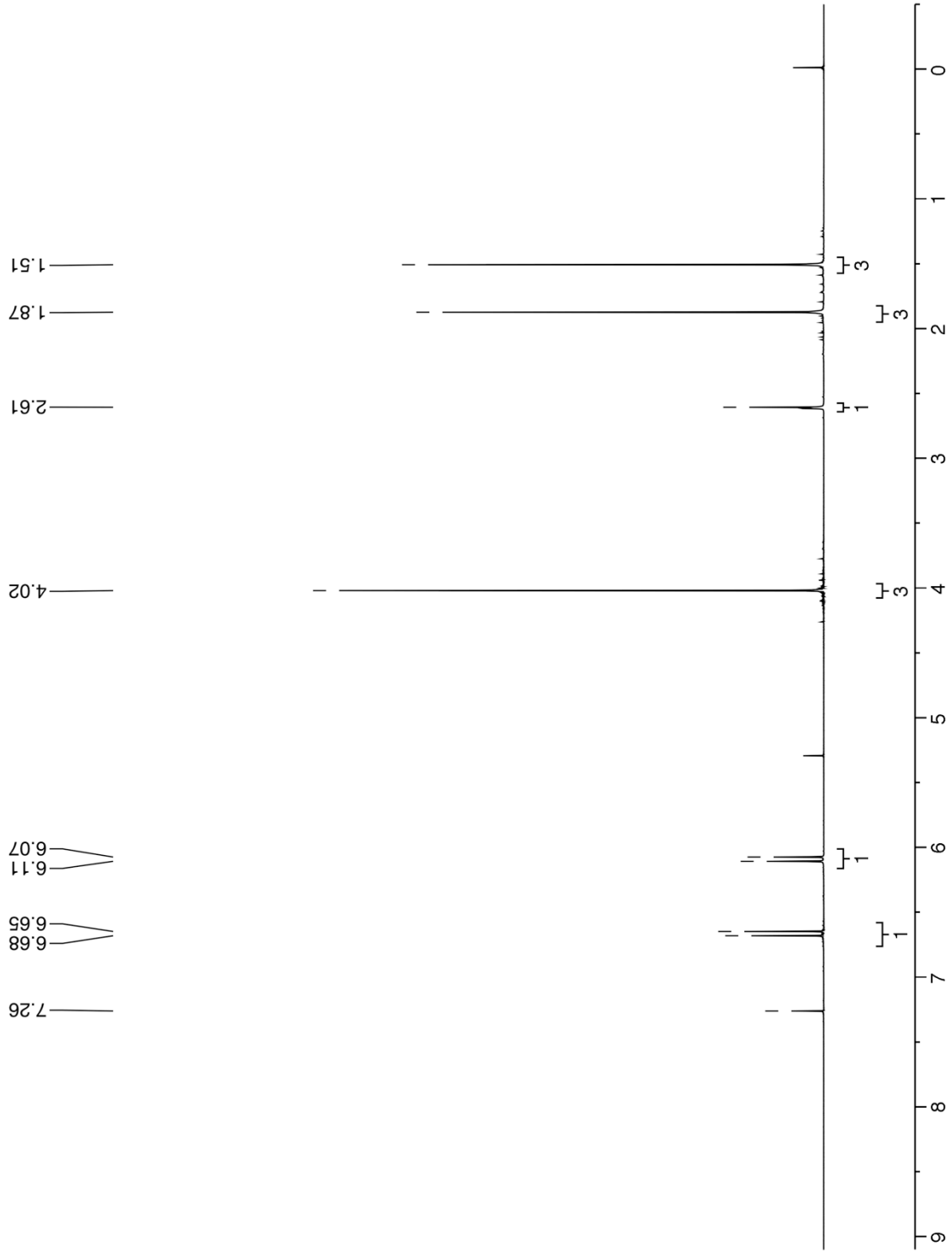

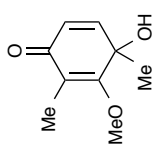

3.42
($CDCl_3$, 300 MHz)

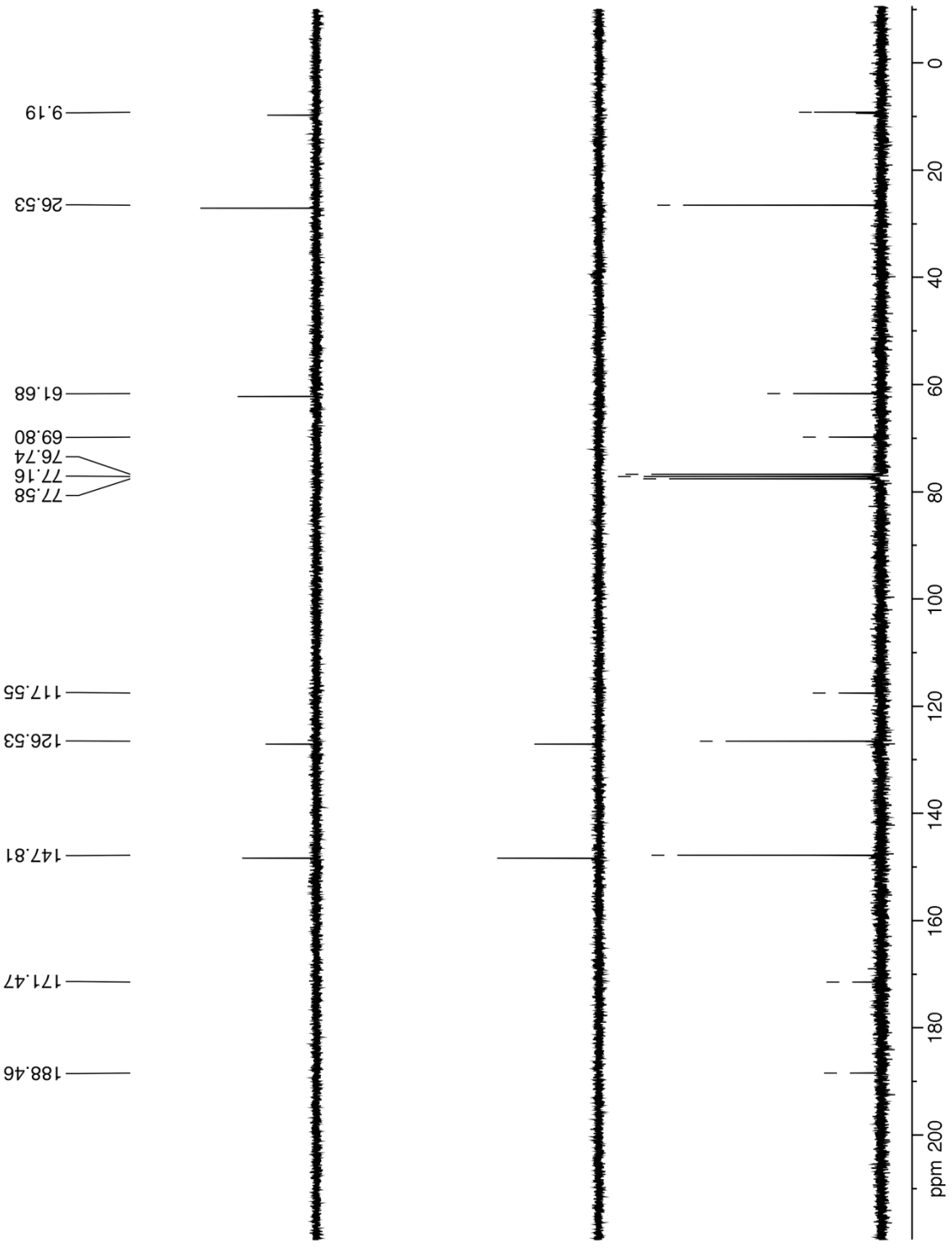

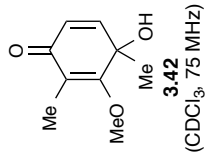

3.42
($CDCl_3$, 75 MHz)

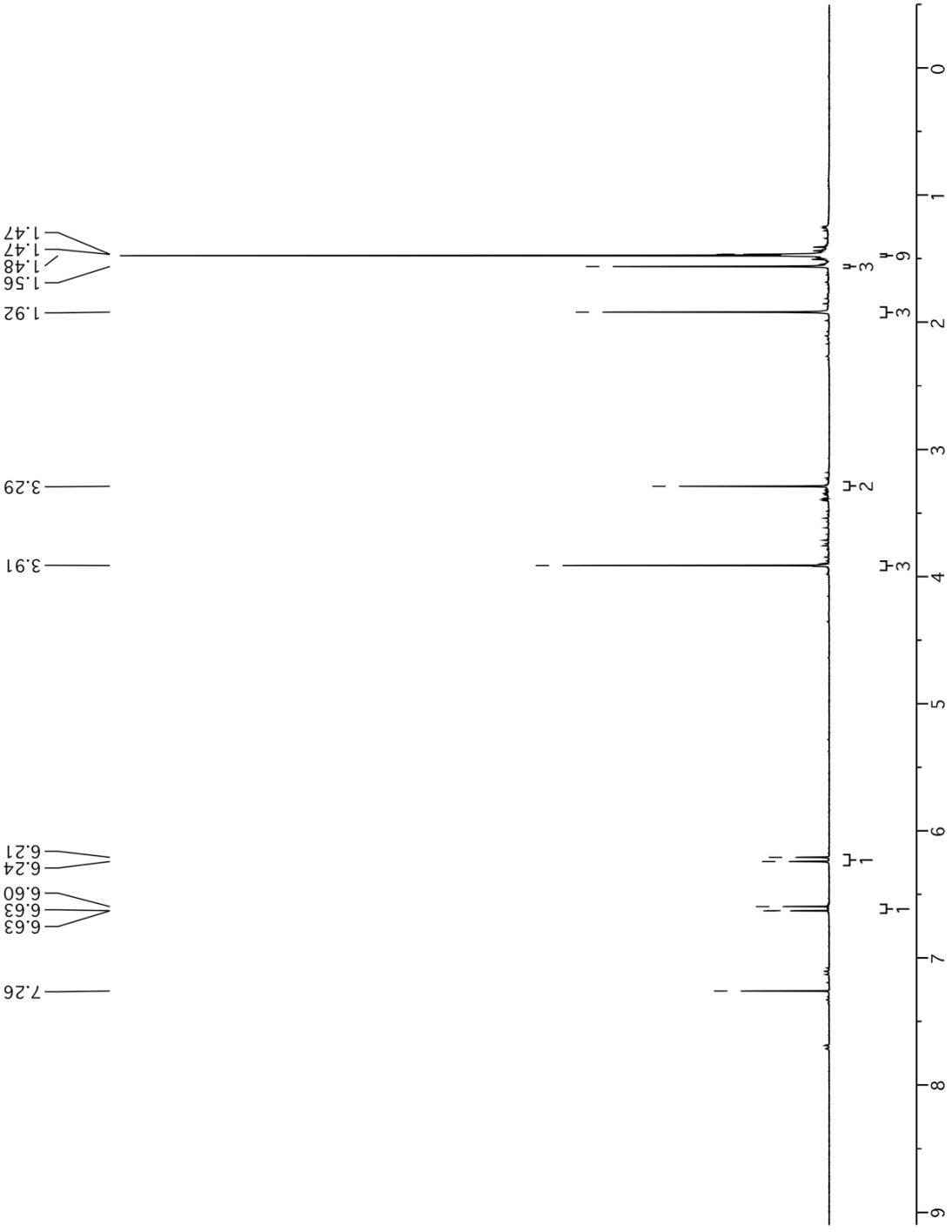

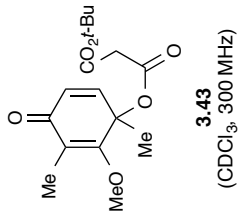

3.43
($CDCl_3$, 300 MHz)

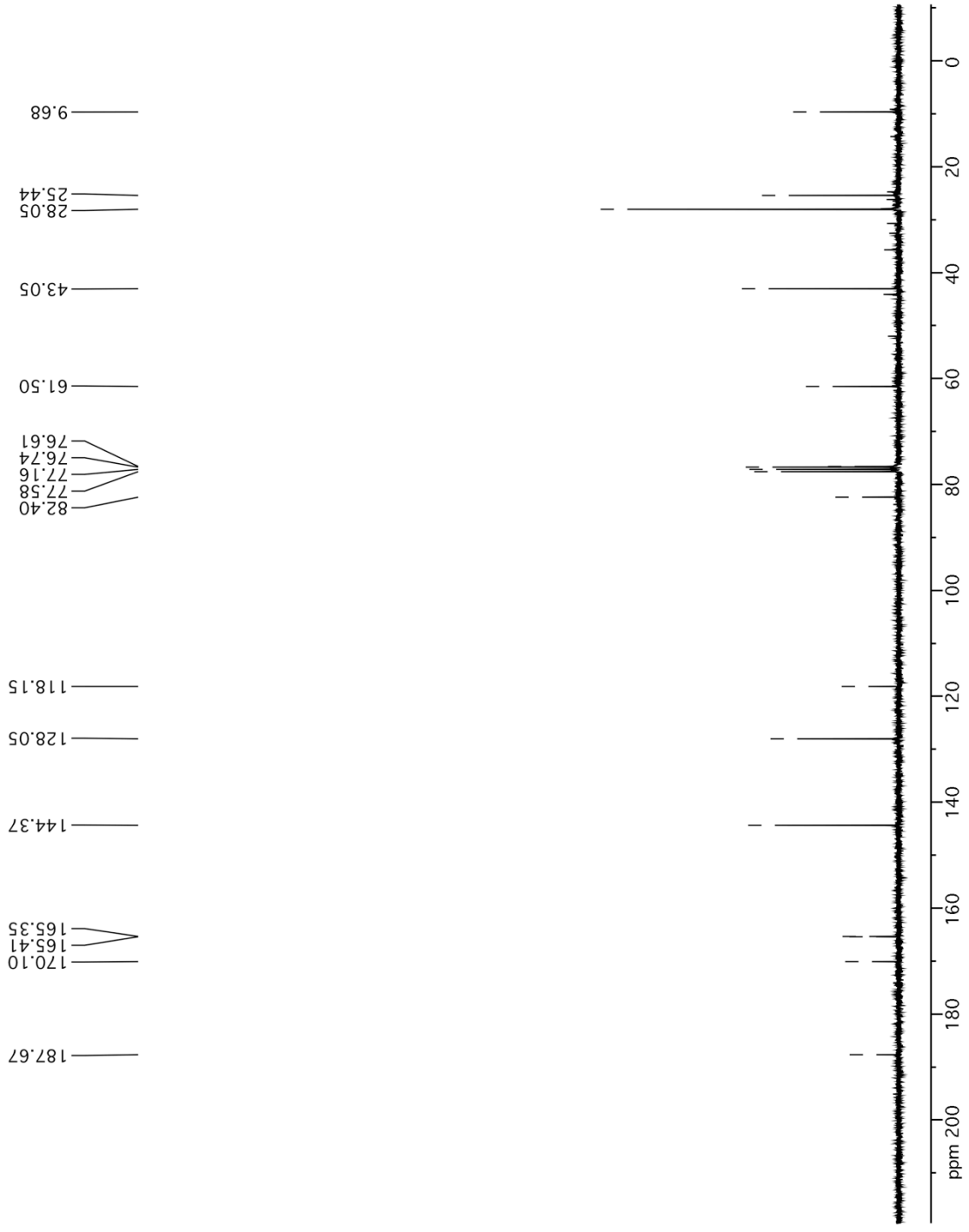

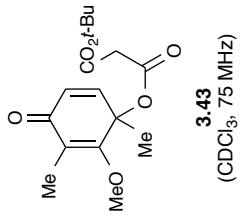

3.43
($CDCl_3$, 75 MHz)

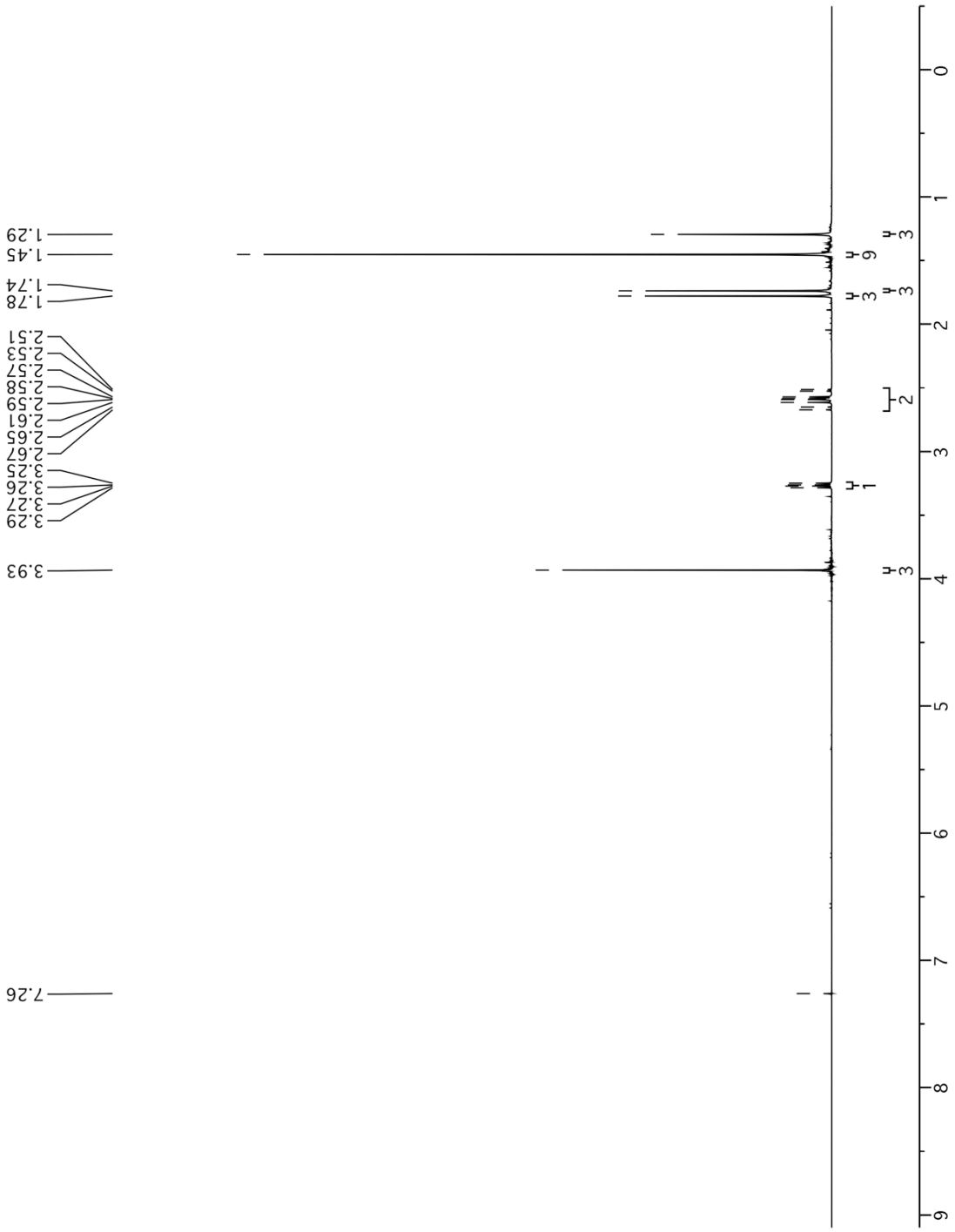

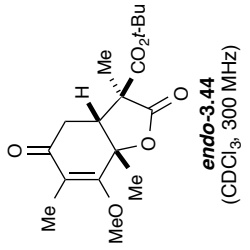

***endo*-3.44**
($CDCl_3$, 300 MHz)

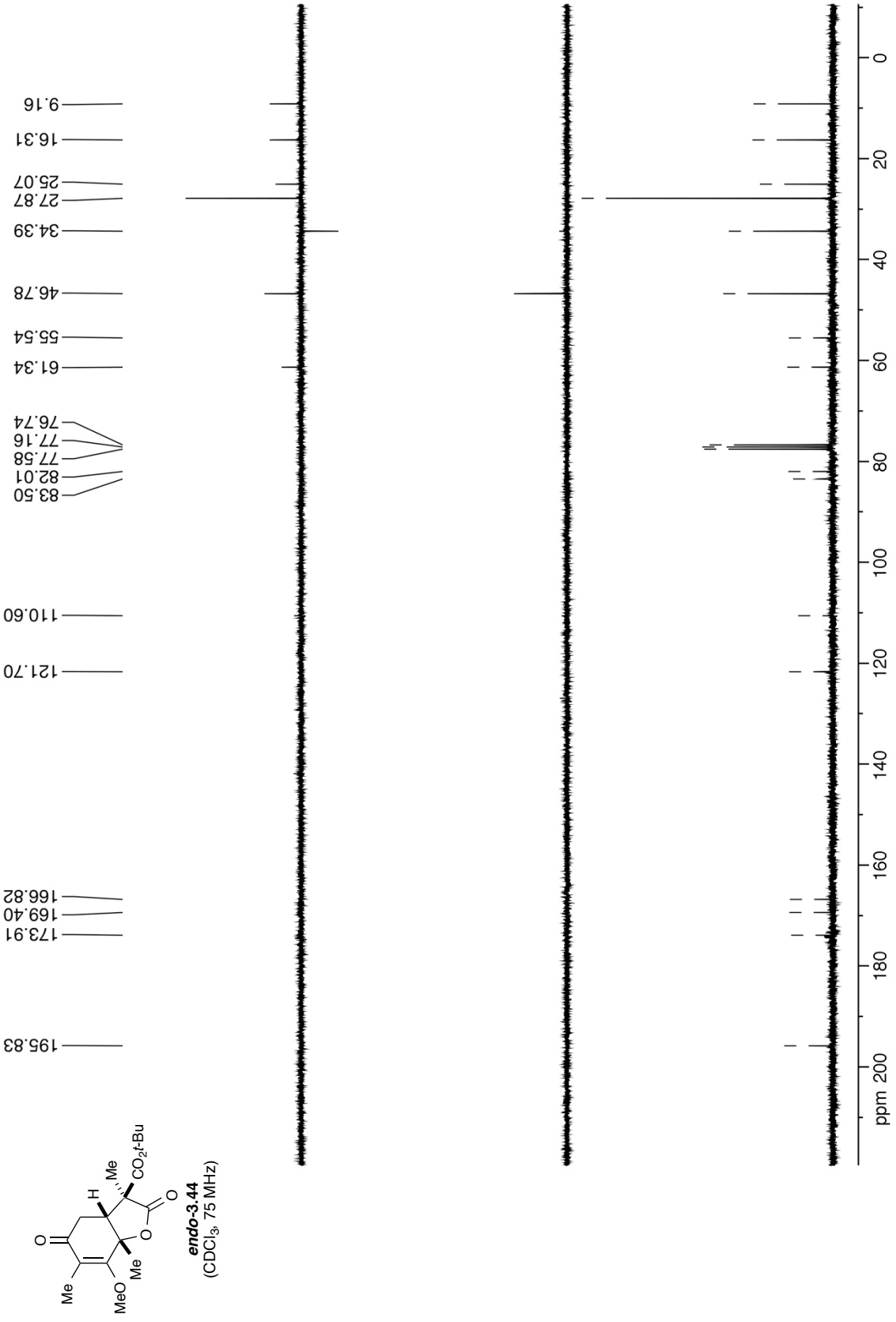

***endo*-3.44**
($CDCl_3$, 75 MHz)

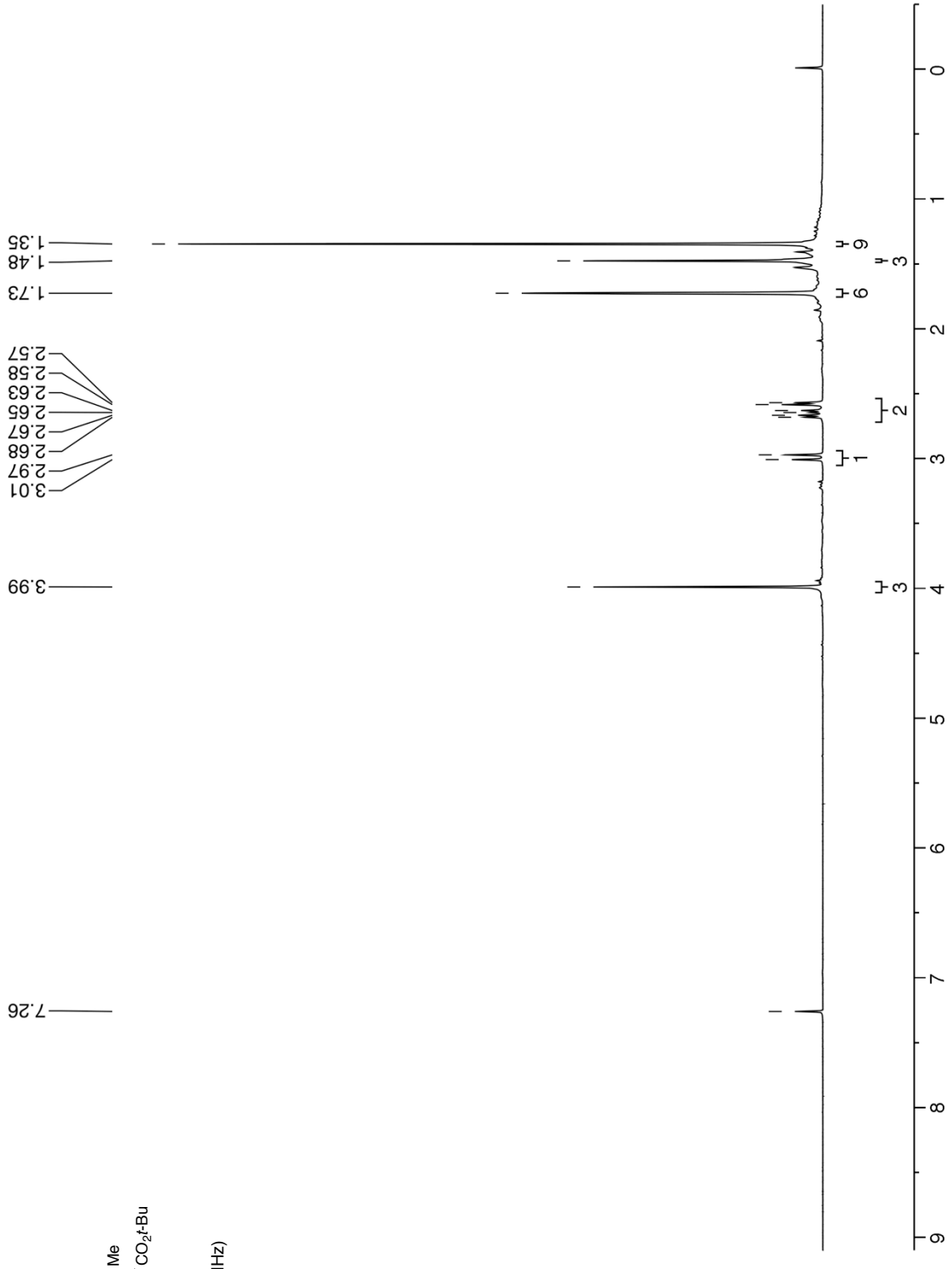

***exo*-3.44**
($CDCl_3$, 500 MHz)

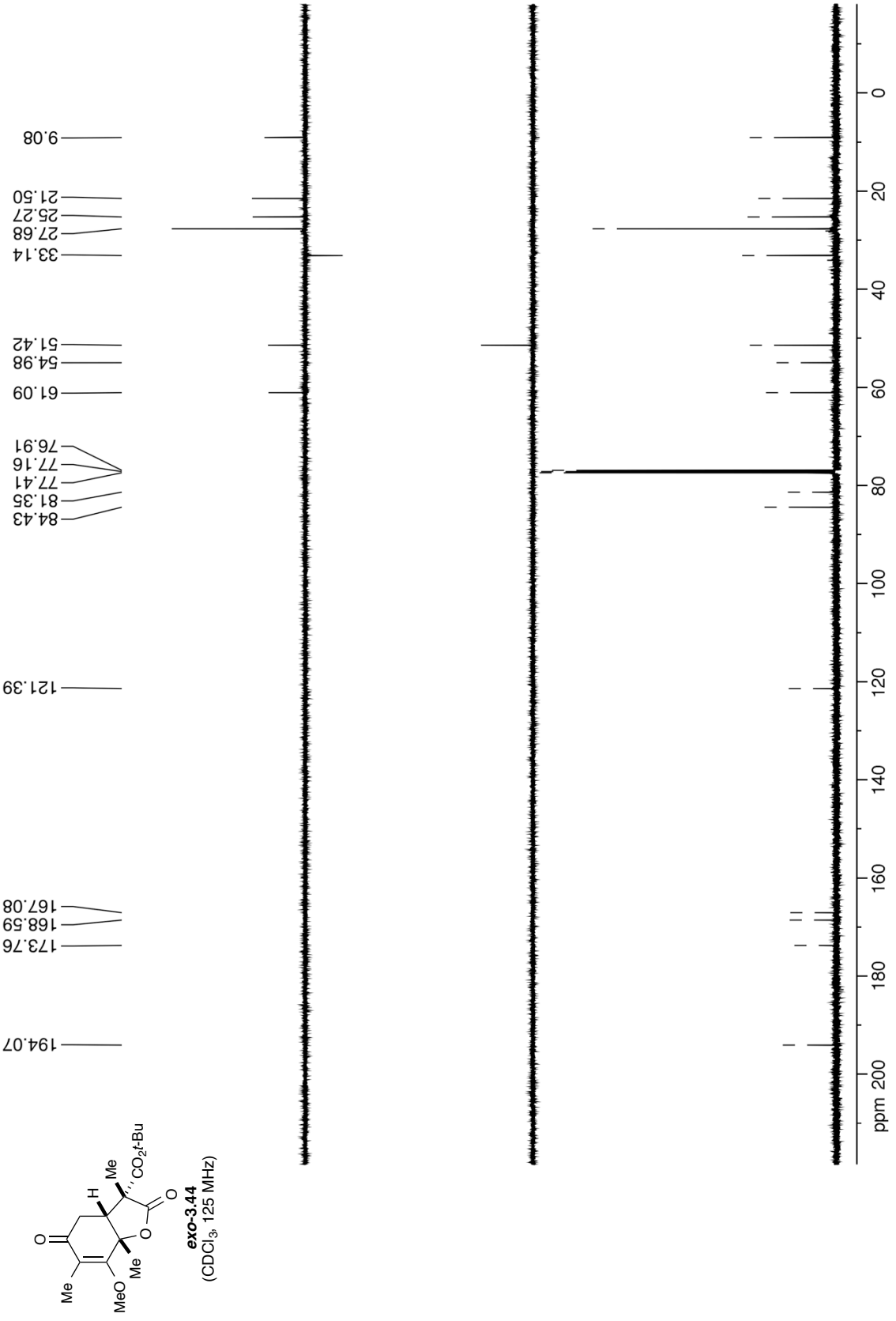

***exo*-3.44**
($CDCl_3$, 125 MHz)

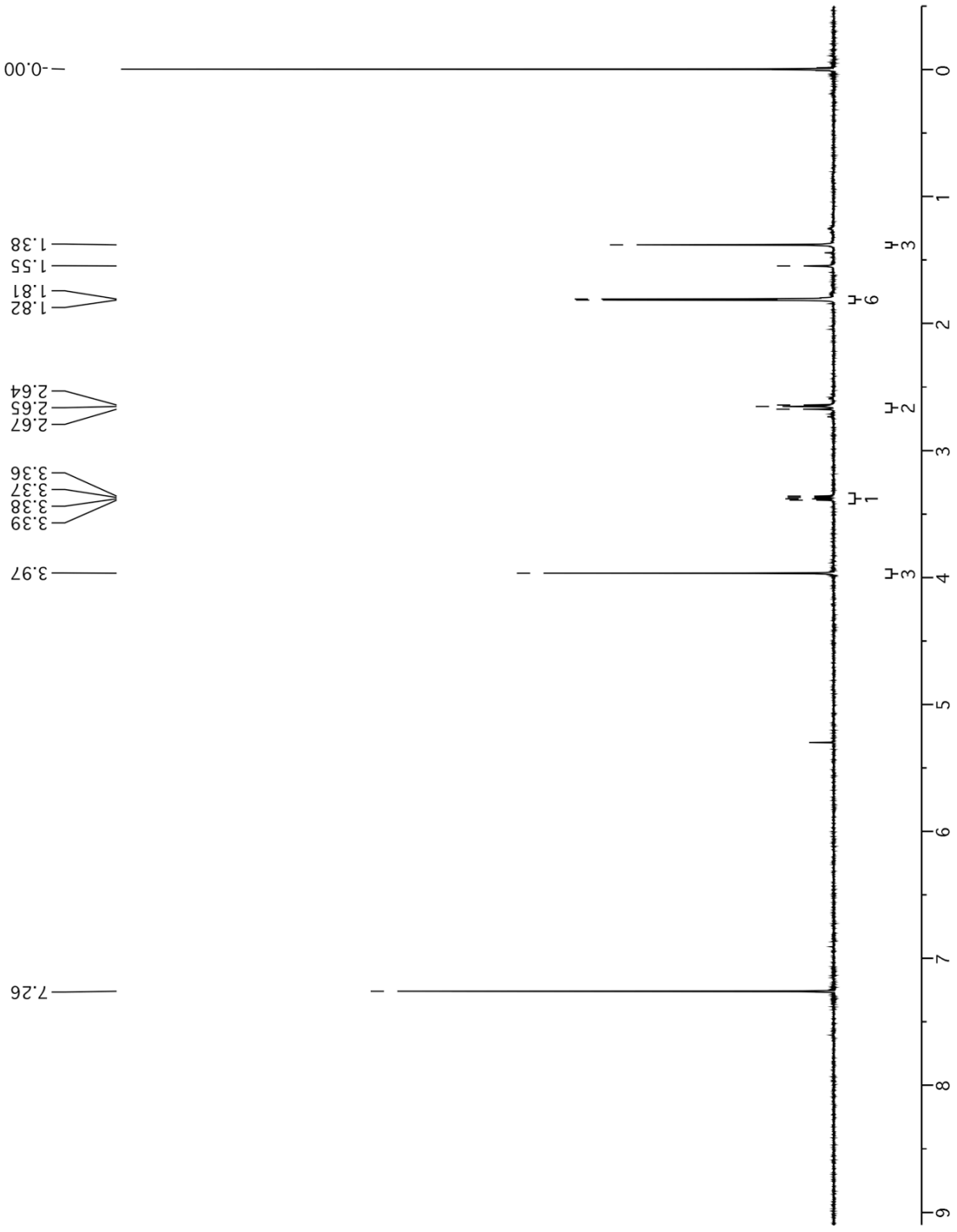

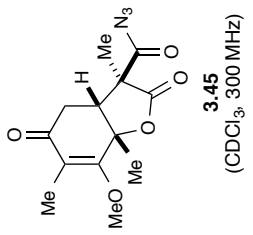

3.45
($CDCl_3$, 300 MHz)

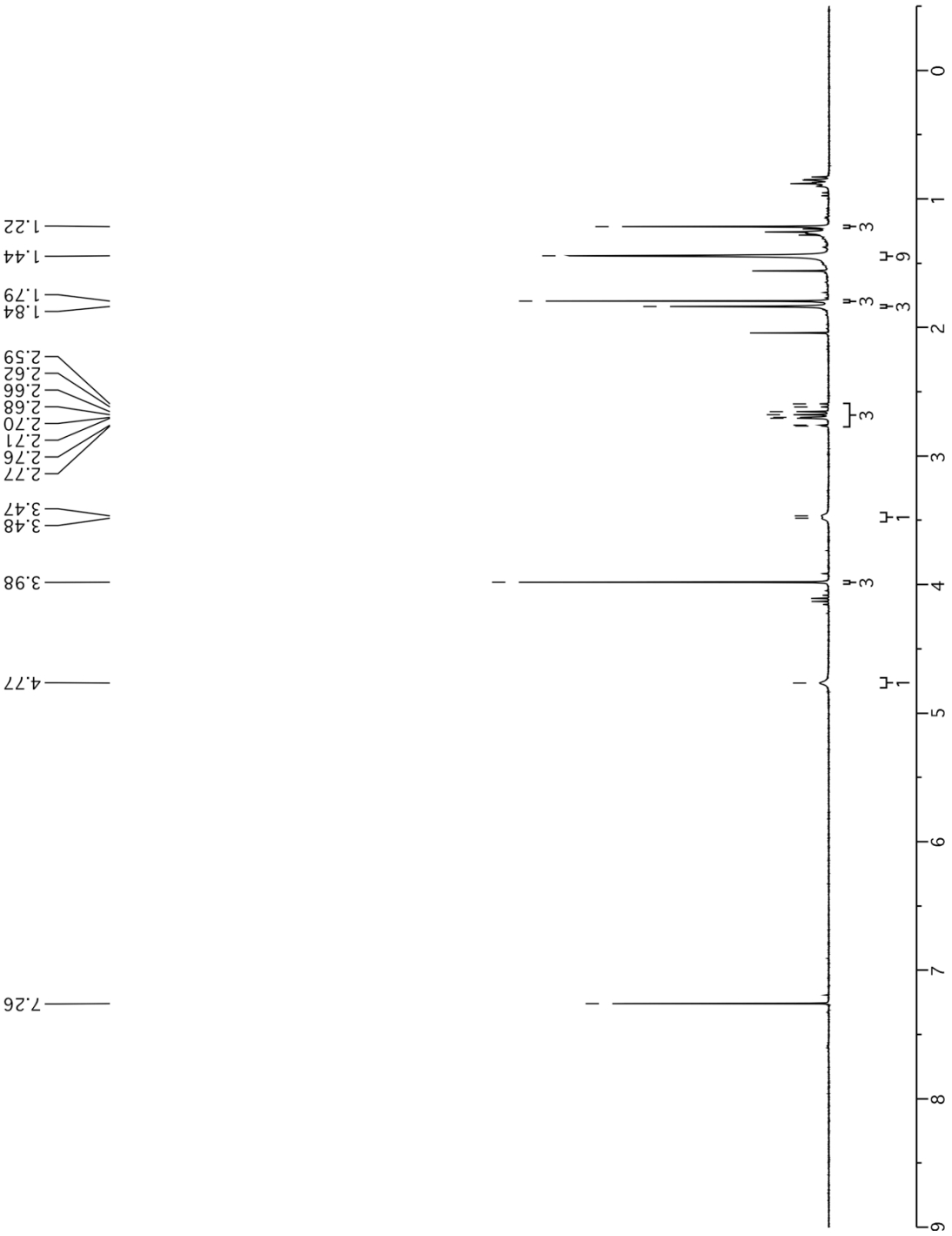

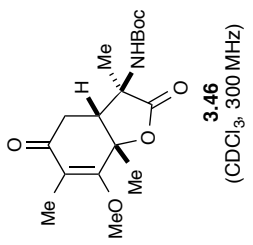

3.46
($CDCl_3$, 300 MHz)

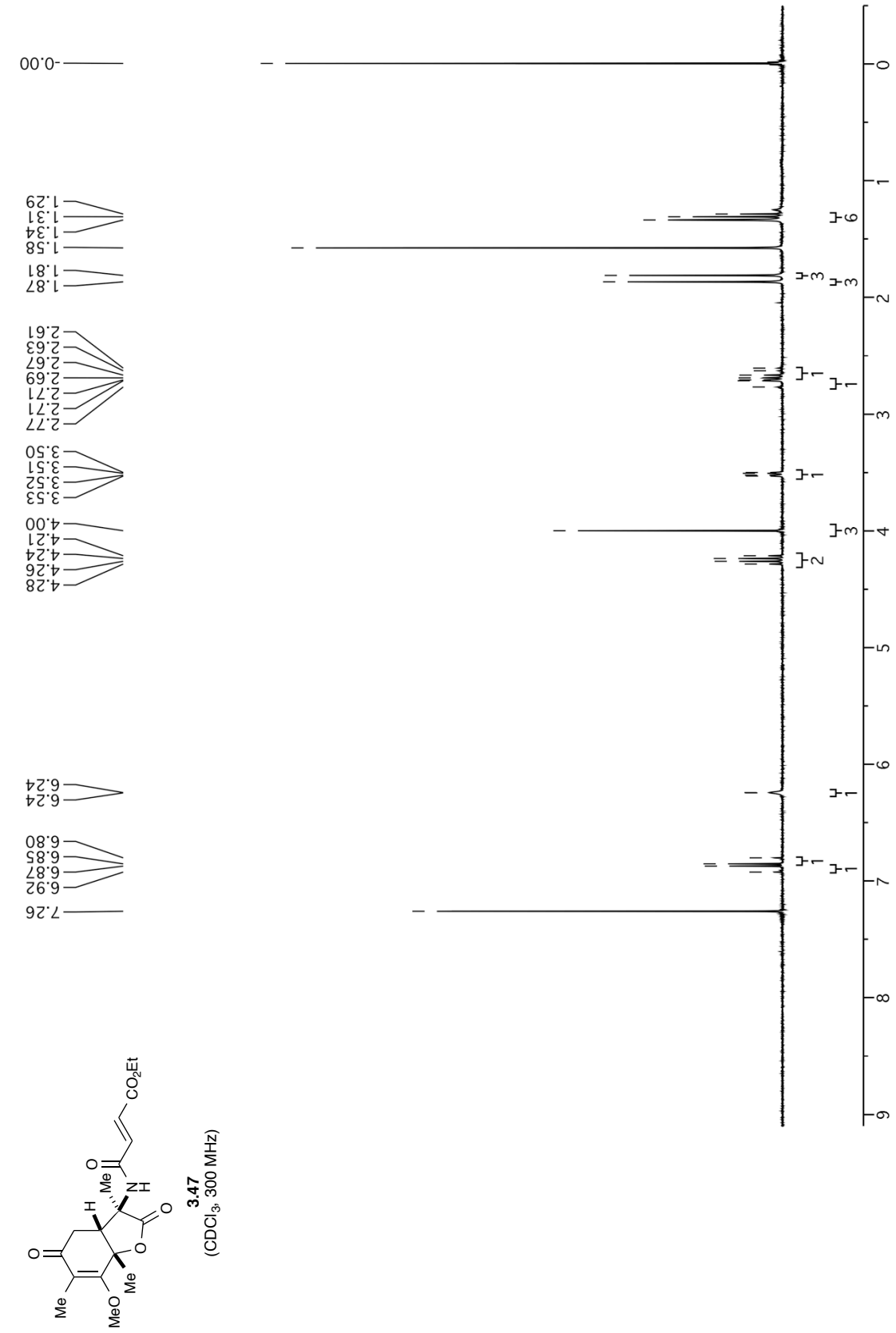

3.47
($CDCl_3$, 300 MHz)

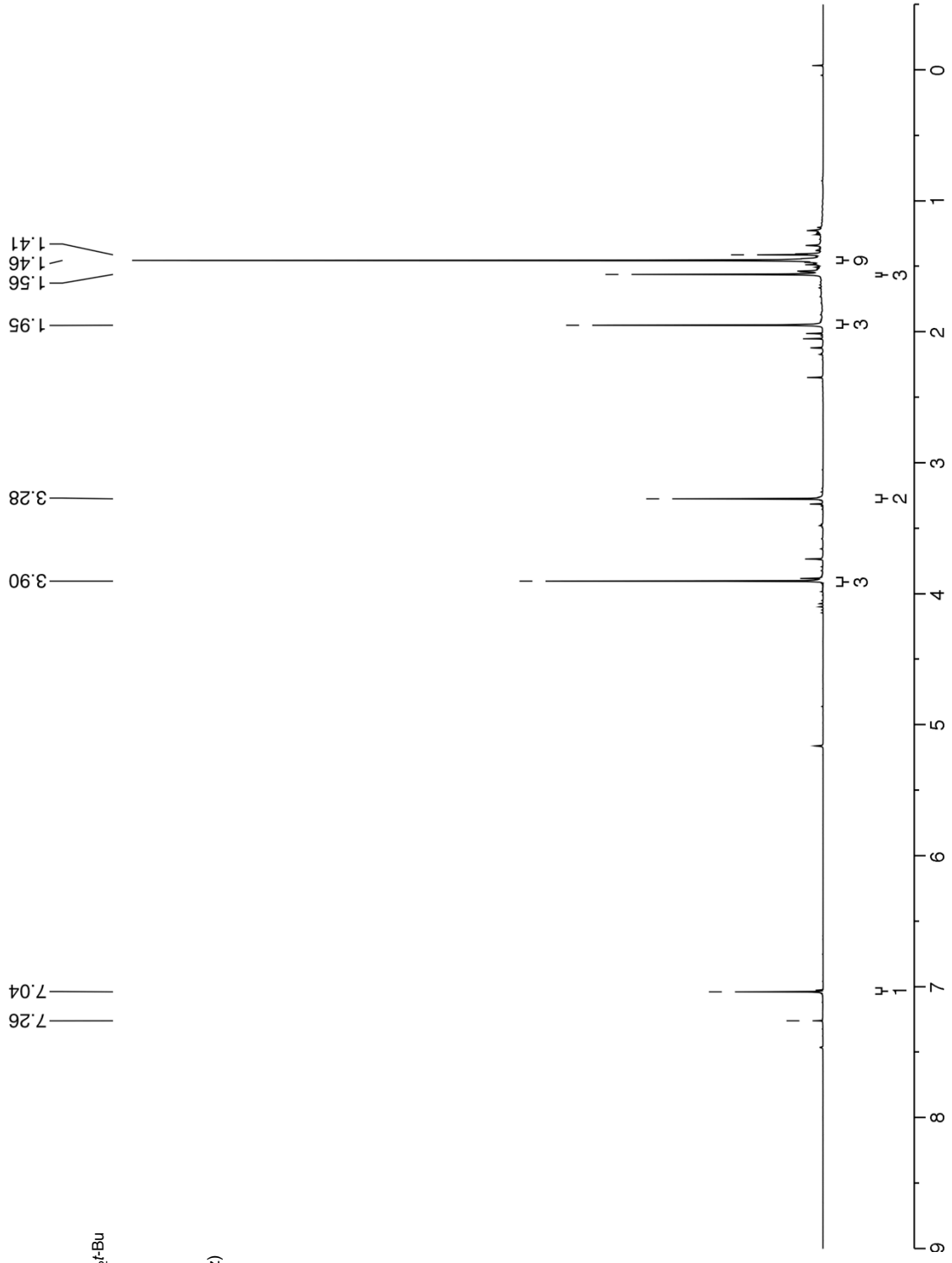

3.53
($CDCl_3$, 300 MHz)

3.53
($CDCl_3$, 75 MHz)

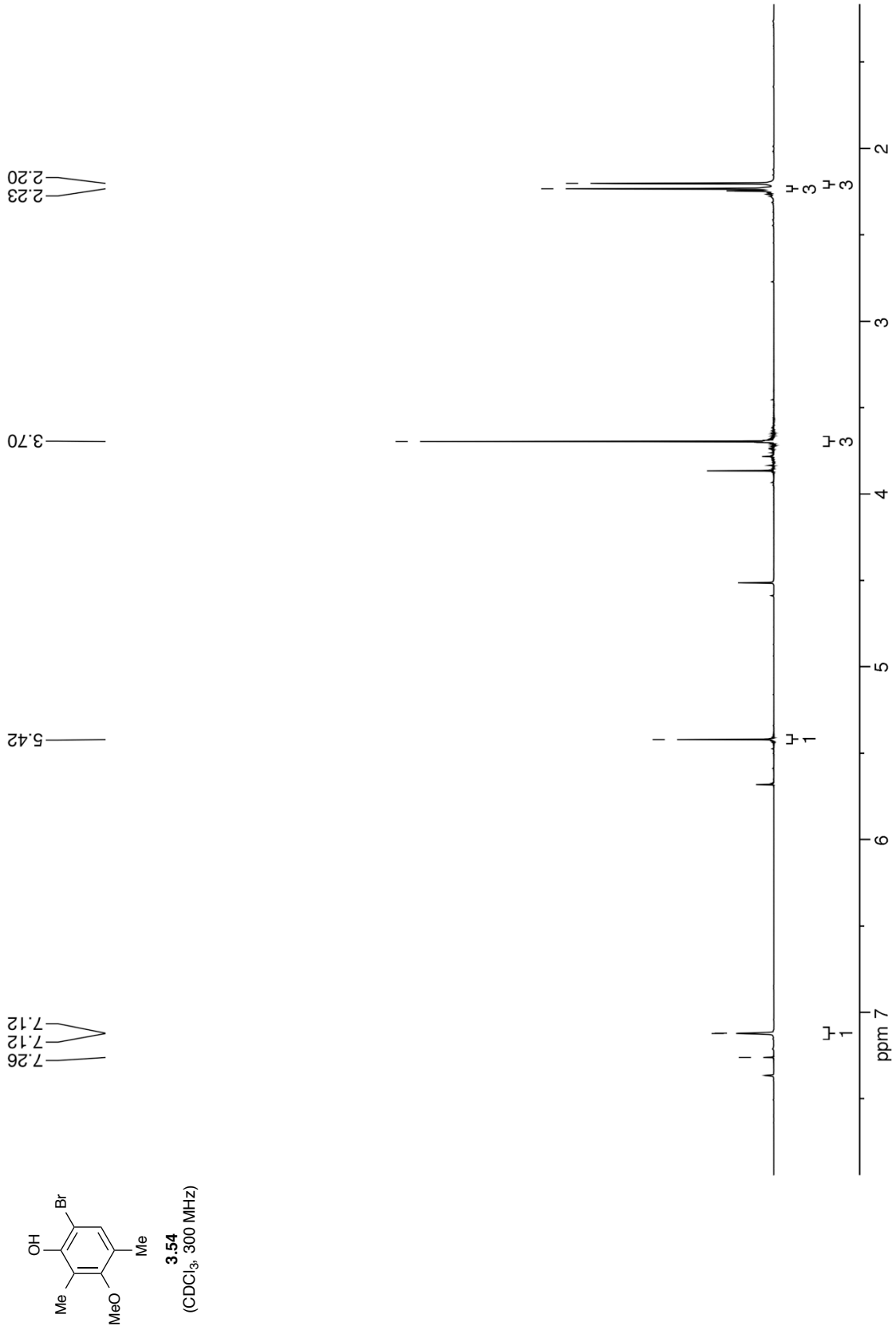

3.54
($CDCl_3$, 300 MHz)

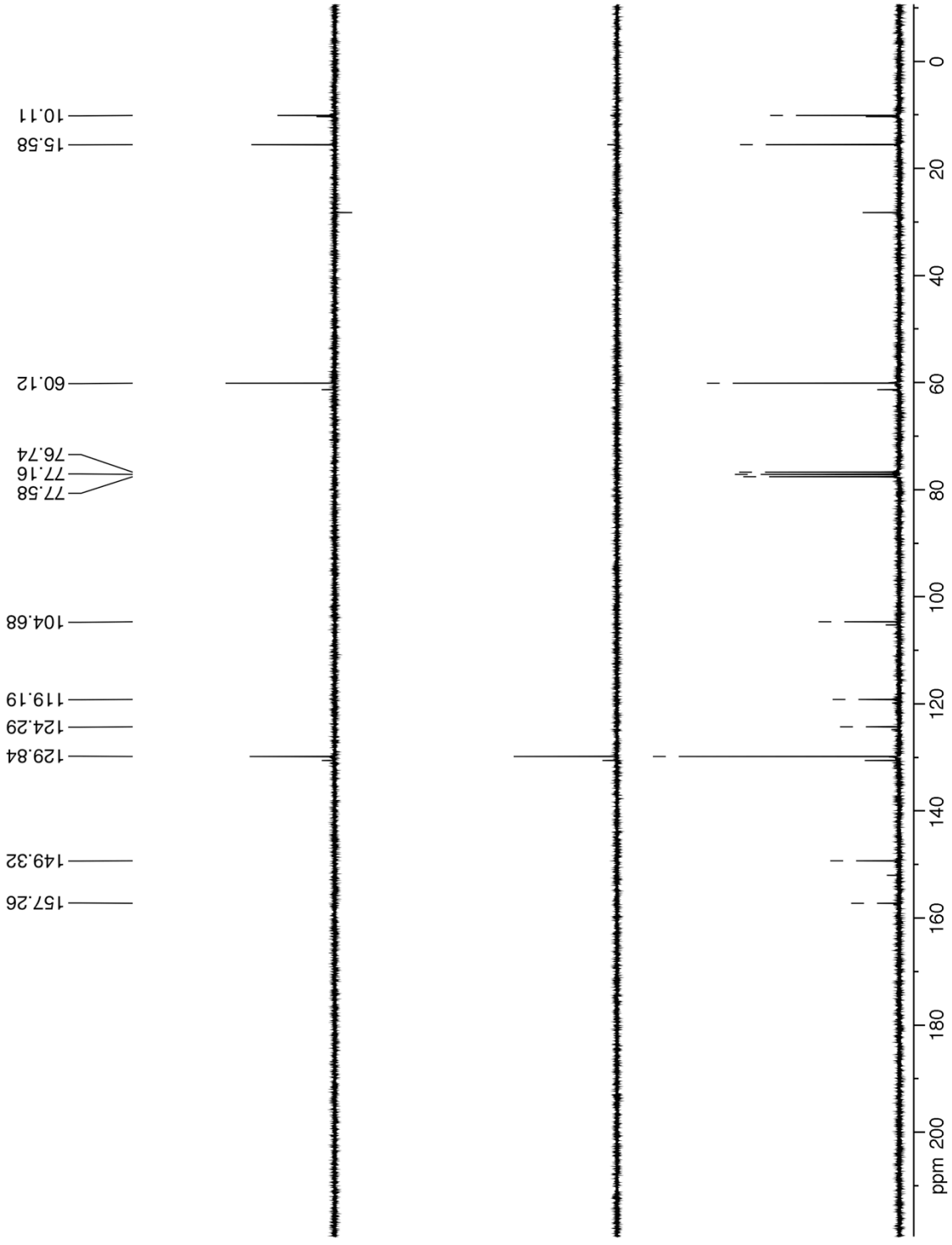

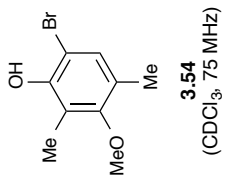

3.54
($CDCl_3$, 75 MHz)

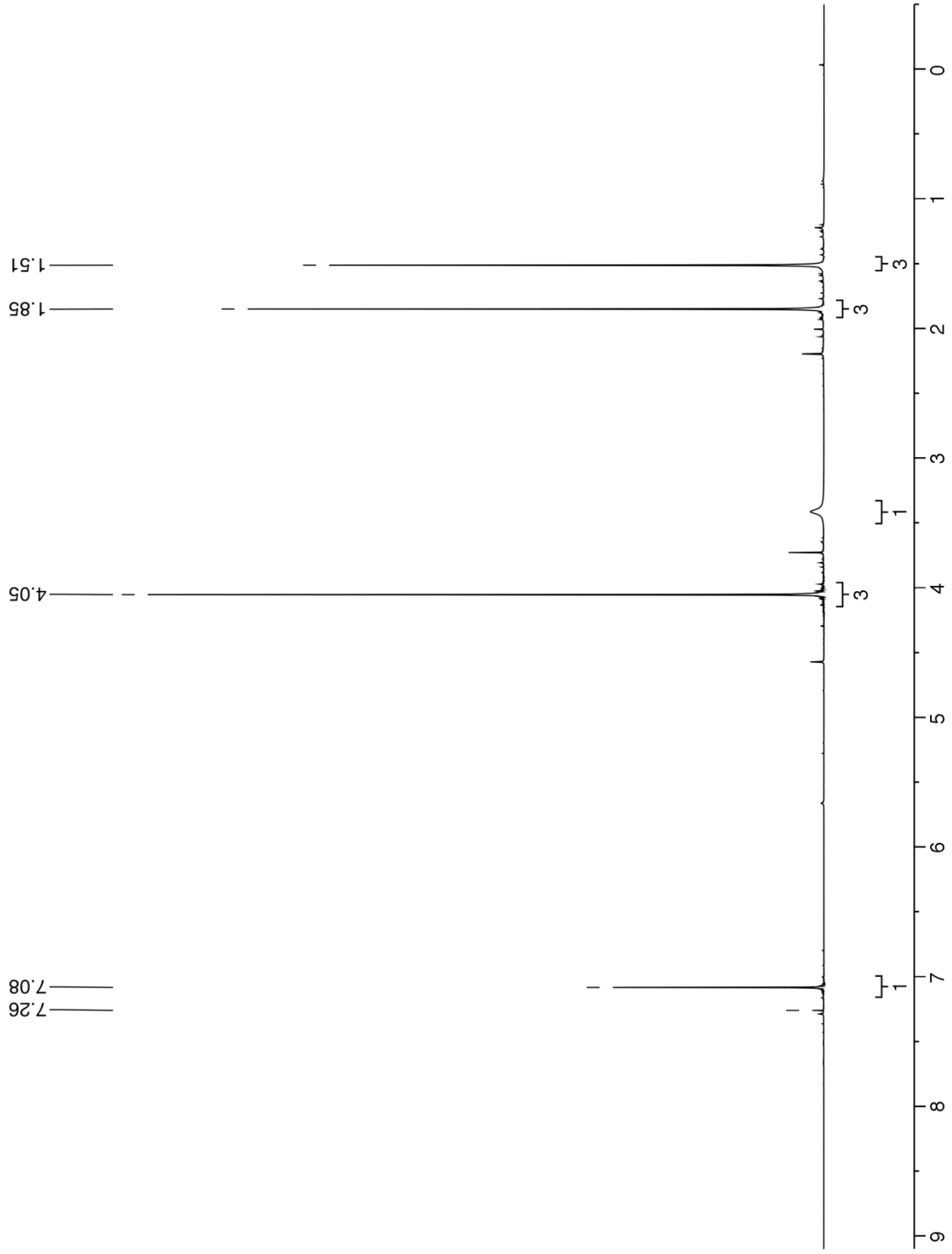

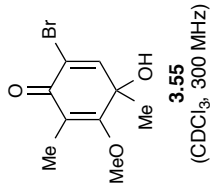

3.55
($CDCl_3$, 300 MHz)

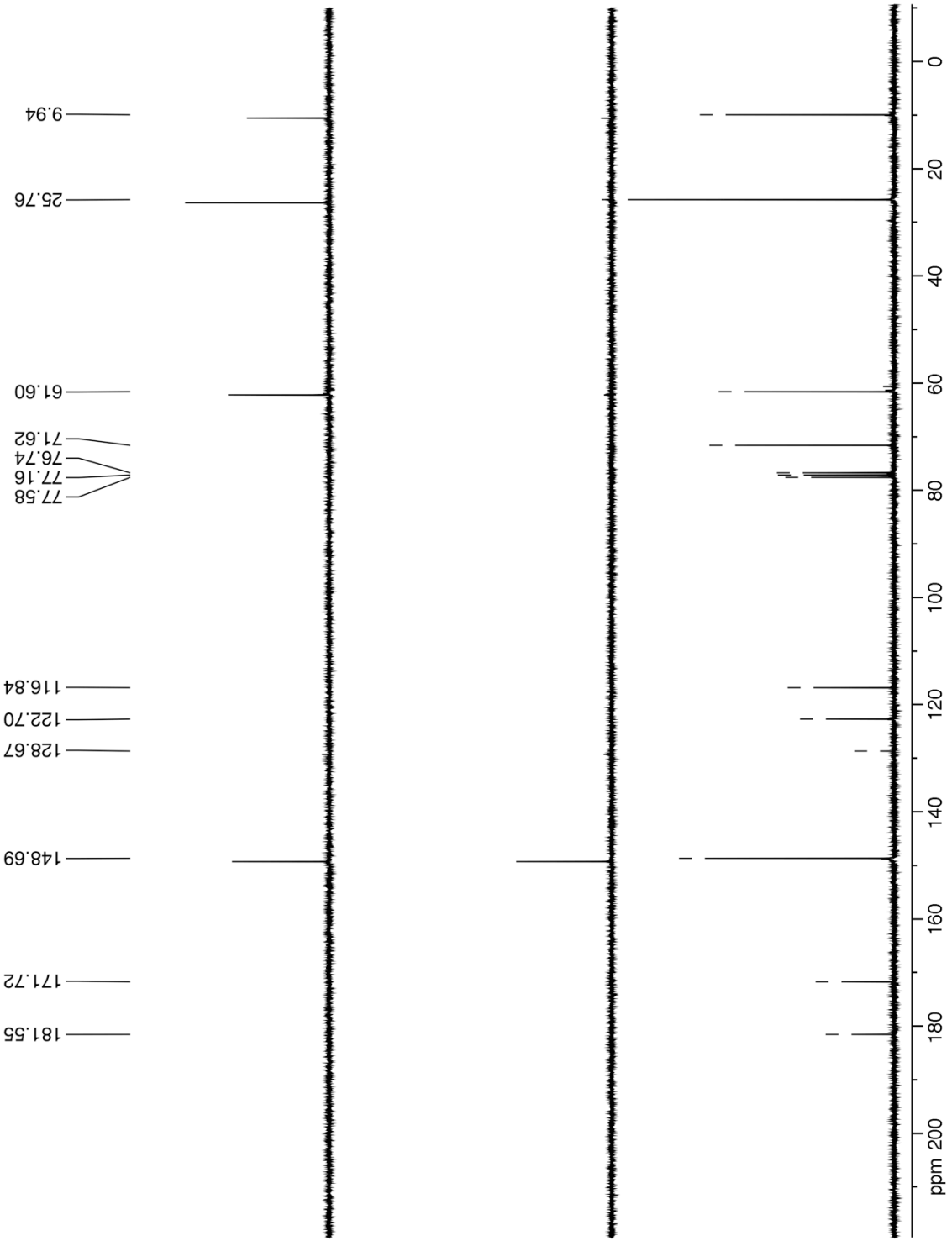

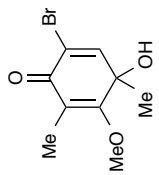

3.55
($CDCl_3$, 75 MHz)

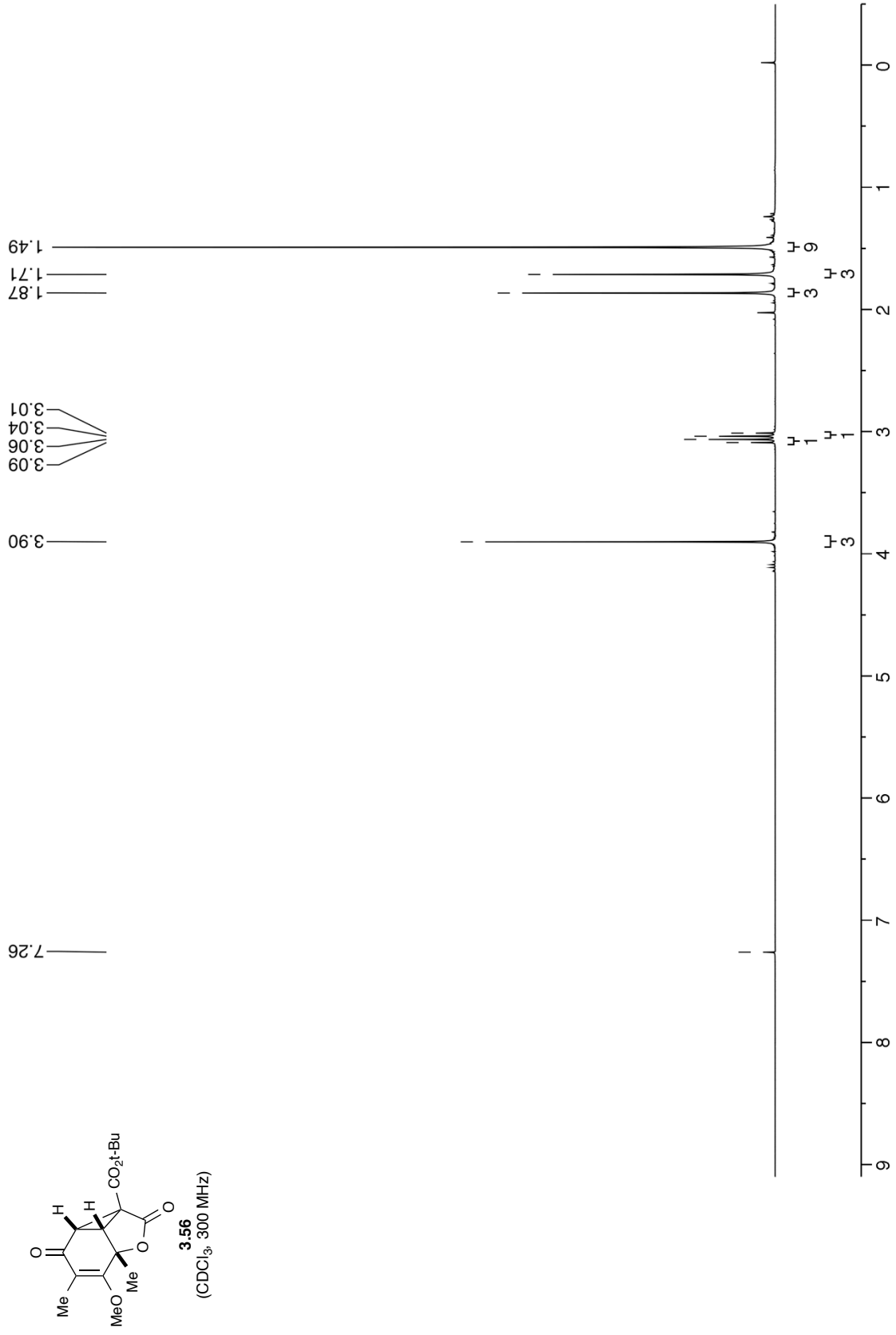

3.56
($CDCl_3$, 300 MHz)

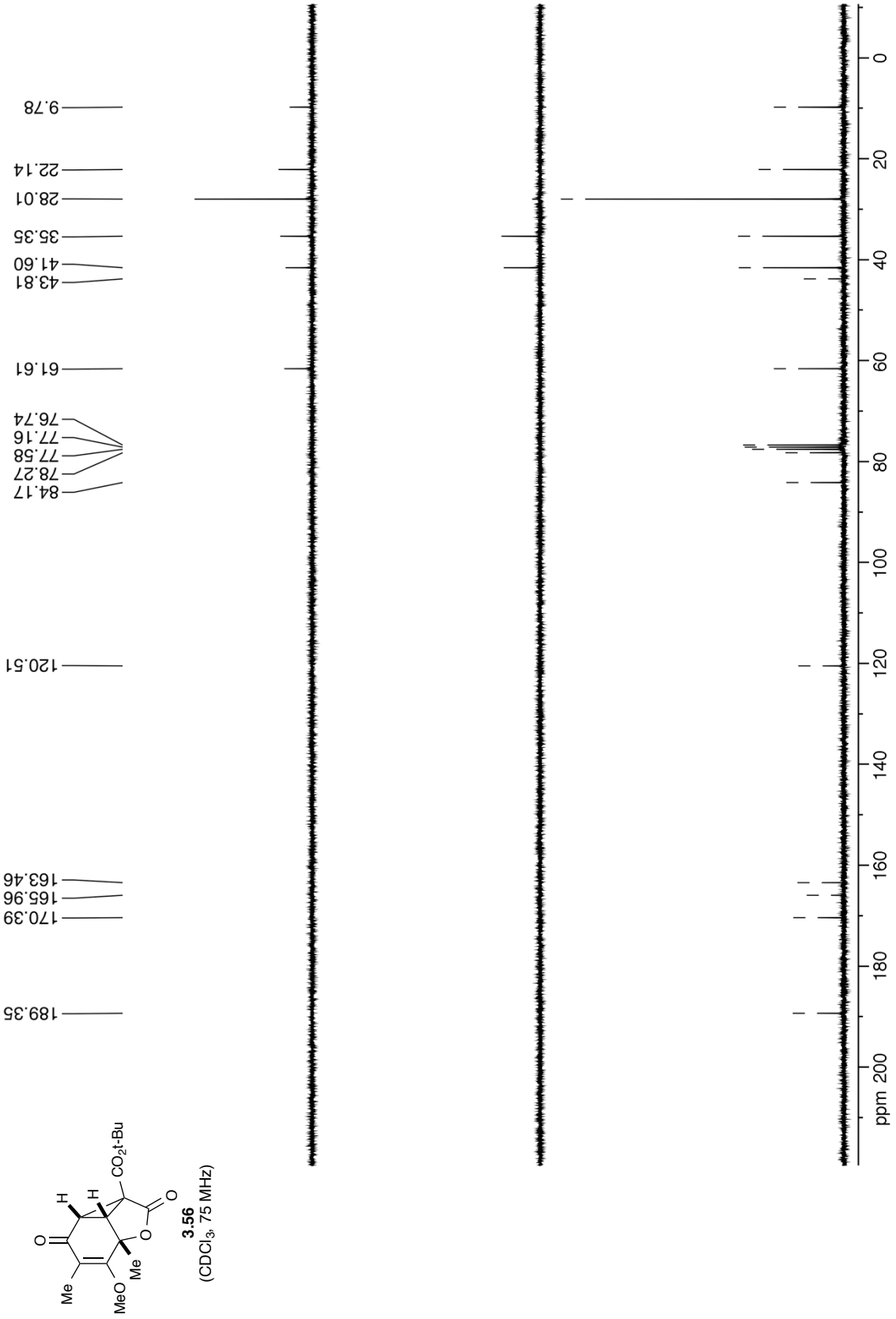

3.56
($CDCl_3$, 75 MHz)

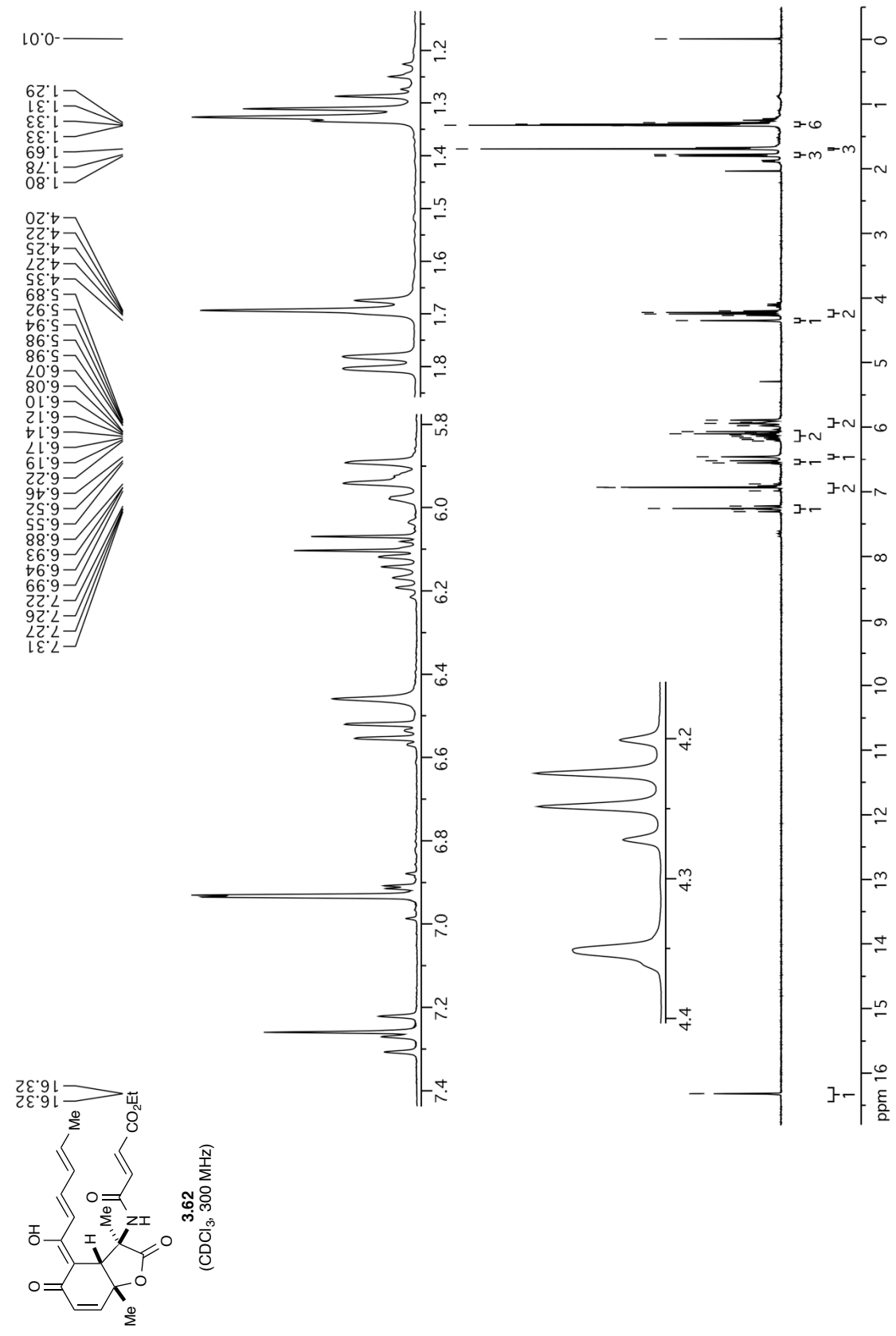
3.62
(CDCl3, 300 MHz)
Me
CO2Et
OH
O
Me
H
N
H
O
O
O
Me
16.32
16.32
7.31
7.27
7.26
7.22
6.99
6.94
6.93
6.88
6.55
6.52
6.46
6.22
6.19
6.17
6.14
6.12
6.10
6.08
6.07
5.98
5.98
5.94
5.92
5.89
4.35
4.27
4.25
4.22
4.20
1.80
1.78
1.69
1.33
1.33
1.31
1.29
-0.01
ppm

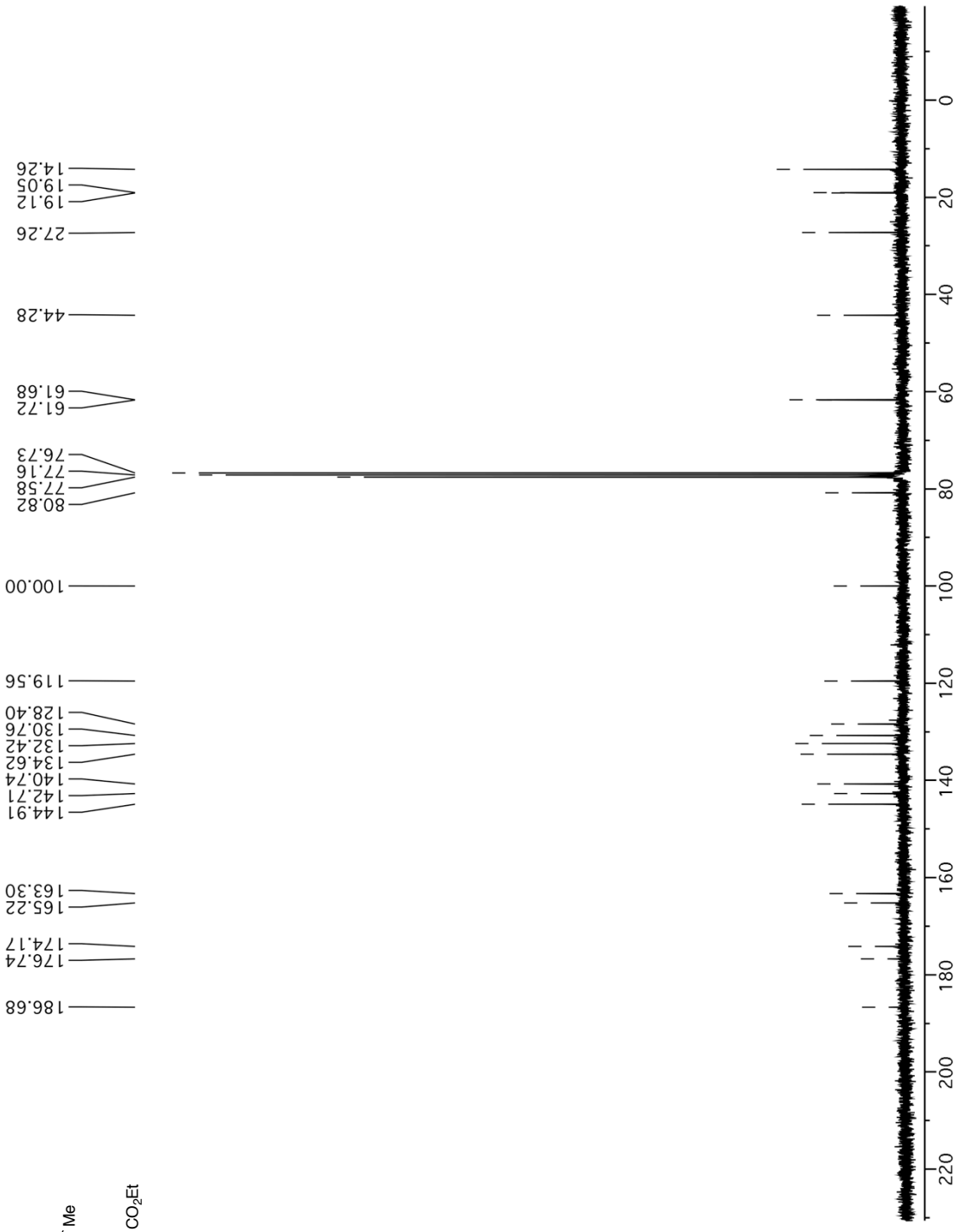

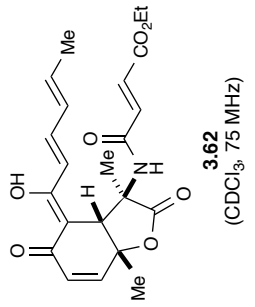

3.62
($CDCl_3$, 75 MHz)

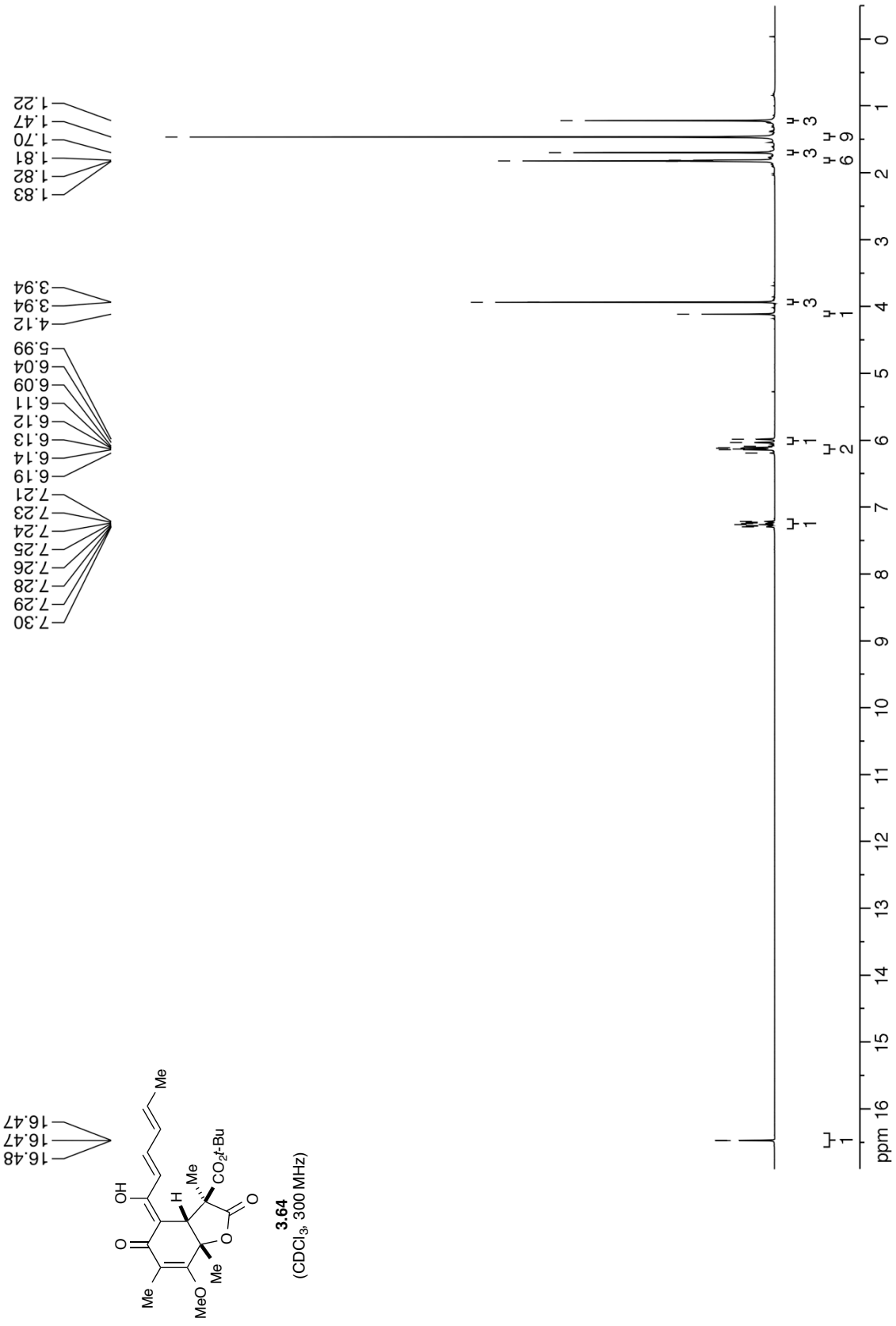

3.64
($CDCl_3$, 300 MHz)

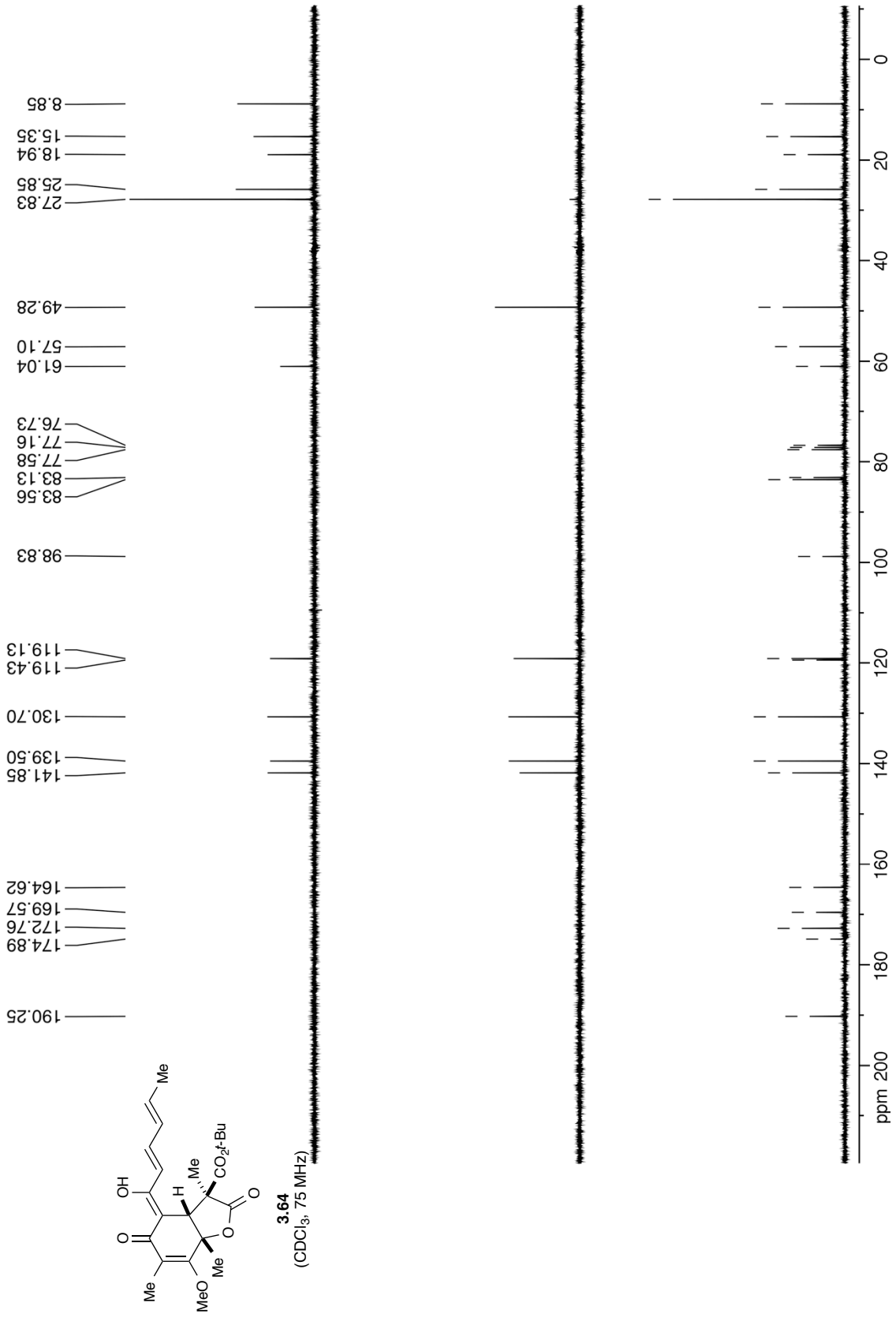
8.85
15.35
18.94
25.85
27.83
49.28
57.10
61.04
76.73
77.16
77.58
83.13
83.56
98.83
119.13
119.43
130.70
139.50
141.85
164.62
169.57
172.76
174.89
190.25
Me
OH
H
Me
CO2t-Bu
O
O
O
Me
MeO
Me
3.64
(CDCl3, 75 MHz)
ppm 200
180
160
140
120
100
80
60
40
20
0

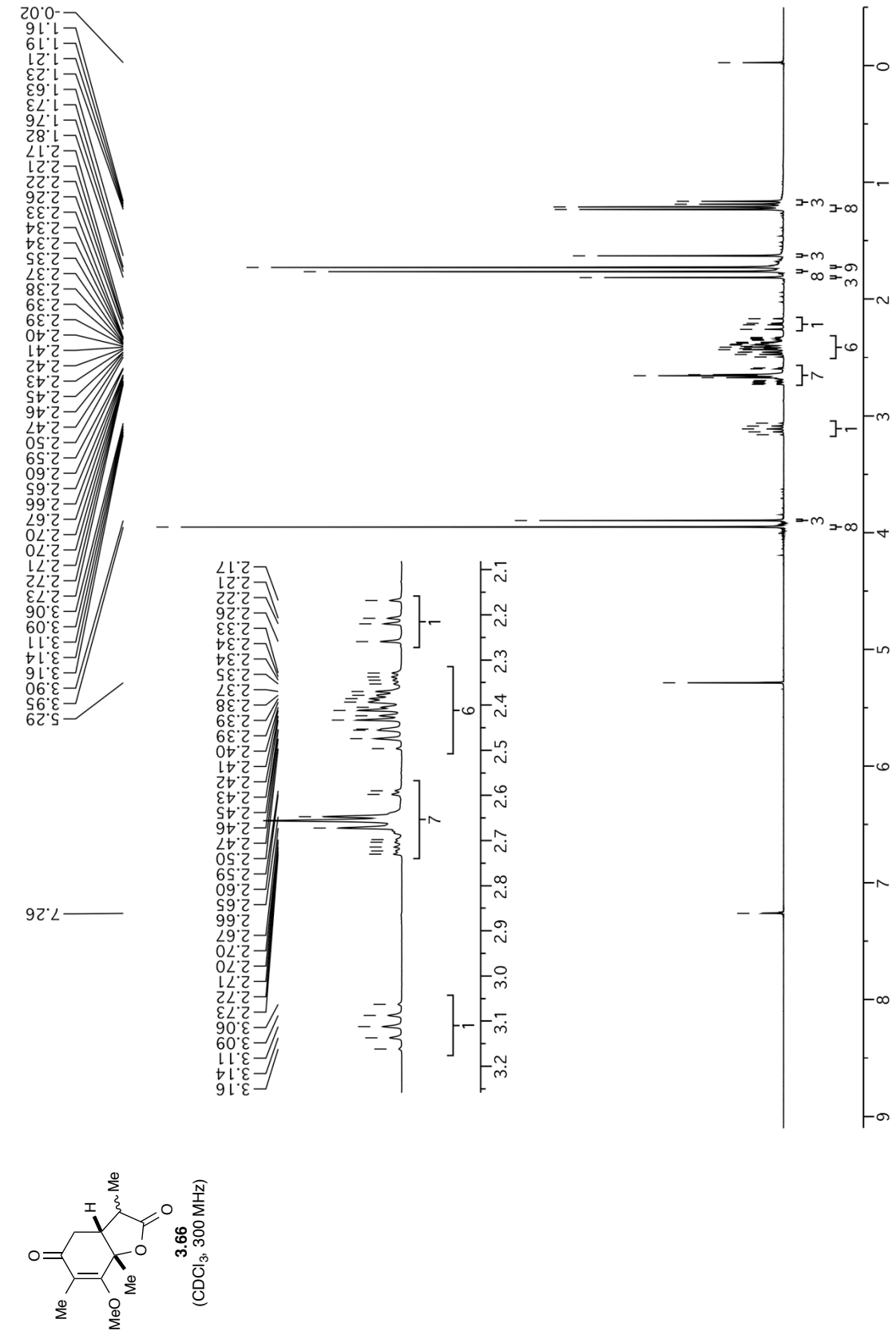
-0.02
1.16
1.19
1.21
1.23
1.63
1.73
1.76
1.82
2.17
2.21
2.22
2.26
2.33
2.34
2.34
2.35
2.37
2.38
2.39
2.39
2.40
2.41
2.42
2.43
2.45
2.46
2.47
2.50
2.59
2.60
2.65
2.66
2.67
2.70
2.70
2.71
2.72
2.73
3.06
3.09
3.11
3.14
3.16
3.90
3.95
5.29
7.26
3.66
(CDCl3, 300 MHz)
Me
MeO
Me
Me
H
O
O
O
O

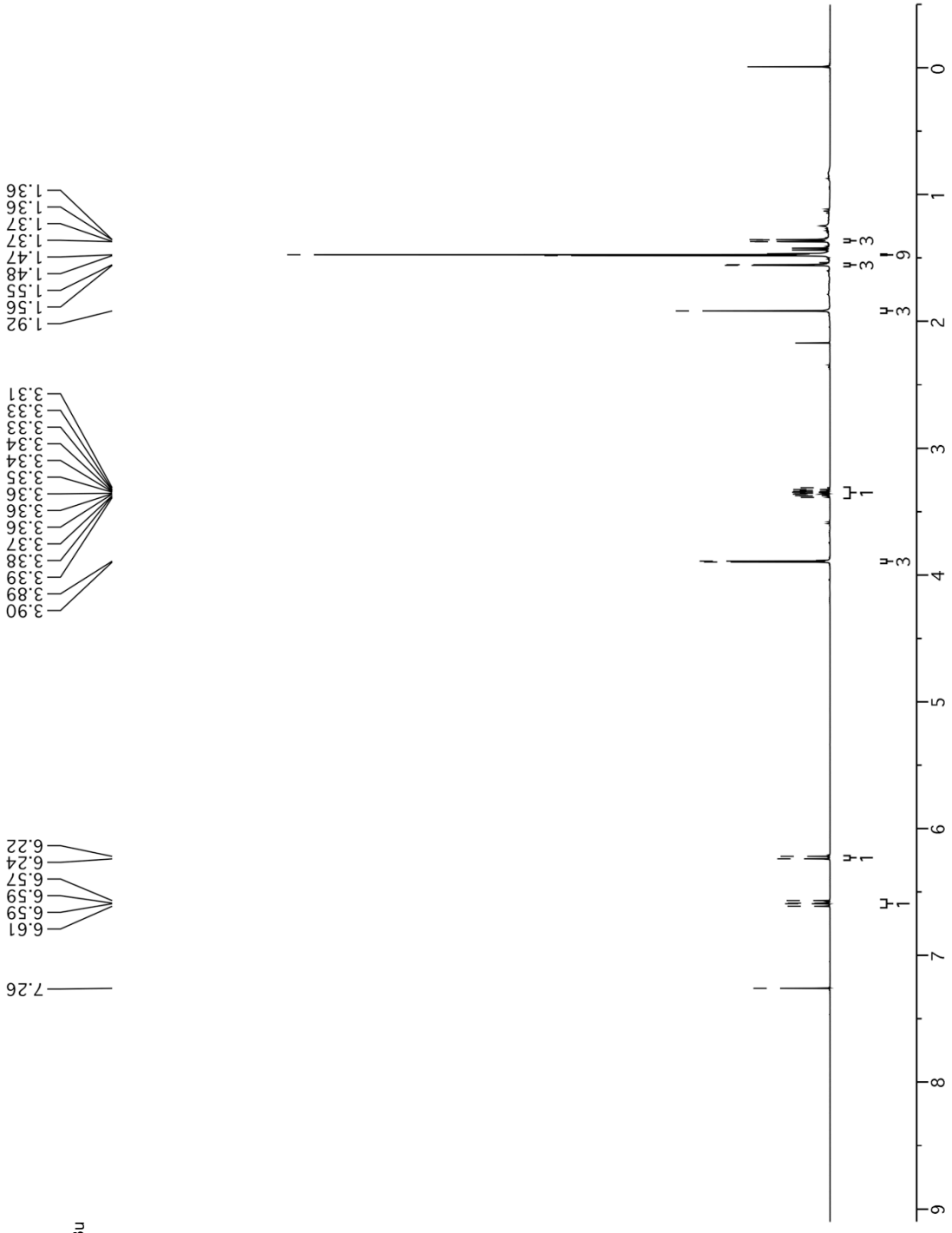

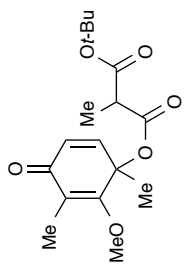

3.67
($CDCl_3$, 500 MHz)

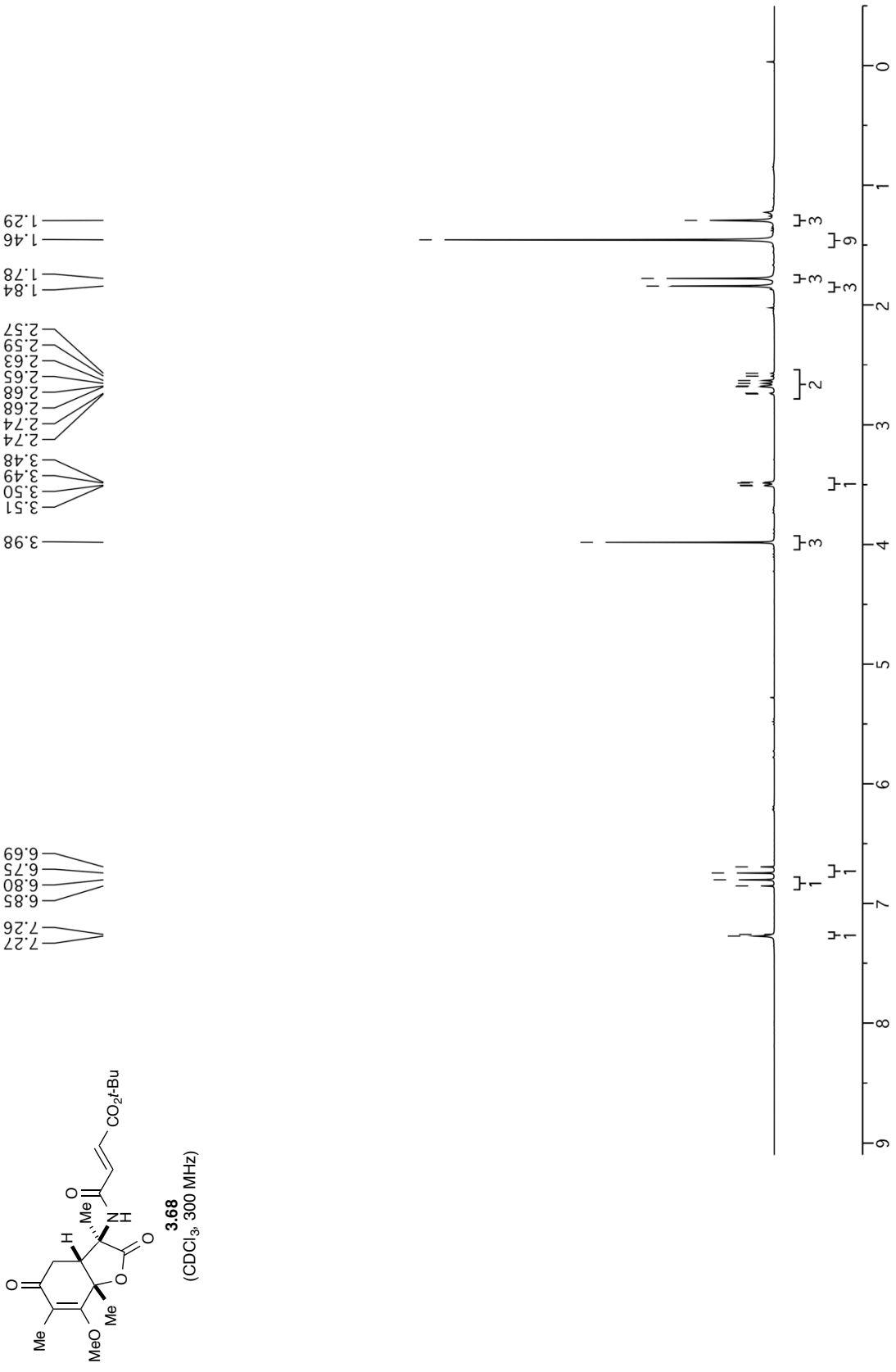
1.29
1.46
1.78
1.84
2.57
2.59
2.63
2.65
2.68
2.74
2.74
3.48
3.49
3.50
3.51
3.98
6.69
6.75
6.80
6.85
7.26
7.27
Me
MeO
Me
O
O
H
Me
O
N
H
O
O
CO2t-Bu
3.68
(CDCl3, 300 MHz)

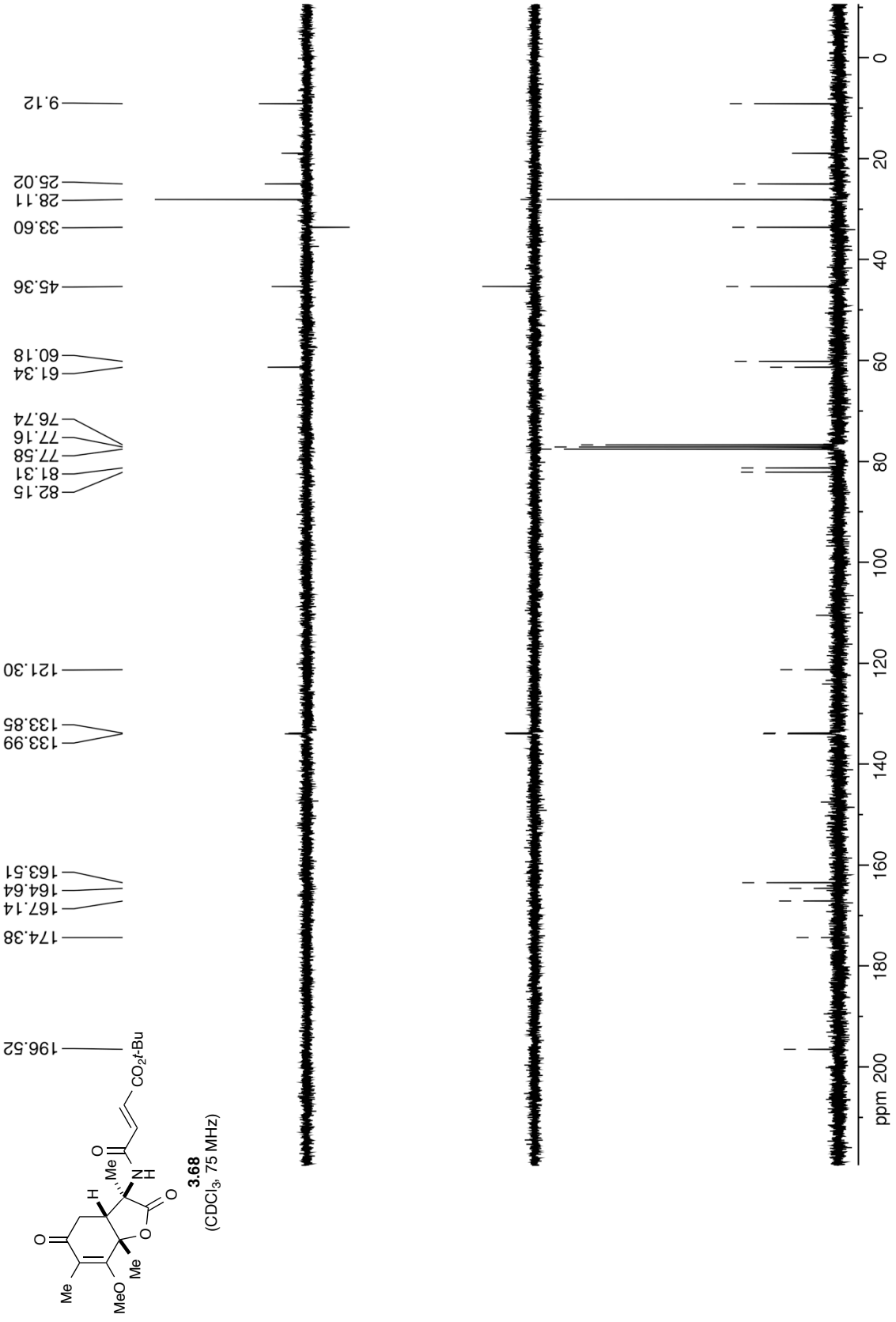
9.12
25.02
28.11
33.60
45.36
60.18
61.34
76.74
77.16
77.58
81.31
82.15
121.30
133.99
133.85
163.51
164.64
167.14
174.38
196.52
CO2t-Bu
Me
MeO
Me
H
Me
O
O
O
O
NH
3.68
(CDCl3, 75 MHz)
0
20
40
60
80
100
120
140
160
180
ppm 200

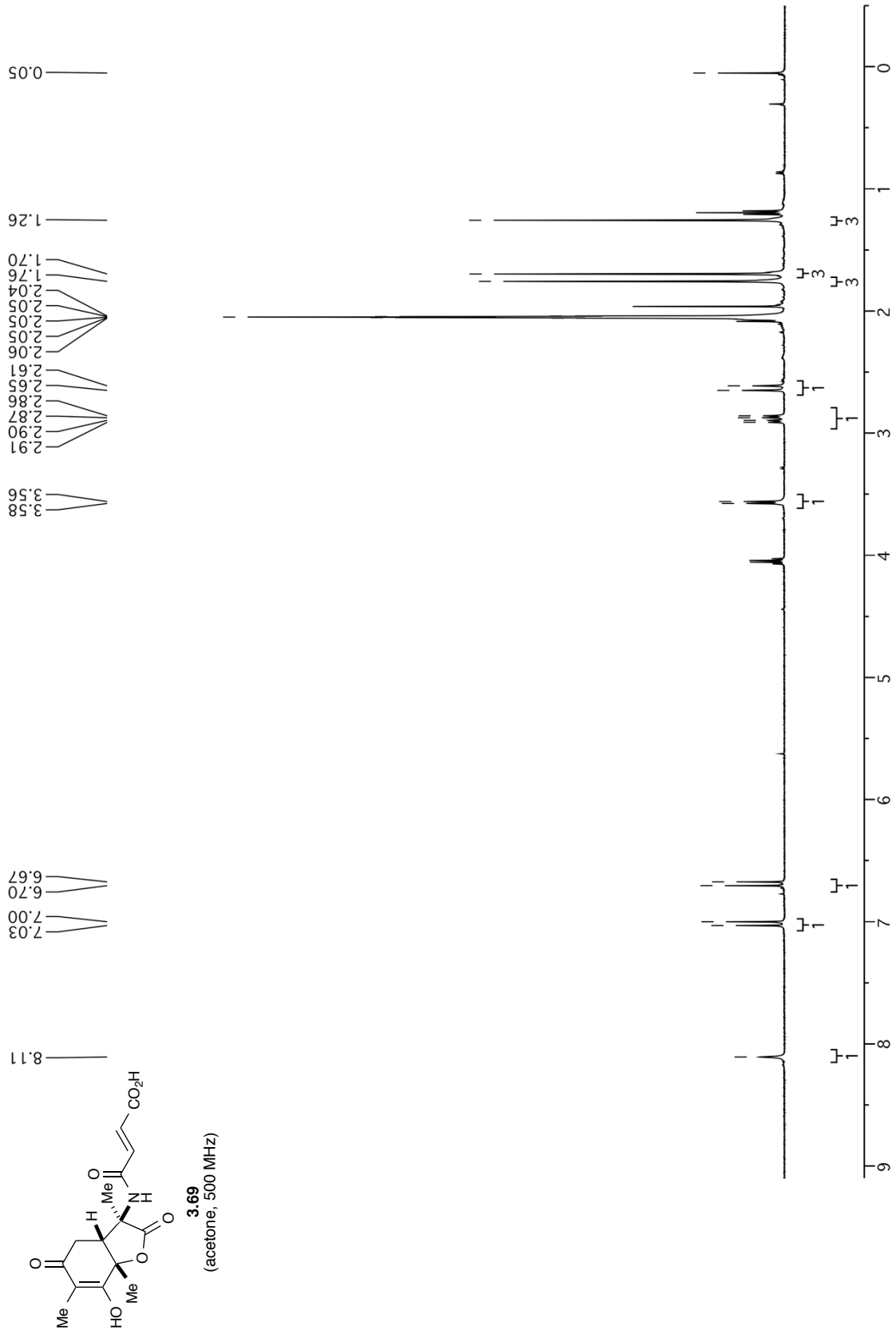
0.05
1.26
1.70
1.76
2.04
2.05
2.05
2.05
2.06
2.61
2.65
2.86
2.87
2.90
2.91
3.56
3.58
6.67
6.70
7.00
7.03
8.11
3.69
(acetone, 500 MHz)

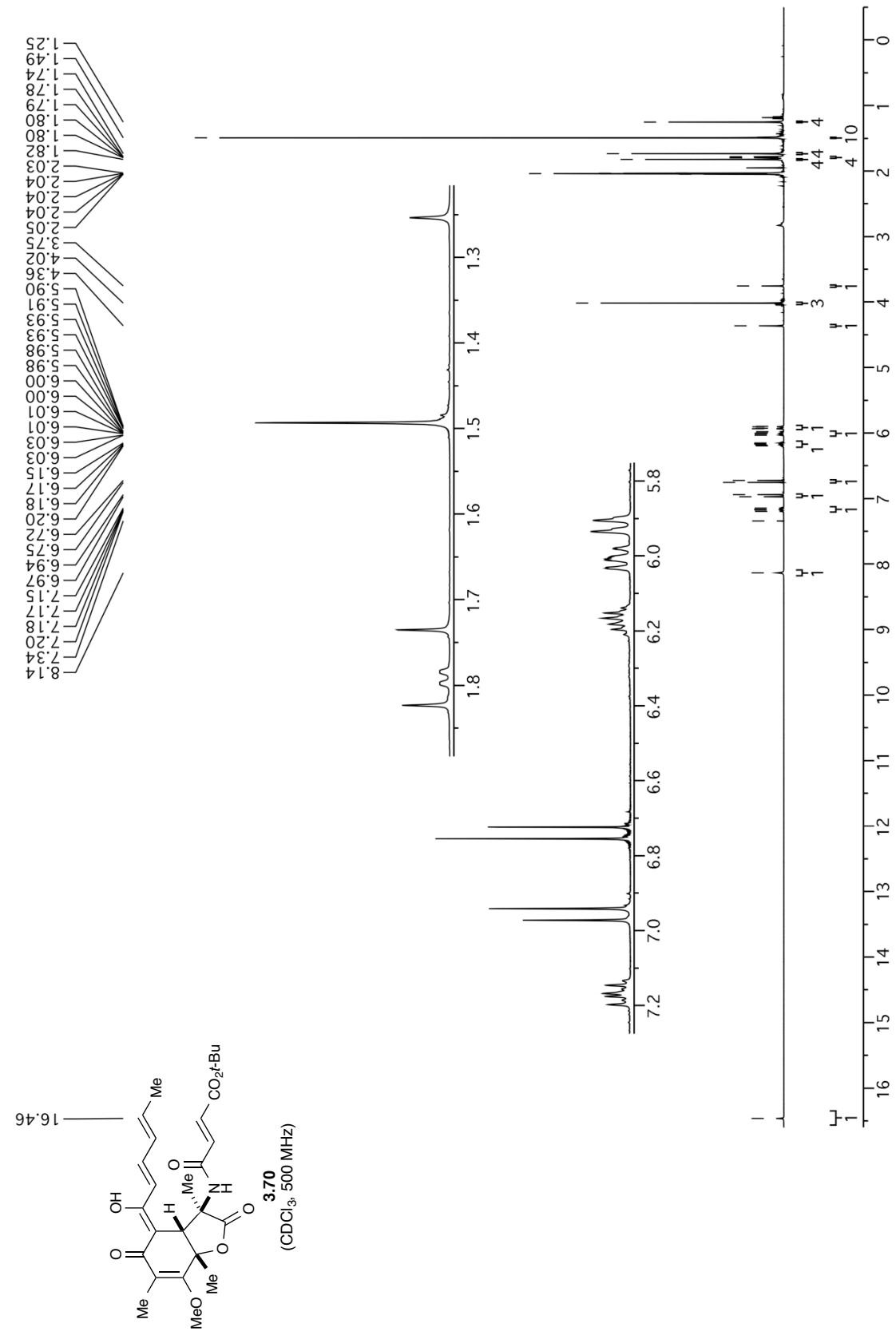
16.46
Me
CO2t-Bu
OH
O
Me
N
H
O
H
O
O
Me
Me
MeO
Me
3.70
(CDCl3, 500 MHz)
8.14
7.34
7.20
7.18
7.17
7.15
6.97
6.94
6.75
6.72
6.20
6.18
6.17
6.15
6.03
6.03
6.01
6.01
6.00
6.00
5.98
5.98
5.93
5.93
5.91
5.90
4.36
4.02
3.75
2.05
2.04
2.04
2.03
1.82
1.80
1.80
1.79
1.78
1.74
1.49
1.25

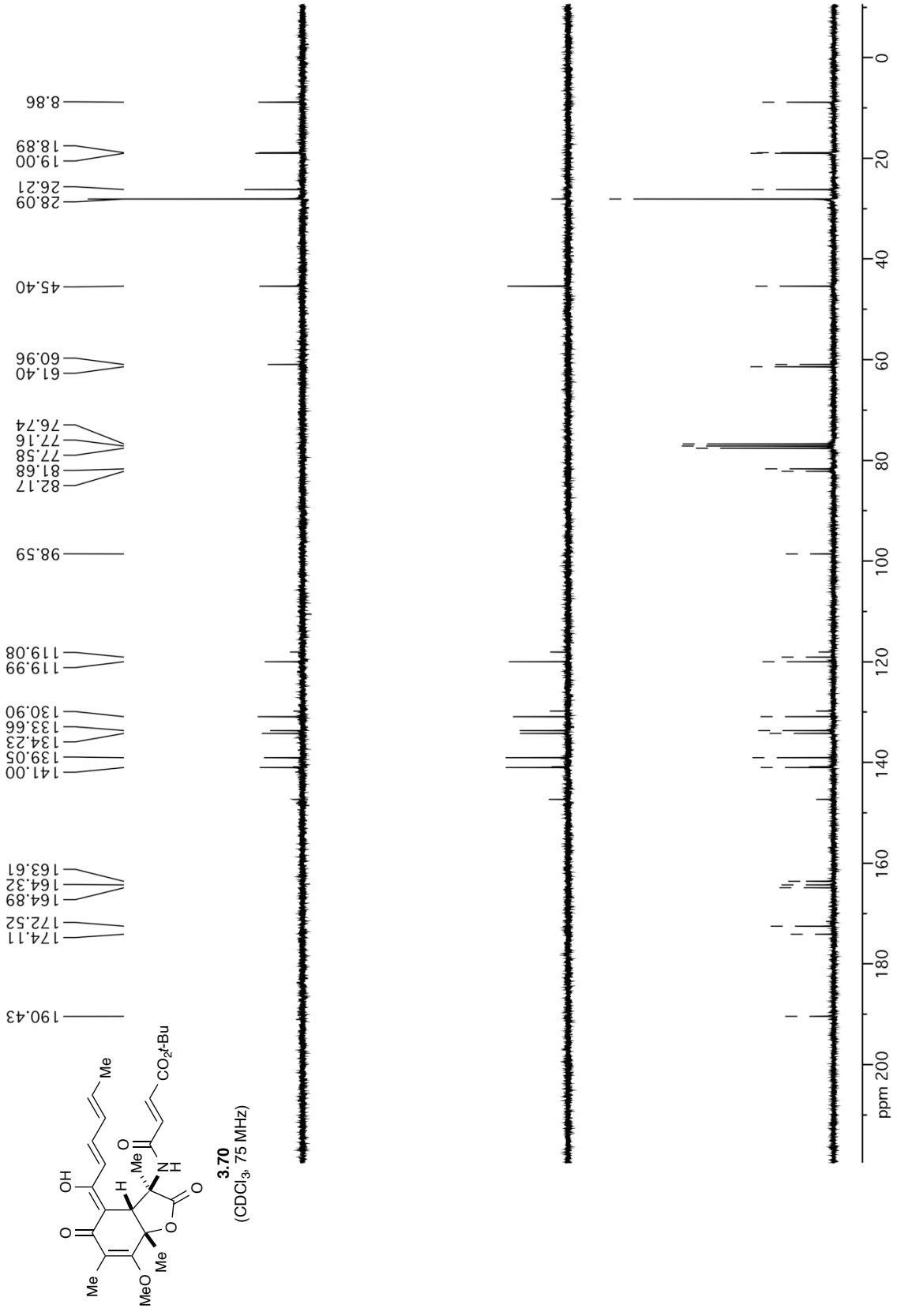
8.86
18.89
19.00
26.21
28.09
45.40
60.96
61.40
76.74
77.16
77.58
81.68
82.17
98.59
119.08
119.99
130.90
133.66
134.23
139.05
141.00
163.61
164.32
164.89
172.52
174.11
190.43
Me
CO2t-Bu
O
Me
N
H
OH
H
O
O
O
Me
Me
MeO
3.70
(CDCl3, 75 MHz)
ppm 200
180
160
140
120
100
80
60
40
20
0

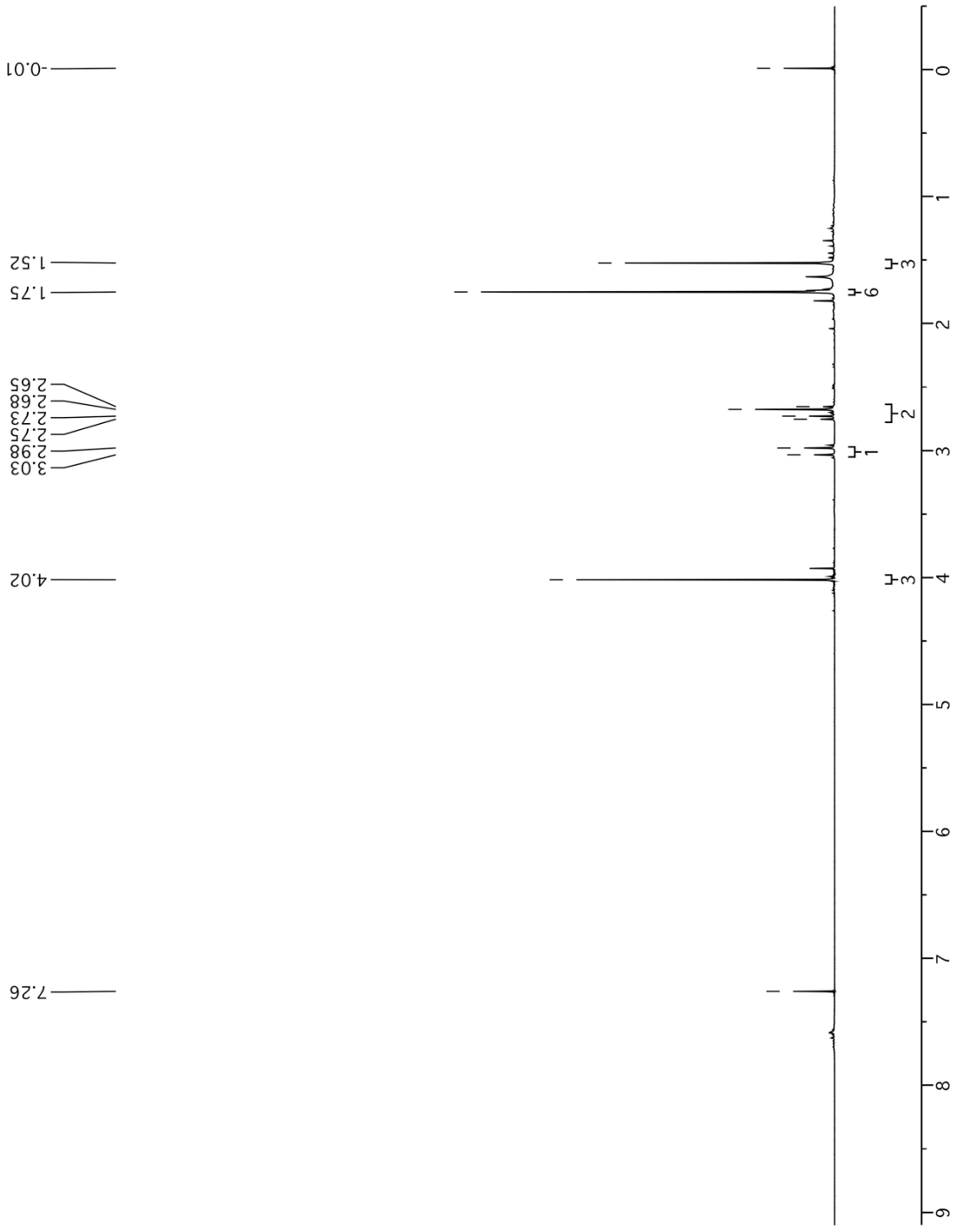

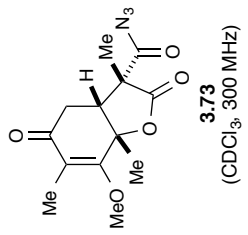

3.73
($CDCl_3$, 300 MHz)

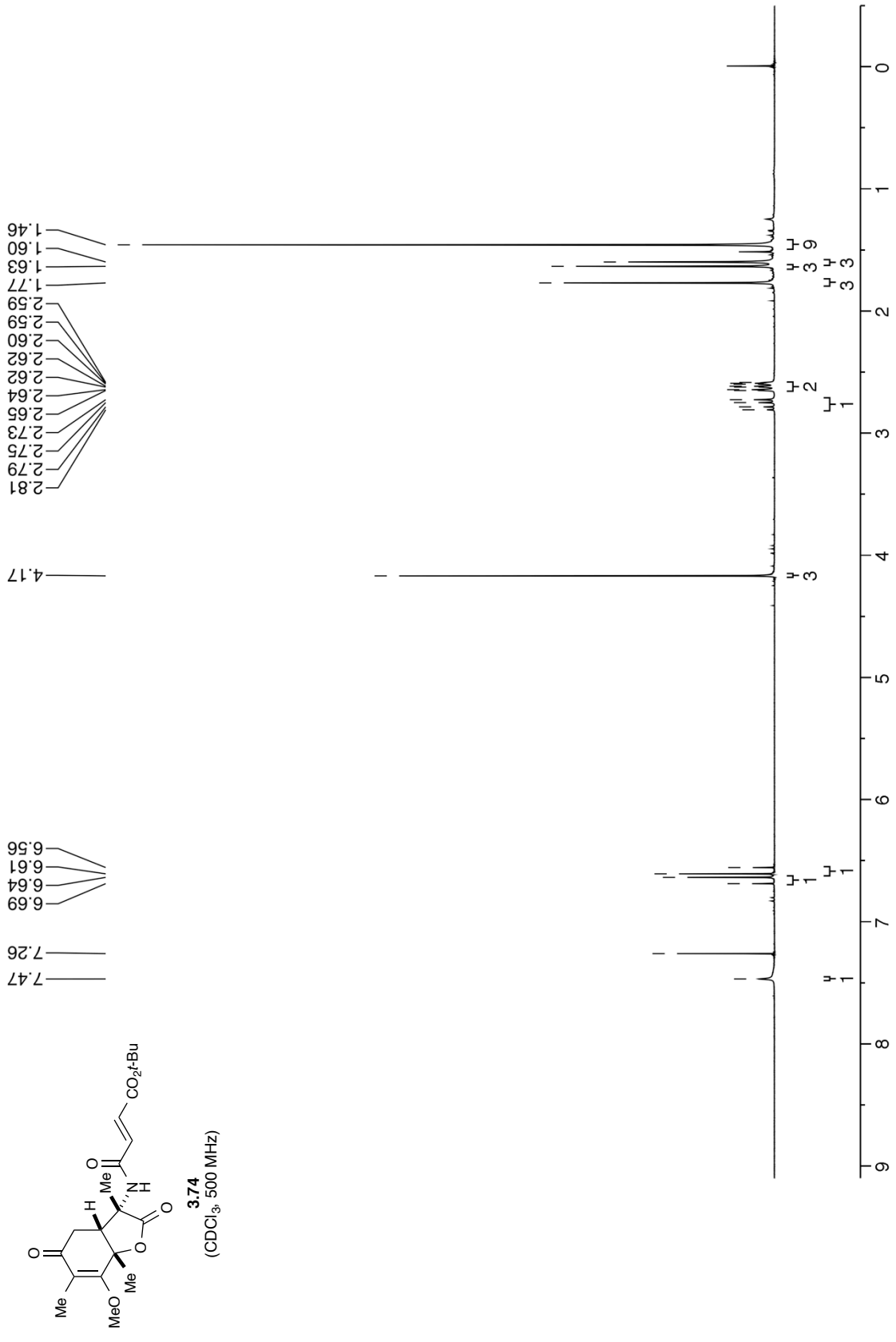
1.46
1.60
1.63
1.77
2.59
2.59
2.60
2.62
2.62
2.64
2.65
2.73
2.75
2.79
2.81
4.17
6.56
6.61
6.64
6.69
7.26
7.47
3.74
(CDCl3, 500 MHz)
Me
MeO
Me
Me
H
O
O
O
O
N
H
O
CO2t-Bu

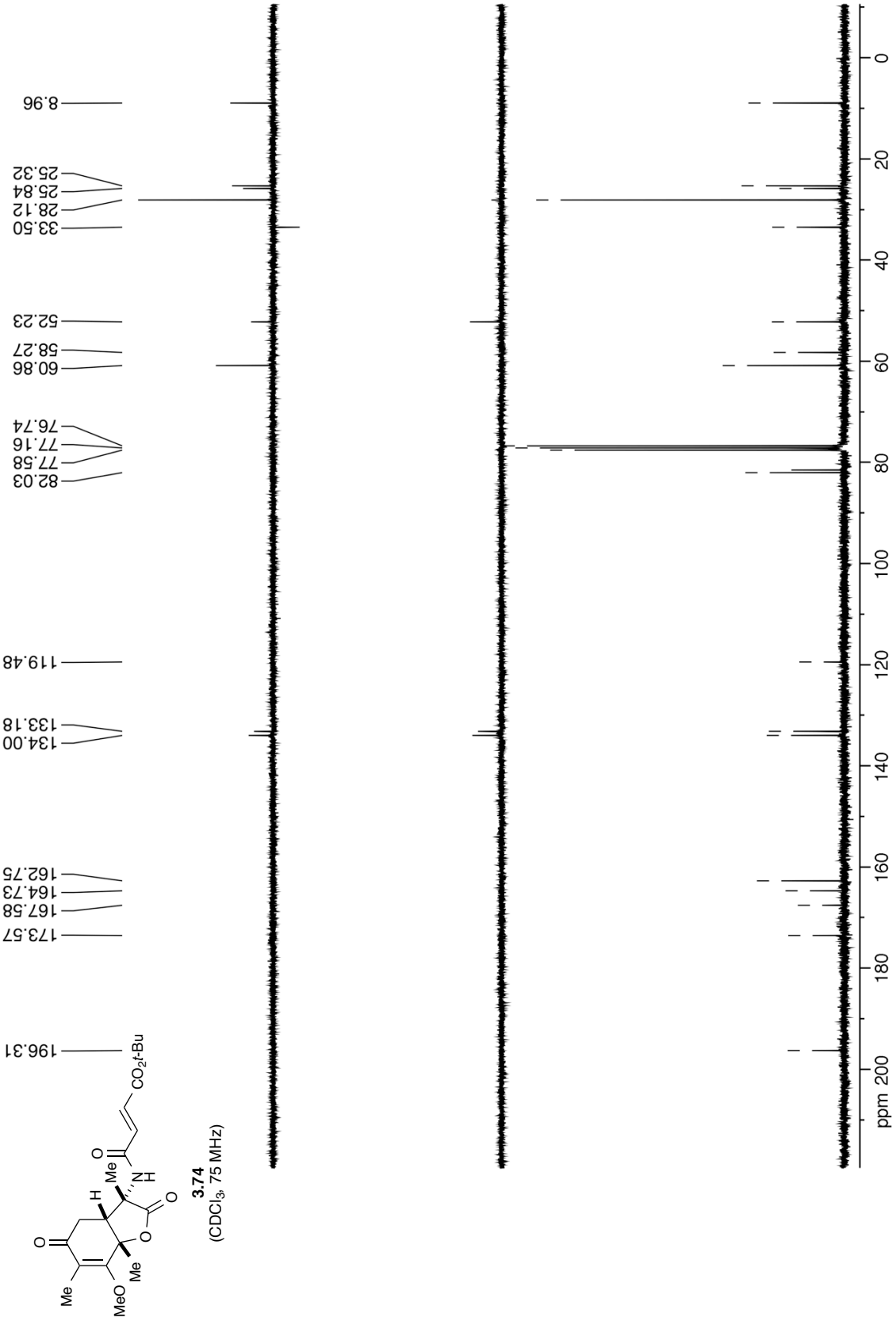

3.74
($CDCl_3$, 75 MHz)

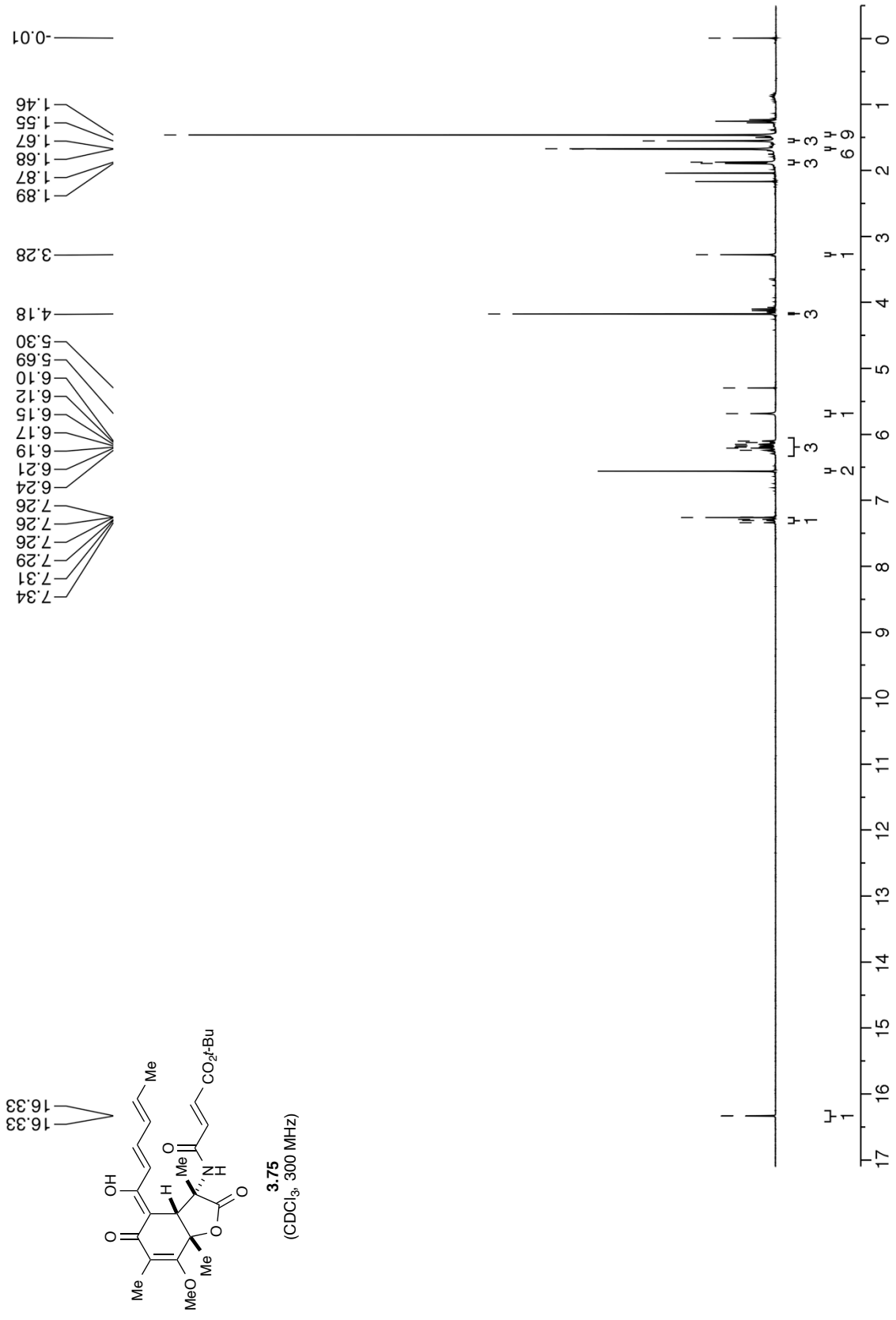
-0.01
1.46
1.55
1.67
1.68
1.87
1.89
3.28
4.18
5.30
5.69
6.10
6.12
6.15
6.17
6.19
6.21
6.24
7.26
7.26
7.26
7.29
7.31
7.34
16.33
16.33
Me
CO2t-Bu
OH
O
Me
H
N
H
O
O
O
Me
Me
MeO
3.75
(CDCl3, 300 MHz)

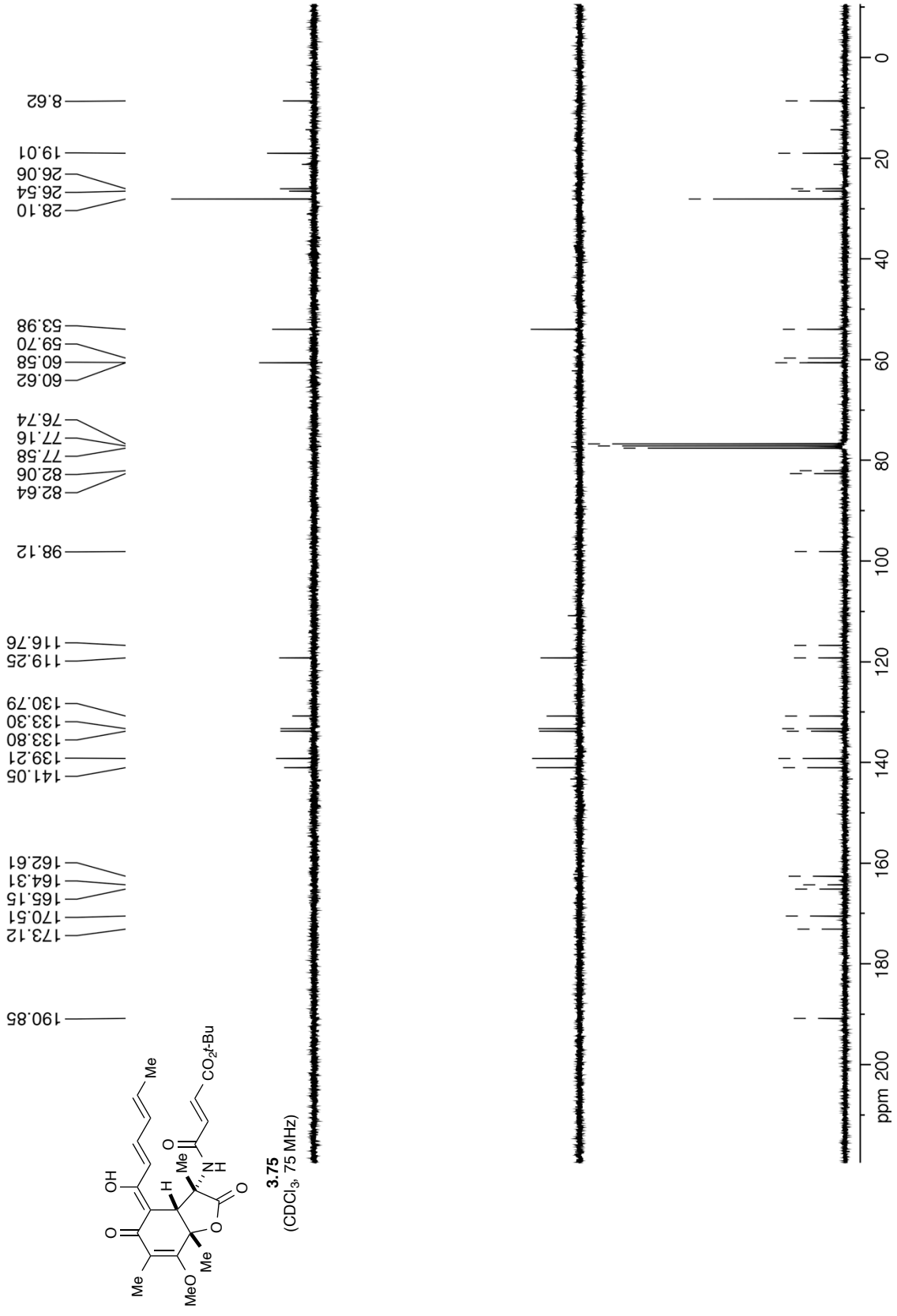
8.62
19.01
26.06
26.54
28.10
53.98
59.70
60.58
60.62
76.74
77.16
77.58
82.06
82.64
98.12
116.76
119.25
130.79
133.30
133.80
139.21
141.05
162.61
164.31
165.15
170.51
173.12
190.85
Me
CO2t-Bu
OH
O
H
Me
O
N
H
O
O
Me
MeO
Me
3.75
(CDCl3, 75 MHz)
0
20
40
60
80
100
120
140
160
180
ppm 200

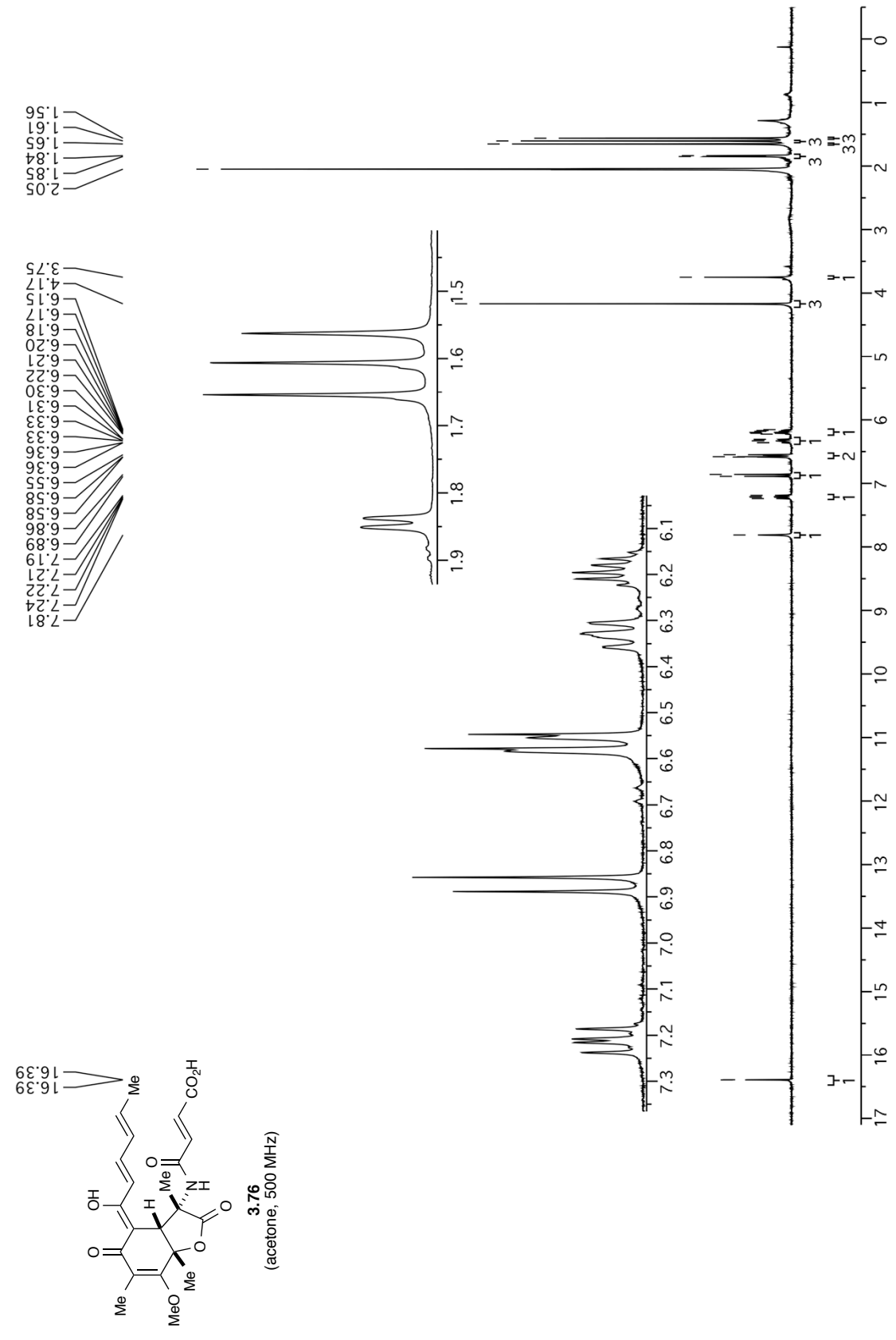
16.39
16.39
Me
OH
O
Me
H
N
H
O
CO2H
O
O
Me
MeO
Me
3.76
(acetone, 500 MHz)
7.81
7.24
7.22
7.21
7.19
6.89
6.86
6.58
6.58
6.56
6.36
6.36
6.33
6.33
6.31
6.30
6.22
6.21
6.20
6.18
6.17
6.15
4.17
3.75
2.05
1.85
1.84
1.65
1.61
1.56

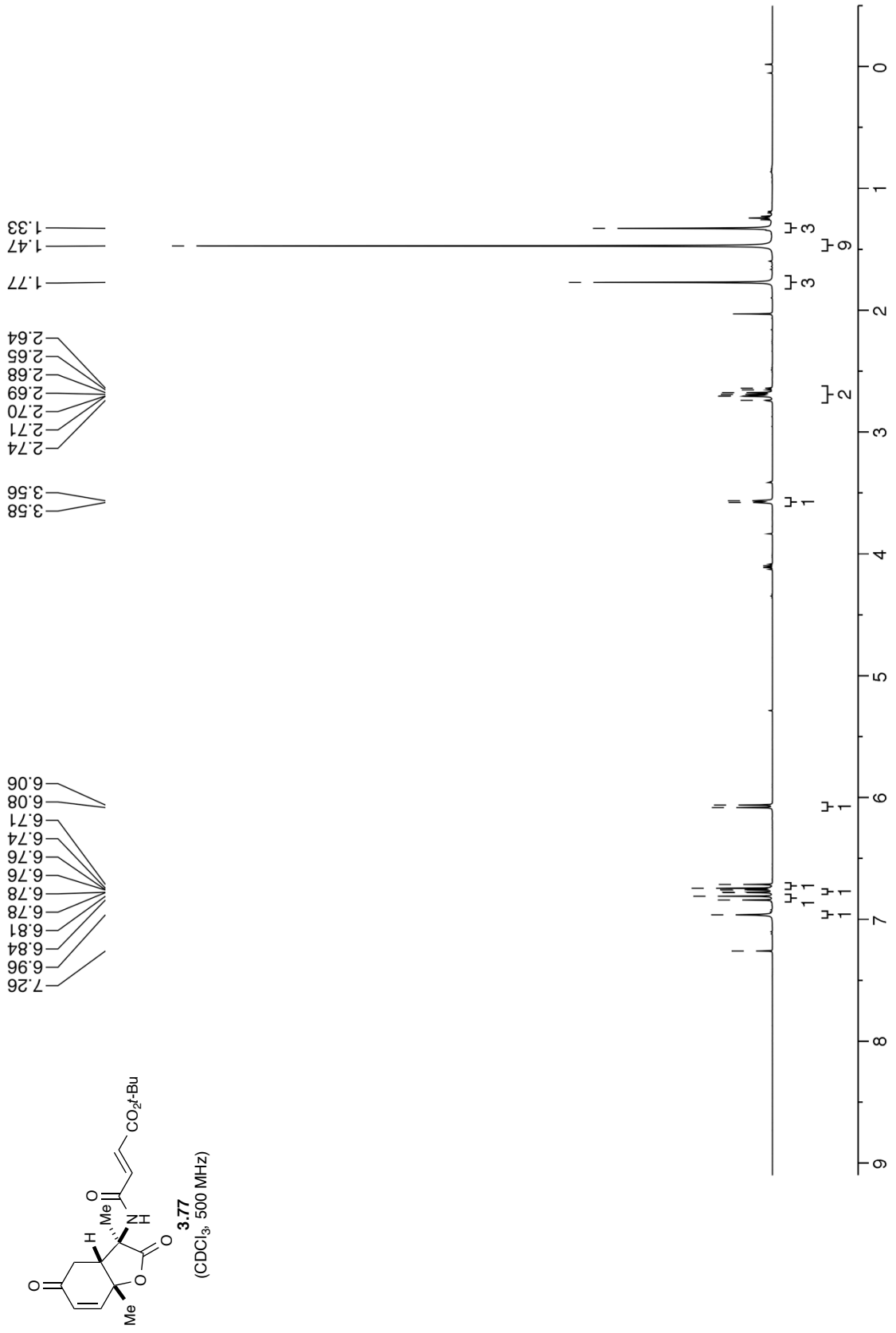

3.77
($CDCl_3$, 500 MHz)

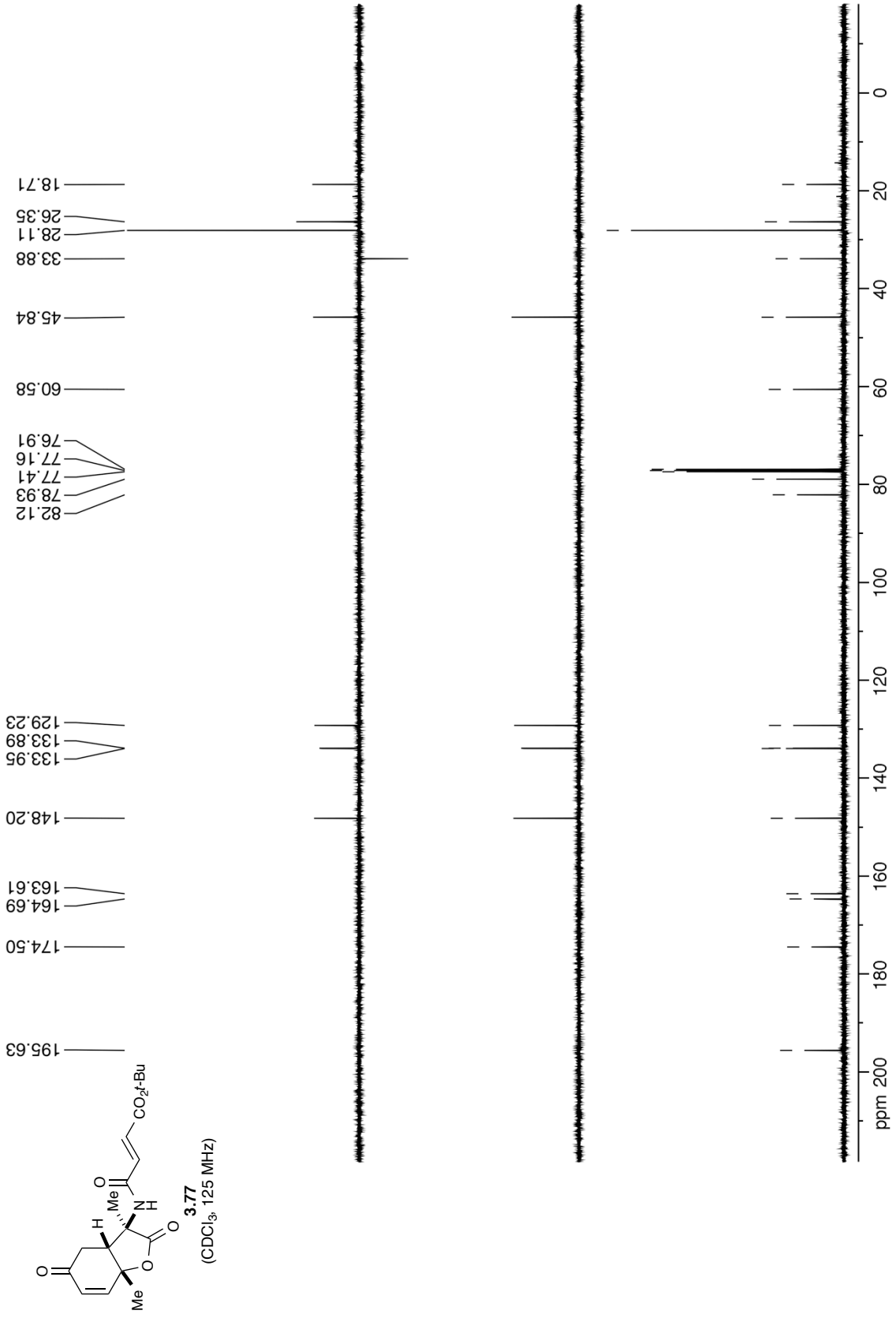
18.71
26.35
28.11
33.88
45.84
60.58
76.91
77.16
77.41
78.93
82.12
129.23
133.89
133.95
148.20
163.61
164.69
174.50
195.63
ppm 200
180
160
140
120
100
80
60
40
20
0
CO2t-Bu
Me
H
N
H
O
O
O
O
Me
3.77
(CDCl3, 125 MHz)

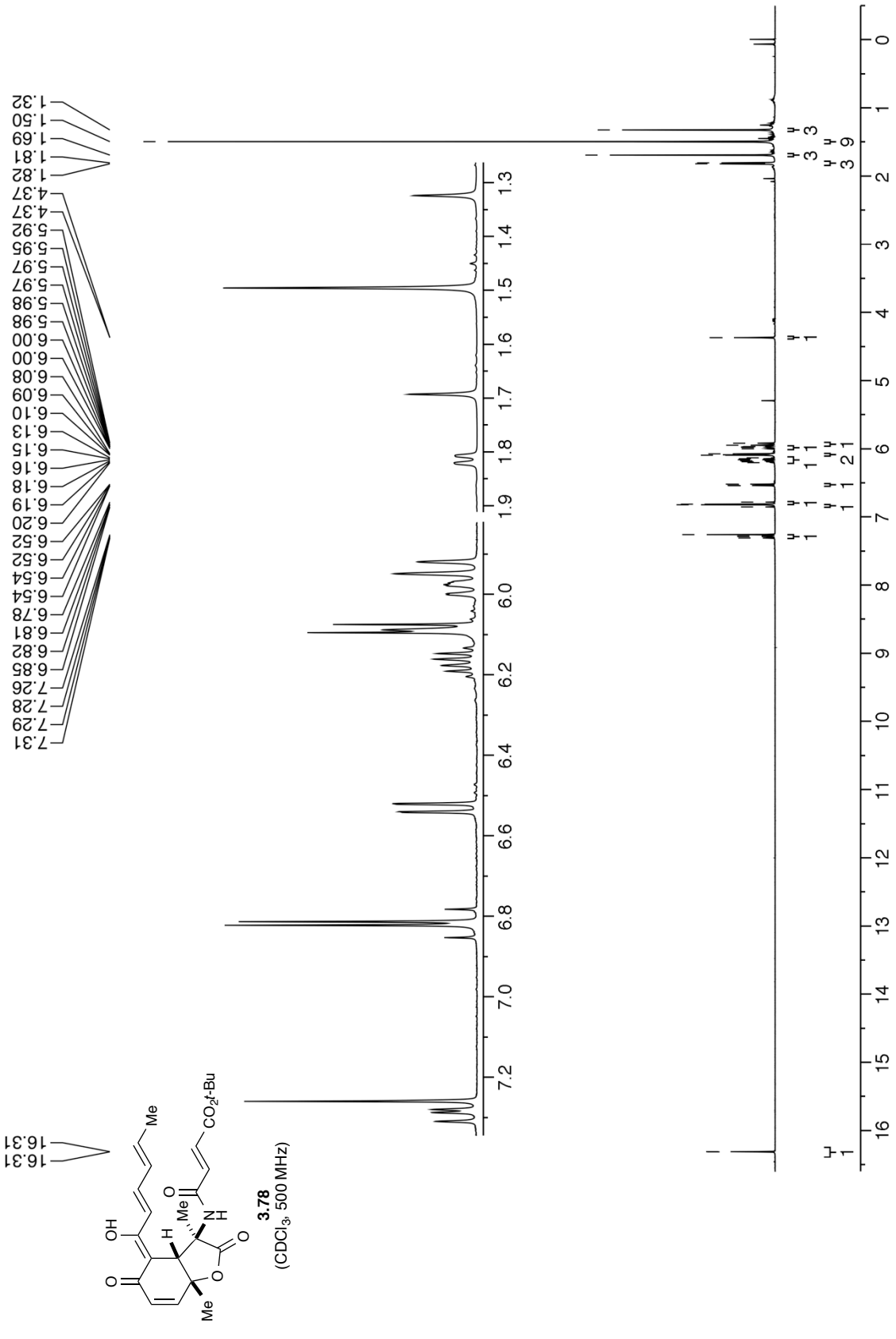
16.31
16.31
Me
CO2t-Bu
OH
O
Me
H
N
H
O
O
O
Me
3.78
(CDCl3, 500 MHz)
1.32
1.50
1.69
1.81
1.82
4.37
4.37
5.92
5.95
5.97
5.97
5.98
5.98
6.00
6.00
6.08
6.09
6.10
6.13
6.15
6.16
6.18
6.19
6.20
6.52
6.52
6.54
6.54
6.78
6.81
6.82
6.85
7.26
7.28
7.29
7.31

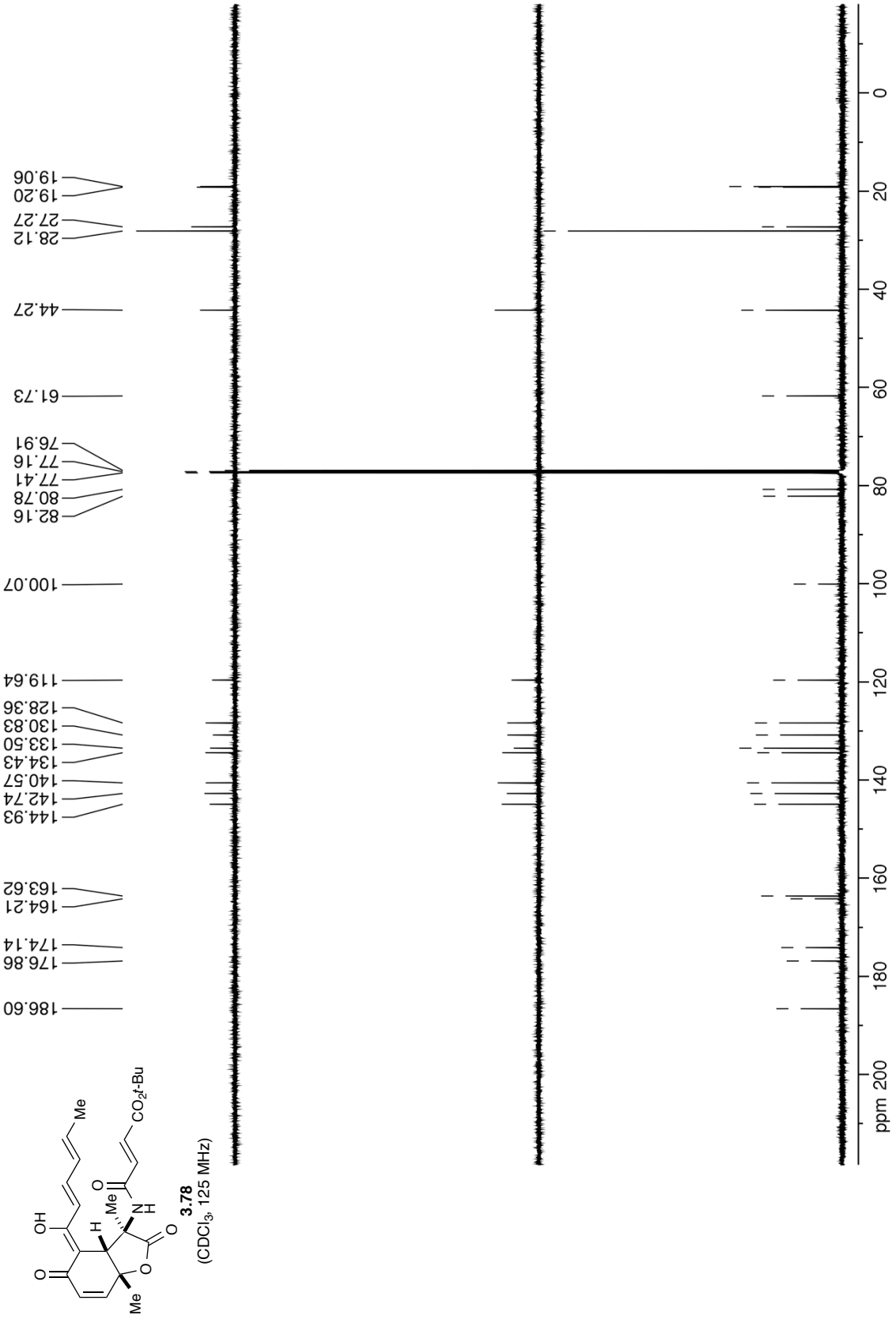
19.06
19.20
27.27
28.12
44.27
61.73
76.91
77.16
77.41
80.78
82.16
100.07
119.64
128.36
130.83
133.50
134.43
140.57
142.74
144.93
163.62
164.21
174.14
176.86
186.60
ppm 200
180
160
140
120
100
80
60
40
20
0
Me
CO2t-Bu
OH
O
H
Me
O
N
H
O
O
O
Me
3.78
(CDCl3, 125 MHz)

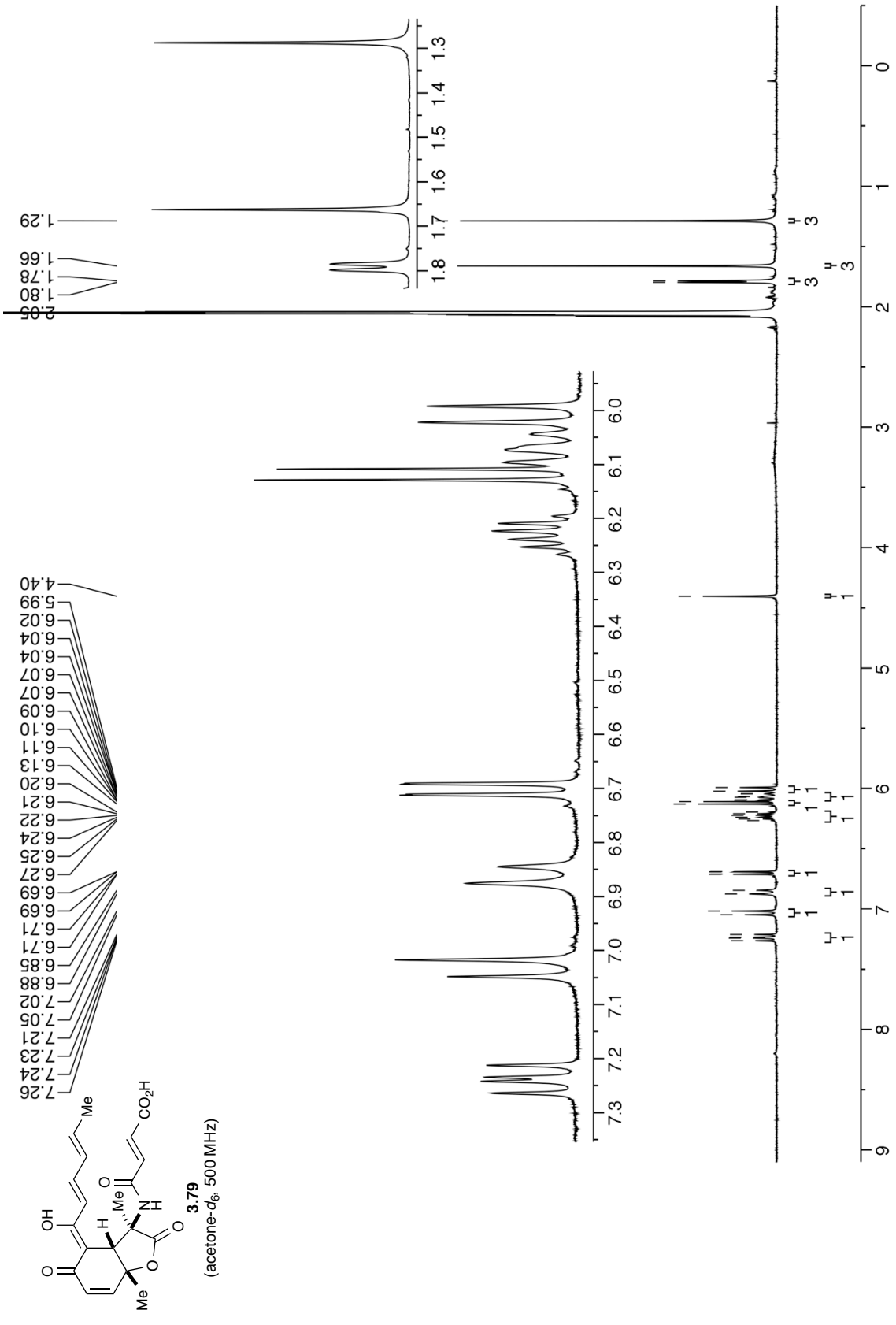
3.79
(acetone-d_6, 500 MHz)

Chapter 4

Spectra

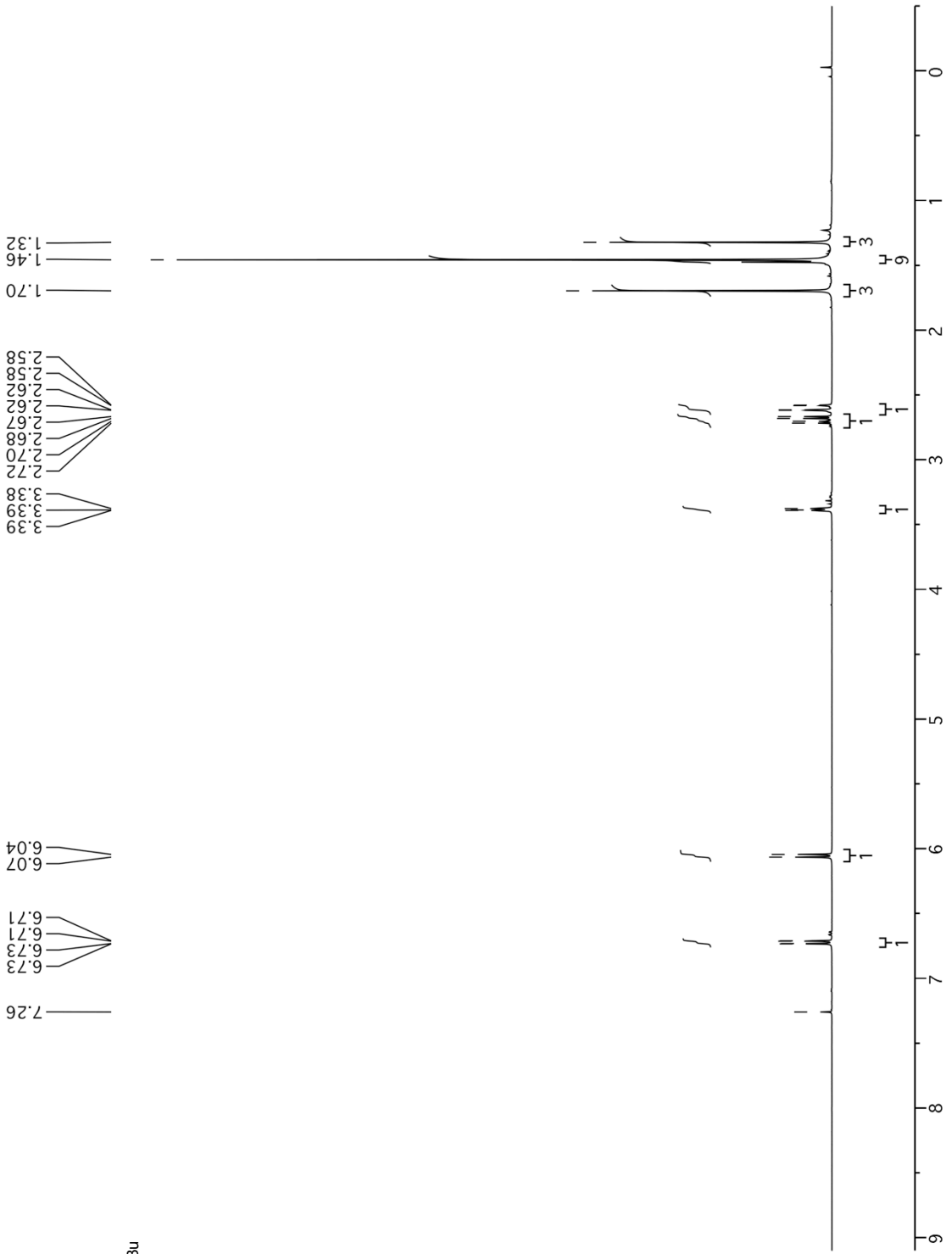

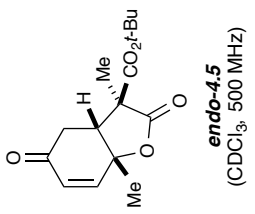

endo-4.5
($CDCl_3$, 500 MHz)

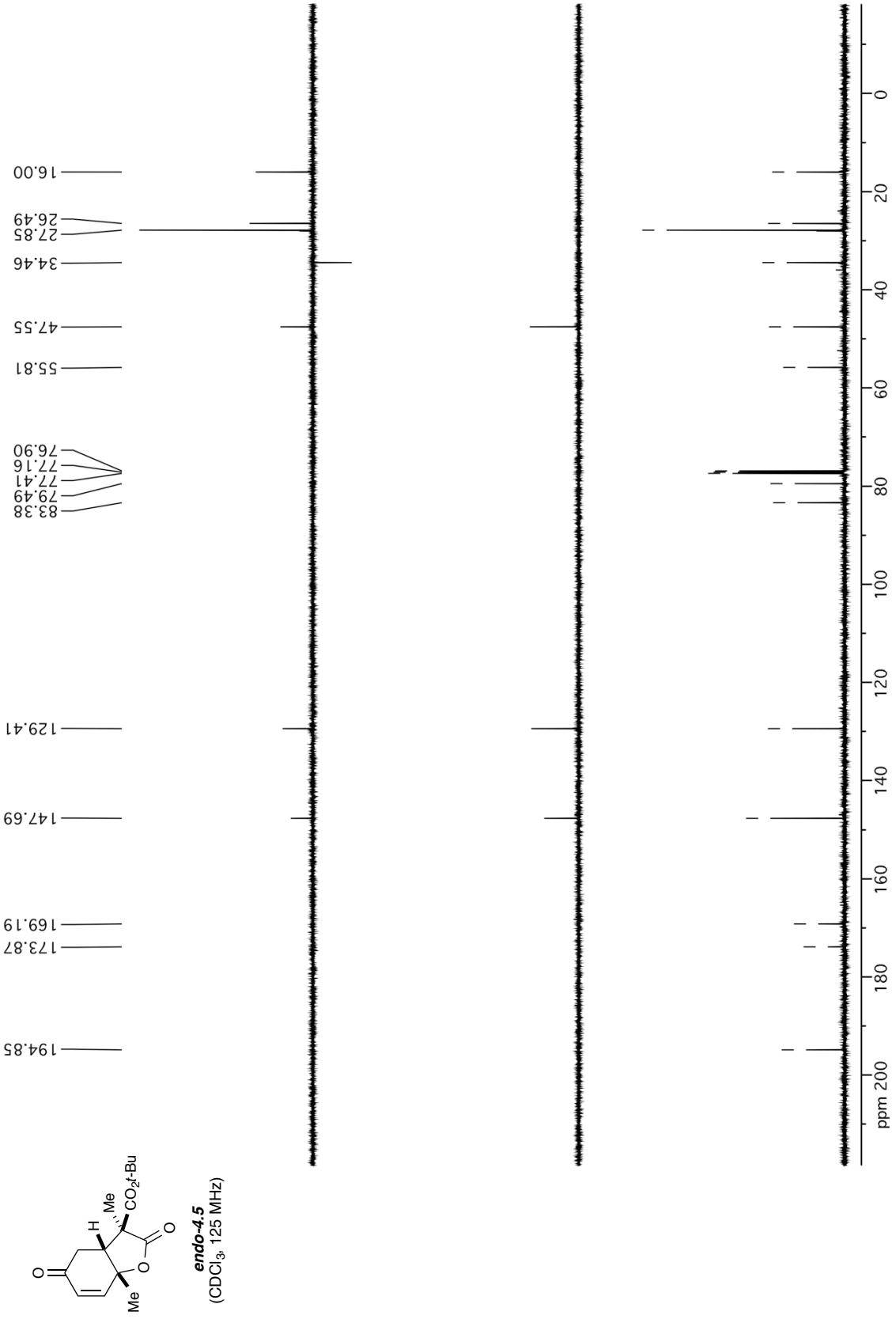

endo-4.5
($CDCl_3$, 125 MHz)

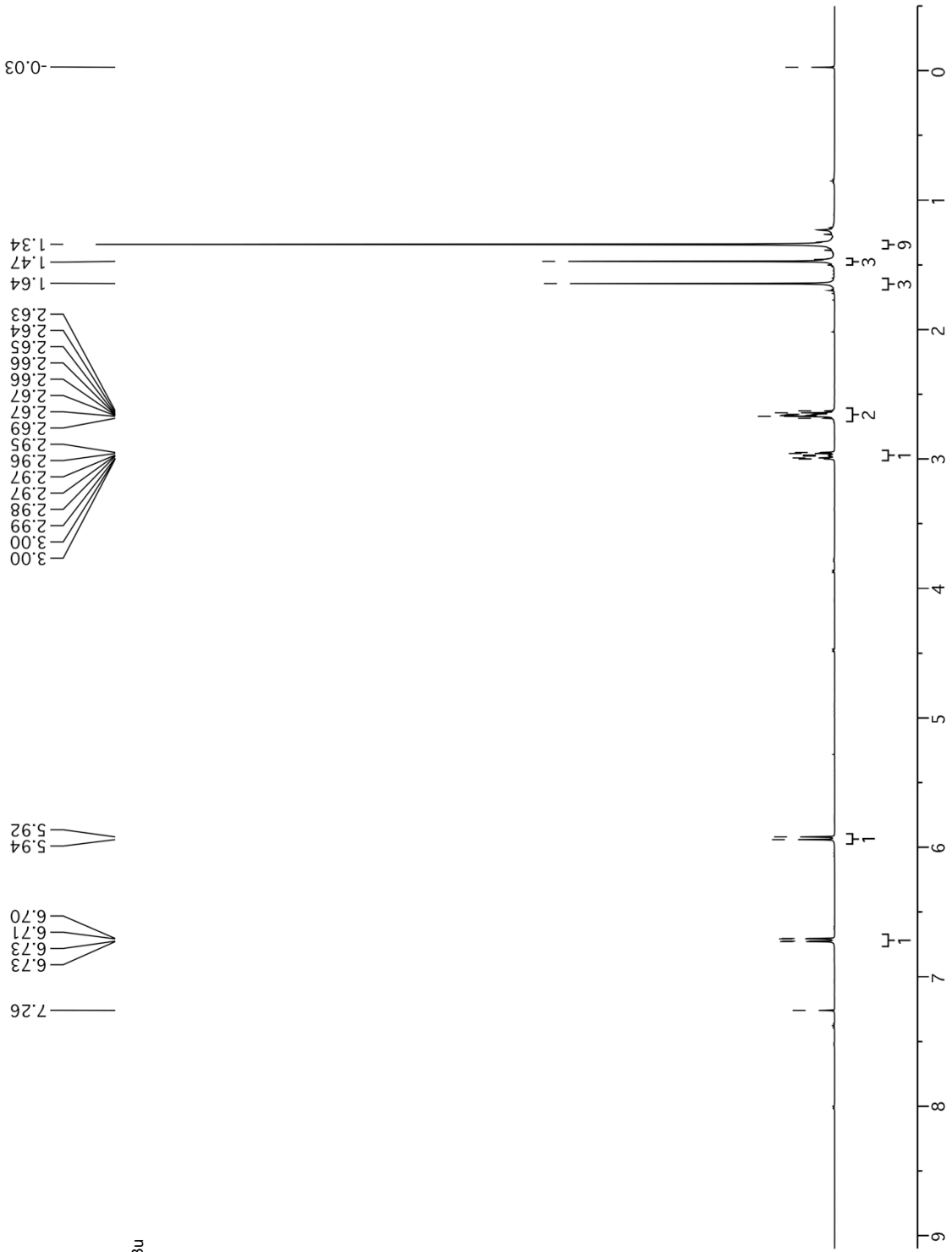

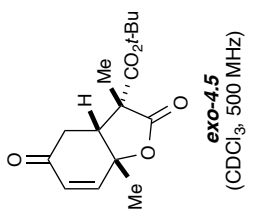

exo-4.5
($CDCl_3$, 500 MHz)

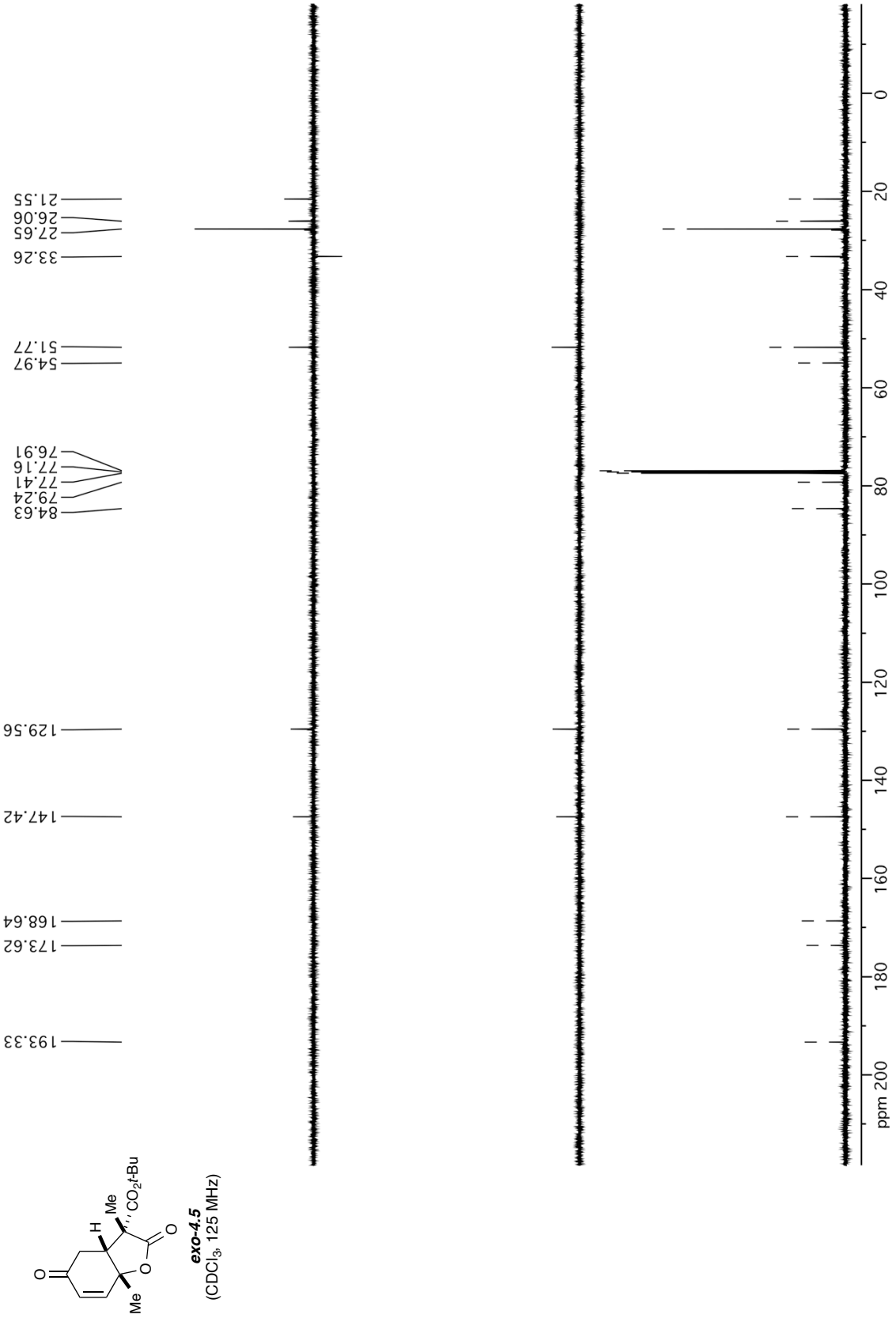
21.55
26.06
27.65
33.26
51.77
54.97
76.91
77.16
77.41
79.24
84.63
129.56
147.42
168.64
173.62
193.33
ppm 200
180
160
140
120
100
80
60
40
20
0
H
Me
CO2t-Bu
O
O
O
Me
exo-4.5
(CDCl3, 125 MHz)

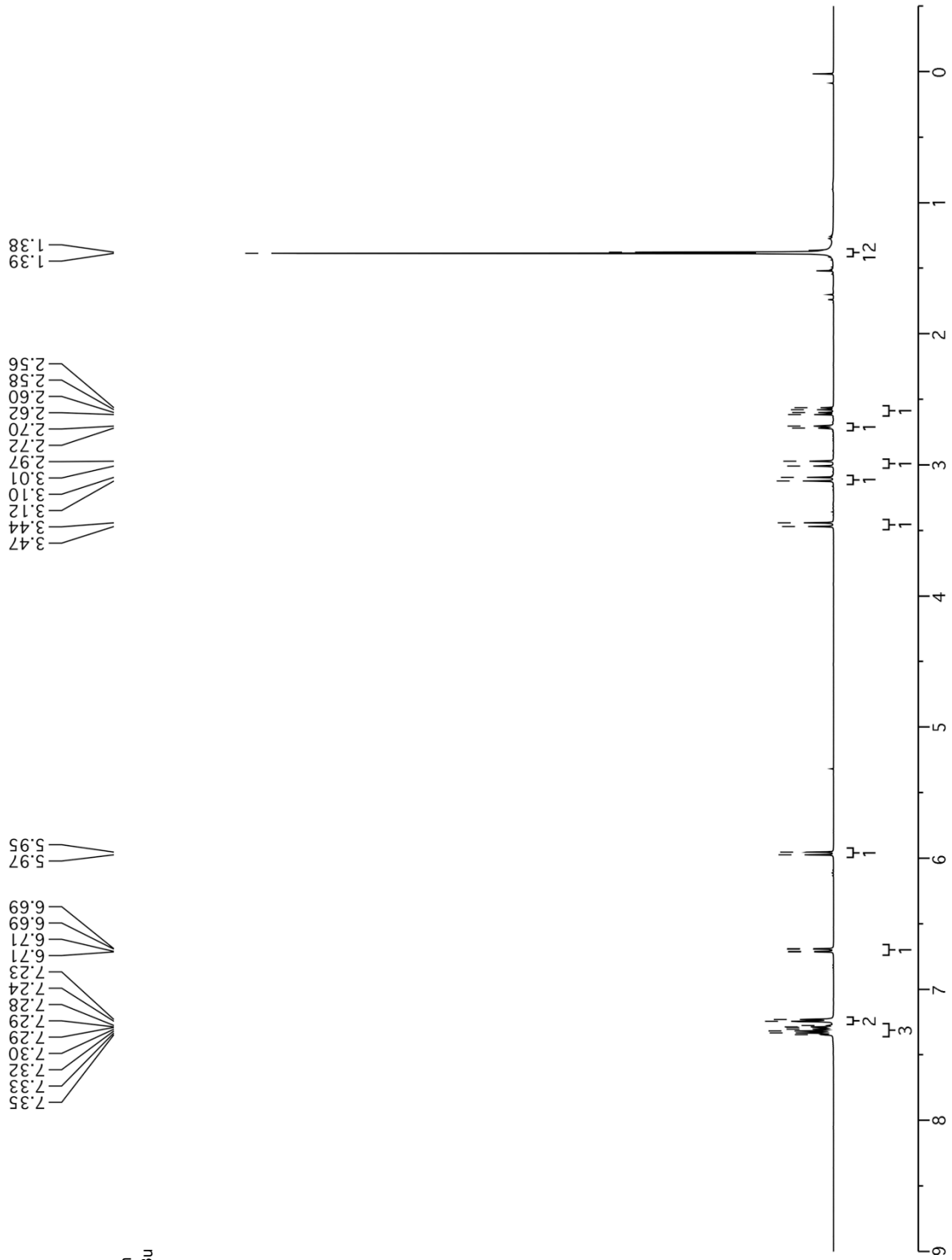

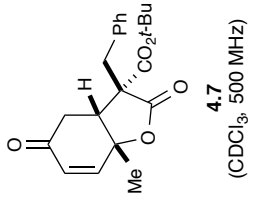

4.7
($CDCl_3$, 500 MHz)

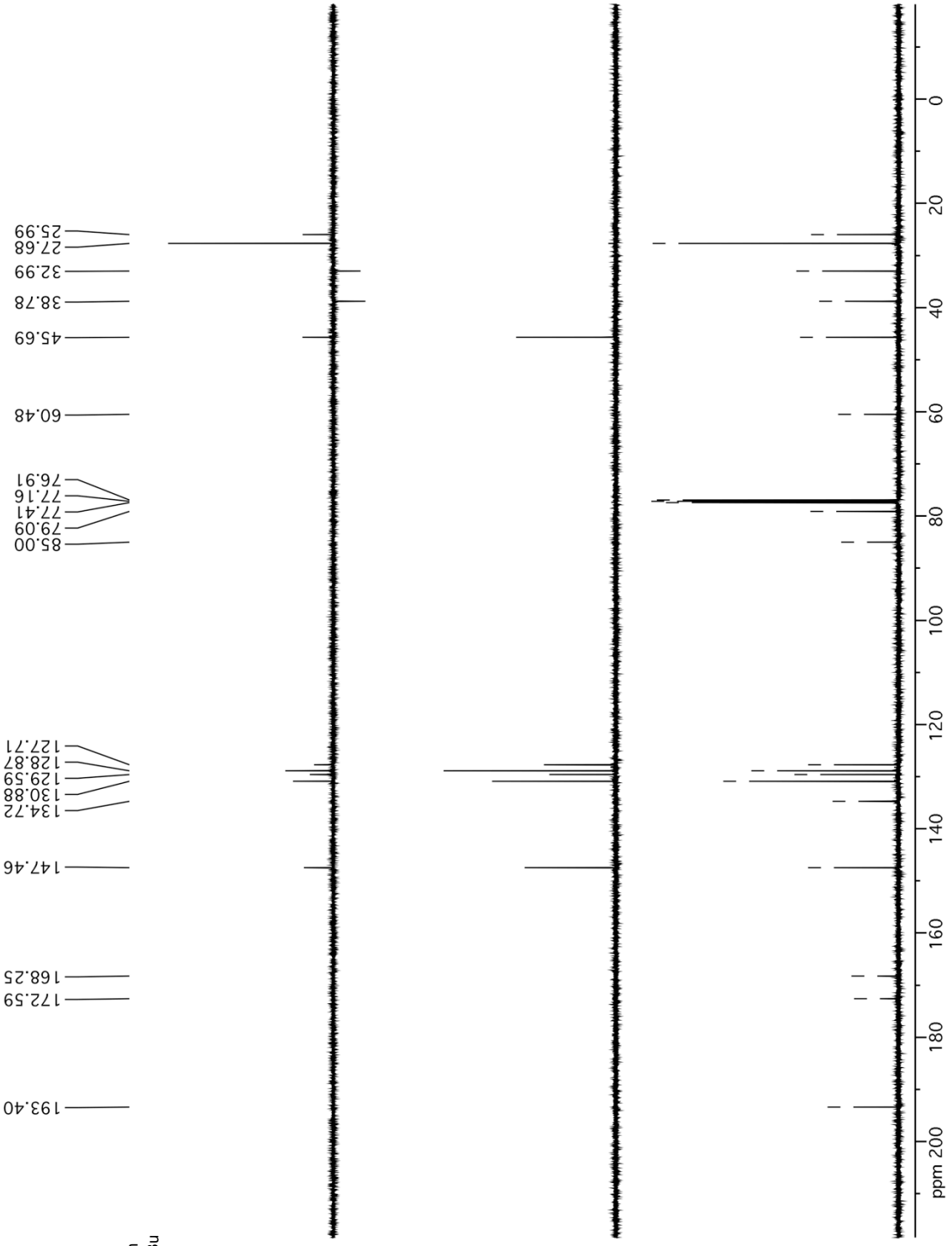

4.7
($CDCl_3$, 125 MHz)

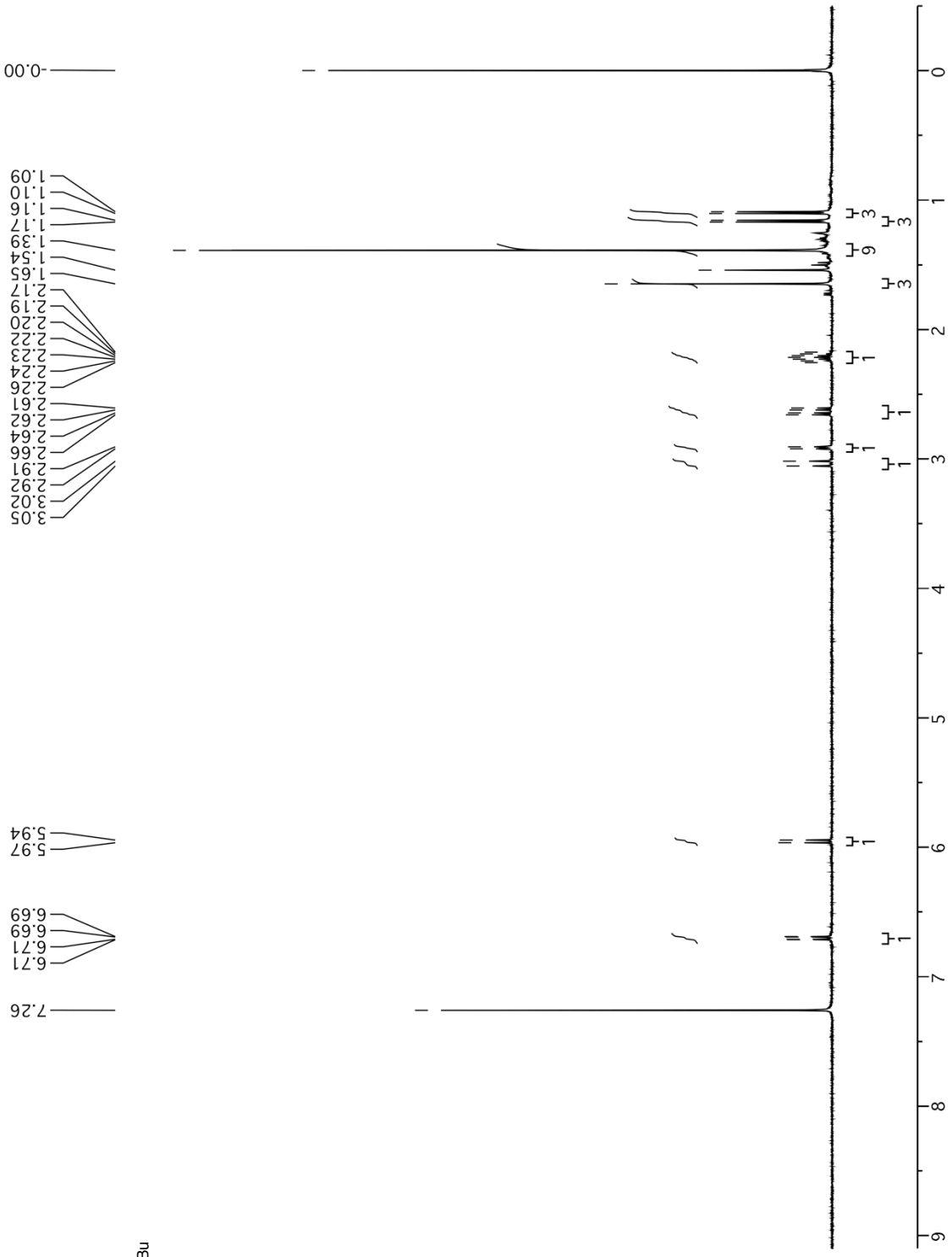

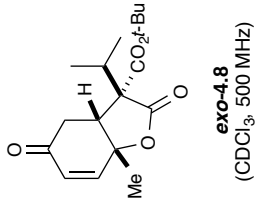

***exo*-4.8**
($CDCl_3$, 500 MHz)

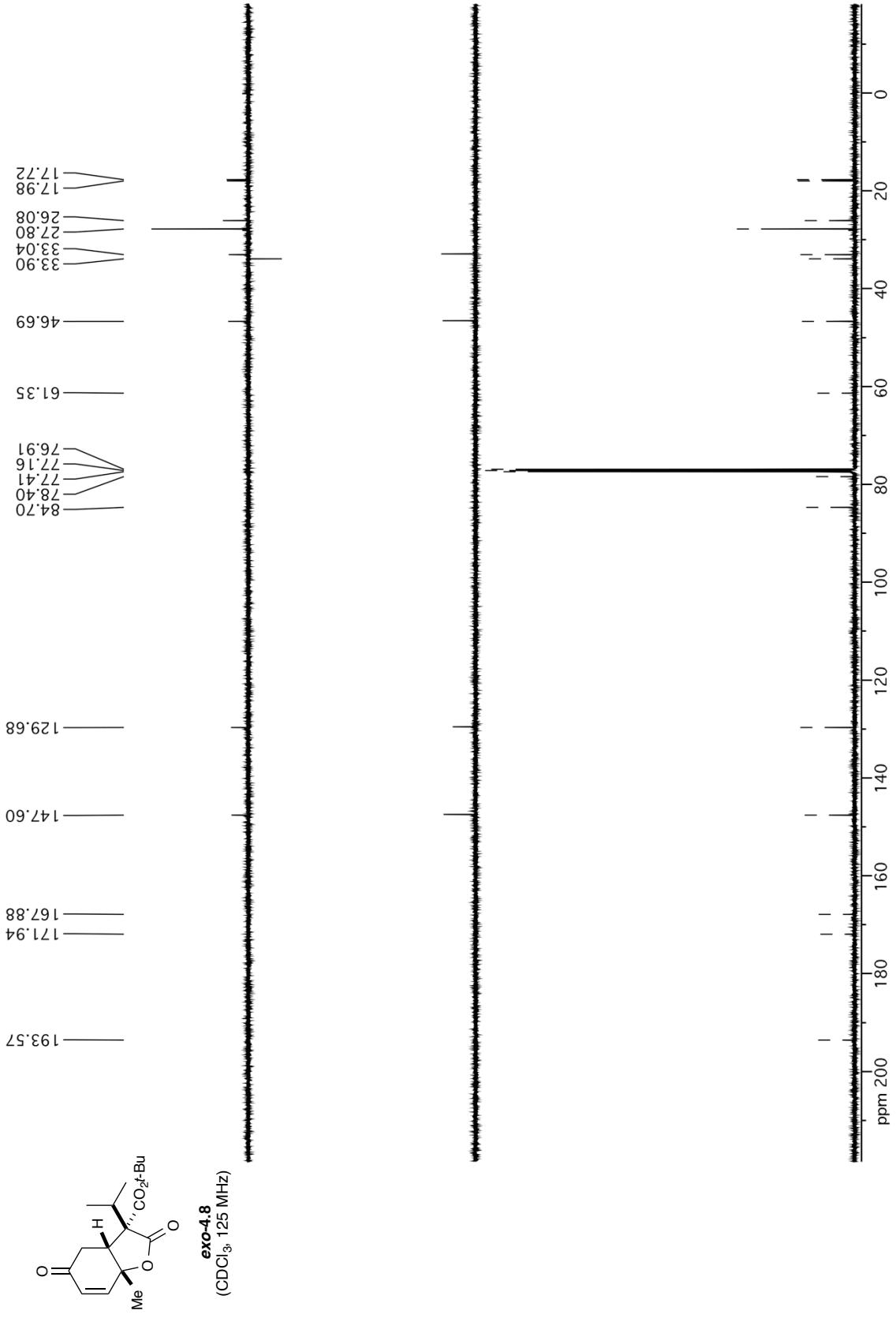
17.72
17.98
26.08
27.80
33.04
33.90
46.69
61.35
76.91
77.16
77.41
78.40
84.70
129.68
147.60
167.88
171.94
193.57
0
20
40
60
80
100
120
140
160
180
ppm 200
CO2t-Bu
H
O
O
O
Me
exo-4.8
(CDCl3, 125 MHz)

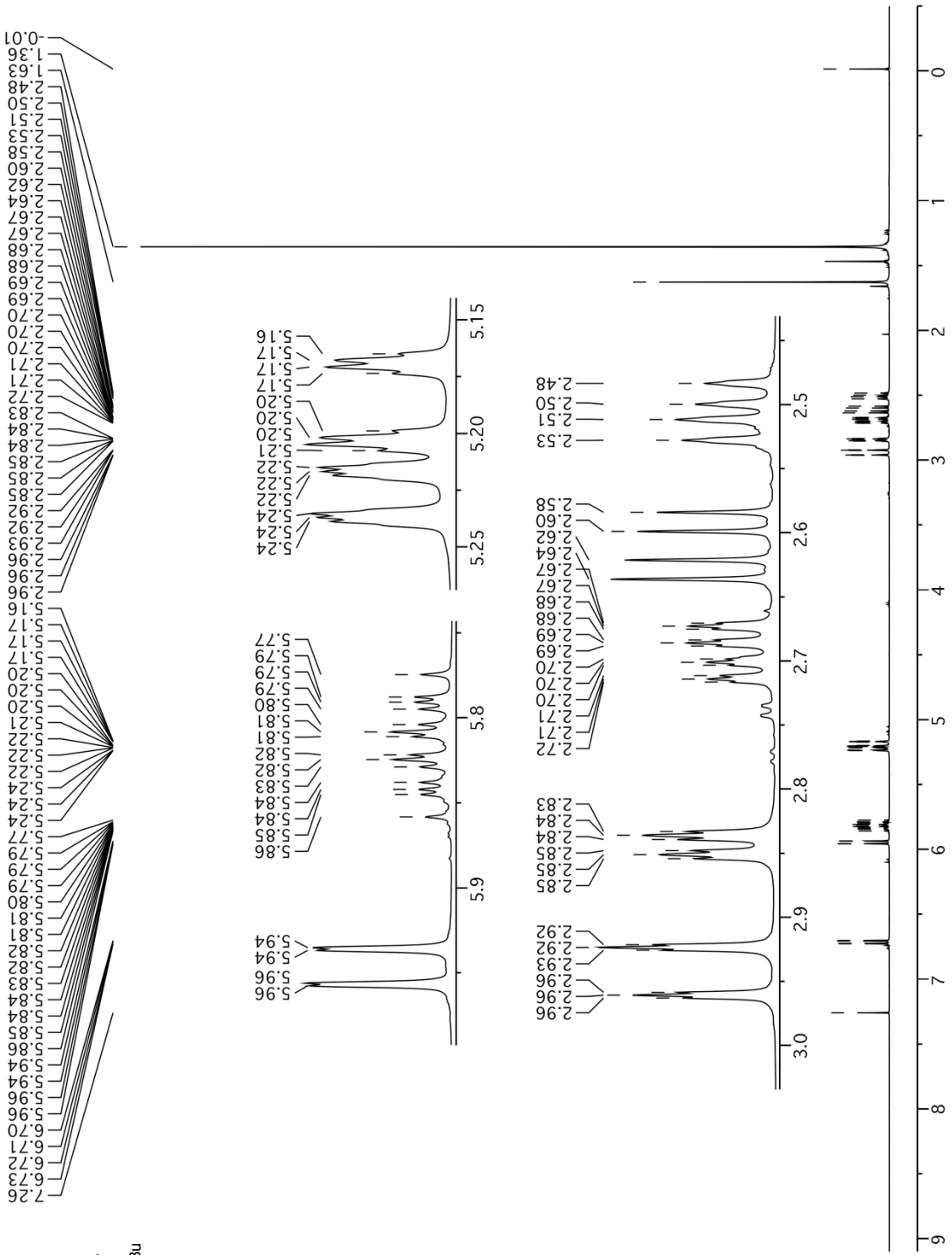
4.9
(CDCl3, 500 MHz)
Me
O
O
O
H
CO2t-Bu

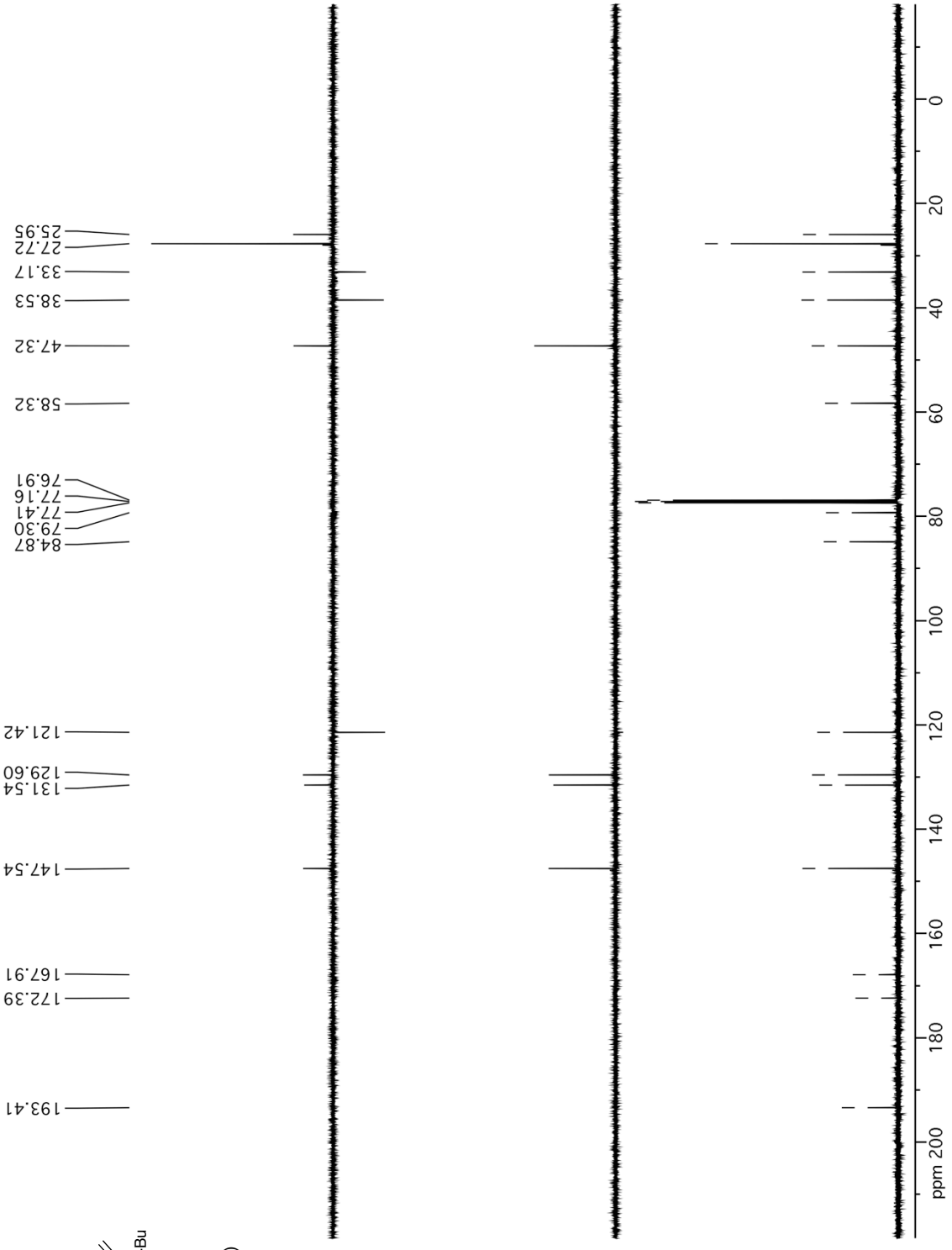

4.9
($CDCl_3$, 125 MHz)

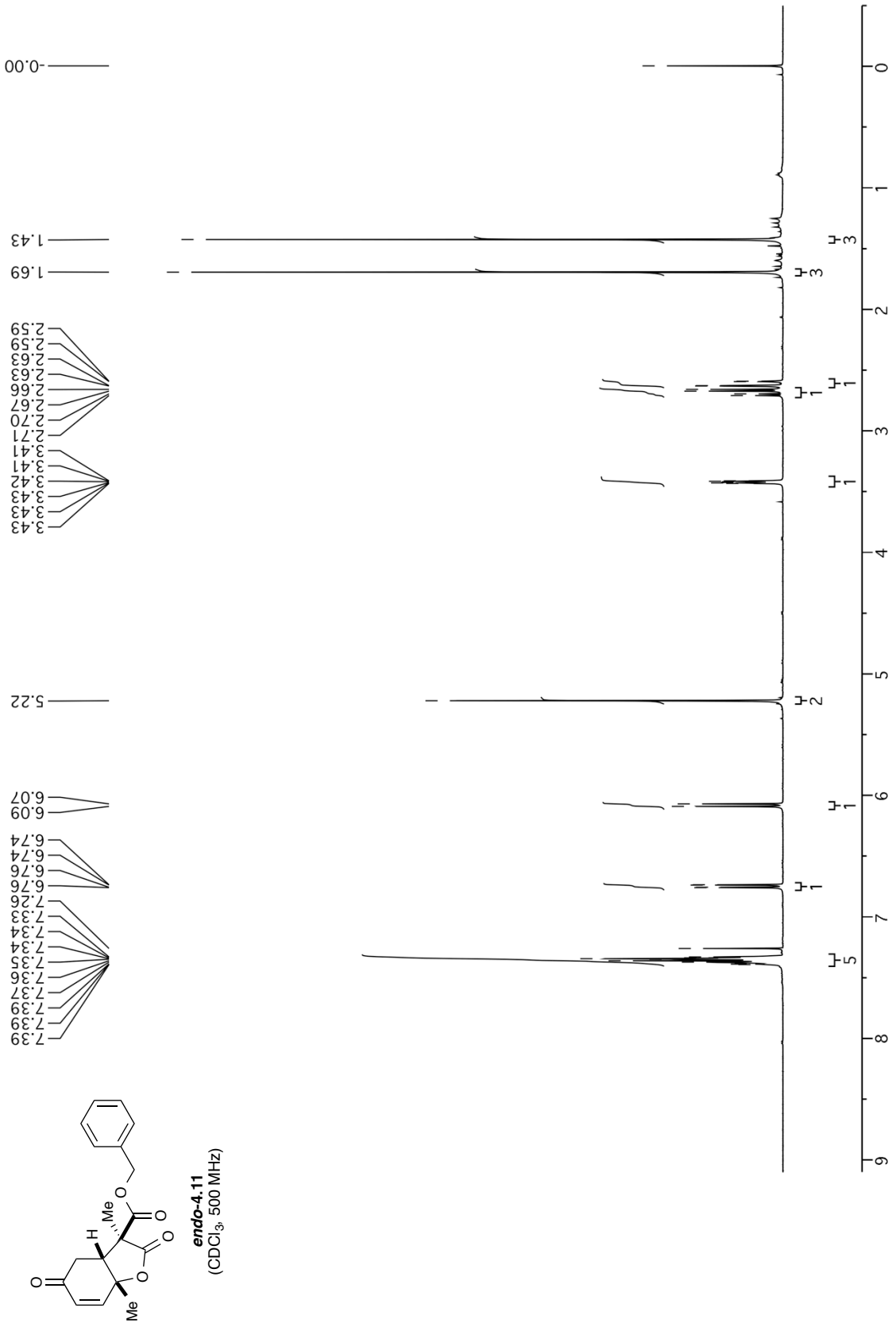

***endo*-4.11**
($CDCl_3$, 500 MHz)

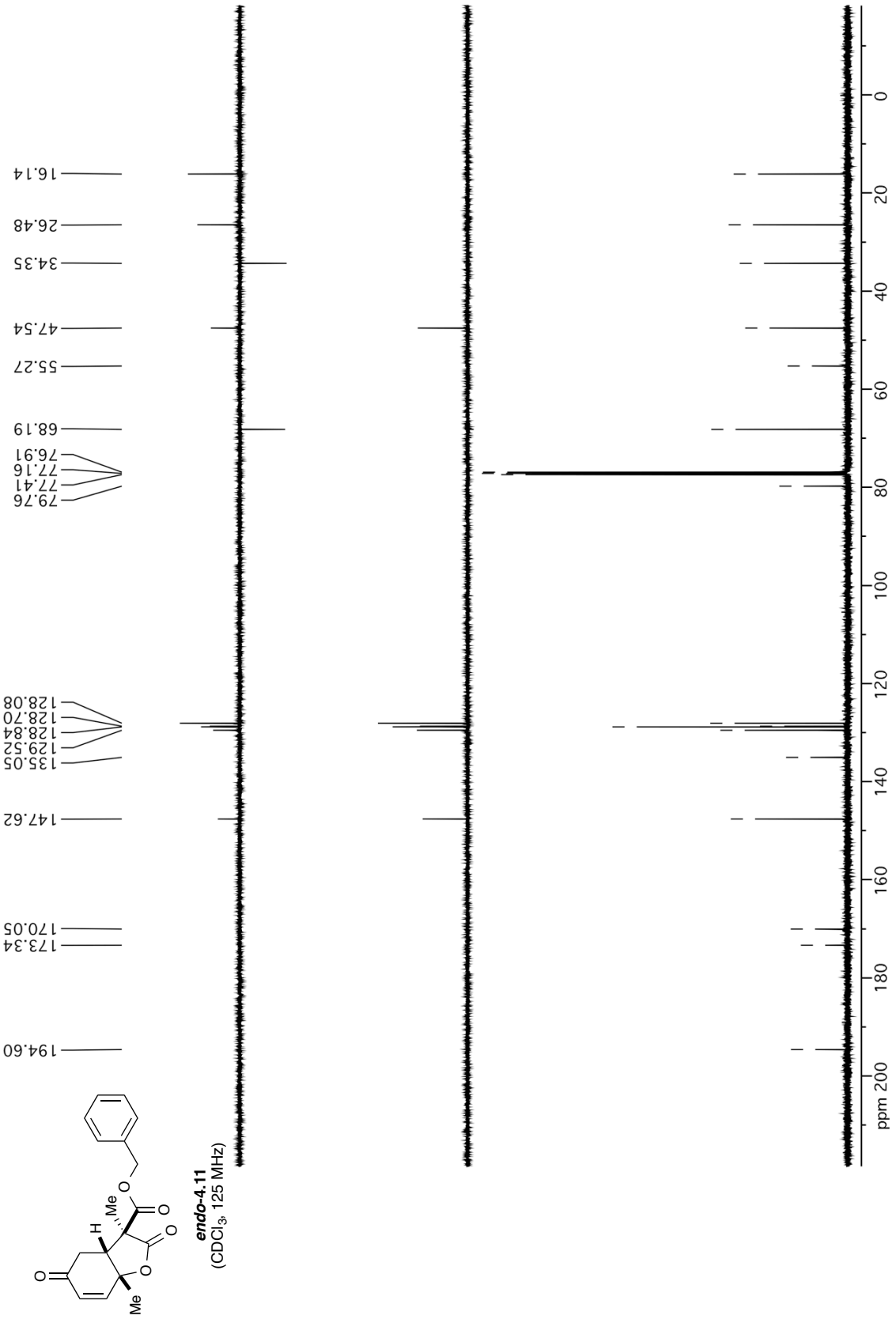
16.14
26.48
34.35
47.54
55.27
68.19
76.91
77.16
77.41
79.76
128.08
128.70
128.84
129.52
135.05
147.62
170.05
173.34
194.60
ppm 200
180
160
140
120
100
80
60
40
20
0
endo-4.11
(CDCl3, 125 MHz)
Me
H
O
O
O
O
O
Me

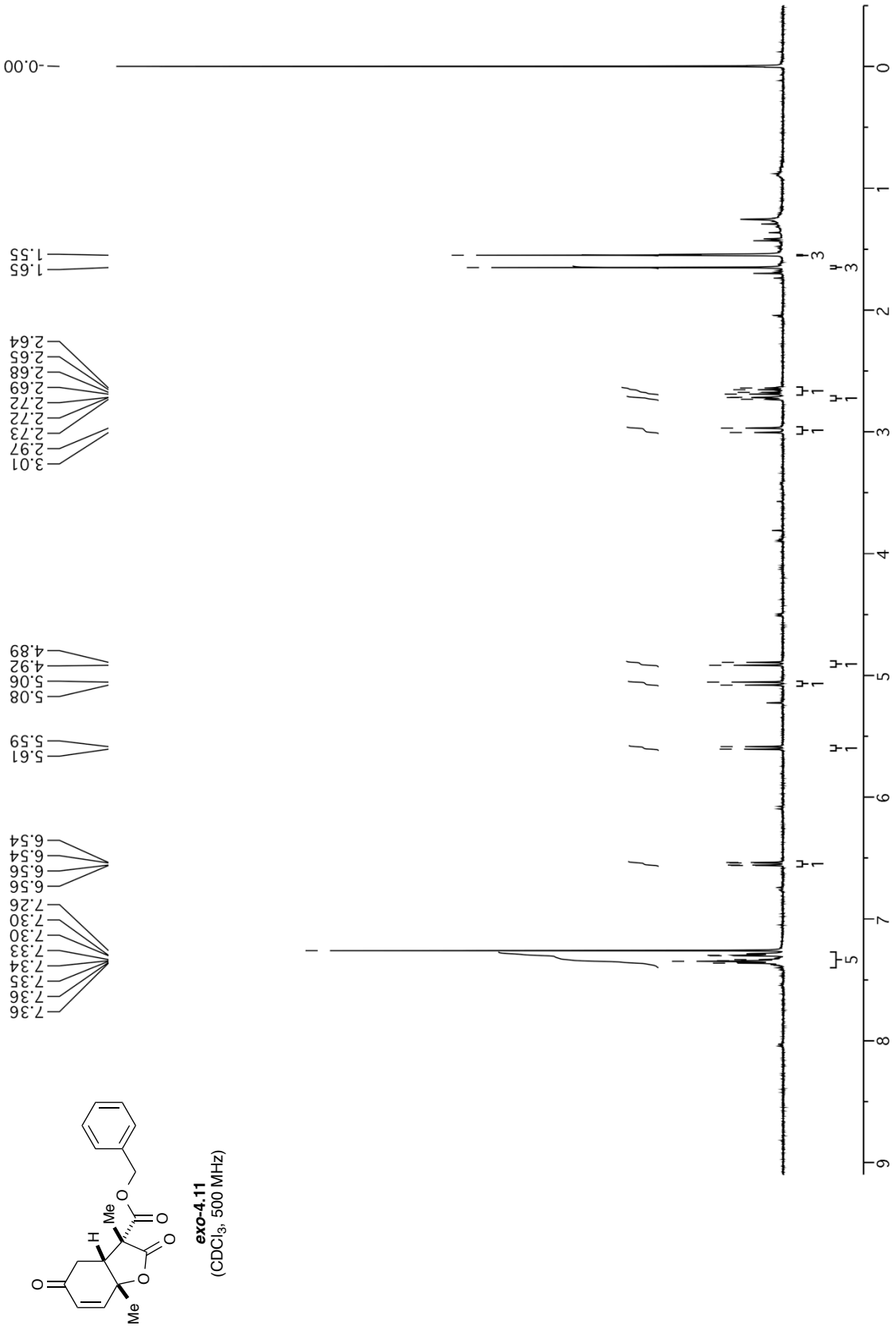
0.00
1.55
1.65
2.64
2.65
2.68
2.69
2.72
2.72
2.73
2.97
3.01
4.89
4.92
5.06
5.08
5.59
5.61
6.54
6.54
6.56
6.56
7.26
7.30
7.30
7.33
7.34
7.35
7.36
7.36
Me
O
O
O
H
O
O
Me
exo-4.11
(CDCl3, 500 MHz)

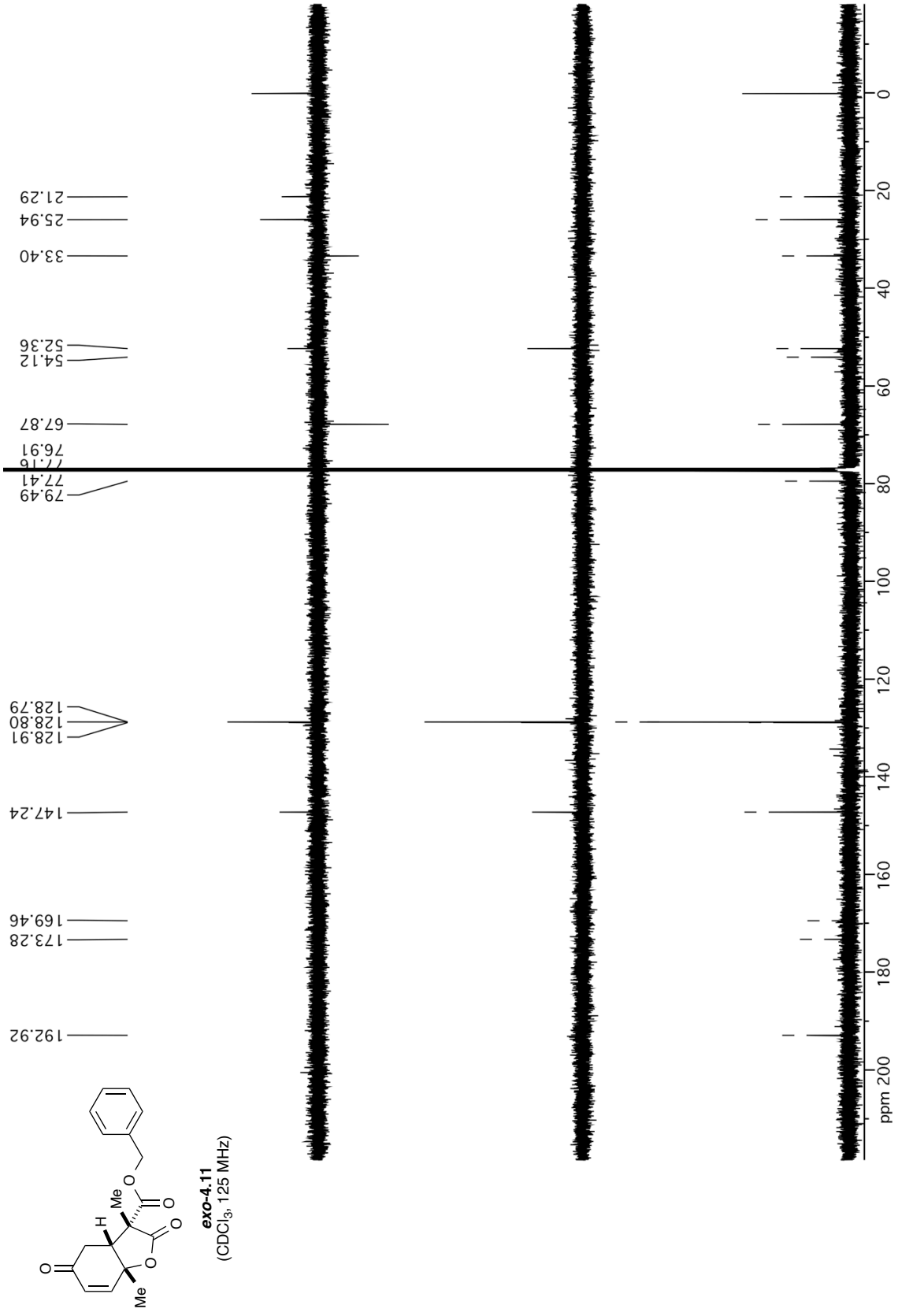
21.29
25.94
33.40
52.36
54.12
67.87
76.91
77.16
77.41
79.49
128.79
128.80
128.91
147.24
169.46
173.28
192.92
ppm 200
180
160
140
120
100
80
60
40
20
0
Me
H
O
O
O
O
O
Me
exo-4.11
(CDCl3, 125 MHz)

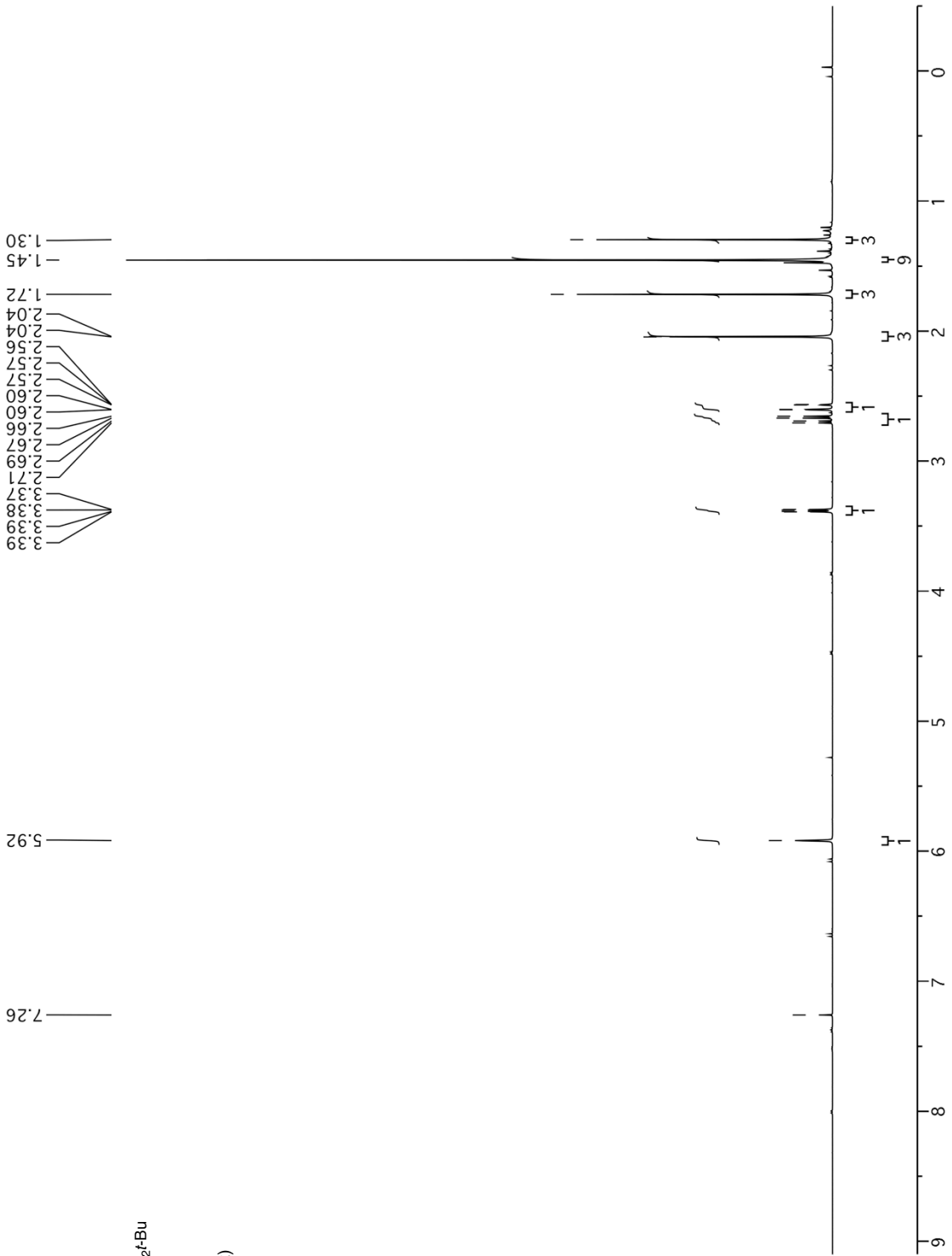

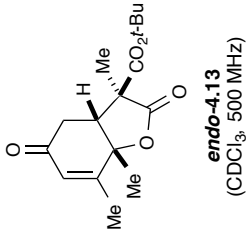

***endo*-4.13**
($CDCl_3$, 500 MHz)

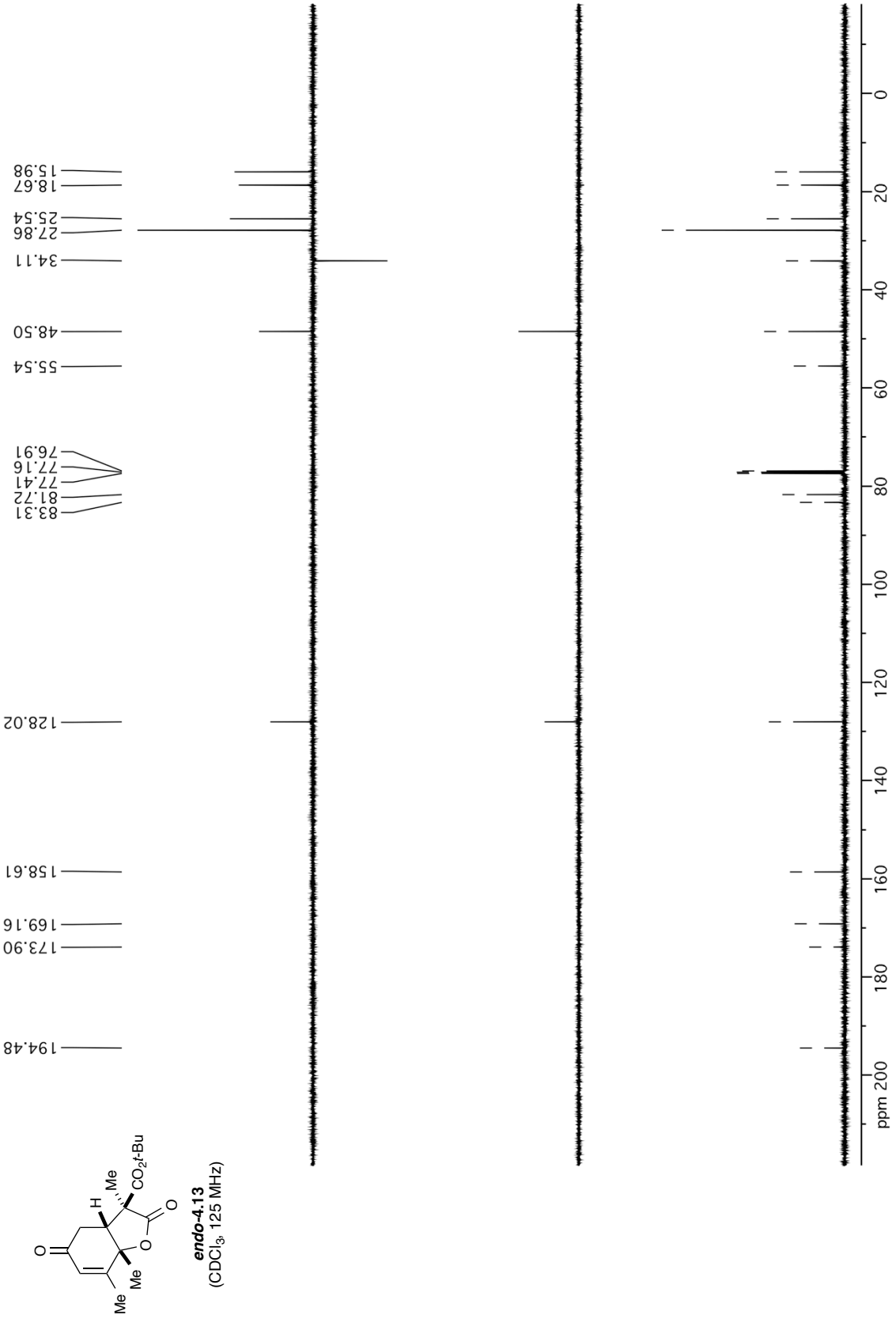
15.98
18.67
25.54
27.86
34.11
48.50
55.54
76.91
77.16
77.41
81.72
83.31
128.02
158.61
169.16
173.90
194.48
ppm 200
180
160
140
120
100
80
60
40
20
0
Me
CO2t-Bu
H
O
O
O
Me
Me
endo-4.13
(CDCl3, 125 MHz)

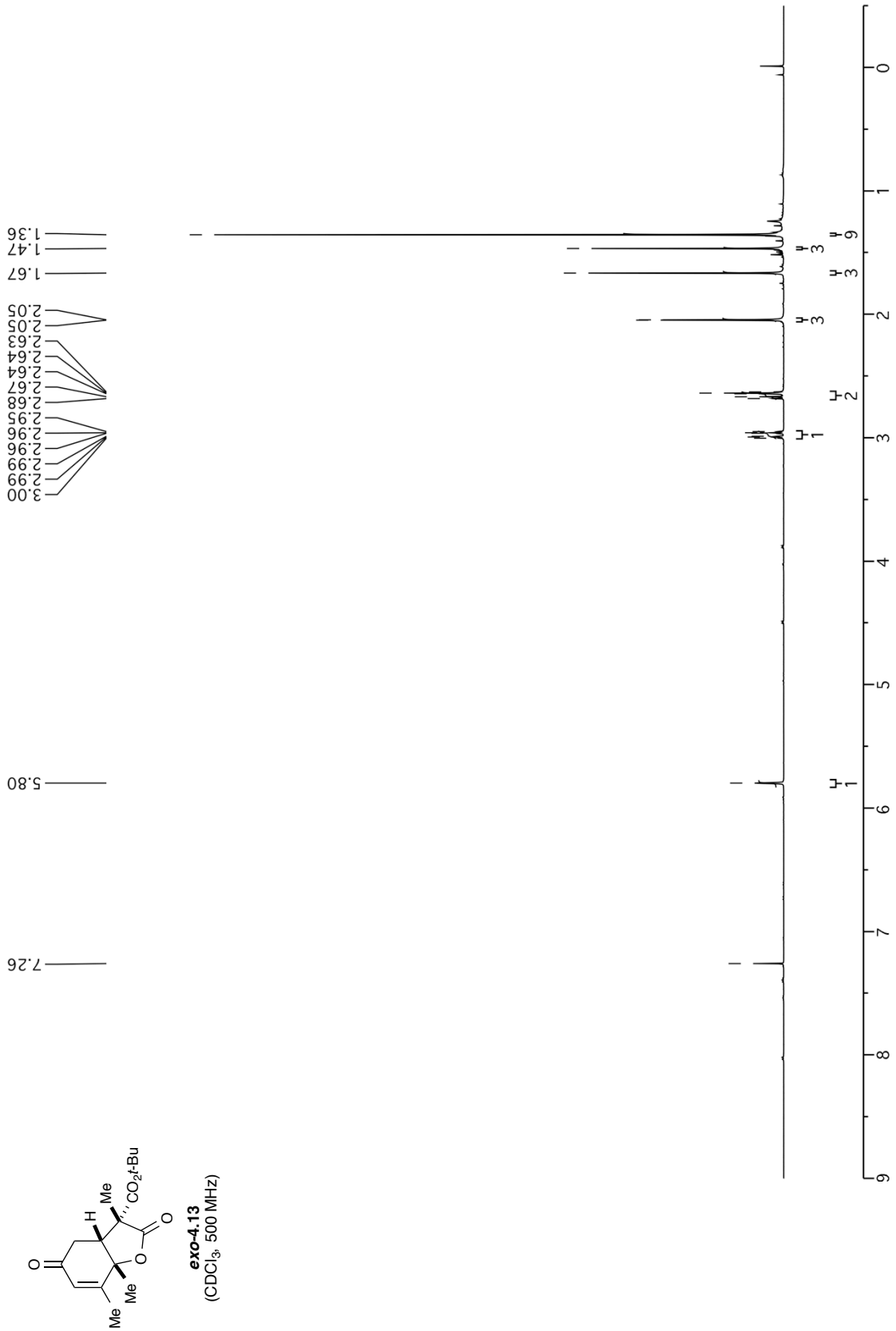
1.36
1.47
1.67
2.05
2.05
2.63
2.64
2.64
2.67
2.68
2.95
2.96
2.96
2.99
2.99
3.00
5.80
7.26
Me
CO2t-Bu
H
O
O
O
Me
Me
exo-4.13
(CDCl3, 500 MHz)

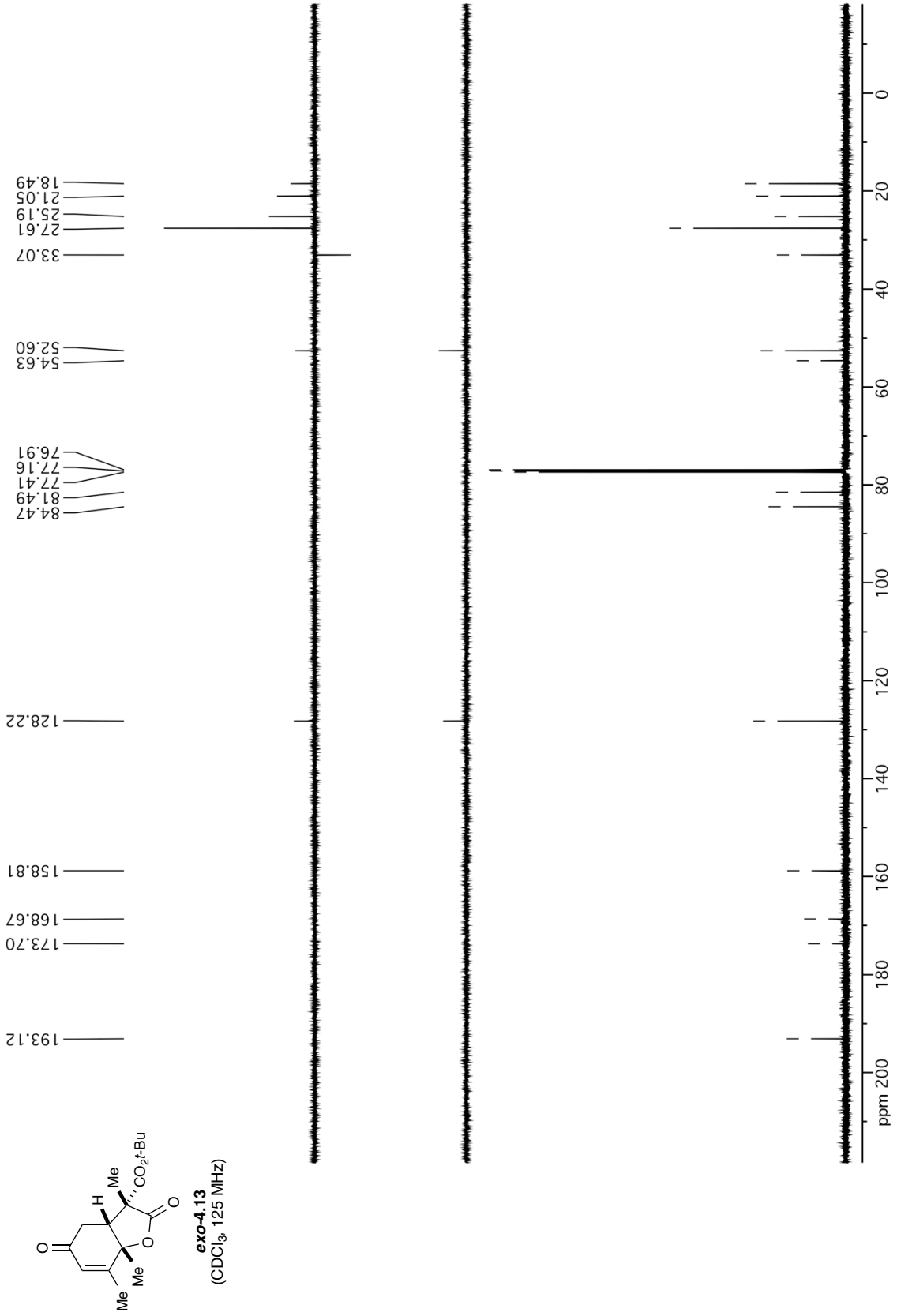

***exo*-4.13**
($CDCl_3$, 125 MHz)

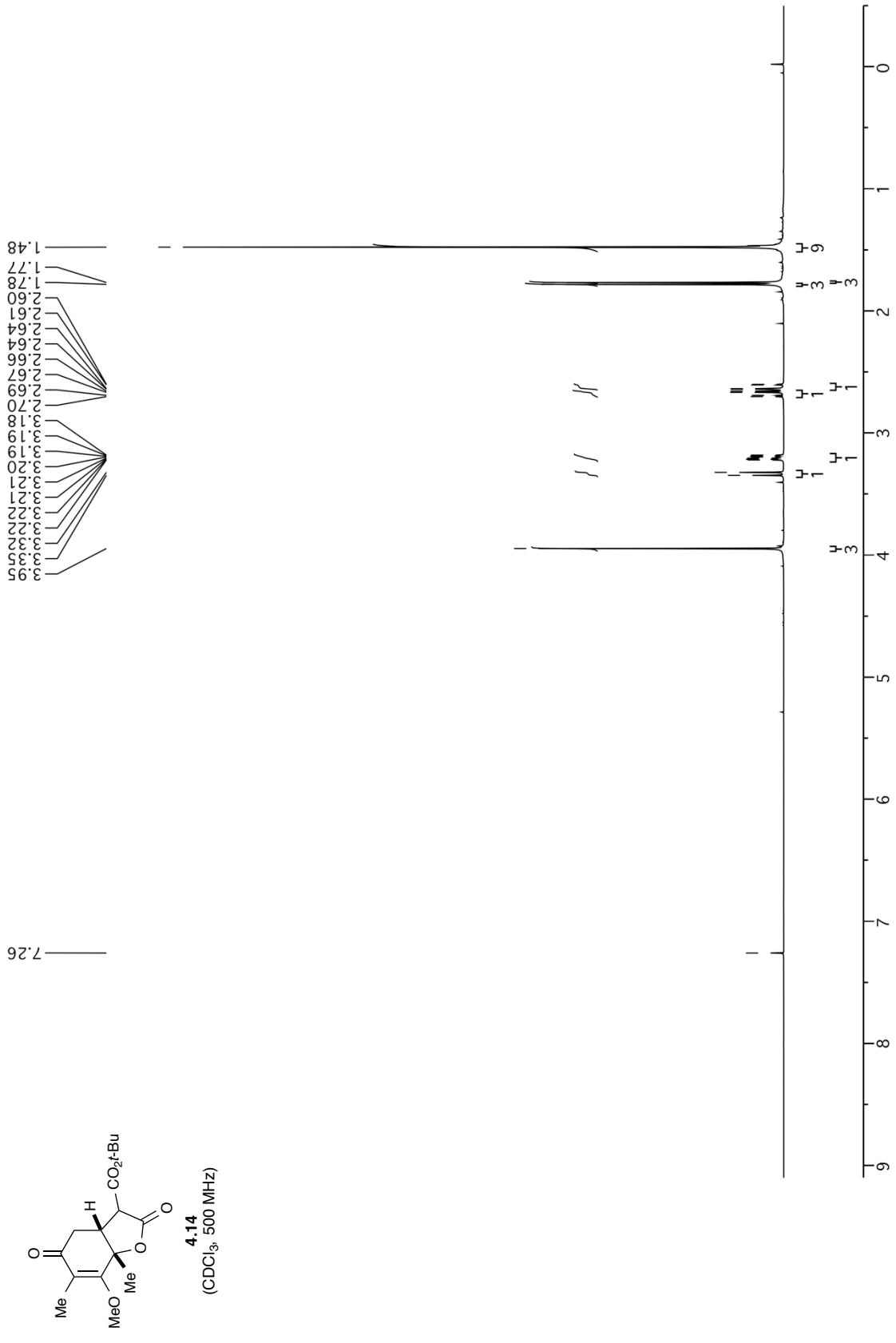

4.14
($CDCl_3$, 500 MHz)

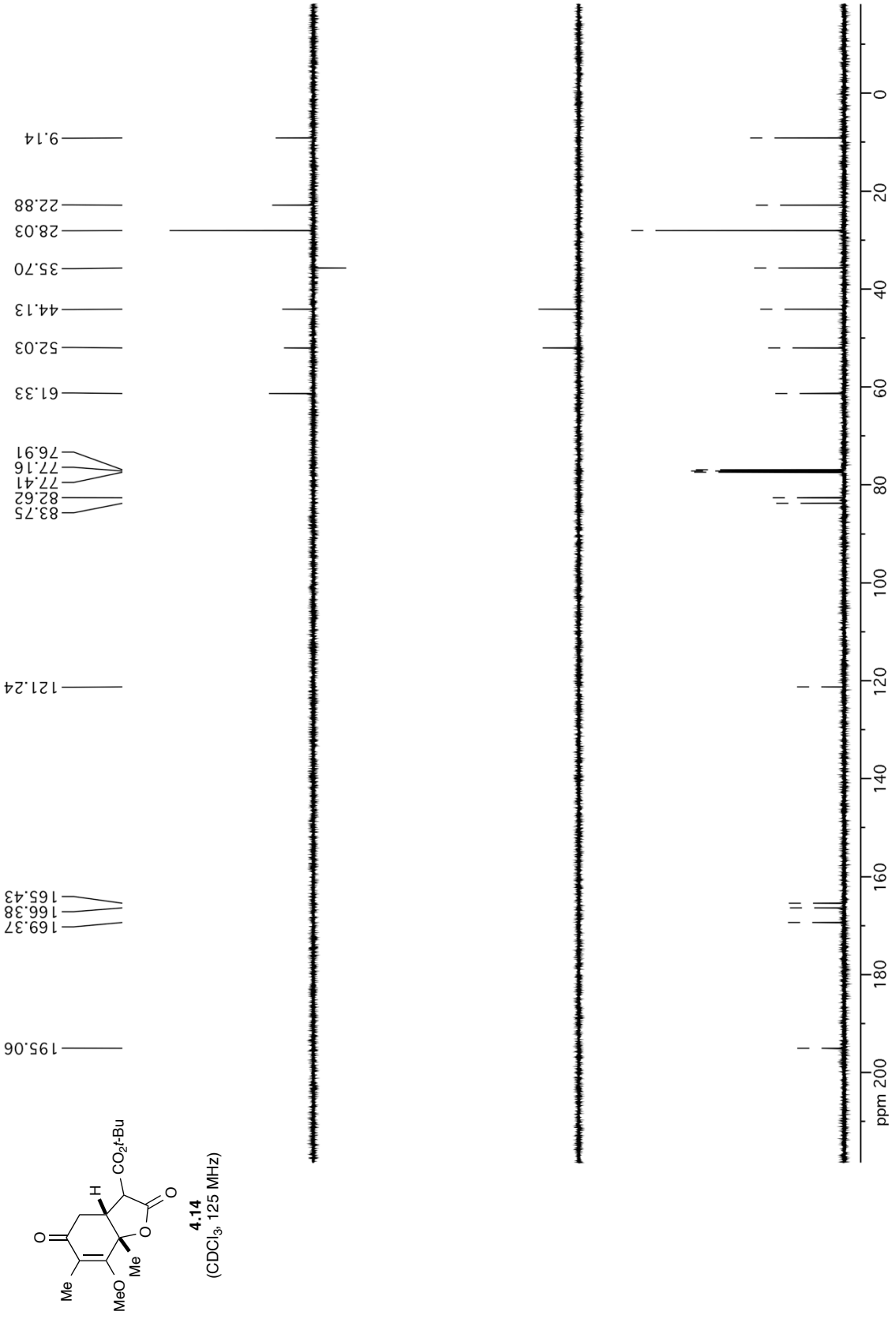

4.14
($CDCl_3$, 125 MHz)

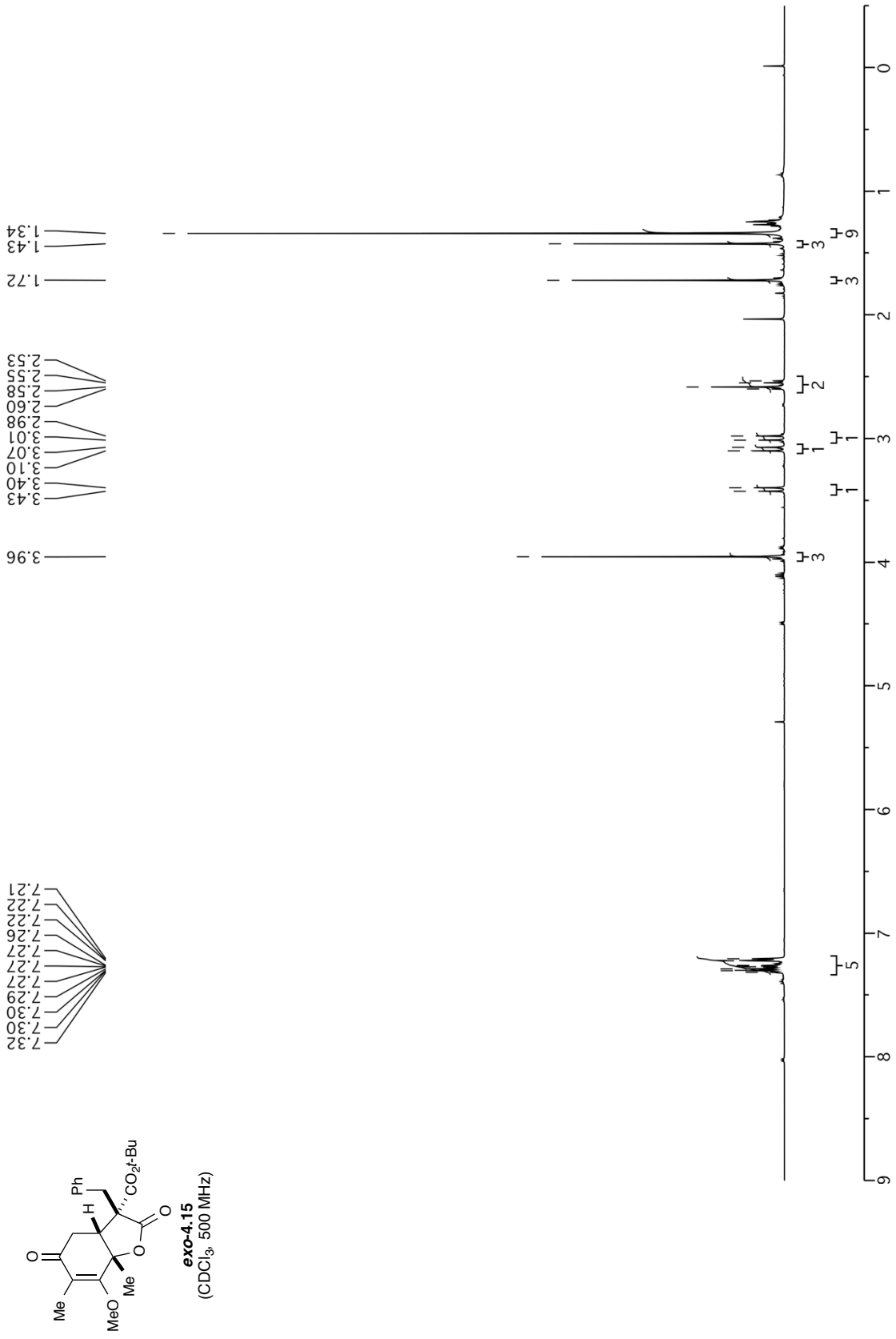

***exo*-4.15**
($CDCl_3$, 500 MHz)

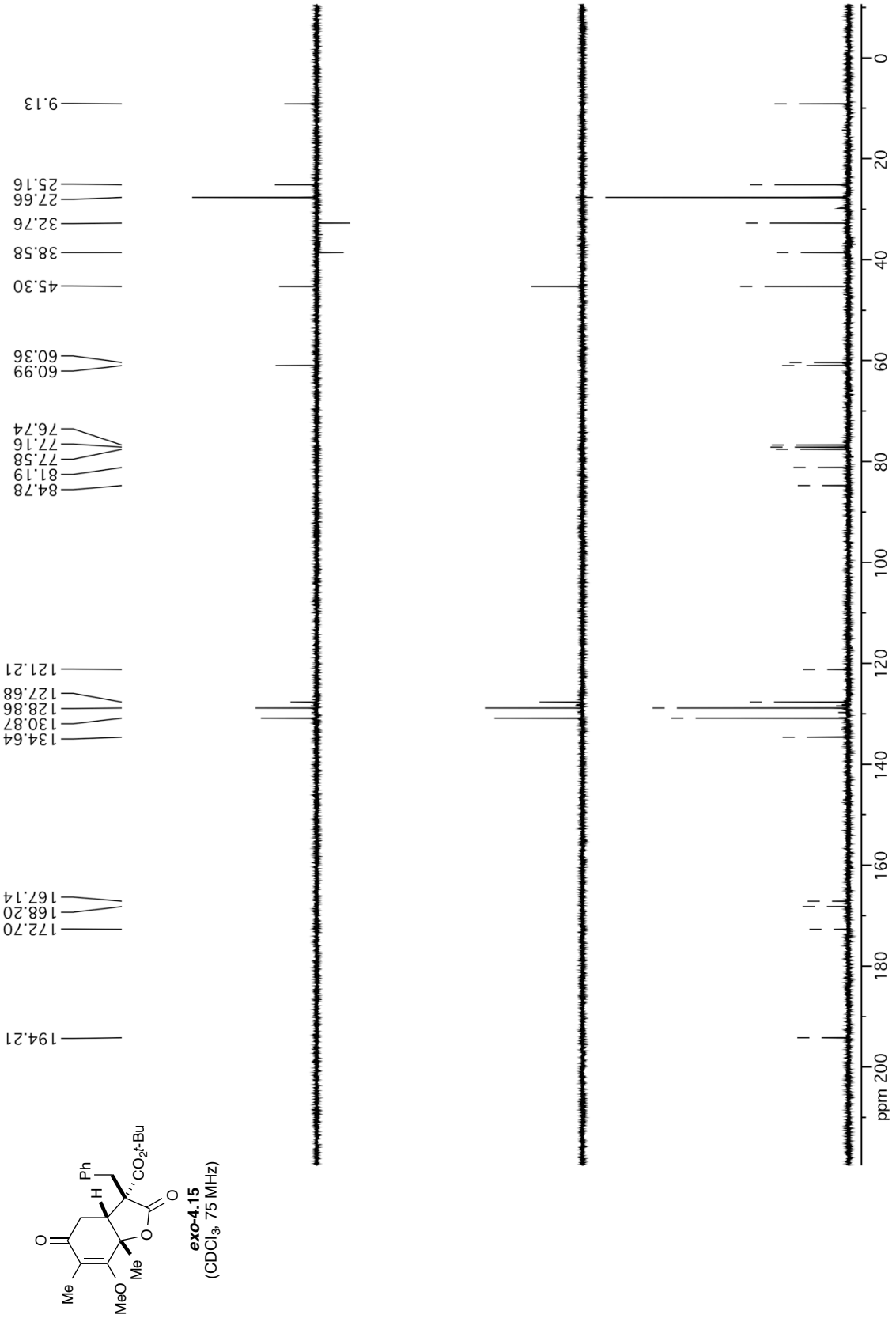

***exo*-4.15**
($CDCl_3$, 75 MHz)

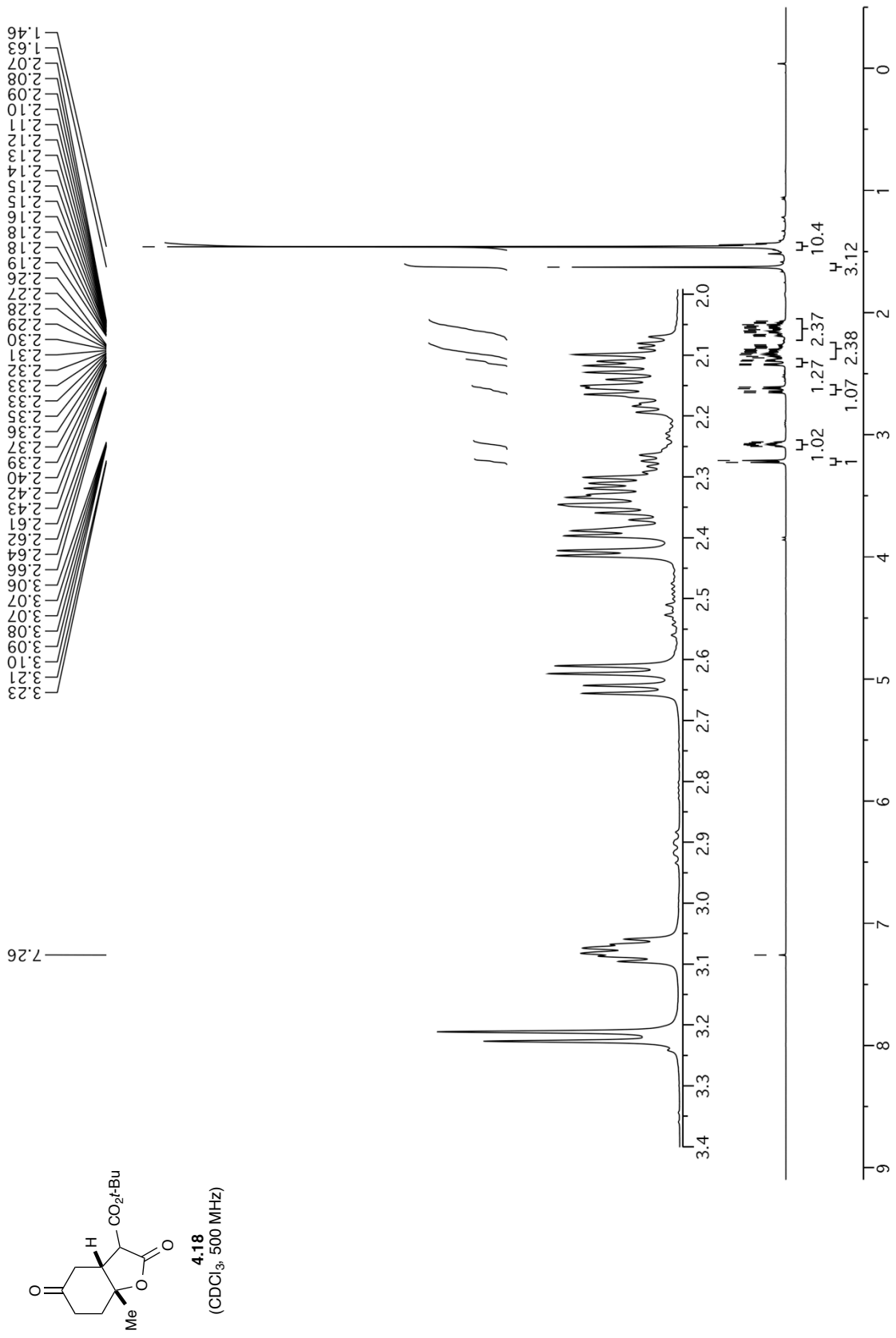

4.18
($CDCl_3$, 500 MHz)

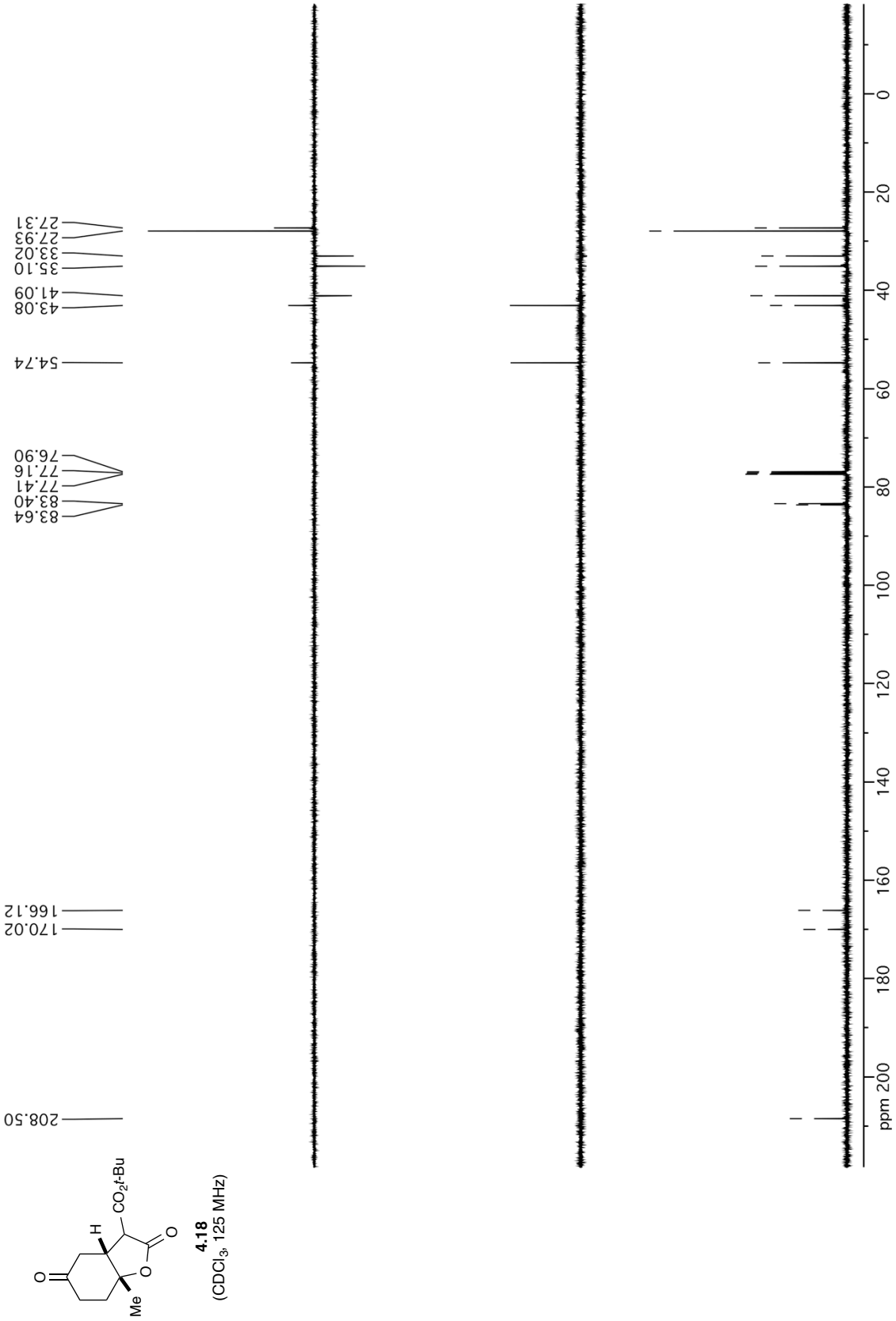

4.18
($CDCl_3$, 125 MHz)

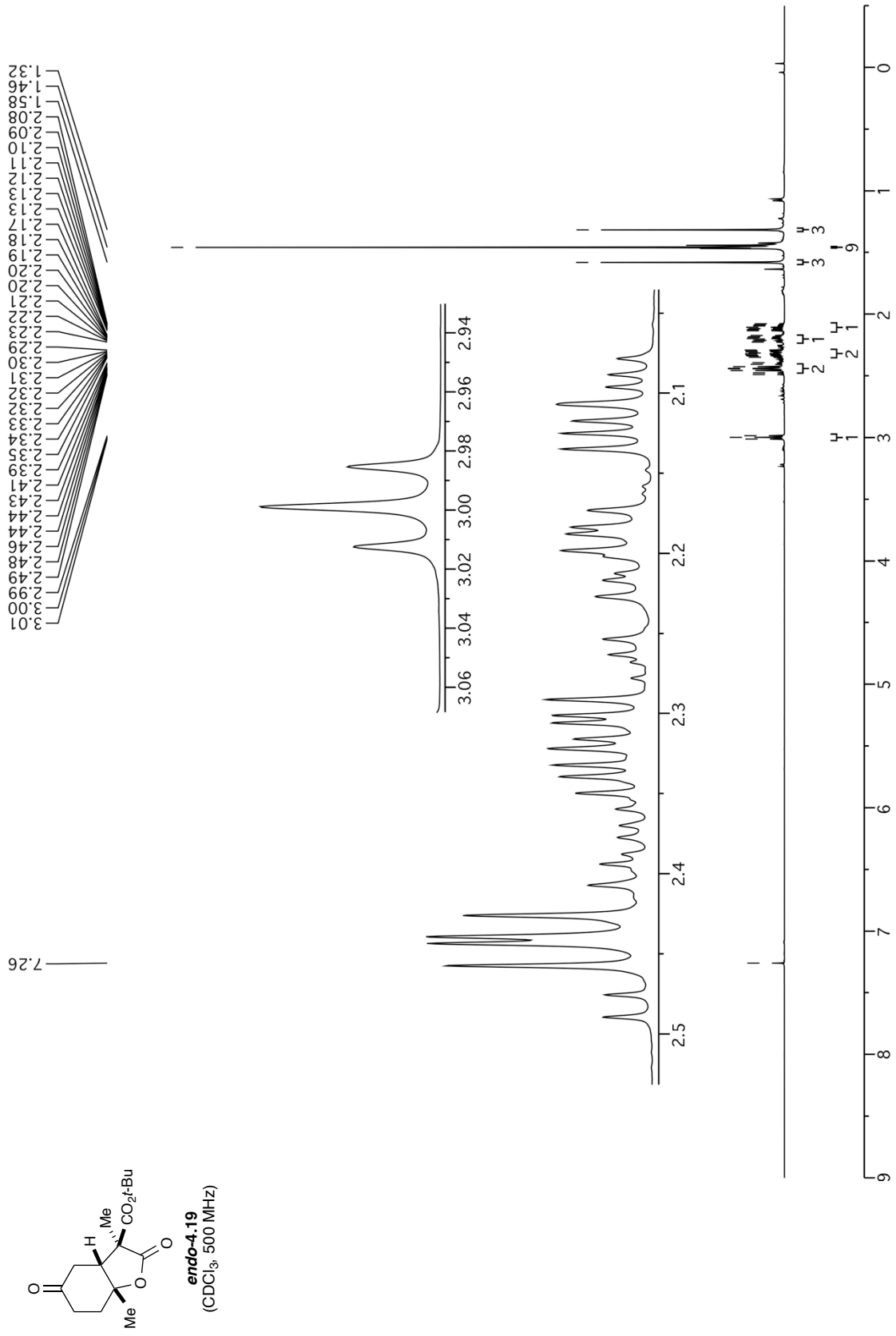

***endo*-4.19**
($CDCl_3$, 500 MHz)

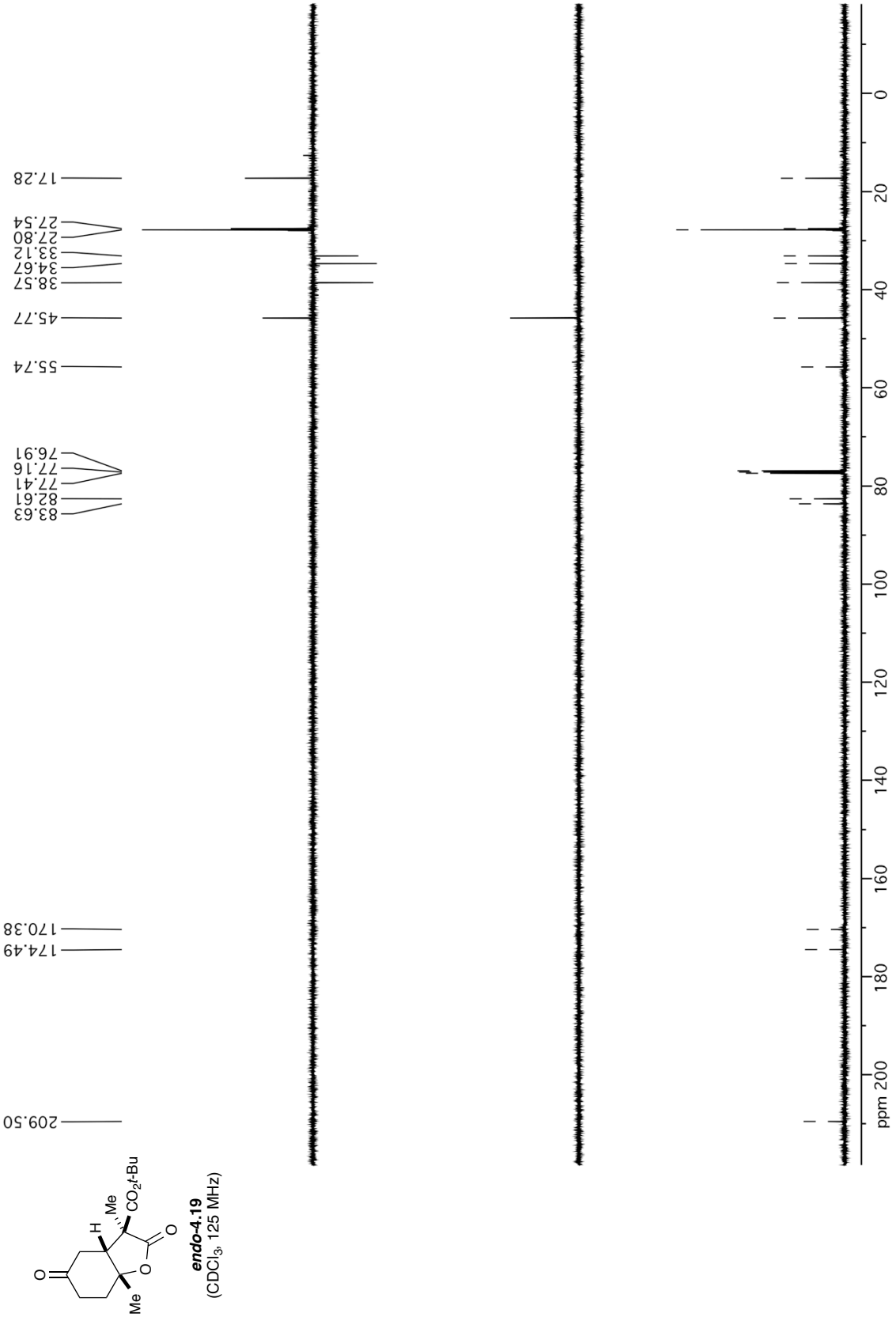

***endo*-4.19**
($CDCl_3$, 125 MHz)

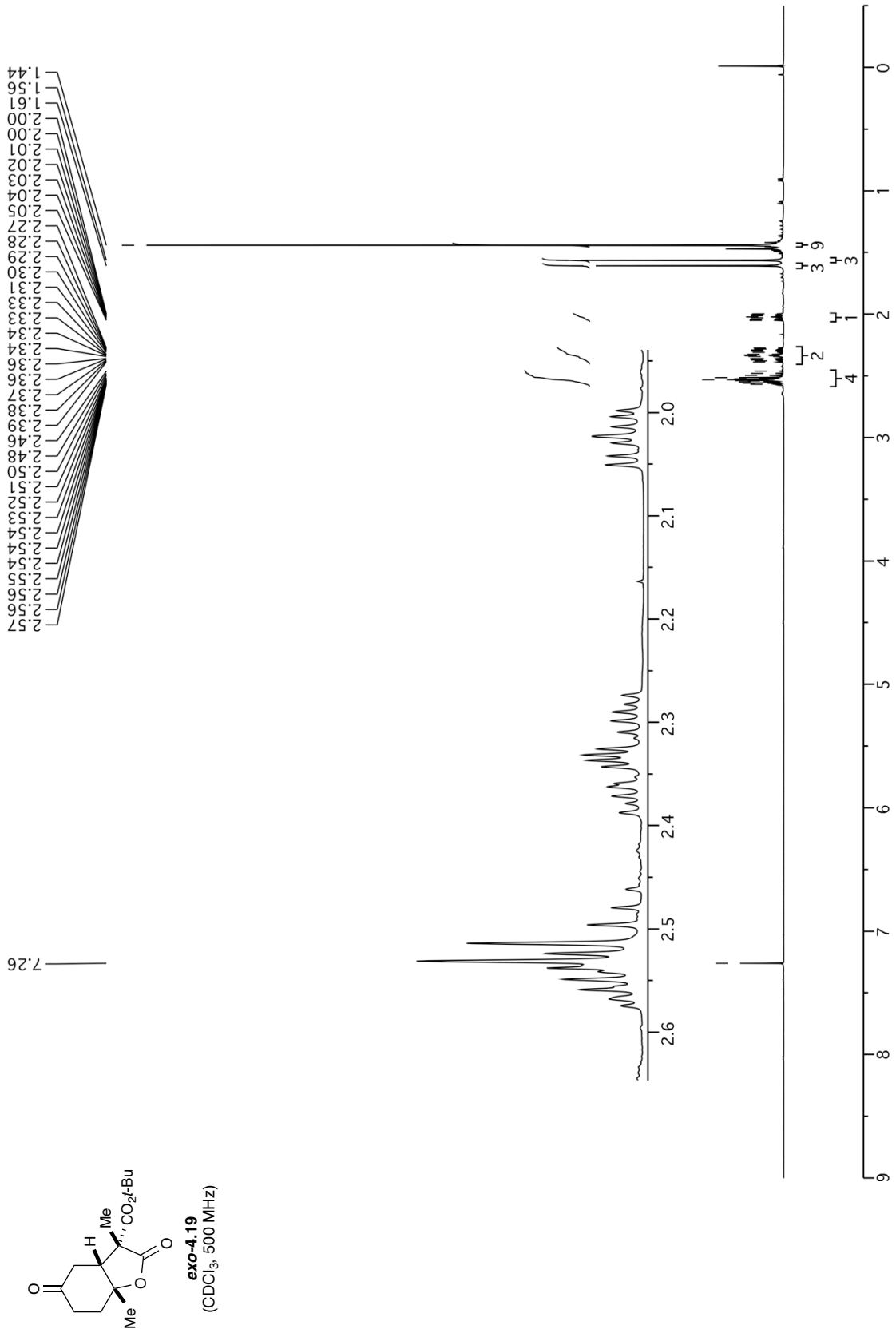
1.44
1.56
1.61
2.00
2.00
2.01
2.02
2.03
2.04
2.05
2.27
2.28
2.29
2.30
2.31
2.33
2.33
2.34
2.34
2.36
2.36
2.37
2.38
2.39
2.46
2.48
2.50
2.51
2.52
2.53
2.54
2.54
2.54
2.55
2.56
2.56
2.57
7.26
Me
H
CO2t-Bu
O
O
O
Me
exo-4.19
(CDCl3, 500 MHz)

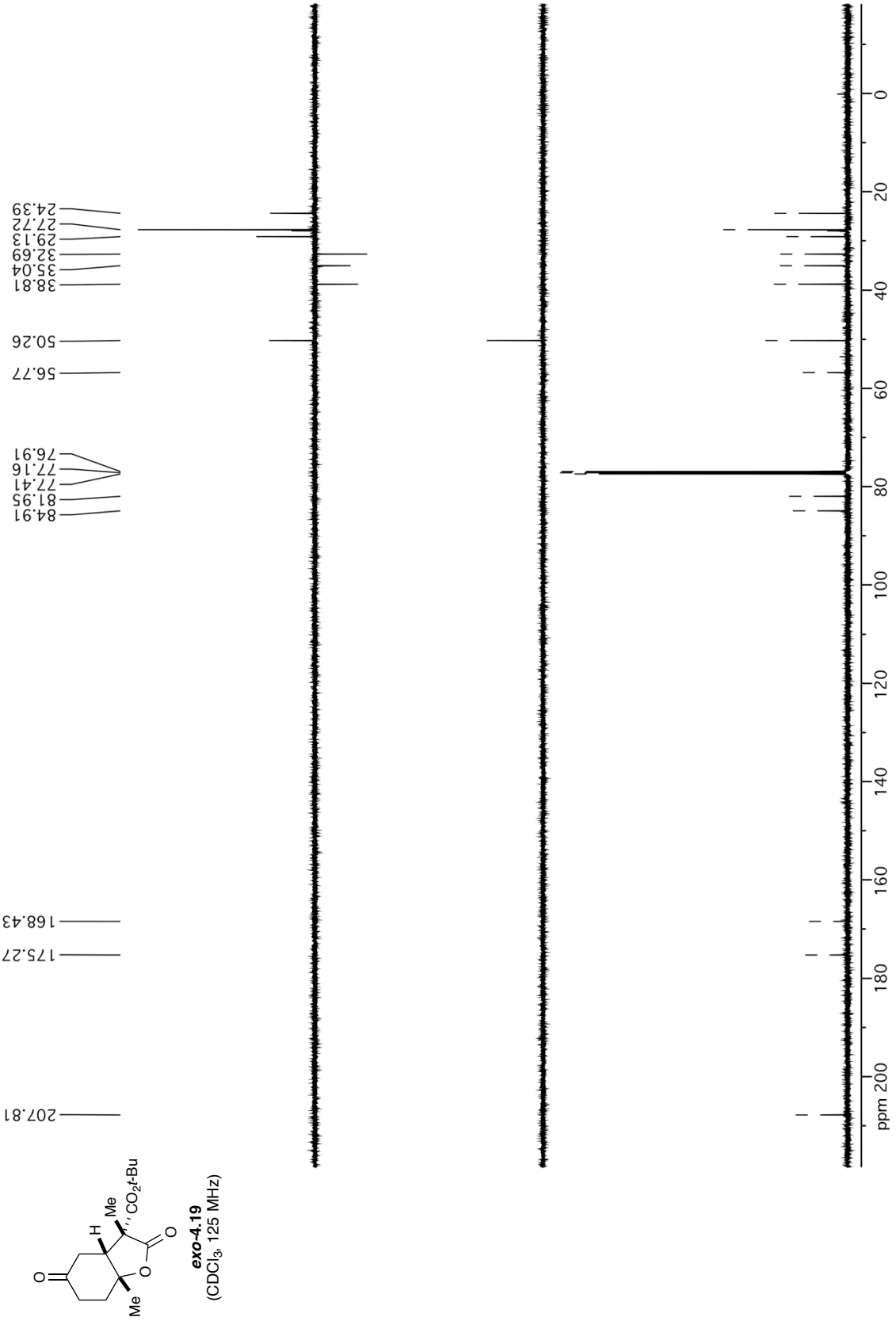

***exo*-4.19**
($CDCl_3$, 125 MHz)

Chapter 5

Spectra

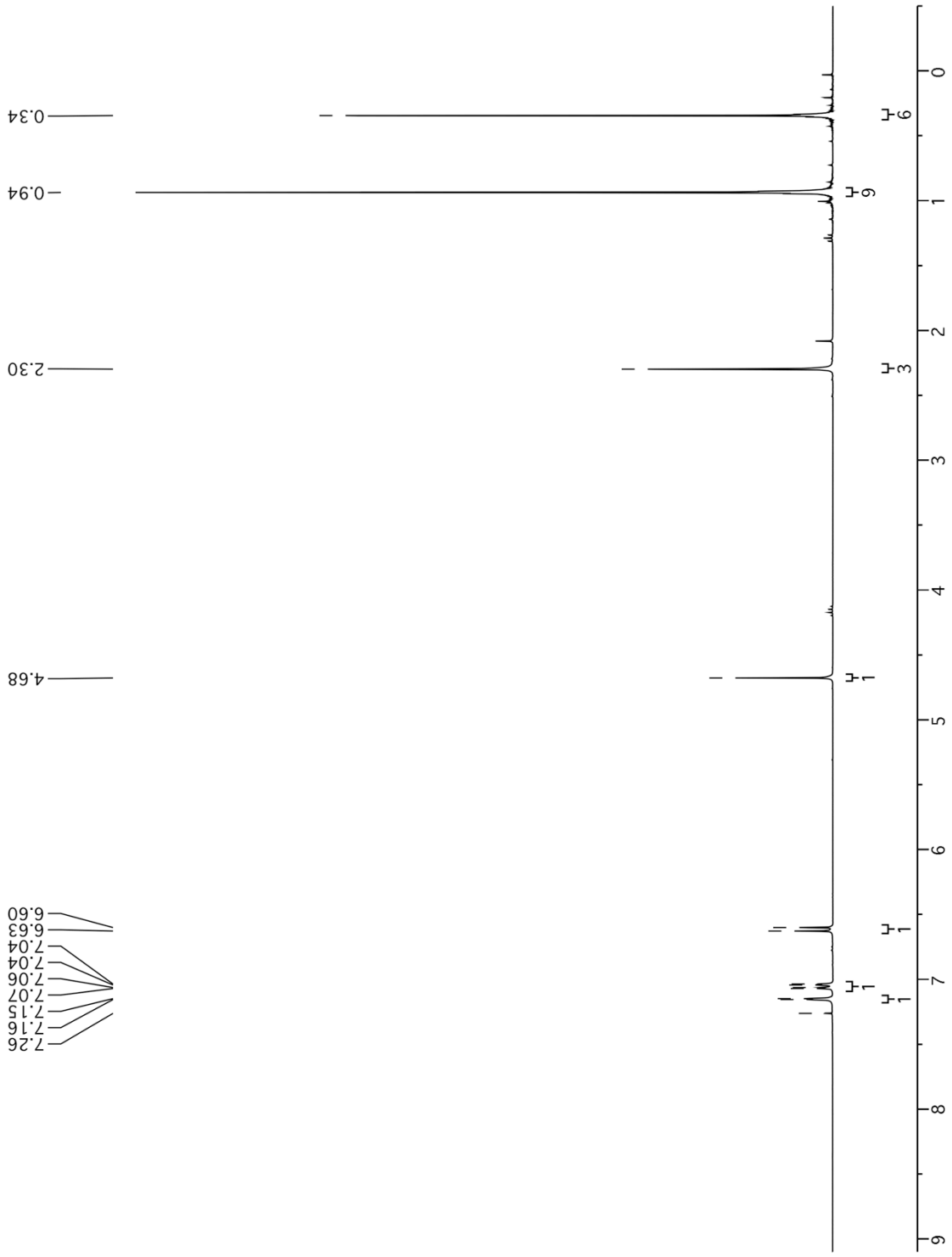

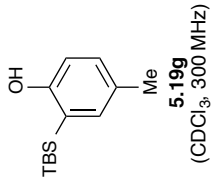

5.19g
($CDCl_3$, 300 MHz)

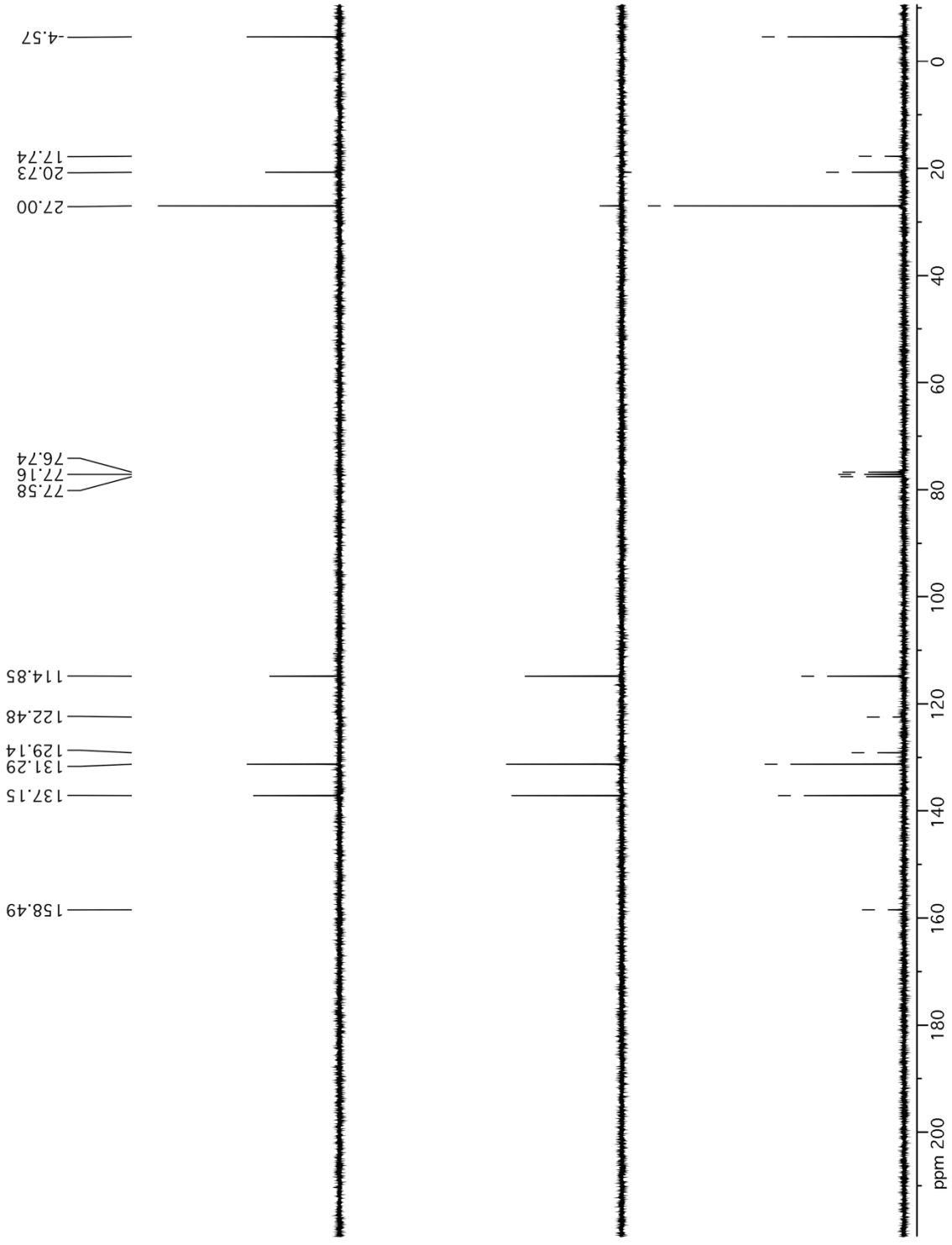

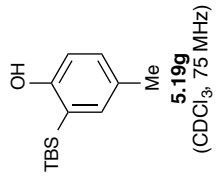

5.19g
($CDCl_3$, 75 MHz)

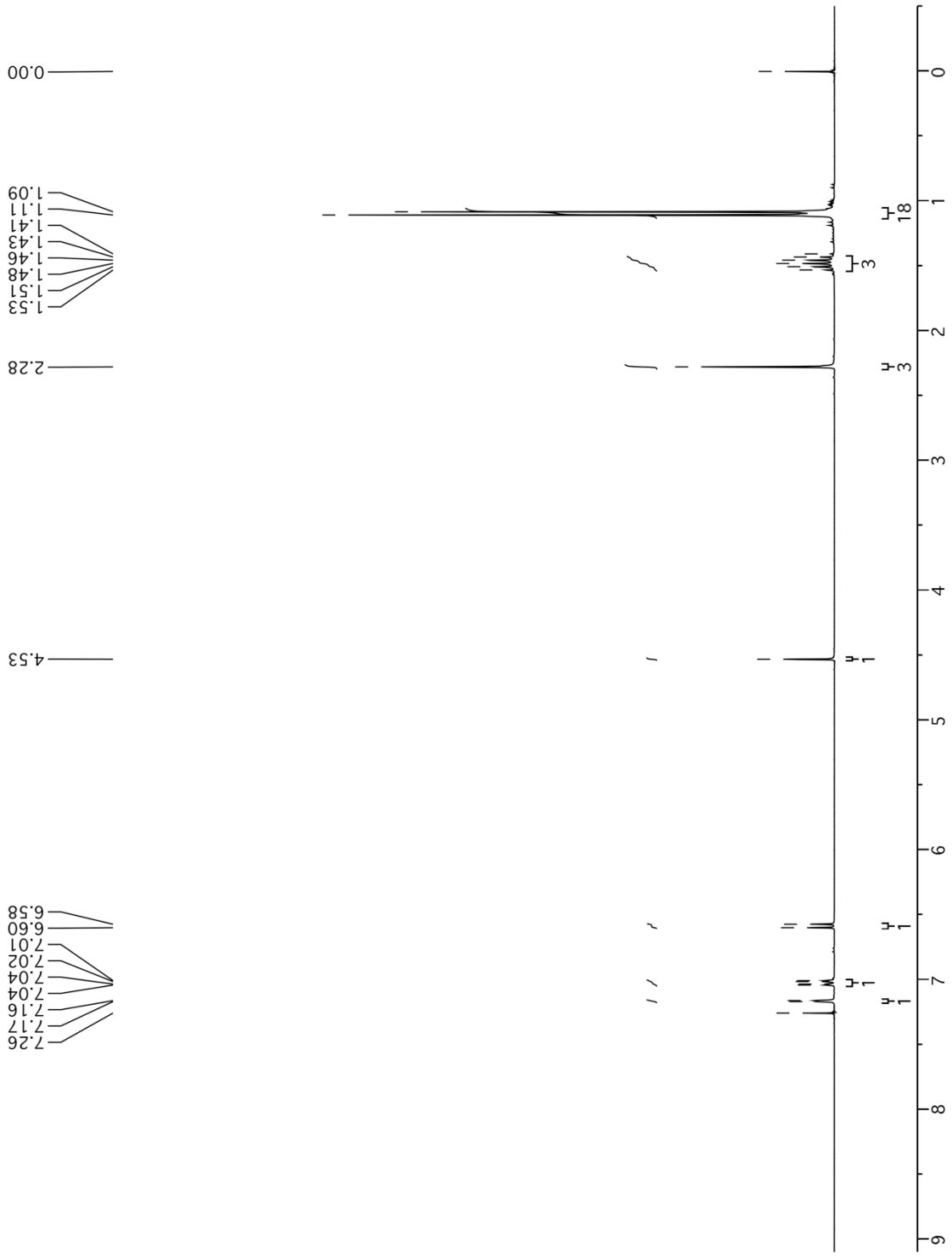

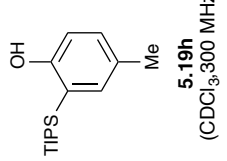

5.19h
($CDCl_3$,300 MHz)

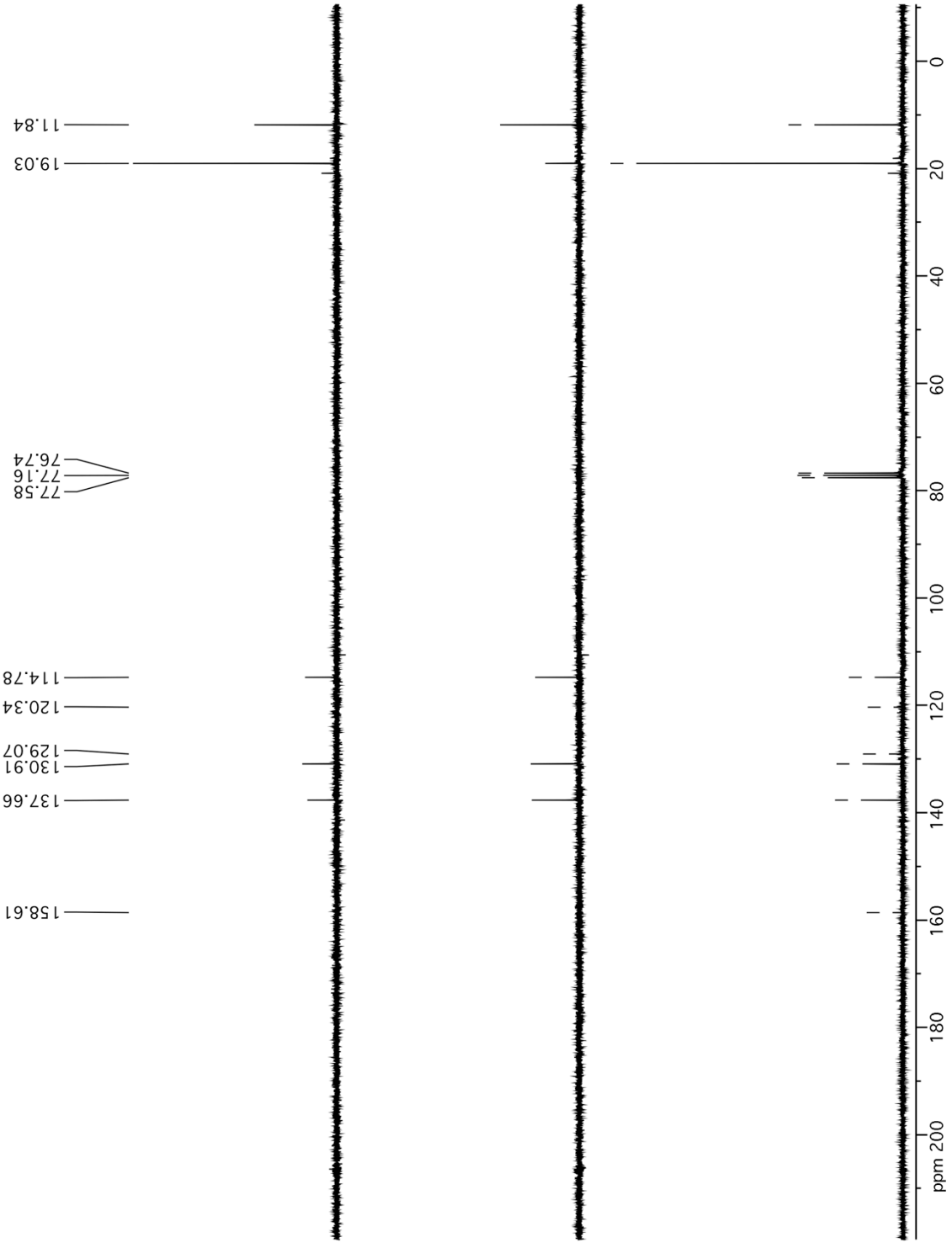

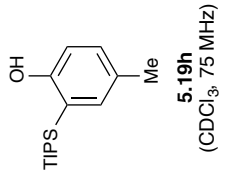

5.19h
($CDCl_3$, 75 MHz)

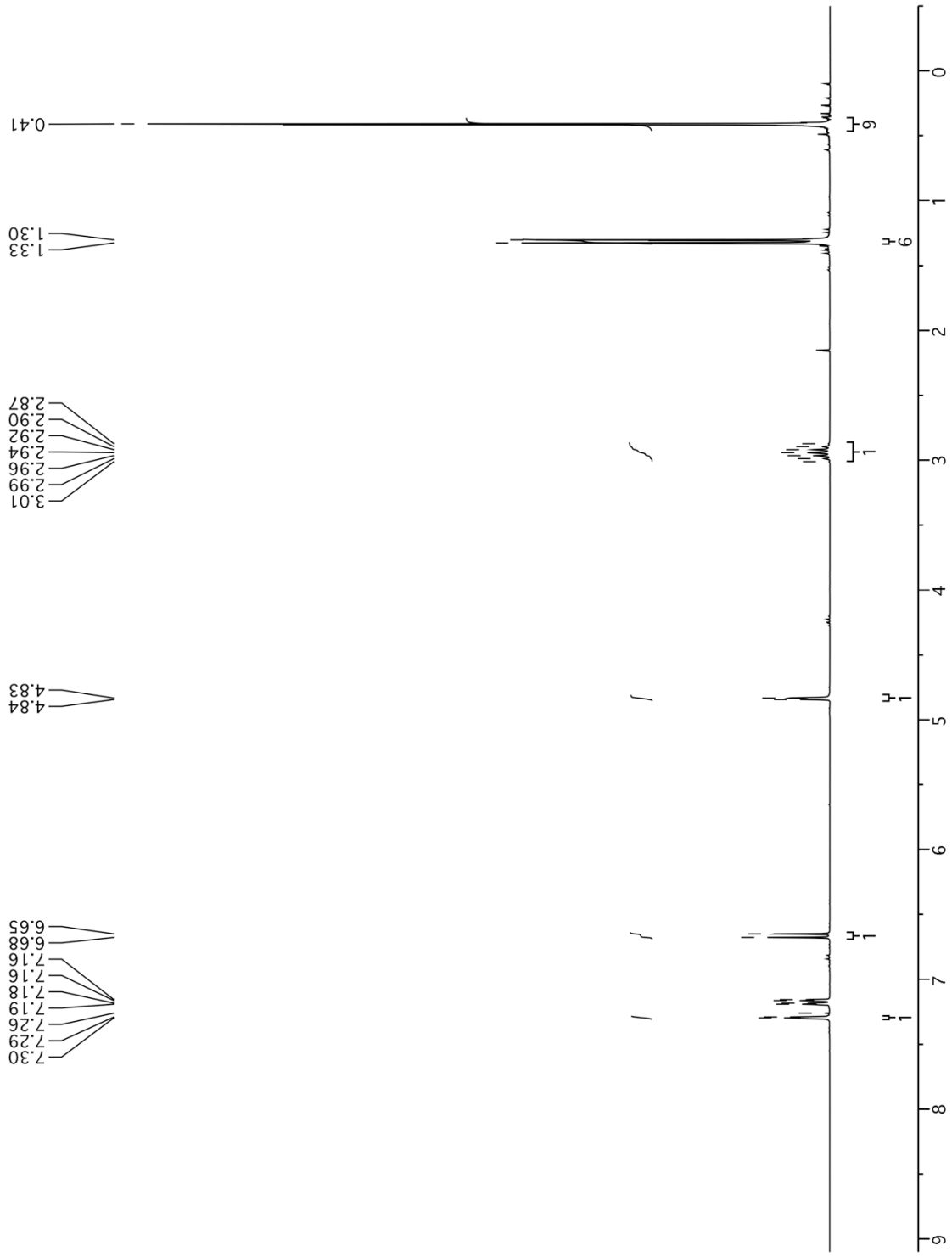

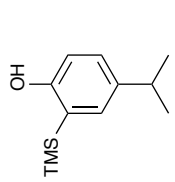

5.19i
($CDCl_3$, 300 MHz)

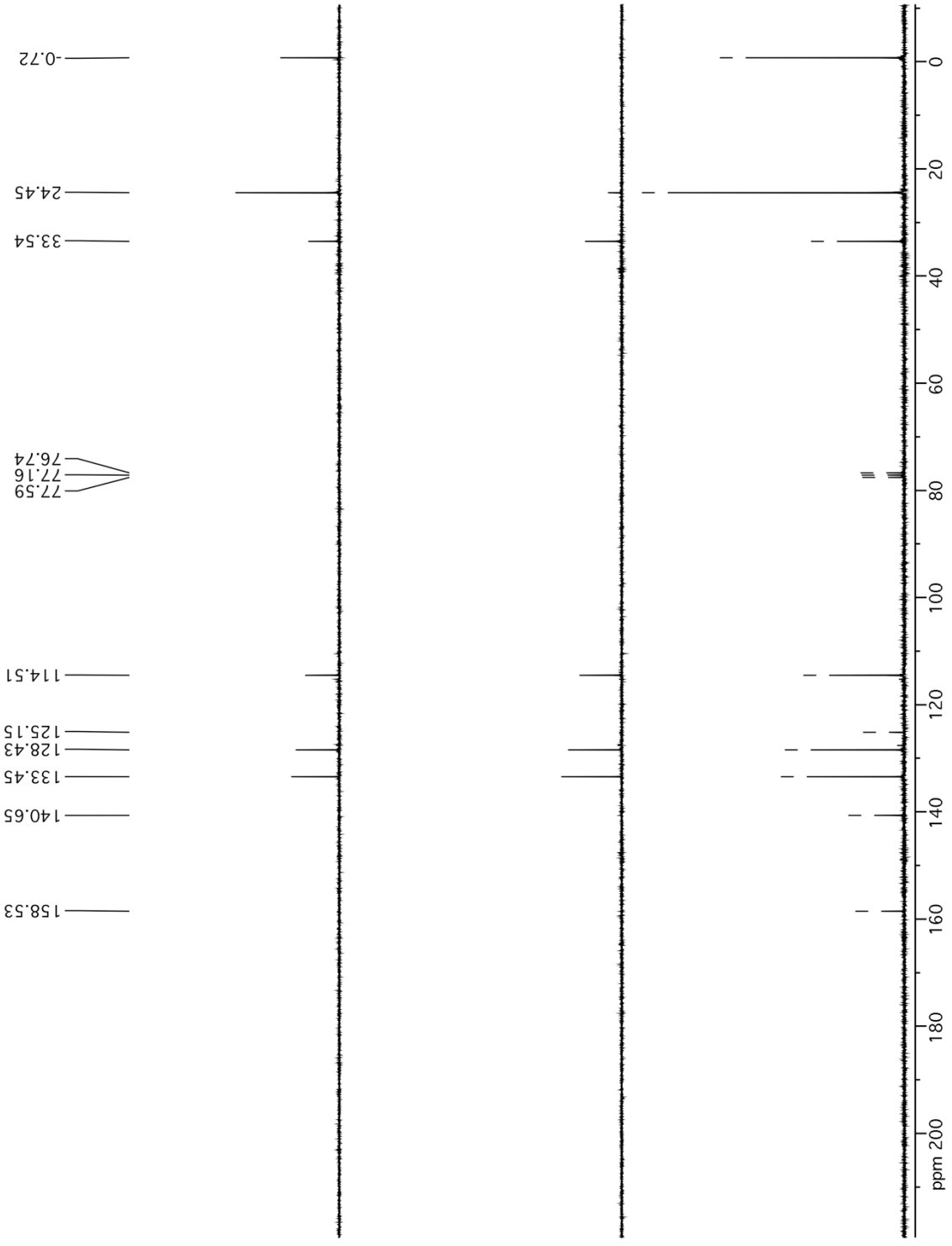

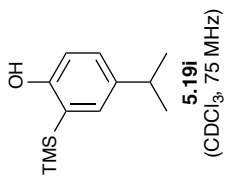

5.19i
($CDCl_3$, 75 MHz)

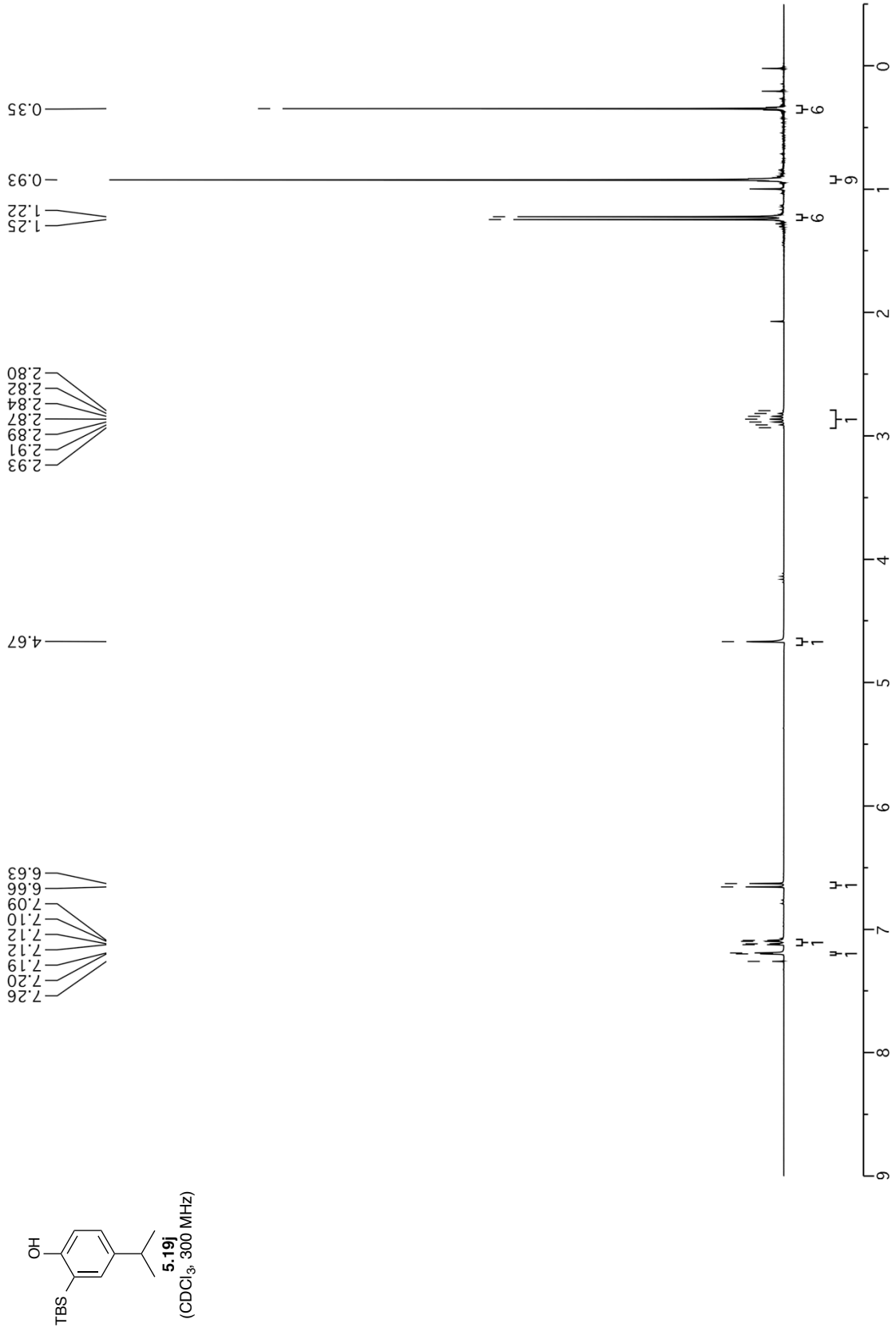

5.19j
($CDCl_3$, 300 MHz)

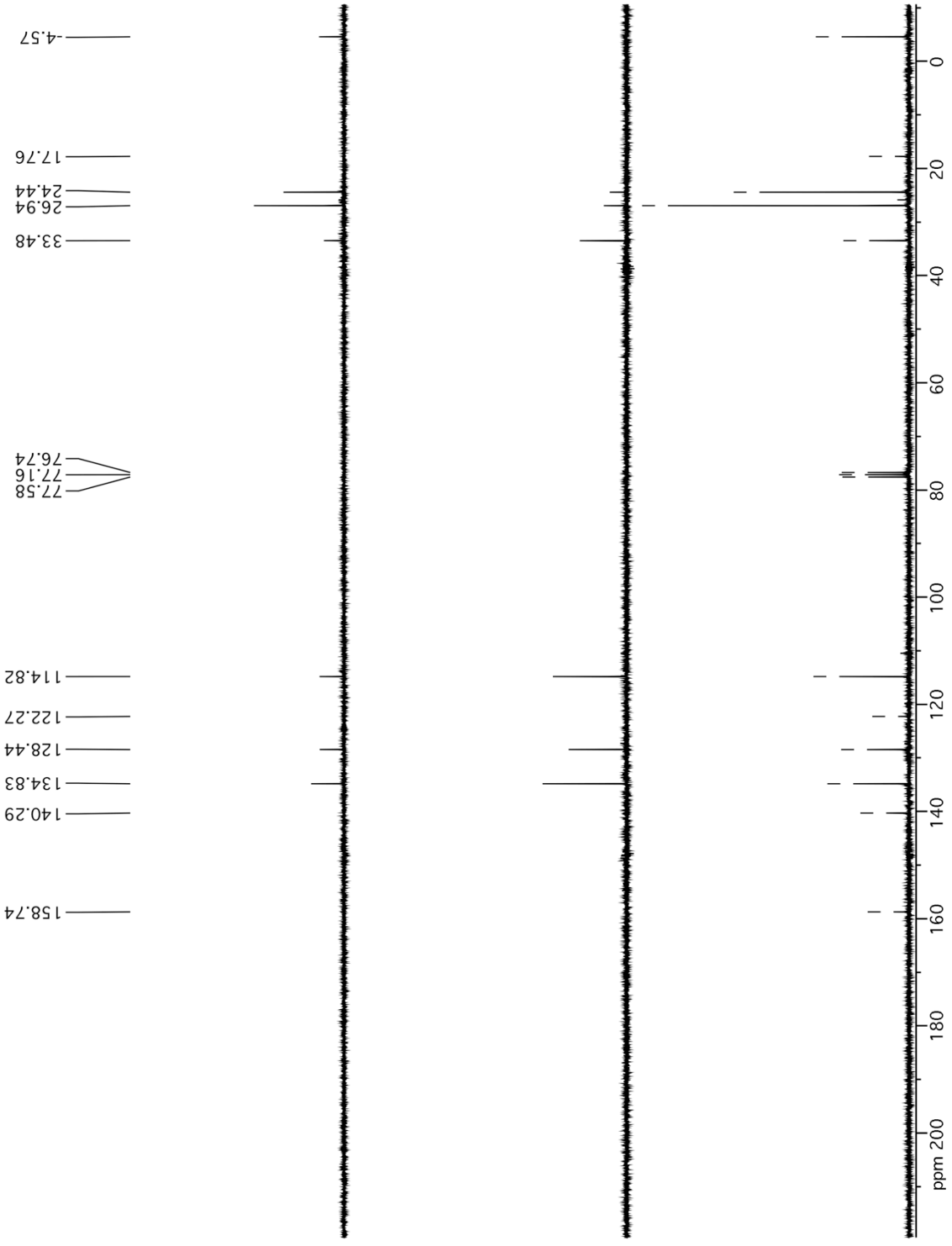

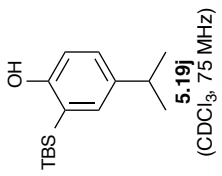

5.19j
($CDCl_3$, 75 MHz)

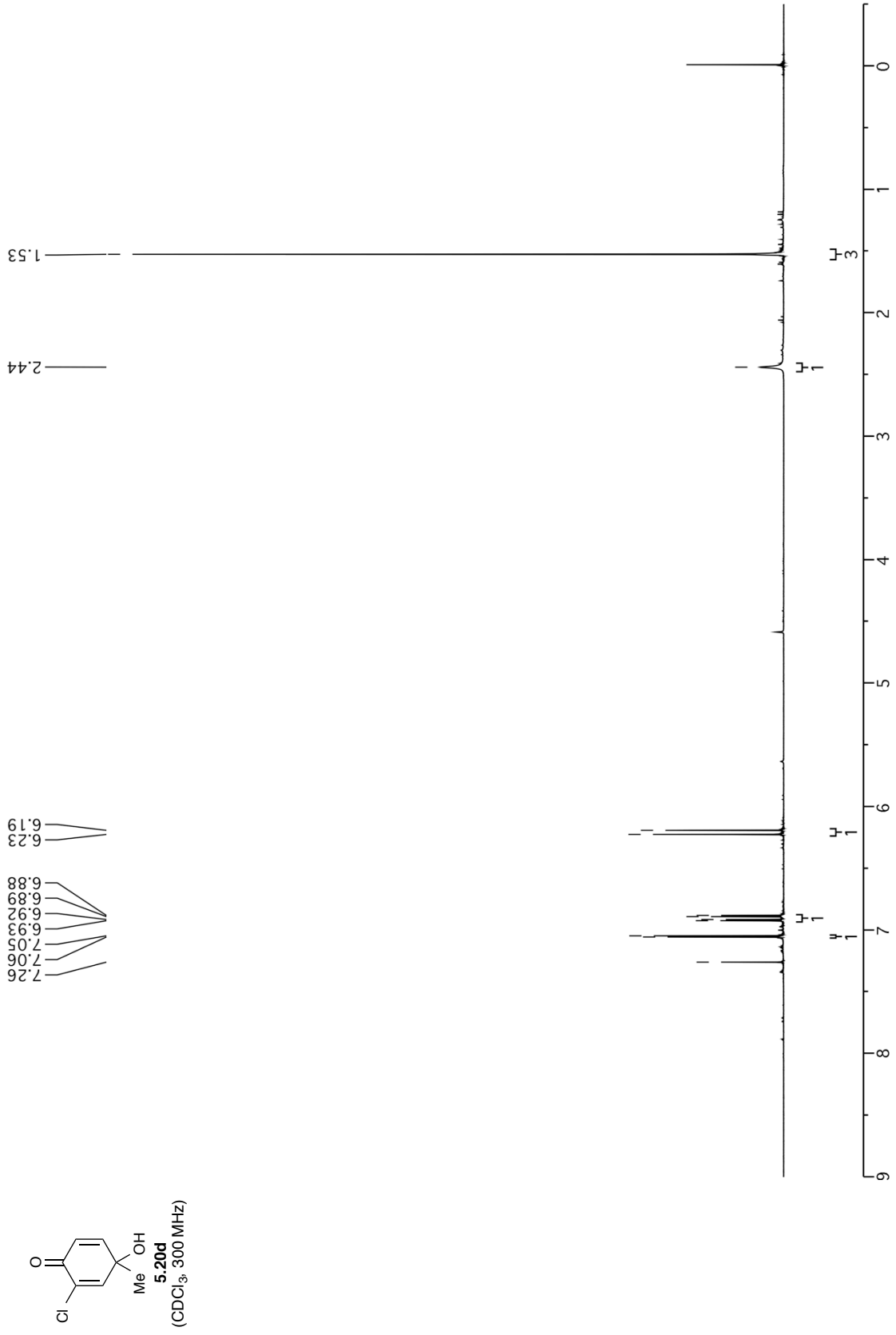

5.20d
($CDCl_3$, 300 MHz)

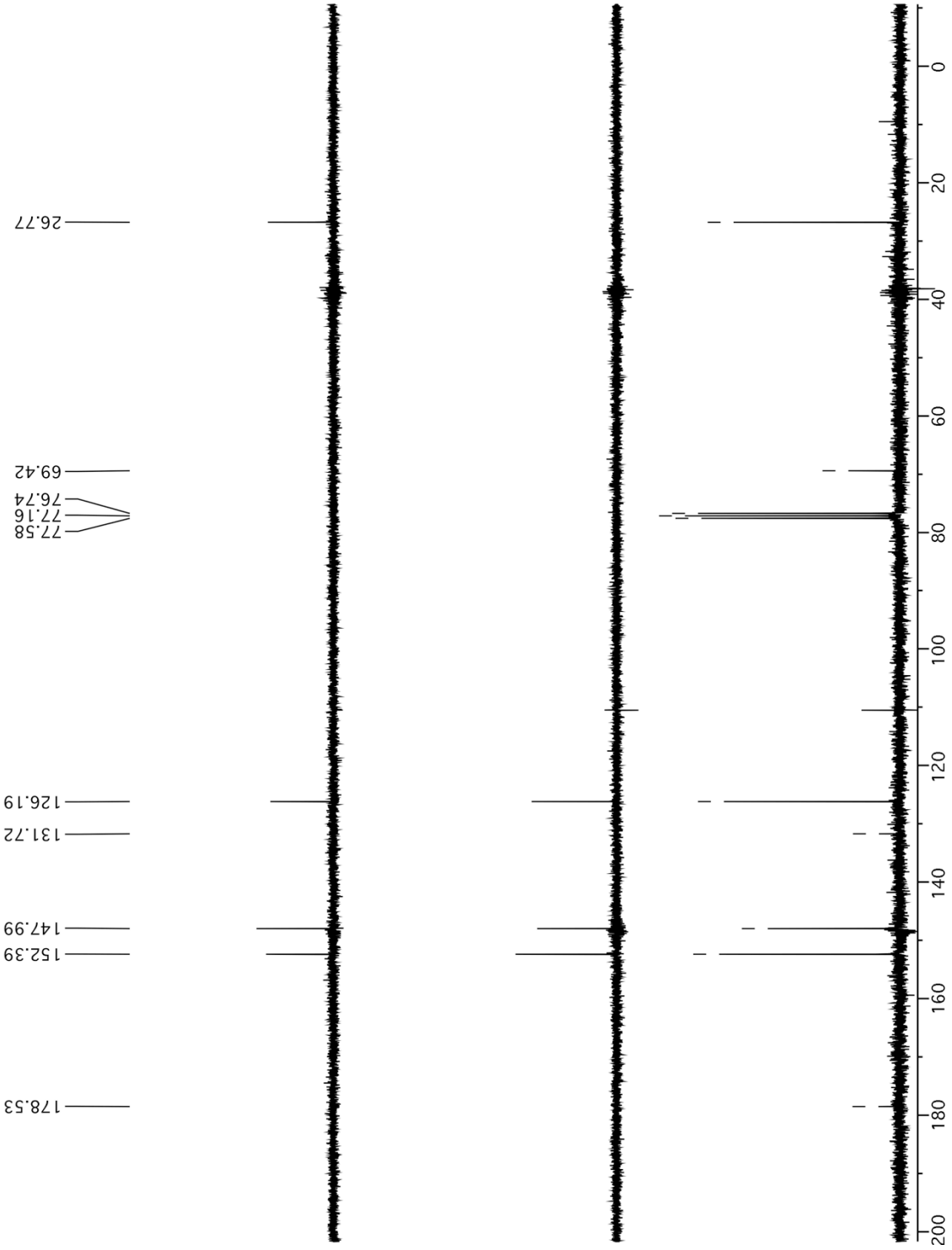

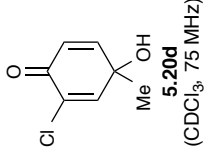

5.20d
($CDCl_3$, 75 MHz)

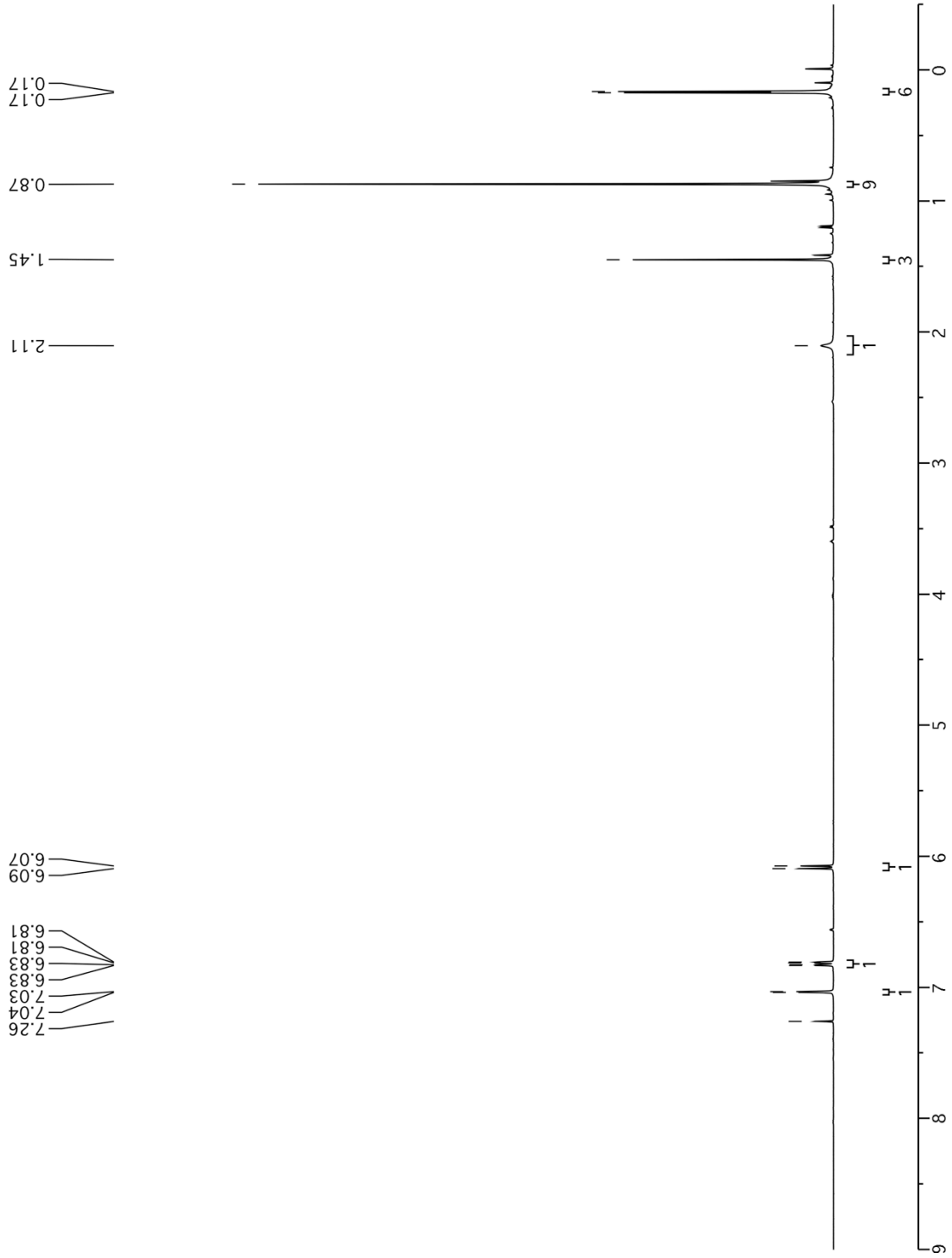
0.17
0.17
0.87
1.45
2.11
6.07
6.09
6.81
6.81
6.83
6.83
7.03
7.04
7.26
6
1
1
1
3
9
6
TBS
Me
OH
O
5.20g
(CDCl3, 500 MHz)

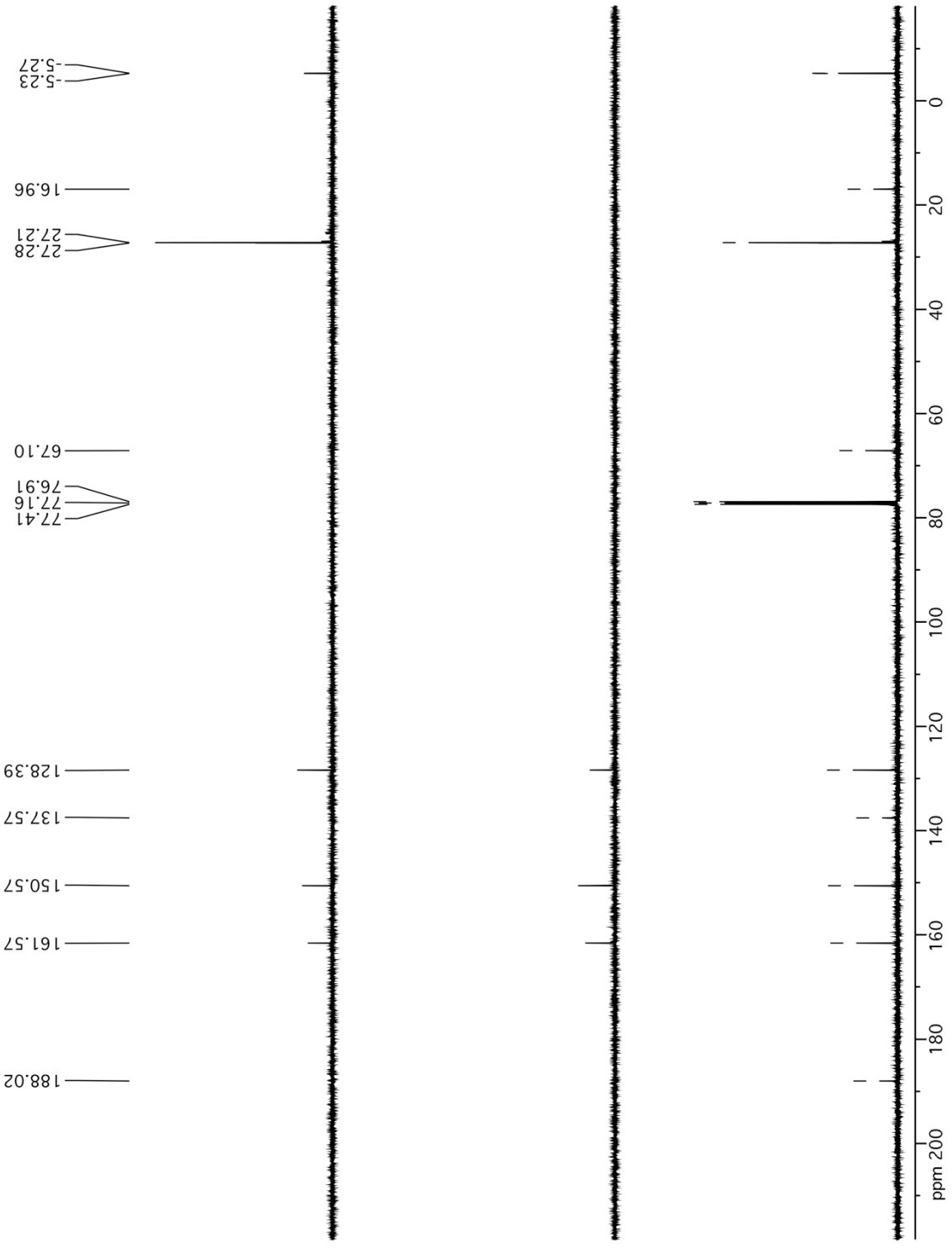

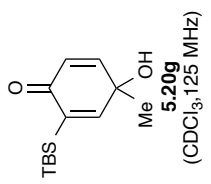

5.20g
($CDCl_3$,125 MHz)

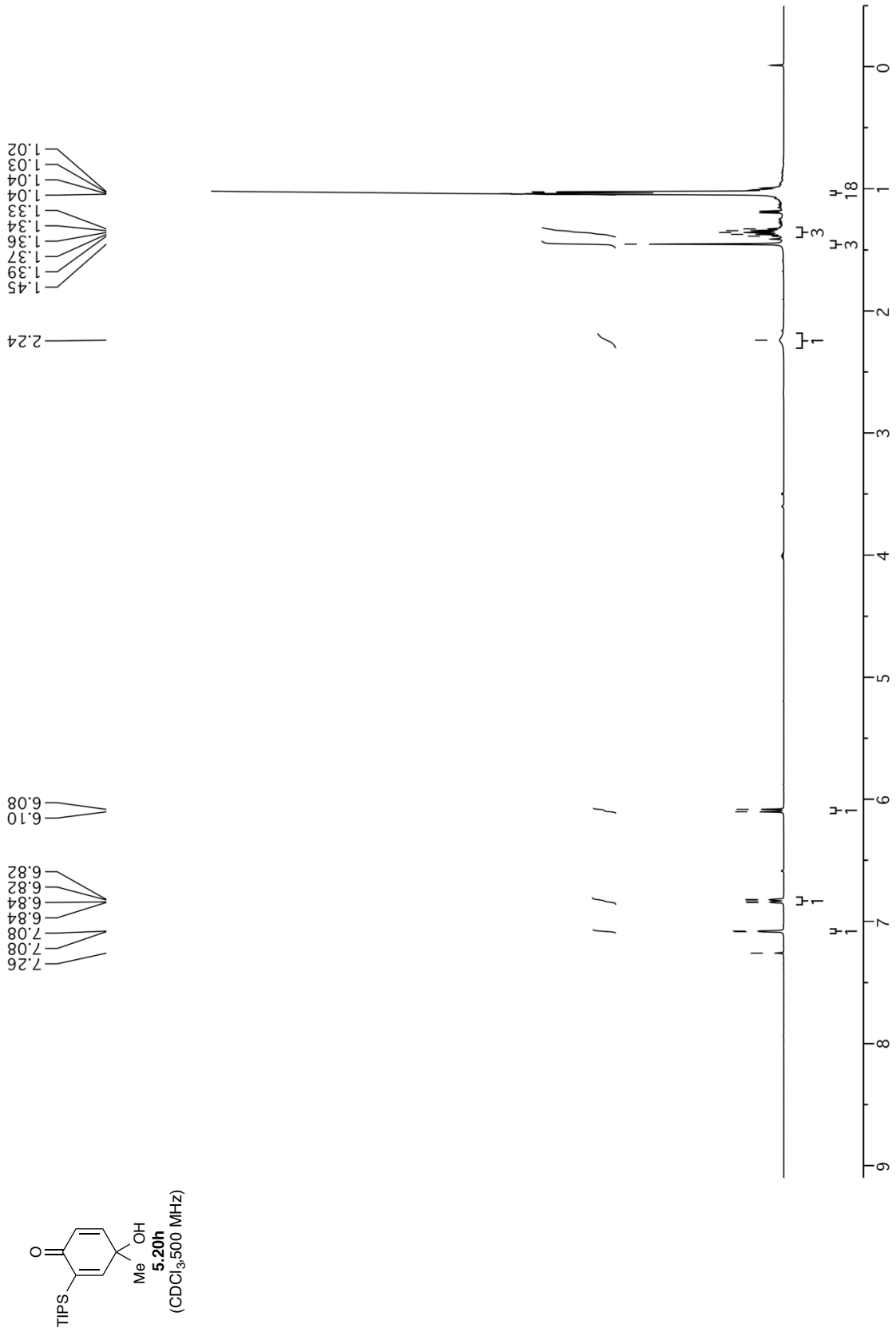

5.20h
($CDCl_3$,500 MHz)

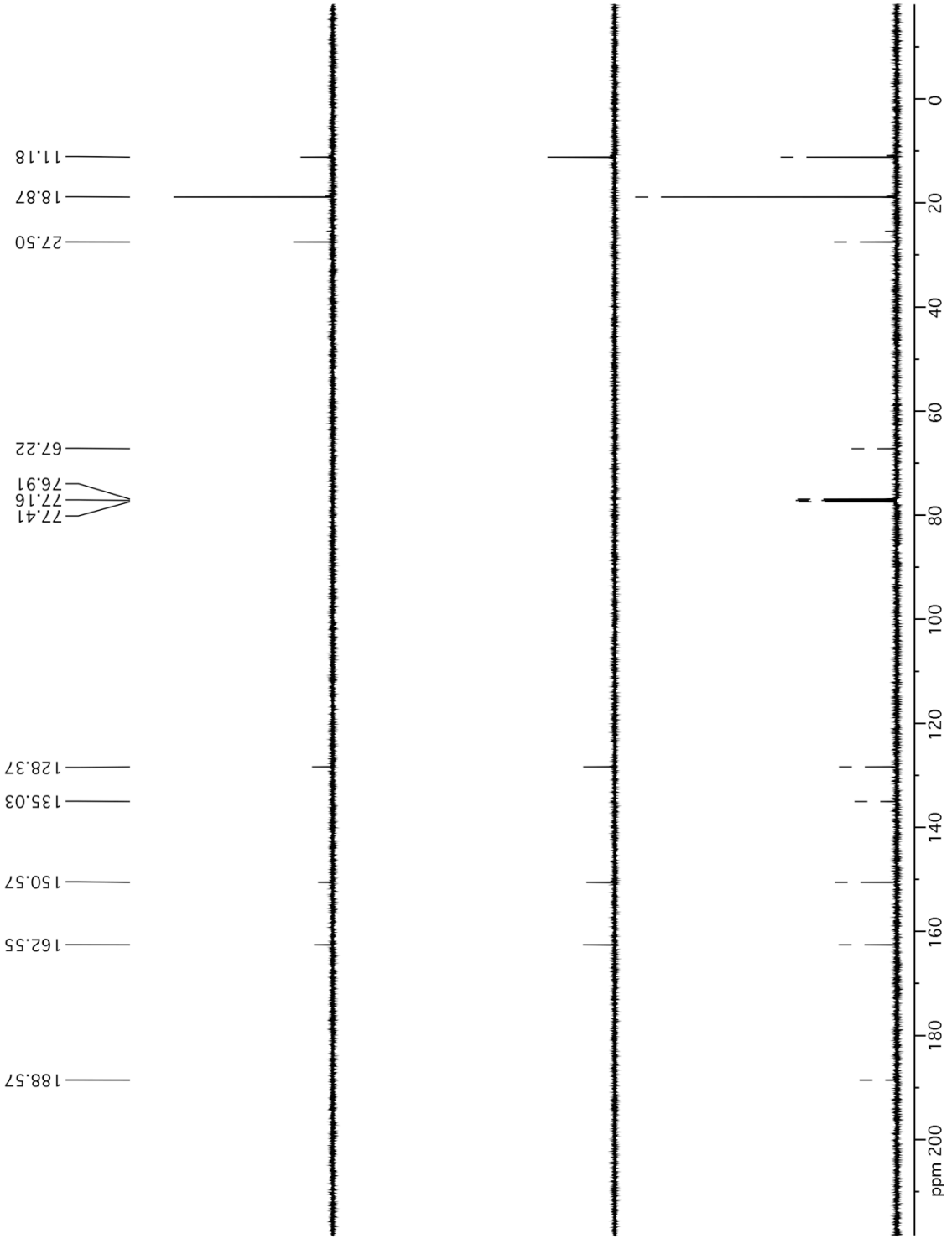

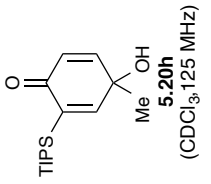

5.20h
($CDCl_3$,125 MHz)

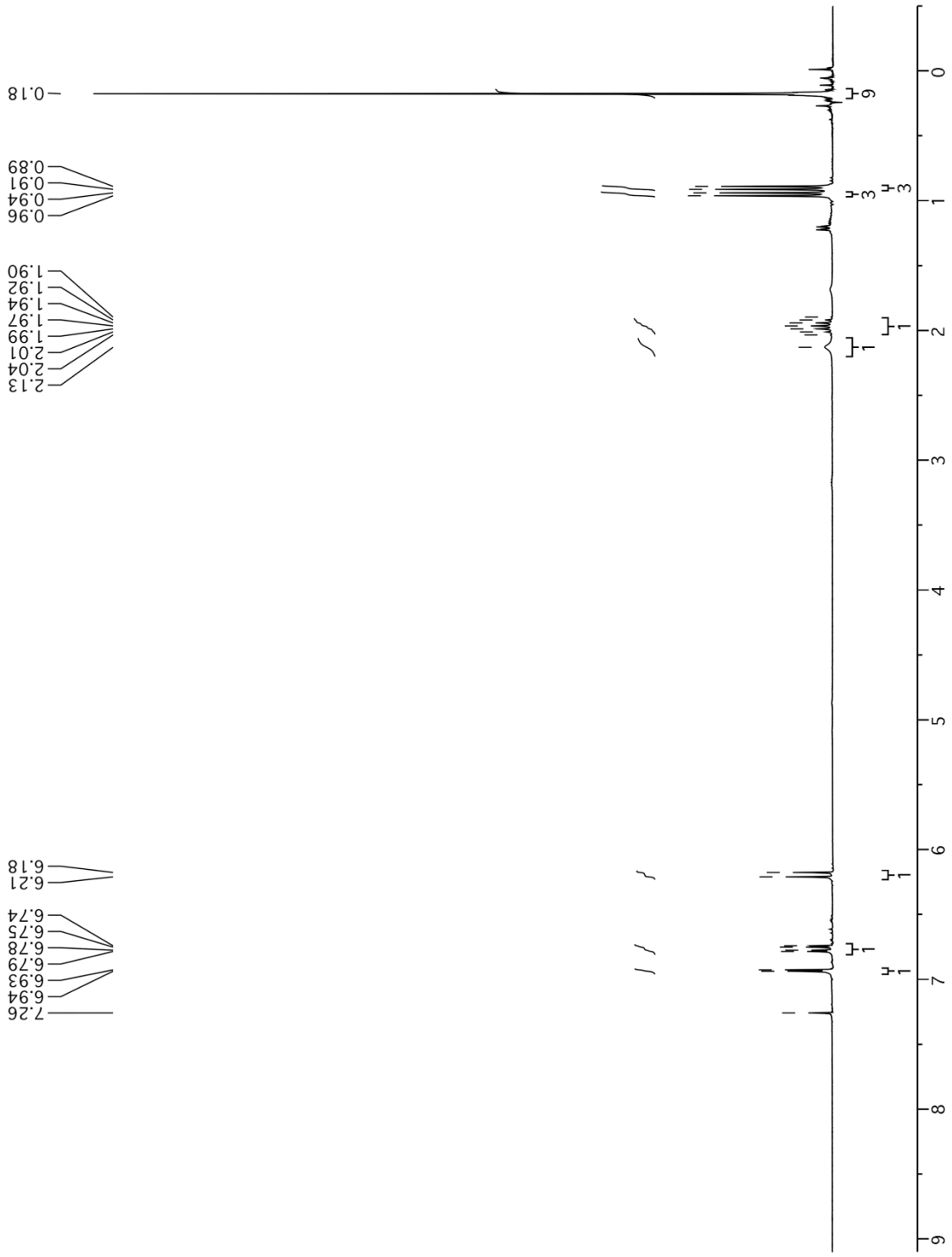

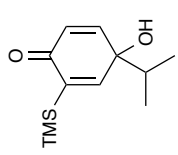

5.20i
($CDCl_3$, 300 MHz)

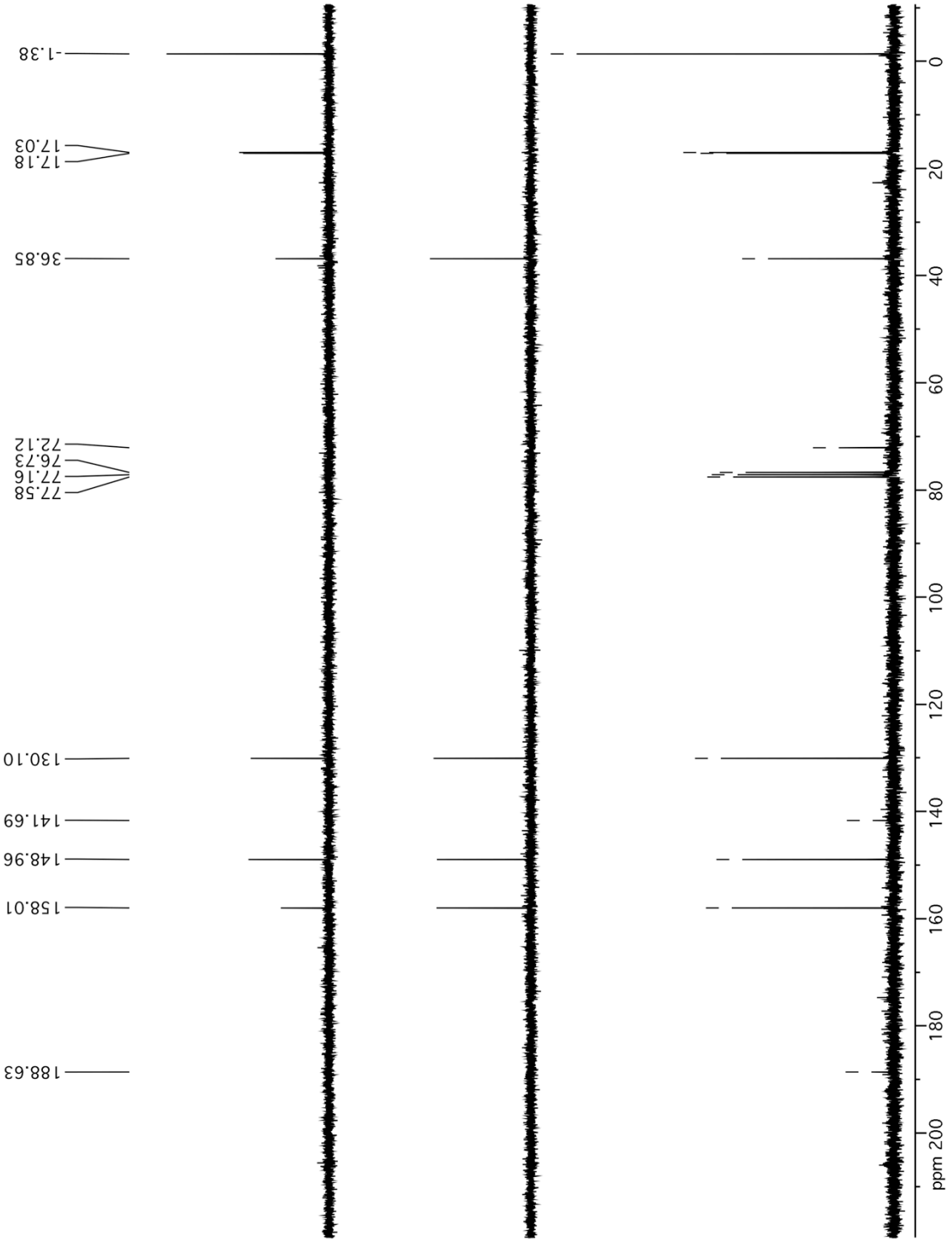

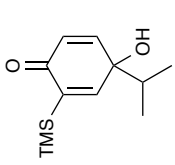

5.20i
($CDCl_3$, 75 MHz)

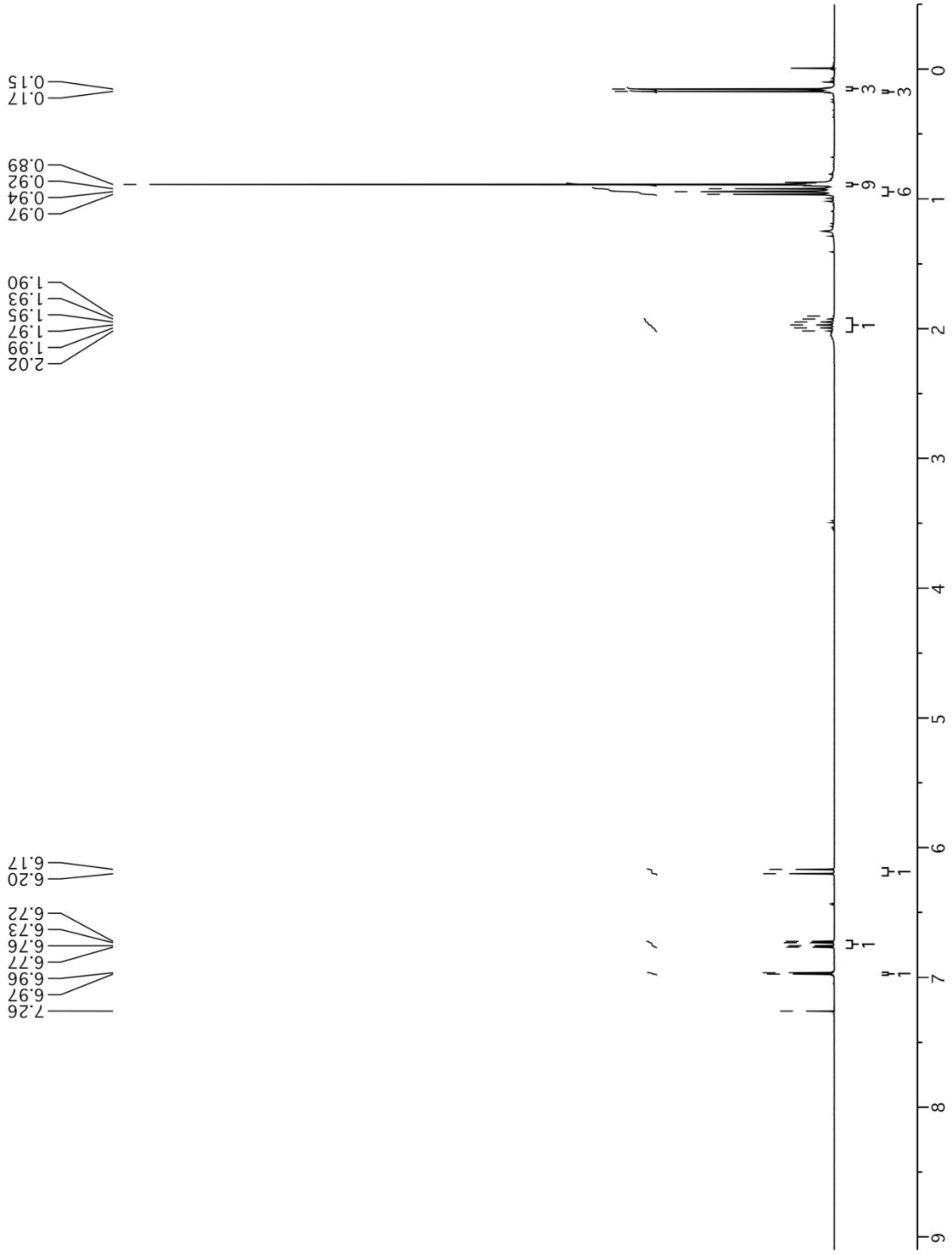

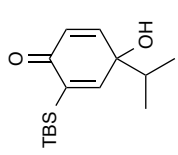

5.20j
($CDCl_3$, 300 MHz)

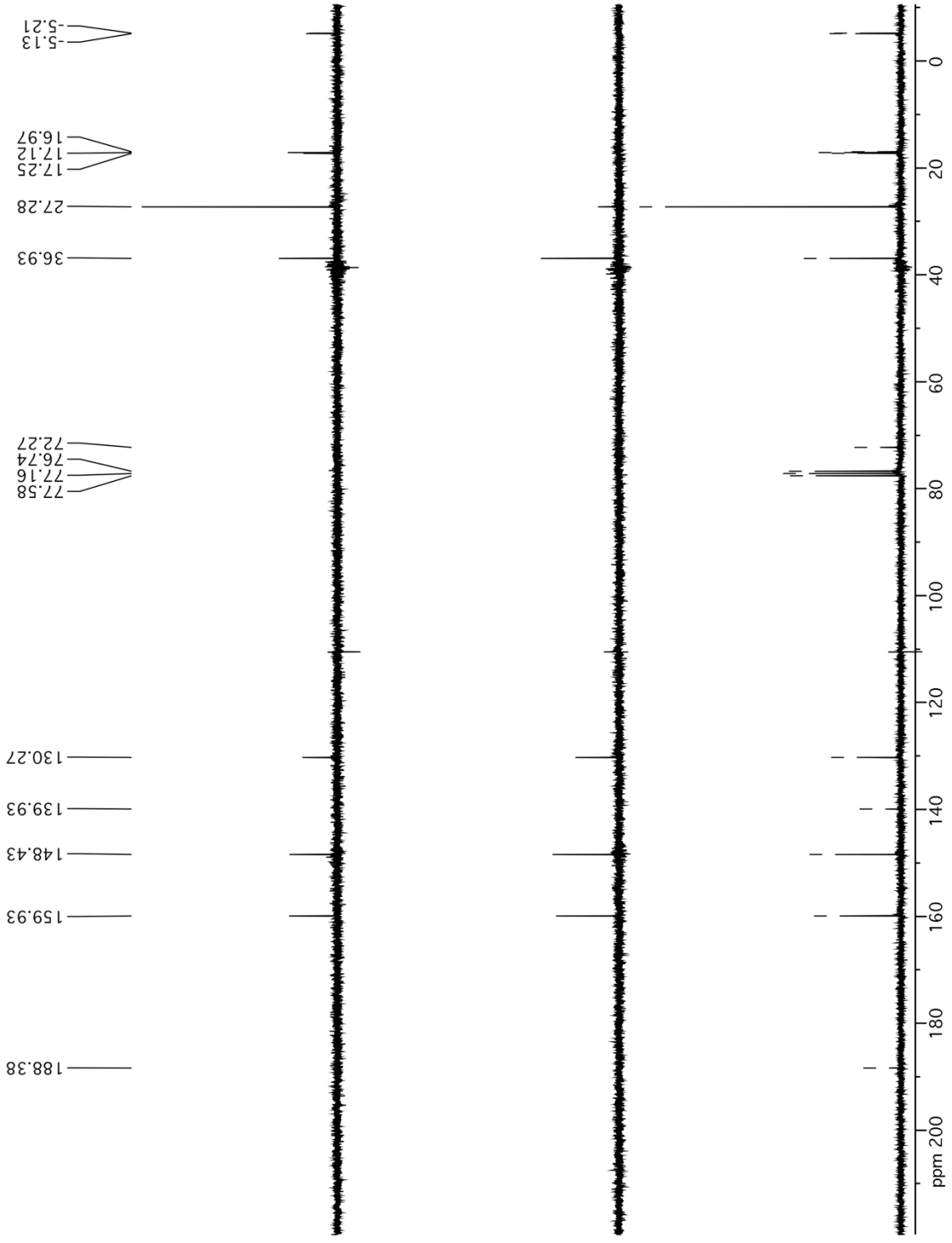

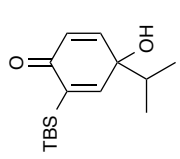

5.20j ($CDCl_3$, 75 MHz)

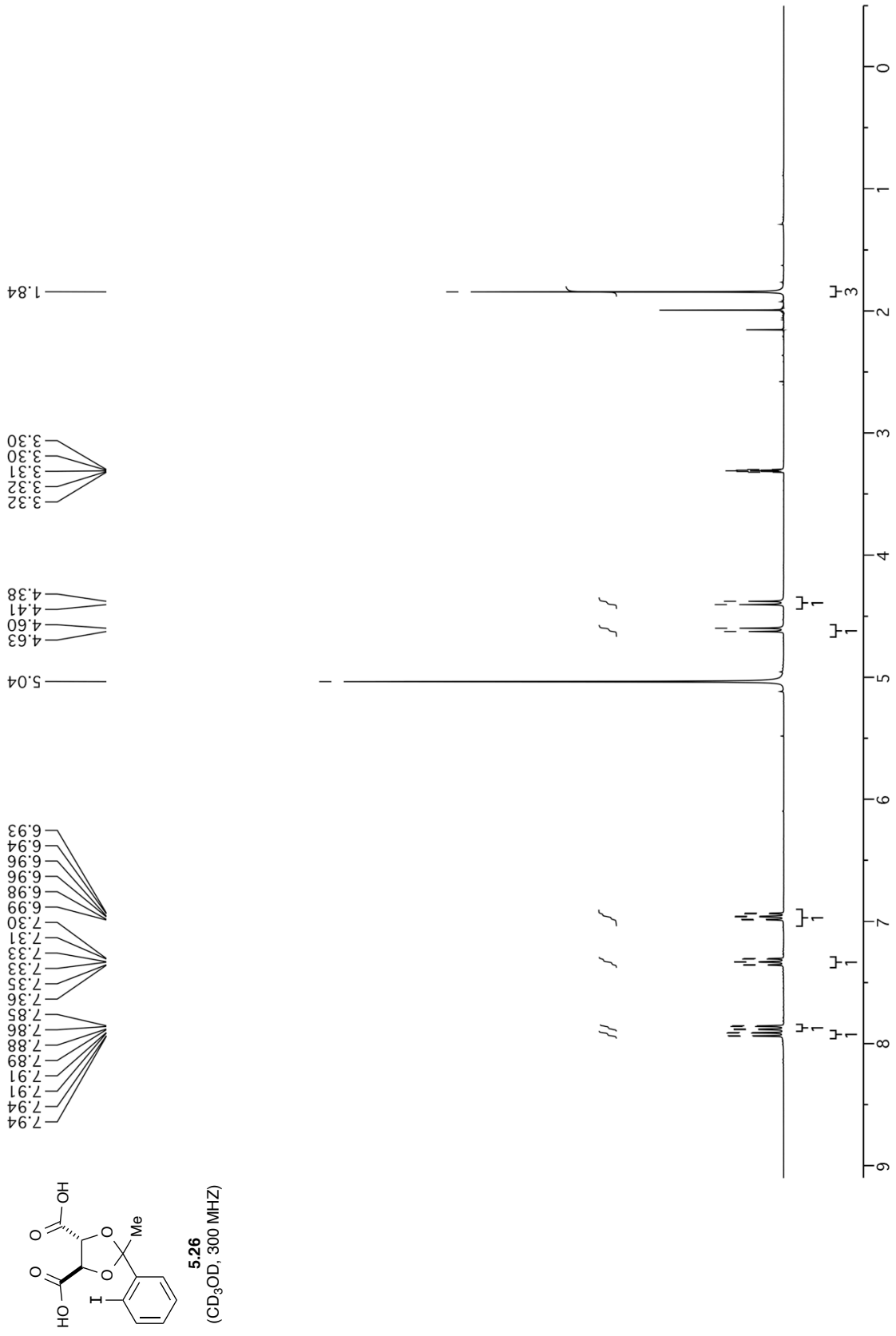

5.26
(CD_3OD, 300 MHZ)

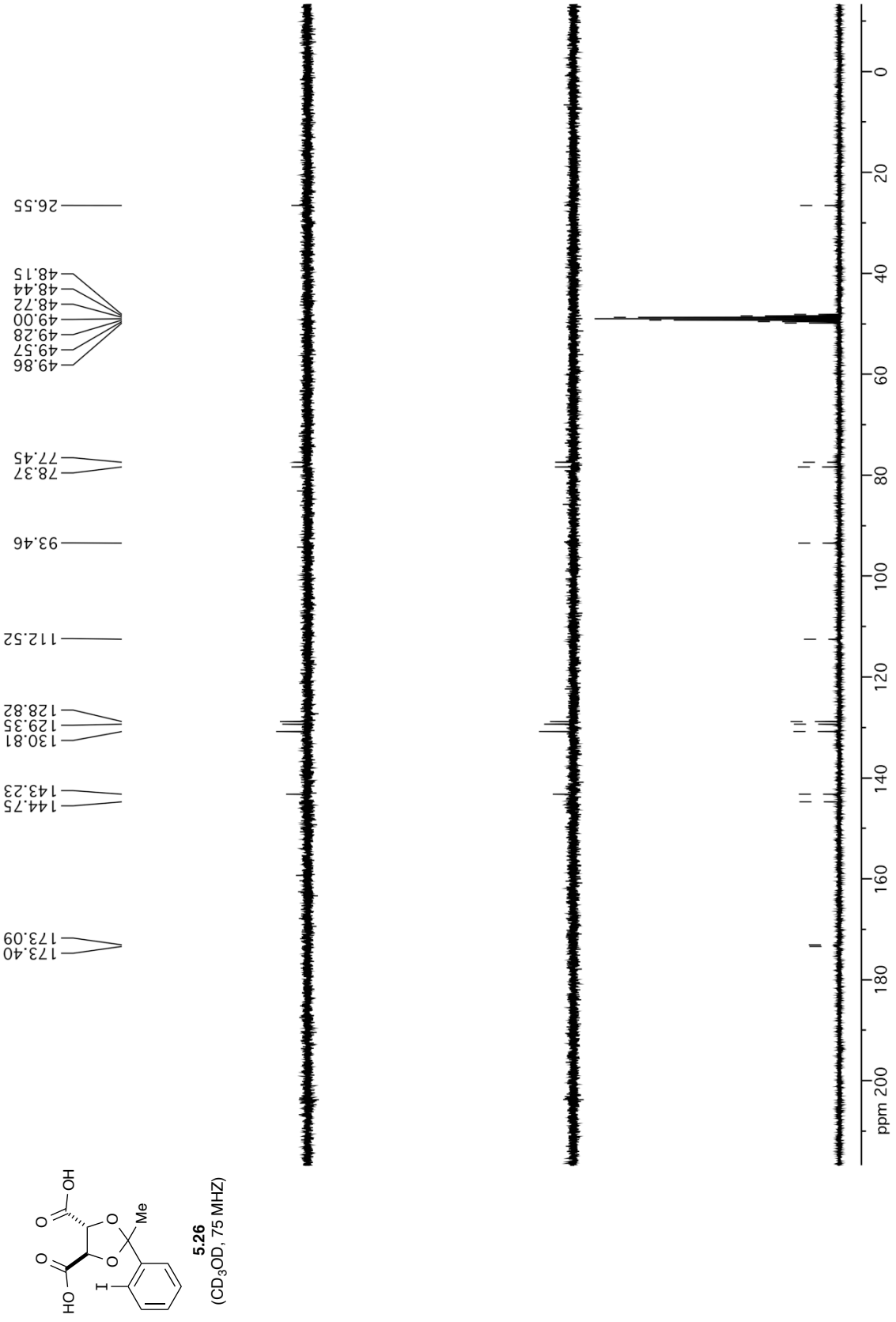

5.26
(CD_3OD, 75 MHZ)

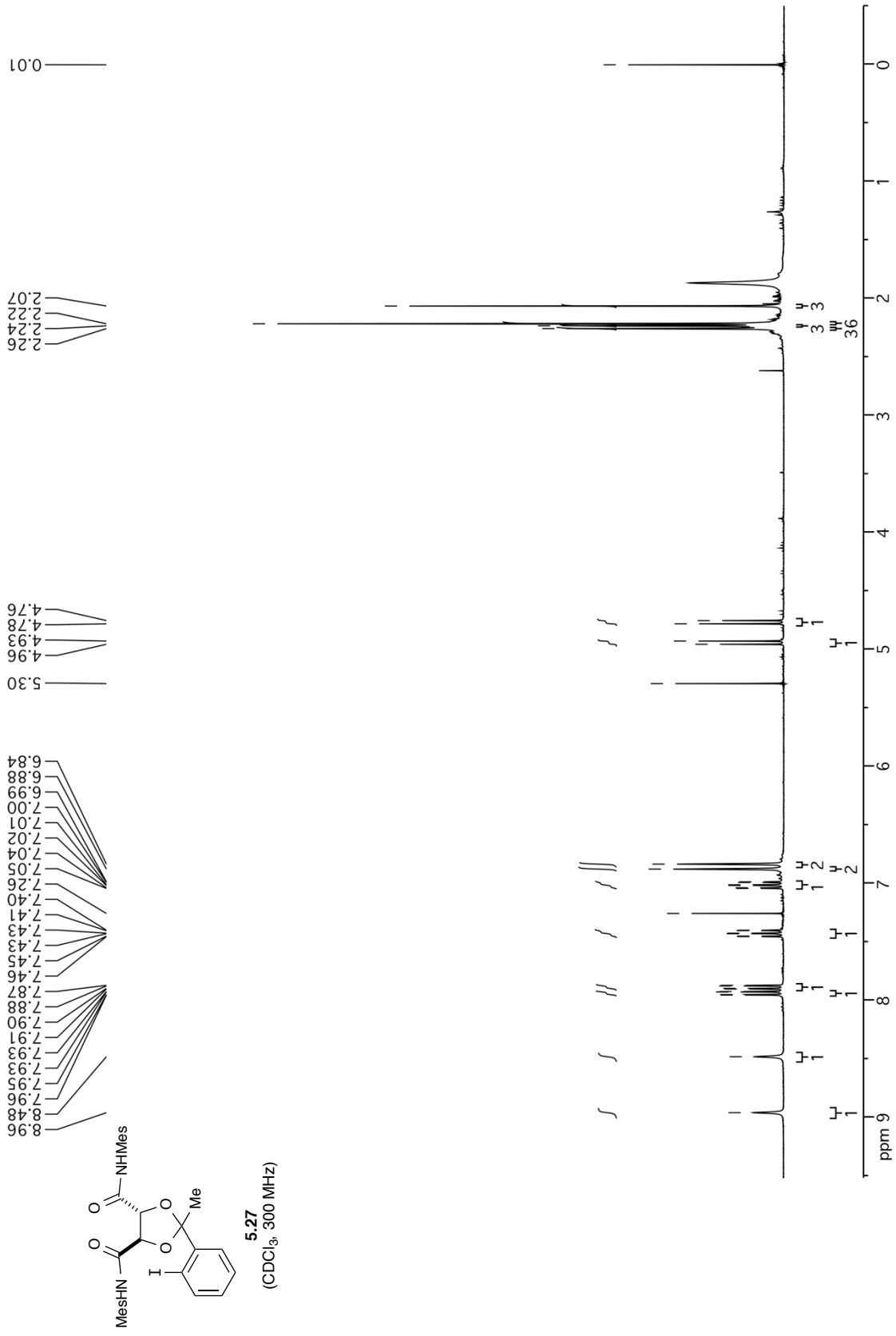

5.27
($CDCl_3$, 300 MHz)

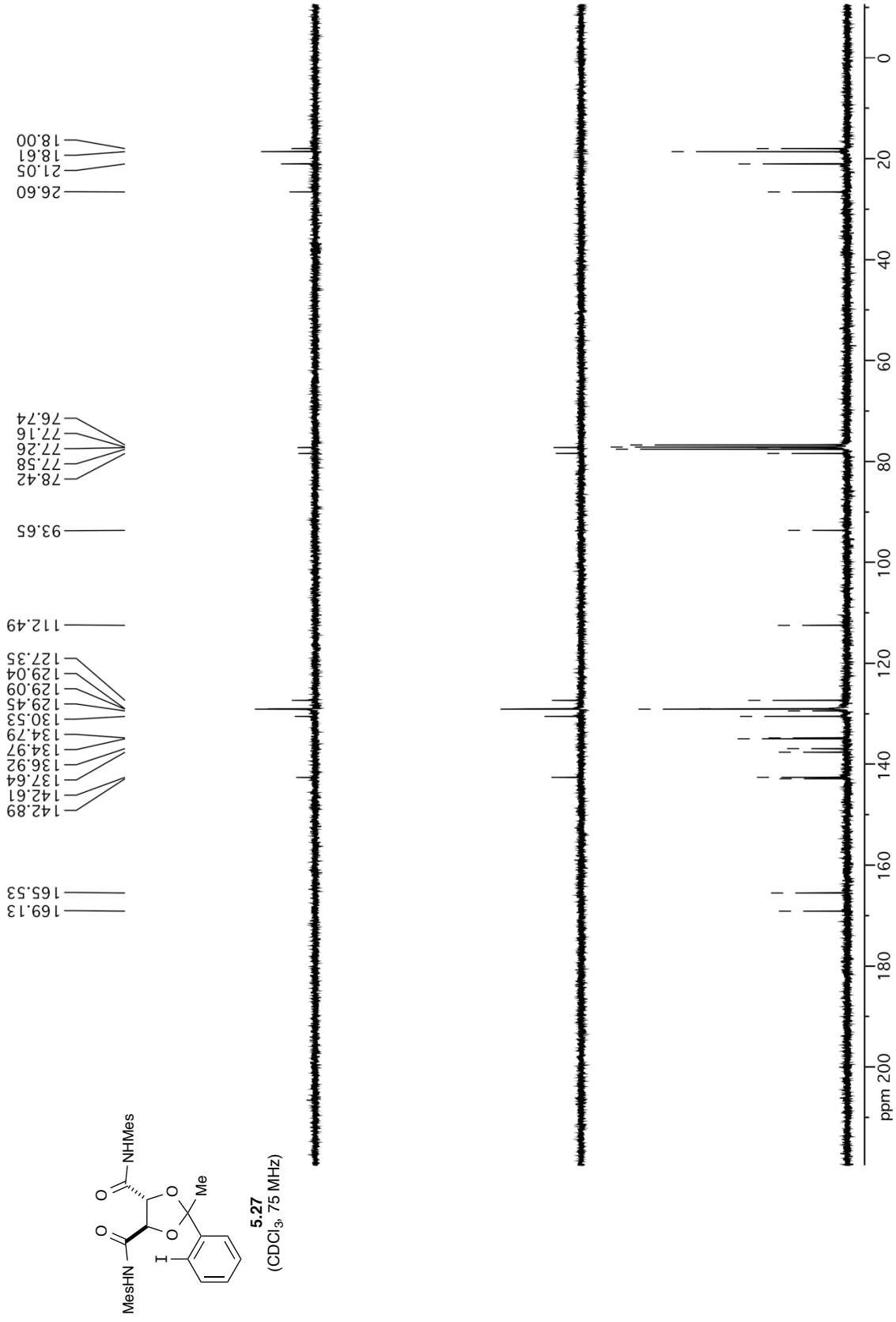

5.27
($CDCl_3$, 75 MHz)

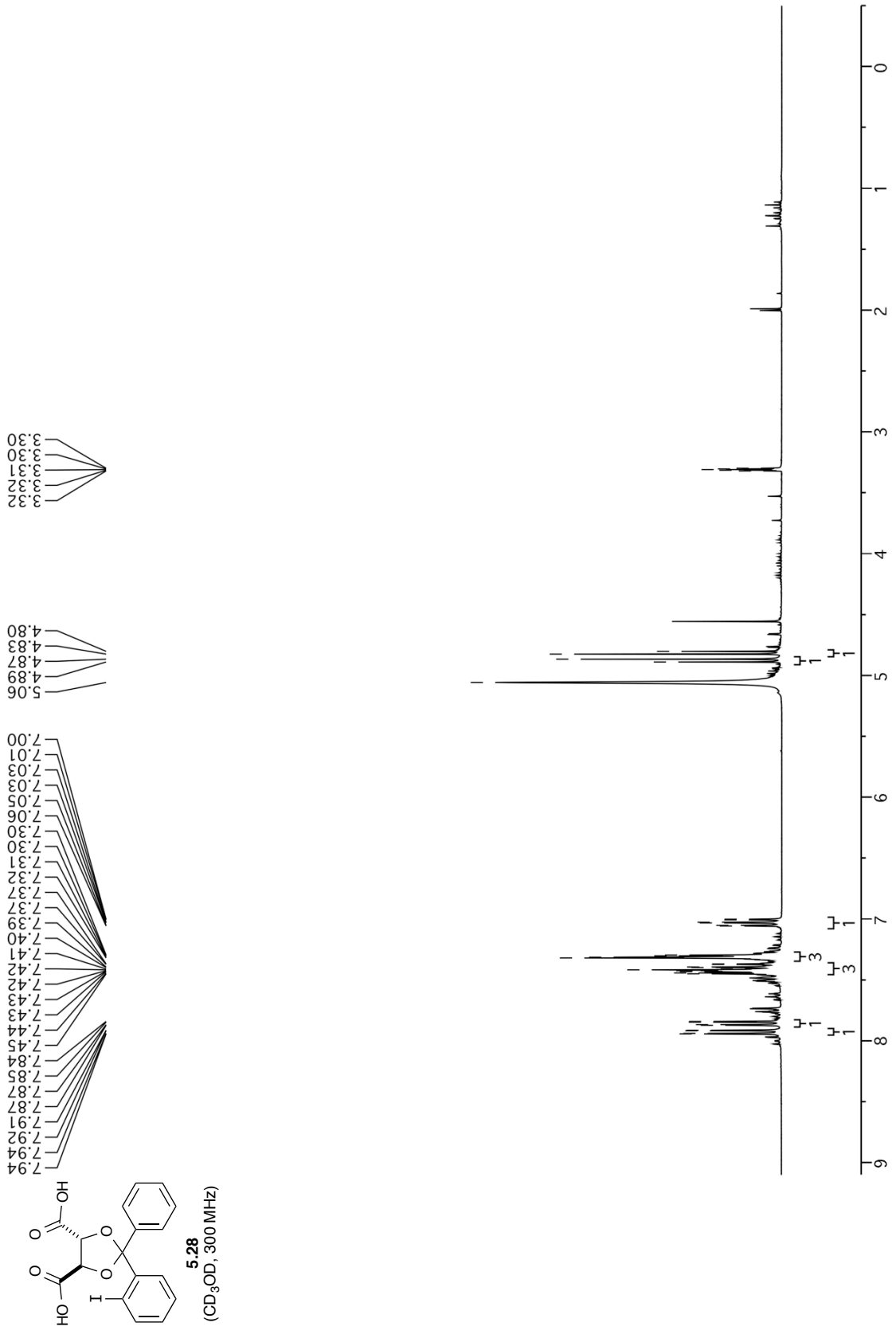
3.32
3.32
3.31
3.30
3.30
4.80
4.83
4.87
4.89
5.06
7.00
7.01
7.03
7.03
7.05
7.06
7.30
7.30
7.31
7.32
7.37
7.37
7.39
7.40
7.41
7.42
7.42
7.43
7.43
7.44
7.45
7.84
7.85
7.87
7.87
7.91
7.92
7.94
7.94
HO
O
O
O
O
I
OH
O
5.28
(CD3OD, 300 MHz)
H 1
H 1
H 3
H 3
H 1
H 1
0
1
2
3
4
5
6
7
8
9

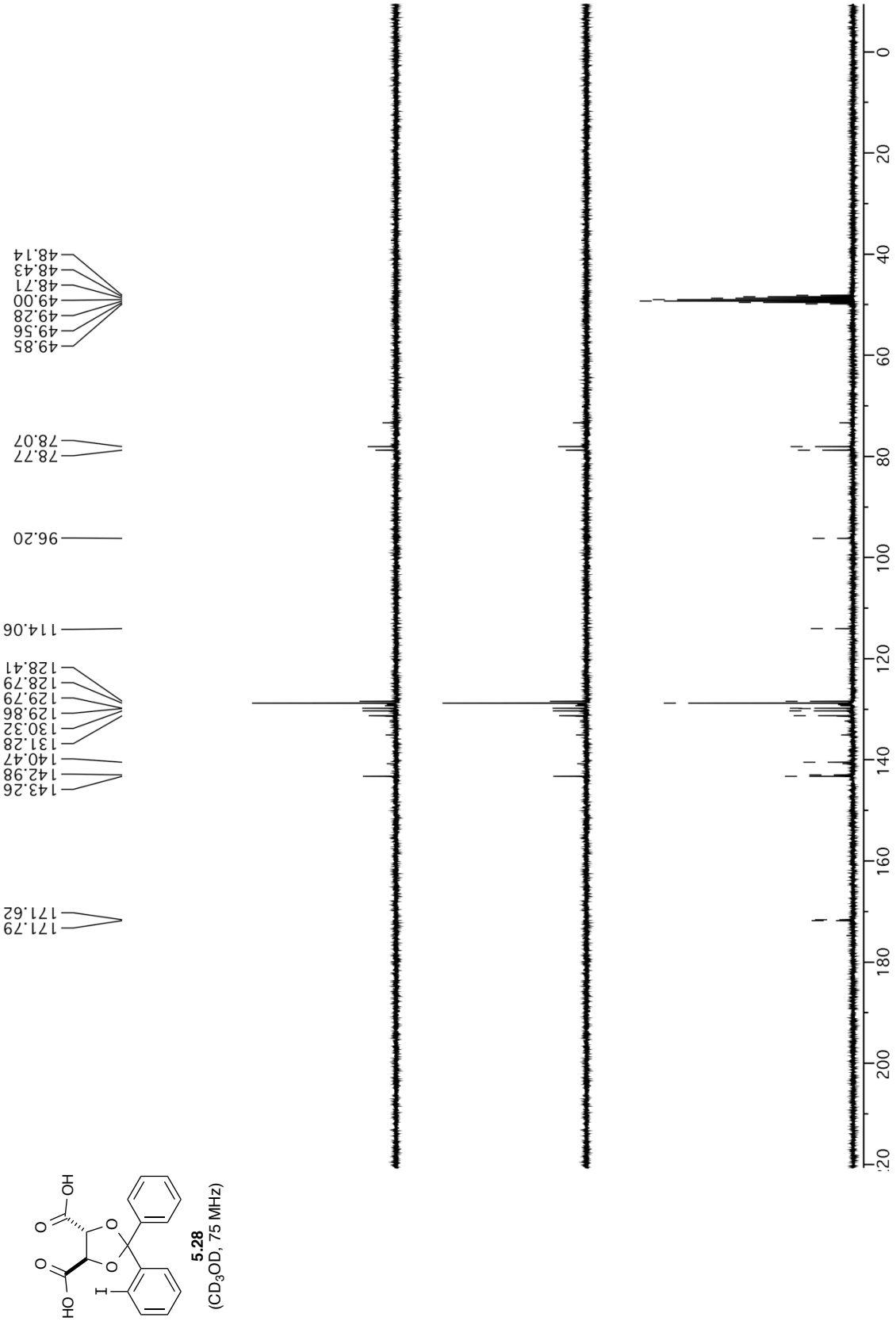

5.28
(CD_3OD, 75 MHz)

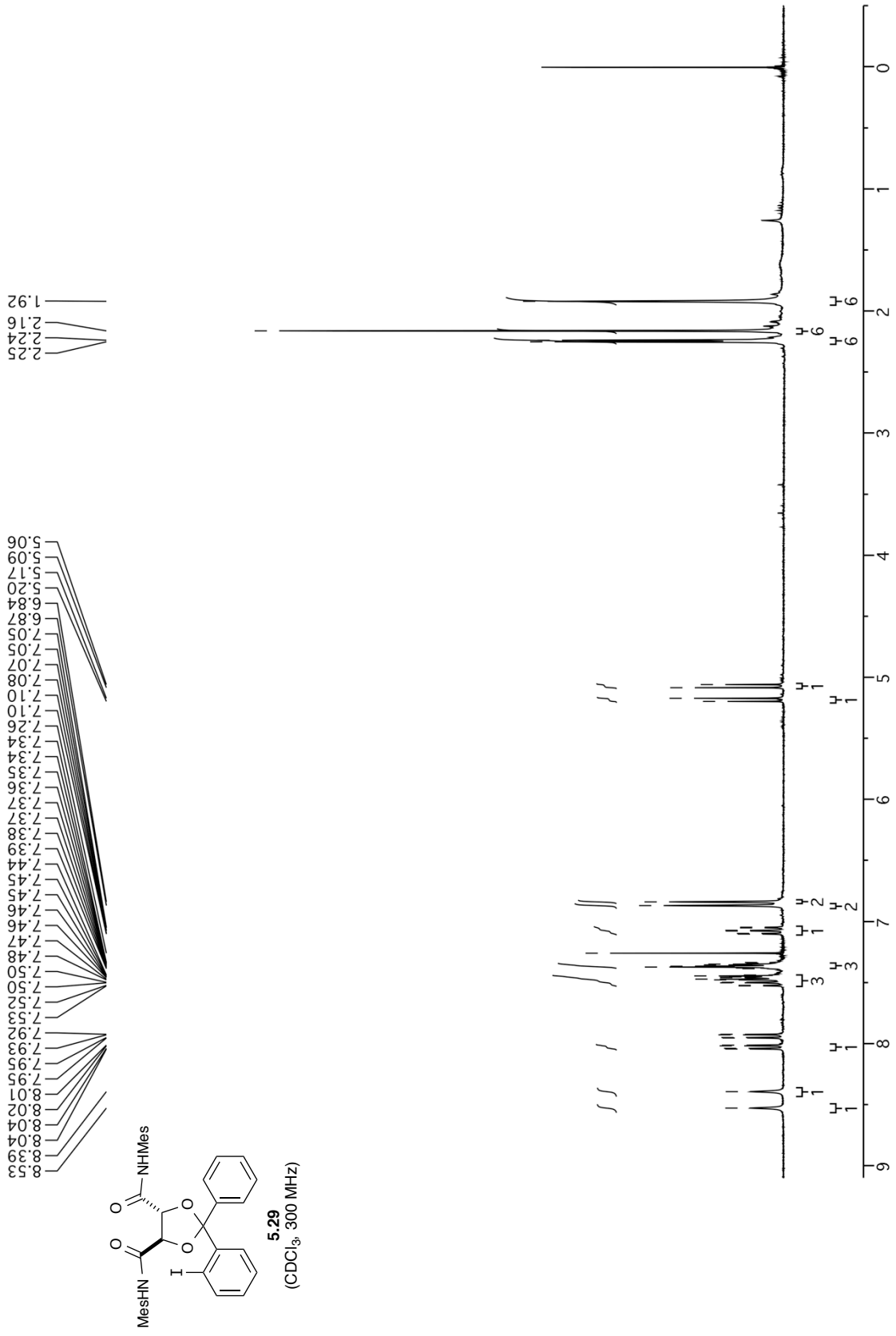
8.53
8.39
8.04
8.04
8.02
8.01
7.95
7.95
7.93
7.92
7.53
7.52
7.50
7.50
7.48
7.47
7.46
7.46
7.45
7.45
7.44
7.39
7.38
7.37
7.37
7.36
7.35
7.34
7.34
7.26
7.10
7.10
7.08
7.07
7.05
7.05
6.87
6.84
5.20
5.17
5.09
5.06
2.25
2.24
2.16
1.92
NHMes
MesHN
O
O
O
O
I
5.29
(CDCl3, 300 MHz)

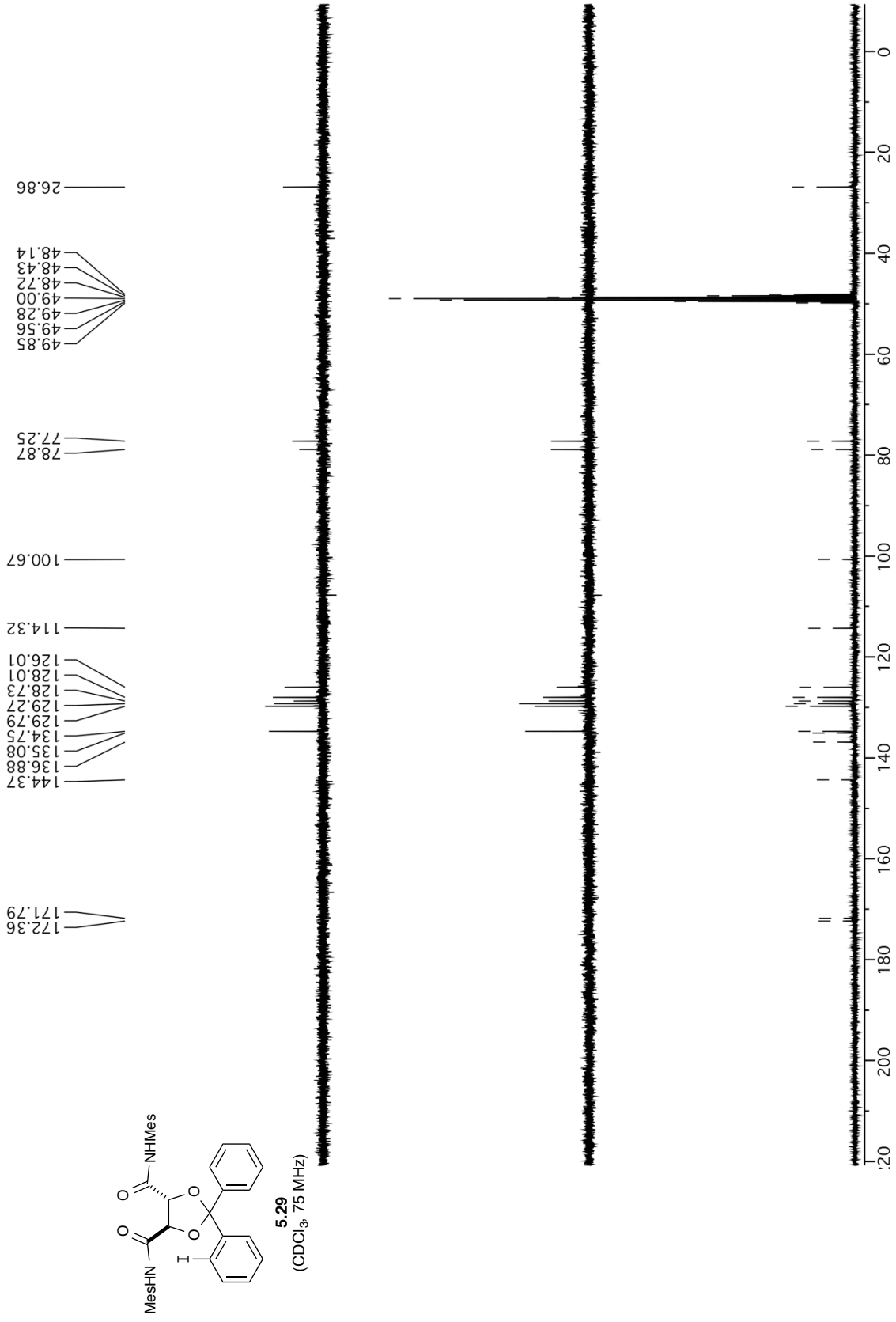
26.86
48.14
48.43
48.72
49.00
49.28
49.56
49.85
77.25
78.87
100.67
114.32
126.01
128.01
128.73
129.27
129.79
134.75
135.08
136.88
144.37
171.79
172.36
NHMes
MesHN
I
O
O
O
O
5.29
(CDCl3, 75 MHz)
0
20
40
60
80
100
120
140
160
180
200
220

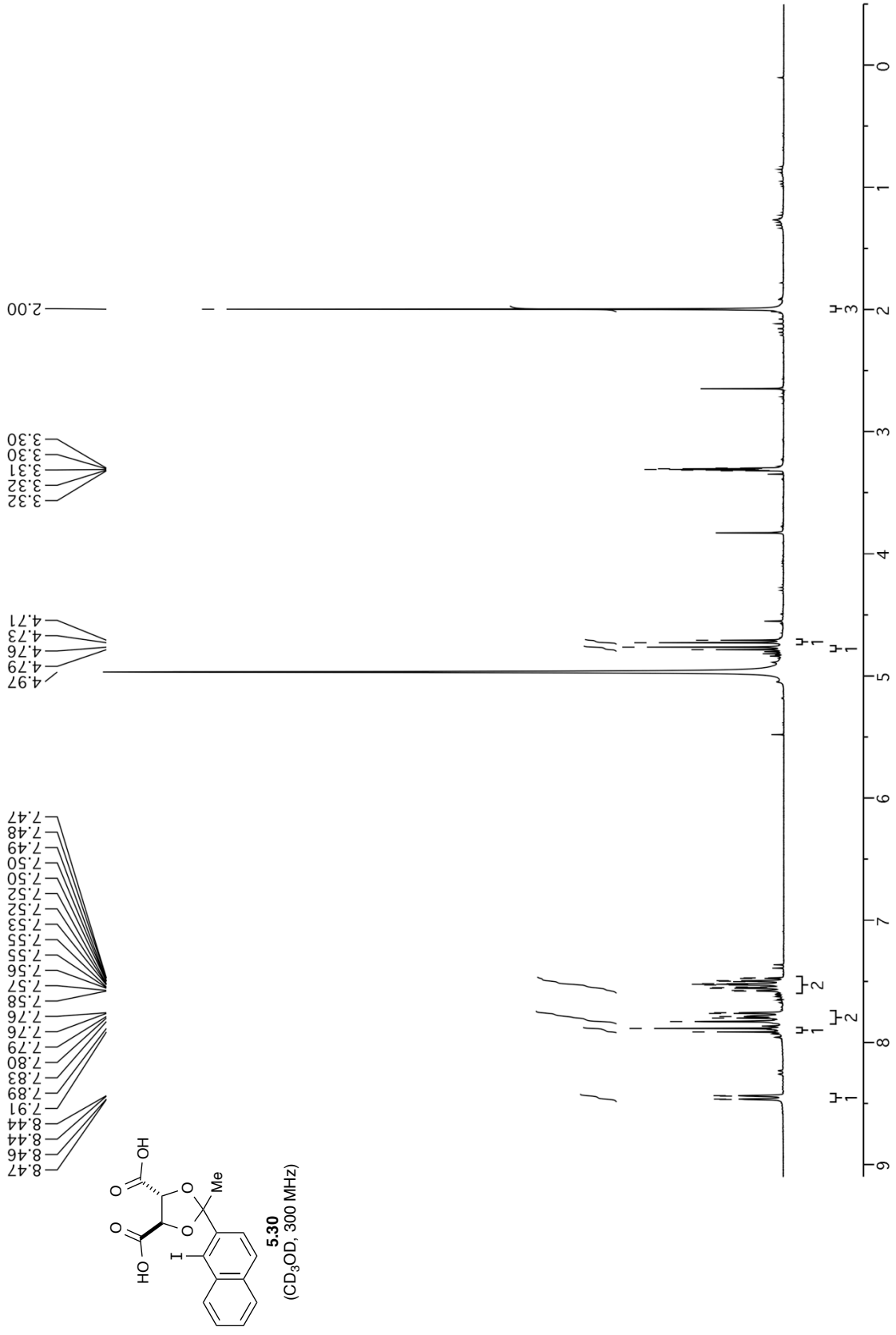
2.00
3.30
3.30
3.31
3.32
3.32
4.71
4.73
4.76
4.79
4.97
7.47
7.48
7.49
7.50
7.50
7.52
7.52
7.53
7.55
7.55
7.56
7.57
7.58
7.76
7.76
7.79
7.80
7.83
7.89
7.91
8.44
8.44
8.46
8.47
HO
O
O
O
O
Me
I
HO
5.30
(CD3OD, 300 MHz)

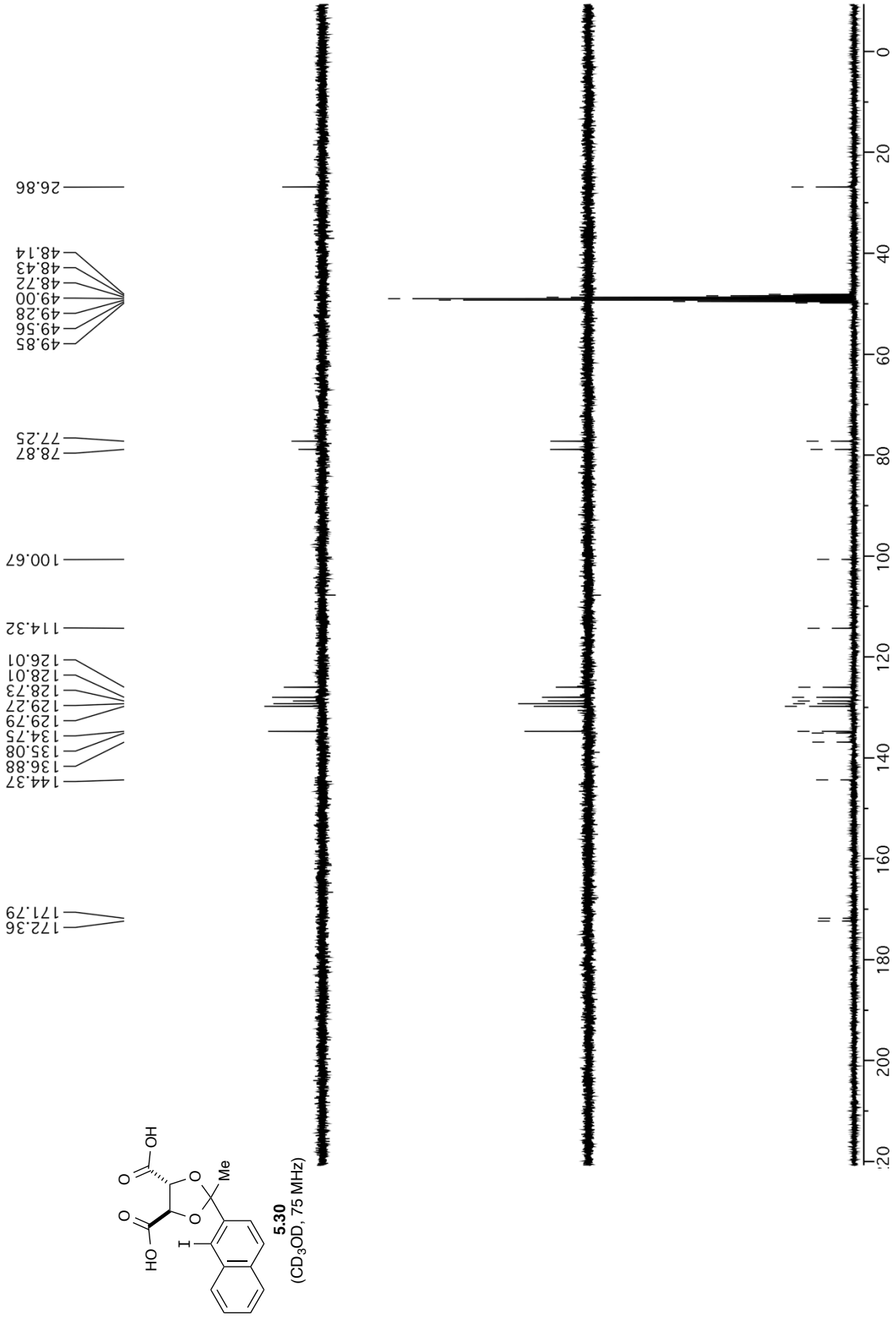
26.86
48.14
48.43
48.72
49.00
49.28
49.56
49.85
77.25
78.87
100.67
114.32
126.01
128.01
128.73
129.27
129.79
134.75
135.08
136.88
144.37
171.79
172.36
HO
O
O
O
O
Me
I
5.30
(CD3OD, 75 MHz)
0
20
40
60
80
100
120
140
160
180
200
220

7.86
7.84
7.83
7.17
7.17
7.15
7.15
6.94
6.92
6.89
5.21
5.18
5.09
5.06
5.00
3.32
3.32
3.31
3.30
3.30
2.87
2.85
2.83
2.24
2.22
2.22
2.20
2.19
2.17
2.16
2.09
2.07
2.07
2.05
1.89
1.87
1.85
1.83
1.81
1.06
1.04
1.08
1.44
2.06
0.849
1.09
2.12
OH
O
O
O
O
I
HO
5.33
CD3OD, 300 MHz

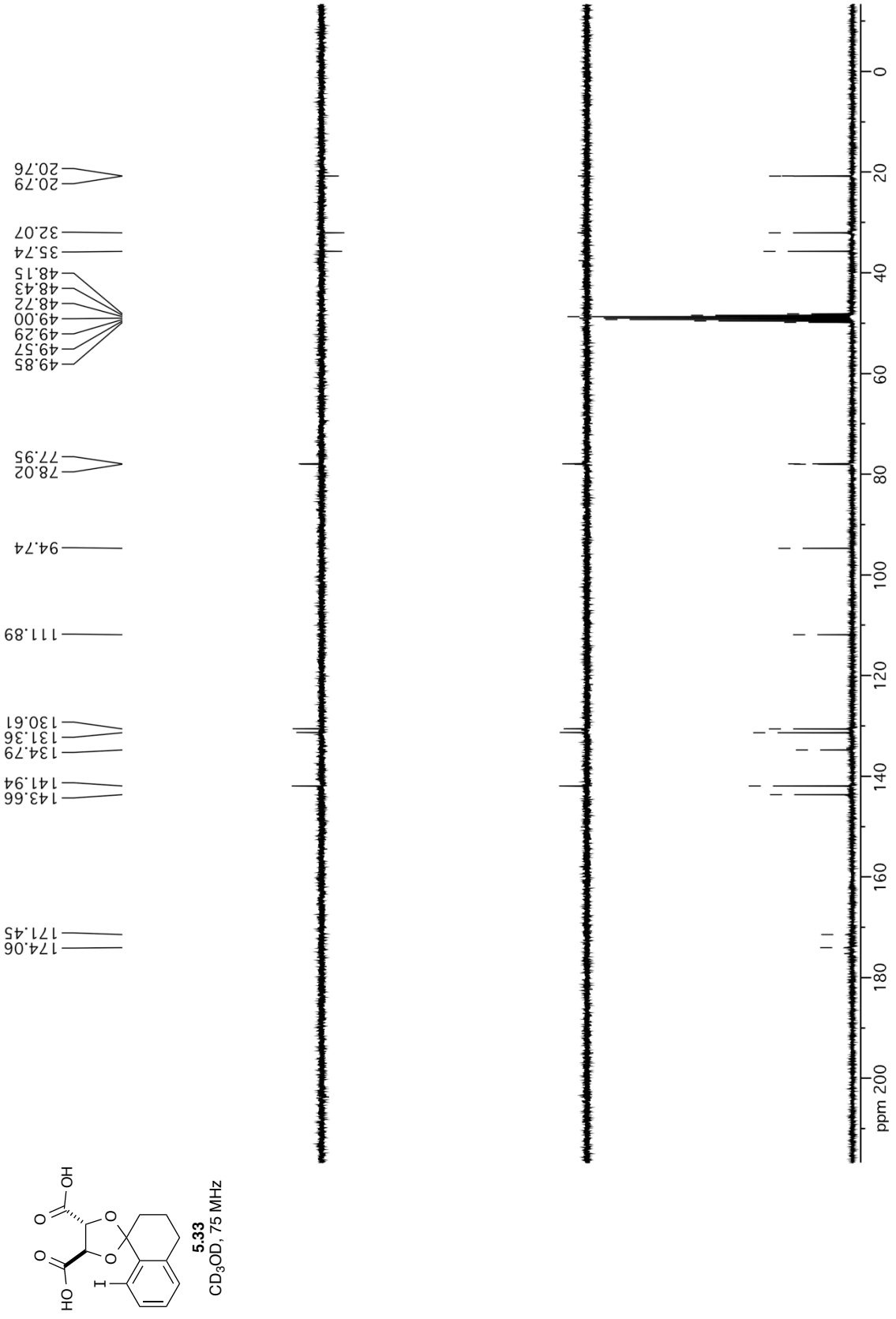
20.76
20.79
32.07
35.74
48.15
48.43
48.72
49.00
49.29
49.57
49.85
77.95
78.02
94.74
111.89
130.61
131.36
134.79
141.94
143.66
171.45
174.06
0
20
40
60
80
100
120
140
160
180
ppm 200
5.33
CD3OD, 75 MHz

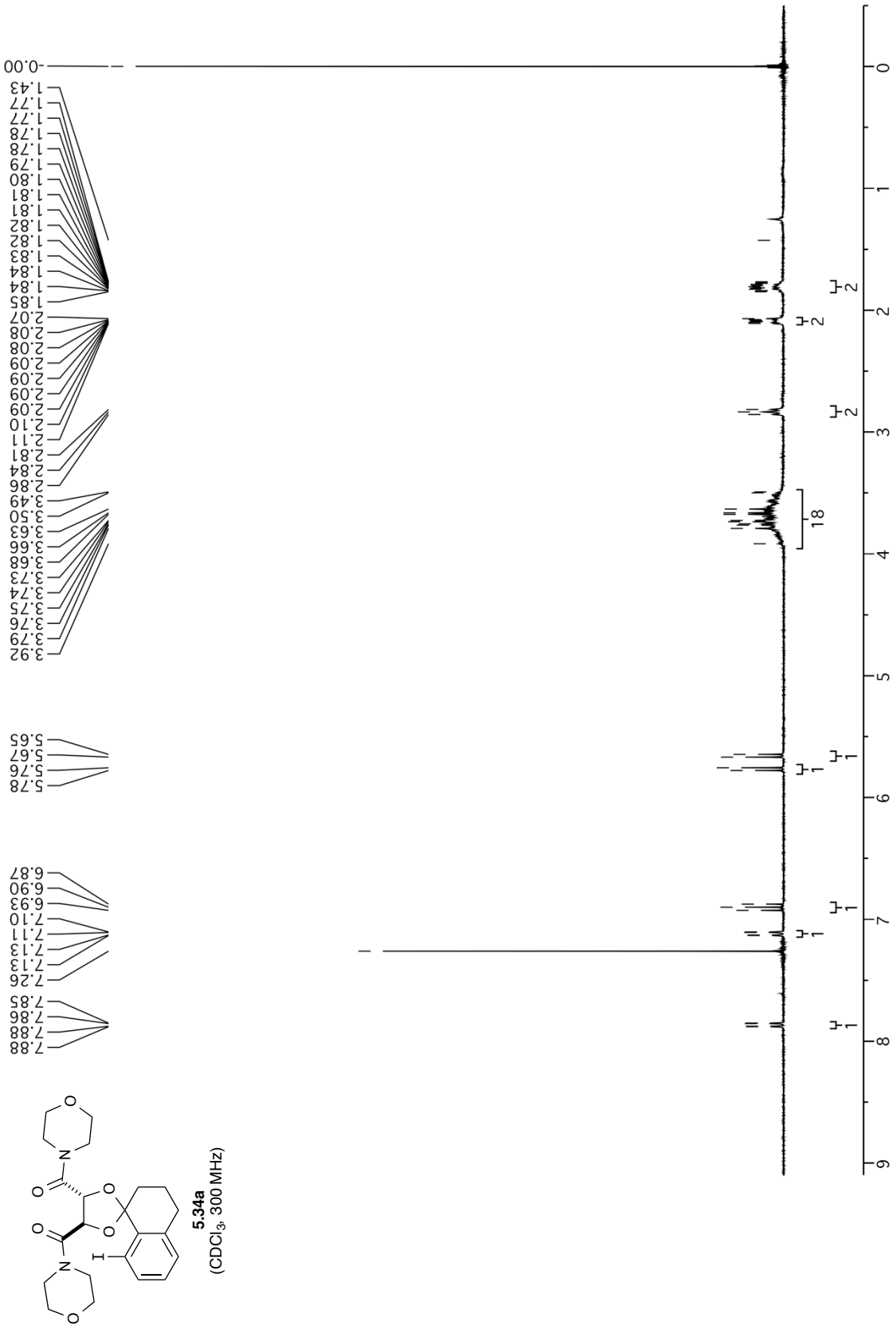
0.00
1.43
1.77
1.77
1.78
1.78
1.79
1.80
1.81
1.81
1.82
1.82
1.83
1.84
1.84
1.85
2.07
2.08
2.08
2.09
2.09
2.09
2.09
2.10
2.11
2.81
2.84
2.86
3.49
3.50
3.63
3.66
3.68
3.73
3.74
3.75
3.76
3.79
3.92
5.65
5.67
5.76
5.78
6.87
6.90
6.93
7.10
7.11
7.13
7.13
7.26
7.85
7.86
7.88
7.88
18
5.34a
(CDCl3, 300 MHz)

0.00
1.87
1.89
1.90
1.91
1.93
1.95
1.97
1.98
2.14
2.15
2.19
2.20
2.22
2.22
2.23
2.24
2.25
2.26
2.27
2.29
2.30
2.85
2.87
2.89
2.90
2.92
2.94
2.95
5.04
5.06
5.24
5.27
6.94
6.97
6.99
7.12
7.14
7.16
7.17
7.17
7.18
7.19
7.20
7.20
7.20
7.21
7.21
7.26
7.33
7.34
7.36
7.39
7.40
7.41
7.63
7.63
7.64
7.65
7.66
7.66
7.67
7.91
7.91
7.93
7.93
8.63
9.03
NH
O
O
O
O
I
NH
5.34b
(CDCl3, 300 MHz)
ppm 9
0
1
2
3
4
5
6
7
8
1
1
1
4
4
1
3
1
1
1
2
2
2

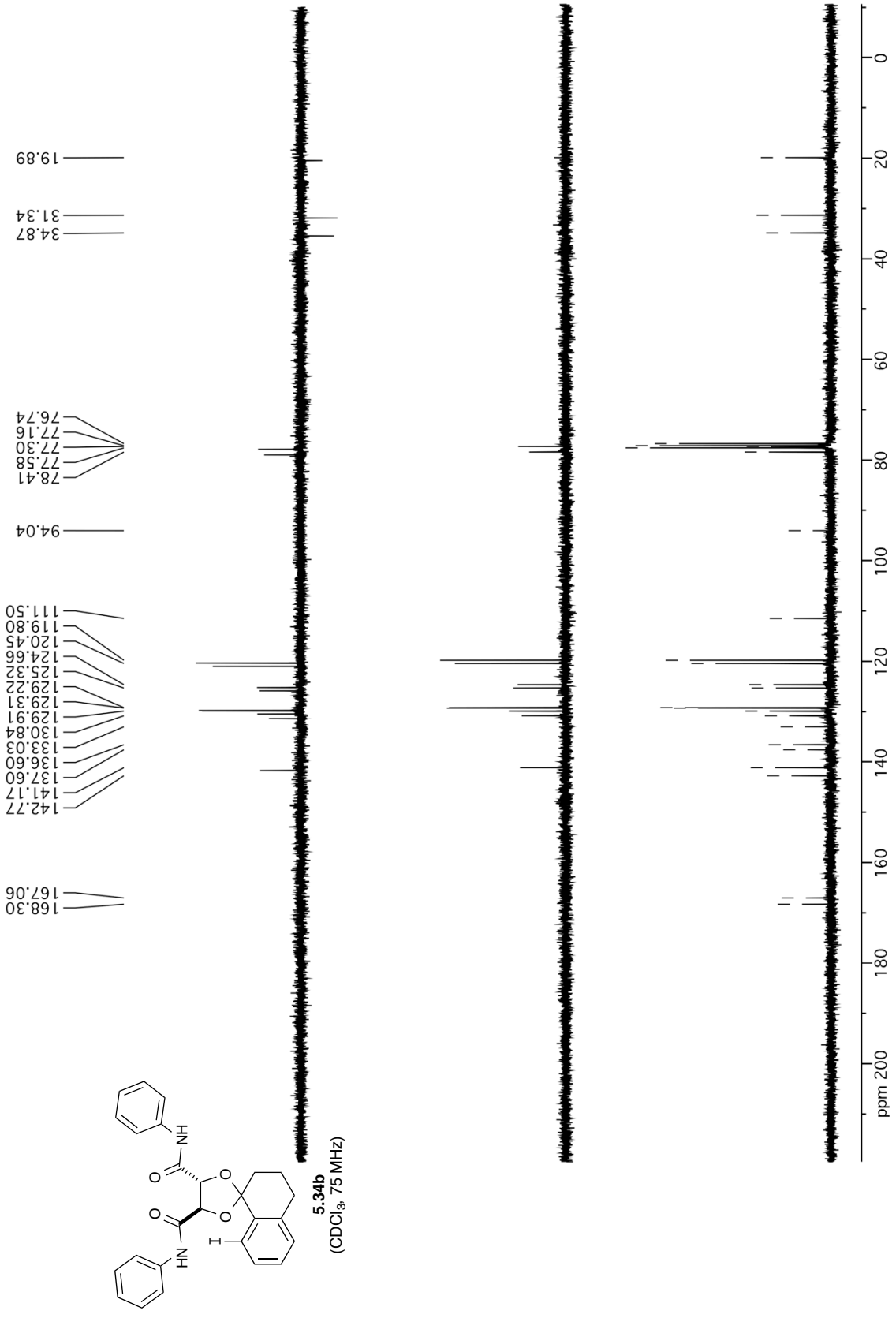
19.89
31.34
34.87
76.74
77.16
77.30
77.58
78.41
94.04
111.50
119.80
120.45
124.66
125.32
129.22
129.91
129.31
130.84
133.03
136.60
137.60
141.17
142.77
167.06
168.30
NH
O
O
O
O
I
NH
5.34b
(CDCl3, 75 MHz)
ppm 200
180
160
140
120
100
80
60
40
20
0

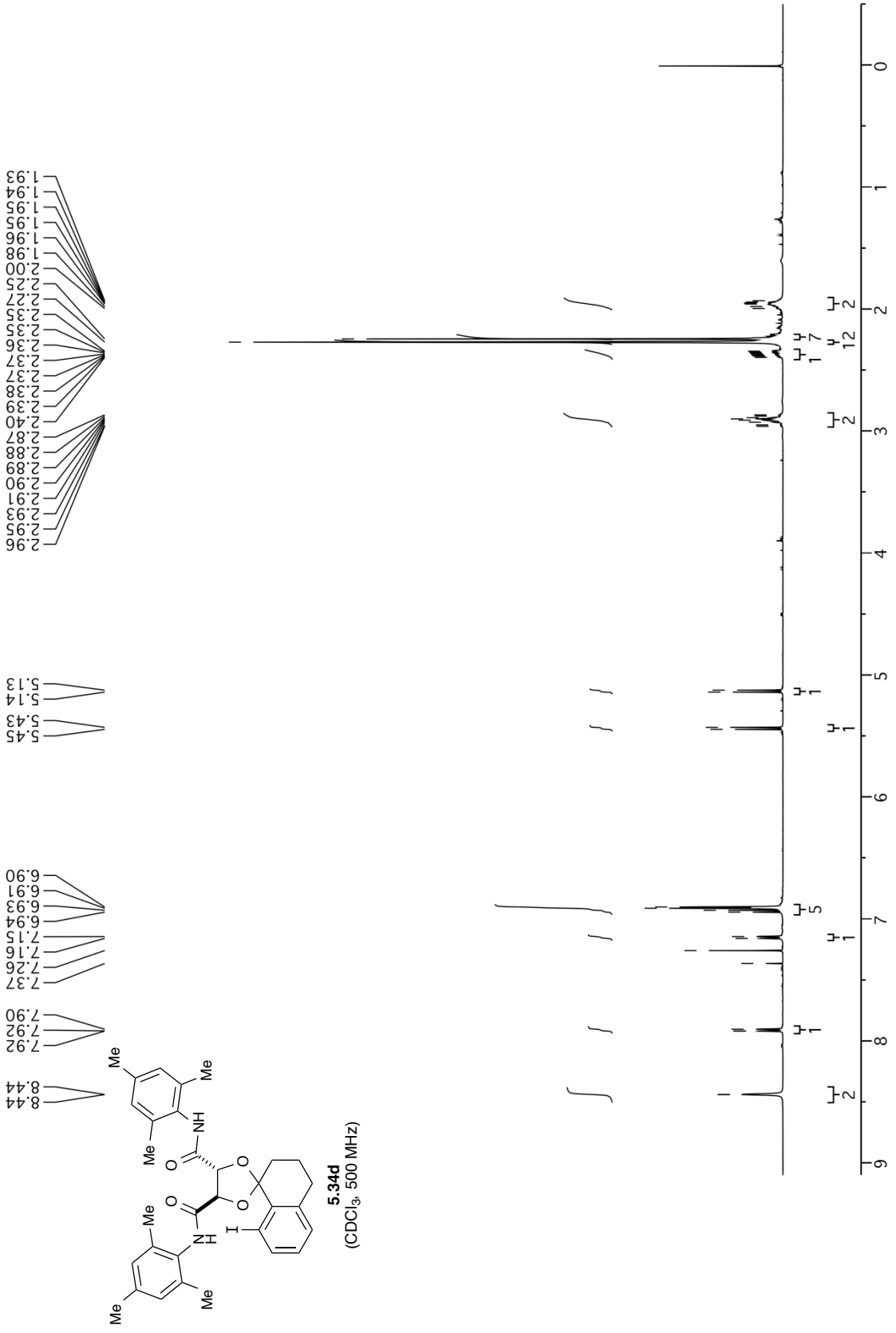
1.93
1.94
1.95
1.95
1.96
1.98
2.00
2.25
2.27
2.35
2.35
2.36
2.37
2.37
2.38
2.39
2.40
2.87
2.88
2.89
2.90
2.91
2.93
2.95
2.96
5.13
5.14
5.43
5.45
6.90
6.91
6.93
6.94
7.15
7.16
7.26
7.37
7.90
7.92
7.92
8.44
8.44
Me
Me
Me
Me
NH
O
O
O
O
O
NH
I
5.34d
(CDCl3, 500 MHz)

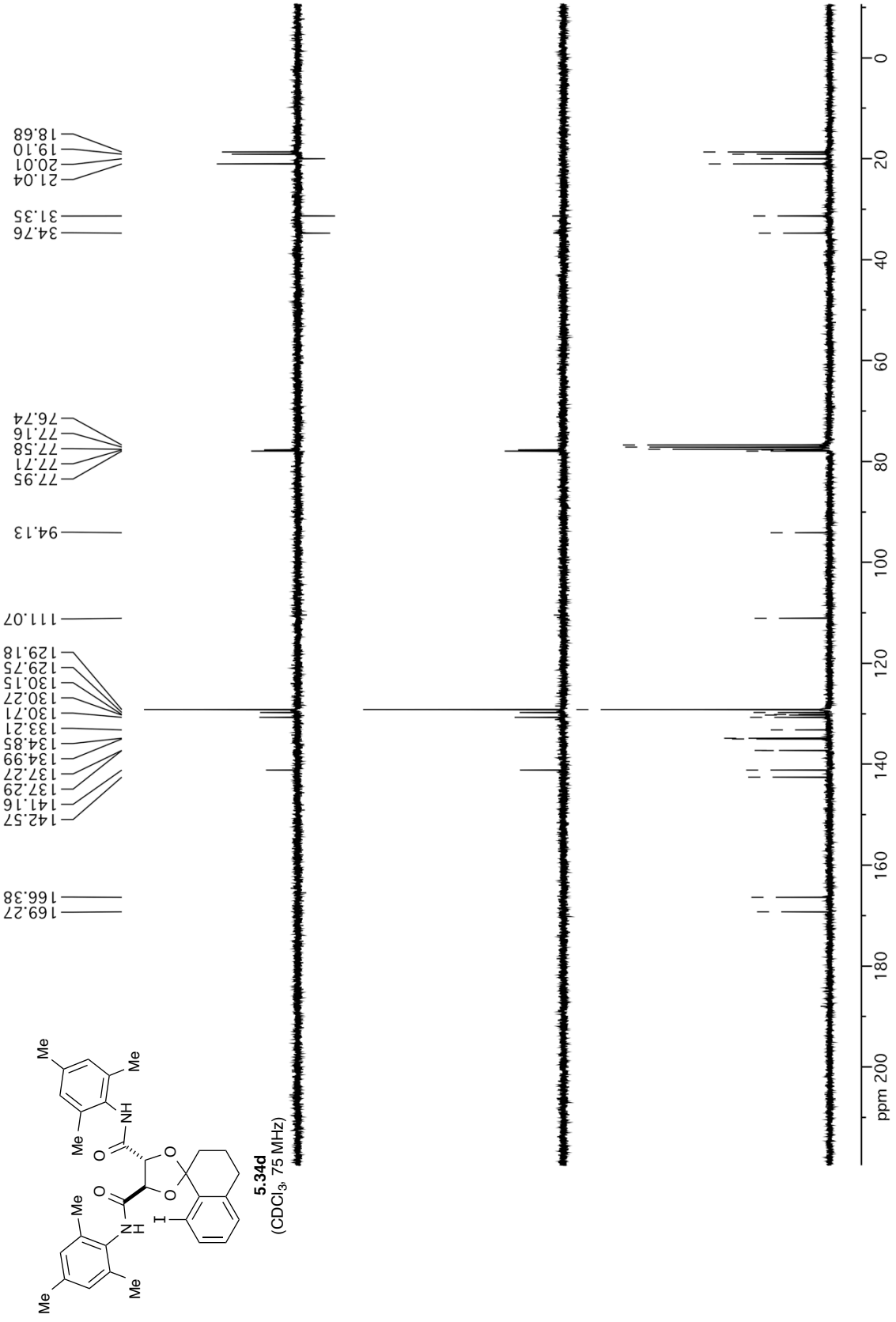
18.68
19.10
20.01
21.04
31.35
34.76
76.74
77.16
77.58
77.71
77.95
94.13
111.07
129.18
129.75
130.15
130.27
130.71
133.21
134.85
134.99
137.27
137.29
141.16
142.57
166.38
169.27
Me
Me
Me
Me
NH
O
O
O
O
N
H
I
5.34d
(CDCl3, 75 MHz)
0
20
40
60
80
100
120
140
160
180
ppm 200

9.11
8.77
8.15
7.93
7.93
7.90
7.70
7.66
7.65
7.26
7.17
7.15
7.00
6.98
6.95
5.31
5.29
5.12
5.10
2.89
2.88
2.85
2.27
2.27
2.26
2.25
2.23
2.22
2.20
2.16
2.15
2.12
2.11
2.08
2.06
1.94
1.93
1.91
F3C
CF3
NH
O
O
O
O
HN
I
CF3
F3C
5.34e
(CDCl3, 300 MHz)
ppm 9
8
7
6
5
4
3
2
1
0

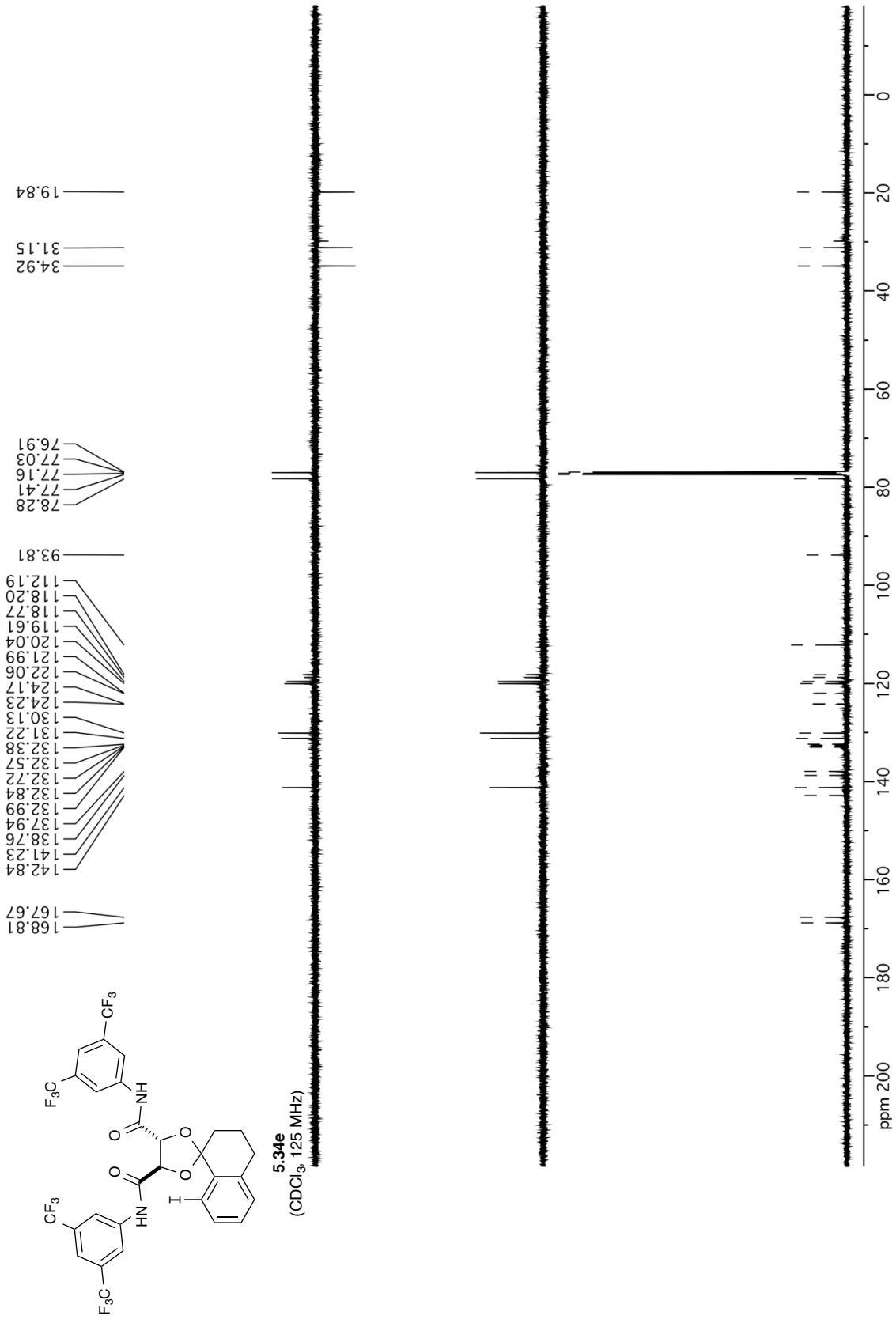
19.84
31.15
34.92
76.91
77.03
77.16
77.41
78.28
93.81
112.19
118.20
118.77
119.61
120.04
121.99
122.06
124.17
124.23
130.13
131.22
132.38
132.57
132.72
132.84
132.99
137.94
138.76
141.23
142.84
167.67
168.81
5.34e
(CDCl3, 125 MHz)
ppm 200
180
160
140
120
100
80
60
40
20
0

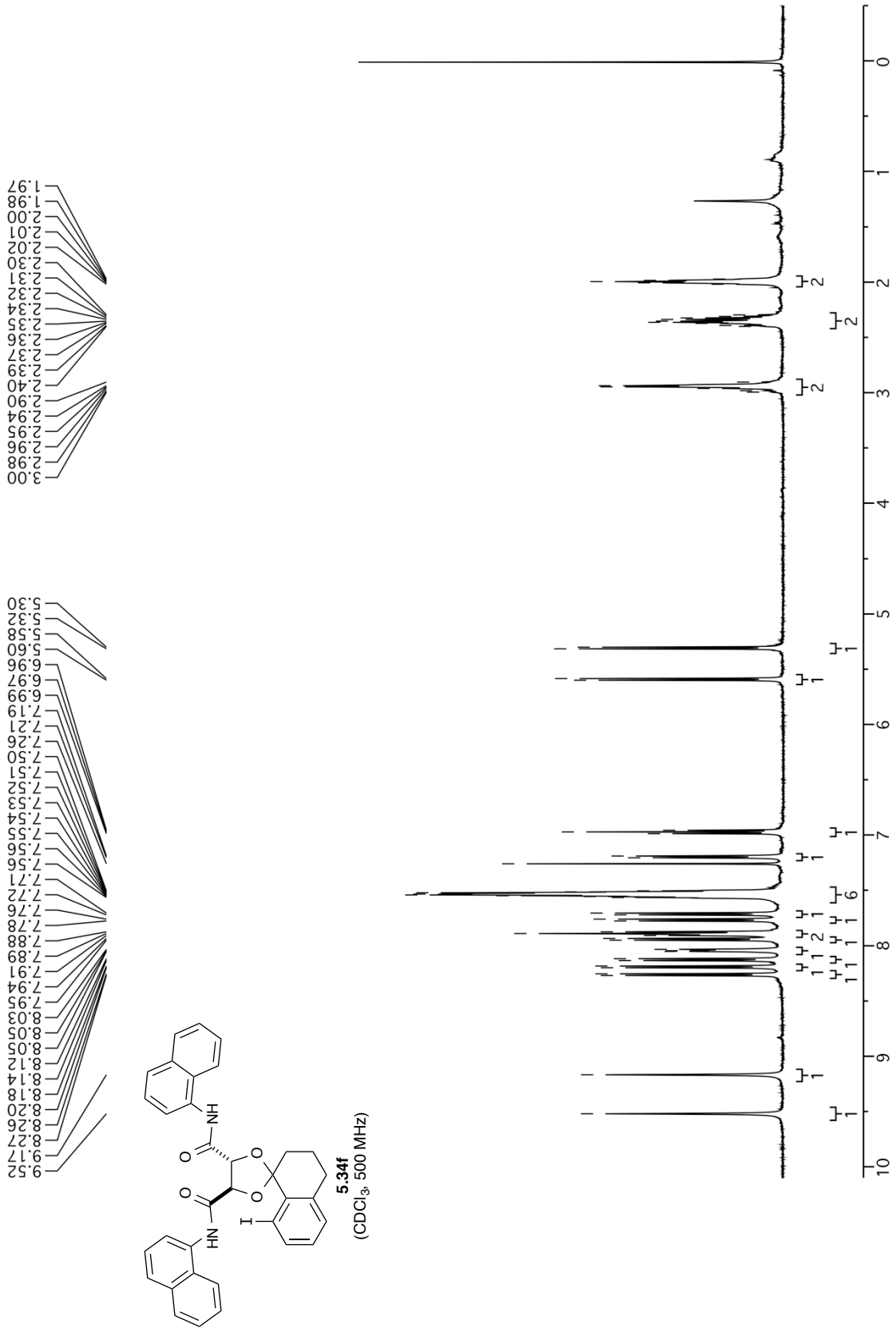
1.97
1.98
2.00
2.01
2.02
2.30
2.31
2.32
2.34
2.35
2.36
2.37
2.39
2.40
2.90
2.94
2.95
2.96
2.98
3.00
5.30
5.32
5.58
5.60
6.96
6.97
6.99
7.19
7.21
7.26
7.50
7.51
7.52
7.53
7.54
7.55
7.56
7.56
7.71
7.72
7.76
7.78
7.88
7.89
7.91
7.94
7.95
8.03
8.05
8.05
8.12
8.14
8.18
8.20
8.26
8.27
9.17
9.52
NH
O
O
O
O
I
NH
5.34f
(CDCl3, 500 MHz)
1
1
2
1
1
1
1
1
1
1
1
1
1
1
1
1
1
1
1
1
1
1
1
1
2
2
2
2
6
0
1
2
3
4
5
6
7
8
9
10

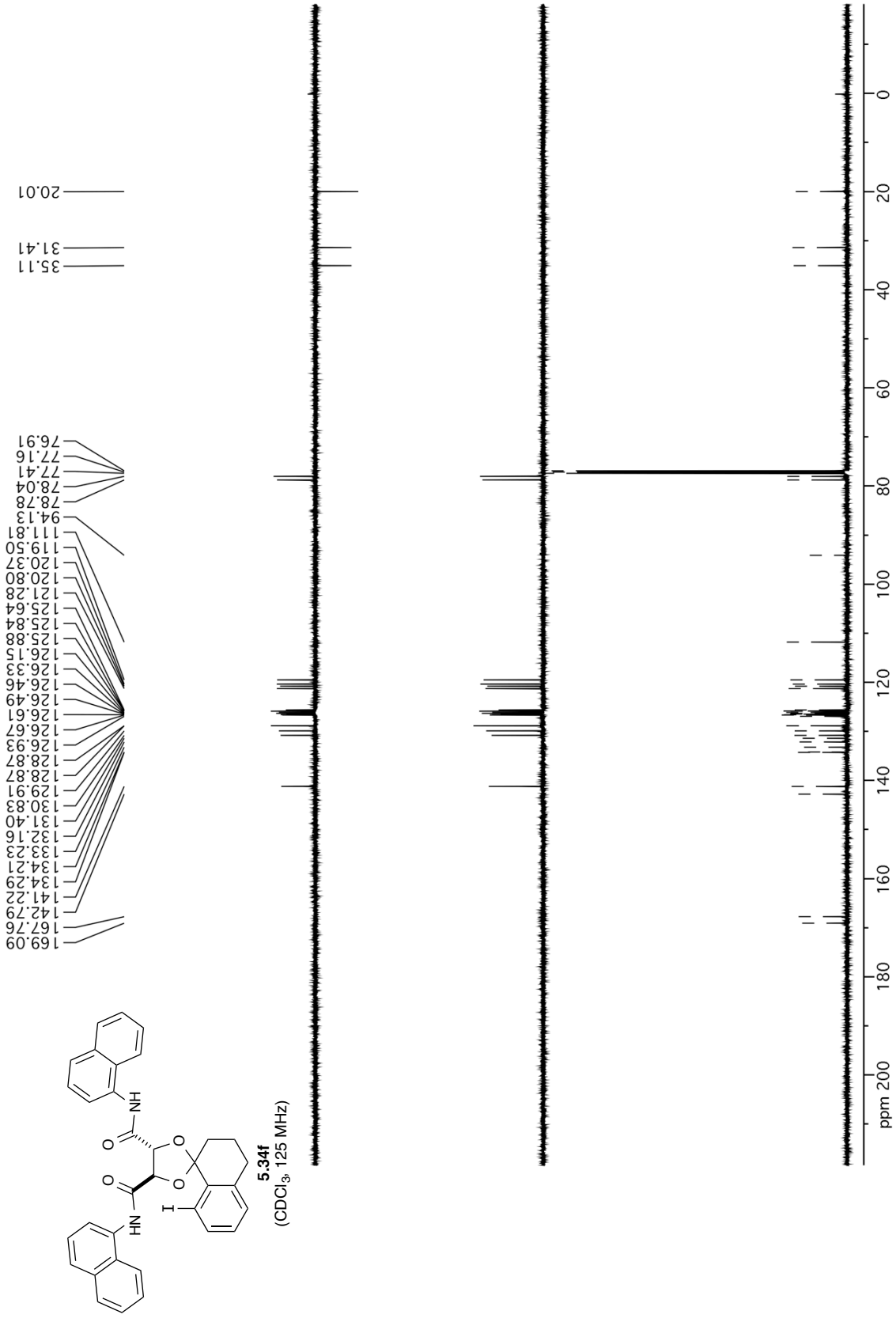
20.01
31.41
35.11
76.91
77.16
77.41
78.04
78.78
94.13
111.81
119.50
120.37
120.80
121.28
125.64
125.84
125.88
126.15
126.33
126.46
126.49
126.61
126.67
126.93
128.87
128.87
129.91
130.83
131.40
132.16
133.23
134.21
134.29
141.22
142.79
167.76
169.09
NH
O
O
O
O
I
NH
5.34f
(CDCl3, 125 MHz)
ppm 200
180
160
140
120
100
80
60
40
20
0

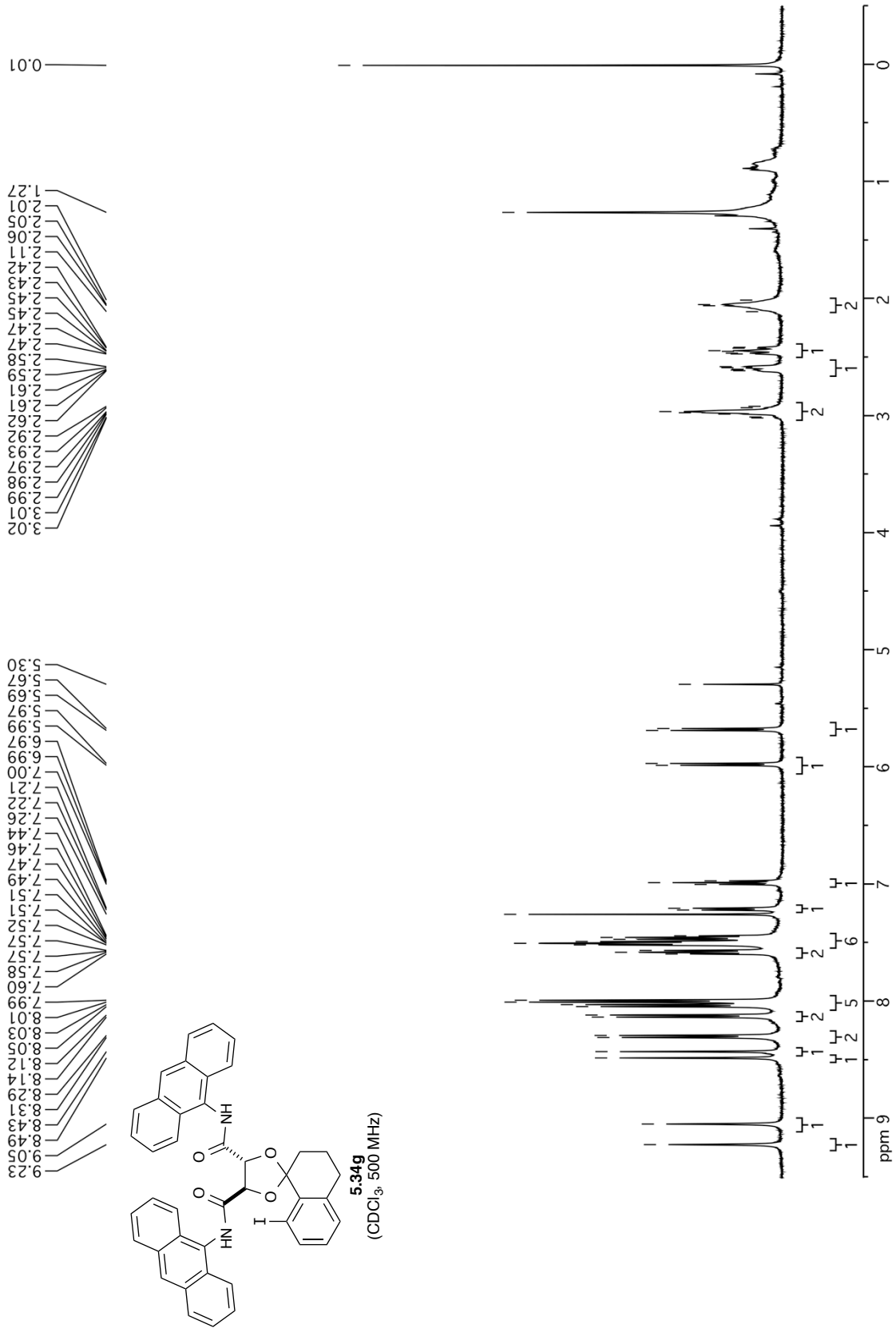
0.01
1.27
2.01
2.05
2.06
2.11
2.42
2.43
2.45
2.45
2.47
2.47
2.58
2.59
2.61
2.61
2.62
2.92
2.93
2.97
2.98
2.99
3.01
3.02
5.30
5.67
5.69
5.97
5.99
6.97
6.99
7.00
7.21
7.22
7.26
7.44
7.46
7.47
7.49
7.51
7.51
7.52
7.57
7.57
7.58
7.60
7.99
8.01
8.03
8.05
8.12
8.14
8.29
8.31
8.43
8.49
9.05
9.23
NH
O
O
O
O
NH
I
5.34g
(CDCl3, 500 MHz)
ppm 9
8
7
6
5
4
3
2
1
0

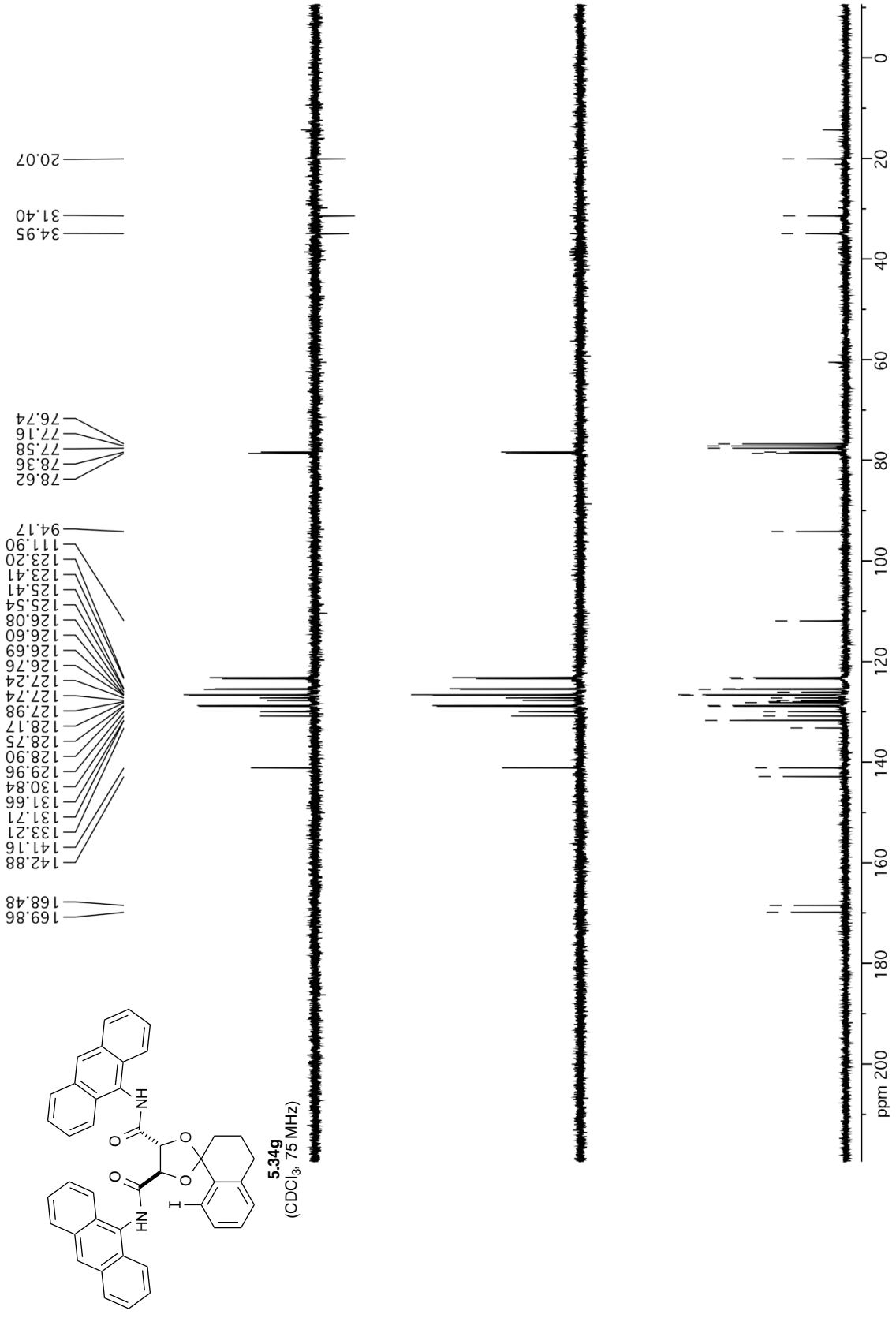
20.07
31.40
34.95
76.74
77.16
77.58
78.36
78.62
94.17
111.90
123.20
123.41
125.41
125.54
126.08
126.60
126.69
126.76
127.24
127.74
127.98
128.17
128.75
128.90
129.96
130.84
131.66
131.71
133.21
141.16
142.88
168.48
169.86
NH
O
O
O
O
NH
I
5.34g
(CDCl3, 75 MHz)
0
20
40
60
80
100
120
140
160
180
ppm 200

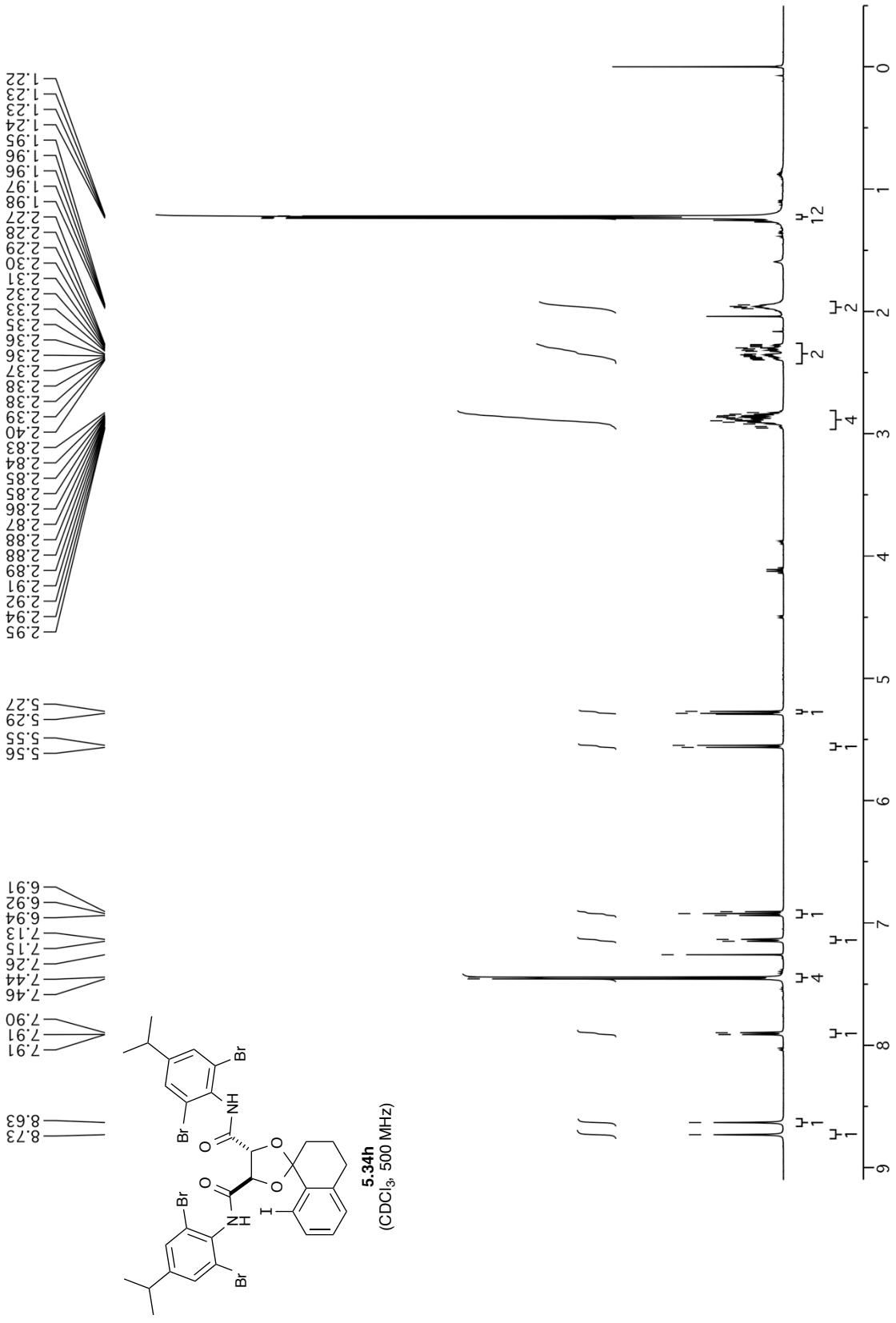
1.22
1.23
1.23
1.24
1.95
1.96
1.96
1.97
1.98
2.27
2.28
2.29
2.30
2.31
2.32
2.33
2.35
2.36
2.36
2.37
2.38
2.38
2.39
2.40
2.83
2.84
2.85
2.85
2.86
2.87
2.88
2.88
2.89
2.91
2.92
2.94
2.95
5.27
5.29
5.55
5.56
6.91
6.92
6.94
7.13
7.15
7.26
7.44
7.46
7.90
7.91
7.91
8.63
8.73
Br
Br
NH
O
O
O
O
NH
Br
Br
I
5.34h
(CDCl3, 500 MHz)
12
2
2
4
1
1
1
4
1
1
1
1
0
1
2
3
4
5
6
7
8
9

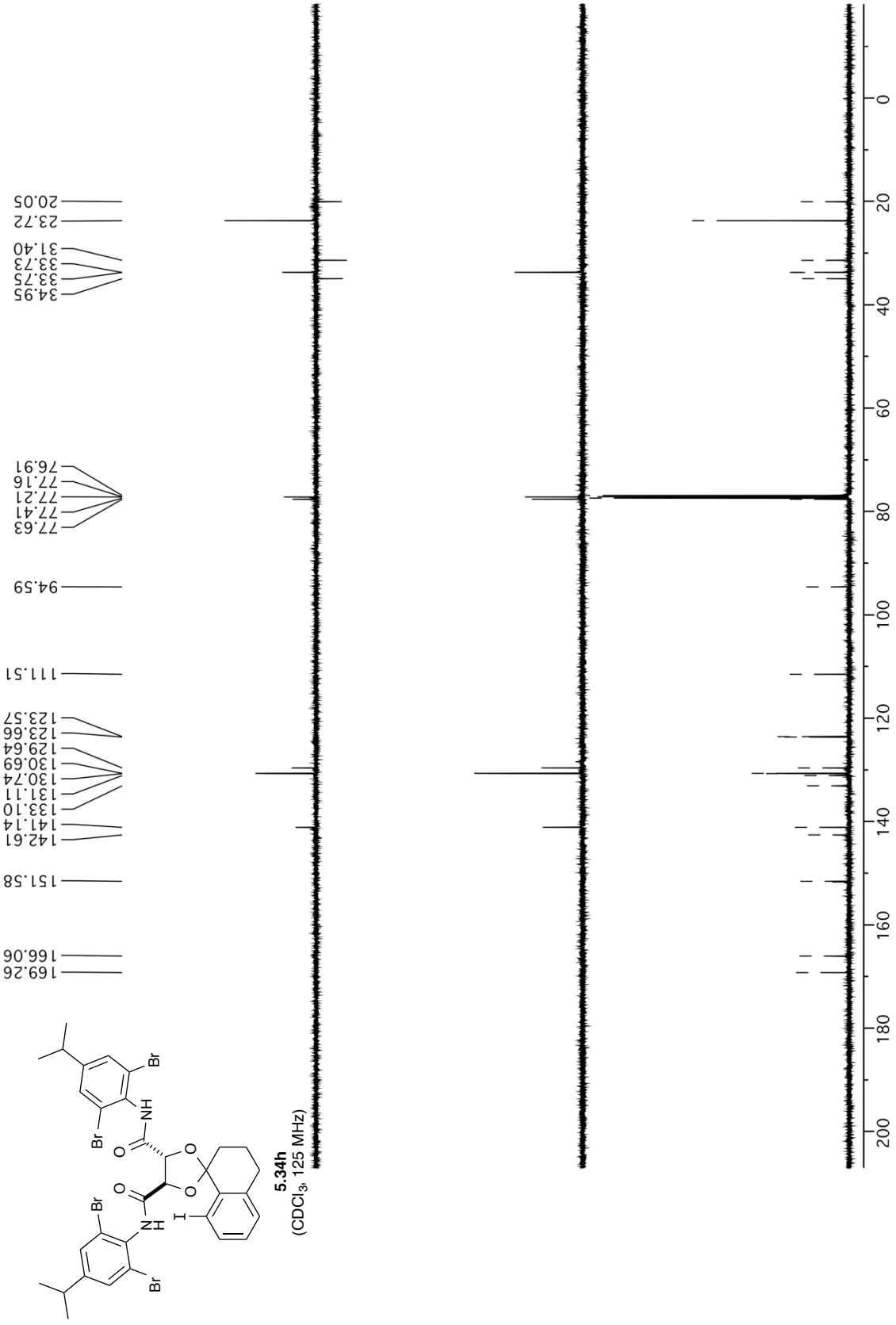
20.05
23.72
31.40
33.73
33.75
34.95
76.91
77.16
77.21
77.41
77.63
94.59
111.51
123.57
123.66
129.64
130.69
130.74
131.11
133.10
141.14
142.61
151.58
166.06
169.26
Br
Br
NH
O
O
O
O
Br
Br
NH
I
5.34h
(CDCl3, 125 MHz)
0
20
40
60
80
100
120
140
160
180
200

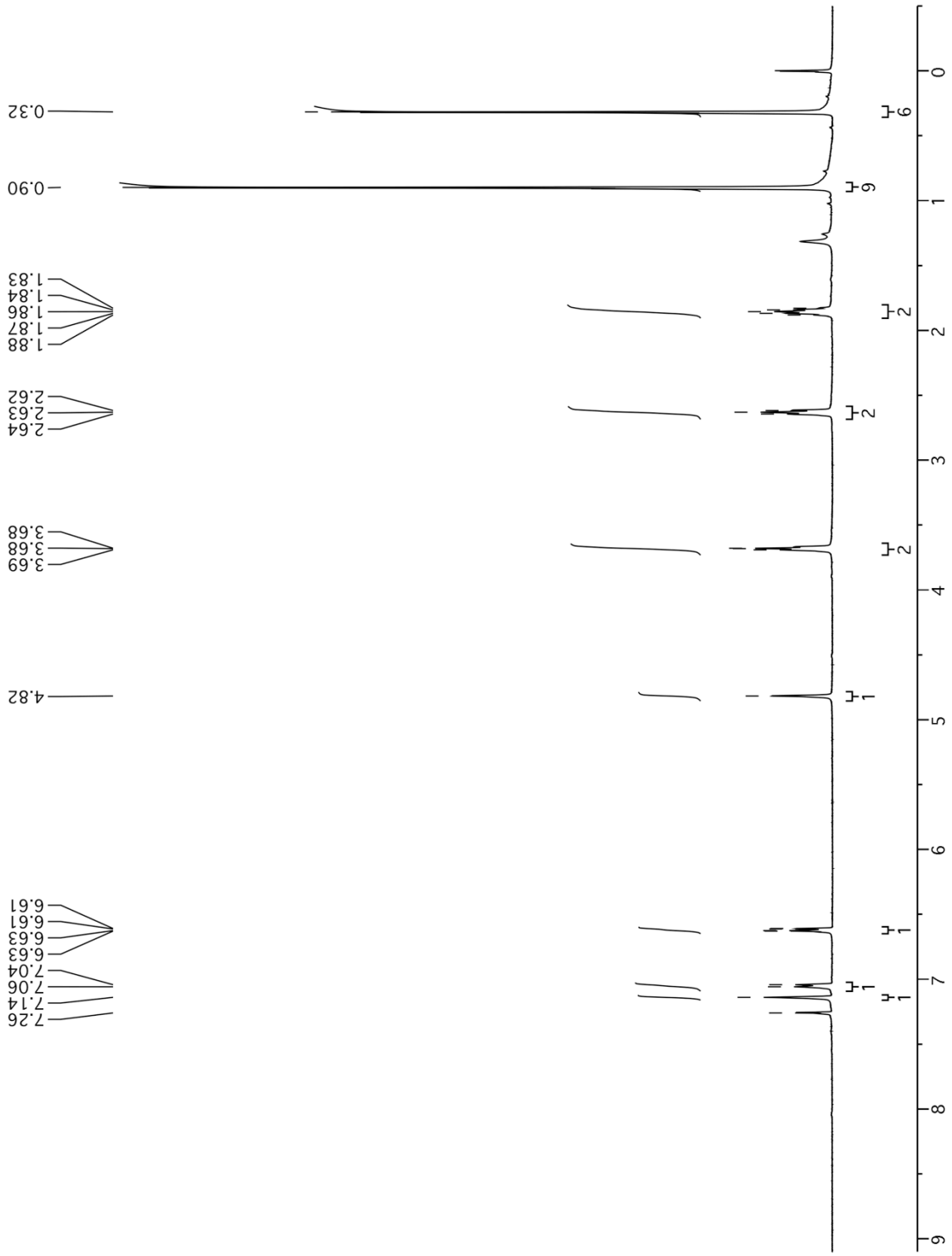

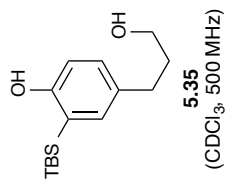

5.35
($CDCl_3$, 500 MHz)

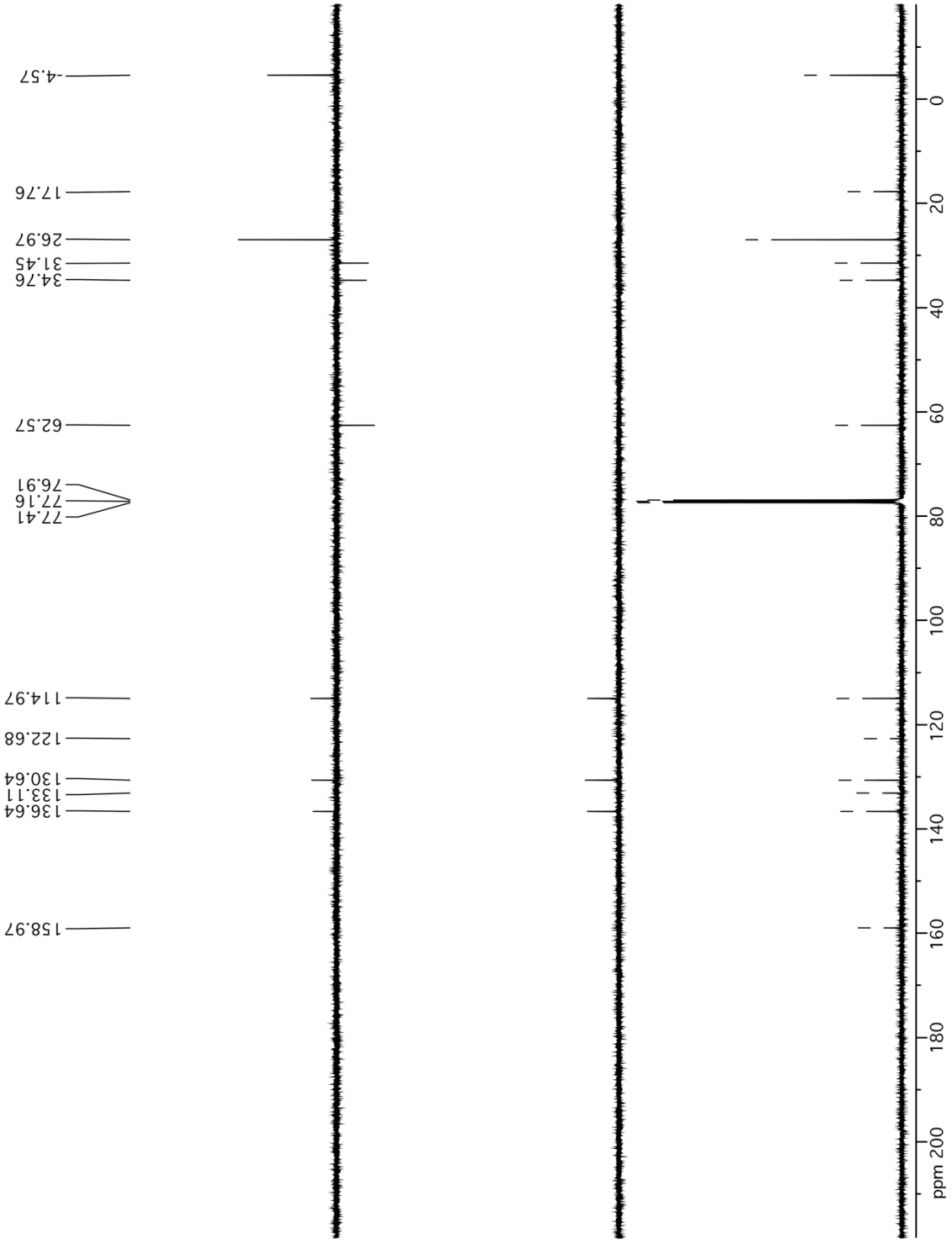

5.35
($CDCl_3$, 125 MHz)

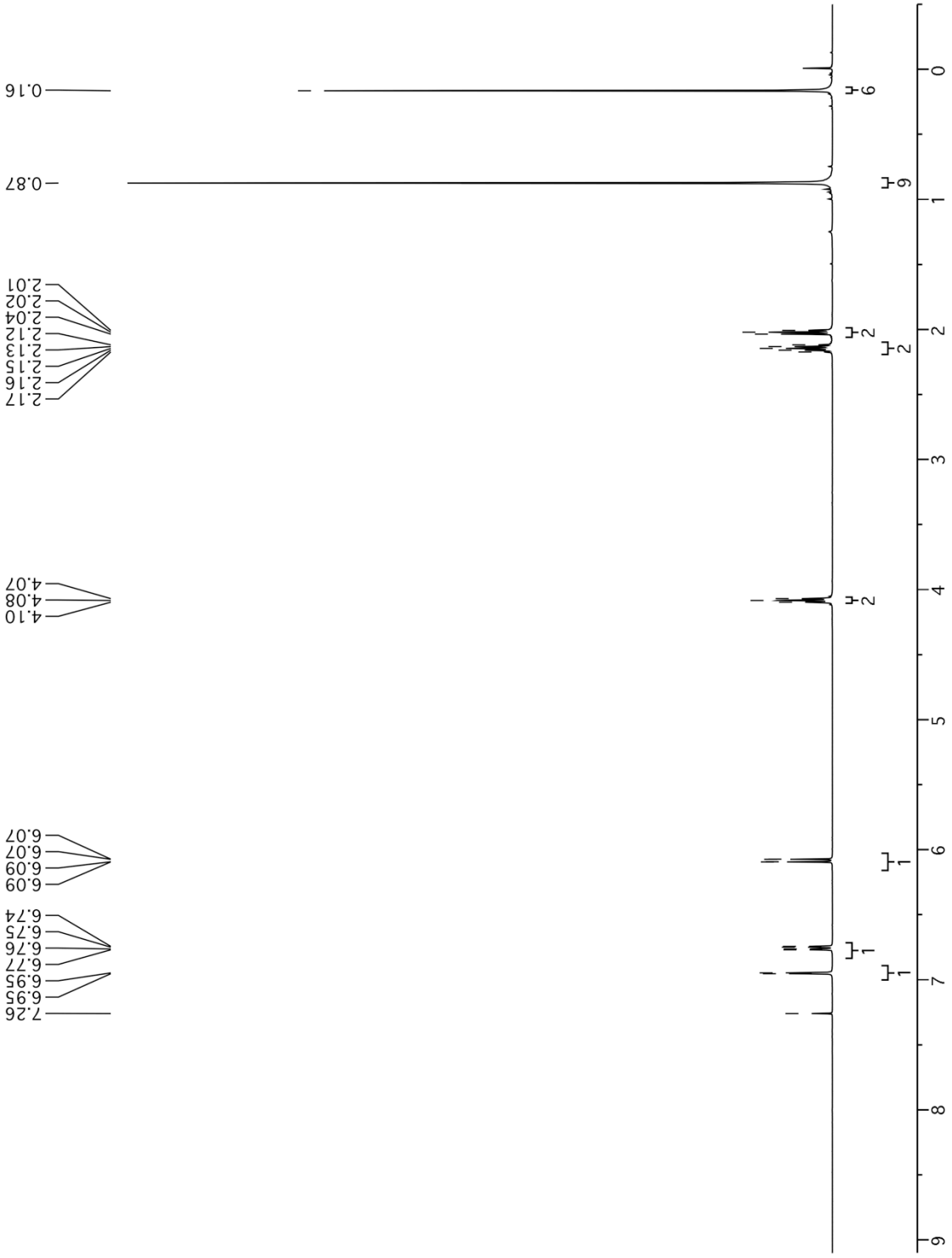

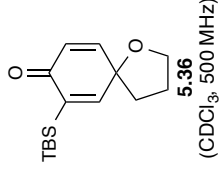

5.36
($CDCl_3$, 500 MHz)

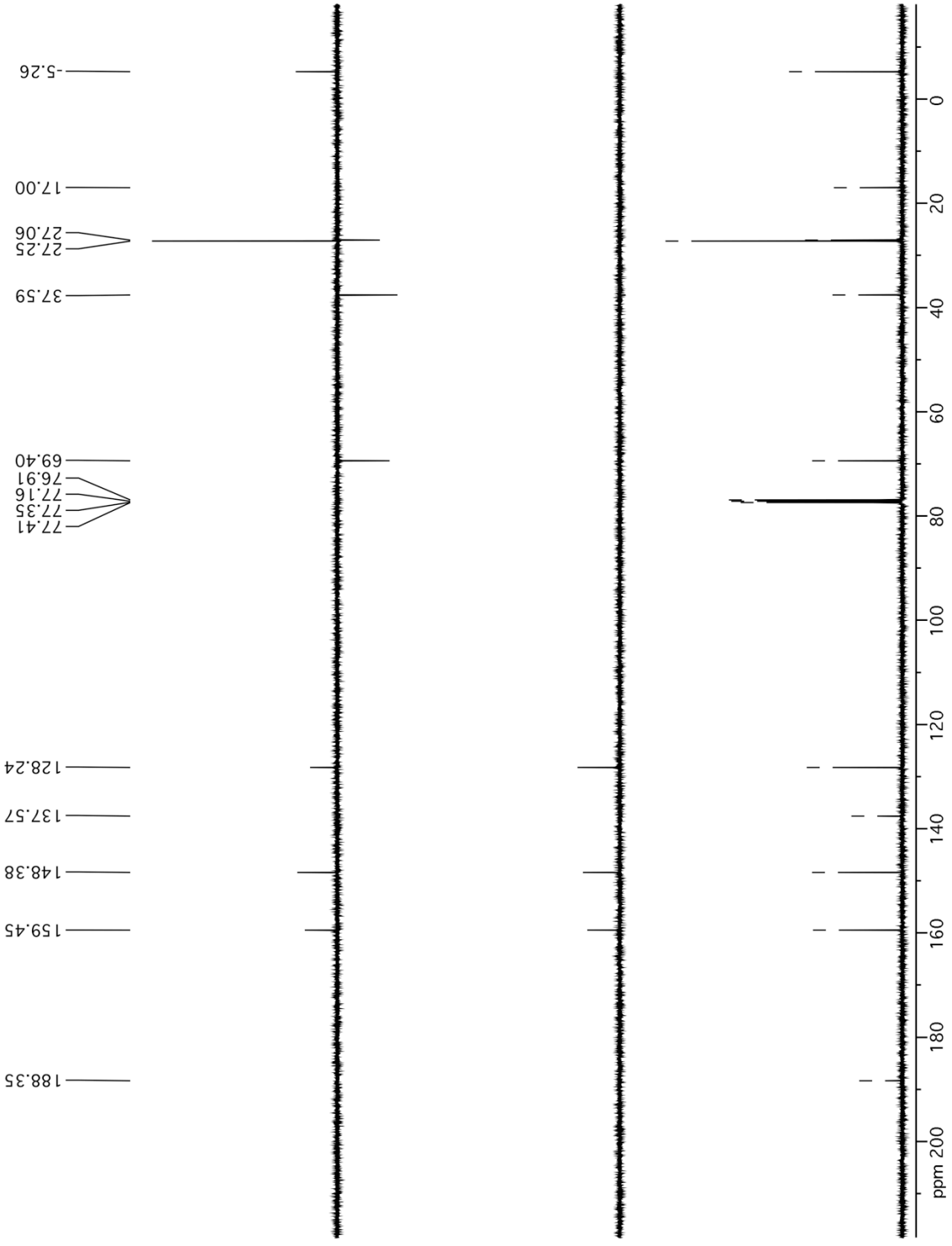

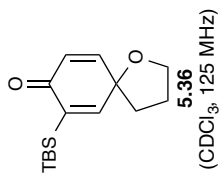

5.36
($CDCl_3$, 125 MHz)